THE UNIVERSITY OF
WARWICK

University of Warwick institutional repository: http://go.warwick.ac.uk/wrap

A Thesis Submitted for the Degree of PhD at the University of Warwick

http://go.warwick.ac.uk/wrap/67279

This thesis is made available online and is protected by original copyright.

Please scroll down to view the document itself.

Please refer to the repository record for this item for information to help you to cite it. Our policy information is available from the repository home page.

Aspects of Bolted Connections in Pultruded Fibre Reinforced Polymer Structures

by

Navroop Singh Matharu

A thesis submitted in partial fulfilment of the requirements for the Degree of Doctor of Philosophy in Engineering

University of Warwick
School of Engineering

Sept 2014

Contents

List of Figures

List of Tables

Acknowledgements

I would like to express my sincere gratitude towards my thesis supervisor, Prof. J. Toby Mottram, for his constant guidance and support throughout this research project. His endless encouragement and enthusiasm has been inspirational, and I am truly thankful to have had such an exceptional mentor during my studies.

I gratefully acknowledge the funding from the UK Engineering and Physical Sciences Research Council (EPSRC) for the research project, "Connections and Joints for Buildings and Bridges for Fibre Reinforced Polymer" (grant number: EP/H042628). Also, I am grateful for technical and materials support from Access Design and Engineering Ltd. (UK) and Creative Pultrusions Inc. (USA). I have benefited from the continued dialogue and discussions with Mr. John Freeman and Mr. Geoff Shinner (of Access Design). I would like to thank Mr. Rusi Russev and Mr. Tim Abbott of Mott MacDonald for their valuable input at our research meetings.

This research would not have been accomplished without the support of so many of the technician staff at the School of Engineering. In particular, special thanks go to Mr. Colin Banks and Mr. Robert Bromley for their tremendous support in preparing test specimens and assistance with testing. Thanks must be given to Dr. Jawed Qureshi and Dr. Behrouz Zafari for their support as a part of our research group. I am grateful to have met so many dear friends and colleagues at the University of Warwick, to them all, I thank you.

I would like to acknowledge my dear friends Mr. Amandeep Sehra, Mr. Jugdip Nandra and Mr. Satnam Sahota for their constant reassurance and support, especially in the difficult times. Above all, none of this would have been possible without my family, brothers, sister-in-law and mother. For all their love and care over the years, I am and always will be in their debt.

Declaration

The work described in this thesis was conducted by the author, except where stated otherwise, at the School of Engineering, The University of Warwick between the dates of October 2010 and March 2014. No part of this work has been previously submitted to the University of Warwick or any other academic institution for admission to a higher degree. All publications arising from this research to date have been listed after this declaration.

N S Matharu

Conference Papers

- Matharu, N.S. and Mottram, J.T. (2012), 'Laterally Unrestrained Bolt Bearing Strength: Plain Pin and Threaded Values,' in the *Proceedings of the 6th International Conference on FRP Composites in Civil Engineering (CICE 2012)*, Rome, Section 14: Codes and Design Guidelines, Paper 311.

- Matharu, N.S. and Mottram, J.T. (2013), 'Laterally Unrestrained Bearing Strength of Hot-wet Conditioned Pultruded FRP Material,' in the *Proceedings of the 6th International Conference on Advanced Composites in Construction (ACIC 2013)*, NetComposites Ltd., Chesterfield, UK, 241-251.

Abstract

This thesis presents an extensive test programme for bolted connections using SuperStructural Pultruded Fibre Reinforced Polymer (PFRP) materials with an emphasis on characterising strengths for the pin-bearing failure mode and linking coupon results to bearing failure in lap-shear bolted connections. The motivation for the research is to address key gaps in knowledge that are known to be hindering the preparation of recognised design guidelines for PFRP (frame) structures, which upon becoming available shall broaden exploitation in civil engineering works.

Prominent among these knowledge gaps has been the need to have statistically verified pin-bearing and bolted connections strengths that are with connection configurations complying with current design practice. Thread in bearing, as found in practice, is investigated together, for the first time, with the plain shaft situation. Both as-received and environmental (hot-wet aging) conditioned PFRP materials are characterized to study long-term behaviour. A non-standard pin-bearing strength test methodology, developed at The University of Warwick, is used to provide targeted test results for a comprehensive test matrix of 150 batches having 5 or 10 nominally identical specimens per batch.

A key contribution from the pin-bearing strength characterisation is that the in-house test method (WUTS) is shown to be suitable for the determination of pin-bearing strengths for flange and web materials, for bolting with or without thread and sizes from M10 to M20, and with a PFRP material orientated at 0^{o}, 45^{o} or 90^{o} to the direction of pultrusion. Thread in bearing does not always have an adverse effect, and it is found that both thread pitch and material orientation have a significant contribution on the measured pin-bearing strength. It is recommended, for the situation when thread is in bearing, a reduction factor of 0.7 is applied to the characteristic plain pin-bearing strength value in the bearing strength equations. Accelerated aging regimes and long-term strength prediction modelling has shown a mean pin-bearing strength reduction of up to 25% over 7.8 years, at UK service temperature of 10.5 °C. This value is found to lie within the bounds set by an American Load and Resistance Factor Design (LRFD) Pre-standard and gives confidence to the mandatory design requirements.

The thesis also reports on a series of strength tests following the methodology for pin-bearing characterization with single and double lap-shear bolted connections having configurations for single and two-rows, and for single and multi-bolts. Reported are a series of open-hole tension tests carried out to characterise the by-pass load situation in multi-rowed connections. A reduction factor of 0.6 between single and double lap configuration is found, with the possibility of multiple mixed failure modes, including block shear. The SuperStructural material has a tri-axial stitched fabric mat reinforcement (usually in pultrudates the mat is a continuous filament mat) which is influencing the strength of bolted connections. Using the procedure in Eurocode 1990, a partial factor of 1.3 for pin-bearing resistance has been calibrated by combining the WUTS and lap-shear bolted connection tests results. Results from an open-hole tension study have shown that the correlation coefficient proposed in the 1970s by Hart-Smith does not satisfactorily relate the isotropic stress concentration factor to the orthotropic stress concentration factor.

The findings and recommendations from the 1500 individual and 230 batch strength test results presented in this thesis have been successful in addressing or partially addressing a number of the key gaps in knowledge.

Notation

b_m	Mean correction factor
C_{op}	Open hole Correlation Coefficient
d	Pin (or bolt) diameter
D	Diffusion coefficient
D_0	Diffusion constant
D_a	Apparent diffusion co-efficient
d_n	Hole diameter
d_w	Washer diameter
e_1	End distance
e_2	Side distance
E_a	Activation energy
$F_{k,\vartheta}{}^{br}$	Characteristic pin-bearing Strength
F_t	Tensile Strength
$F_\vartheta{}^{br}$	Pin bearing strength with respect to orientation
g	Gauge Spacing
G	Time dependent parameter
g_s	Staggered gauge spacing
k_r	Reaction rate at interval r
k_{tc}	Orthotropic stress concentration factor
k_{te}	Isotropic stress concentration factor
l_s	Stagger distance
$M(s)$	Moisture Content
M_{cond}	Specimen mass after hot-wet conditioning
M_{dry}	Dry specimen mass
M_i	Moisture content at a given interval i
M_m	Maximum moisture content
n	Number of tests
p	Pitch spacing
P	Thread pitch
R	Universal gas constant
R_{br}	Pin-bearing Resistance
$R_{br,ff}$	Pin Bearing First Failure load

$R_{br,mn}$	Pin Bearing maximum load
r_e	Experimental resistance value
R_{nt}	Open-hole tensile strength
r_t	Theoretical resistance value
s	time
T	Temperature
t	Material thickness
t_f	Thickness of flange material
T_g	Glass transition temperature
t_w	Thickness of web material
V_{Xi}	Co-efficient of variation
V_δ	Co-efficient of variation of the errors
w	Width of material
w	width
W_d	Dry weight of specimen
W_w	Wet weight of specimen
γ_M	Partial safety factor
δ	Error
Δ_i	Estimator
ϑ	Material orientation

Abbreviations

ASCE	American Society of Civil Engineers
ASTM	American Standard Test Method
BSI	British Standards Institute
CFM	Continuous Fabric Mat
CoV	Coefficient of Variation
CP	Creative Pultrusions
CSM	Chopped Strand Mat
CV	Characteristic Value
CW	Cross Wise
EC3	EuroCode 3
EN	EuroNorm
FF	First Failure
FRP	Fibre Reinforced Polymer
FVF	Fibre Volume Fraction
GRP	Glass Reinforced Polymer
ISO	International Organization for Standardization
LRFD	Load and Resistance Factor Design
LW	Length Wise
MPa	MegaPascals
NI	National Instruments
PFRP	Pultruded Fibre Reinforced Polymer
SD	Standard Deviation
SV	Surface Veil
TSFM	Tri-axial Stitched Fabric Mat
UD	Unidirectional
UNC	Unified Course
UoW	University of Warwick
WF	Wide Flange
WUTS	Warwick University Test Setup

CHAPTER 1

Introduction

The manufacture of composite materials is arguably one of the oldest man-made engineering endeavours. From antiquity the use of straw to strengthen clay bricks through to 'wattle and daub' during the middle ages and more recently fibre reinforced concrete have all formed a key part of civil engineering resources. These materials all harness the strength of a fibrous phase whilst utilising the binding nature of often a weaker or brittle continuous matrix phase, thereby providing increased performance not available in either unmodified material alone. This technology has been replicated throughout the ages up to the modern era that has spurned the age of Fibre Reinforced Polymer (FRP) composite materials.

Figure 1.1 shows a schematic of materials that typically enclose in a continuous resin-matrix system inter-dispersed layers of high strength, high modulus fibres. These fibres can be commonly of glass, carbon, or aramid. Alternatively, naturally occurring fibrous materials such as jute, hemp or flax to name a few, can be used although their mechanical properties are considerably different than the aforementioned fibres. Similarly, a range of resin systems are used including thermoset resins such as polyester, vinylester or polyurethane and more

recently thermoplastics such as polybutylene terephthalate (PBT) or polyethylene terephthalate (PET).

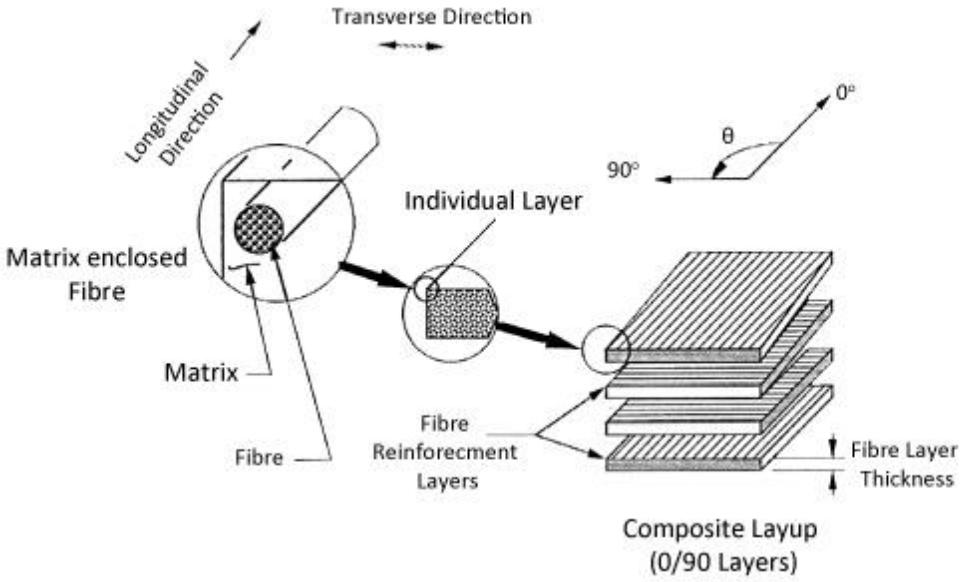

Figure 1.1: Schematic of a Composite Material

The key advantage of FRPs is their high strength-to-weight ratio. In addition, they can provide corrosion resistance, good electrical and thermal insulation and low maintenance over a long life cycle (Kim, 1995). A designer has a combination of properties not generally available in traditional structural materials, with the advantage that the material can be tailored to the specific application using modern manufacturing technologies. Ultimately these materials give considerable benefits to clients, contractors and designers alike.

The marine and aerospace industries have both used advanced composites for many years. Having developed a wide variety of manufacturing techniques, design analyses and multitudes of constituent combinations, FRPs have been successfully exploited in these industries. However, this has led to the fallacy to some extent that the material technology, analysis and design methods can be readily applied and adopted by structures in civil engineering as it is significantly mature in other industries.

There are several reasons that this misconception can be attributed and can be expanded by an abridged comparison of aerospace composites with those found in construction. At the outset, the aerospace industry typically utilises carbon FRP laminates whereas in construction, glass FRP material is generally used. Both types of FRP typically have different fibre architecture (layup), which affects the structural performance (Bank, 2006). Secondly, expensive and high strength fibres and resins are used in aerospace, whereas civil engineering composites are relatively cheaper and the matrix can often include fillers, such as calcium carbonate in order to reduce costs. Finally, the scale of joints and components can be considerably larger in civil engineering and this is reflected in the material thickness typically ranging from 6 mm to 25 mm thick compared to thicknesses as low as 2 mm used in aerospace. In addition, the shape of the connections and joints can differ significantly between the two industries.

As a result of these key differences in the material and methods of each industry, it is accepted that extrapolation of test results from characterisation work in the aerospace industry to civil engineering applications should be treated with caution (Mottram and Turvey 1998). This realisation has resulted in a significant movement of experimental and analytical studies being conducted with regard to the growing field of all-FRP shapes and systems in civil and structural engineering applications.

1.1 Composites in Construction

FRPs have been used in a limited capacity in civil engineering projects for over half a century, particularly for rehabilitation and repair of structures. Initially, specialist structural engineers in

FRP materials, who had visionary concepts, designed with these materials based on experience of in-house procedures from composite manufacturers (Bank, 2006).

As the industry grew, other mainstream (non-specialist) structural engineers and architects utilised FRP sections that were manufactured on a commercially large scale, with aid of published design guides, proof testing and in-house FRP manufacturer's assistance (Bank, 2006). This expansion since the 1990's allowed designers to exploit the technology and further develop an applied understanding. As a result, the present situation whereby some primary, but mainly secondary, load bearing structures, as well as building facades, are being made of FRP components as they have become more competitive (Turvey, 2000). One of the more widely exploited FRP manufacturing technologies for composites within construction is pultrusion and the next section introduces this cost effective building material and process.

1.1.1 Pultrusion

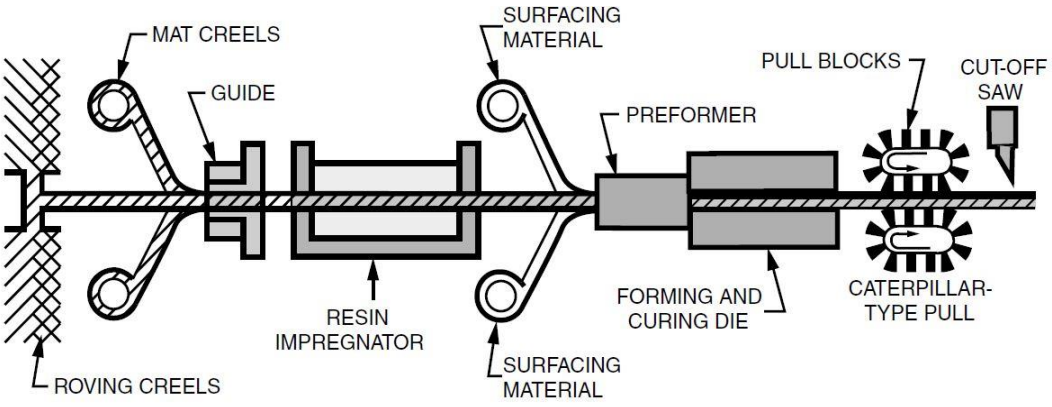

Figure 1.2: The Pultrusion Process (courtesy of Strongwell, 2013)

The portmanteau term 'pultrusion' was fashioned from the manufacturing process that combines to some extent a pulling and extrusion type action upon a part. The automated FRP processing method utilising the caterpillar type pulling action, as shown schematically in Figure

1.2, can be used to fabricate standard structural shapes. The figure shows the process (from left to right) of fibre reinforcement in both roving bundles and mat creels passing through guide plates and into a resin bath that impregnates them prior to being formed. The guide plates accurately align the reinforcement layers before the material is pulled into the heated die. A surface veil is added before the consolidation of the FRP shape occurs in the forming and curing die, after which the finished shape is cut to size. These shapes are often referred to as Pultruded Fibre Reinforced Polymer (PFRP) profiles.

Figure 1.3: Pultruded FRP Profiles (courtesy of Creative Pultrusions, 2010)

Inherently, the process lends itself to a variety of constant cross-sectional shape (along its length), thickness and size. The typical (or 'standard structural') shapes formed by pultrusion are I-beams, wide-flange sections, channels and leg angles as found in steel construction and as shown in Figure 1.3. The key driver for using this FRP manufacturing technique is the simple and relative low-cost continuous method, which can provide tailored custom profiles for customers, often referd to as 'second generation' shapes. The scope of the experimental work presented in this thesis is for standard structural shapes but does also extend to the more tailored profiles.

1.1.2. Pultruded FRP Applications

The application of PFRP materials, such as those shown in Figure 1.2, has become more wide ranging in recent years for civil engineering projects. Pultruded materials have been used for applications ranging from railway platforms to bridge decks and building facades to cooling towers. In 2012, the exploitation of PFRP material in the mainstream residential market led to the building of the "Startlink Lightweight Building System". The aim of the project was to provide an energy efficient and low cost solution to the ever expanding UK accommodation shortfall. There is certainly a clear demand for these materials and Figure 1.4 presents just a few examples of the aforementioned applications, with the future promising to deliver more innovative and unique structural applications utilising PFRPs.

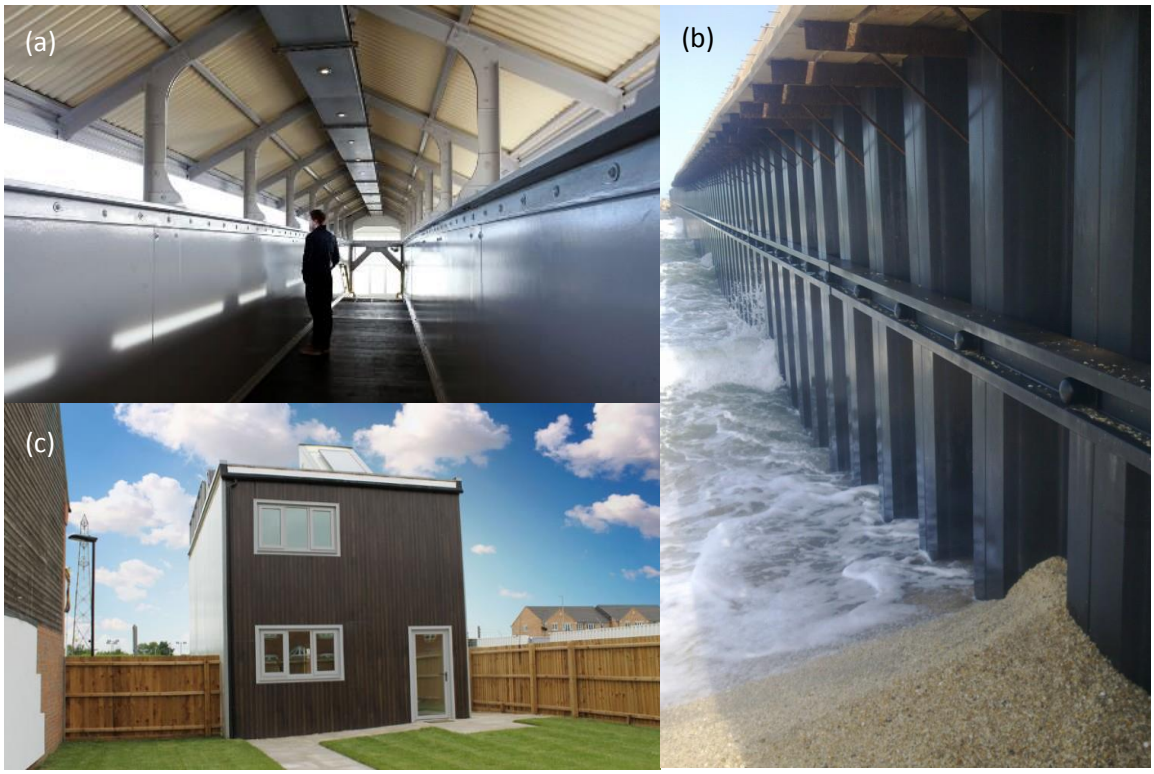

Figure 1.4: Applications of Pultruded Fibre Reinforced Polymer Materials including (a) The Dawlish Station Footbridge (courtesy of rail.co.uk), (b) SuperWaleTM Composite Sheet Pile Wall (courtesy of Creative Pultrusions) and (c) the Startlink Lightweight Building System (courtesy of building4change.com)

1.2. Aims and Objectives

Arguably the key barriers to wider implementation of the relatively novel construction materials, such as PFRP, are well founded design rules in the form of published standards – as can be found in the Eurocode suite (Mottram, 2009a). A designer will have an increased confidence to execute design in FRP if mature and verifiable design rules are available, which moreover, allow appropriate margins of safety and economical design concepts to be established.

Recognising this need, in 2007 the American Society of Civil Engineers (ASCE) and the American Composites Manufacturers Association (ACMA) signed a three-year agreement for a project to develop a pre-standard for the "*Load and Resistance Factor Design (LRFD) of Pultruded Fiber-Reinforced Polymer (FRP) Structures*." This LRFD standard is expected to help structural engineers and architects use pultruded FRP composites (standard shapes) in the design of buildings and infrastructure. In November 2010, the ASCE project delivered a pre-standard which was revised in 2012 (ASCE, 2012) and currently, the final clauses are being verified to allow this guidance to achieve an incorporated status as a full standard. Although this PhD work has not been specifically design code driven, the identification of a structural research framework (Mottram, 2009a) for "*Chapter 8. Design of Bolted Connections*" of the LRFD Pre-standard (ASCE, 2012) has influenced the aims and objectives of this PhD to allow congruent transfer of knowledge for use in design.

It is generally accepted that the verification of bolted connections in PFRP frames is a challenging exercise which is critical in establishing the safe design of a load bearing structure. The task has considerable gaps in knowledge (Mottram, 2009b), particularly ensuing to the many parameters influencing the stiffness and strength of connections and joints in PFRP. It is

the aim of the author's PhD work to address some of these issues by way of experimental testing, analysis and evaluation of targeted test results. This will allow either the revision or modification of current design provisions so that risk of structural failure can be minimised and improve the economy of the design. The work reported in this thesis is split into two major experimental themes with the following key objectives:

- to further develop the test methodology used for the determination of pin-bearing strength (without lateral restraint), and to characterise this key strength property for use in the design of bolted connections in FRP shapes;
- to conduct a series of plate-to-plate tests that characterise the resistance of bolted connections of Pultruded material, which shall lead to the proposal of new or improved design guidance.

The next section describes the thesis structure and some of the areas found in each chapter that address the aforementioned aims of this PhD research.

1.3. Thesis Structure

This thesis is divided into seven chapters. This chapter has given general background information on FRP materials and the pultrusion process. For a more in-depth review of the pultrusion method and FRP processing technologies refer to Starr (2000); equally a wide variety of topics including material properties, theoretical modelling and design of PFRP are discussed by Bank (2006) with specific regard to composites in construction.

Presented in Chapter 2 is a literature review of bolted connections in pultruded fibre reinforced polymer structures, covering testing from previous studies, particularly for pin-

bearing strength. The chapter highlights the key research questions to be addressed in this PhD thesis.

Chapter 3 covers material properties, firstly by way of describing a series of resin burn-off tests to establish the constituent properties of the FRP material. Tensile tests on longitudinal and transverse coupons are reported, which are further developed alongside open-hole tensile results to assess the suitability of the Hart-Smith approach (1978). In addition, compression coupons are tested which allow a comparison to be drawn with the main pin-bearing strength study and the manufacturers reported values as testing uses a non-standard compression test setup developed by Mottram (1994). The final section of the research in this chapter is a moisture diffusion study, which establishes the moisture diffusion co-efficient for the PFRP material with distilled water and various conditioning temperatures. Furthermore, an estimation of the activation energy of the material is presented in order to further develop the results and analysis in Chapter 5 for the long term pin-bearing strength performance of the material.

The fundamental material characterisation research presented in Chapter 4 is an extensive pin-bearing strength study with the aim of investigating this key strength property for use in the design. The study includes the effect of thread and material orientation with respect to the pultrusion axis on pin-bearing strength. Testing is conducted using the Warwick University Test Setup (WUTS) for pin-bearing strength testing, which is a non-standard method. Four pin sizes of M10 to M20 and a clearance hole are considered along with loading in the longitudinal (0°) and Transverse (90°) directions with respect to the material orientation. Furthermore, an in-depth analysis of the threaded failure mode and a novel study on thread pitch supplement the main investigations. The research data is vital in bridging the knowledge gaps for use in design equation calibration to give characteristic values.

Chapter 5 presents a study of the effect of environmental conditioning on pin bearing strength using a similar test matrix as Chapter 4 for non-aged material. The effect of thread in bearing is considered along with the aging regime to give a novel database of pin-bearing strength values. This allows the verification of a mandatory reduction factor to the plain pin bearing strength for thread in bearing as found in the ASCE Pre-standard (2012) to be checked for both the aged and non-aged situation. The specific parameters of the effect of high temperature and moisture are studied with the aim of estimating the long term degradation of pin-bearing strength due to environmental aging. The material is conditioned in distilled water for 3 and 6 months and at 30, 40 and 50°C. Comparisons are drawn with the non-aged test results from Chapter 4 to establish the influence of the conditioning with respect to others variables, such as pin size and material orientation on pin-bearing strength.

Chapter 6 is concerned with a series of double and single-lap shear plate-to-plate connection tests with five different bolting arrangements and mainly testing with a single size bolt. The bolting arrangements of single, two and four bolts along with connection geometry specifications are in line with the minimum requirements of the LRFD Pre-standard (ASCE, 2012). The results are analysed against the current design formula for bearing from the ASCE Pre-standard (2012) using the characteristic pin-bearing strengths presented in Chapter 4. A preliminary partial factor calibration is presented for the bearing failure mode and compared with current design provisions.

Concluding remarks from the PhD research are given in Chapter 7 along with a brief exploration of possible opportunities for further work in the field of connections and joints for PFRP structures.

CHAPTER 2

Literature Review

2.1. Introduction

Presented in this chapter is a literature review of fibre reinforced polymer materials with specific regard to construction and civil engineering. A general background has been given in the introductory chapter, from which attention was drawn to pultrusion technology and its applications. Hereafter, the emphasis is on bolted connections in PFRP materials, with an appraisal and collation of pertinent previous research with specific relevance to plate-to-plate connection design. Further in-depth review for specific information will be given in individual chapters where necessary.

This review shall firstly consider using bolted connections in PFRP structures, with a brief comparison with an alternative – adhesive bonding. Following on from this introduction to bolting in PFRP structures, next the failure modes are presented and specifically bearing failure which is associated with its own 'unique' pin-bearing strength formula (Bank, 2006) as specified in the LRFD Pre-Standard (ASCE, 2012). The majority of this thesis is dedicated to

characterising, analysing and developing guidance for this specific failure mode, as it is the most benign of the failure modes found in PFRP bolted connections (Mottram, 2009b). Previous investigations are reviewed for the bearing failure mode and strength characterisation as well as bolted connections studies. In addition, a brief overview of guidance available for the designer of PFRP bolted connections is given. Finally, a summary presents some of the key gaps in knowledge and further develops the research questions, outlined in the introductory chapter, which are to be addressed in the proceeding chapters.

2.2. Bolted Connections in Pultruded FRP Structures

Standard pultruded structural sections, imitating those found in conventional steel construction, are often used in civil engineering for non-sway braced frames (Turvey, 2000). PFRP sections are often connected together by conventional (stainless) steel bolting. These mechanical connections joining either pultruded profiles, such as single leg-angle and channels, or pultruded plate material (such as bracing members) are often referred to as "pultruded connections" (Bank, 2006). It should be noted that here, and onwards, the term connection and joint are with respect to terminology used for steel construction (EC3) as described in BS EN 1993-1-8 (British Standards Institute, 2001). A connection is two or more elements meeting, and for design proposes is the assembly of the basic components transferring actions. A joint can contain several individual connections and is where two or more members are interconnected together.

Bolted connections in PFRP structures provide ease of assembly and maintenance, as well as being capable of transferring the actions experienced in primary load bearing structures. The types of pultruded connections accepted in the ASCE pre-standard (ASCE, 2012) are shown in

Figure 2.1, with frame joints, such as web-cleated connections, in part (a) and plate-to-plate connections, such as the bracing members in part (b).

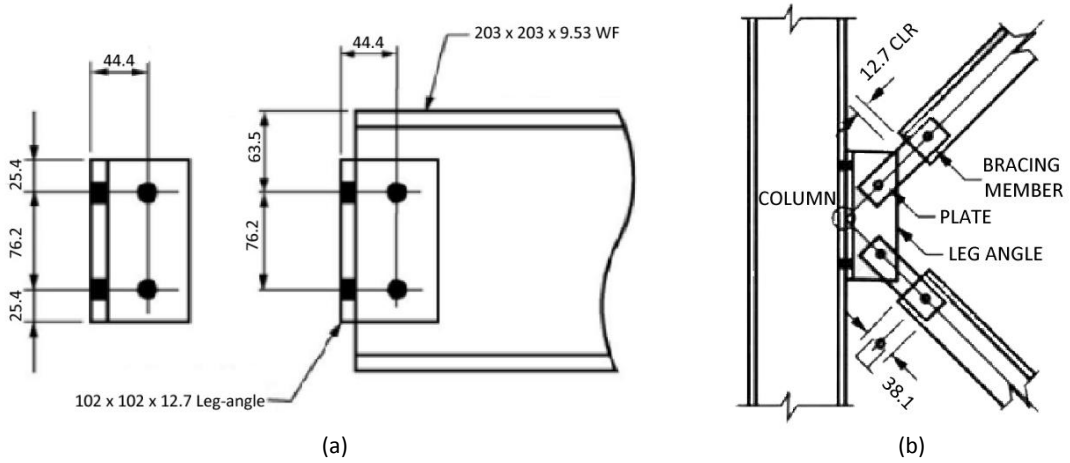

Figure 2.1: Typical Frame Connection Detailing adapted from Strongwell (2013) showing (a) Beam-to-Column and (b) Bracing Members

It is known that in PFRP structures the weakest part of a structure can be the connections (Turvey, 1998). Furthermore, the characterization of the strength and stiffness of FRP materials is complicated, mainly as a result of the number of material variables involved, with Godwin and Matthews (1980) going as far as stating:

> *"…in view of the very large number of variables involved, a complete characterisation of connection behaviour is impossible".*

These variables can include considering the directional mechanical properties in the three principle material axes and an elastic response with the material yielding (rupturing) without significant ductility. Therefore, design of joints with FRP materials must account for parameters related to the type of connection and its associated geometry as well as the directional strengths; the situation is more complex than traditional materials, like steel.

Godwin and Matthews (1980) set out bolted connection parameters and subjectively divided them into the three groups of: material parameters; fastener parameters; design parameters. The mass of published information on mechanically fastened connections in glass FRP (including material manufactured by pultrusion) is largely related to experimental results. Although, there have been prominent computational and analytical models of PFRP bolted connections (McCathy *et al.*, 2005; Hassan et al. 1996), stress analysis through finite element methods proves complex due to the various complications mentioned. Moreover, the prediction of local stress concentrations and verification with empirical testing is equally challenging both of which are paramount to understanding the structural behavior of the connections.

There are three conventional methods of connection adopted with PFRP shapes and systems. They are mechanical fastening; adhesive bonding and a combination of both mechanical fasteners (including the mechanical interlock of PFRP shapes) and bonded connections. The type of connection used requires careful deliberation of all the relevant parameters affecting the performance of the connection. For example, if dismantling is required this excludes bonded connections, whereas if thin section members (not commonly found in civil engineering structures) are to be joined it would be implausible to use mechanical fasteners. Mechanical fasteners can be found of FRP or stainless steel, with the latter being more commonly used due to the financial economy achieved, but in corrosive environments or the need for electromagnetic transparency is required the former has clear advantages. Some of the main advantages and disadvantages (Broughton *et al.*, 2002) of bolted and bonded connections are summarised in Table 2.1.

Table 2.1: Review of Bolted Connections in FRP

Advantages	Disadvantages
• No surface preparation is required • Easily disassembled with component damage • Straightforward manufacture and inspection • Full strength developed immediately • Insensitive to peel forces • Simple connection configuration • Residual stress generally not a problem	• High stress concentrations due to drilled holes • Added weight of mechanical fastener • Metallic parts have poor fatigue resistance • Special sealants needed for weather tightness • Possible corrosion of the metallic fasteners • Difficult to achieve high connection strength

Table 2.2: Review of Bonded Connections in FRP

Advantages	Disadvantages
• Lightweight • Good fatigue life • Smooth surface contours of connection • Relatively high stiffness • Damage tolerant to certain degree	• Cannot be disassembled • Weakened by environmental degradation • Require surface preparation • Difficult to inspect for connection integrity • Takes time to develop full strength • High quality control required • Sensitive to peel and cleavage stresses • Difficult in bonding thick sections

Although, adhesively bonded connections are known to provide a higher efficiency than mechanically fastened connections; preference is given to the latter for its simplicity and hence most pragmatic solution. The key disadvantage of mechanical fastening (Eriksson, 1998) is the inability of the connection capacity to be more than 50% of the material. In bolted lap-connections of FRP material, with current factors of safety (Strongwell, 2013 and Creative Pultrusions, 2010) maximum working loads is <15% of the material strength available. Therefore, the need arises for the engineering uncertainties to be diminished through further targeted research of these connections (Turvey, 1998). Despite, some challenges for wider exploitation of bolted connections, the use of adhesive bonding is rarely used in pultruded structures due to durability issues (Bank, 2006). Considering civil engineering structures have life spans of tens of years, up to say 50 years, the long-term properties of pultruded adhesively bonded connections are still unknown and subject to research (Cadei and Stratford, 2002).

2.3. Failure Modes of PFRP Bolted Connections

The basic building blocks for a bolted connection will now be considered with an exploration of the failure modes, which inform Chapters 4 to 6. The discussion will be limited to plate-to-plate connections which have a double-lap shear configuration with in-plane loading. Although, the single-lap configuration, as shown in Figure 2.1b for bracing members, is detailed within Chapter 6, most testing prefers the double-lap arrangement due to the limited detrimental effect of the geometrical discontinuity, as found in the former.

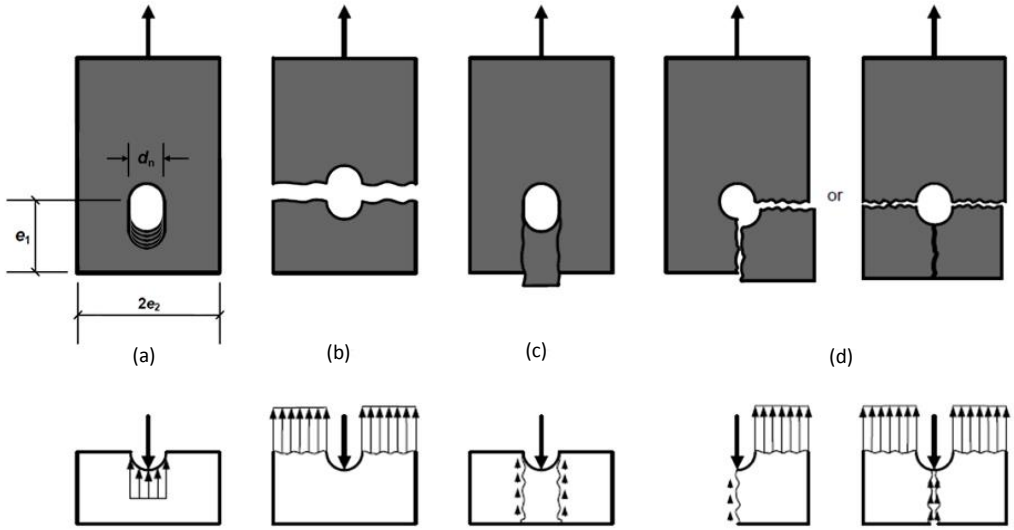

Figure 2.2: Failure Modes of PFRP Bolted Connections under Shear Loading showing (a) Bearing, (b) Net-section, (c) Shear-out and (d) Cleavage Failure (Mottram, 2009b)

As already established (Mottram 2009a), the design of bolted connections with PFRP is critical in ensuring sound structural performance and involves a fundamental understanding of connection and joint failure modes. Furthermore, due to the orthotropic and layered nature of PFRP, failure modes can vary significantly (Mottram and Turvey, 2003). The damage and mode of failure is dependent on connection detailing, material and fastener specifications, such as geometry, fibre volume fraction, bolt torque and loading conditions, etc. The fracture

mechanisms of PFRP include delamination, intra-laminar matrix cracking, longitudinal matrix splitting, fibre/matrix de-bonding, fibre pull-out, and fibre fracture (Bank, 2006).

PFRP bolted connections experience failure modes which are similar to those found in conventional structural steel bolted connections. The basic modes include net-tension, shear-out and bearing as shown in Figure 2.2 parts (a), (b) and (c) respectively. In addition to these basic failure modes, a fourth known mode is cleavage or splitting failure, shown in Figure 2.2d. Combinations of failure modes are also possible with special cases of shear-out and cleavage leading to 'block-shear' found with multiple rows of bolts. Also, it should be noted that these distinct singular failure modes are expected to occur in PFRP when loaded in 0 or 90° direction (either parallel or perpendicular to the pultrusion axis). Loading that occurs in off-axis orientations (for example within a truss member) failure will generally occur in combined net-tension and shear-out along the plane parallel to the UD rovings (Cooper and Turvey, 1995).

Mottram and Turvey (2003) and many previous researchers state that bearing failure is most preferred in design due to its potential to give a progressive pseudo-ductile response, when compared to the sudden failure and often without damage tolerance of the other modes. The term pseudo-ductile is used because yield or ductility is a misleading term if applied to PFRP connections. Within the context of PFRP engineering the term ductility would be used to differentiate between the sudden failures of a connection, e.g. net-section, from a failure which continues to resist the connection yield load at increased displacement (stroke), e.g. bearing. However, in the latter case the energy absorbed in the deformation of a PFRP connection cannot be regained since the crushing of fibres under the bolt is permanent and therefore no further energy is available from that portion of material at the connection

Table 2.3: Recommended Geometric Relations for Plate-to-Plate Connections (Bank, 2006)

	Research Data		Manufacturer	
	Recommended	Minimum	Recommended	Minimum
End distance to bolt diameter (e_1/d)	≥3	2	≥3	2
Width to bolt diameter (w/d)	≥5	3	≥4	3
Side distance to bolt diameter(e_2/d)	≥2	1.5	≥2	1.5
Pitch distance to bolt diameter (p/d)	≥4	3	≥5	4
Gauge distance to bolt diameter (g/d)	≥4	3	≥5	4
Bolt diameter to thickness (d/t)	≥1	0.5	≥2	1
Washer diameter to bolt diameter (d_w/d)	≥2	2	-	-
Bolt-hole clearance (d_n-d)	Tight-fit (0.05d)	1.6 (Max)	1.6	-

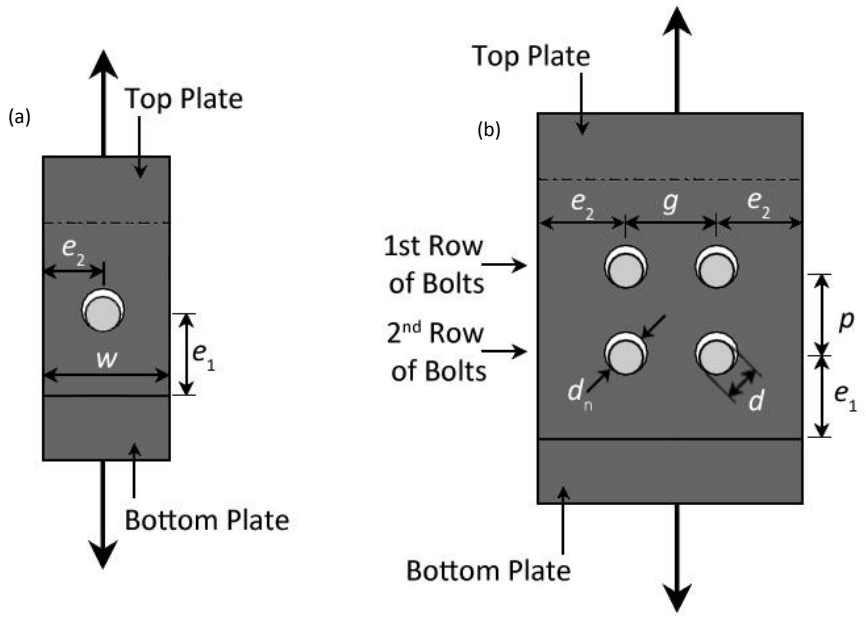

Figure 2.3: Geometric Relations for (a) Single Bolt and (b) Multi-bolt Plate-to-Plate Connections

Bearing failure is achieved by design of a connection with large end distances and widths relative to the bolt-hole. The key geometric relations, as shown in Figure 2.2, are the side distance, e_2, (where the width, w is equal to $2e_2$), the end distance, e_1, the bolt-hole diameter, d_n and the thickness of the PFRP plate, t (not-shown). In Table 2.3 are recommended and minimum geometric relations for plate-to-plate connections with in-plane loading, as compiled by Mottram and Turvey (2003) from manufacturers design manuals and research data. Figure 2.3 shows a schematic of the geometric relations found in Table 2.3. (Note, these values are not the same as those presented in Chapter 6 for the ASCE Pre-standard) These values are

from tests on pultruded plate (flat sheet) material and are expected to differ from structural shapes, which is one of the reasons for the research presented in Chapter 6.

The design of bolted connections of PFRP structures involves considering all of the distinct failure modes, as presented in Figure 2.2, each of which have their own associated 'simple' design formulae. Simplified design equations based on structural mechanics with idealised stress contributions for the design of PFRP bolted connections have been proposed by many (Chamis, 1988; Hart-smith, 1978); although, these methods are still difficult for designer to apply (Mottram, 2009b). The simple closed formed solutions presented in this chapter are based on the ASCE Pre-standard and developed through the endeavours of collating previous research by Mottram (Mottram and Turvey, 2003). It is currently required to establish a unique structural property of 'pin-bearing strength' for use with the preferred bearing failure mode. This distinct strength property is the specific topic of Chapters 4 and 5 and used in Chapter 6. Therefore, having considered the basic failure modes, next, an overview of bearing strength and previous research studies into this distinct failure is presented. The simple closed-form equation, as specified for use in design (Bank, 2006) and in accordance with the ASCE Pre-standard is given along with a discussion of the factors affecting pin-bearing strength.

2.3.1. Pin-bearing Failure

The pin-bearing strength is the laterally unrestrained strength value when a loading pin, representing the plain shaft of a bolt, bears against the bolt-hole of a PFRP. Pin-bearing strength is not a pure material property, but a system property, which forms a convenient concept for design. Due to it not being a pure material property, pin-bearing strength is dependent upon: the specific fibre architecture and composition of the material; diameter of the fastener; angle between resultant force and material (fibre) orientation; and friction

between fastener and FRP (Mottram, 2009b). The pin-bearing strength measure (where there is no lateral restraint or clamping force) is chosen to calculate the bearing resistance (R_{br}) per bolt (ASCE, 2012; also see Mottram, 2009b; Bank, 2006) as given in Equation (2.1).

$$R_{br} = tdF_{\theta}{}^{br} \tag{2.1}$$

The strength formula (given in Eq. (2.1)) requires the specific pin-bearing strength ($F_{\theta}{}^{br}$) to be calculated, with respect to the direction of pultrusion (θ), from the bearing resistance (R_{br}) measured from a failure load given in a bearing test. Conventionally, the orientation of the applied force, when parallel to the pultrusion direction, is noted as θ = 0° (longitudinal or lengthwise) and when orthogonal, θ = 90° (transverse or cross-wise). The projected area of bearing is given by the thickness of the material (t) multiplied by the diameter of the bolt or pin (d).

Pin-bearing failure due to the bolt connection force, involves the crushing and delamination of material directly beneath the bolt contact in PFRP materials. Considering the dependency of the bearing strength, it is unsurprising that the response of bolted connections that failed in bearing are sensitive to bolt diameter, material thickness, fibre orientation and architecture, clearance-hole size and environmental conditioning (Mottram and Turvey, 2003). In this thesis 'bearing' is when bolt torque and lateral restraint is present; pin-bearing is without lateral restraint and a plain pin situation; and threaded pin-bearing is with a thread in bearing, but with no lateral restraint. It is known, when lateral restraint is applied through a bolt torque, a higher bearing strength is found (Turvey, 1998; Mottram, 2004). This is due, somewhat, to the added stiffness that opposes inherent through-thickness deformations – which if inhibited would lead to delamination between the material's fibre reinforcing layers. The favourable effect of lateral restraint from bolt torque needs to be considered in relation to the reduction

found from creep relaxation (Thoppul et al., 2009; Mottram, 2004). Therefore, in order to ensure premature failure of a bolted connection does not occur, the lower bound strength value of pin-bearing strength should be used, with respect to design variables as found in practice (Mottram, 2009b).

2.3. Bearing Strength Studies

In this section previous research on bearing strengths of FRP material along with factors affecting this strength measure are presented. This section informs both Chapter 4 and 5 on pin-bearing strength characterisation and environmentally conditioned pin-bearing strengths, respectively. First, a short review of work conducted by Johnson and Mathews (1979), which proposed the various ways of defining a failure load for bearing strengths, is given. Next test methods of characterising bearing strength shall be given, with an emphasis on giving a background for the non-standard test setup used within the proceeding chapters. There has been, historically as noted by Mottram and Zafari (2011), an inconsistency in the specification of pin-bearing test methodology. Hence a brief overview of the methodologies employed will both give context to the need for the non-standard setup used within this thesis. Finally, this section widens the discussion to the key factors affecting bearing strength in particular for the areas of pin size, clearance, thread bearing, material orientation and environmental conditioning.

2.3.1. Failure Load Definition in a Pin-bearing Test

The bearing strength is by description the mean stress at bearing failure, however, the failure load criterion for this mean stress value is defined. Figure 2.4 shows the typical load/extension plot recorded by Johnson and Matthews (1979) for testing of single bolt e-glass/epoxy FRP

plates. The problem can fundamentally be seen in the seven possible ways of defining the failure load from load/extension plots. These can be split between a strength criterion and a displacement criterion. It must be noted that the load/extension response of a connection will be dependent on the specific detailing and environmental conditioning of the connection testing.

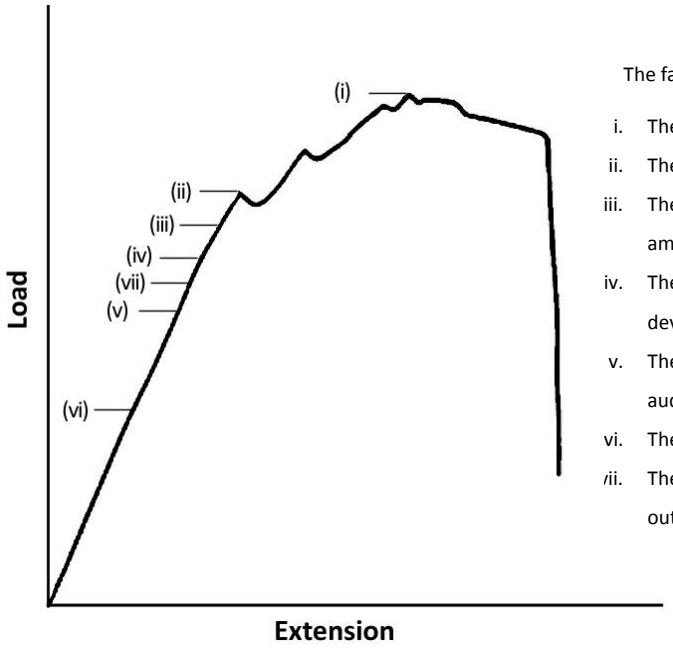

The failure load definition was noted as:

i. The maximum load;
ii. The first peak in load/extension plot;
iii. The load corresponding to a specified amount of hole elongation;
iv. The load at which load/extension plot first deviates from linearity;
v. The load at which cracking first becomes audible;
vi. The load at which cracking is initiated;
vii. The load at which cracks become visible outside the washer.

Figure 2.4: Failure Definition from the load-extension curve (Johnson and Matthews, 1979)

The three clearly objective methods of choosing a failure loads from Figure 2.4 are (i) to (iii), with the other methods dependent on individual test criteria. The failure loads based on strength criterion include the maximum load which is taken usually after considerable damage has already occurred. Similarly, the first-peak in the load-displacement curve is concurrent with damage which is not trivial. The displacement criterion includes a specified amount (%) of hole-elongation. This criterion has been used by various research test methodologies (ASTM D953-10; MIL-HDBK-17-3F; ASTM D5961-05; Thoppul *et al.*, 2009). Johnsons and Mathews stipulated that some of the aforementioned load definitions would be subject to variability

and therefore they placed the measurement of bolt-hole deformation, definition (iii), as the most reliable approach. This method has often been consistently found in the aerospace industry and test standards, such as ASTM D953-10 which specifies a 4% hole-diameter offset. Although this standard (ASTM D953, 2010) has been used for the characterization of pultruded FRP materials, its scope actually lies within rigid plastics.

Mottram and Zafari (2011) note that Vangrimde *et al.* (2003) explained that the use of the 4% hole elongation was flawed as design parameters rely on bearing deformation that is dependent on a 'bearing' displacement and not hole elongation. This displacement is to be measured from the point, remote from the bolt hole, at which the stress concentrations have disappeared. This observation has been a contributing factor to why load/displacement plots cannot be readily compared (Mottram, 2001). Mottram and Zafari (2011) revisited the original definition of failure by Johnson and Matthews (1979) in a historical survey of tests methods and advocated that the definition (iii), in Figure 2.4, was not suitable as determination is uncertain due to the reliance on the gauge length used to measure the hole-elongation. Furthermore, they identified that failure definitions (iv) to (vii) were not observed in pultruded materials for pin-bearing tests and (ii) did not occur for the longitudinal direction. Therefore, the bearing strengths should be determined using failure load (i), the maximum load. This is the method selected for the pin-bearing study presented in Chapters 4 and 5.

2.3.2. Pin-bearing Test Methods

Prior to presenting an overview of test methods, it would be useful to summarize the scope of bolted connections in the ASCE LFRD Pre-standard (2012). Material is specified as plate (flat sheet) or structural profiles (I, H etc. sections) between 6.35 mm and up to and including 25.4 mm with E-glass reinforcement. The structural profiles are likely to have higher Fibre Volume

Fractions (FVF) of UD rovings (Creative Pultrusions, 2010). Bolting is permitted for ASTM standards A193, A304, A307 and A316, with bolt diameters, *d*, ranging from 9.53 mm up to and including 25.4 mm. At least one hardened flat circular washer, with a minimum outer diameter of 2*d,* is to be used at either the head of the bolt or the nut. A 'snug-tight' level of bolt torque is specified, as defined by the Research Council on Structural Connections (RSCS) guidelines for steel bolting (RCSC, 2009). The nominal clearance-hole diameter, d_n, is to be 1.6 mm larger than the bolt diameter, *d*, with the holes being reamed or drilled. The use of a pin-bearing strength when a light torque is specified has been discussed with regards to loosening of this clamp-up pressure over time due to relaxation (Mottram, 2004).

With regard to the testing for bearing strength PFRP material there is a variation in approaches. This has led to reported bearing strengths for PFRP (Creative Pultrusions, 2010; Zafari, 2013) being disparate and not always with their derivation known (Mottram, 2009a). Traditionally, testing has been in accordance with aerospace testing procedures as documented by Thoppul *et al.* (2009), with the use of test methods such as ASTM D5961-13 (2013) and conforms to MIL-HDBK-17 (2002). This standard has provisions for both single-lap and double-lap shear configurations, and corresponds to the aerospace bolted connections with composite laminates. Mottram (2009b) notes that end distance of 3*d* may not be large enough for the bearing mode to govern for PFRP instead of the symmetrical laminates for which test method is written.

The more common methodology detailed in D953-10 (2010), as shown in Figure 2.6, utilises a double lap shear connection configuration under static tensile loading, with a hardened steel pin of 6.35mm diameter only, in order to establish load/extension plots. Considering that pin size can significantly affect bearing strength, as shown by studies to be highlighted later, this is a key reason of dismissing this test standard for characterisation of pin-bearing strengths. The

maximum hole diameter is specified as d_n = 1.012d, which gives an almost tight fitting clearance hole of 0.012d_n and doesn't comply with current practise, and guidance on minimum clearances of 1.6 mm (ASCE Pre-standard, 2012). This test standard is written for rigid plastics; although, as Mottram (2009b) reported, a majority of manufacturers of pultruded materials have and continue to test bearing strength using this standard, as given within pultruder's design manuals (Creative Pultrusions, 2010). The test specimen thickness is specified at 6.4mm, e_1/d = 3 and e_2/d = 1.85d. A gauge length behind the hole is 100 mm, although some of this length is used for gripping the specimen. The failure load specification is taken as the 4% bolt-hole elongation from extensometer readings, which has been deemed unreliable (Mottram, 2009b).

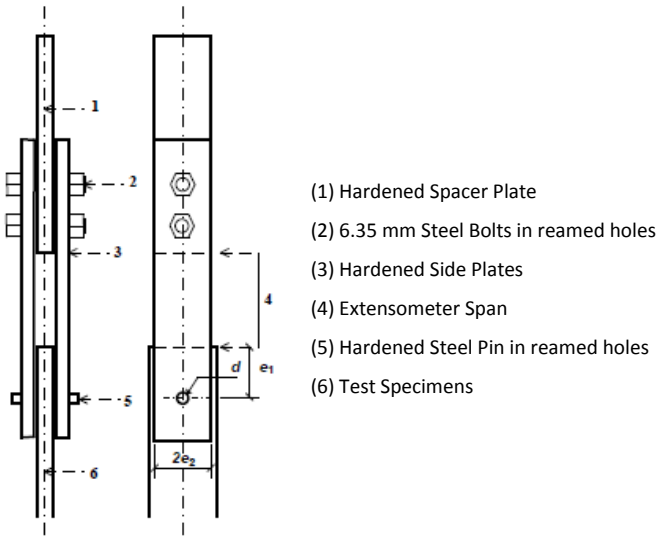

Figure 2.5: ASTM D953 Bearing Test Setup with a Steel Tension Loading Fixture (ASTM D953-10)

To address the need for a standardised specification for pultruded materials in Europe there is BS EN 13706-2:2002, Annex E of Part 2, produced with guidance for a bearing strength test method (British Standards Institute, 2002). This test procedure is for double-lap shear configuration with tensile loading and requires only the maximum bearing stress to be calculated. The key difference between ASTM D953-10 and BS EN 13706-2 is the test coupon

dimensions of the latter have an end distance to bolt diameter (e_1/d) of 6, twice the specification of the former. This requires particularly large specimen sizes for testing coupons, especially when the direction of pultrusion is normal to the direction of testing and a large bolt diameter is used. It must be noted that test coupons can readily be manufactured from standard pultruded plate material (with the constituents of structural shapes); because the fibre architecture is different this option could produce inappropriate bearing strengths for use with structural shapes. The pin diameter is 6 mm (not specified with a clearance-hole of the small size). It is of interest that part 3 of this standard specification stipulates that a material is required to have minimum pin-bearing strength in the longitudinal and transverse directions of 150 and 90 N/mm^2 (Grade 23) or 90 and 50 N/mm^2 (Grade 17). This thesis considered material that may be assumed to have material of Grade 23.

Amongst the literature an alternative arrangement to the double-lap shear configuration is a compression testing procedure developed by Wang et al. (1996) that utilises a semi-circular notch instead of a full circular hole within a comparatively smaller specimen, as shown in the sketch in Figure 2.6.

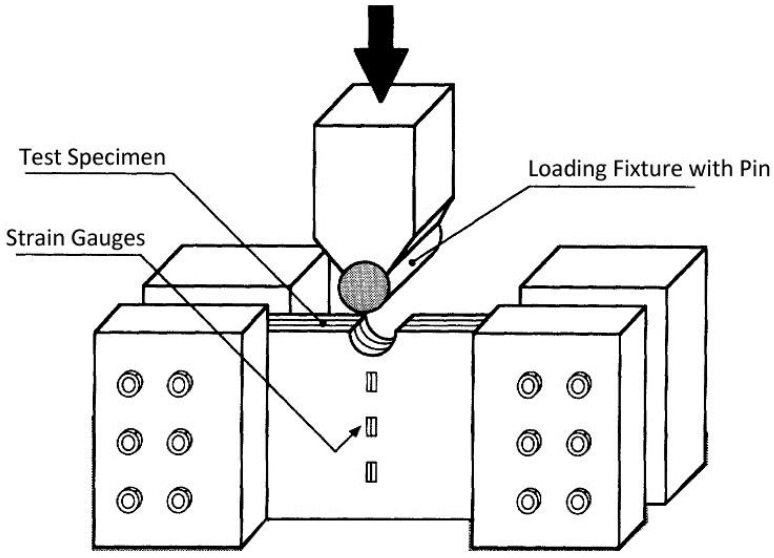

Figure 2.6: Wang et al. (1996) Pin Bearing Test Setup

The load is applied through a cylindrical steel rod (representative of the bolt shaft) attached to the load head, and the setup allows the specimen to deform freely as the in-plane load is applied. This method ensures that the material fails only in the bearing mode for the given static loading conditions (low stroke rate of 0.02mm/s). It can be noted that the procedure is somewhat adapted from ASTM D5764-07. Furthermore, in a bolted connection, flexure of the bolt can and does occur, which is inhibited by ASTM D5764-07 and could be seen as limitation of this dowel bearing type test method. Wang et al. (1996) also performed bolted connection tests and a comparison with the pin-bearing strength results showed a marked change in the type of bearing failure with a more benign failure with lateral restraint. This provides another reason to specify the pin-bearing method, without lateral restraint, as it determines a lower (safer) strength value.

Now returning to the Pre-standard specification for bolted connections (ASCE, 2012); the short overview of bearing strength test methodologies (ASTM D5961; ASTM D953; BS EN 13706) has highlighted several key issues. Firstly, the size of specimens would need to be smaller than specified in the European specification, such that specimens could be manufactured from web and flanges of structural shapes and not only flat sheet. Moreover, there should be no lateral restraint for the determination of safe design strength with the measurement meeting appropriate to field conditions. One such condition is for a clearance hole which is specified within the Pre-standard (1.6 mm) but doesn't feature in either D953-10 or BS EN13706-2:2002. In addition, in practice, a range of pin diameters are used and hence an appropriate test methodology should accompany this range, with previous research indicating a conservative value (worst case) will be found for the largest pin-to-thickness ratio (Mottram and Zafari, 2011). To consider this aspect and other factors affecting pin bearing strength a review of previous studies is given next.

2.3.3. Factors Affecting Pin-bearing Strength

Presented next are various studies pertaining to the effect of thread in bearing, clearance-hole size and pin-size on bearing strength. These studies are useful for informing Chapters 4 and 5 on pin-bearing strength characterisation. Firstly a series of tests by Troutman and Mostoller (2010) will be discussed. A programme of pin bearing tests conducted a study to investigate the effects of bolt diameter, clearance hole and thread in bearing. They conducted pin-bearing tests for longitudinal material only for thread in bearing, on three different PFRP structural shapes of thickness 6.35, 12.7 and 15.9 mm. Bolt diameters ranged from 6.35, 12.7 and 15.9 mm and testing utilised a modified D953 (Procedure B) configuration with no bolt torque. The pin diameter study showed as the pin diameter increased, the pin-bearing strength decreased, by as much as 29% between the largest and smallest pin size. The clearance study showed the larger the hole-diameter the lower the pin bearing strength. The threaded-pin study showed that the largest reduction in bearing strength due to thread in bearing was 37%. The study used UNC bolts of size 12.7 mm and 15.9 mm which have TPI values of 13 and 11, respectively. The largest reduction was found for a laterally unrestrained 12.7 mm pin with a 6.35 mm thick polyester resin matrix pultrusion (the fibre architecture is unknown).

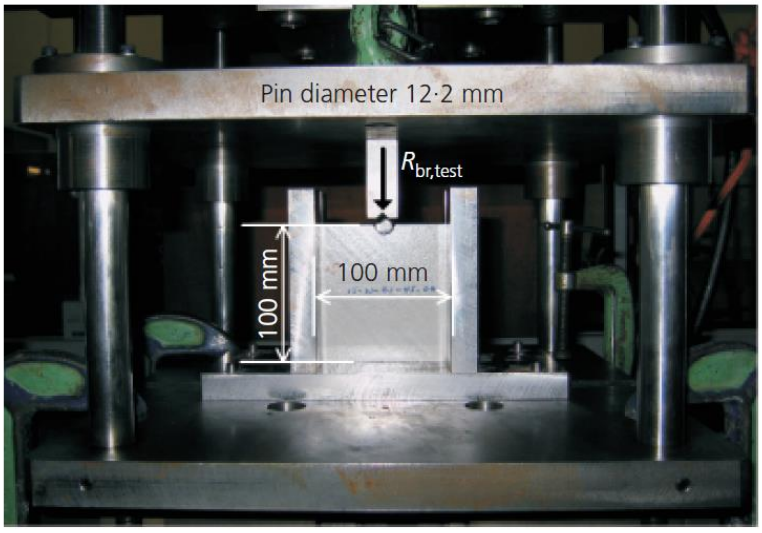

Figure 2.7: Warwick University Test Setup (WUTS) for Pin Bearing Strength Tests (Mottram and Zafari, 2011)

Mottram and Zafari (2011) studied the effect of pin diameter on the pin-bearing strength. They used a non-standard compression test setup, as shown in Figure 2.8, similar to Wang *et al.* (2006) for evaluating pin bearing strength values from web material of a 203 x 203 wide flange section with 9.53mm thickness from Creative Pultrusion Inc. The bolt diameter was varied from 9.7mm to 25.4mm with 1.9mm minimum clearance holes and results were taken with θ at 0°, 45° and 90°. The results based on the minimum characteristic strength values indicated a decrease of 50-60% found on changing *d* from 9.7mm to 25.4mm pin size. The earlier reported pin-bearing strength ratio for (F_0^{br}/F_{90}^{br}) gave a new minimum value of 1.13. In addition, the study reported that the aforementioned strength ratio was not proportional to the ratio of the moduli of elasticity at 1.7 (Lane, 2002). The proposed explanation was that the failure mechanism for the bearing mode had changed with orientation.

A key factor effecting pin-bearing strength is the changing the fibre orientation angle, θ, in the off-axis direction with respect to the axis of loading. This shall be discussed next. Zafari and Mottram (2012b) reported results from a series of test at three θ values of 5, 10 and 20°, with four pin diameter-to-thickness ratios ranging from 1.05 to 2.76, for specimen taken from a PFRP section. They alluded to a linear decrease in strength as θ increases. Ascione *et al.* (2009) conducted testing for bearing strength using a FRP plate with similar fibre architecture to PFRP material. Measurements were made at for various θ values with respect to the load. They showed that a significant decrease in bearing failure load occurred when the fibre inclination angle, θ, increases. For example a 15% reduction (of maximum recorded value) was found for a θ value of 10°. In a survey of various bolted connection tests (Mottram, 2009b), it was noted that the strength ratio from 0° to 90° ratio bearing strengths can be between 1.2 and 1.5 depending on how orthotropic the material. The strength trend was not linear but rapidly decreased within the 0 to 20° range and steady fell to the 90° value.

Having discussed the effects of pin and material parameters, next a brief overview of environmental conditioning, on pin-bearing strength shall be given. Karbhari et al. (2003) asserted that although the term 'durability' is widely used, its meaning and implications are often ambiguous. The authors defined the durability of a material or structure as,

> *"…its ability to resist cracking, oxidation, chemical degradation, delamination, wear, and/or the effects or foreign objects damage for a specified period of time, under the appropriate load conditions, under specified environmental conditions."*

One of the key factors that affect the performance of PFRPs is their durability and resilience against environmental conditions. Previous research (Apricella *et al.* 1983; Schutte, 1994; Bank *et al.*, 1995; Liao *et al.*, 1999; Nishizaki and Meirashi, 2002; Robert *et al.*, 2010) has been conducted to expose composites to an aggressive environment for extended periods of time, with results indicating significant loss in mechanical properties (Sridharan *et al*., 1998) and material degradation (Ghorbel and Valentin, 1993). It was noted by Karbhari (2007), there are 7 key environmental conditions that can lead to material degradation: thermal effects; an alkaline environment; creep relaxation of the material; moisture or solution ingress; fatigue; UV exposure; and fire.

There is need for long-term durability and performance data in order for a larger exploitation of PFRP shapes and systems. FRP materials have favourable properties that make them ideal for sustainable construction (Daniel, 2003) and pultruded shapes are known to resist chemical agents (Creative Pultrusions, 2010). This data cannot be provided from existing applications because they are too young. A common method of simulating field conditions is the use of accelerated form of aging. This method provides an acceleration factor to reduce the actual time to when 'long-term' mechanical properties can be measured. Acceleration is usually

achieved through increased temperature in accordance with the Arrhenius law (Karbhari, 2007).

2.4. Bolted Connection Studies

Test configurations for plate-to-plate connections (for single or multi-bolt) under tension loading seem to be derived from testing for steel connections in tension (Turvey, 1998). In general, the double lap configuration, as shown in Figure 2.5, is used as it eliminates bending effects (Turvey, 2000). Reviewing the literature it is found that researchers have differed in their approaches. Previous tests have used a single inner plate of PFRP and steel outer plates (Cooper and Turvey, 1995; Turvey and Wang, 2003) in order to conduct one bolted connection at a time. In contrast, outer plates of FRP and a single inner plate of steel can be used (Rizkalla and Rosner, 1995a), which can efficiently test two single bolted connections at one time. Furthermore, both inner and outer plates can be tested with PFRP material (Erki, 1995). The aforementioned test configurations can differ in the level of separation of the plates ranging from being in contact to using several washers; intrinsically, full surface contact between overlapping plates is representative of actual connections within industrial applications.

2.4.1. Factors Affecting Bolted Connections

The structural performance of a bolted connection in PFRP material can be affected by the geometric parameters relating end, side, pitch and gauge distances with respect to bolt diameter, as shown in Figure 2.3. Various studies have investigated variables such as type of loading; materials (bolts and PFRP); plate thicknesses, orientations and connection geometries; the bolt arrangements and interface conditions (washer, torque and clearance hole) (Mottram and Turvey, 2003). Presented and discussed are a few prominent investigations on the effect

of geometric relations, clearance-hole, material orientation and bolt torque on the strength of bolted connections.

Some of the first testing was conducted by Rizkalla and Rosner (1995a and 1995b). The investigation included a series of 102 single bolt tension tests on EXTREN™ 500 series (polyester matrix with e-glass fibres) flat sheet material of thicknesses 9.53, 12.7 and 19.05mm. The key testing parameters included varying of the geometric relations (e_1/d) and (w/d) as well as testing in 0°, 45° and 90° to the direction of pultrusion. Bolts were placed such that (w) was equal to ($2e_2$). In addition, a modified semi-empirical model first proposed by Hart-Smith (1979) for failure criterion was developed. The study concluded that increasing both (e_1/d) and (w/d) beyond 5 had an insignificant effect on the ultimate load capacity of the connection. The measured material strength decreased as the fibre orientation varied from 0° to 90° and this decrease was more predominant than the decrease in ultimate load capacity of the connection. Mottram (2009b) identifies that, the minimum geometric ratios for the promotion of bearing failure should be 4 for both (e_1/d) and (w/d). However, the minimum geometric ratios are still a matter of dispute as no clear consensus has been achieved, in light of this Chapter 6 was based on the specified values from Bank (2006) given in Table 2.3 and the ASCE Pre-standard (2012).

The need for additional test data when the pultrusion and connection force direction do not coincide was identified by Turvey (1998), and as a result a series of 54 single bolt tests in tension were conducted. The study looked at the angle, θ, between the aforementioned axes at 30, 45 and 90° for EXTREN 500 series 6.4mm material. The results of the study showed that the load capacity of the connection increases as the off-axis angle, θ, decreases. The failure modes observed within the 30° and 45° orientations showed that cracks propagate along the rovings. This fibre reinforcement may be viewed (negatively) as zones of weakness, or

alternatively (positively) as crack guides and/or arresters. It was noted that bolt slip occurs even for a nominally tight fit, which was attributed to the tolerances achieved during manufacture of the specimens and drilling procedures.

The effects of bolt torque on connection strength were studied by Cooper and Turvey (1995) in 81 tension tests on a single bolt double lap connection with a thickness of 6.53mm for the EXTREN™ 500 series material. The tests characterised the effect of three different bolt torque levels of 0 Nm (pin-bearing), 3 Nm (lightly clamped) and 30 Nm (fully clamped) failure load. The material was only tested with the tension axis coincident to the direction of pultrusion and the (e_1/d) and (w/d) ratios were varied in order to establish a critical ratio when bearing failure happened. The beneficial effect of applying a lateral constraint to the bolted connection increased the mean failure load (i.e. strength) by 50 % for the fully torqued situation compared to the pin bearing condition. The study concluded that the minimum geometric relations required for bearing of to occur increased as the bolt torque increased with recommendations for (e_1/d) and (w/d) ratios of 3 and 4, respectively.

An analytical study of pin elasticity, clearance and friction conducted by Hyer *et al.* (1987) suggested that a co-sinusoidal stress distribution can be used to model the stresses around a bolt hole in a pin-loaded orthotropic plate. The results of their study indicated that both clearance and friction significantly affect the distribution and magnitude of stresses in a way that degrades the load capacity. They noted that clearance affects the location and direction of the peak stresses as well as magnitude and pin elasticity is not as important as the aforesaid variables.

The effect of bolt-hole clearance was studied by Yuan *et al.* (1996) in a series of tests on single bolt tension connections of EXTREN™ 500 series pultruded plate, 9.5mm thick. An untorqued

smooth shank steel bolt was used in holes with clearances ranging from 0 to 6.35mm. In order for the connection to fail only in the bearing mode, the investigation used geometric relations (e/d) and (w/d) of 4 and 8 respectively. The results showed that the ultimate load and load at the onset of bearing failure both decreased as the bolt-hole clearance increased (i.e. a larger clearance results in lower connection strength).

2.5. Design Guidance for PFRP Bolted Connections

PFRP structures have been used in civil engineering applications and other engineering industries for almost 40 years, particularly as secondary load bearing structures, such as platforms. It is within the last 15 years, that we have witnessed the emergence of primary load-bearing structures such as footbridges, cooling towers, and building frames (Turvey, 2000). This may be attributed to the level of confidence designers have with employing PFRP shapes and systems with limited design guidance at their disposable relative to other traditional and more established structural materials.

FRP materials are used in the aircraft and aerospace industries with most of the in-design guidance for bolted connections provided by design manuals such as 'The Department of Defence: FRP Materials Handbook' known as the MIL-HDBK-17 (2000). The design guidance is for procedures relating to laminated FRPs and correlates to design standards such as ASTM D5961, as explored earlier in the review. This design guidance has been specifically developed for aerospace materials and testing procedures with a vast amount of empirical and analytical research to support their recommendations. Although, the MIL-HDBK-17 gives comprehensive information in order to guide designers, they do not reflect the type of FRP material and structural forms for construction.

The EUROCOMP design code (Clarke, 1996) utilises the limit state approach in order to provide general design guidance to the construction industry for materials processed using pultrusion, hand lay-up, filament winding and several others. The design guidance was based on a heuristic approach with the compilation of best known practises, research and in-house expertise from pultruder's. The simplified design approach for connections include the most basic building block of plate-to-plate connections for both bolted and bonded connections. A detailed critique of the simplified design method used by the EUROCOMP design code has been conducted by Wang (2004). The second rigorous design procedure, given in the accompanying handbook, utilises damage tolerance, finite element stress calculations and knowledge of characteristic distances similar to the aerospace procedures (MIL-HDBK-17). It should be noted that the partial safety factors given in the EUROCOMP Design Code (Clarke, 1996) are based on the limited experience and knowledge and could not be calibrated using reliability analysis and specific test results.

Specific guidance for PFRP is given in the form of design manuals from pultruder's, based on in-house levels of knowledge and understanding (Mottram, 2001). It was observed that through scrutiny of simple minimum geometric recommendations for single bolt connections, manufacturers design manuals have specified values based on parameters from early research of marine hand lay-up GFRP (Mottram, 2001). The design guidance is based on non-standardised test data with little or no clear provenance.

2.6. Summary

An overview of bolted connections has been presented with a focus on the failure modes, specifically pin-bearing failure. The salient features of previous test methodologies and failure

load definitions have been summarised; a justification of the need for a revised pin-bearing methodology that encompasses all factors affecting bearing strength has been given. This forms part of the reasoning for use of the Warwick University Test Setup (WUTS) in Chapter 4 towards the determination pin-bearing strengths. In addition, several key studies into bolt, material and design parameters affecting pin-bearing strength have been presented. Following on from the pin-bearing strength review, the area of bolted connections has been explored with a focus on describing some of the influences affecting the strength of connections in PFRP materials. Finally, attention has been drawn towards the recognised guidance currently available to structural engineers to design in PFRP.

The key research questions drawn from the literature to be addressed in the proceeding chapters of this thesis are:

- Are there any limitations on strength and durability of PFRP material in allowing bolt thread to bear against the material?
- What is to be the standard test method that shall be specified to determine pin-bearing strength?
- How does pin-bearing strength vary with environmental conditioning, material architecture type, and orientation of 'bearing' force relative to the orientation of the FRP material?
- What details are recommended for connection geometries (e.g. end distance (e_1), side distance (e_2), etc.); bolt, nut and washer types; bolt installation torque?
- Is it acceptable to have a joint with a single bolt?
- What is the strength reduction to the double-lap test arrangement for the single-lap plate-to-plate situation, considering the basic resistance formulae are based on the former configuration rather than the latter?

- How do we predict strength when there are two or more rows of bolting (i.e. when the by-pass loading exists and there is a requirement to know the open-hole stress concentration factor)?
- What information do we need to prepare mandatory text for staggered bolt arrangements?
- Are the closed formed formulae for clearly defined modes of failure, such as bearing, necessary and/or sufficient (adequate)?

CHAPTER 3

Material Properties

3.1. Introduction

Described in this chapter are physical and mechanical properties of the pultruded Wide Flange (WF) section used in the experimental programmes found in Chapters 4 to 6. The fibre architecture and resin properties of the material are given along with both measured and modelled mechanical properties of these constituents. The majority of this thesis is concerned with the system strength property of pin bearing strength and associated variables which affect the determination of this strength measure. This system strength is known to be affected by the material architecture and hence it is useful to understanding the behaviour of bolted connections if details of each of these constituent parts are presented. Furthermore, the test programme included artificial aging of the material, in Chapter 5, and consideration of the environmental degradation as a result of exposure to moisture. Thus, a supplementary investigation into the moisture kinetics of the material is detailed and discussed.

This chapter first sets out a description of the PFRP material with a description of both the fibre reinforcement and resin matrix. The two components are further examined with respect to the results of resin burn-off testing to calculate the Fibre Volume Fraction (FVF) and relative

dimensions and properties of each layer. Following on from the material specification, the salient results from a series of compression tests, conducted using a compression die set, developed at the University of Warwick (Mottram, 1994), is given. Moreover, a short discussion of the shear strength of the material is given, after which tensile strength tests which inform a further series of open-hole tension tests are presented. These tests were preliminary investigations to verify the use of the Hart-Smith (1978) approach, developed for Aerospace bolted connections, and promoted by Mottram (2010) for use with PFRP bolted connections. Finally, before the chapter summary, a presentation of a moisture diffusion study is given. This study determined both coefficients of diffusion and activation energies for the PFRP material and is used in Chapter 5 for long term strength predictions.

3.2. Pultruded Material

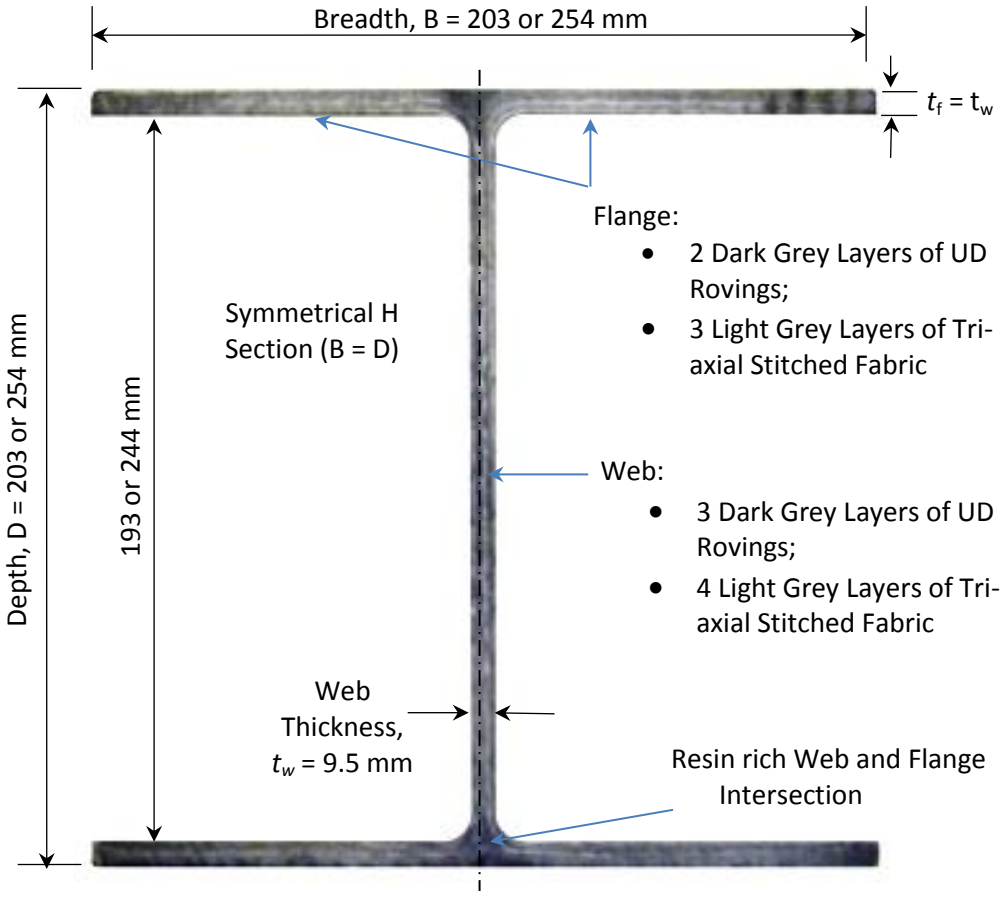

Figure 3.1: Cross-section of Wide-Flange Pultruded SuperStructural H-Section with nominal dimensions

The material used is a Creative Pultrusions (CP) Pultex® SuperStructural 1525 WF section, as shown in Figure 3.1. It has been manufactured using traditional continuous pultrusion (Bank, 2006) with the addition of closed mould resin injection instead of an open resin bath. This method is known to ensure there is an effective saturation of the resin matrix throughout the E-glass fibre reinforcement and less voids (Starr, 2000). The material is a slate (dark) grey colour, in the form of an H-section beam. It has a flame spread rating of 25 or less when tested per ASTM E84-01 (or Class FR1) (ASTM, 2001) plus good chemical resistance combined with high mechanical and electrical properties as stated by the manufacturer (Creative Pultrusions, 2010). The property portfolio for this particular section makes it attractive for use in building applications, such as chemical plants and cooling towers, as well as railway platforms (Creative Pultrusions, 2010). According to the manufacturers design manual (Creative Pultrusions, 2010), the material has the mechanical properties detailed in Table 3.1.

Table 3.1: Material Properties of 1525 SuperStructural Pultruded WF Sections (Creative Pultrusions, 2010)

Mechanical Property	Units (ASTM Test Method)	Longitudinal (LengthWise - LW)	Transverse (CrossWise – CW)
Flange Section			
Tensile Strength	N/mm^2 (D638)	275	-
Tensile Modulus	kN/mm^2 (D638)	28.6	-
Compressive Strength	N/mm^2 (D695)	316	122
Compressive Modulus	kN/mm^2 (D695)	26.5	13.1
Shear Strength (by Punch)	N/mm^2 (D732)	37.8	-
Inter-laminar Shear	N/mm^2 (D2344)	27.5	-
Maximum Bearing Strength	N/mm^2 (D953)	227	158
Poisson Ratio	- (D3039)	0.35	0.12
Web Section			
Tensile Strength	N/mm^2 (D638)	208	72.2
Tensile Modulus	kN/mm^2 (D638)	21.3	9.6
Compressive Strength	N/mm^2 (D695)	258	97.6
Compressive Modulus	kN/mm^2 (D695)	19.2	13.1
Shear Strength (by Punch)	N/mm^2 (D732)	37.8	-
Inter-laminar Shear	N/mm^2 (D2344)	23.4	-
Maximum Bearing Strength	N/mm^2 (D953)	234	206
Poisson Ratio	- (D3039)	0.35	0.12

The material used in the experimental studies in Chapters 4 to 6, was sourced from two readily available (off-the-shelf) WF sections. It should be noted that the material used in this thesis was sourced from the same batch from the manufacturer. They included 254 x 254 x 9.53 mm

and 203 x 203 x 9.53 mm nominally sized pultruded sections with multi-layered fibre architecture and a complex chemical formula resin matrix. The fibre architecture, in terms of layering, was assumed to be the same for both sizes of section (as confirmed by the manufacturer in a private communication). The properties of the fibre reinforcement and resin matrix are reported next and subsequently the material strength tests.

3.2.1. Fibre Reinforcement

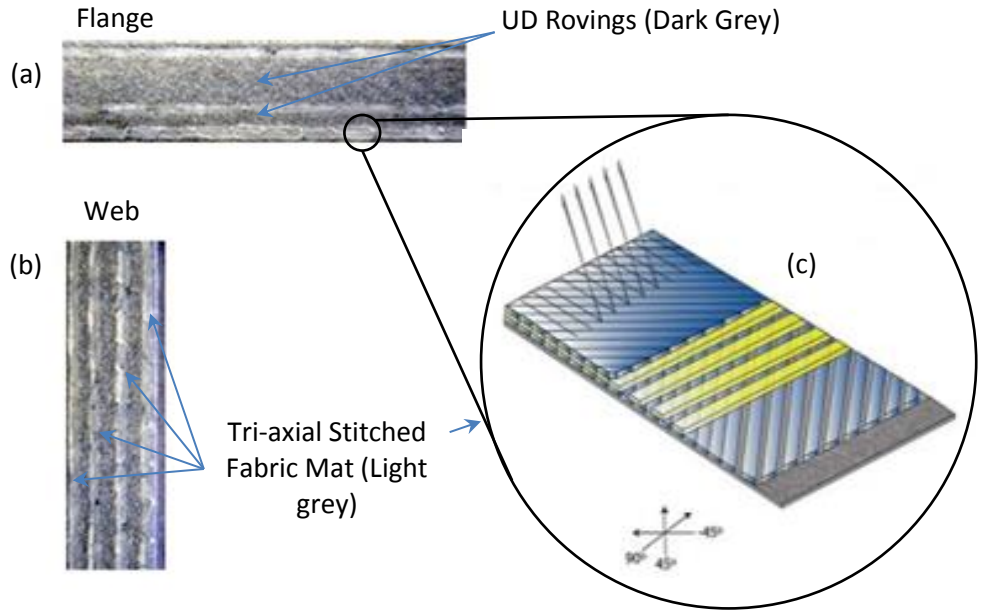

Figure 3.2: Sections of PFRP WF Beam showing (a) Flange Material, (b) Web Material and (c) Tri-axial Stitched Fabric Sketch (Vectorply, 2005)

The PFRP shape shown in Figure 3.1 has a cross section of a thin walled WF section. Panels have a combination of the fibre reinforcement systems including UniDirectional (UD) rovings and Tri-axial Stitched Fabric Mat (TSFM), as shown in Figure 3.2. A close-up of fibre a reinforcement layer is shown in Figure 3.2c with photographs of the sections in Figure 3.2a and 3.2b, for flange and web, respectively. As shown, layers of UD and TSFM are alternated to provide off-axis strength. TSFM layers are formed from a cross stitched continuous fabric as

shown in the schematic in Figure 3.2c, and has four layers with the fibre layup sequence of +45°/90°/-45°/random Chopped Strand Mat (CSM). The UD rovings are bundles of E-glass fibre made from calcium-alumina boro-silicate glass with alkali content <1% (Starr, 2000; also see Bank, 2006). It is known from the pultruder that 56 yield rovings are used for the roving layers in the 9.53mm thickness. The PFRP fibre architecture consists of mat layers interspersed with nominally constant (although this is not the case for flange sections see Figure 3.2a) thickness layers of UD and covered with an outer (relatively thin) surface veil (non-structural). The NEXUS® veil is resin-rich and consists of randomly orientated short fibres in the plane, which has a quantity mass per unit area of <100 g/m^2 and a semi-glossy finish that allows the pultrusion to be easily handled. It is found that the PFRP shapes, in the web, have four TSFM layers and three layers of UD. The flange has three TSFM layers and two layers of UD. Consequently, the mechanical properties are different between the web and flange materials. Test for pin-bearing characterisation and bolted connections will be for both materials cut from the WF sections.

3.2.2. Resin Matrix

The thermoset resin is a Reichhold 31031 unsaturated isophthalic (an isomer of phthalic acid benzene-1 and 3-dicarboxylic acid) polyester resin which contains additives to form the matrix for use in the pultrusion process. Clay filler is added and assumed to be aluminium silicate, which is commonly known as kaolin clay (Lane, 2002). This filler is used, in addition to economic purposes, to improve chemical resistance, opacity, surface finish and insulation properties (Creative Pultrusions, 2010). The fire retardant material, antimony trioxide, is added to the resin mixture and acts alongside the other resin base of brominated polyester to provide fire protection. Other additives include a mould releasing agent, and low, mid and high range catalysts which are activated during the pultrusion process. Finally, internal stresses and

cracking issues are dealt with the addition of glass beads. UV inhibitors are present as well. The largest proportion of the resin formula, which consist of 13 constituent parts, are the polyester resins, known to be approximately 80% of the bulk matrix (Creative Pultrusions, 2013 – private communication).

3.2.3. Constituent Material Properties

A series of resin burn-off tests were conducted to estimate the volumetric proportions of UD, TSFM and resin matrix, as well as the nominal thicknesses of each reinforcement layer within the flange and web material. Specimens were prepared from both the web and flange of a 254 x 254 x 9.53 mm WF section using a milling process to give finished dimensions of 25 mm length and 15 mm width (the specimens varied in thickness in the as-received pultrusion). The resin burn-off procedure was adapted from the method described in Appendix B of PhD thesis by Lane (2002), and reference made to ASTM D2584-11 and Ye *et al*. (1995). Presented in Tables 3.2 and 3.3 is a summary of the results from the resin burn-off tests.

Table 3.2: Web Material Constituent Properties

Constituent Part (1)	Number of Layers (2)	Fibre Architecture (3)	% of Material (4)	% Total of Fibre Reinforcement (5)	Nominal Layer Thickness (mm) (6)
SV	2	Random Fibre Veil	3	5	0.03
CFM	4	45/90/-45/CSM	34	48	1.4
UD	2[a]	156 (56 yield)	33	47	2.0
Matrix	-	-	30	-	-

Table 3.3: Flange Material Constituent Properties

Constituent Part (1)	Number of Layers (2)	Fibre Architecture (3)	% of Material (4)	% Total of Fibre Reinforcement (5)	Nominal Layer Thickness (mm) (6)
SV	2	Random Fibre Veil	3	5	0.03
CFM	3	45/90/-45/CSM	27	36	1.4
UD	2	156 (56 yield)	45	59	3.4 and 1.7*
Matrix	-	-	25	-	-

In column (1) of Tables 3.2 and 3.3 are the names of the constituent parts of the PFRP material, the respective number of layers for each Fibre reinforcement type given in column (2). Column (3) describes the type of fibre reinforcement. Column (4) gives the percentage weight of each constituent as part of the whole material specimen tested. The values in Column (4) if summed together and considered for the specimen volume, this gives the total FVF of approximately 50% for the material. The calculated (Mottram – private communication) layer thickness is given in column (6). The flange material has a thicker layer of UD (as shown by * in Table 3.3) on the outer edge (remote from the Neutral Axis) of the material, which is thought to improve the section properties with regard to buckling and flexure. There was no UD layer found (shown by ([a]) in Table 3.2) in between the middle TSFM layers as was expected from observation of the cut surface in Figure 3.2b.

3.3. Mechanical Strength Properties

For Isotropic steels, the tensile yield and ultimate strength is generally used for the purposes of design of bolted connections (BS EN 1993-1-8:2007). The design of PFRP bolted connections requires four additional material strength properties to be established. They are the tensile, the in-plane shear, the pin bearing (structural system strength), and through-thickness tensile. A fifth strength property for open-hole or notched tensile strength is required for a design procedure adopted from Hart-Smith (1979) for the design of bolted connections of aerospace FRP materials. The material properties are more complex in PFRP than for steel due to the inhomogeneity and anisotropic nature, as explained previously in Chapter 2. Mechanical properties are measured with respect to the axis of pultrusion in the longitudinal and transverse directions for reliable estimates to be used in characteristic analyses, which in turn are used in theoretical closed formed design solutions. This forms the basis of subsequent chapters on the determination of pin-bearing strength for the reasons outlined in the

literature review in Chapter 2. This research does not need to consider through-thickness tension and so testing is limited to the four other strengths. Because, Chapters 4 and 5 provide a comprehensive study on pin-bearing strength this design strength is omitted from the following presentation.

A series of tension and compression coupon tests were conducted using modified test methods. It should be noted that compression strength is given for fullness of mechanical properties and to provide a comparison with pin bearing strengths reported in Chapter 4 and 5. Only compression, tension and open-hole tension tests were conducted at the University of Warwick (UoW); the data for in-plane shear strength was taken from standard tests conducted by D'Alessandro (2009) on the same 203 x 203 x 9.53 mm sized WF section.

3.3.1. Compressive Strength Tests

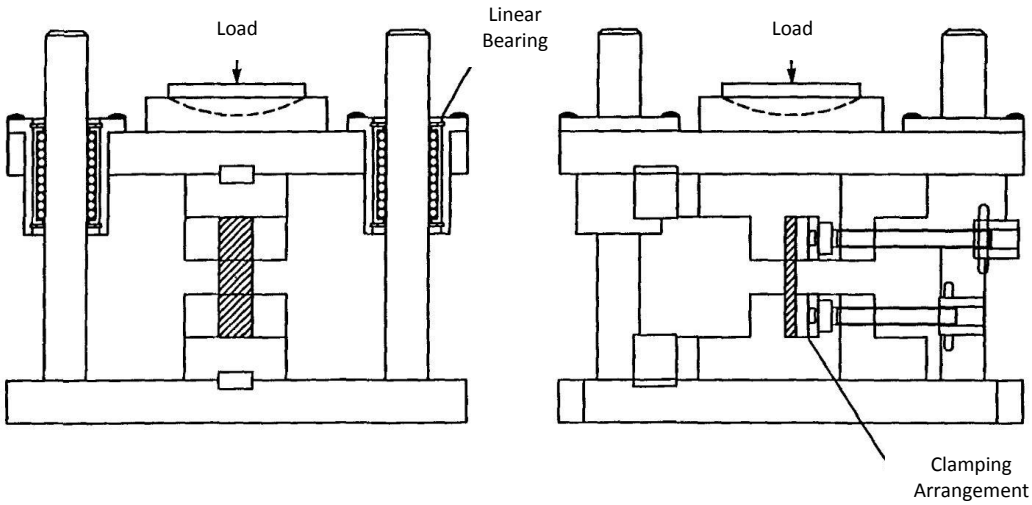

Figure 3.3: Compression Test Rig and Clamping Arrangement Drawing (Mottram, 1994)

The test rig, shown in Figure 3.3, was designed and manufactured at the University of Warwick as a modified version of the apparatus used by Barker and Balasandaram (1987), which was

later used by Haeberle and Matthews (1990). Some advantages of this setup as stated by Mottram (1994) are the elimination of end effects, no need for end tabs and failure occurs within the gauge length. The test rig was clamped into a load-controlled 40 metric tonne Amsler universal testing machine and specimens were set within the clamps. The load rate was applied at approximately 10 kN/min and ultimate load recorded. It should be noted that when calculating the average compressive strength of coupons, the small stress due to the dead weight of the top platen of the test rig was not included. It was deemed acceptable because the cross section is about 500 mm^2. Tests were conducted at ambient laboratory temperatures. The results of compression tests are presented in Tables 3.4 and 3.5.

Table 3.4: Longitudinal and Transverse Compressive Strength Test Results for Web Material

Specimen (1)	Thickness (mm) (2)	Width (mm) (3)	Area (mm^2) (4)	Maximum Amsler Load (t) (5)	Maximum Specimen Load (kN) (6)	Compressive Strength (N/mm^2) (7)
Longitudinal (0°)						
W/0-01	9.56	50.0	478	15.1	149	311
W/0-02	9.60	50.0	480	14.2	140	291
W/0-03	9.54	50.0	477	13.8	136	285
W/0-04	9.54	50.0	477	14.8	145	304
W/0-05	9.56	50.0	478	13.6	134	280
W/0-06	9.52	50.0	476	16.1	158	333
W/0-07	9.58	50.0	479	16.0	157	328
W/0-08	9.59	50.0	480	13.7	135	281
W/0-09	9.58	50.0	479	15.8	155	323
W/0-10	9.56	50.0	478	15.9	157	327
Transverse (90°)						
W/90-01	9.57	50.0	479	4.80	47.3	98.8
W/90-02	9.56	50.0	478	6.85	67.4	141
W/90-03	9.54	50.0	477	6.83	67.2	141
W/90-04	9.56	50.0	478	7.44	73.2	153
W/90-05	9.57	50.0	479	6.30	62.0	130
W/90-06	9.55	50.0	478	6.42	63.1	132
W/90-07	9.57	50.0	479	6.36	62.6	131
W/90-08	9.56	50.0	478	6.90	67.9	142
W/90-09	9.58	50.0	479	6.65	65.4	137
W/90-10	9.59	50.0	480	6.25	61.5	128

All specimens failed within the gauge length initially with audible inter-layer splitting followed by an angled shear crack at approximately 45° throughout the cross-section of the coupon. This crack initiated from one of the loaded-face corners and extended through the thickness and was the predominate-failure mode of most specimens. Presented in Figures 3.4 to 3.7 are failed specimens; the typical 45° shear cracks can be seen. The exception is flange material

orientated with the load and pultrusion axis parallel where two 45° crack propagate from either face of the specimen and terminate into a V-shape, as shown in Figure 3.5.

Table 3.5: Longitudinal and Transverse Compressive Strength Test Results for Flange Material

Specimen (1)	Thickness (mm) (2)	Width (mm) (3)	Area (mm^2) (4)	Maximum Amsler Load (t) (5)	Maximum Specimen Load (kN) (6)	Compressive Strength (N/mm^2) (7)
Longitudinal (0°)						
F/0-01	9.55	50.0	478	18.5	181	380
F/0-02	9.79	50.0	490	17.2	169	345
F/0-03	10.3	50.0	514	19.7	193	377
F/0-04	9.86	50.0	493	14.6	143	291
F/0-05	9.59	50.0	480	17.0	167	349
F/0-06	9.57	50.0	479	17.8	175	366
F/0-07	9.61	50.0	481	17.5	171	357
F/0-08	9.60	50.0	480	16.6	163	340
F/0-09	9.59	50.0	480	17.8	175	365
F/0-10	9.57	50.0	479	18.4	180	377
Transverse (90°)						
F/90-01	10.2	50.0	511	5.24	51.6	101
F/90-02	9.57	50.0	479	3.65	36.0	75.2
F/90-03	9.82	50.0	491	5.22	51.4	105
F/90-04	9.58	50.0	479	5.13	50.5	105
F/90-05	9.59	50.0	480	5.38	52.9	110
F/90-06	10.3	50.0	514	4.84	47.7	92.8
F/90-07	9.60	50.0	480	5.35	52.7	110
F/90-08	10.2	50.0	512	5.56	54.7	107
F/90-09	9.58	50.0	479	5.29	52.1	109
F/90-10	9.81	50.0	491	5.33	52.5	107

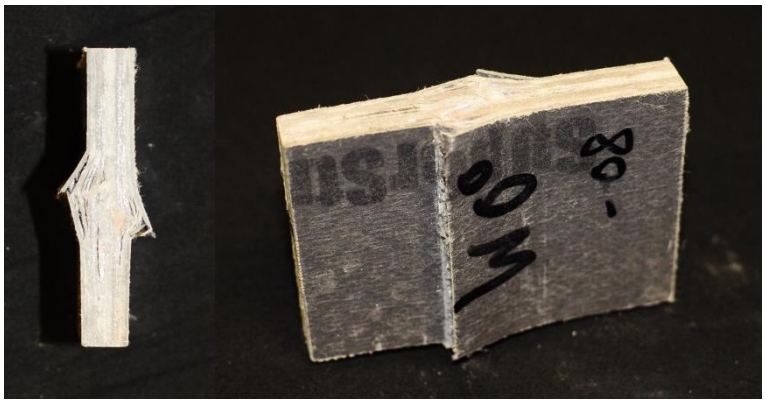

Figure 3.4: Failed Compression Test Specimen for Web Material Orientated at 0°

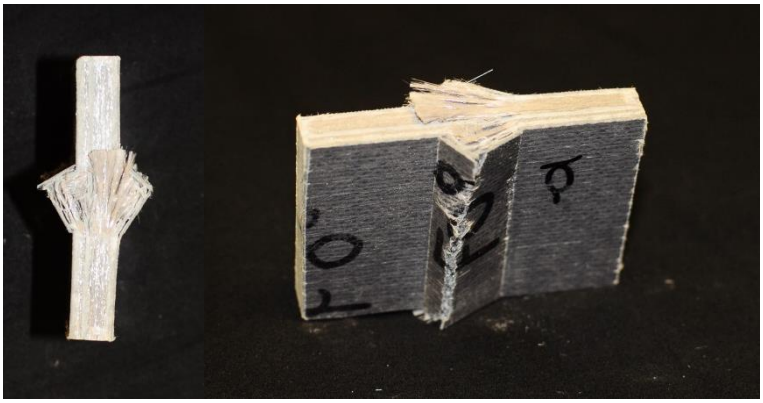

Figure 3.5: Failed Compression Test Specimen for Flange Material Orientated at 0°

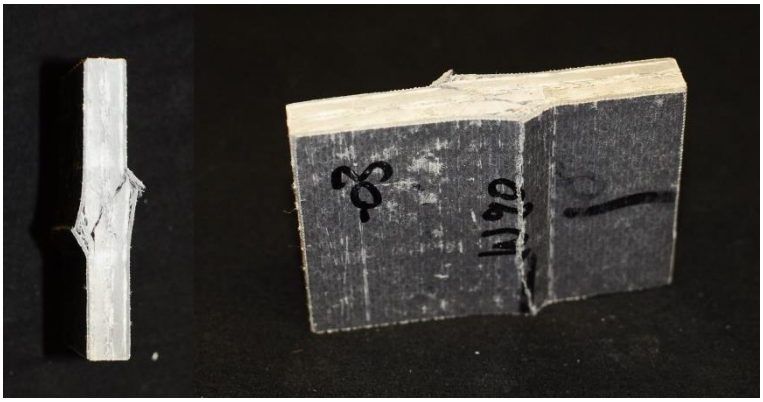

Figure 3.6: Failed Compression Test Specimen for Web Material Orientated at 90°

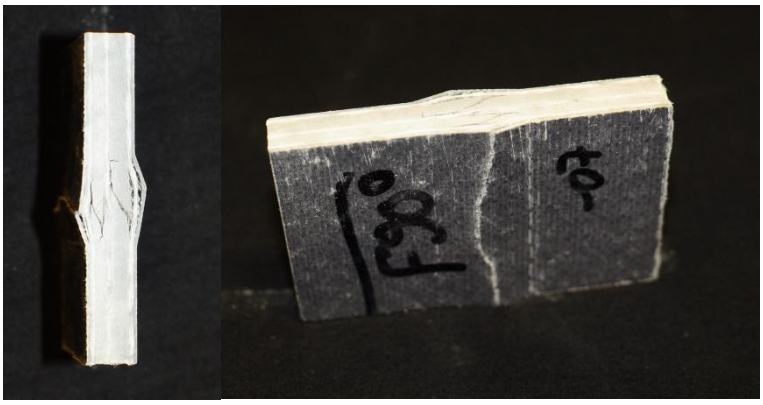

Figure 3.7: Failed Compression Test Specimen for Flange Material Orientated at 90°

The mean compressive strength from the Tables 3.4 and 3.5 are calculated next. Column (5) of each table is the maximum load in tons attained by each specimen, which are converted to kilonewtons in column (6). The ultimate compressive strength is calculated in column (7) by dividing the values the maximum load (Column (6)) by the cross-sectional area (Column (4)). The mean strength from the average of column (7) for web 0° (90°) and flange 0° (90°) is 306 (133) N/mm^2 and 355 (102) N/mm^2 .

The longitudinal strength for web material ranges from 280 to 328 N/mm^2 and almost double the range from 291 to 380 N/mm^2 is obtained for the flange. The transverse strength ranges from 98.8 to 153 N/mm^2 and 75.2 to 110 N/mm^2 for web and flange, respectively. Although the four batches of ten specimens had a large co-efficient of variation (CoV ≈ 10%), no value was removed from further analysis as they all lay within the acceptable bounds as determined by the Chauvenet criteria (Kennedy and Neville, 1986).

Comparing ultimate mean compressive strength values, it is found that the ratio of longitudinal to transverse values is 2.3 and 3.5 for web and flange material, correspondingly. The mean longitudinal compressive strength of the web is 14% lower than equivalent flange material, conversely a 23% higher value for transverse web when compared to flange material. These differences between web and flange can be attributed to the higher fraction of UD in the flange and four layers of TSFM in the web when compared to three in the flange.

The results were analysed with the protocol outlined in Annex D of BS EN 1990:2002 to determine Characteristic Values (CV), and these are given in column (8) of Table 3.6. The test result shall be compared with the equivalent pin-bearing strength in Chapter 4. In comparing the co-efficient of variation (CoV) given in column (7), a higher value of approximately 3% is observed in the transverse direction when compared to the longitudinal; the reason for this is

yet to be determined. A comparison of mean compressive strengths from the pultruder's design guide, presented in Table 3.1 (CP) and the study presented in this chapter (designated University of Warwick (UoW) values in the figure) are shown in Figure 3.8, along with the characteristic values given in Table 3.6.

Table 3.6: Summary of Compression Test Results

Specimen Batch	Thickness (mm)	Width (mm)	Specimen Load (kN)	Compressive Strength (N/mm^2)	SD (N/mm^2)	CoV (%)	EN 1990 Char. Value (N/mm^2)	ASTM D2970 Char. Value (N/mm^2)
(1)	(2)	(3)	(4)	(5)	(6)	(7)	(8)	(9)
Web 0°	9.56	50.0	146	306	21.0	6.86	270	249
Web 90°	9.57	50.0	63.7	133	14.3	10.7	109	100
Flange 0°	9.70	50.0	172	355	26.3	7.43	309	298
Flange 90°	9.83	50.0	50.2	102	10.8	10.6	84	83

The mean compressive strengths in the longitudinal direction for both web and flange material and for transverse web specimens as found in this study are 25% higher than the pultruder's values, the reverse trend is observed for the transverse flange. If we compare characteristic values it can be seen that for material orientated at 0°, is within 4% of CP value; the trend is not as matched in the transverse with the web 90° 10% higher and the flange 90° 45% lower. From inspection of Table 3.6 characteristic values are 15% lower than the mean.

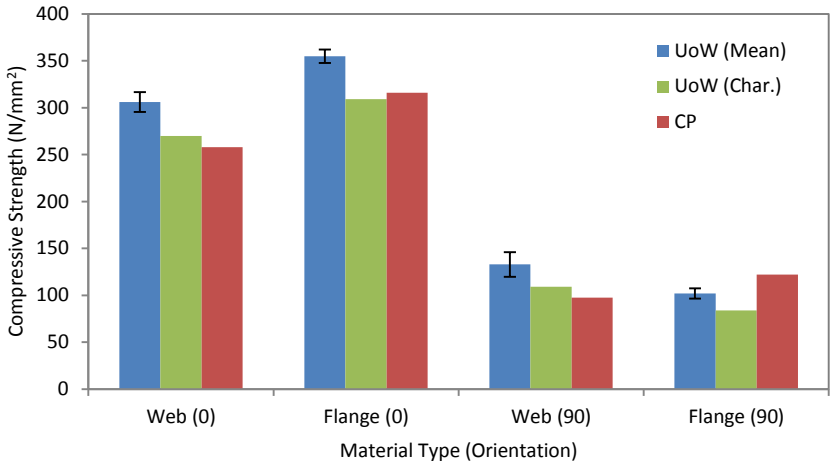

Figure 3.8: A Comparison of Mean Compression Strength test Results from Creative Pultrusions (2010) and the University of Warwick

3.3.2. In-Plane Shear Strength

A series of in-plane shear strength tests were conducted by D'Alessandro (2009) on the same size section and type of WF pultruded beam as used in this investigation. The tests were conducted in spirit of ASTM D5379 (M), "Shear Properties of Composite Materials by the V-Notched Beam Method" for 10 longitudinal web specimens only. The use of an Iosipescu test fixture was employed with the in-plane strength and in-plane stiffness (for shear modulus) being measured. The procedure and further details on the test setup are given in D'Alessandro's MSc thesis (2009) and only salient strength and modulus are given here. From a batch of 10 specimens, it was found the mean in-plane shear strength for web material (0°) is 90.6 N/mm^2 with a standard deviation (SD) and CoV of 2.8 N/mm^2 and 3.1%, respectively. Using EN 1990 (British Standards Institute, 2002), a CV was calculated of 86 N/mm^2.

3.3.3. Tensile Strength Tests

Tensile coupons were prepared in two operations, firstly a rough cut to nominal dimensions using a diamond edged circular saw with water coolant. The specimens were then machined using a fluted carbide end mill to finished dimensions of 250 mm length by 25 mm width having a tolerance of ± 0.2 mm. The thickness of specimens was measured using digital vernier callipers and ranged from 9.59 to 10.3 mm with a mean of 9.71 mm. A grip length of 50 mm on either end on the specimen gave a gauge length of 150 mm. A total of 10 longitudinal specimens, five from both the web and flange were prepared, along with 10 transverse specimens from the web. Specimens were labelled using the convention: material type (web or flange) /material orientation (0 or 90°) – specimen number. Therefore, F/90-03 represents the third flange specimen tested with the material orientated at 90° to the loading axis.

The tests were conducted using a load-controlled Amsler universal testing machine; the loading was applied at a rate of approximately 10 kN/min. The ultimate load was recorded. Acoustic Emissions (AE) could be heard prior to ultimate load being attained, especially in the longitudinal specimens. Ultimate failure was always by fibre rupture across the specimen width. Results from longitudinal testing are given in Table 3.7 and from transverse testing they are presented in Table 3.8. The load was converted from metric tons (t), as read off from the testing machine, to kilo newton by multiplying the load reading by 9.81 m/s^2, as given in column (6). Following the tables, a failed web 90° specimen is shown in Figure 3.9, with the typical failure mode of rupture across the specimen width.

Table 3.7: Longitudinal Tensile Strength Test Data for Web and Flange Material

Specimen	Thickness (mm)	Width (mm)	Area (mm^2)	Maximum Amsler Load (t)	Maximum Specimen Load (kN)	Tensile Strength (N/mm^2)
(1)	(2)	(3)	(4)	(5)	(6)	(7)
Web Material						
W/0-01	9.60	25.1	241	6.94	68.1	282
W/0-02	9.60	25.1	241	6.23	61.1	254
W/0-03	9.59	25.1	241	7.22	70.9	294
W/0-04	9.64	25.1	242	7.32	71.8	297
W/0-05	9.66	25.1	243	7.50	73.6	303
Flange Material						
F/0-01	9.59	24.8	237	7.65	75.1	316
F/0-02	9.58	25.2	241	8.87	87.0	361
F/0-03	10.3	25.2	259	9.45	92.7	358
F/0-04	10.3	25.2	260	8.25	80.9	311
F/0-05	9.59	25.1	241	7.98	78.3	325

Table 3.8: Transverse Tensile Strength Test Data for Web Material

Specimen	Thickness (mm)	Width (mm)	Area (mm^2)	Maximum Amsler Load (t)	Maximum Specimen Load (kN)	Tensile Strength (N/mm^2)
(1)	(2)	(3)	(4)	(5)	(6)	(7)
W/90-01	9.63	25.0	241	2.40	23.5	97.8
W/90-02	9.63	25.0	241	2.19	21.5	89.2
W/90-03	9.61	25.0	240	2.18	21.4	89.0
W/90-04	9.66	25.0	242	2.19	21.5	89.0
W/90-05	9.64	25.0	241	2.23	21.9	90.8
W/90-06	9.61	25.0	240	1.97	19.3	80.4
W/90-07	9.71	25.0	243	1.99	19.5	80.4
W/90-08	9.68	25.0	242	1.95	19.1	79.1
W/90-09	9.63	25.0	241	2.12	20.8	86.4
W/90-11	9.64	25.0	241	1.88	18.4	76.5

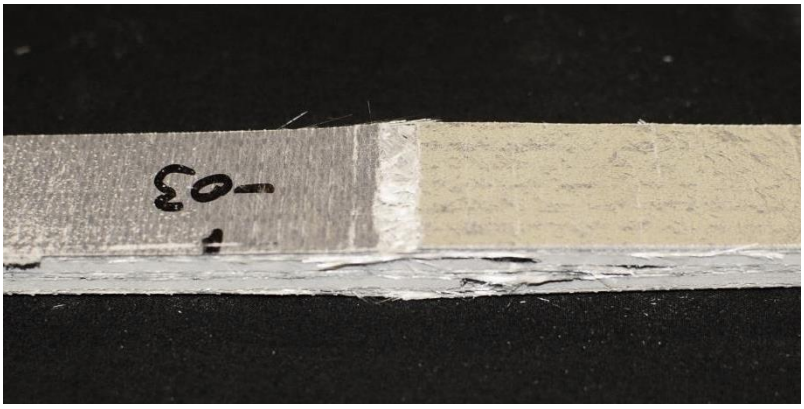

Figure 3.9: Failed Tensile Test Specimen for Web Material Orientated at 90°

As expected the flange material in the longitudinal direction exhibits a higher strength than the web in this direction. This is mainly due to the higher volume content of fibres, specifically UD, giving the flange, on average, a 17% higher tensile strength.

Prior to calculating a CV, the batch data was analysed to identify the reliability of the sample in the population. The individual tests were assessed against the Chauvenet criteria (Kennedy and Neville, 1986), to identify the possibility of outliers, by analysing the data based within a specific probability band centred on the mean. The criterion stipulates that each absolute test value must lie within the band of the mean ± 1.65SDs or 1.96SDs for five and ten samples per batch, respectively.

The results of this analysis showed that no individual test value from the transverse web or longitudinal flange of the sample populations lay outside of the acceptable probability band. Hence no data was rejected as outliers from these batches for further analysis. However, it was found using the criteria that strength value from row two of Table 3.7, for specimen W0-02, (longitudinal web) was out of the specified criteria. The value is 1.8SDs lower than the mean value of 286MPa, which is 9% lower than the lower band to the criterion. If this value is eliminated from the batch and the mean, SD and CV recalculated for a batch of four

specimens, their values now become 294 N/mm^2, 7.6 N/mm^2 and 280 N/mm^2, with a CoV of 2.6%.

Reported in Table 3.9 is a summary of the tensile testing study with the adjusted values for the longitudinal web series. The same convention for column content as Table 3.8 is used. From the batch of nominally identical specimens, the SD and CoV are determined. They are used to calculate the CV according to the procedure in EN 1990 (British Standards, 2002) using the mean minus 1.8 SDs or 1.72 SD for batches of five or ten specimens, respectively. The CoV ranges between 3 and 10%, with the largest dispersion of data found in the transverse direction. Because CoV values are not larger than 10%, it was assumed acceptable to calculate characteristics strengths on the basis that the CoV is known beforehand. The values in Table 3.9 are plotted in Figure 3.10 along with CP values for both flange and web material.

Table 3.9: Summary of Tensile Test Results

Specimen Batch (1)	Thickness (mm) (2)	Width (mm) (3)	Specimen Load (kN) (4)	Tensile Strength (N/mm^2) (5)	SD (N/mm^2) (6)	CoV (%) (7)	EN 1990 Char. Value (N/mm^2) (8)
Web 0°	9.62	25.1	69.1	294	7.6	2.6	280
Web 90°	9.64	25.0	20.3	84	8.6	10	69
Flange 0°	9.87	25.1	82.8	334	23.6	7.1	294

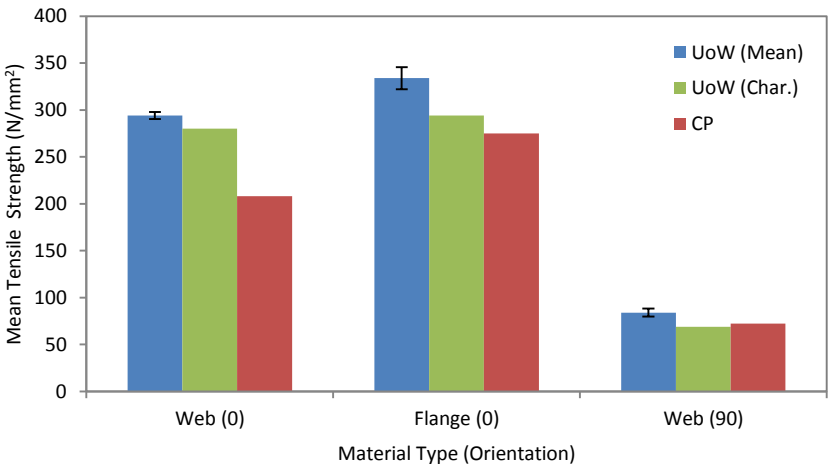

Figure 3.10: A Comparison of Mean, Characteristic and Manufacturers Tensile Strength Values for Web and Flange Material

The mean tensile strengths in the longitudinal direction for both web and flange material are 18 and 30% higher, respectively than the pultruder's values; similarly transverse web is 14% higher. From inspection of Table 3.6 characteristic values are 5, 18 and 12 % lower than the mean for the web 0°, 90° and flange 0°, respectively.

3.3.4. Open Hole Tensile Strength Tests

Prior to setting out the test method for determining open-hole tension strength, it will be prudent to give a brief background to the need for this strength. An aim of the research presented in this thesis is to provide relevant and reliable data to support the design of bolted connections, in order to assess the performance of current and proposed design procedures. One challenge for the writers of the ASCE Pre-standard for "Load and Resistance Factor Design (LFRD) of Pultruded Fiber-Reinforced Polymer (FRP) Structures" (ASCE, 2012) has been to have a 'closed-form equation' that is acceptable to reliably predict the resistance of multi-row bolted connections failing with the net-tension mode at the first bolt row. Hart-Smith (1979) developed a semi-empirical method, commonly used in the Aerospace industry, and postulated that a simple correlation coefficient can relate the isotropic stress concentration factor (for material such as steel) to the orthotropic stress concentration factor (for an FRP material). One term in the expressions for the closed-form equation is for the stress concentration for an open notch that is for the by-pass load contribution (not resisted by bolt bearing) at the net-tension plane of failure.

In the Hart-Smith (1979) approach the open hole elastic stress concentration factor, $k_{\mathrm{te,op}}$, for an isotropic material, is given by:

$$k_{\mathrm{te,op}} = 2 + (1 - \frac{d_n}{w})^3 \qquad (3.1.)$$

The geometric relations of hole-diameter, d_n and specimen width, w, are shown in Figure 3.11.

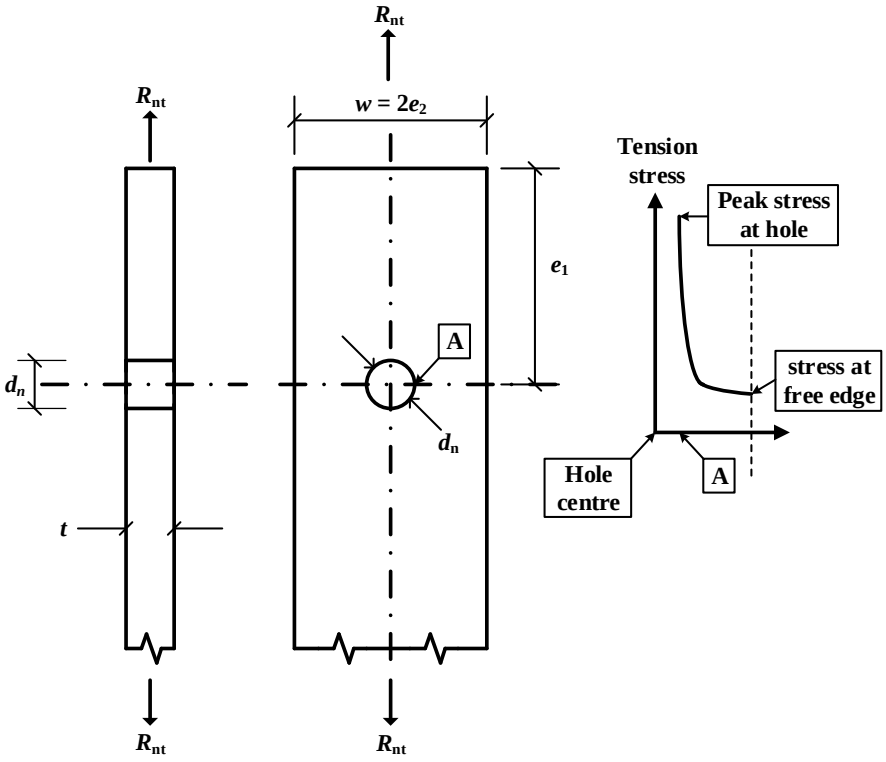

Figure 3.11: Diagram of the Open-hole Tensile Specimen under load (adapted from Mottram, 2010)

The orthotropic stress concentration factor, k_{tc}, for an FRP material was empirically determined by Hart-Smith (1979) as given in Equation (3.2). It requires test data for the tensile strength, F_t, which has been determined in the previous section and the failure load from an open-hole tensile strength test, R_{nt}. The material thickness, t is measured too.

$$k_{tc} = \frac{t(w - d_n)F_t}{R_{nt}} \tag{3.2.}$$

It was proposed by Hart-Smith (1979) that the isotropic stress concentration factor $k_{te,op}$ can be related to the orthotropic stress concentration factor k_{tc} by way of a correlation coefficient, C_{op}, using the linear relationship:

$$k_{tc} - 1 = C_{op}(k_{te,op} - 1) \tag{3.3.}$$

Furthermore, in characterising this relationship, Hart-Smith stated that when C_{op} = 1, the failure is perfectly brittle, and when C_{op} = 0, the failure is perfectly plastic or ductile. It has been found by Mottram (2010) using test data from Turvey and Wang (2003) that the open-hole correlation coefficient had a mean value of 0.37 for a specific ¼ in. PFRP flat sheet material. Hart-Smith stipulates that C_{op} is a material constant, with the assumption this co-efficient is independent, for example, of the bolt-hole to diameter ratio. The approach used to establish C_{op} in what follows has been set out by Mottram (2010).

A series of open-hole tensile strength tests were conducted on 0^{o} material from the web and flange of a 254 x 244 x 9.53 mm WF section. Specimens were prepared by initially machining blanks to approximate dimensions using a diamond edged circular cutting saw, and then finished to within ±0.2 mm of 50 mm width by 250 mm length. The holes within coupons were located centrally, as shown in Figure 3.12, and milled to the finished hole diameters, d_n, of 5, 10, 15, 20, 25 and 30 mm, having ± 0.1 mm tolerance. The dimensions of the test coupon thickness, width, and hole diameter were measured using a vernier callipers and the mean results from five specimens per batch are reported in columns (2), (3) and (4) of Table 3.10. Batches were labelled with W or F for web or flange, followed by the nominal hole diameter. For example, W10 is for a web specimen with a 10 mm hole (column (1) of Tables 3.10 and 3.11).

In total, 60 specimens were tested in tension using a 100 kN Testometric universal testing machine, with the exception of batches W05 and F05 that were failed using an Amsler universal testing machine with a larger load range (capacity 400 kN) than the Testometric. Tests were conducted until failure, as indicated by fibre rupture in the net section. The mean results for the 12 batches are presented in Table 3.10. Column (5) gives the hole-diameter to width ratio (d/w) for each specimen batch, and column (6) the net section area equal to the

width minus the hole-diameter. Finally the gross section strength in column (7) is obtained by the failure load (6) (in kilo Newtons) divided by ((3) multiplied by (4)).

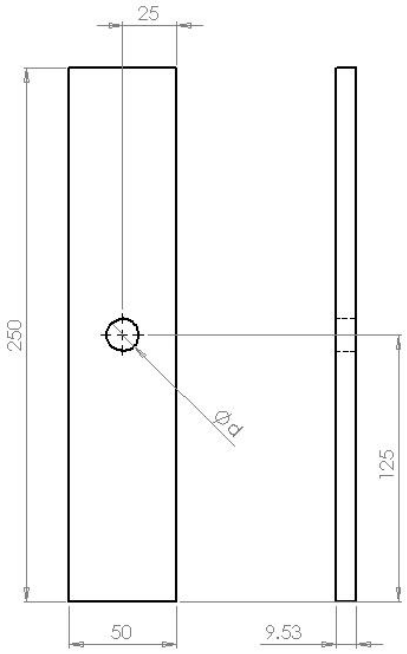

Figure 3.12: Open-hole tension Specimen with Dimensions

Table 3.10: Open-hole Tensile Strength Results for Longitudinal Flange and Web Material

Specimen Batch (1)	Coupon Thickness, *t* (mm) (2)	Coupon Width, *w* (mm) (3)	Hole Diameter, *d* (mm) (4)	*d*/*w* (5)	Net Section Area (cm^2) (6)	Mean Specimen Load (kN) (7)	Mean Gross Section Strength (N/mm^2) (8)
Web Material							
W05	9.62	50.1	4.93	0.10	45.2	120	249
W10	9.63	50.1	9.95	0.20	40.1	102	211
W15	9.62	50.1	14.9	0.30	35.1	79.2	164
W20	9.63	50.0	19.8	0.40	30.2	66.4	138
W25	9.63	50.1	24.7	0.49	25.4	47.6	98.7
W30	9.63	50.1	29.7	0.59	20.4	37.4	77.6
Flange Material							
F05	9.77	50.2	4.73	0.09	45.4	140	287
F10	9.71	50.2	9.92	0.20	40.3	119	244
F15	9.96	50.1	14.9	0.30	35.2	89.0	178
F20	10.0	50.1	19.8	0.40	30.3	78.3	156
F25	9.64	50.2	24.8	0.50	25.3	59.1	122
F30	9.90	50.1	29.7	0.59	20.4	47.5	95.7

Table 3.11 presents the open-hole correlation coefficient analysis for flange and web materials. Column (2) provides the mean net-section strength from dividing the mean failure load in column (7) by the net section area from Table 3.10 column (6). The efficiency is the

ratio of the gross section to the measured strength. The tensile strength of the material is taken from Table 3.9. Columns (4) and (5) are calculated based on Eqs. (3.2) and (3.1), respectively. Similarly, C_{op} in Column (8) is the ratio of the values reported in columns (6) and (7).

Table 3.11: Open-hole Stress Concentration Correlation Coefficient for Flange and Web Material

Specimen Batch	Mean Net Section Strength (N/mm^2)	Efficiency	k_{tc}	k_{te}	$k_{tc}-1$	$k_{te,op}-1$	C_{op}
(1)	(2)	(3)	(4)	(5)	(6)	(7)	(8)
Web Material							
W05	276	0.87	1.04	2.73	0.04	1.73	0.03
W10	263	0.74	1.09	2.52	0.09	1.52	0.06
W15	234	0.57	1.23	2.35	0.23	1.35	0.17
W20	228	0.48	1.26	2.22	0.26	1.22	0.21
W25	195	0.35	1.47	2.13	0.47	1.13	0.42
W30	190	0.27	1.52	2.07	0.52	1.07	0.48
Flange Material							
F05	317	0.86	1.06	2.74	0.06	1.74	0.03
F10	304	0.73	1.10	2.52	0.10	1.52	0.07
F15	254	0.53	1.32	2.35	0.32	1.35	0.24
F20	257	0.46	1.30	2.22	0.30	1.22	0.25
F25	242	0.36	1.39	2.13	0.39	1.13	0.34
F30	236	0.29	1.42	2.07	0.42	1.07	0.40

Presented in Figure 3.13 are plots for Eq. (3.3) for the relationship between the isotropic and orthotropic stress concentration factors. A negative relationship exists, the reason for which is to be determined. The finding does indicate a significant limitation of the linear assumption in Eq. (3.3) for PFRP materials, as Hart-Smith (1979) had shown this relationship to be positive for a CFRP/epoxy material.

The Hart-Smith approach assumes C_{op} to be a material constant, which is independent of *d*/*w*. This is not the case from this current experimental study. It can be seen from Table 3.11 and Figure 3.14 that the coefficient varies, significantly, with *d*/*w*. It should be noted that in the ASCE Pre-standard (2012) currently specify the Hart-Smith approach to establish the strength for net-tension failure, with C_{op} = 0.5 for PFRP (standard structural) shapes. From Figure 3.14, using the range of bolt diameters and minimum widths specified in the pre-standard (ASCE,

2012), (d/w) is between 0.33 and 0.25, the C_{op} value for the SuperStructural material is lower at approximately between 0.3 and 0.2. This result can be explained by reasoning that the tri-axial mat that has replaced continuous filament mats in standard structural shapes has given the PFRP material a higher level of damage tolerance (Mottram, 2010). The choice of C_{op} = 0.5 in the ASCE pre-standard is on the high side and towards the brittle failure condition for lowest design strength.

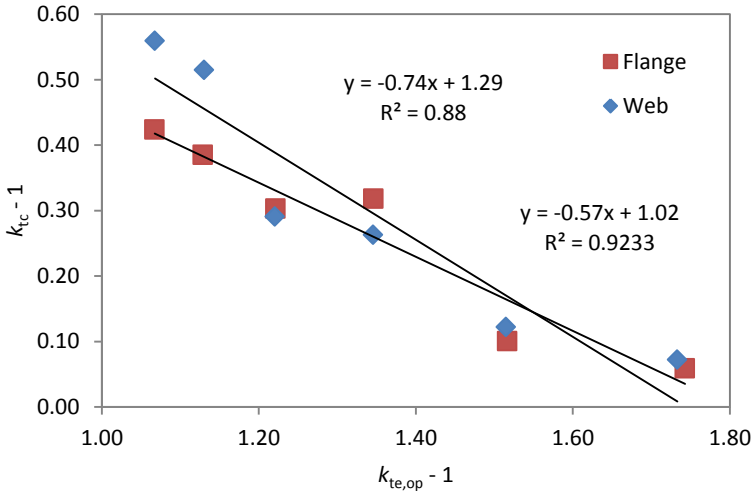

Figure 3.13: A Comparison of $k_{te,op}$ - 1 plotted against k_{tc} - 1 for Flange and Web Material

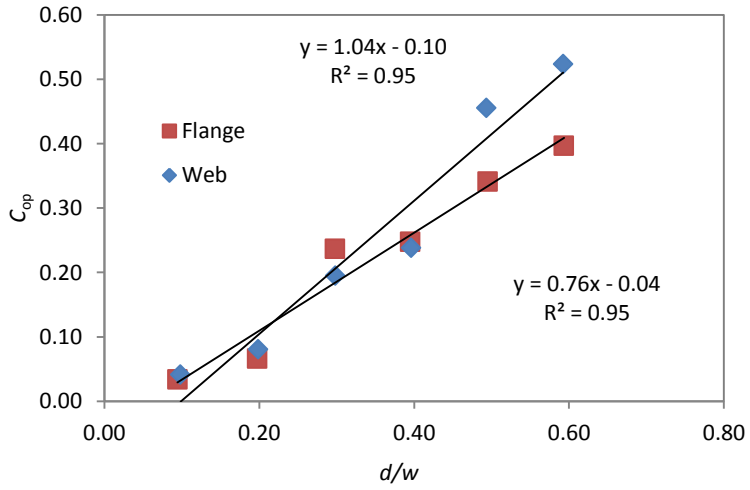

Figure 3.14: Open-hole Stress Concentration Correlation Coefficient plotted against hole-diameter to specimen width ratio

3.4. Moisture Sorption Tests

A series of moisture absorption tests were conducted in order to determine the moisture diffusion coefficient, *D*, of the PFRP material for use in the environmental aging analysis presented in Chapter 5. Bank *et al. (*2003) present a procedure for the long term material property qualification of FRP through the use of accelerated aging. The modelling of the accelerated aging regime by Bank *et al.* (2003) and others (Litherland, 1981; Koerner et al. 1992; Hassan and Iskander, 2001; Surathi and Karbhari, 2006) are based on Arrhenius relationships where a higher aging temperature can be related to a lower service temperature. The specification given by Bank et al. (2003) requires specimens to be hot-wet conditioned at least four accelerated temperatures and periodic readings over a duration of eight months. This method requires a high number of data points over long time duration (relative to this research project duration) for use in the regression analysis and subsequent data processing to achieve Arrhenius plots of reaction rates against the inverse of temperature, which in turn produce the activation energy for use in long-term predictions.

Due to the limitations of time, an alternative method, moisture diffusion, was chosen as presented in this section to establish the activation energy of the material due for hot-wet conditioning. Firstly, consider Equation (3.4) for the Arrhenius relationship in terms of the diffusion coefficient, *D* (Surathi and Karbhari, 2006) and as a function of temperature, *T* (in degrees Kelvin).

$$D = D_0 \exp(-E_a/\mathrm{R}T) \qquad (3.4.)$$

where D_0 is a constant, E_a is the activation energy of the diffusion process and R is the universal gas constant (8.3144 J mol^{-1} K^{-1}). This relationship is based on a Fickian diffusion process, which is often found in FRP materials (Karbhari, 2007); however empirical data is required to confirm

this for the PFRP material used in Chapter 5. To this end, a moisture diffusion test regime was undertaken, adopted from guidance from BS EN 2378:1995 and ISO EN 62.

A total of 132 nominally square PFRP specimens were cut, using similar procedures as presented for material properties tests, from a 203 x 203 x 9.53 mm WF section. Three sizes of specimen were selected with nominal square dimensions of 40, 60 and 80 mm and both web and flange material. Due to the complex fibre architecture, it was expected the diffusion mechanisms varied between the flange and web. The thickness, length and width of each specimen was measured and recorded. Three control specimens, one of each size were, kept in ambient laboratory conditions.

The remaining 129 specimens were firstly, dried in an oven to remove the initial moisture content and provide a datum to record moisture uptake. Specimens were weighed, using a calibrated electronic balance, accurate to 0.01g. 15 specimens, in batches of five for each of the three sizes (40, 60 and 80 mm), for both web and flange were immersed in SUB Grant water baths of distilled water at temperatures of 22 (9 Flange specimens only), 30, 40, 50 and 60°C.

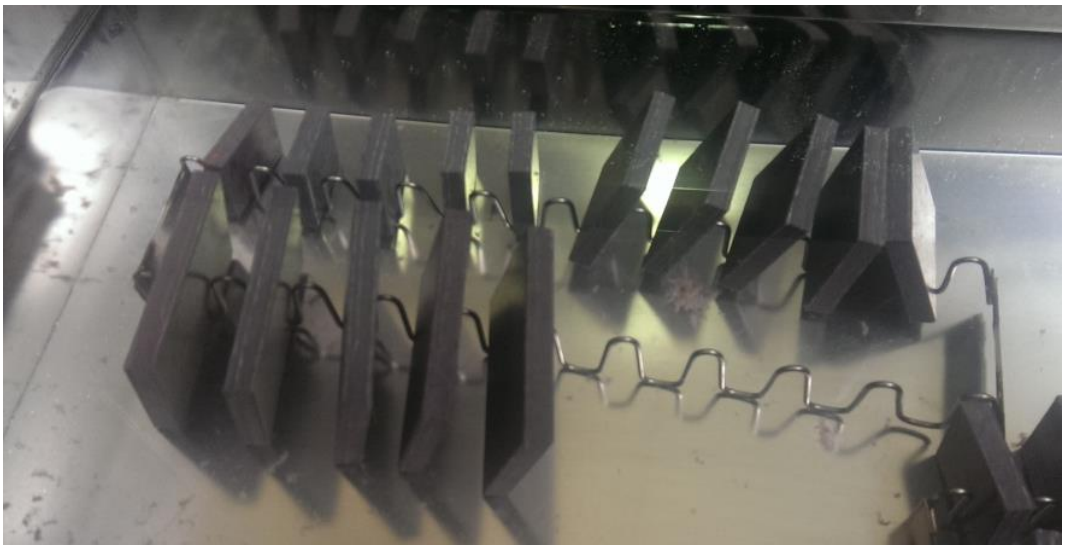

Figure 3.15: Moisture Absorption Test with Specimens immersed at 22°C in Distilled Water

A photograph of specimens on test racks, in distilled water, is shown in Figure 3.15. Specimens were removed periodically from the water baths, their surface wiped dry and weighed. Specimens were returned to the water baths. The test standards (BS EN 2738:1995) classify removal specimens from immersion conditions for weighing as continuous diffusion, if the time out of water is short)less than 2 minutes). Readings were taken after 1, 2, 4, 8, 16, 24, 48, 96, 168 hours and then every two weeks until a total period of 4 months. This was in line with the test standards for moisture absorption (BS EN 2378:1995). The moisture uptake was calculated using Equation (3.4).

The moisture uptake, *M*, at a given time, s, is defined as

$$M = M(s) = \left(\frac{W_w - W_d}{W_d}\right) \times 100 \qquad (3.5.)$$

where, W_w, is the wet weight of the specimen after immersion and W_d, the dry weight. The maximum moisture or saturation mass, M_m, is defined as when weight gains from three successive measurements differ less than 1% of the overall weight gain due to moisture uptake. It should be noted that no specimens reached a saturation level after four months immersion, which is estimated by Springer to be in the duration of decades (Springer, 1977). Presented in Tables 3.12 and 3.13 are the batch mean (of five specimens) percentage moisture uptake for temperatures of 22, 30, 40, 50, and 60°C, over time for the 80 x 80 mm specimens, only. The largest specimen sizes were chosen to match the pin-bearing strength coupons and hence further analysis and discussion is presented for this size specimen only. A full set of test results is presented in Appendix A.

Table 3.12: Summary of Mean Moisture Absorption Results for Flange Material

		Mean % Moisture Gain for given Temperature				
Time Period	Time, √t (days)	22°C	30°C	40°C	50°C	60°C
(1)	(2)	(4)	(5)	(6)	(7)	(8)
0hr	0.00	0.00	0.00	0.00	0.00	0.00
1hr	0.20	0.07	0.05	0.04	0.05	0.05
2hr	0.29	0.12	0.05	0.05	0.06	0.07
4hr	0.41	0.12	0.06	0.07	0.09	0.10
8hr	0.58	0.19	0.09	0.10	0.13	0.13
16hr	0.82	0.11	0.11	0.12	0.17	0.18
24hr	1.00	0.18	0.11	0.15	0.18	0.19
48hr	1.41	0.18	0.14	0.21	0.24	0.26
96hr	2.00	0.20	0.21	0.27	0.31	0.34
168hr	2.65	0.26	0.26	0.31	0.37	0.42
2wk	3.74	0.33	0.34	0.41	0.47	0.55
4wk	5.29	0.43	0.43	0.50	0.60	0.70
6wk	6.48	0.48	0.50	0.59	0.70	0.77
8wk	7.48	0.54	0.53	0.64	0.75	0.86
10wk	8.37	0.58	0.59	0.69	0.79	0.88
12wk	9.17	0.58	0.62	0.71	0.83	0.90
14wk	9.90	0.61	0.63	0.75	0.86	0.93
16wk	10.58	0.64	0.67	0.77	0.90	0.91

Table 3.13: Summary of Mean Moisture Absorption Results for Web Material

		Mean % Moisture Gain for given Temperature			
Time Period	Time, √t (days)	30°C	40°C	50°C	60°C
(1)	(2)	(4)	(5)	(6)	(7)
0hr	0.00	0.00	0.00	0.00	0.00
1hr	0.20	0.05	0.06	0.05	0.05
2hr	0.29	0.06	0.07	0.07	0.08
4hr	0.41	0.08	0.10	0.10	0.10
8hr	0.58	0.10	0.13	0.13	0.16
16hr	0.82	0.13	0.16	0.17	0.22
24hr	1.00	0.15	0.18	0.19	0.25
48hr	1.41	0.20	0.24	0.27	0.33
96hr	2.00	0.28	0.34	0.36	0.46
168hr	2.65	0.33	0.43	0.45	0.54
2wk	3.74	0.45	0.54	0.56	0.73
4wk	5.29	0.57	0.65	0.73	0.86
6wk	6.48	0.68	0.75	0.80	0.97
8wk	7.48	0.73	0.79	0.89	1.01
10wk	8.37	0.79	0.84	0.92	1.08
12wk	9.17	0.82	0.88	0.94	1.13
14wk	9.90	0.86	0.92	1.00	1.17
16wk	10.58	0.91	0.96	1.03	1.15

From inspection of Tables 3.12 and 3.13 it can be seen than moisture gain steadily increase with respect to duration and in comparing the last row of each table, it becomes apparent the role of test temperature in increasing absorption. Plotted in Figure 3.16 are the percentage moisture uptake curves for (a) Flange and (b) Web material. The initial stage of the diffusion process, the moisture content, as shown in Figure 3.16 linearly increases and then an exponential decline is observed, which if the process follows a Fickian behaviour will reach a

plateau at M_m (Surathi and Karbhari, 2006). The web material had a higher rate of moisture absorption when compared to web; this is due to the differences in fibre architecture.

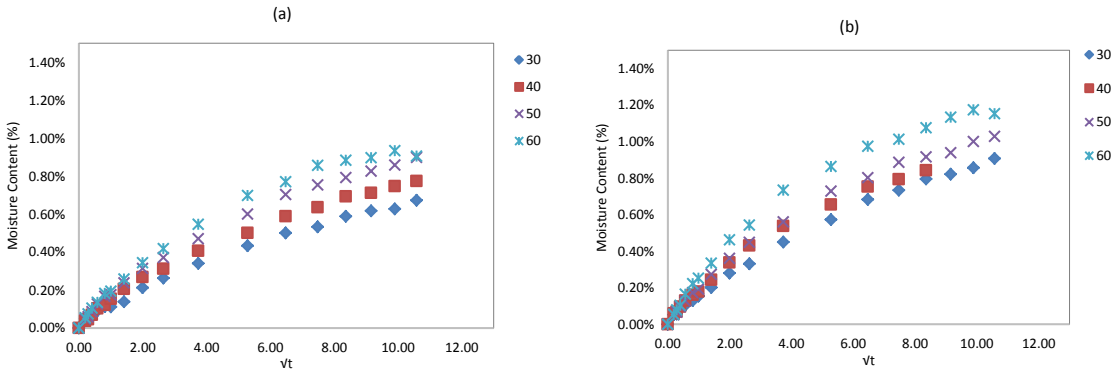

Figure 3.16: Percentage Moisture uptake over the square root of Time for (a) Flange and (b) Web material

3.4.1. Determination of Diffusion Co-efficient and Moisture Saturation Content

Presented next is a derivation of the method used to estimate the maximum moisture content, M_m, of the specimens, which is fundamental to establishing the diffusion coefficient and hence activation energy. The total mass of the moisture absorbed $M(s)$ at time s, can be expressed as (Shen and Springer, 1977)

$$M(s) = G\,(M_m - M_i) + M_i \qquad (3.6.)$$

where M_i the initial moisture content, M_m is the maximum moisture content that can be attained under the given conditions and G, is a time dependent parameter expressed by (Surathi and Karbhari, 2006; Crank, 1975):

$$G = 1 - \frac{8}{\pi^2}\sum_{n=0}^{\infty}\frac{\exp\left[(2n+1)^2\pi^2\left(\frac{-Ds}{t^2}\right)\right]}{(2n+1)^2} \qquad (3.7.)$$

where t, is the material thickness and D is the diffusion coefficient. The initial condition of specimens within this study was that of being dried within a low heat oven until mass was not

changing from three consecutive readings, taken five minutes apart. It can be assumed that the initial moisture content was zero. With $M_i = 0$:

$$M(t) = M_m \left[1 - \frac{8}{\pi^2} \sum_{n=0}^{\infty} \frac{\exp\left[(2n+1)^2 \pi^2 \left(\frac{-Dt}{s^2} \right) \right]}{(2n+1)^2} \right] \tag{3.8.}$$

An approximation for the initial phase of absorption or when $(\frac{Dt}{h^2}) < 0.04$, equation (3.7) simplifies to:

$$M(t) = M_m \left[1 - \exp\left[-7.3 \left(\frac{-Dt}{s^2} \right)^{0.75} \right] \right] \tag{3.9.}$$

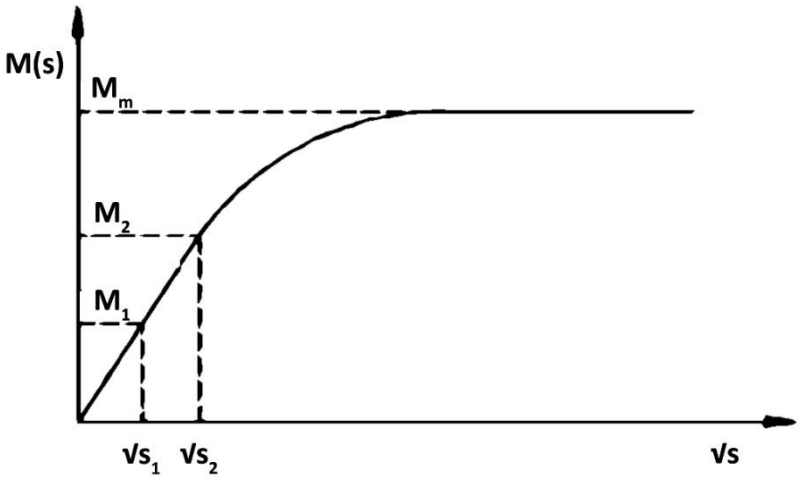

Figure 3.17: Characteristic Fickian Diffusion Process

Alternatively, an approximation to the initial linear phase of absorption, as shown in Figure 3.17, is given in the following form (Duncan and Broughton, 2007):

$$M(t) = M_m \left[\frac{4}{\pi} \sqrt{\frac{-Dt}{s^2}} \right] \tag{3.10.}$$

Rearranging equation (3.10), the diffusion co-efficient can be calculated using two time points (s_1 and s_2) points that lie within the initial linear part of the curve, from:

$$D = \pi \left(\frac{t}{4M_m} \right)^2 \left(\frac{M_1 - M_2}{\sqrt{s_1} - \sqrt{s_2}} \right)^2 \tag{3.11.}$$

3.4.2. Estimation of Activation Energy

The moisture diffusion curves, as shown in Figure 3.16 were curve fitted using a MatLab protocol with a simple exponential function to estimate the maximum moisture content. Using Equation (3.11), the % moisture uptake over the estimated maximum moisture value ($M(s)/M_m$) was plotted against ($4/t^2\pi\sqrt{s}$) to give the slope of the best fit line equal to the diffusion coefficient. A correction factor was applied to the coefficient as stipulated by Shen and Springer (1976).

Table 3.14: Calculated Diffusion Coefficients for Moisture Absorption in Web and Flange Material

	Diffusion coefficient, *D* (mm/s)	
Temperature	Flange	Web
30	2.16E-09	3.73E-09
40	2.57E-09	4.43E-09
50	2.82E-09	4.76E-09
60	3.02E-09	6.02E-09

The diffusion coefficients for web and flange material at different temperatures are given in Table 3.14. The diffusion coefficient is proportional to temperature; doubling the temperature from 30 to 60° results in a 30 and 40% increase in diffusivity of moisture for flange and web, respectively. The values in Table 3.14 were used to produce an Arrhenius plot (All plots are given in Appendix A) of the ln D against 1/T (in Kelvin) from which the gradient of the best fit line was equal to the activation energy, E_a. This was found to be 46 and 59 kJ per mol for flange and web material, respectively. The range of activation energy for pultruded materials immersed in water have be found by Purnell (2008) to range from 40 to 100 kJ per mol for various FRP and GRC materials. Therefore, there is confidence the values calculated within this study can be used in Chapter 5 for the prediction of long-term service periods at lower service temperatures for accelerated aging regimes.

3.5. Summary

This chapter has presented a series of experimental tests to determine the material properties of the WF pultruded sections used in the main experimental chapters of this thesis. It has been shown the material exhibits a complex material architecture with a FVF of 70 and 75% for the web and flange material, respectively. The results of resin burn-off tests have indicated that in the flange the two UD layers are not symmetrical, with the layer furthest away from the neutral axis being almost twice the thickness of the other. This has an effect on the material properties with strengths and in particular for the pin-bearing strength characterisation, due to the possibility of failure being propagated from the smaller UD layer.

A series of compression tests have been successfully conducted using a non-standard compression test rig developed by Mottram (1994). The test setup is based on a high precision die set using rectangular coupons loaded through the ends with the key advantages being an elimination of end effects, no need for end tabs and failure occurring within the gauge length. All specimens failed with a characteristic 45° shear crack throughout the section with an exception found for batches of flange material orientated with the pultrusion and testing axis parallel; In this situation a double shear crack occurs in a V-shape through the specimen thickness. The mean strength values are found to be on average 20% higher than the pultruder's stated values with characteristic values similar.

Tensile tests have produced characteristic and mean strengths which were further employed in the determination of open-hole tension strength. The Hart-Smith method (1979) for determining the open-hole correlation coefficient has been applied and found, for the PFRP shape characterised in this chapter, it may not be suitable. The method, when applied, does not satisfactorily relate the isotropic stress concentration factor to the orthotropic stress

concentration factor. The previously thought material 'constant' C_{op} is shown to vary. This finding has implications of the reliability of using the Hart-Smith approach in determining the design resistance of bolted connections that fail in the net-section.

Moisture diffusion tests have been used to establish the diffusion coefficients of the material when immersed in distilled water. The semi-empirical approach has been successfully used to establish the activation energy for web and flange material and can be used in subsequent analysis of environmental conditioning of PFRP, as to be found in Chapter 5.

CHAPTER 4

Plain and Threaded Pin-Bearing Strength Characterisation

4.1. Introduction

Pultruded structures are often connected together by conventional stainless steel bolting (Mottram and Turvey, 2003). These connections provide ease of assembly and maintenance, as well as being capable of transferring the actions in primary load bearing structures. The design and verification of bolted connections in PFRP frames is a complex exercise (Mottram and Turvey, 2003, and Mosallam, 2011) that has considerable gaps in knowledge (Mottram, 2009a). One key knowledge gap is that designers and/or fabricators often allow bolt thread to be in bearing, in particular when several different material thicknesses are connected within a pultruded frame. The effect this has on bearing strength of PFRP material, if any, is not fully understood (Troutman and Mostoller, 2010 and Matharu and Mottram, 2012). Furthermore, the relationship between the pin-bearing value, when there is a smooth bolt shank in bearing, and a threaded bearing value has yet to be established. It is relevant to discuss now the meaning of 'pin-bearing'. Not only is this term for the situation when the bolt is laterally

unrestrained, its meaning implicitly implies a 'pin' with a smooth shank. This poses a difficultly when wanting to use the term for the situation of an unrestrained bearing strength when thread is present. For convenience in this thesis the author uses the descriptor 'pin-bearing' preceded by plain and threaded to represent the situation without and with thread in bearing.

Recent studies for bearing strength of as received material (non-aged) have focused on plain shafts for pin-bearing (Mottram, 2009b, Mottram and Zafari, 2011). Considered in this chapter is the laterally unrestrained (pin) bearing strength property with and without bolt thread present for a non-aged PFRP material. Furthermore, thread in bearing is considered for the first time in the off-axis direction with respect to the loading and direction of pultrusion.

The design of bolted connections of PFRP structures involves considering several distinct failure modes which have their own associated design formulae. The bearing mode requires the pin-bearing strength ($F_{\vartheta}^{\mathrm{br}}$) for use with Eq. (2.1). To be classified as pin-bearing, this lower bound strength is for no lateral restraint or through thickness constraint from a bolt tightening, which is known to significantly increase the bearing force prior to ultimate failure (Cooper and Turvey, 1995 and Mottram and Turvey, 2003).

For use in design calculations, Eq. (2.1) requires a characteristic pin-bearing strength. It has been recommended in the LRFD pre-standard (ASCE, 2012) that for a threaded pin in bearing its pin-bearing strength in Eq. (2.1) shall be 0.7 of the characteristic plain pin-bearing strength. One of the objectives of the work presented in this chapter is to check this mandatory guidance. This requires the determination of characteristic strengths for different pin sizes with and without thread in bearing. To have the flexibility to use recognized statistical procedures in this work (e.g. ASTM D7290) to establish characteristic values the number of specimens per batch is 10.

One of the aims of the study was to develop further the test methodology to be used in determining the pin-bearing strength measure. The disparate results and test methods for determining bearing strengths over the years (Mottram, 2009b) has meant drawing parallels between the characterisation of bearing strengths for use in design and calibration for partial (safety) factors is unreliable.

The author's investigations have studied the behavioural effects of pin-diameter to material thickness ratio, material (fibre) orientation with respect to load axis, material (architecture) type, and environmental conditioning on pin-bearing strength. The environmental conditioning study is covered in Chapter 5. Furthermore, the characterisation of bolt thread in bearing, as well as the effect of thread pitch on the bearing resistance of the material, is considered for a fundamental understanding of the failure mechanism. The studies of the effect of thread pitch and off-axis material orientation with respect to loading direction are separate studies that complement the main investigation to establish characteristic values for plain and thread pin-bearing strengths.

The new test results presented in this chapter form a considerable addition to the existing database of pin-bearing strengths, and subsequently a discussion is presented of these findings from the extensive experimental programme, with more than 500 individual pin-bearing strength tests. A focus is drawn to the situation of thread in bearing, including a unique study into thread pitch and its associated effect on pin-bearing strength. Furthermore, the effect of material orientation, with respect to the axis of pultrusion, is explored. Finally, conclusions are drawn from the discussion and evaluation of all the test results; they look to provide guidance towards use of the pin-bearing strength in the design of bolted connections.

4.2. Test Specimen Preparation

A Wide Flange (WF) beam section was cut into five pieces by removing the four flanges from the web to produce flat plate sections that were further processed into specimen blanks. Material was utilised from both 254 x 254 x 9.53 mm and 203 x 203 x 9.53 mm sections, having the same fibre architecture and nominal material properties as detailed in Chapter 3. Figure 4.1 shows the locations of plate sections produced from removing the flanges from the web, with approximately 10 mm removed from the outer edge of the flange as this volume, along with the region between the flange and web, is a resin rich zone with less volume of fibre reinforcement. It should be noted that the material has not been conditioned prior to testing, other than stated during the manufacture of specimens, and so has effectively been tested as-received from Creative Pultrusions Inc. In the rest of the chapter the abbreviation CP is for Creative Pultrusions Inc.

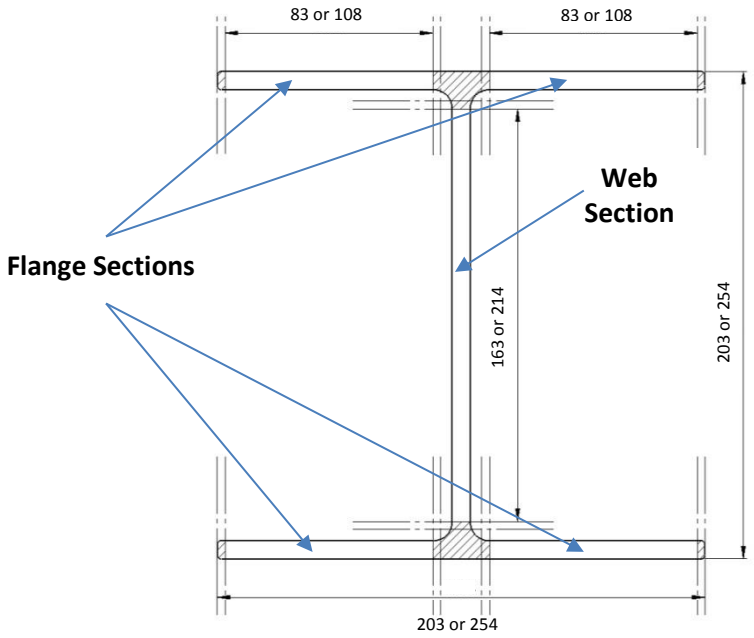

Figure 4.1: WF Section cutting up diagram for Pin-bearing Specimen Preparation

Specimen blanks of 80 mm × 100 mm were prepared from the web and flange materials, as shown in Figure 4.1, using a diamond edged circular saw with water coolant to minimise machining-induced damage. Mottram and Turvey (2003) have noted that bearing failure is most likely to occur when the end distance (e_1) and width (w) are, at least, four times the pin diameter. To accommodate the maximum pin size of 20 mm, the finished specimens were set to have a plan size of 80 by 80 mm. The exact location of each specimen from within the WF section was not recorded. It is noted that specimens within the same batch tended to be from the same vicinity (adjacent) to each other when cut from the section. Furthermore, all specimens were cut from the same run (120m batch) of pultruded material. A schematic of the principal dimensions of a semi-notched specimen are shown in Figure 4.2b. Due to the restriction in the width of flange sections to 108 mm, specimens at 45° orientation were only prepared with web material; the width dimension being 215 mm for the larger 254 x 254 x 9.53 mm section.

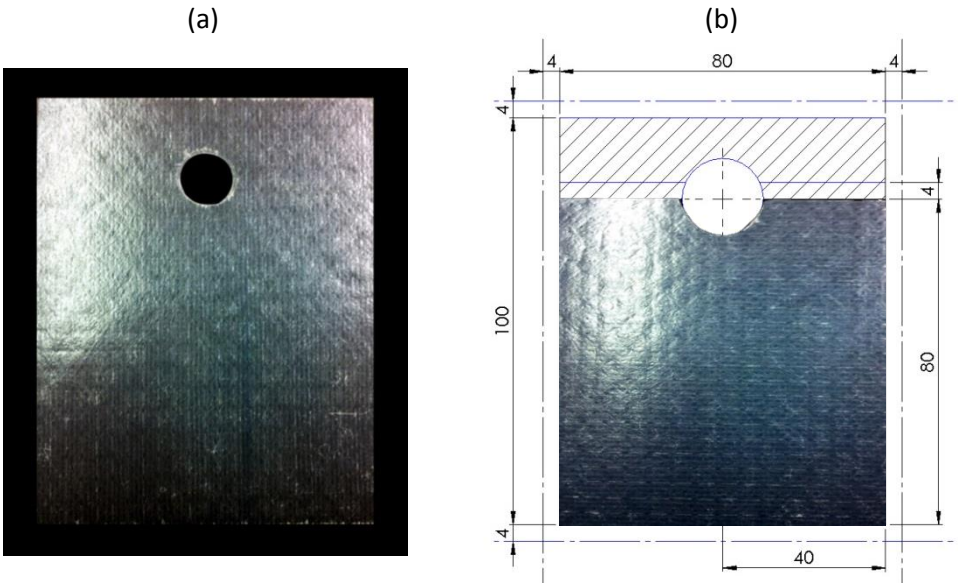

Figure 4.2: Pin-bearing Specimen Preparation (a) Uncut Drilled Specimen and (b) Finished Specimen and Dimensions

Specimen blanks were placed into a specifically designed drilling jig, which allowed 10 specimens to be drilled at once, and in-turn was affixed to the moveable bed of a Cincinnati

Arrow 750 vertical milling machine. For every specimen the hole-centre was located centrally within the width (w) at a 40 mm side distance (e_2), and 80 mm end distance (e_1). The major specimen dimensions are shown in Figure 4.3.

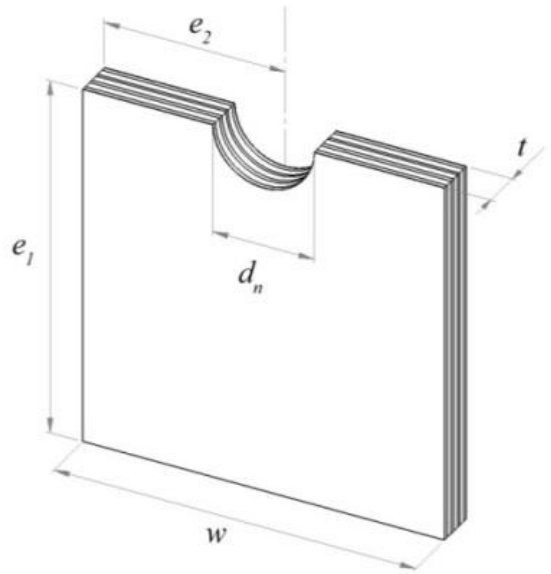

Figure 4.3: Schematic of Test Specimen and Major Geometry Variables

Figure 4.4(a) shows the milling machine and in Figure 4.4(b) the machine has a batch of 10 unprepared specimens. The drilling process, firstly, uses a solid carbide 10 mm stub drill bit to rough-out the centre of each hole. This operation was conducted at a speed of 1000 rpm and a feed rate of 100 mm/min. Secondly, a four flute end mill enlarged the hole to within 0.5 mm of the required diameter. This second roughing-out operation was conducted at a speed of 1500 rpm and a feed rate of 150 mm/min. The holes were finished with a second end mill (used only for this finishing drill pass) of 10 mm for clearance hole (d_n) diameters of 12 mm and 14.4 mm, and a 16 mm end mill for the 18.4 mm and 22.4 mm hole sizes. The final operation used a speed of 1500 rpm with a feed rate of 400 mm/min. The complete procedure for a clearance hole of 12 mm involved drilling a 10 mm hole, the roughing out the hole leaving 1 mm to finish the hole, i.e., a 12 mm diameter hole was first 10 mm, next 11 mm and finally milled out to 12 mm with a tolerance of +/- 0.1 mm.

(a)

(b)

Figure 4.4: Machining Setup with (a) Cinccinati Arrow 450 Milling machine and (b) Specimen Blanks in the drilling Jig

Support given at the tool exit side by the drilling jig minimised surface rupture and potential FRP delamination, as well as the use of soluble oil to reduce excessive tool wear. The drilling method of circular pocketing (also known as orbital drilling) was used at 1800 rpm and a feed rate of 100 mm/min. This minimised thrust force; a key factor known to affect drilling induced delamination failure (Singh and Bhatnagar, 2006). Using a four fluted end mill the specimens were milled around the perimeter edges to give a finished size specimen of 80 x 80 mm within

a tolerance of +/- 0.1 mm using a speed of 1500 rpm and feed rate of 200 mm/min. Post-drilling, the specimens were finalised by cutting at 80 mm (e_1) to obtain the semi-circular notched coupon.

The fabrication procedure ensured longevity of drill bits, and optimised time and tolerances of the test specimens. This was confirmed by measurements taken using an internal micrometer for each hole prior to final cutting; the largest variation being an under-sizing of the clearance hole by a maximum of 0.02 mm.

The thickness of each specimen was measured using an external micrometer to the nearest 0.01 mm, and found to range from 9.58 mm to 9.75 mm (0.17 mm) for web material and 9.57 mm to 10.32 mm (0.75 mm) for flange material. Measurements of length, width and position of the hole for each specimen were taken using digital vernier callipers to the nearest 0.01 mm, which was needed to allow the specimen to be aligned within the test rig. Further information on detailed measurements of specimens is given in Appendix B.

Specimens were labelled using the format W/0/P/M10-01; this label is for a specimen from web material (W) with the hole cut to be coincident with the longitudinal axis relative to pultrusion (0°). This specimen would be tested with a plain (P) M10 sized pin and would be the first (01) in a batch of 10.

4.2.1. Test Matrix

A total of 380 specimens were tested to determine the effect of ‘pin’ type, both threaded and plain, on the bearing failure load for three material orientations of 0, 45 and 90° and four pin diameters. Loading pins were cut from standard A4 (314) stainless steel bolts of M10, M12,

M16 and M20 size diameter (*d*), with 1.5, 1.75, 2 and 2.5 mm (coarse) pitch, respectively. (Note that specific pin diameter measurements to the nearest 0.01 mm are stated in Tables 4.1 to 4.4. for all pins). An unthreaded pin represents the smooth shaft of a bolt, whereas a threaded pin is for a conventional threaded bolt. Because increasing the hole diameter is known to reduce failure load (Yuan *et al.*, 1996; Mottram, 2009b) the test programme considered the largest acceptable hole clearance according to ASCE Code of Standard Practice for Fabrication and Installation of Pultruded FRP Structures (2013). The nominal clearance (d_n – *d*) is 2.2 mm (given by 1.6mm clearance + 0.4mm tolerance) for M10 and 2.6 mm (1.6mm clearance + 0.8mm tolerance) for M12, M16 and M20 sizes. Testing was conducted at ambient laboratory temperatures for the 38 batches of 10 specimens (22 from web and 16 from flange material). Because of a dimension constraint the 45° specimens were only cut from the web material for all four plain pin sizes and for M10 and M20 threaded pin sizes.

4.3. Test Setup and Procedure

The Warwick University Test Setup (WUTS) for the determination of pin-bearing strength was first presented by Mottram (2009b) and has been used in the PhD work of Zafari (2012) to characterise pin-bearing strengths for a web material pultruded by CP in the 1990's (before the SuperStructural range of shapes existed).

The key differences between the WUTS and other methodologies such as ASTM D953 (American Society for Testing and Materials, 2010) or BS EN 13706 (British Standards Institution, 2002) are the following features:

- it accommodates a smaller coupon, such as, specimens cut from web and flanges of structural shapes and not only flat sheet.

- there is no lateral restraint which is known to increase bearing strength by preventing onset of delamination failure; it may not always be present (due to creep relaxation and loosing of torque), and for safe design the strength measurement needs to be appropriate to field conditions.
- the use of a clearance hole that is known to reduce a bearing strength.
- the use of a variety of pin sizes between M6 to M24 as found in practice.
- the WUTS reduces the influence of any pin flexure.

A critical discussion on worthiness of the WUTS (for PFRP materials) has been given by Mottram (2009b), and Mottram and Zafari (2011). The same test rig was used for all tests detailed in this chapter. An adjustment to the original set-up was made to accommodate a more accurate loading alignment on a specimen. This included a horizontal alignment system that allows the specimen within the holder to be centrally located and to be coincident with the longitudinal axis of the loading pin.

4.3.1. Test Setup

The compression die set and specimen holder has been used to conduct several previous investigations (Mottram and Zafari, 2011 and Zafari and Mottram, 2012a). A test methodological issue arose that the specimens should be precisely aligned so that the line of action of the pin is directly in line with the centre of the notch (Lutz, 2004). The implication of being off-centre is first and foremost for a less reliable strength measurement because position provides another test uncertainty. Figure 4.5 shows a spring (left-side), a micrometre (right-side) and specimen holder (middle) arrangement that is used to centre the holder. In addition, to accommodate the threaded pins (so as to reduce damage to the die set), a new v-notch top fixture (see Figure 4.5) made of tool steel (gauge plate) was manufactured. The

testing required fabrication of a spacing-block to accommodate the smaller specimen size (compared to previous specimen size of 96 by 73 mm), and re-milling of the anti-buckling side plates in the specimen holder to hold the nominally thicker flange material.

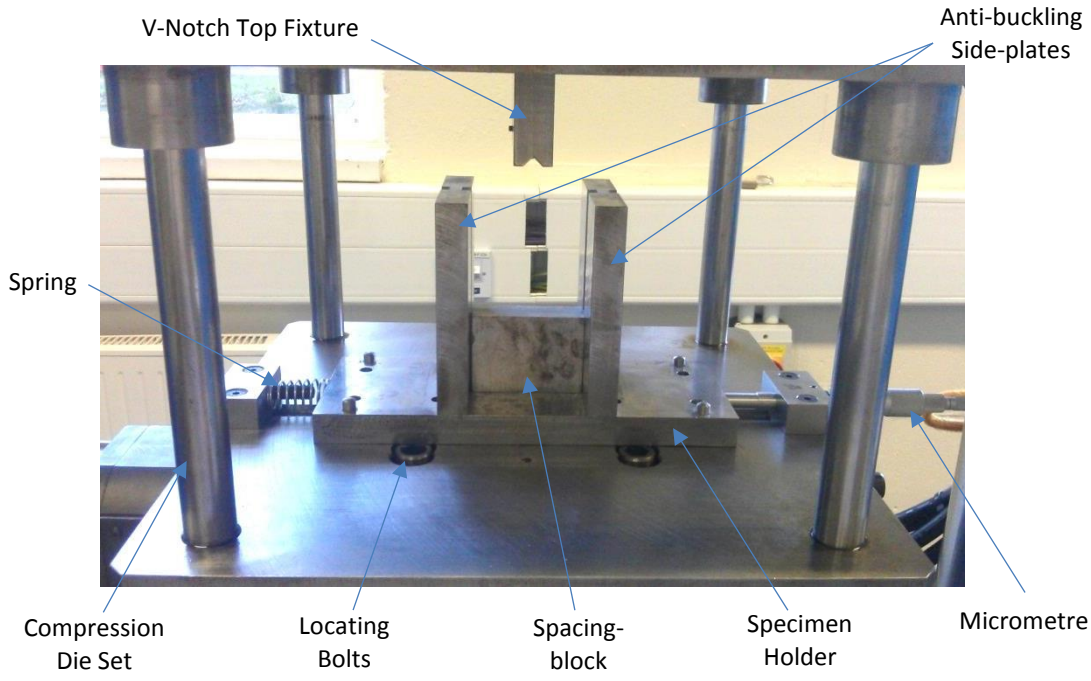

Figure 4.5: Specimen Holder and Alignment Mechanism

It was identified that the influence of the relative horizontal positioning of the thread profiles to the layers within the PFRP material is unknown using the previous v-notch top fixture. Hence, a stop was placed within the top fixture to ensure the pin was located in the same positon in every test; the thickness of the specimens with respect to this pin positioning was not adjusted. It is expected that the effect would contribute to the failure mode, but not necessarily be a direct cause for the usual delamination failure.

4.3.2. Test Procedure

Each test was performed using a DARTEC 9500 servo-hydraulic testing machine with a 250 kN load cell equipped with WUTS as shown in Figure 4.6. The test procedure involved, firstly, a

specimen being placed into the holder and the pin located within the notch. The specimen was next aligned by adjusting the micrometer to the required distance with respect to the measurements taken for locating centrally the notch (Appendix B). The top crosshead of the testing machine was lowered so that the upper platen and top v-notch fixture rested upon the specimen and pin. The load and stroke readings were then zeroed and the static strength test was commenced.

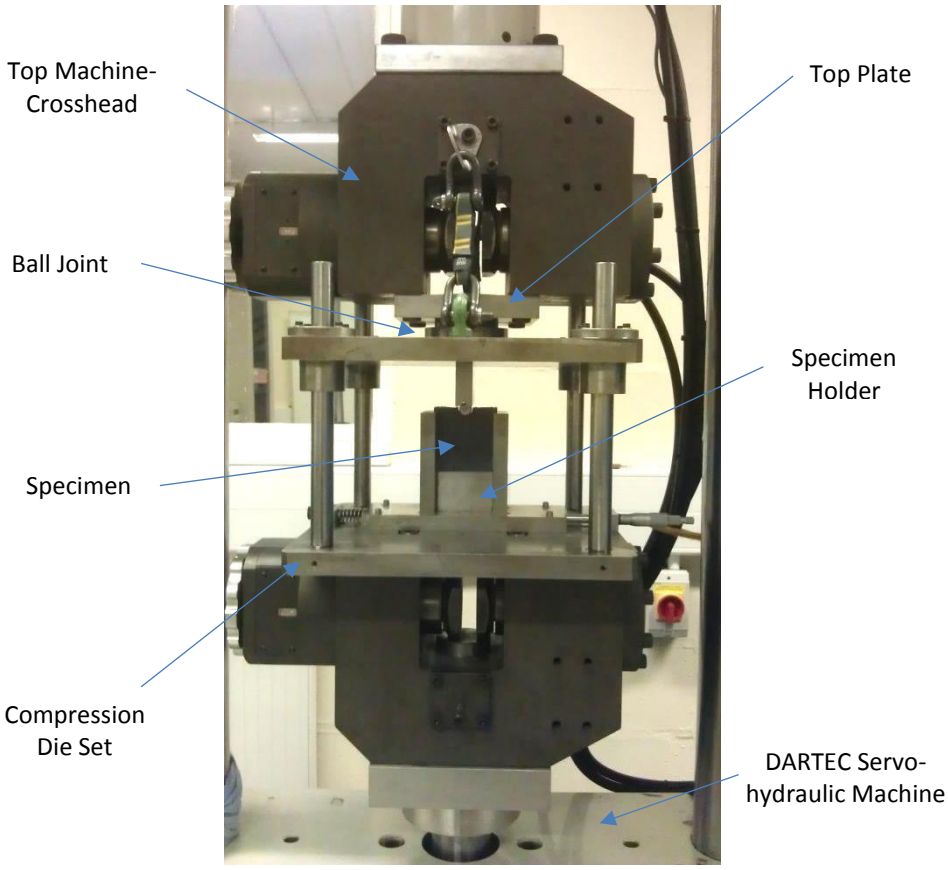

Figure 4.6: WUTS for Pin-bearing tests in the DARTEC 9500 Machine

Loading transfer is completely in-plane ensuring purely bearing damage will occur. The uniaxial compressive load was applied under a constant stroke rate of 0.01 mm/s and load and machine stroke recorded once every half-second by National Instruments (NI) data acquisition equipment. The maximum failure load was recorded and the (NI) data exported to form load-stroke plots.

The machine stroke is predominately governed by the compressive deformation of the specimen, due to the relatively high axial stiffness of the machine's frame, test fixtures and pins. The maximum compressive force takes account of the dead weight of the top plate and rocker fixture, at 0.321 kN. The specimens were tested to failure, defined as the maximum load which is known (Mottram and Zafari, 2011) to be often followed by a precipitous drop in the load/displacement plot particularly for specimens tested in the longitudinal direction but not always for off-axis testing. First Failure is defined as first peak or a deviation from linearity of the plot load-stroke curve. The load used to determine the pin-bearing strength is the maximum load (Mottram, 2009b; ASCE, 2012).

4.4. Test Results

4.4.1. Plain and Threaded Pin-bearing Strength Characterisation

Presented in this section are results with plain and threaded pins using web and flange material orientated at 0° and 90°. In addition, results for web material orientated at 45° are reported. The pin-bearing strengths for specimens and batches of specimens were calculated using Eq. (2.1). Furthermore, for the first time a new set of load-stroke plots for thread in bearing is presented. General trends are identified, which are graphically represented, drawing comparisons between pin-bearing strength and ratio d/t, as well as the ratio of longitudinal-to-transverse strengths (F_0^{br}/F_{90}^{br}) from similar batches of the same material and test conditions. The strength differences between having either a plain or threaded pin is further developed in the discussion on the effect of thread in sub-section 4.5.1.

The pin-bearing test results are analysed by computing means, standard deviations and coefficients of variation, in order to assess the quality of the data. Furthermore, batch results

are conditioned appropriately to identify if there are any anomalous test results within batches. This was done before calculation of characteristic values in accordance with BS EN 1990 Annex D (British Standards Institute, 2002). Finally in this section, a broad comparison is made between characteristic values and manufacturers supplied data for pin-bearing strengths, which leads onto a wider discussion with other pin-bearing strength studies for thread pitch and material orientation.

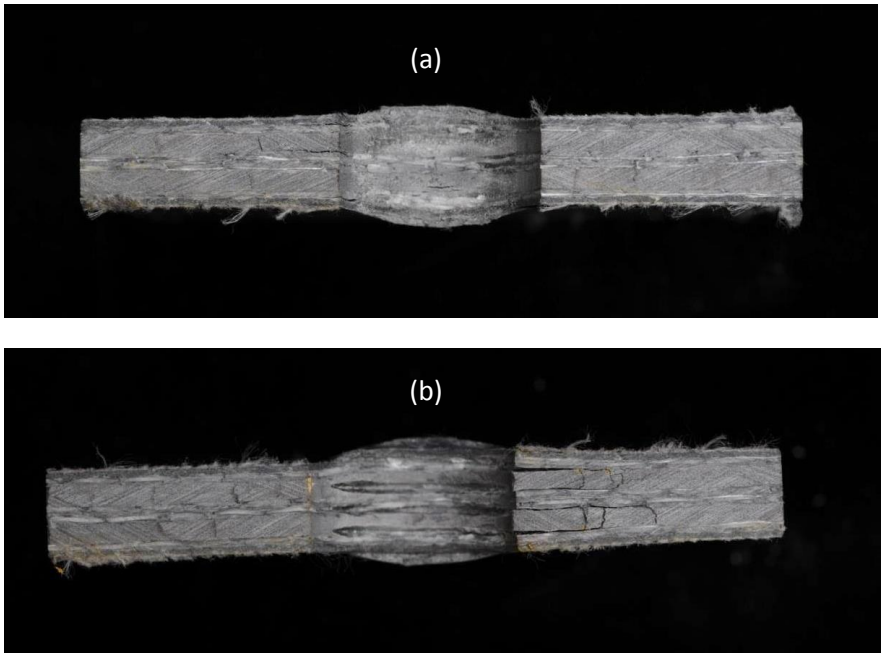

Figure 4.7: Failed Pin-bearing Specimen tested with (a) Plain Pin and (b) Threaded Pin

Figure 4.6a shows the typical failure with a plain pin when view normal to the bearing area. Figure 4.6b is for the threaded situation with the same web material oriented at 45°. The specimens in this figure were tested until just after there is a sudden 'drop-off' in compressive load, as found in conventional load-stroke plots (particularly in the 0° direction (Mottram and Zafari, 2011), and which represents bearing failure that often coincides with the maximum attained load. Similar overall failure with localised brooming after delamination fractures was observed with 0^o and 90^o specimens. It can be seen in Figures 4.6a and 4.6b that the bearing areas are not equal, and what is clearly visible is the contrast from the difference in the

geometric profiles of the plain and threaded pin. Figure 4.6(b) shows that thread in bearing reveals greater peripheral cracking on the top of the specimen, thereby suggesting a different internal crack structure has developed from the embedment of the thread pitch profile. This fundamental difference between plain and threaded bearing will be discussed further in sub-section 4.5.1. Specimens exhibit the archetypal bearing failure shown in Figure 4.7, consisting of a splaying of material in the out-of-plane direction at the material-pin interface. The failure mechanism is thought to as a result of interface friction creating a localised three-dimensional stress field, with eventually the through-thickness strength (or fracture toughness) being overcome and instantaneously initiating delamination cracks for the characteristic bearing failure.

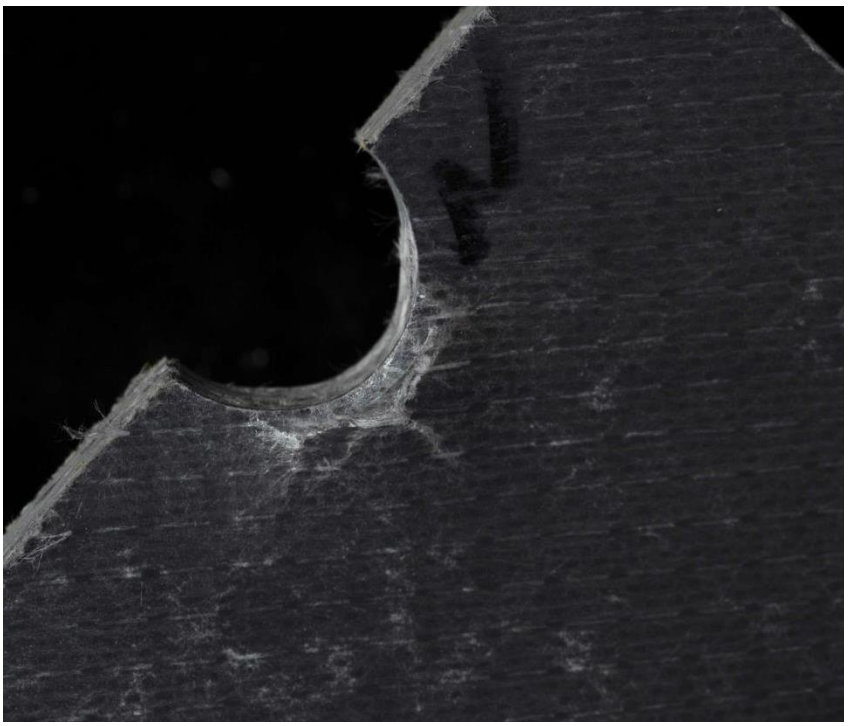

Figure 4.8: Typical Failure Face of Pin-bearing Specimen

Tables 4.1 to 4.4 present a summary of the test results for both web and flange material at 0°, and 90° orientations, and 45° (web only) orientation. In Columns (1) and (2) are reported the pin diameter (*d*) and the mean specimen thickness (*t*), as measured with vernier callipers and

outside micrometer respectively. The average ratio of diameter-to-thickness is 1.02, 1.23, 1.65 and 2.05 for pin sizes M10, M12, M16 and M20. These values for d/t correspond to the first four rows and are in same order for subsequent four rows down a table. The mean maximum failure load ($R_{br,mn}$ in kN) is given in column (3). Using the individual R_{br}s the mean pin-bearing strength in N/mm^2 (MPa) is calculated using Eq. (2.1) and its batch mean is reported in column (4). For each batch the Standard Deviation (SD) is given in column (5) and its Coefficient of Variation (CoV) in column (6). The full set of specimen results are given in Appendix C for the main results summarised in Tables 4.1 to 4.4.

In column (7) of the tables the characteristic value, in accordance with Annex D7 (General Principles for Statistical Evaluation) BS EN 1990 (British Standards Institute, 2002) is given. This value is determined with the assumptions that the property distribution fits a Gaussian (normal) distribution and the CoV is known. Previous test results (Mottram and Zafari, 2011) have shown that the CoV is often ≤ 10%, and this finding concurs with the CoVs in Tables 4.1 to 4.4. Moreover, CL D7.2 (2) in EN1990 states that "a realistic upper bound of it (CoV), is known from prior knowledge" the approach is deemed acceptable. Hence Table D1 in EN 1990 is used to obtain k_n (characteristic fractile factor) required to determine the 5th percentile characteristic value. Based on procedure for a known CoV and a batch size of 10 specimens the characteristic value is equal to (mean – 1.72×SD); where k_n is 1.72. The calculated characteristic strengths may be used as the pin-bearing strength in Eq. (2.1) for the design of bolted connections when the FRP material is that in SuperStructural® shapes. It is observed that the characteristic values are generally 10% lower than the mean value.

It is noteworthy that the largest CoV at 5.9 to 10.4% from Table 4.1 and 6.4 to 11.6% from Table 4.3 are for 0° (web and flange) material when the 'pin' is plain. Overall, the populations have considerably less scatter for pin-bearing strength determined with thread than without.

The largest variations (spread) in batch results giving CoVs of 10.4% and 11.6%, respectively, are found with the plain M12 pin and both web and flange material.

Table 4.1: Plain Pin-bearing Strength Test Results for Web Material

Pin Diameter, d (mm) (1)	Mean Thickness, t (mm) (2)	Mean Max. Failure Load, $R_{br,mn}$ (kN) (3)	Mean Pin-bearing Strength, F_{ϑ}^{br} (N/mm^2) (4)	Standard Deviation, SD (N/mm^2) (5)	Coefficient of Variation, CoV (%) (6)	Characteristic Value, $F_{k,\vartheta}^{br}$ (N/mm^2) (7)
Longitudinal (0°)						
9.81 (M10)	9.61	18.7	198	16.3	8.2	170
11.8 (M12)	9.63	21.7	191	19.8	10.4	157
15.9 (M16)	9.63	28.1	184	10.8	5.9	165
19.8 (M20)	9.65	33.5	175	15.5	8.8	148
45°						
9.81 (M10)	9.63	15.3	162	4.94	3.0	154
11.8 (M12)	9.62	14.8	130	6.63	5.1	119
15.9 (M16)	9.65	18.6	122	4.21	3.5	115
19.8 (M20)	9.66	22.9	120	4.85	4.1	112
Transverse (90°)						
9.81 (M10)	9.62	15.0	159	7.09	4.5	147
11.8 (M12)	9.64	15.5	136	3.27	2.4	130
15.9 (M16)	9.63	19.4	127	8.76	6.9	112
19.8 (M20)	9.64	20.3	107	5.01	4.7	98

Table 4.2: Threaded Pin-bearing Strength Test Results for Web Material

Pin Diameter, d (mm) (1)	Mean Thickness, t (mm) (2)	Mean Max. Failure Load, $R_{br,mn}$ (kN) (3)	Mean Pin-bearing Strength, F_{ϑ}^{br} (N/mm^2) (4)	Standard Deviation, SD (N/mm^2) (5)	Coefficient of Variation, CoV (%) (6)	Characteristic Value, $F_{k,\vartheta}^{br}$ (N/mm^2) (7)
Longitudinal (0°)						
9.81 (M10)	9.61	18.3	194	12.4	6.4	173
11.8 (M12)	9.62	19.6	173	11.4	6.6	153
15.8 (M16)	9.63	24.3	160	13.1	8.2	138
19.8 (M20)	9.64	24.1	126	8.97	7.1	111
45°						
9.81 (M10)	9.65	15.9	168	9.65	5.8	151
19.8 (M20)	9.64	22.9	124	6.95	5.6	112
Transverse (90°)						
9.81 (M10)	9.61	16.6	176	8.87	5.1	161
11.8 (M12)	9.63	18.7	165	4.10	2.5	158
15.9 (M16)	9.63	23.2	152	7.58	5.0	139
19.8 (M20)	9.63	22.3	117	7.46	6.4	104

The means in Tables 4.1 to 4.4 are based on all 10 specimens in the batch. It should be noted that an analysis on the spread in each batch was conducted against the Chauvenet criterion (Kennedy and Neville, 1986), with the objective of rejecting specific data points, if deemed appropriate. Although there were some points classified as outliers, typically a single point in a

few batches, the removal of these selected few points made no significant difference (± 4%) to the means. It was therefore deemed acceptable to include all results when determining the characteristic strength of a batch of 10 specimens. It should be noted that because there has historically been observed a relatively large variation in material test results for batches of PFRP material this lead (Zureick *et al.* (2006) to specify larger batch sizes (minimum 10 and recommended 30 nominally identical specimens). The results of the Chauvenet test are given in Appendix C, along with suspected outliers and recalculated values with the outliers removed.

Nevertheless, a testament to the low variability in this pin-bearing investigation, particularly with thread present, is the relatively 'low' CoV, often well below 10%, with the exception of the two batches with plain M12 pin. The reason for this larger spread shall be discussed later. It is seen that the scatter, in general, for batches without thread are higher than the equivalent with thread. It is believed this finding is interconnected with the 'brittle' behaviour of the 0° material, typified by a precipitous drop in load on a load-stroke plot, immediately after bearing failure (Mottram and Turvey, 2003).

From inspection of information in Table 4.1 it can be observed that for web material the minimum mean F_0^{br} and F_{90}^{br} is 175 and 107 N/mm^2, respectively. These are significantly lower than 234 and 206 N/mm^2, for the longitudinal and transverse pin-bearing strengths, taken directly from the pultruder's Design Manual (Creative Pultrusions, 2010). In the design manual they are described as a maximum bearing strength. Similarly, in Table 4.3, the minimum means for the flange material of 186 (F_0^{br}) and 92 (F_{90}^{br}) N/mm^2 are considerably lower than the stated strengths from CP of 227 and 158 N/mm^2. There are a number of reasons that justify why the strengths given by CP, who used standard ASTM D953 to determine them, can be more than doubled. They are developed by Mottram and Zafari (2011) with key reasons being that CP

used a 6.35 mm pin size and no clearance, and report average values based on random sampling and testing of production lots. CP also used the 4% hole-elongation as the criterion to establish failure load, and it is known to be less reliable. It is clearly up to the design engineer to decide what value of pin-bearing strength is to be used as the characteristic strength in Eq. (2.1) for the reliable design of bolted connections.

Table 4.3: Plain Pin-bearing Strength Test Results For Flange Material

Pin Diameter, d (mm) (1)	Mean Thickness, t (mm) (2)	Mean Max. Failure Load, $R_{br,mn}$ (kN) (3)	Mean Pin-bearing Strength, F_{ϑ}^{br} (N/mm^2) (4)	Standard Deviation, SD (N/mm^2) (5)	Coefficient of Variation, CoV (%) (6)	Characteristic Value, $F_{k,\vartheta}^{br}$ (N/mm^2) (7)
Longitudinal (0°)						
9.81 (M10)	9.77	20.1	210	19.9	9.5	176
11.8 (M12)	9.77	21.5	186	21.5	11.6	149
15.8 (M16)	10.0	32.7	205	13.1	6.4	182
19.8 (M20)	9.66	37.9	198	17.6	8.9	168
Transverse (90°)						
9.81 (M10)	9.96	13.9	142	5.31	3.8	133
11.8 (M12)	9.81	14.4	125	5.59	4.5	115
15.8 (M16)	10.3	18.2	111	4.15	3.7	104
19.8 (M20)	9.61	17.6	92	3.01	3.3	87

Table 4.4: Threaded Pin-bearing Strength Test Results for Flange Material

Pin Diameter, d (mm) (1)	Mean Thickness, t (mm) (2)	Mean Max. Failure Load, $R_{br,mn}$ (kN) (3)	Mean Pin-bearing Strength, F_{ϑ}^{br} (N/mm^2) (4)	Standard Deviation, SD (N/mm^2) (5)	Coefficient of Variation, CoV (%) (6)	Characteristic Value, $F_{k,\vartheta}^{br}$ (N/mm^2) (7)
Longitudinal (0°)						
9.81 (M10)	9.76	18.7	195	12.42	1.9	174
11.8 (M12)	9.70	21.0	184	15.33	8.3	158
15.8 (M16)	9.78	24.9	161	12.62	7.8	139
19.8 (M20)	9.64	27.0	141	6.29	4.5	130
Transverse (90°)						
9.81 (M10)	9.96	15.4	158	7.22	4.6	146
11.8 (M12)	9.82	16.5	143	9.49	6.7	127
15.8 (M16)	9.65	18.8	123	7.70	6.2	110
19.8 (M20)	10.3	20.4	100	3.25	3.2	94

Figures 4.8a to 4.8d show a graphical representation of mean strengths with standard deviation error bars with plain and thread pin batches next to each other. The general trend seen from this presentation is that as the pin size increases the strength decreases. Intuitively, this relationship would seem paradoxical. It is to be noted that the bearing strength is a

function of both pin diameter and material thickness (the projected bearing area being *dt*), and hence the bearing resistance $R_{br,mn}$ in kN (column (3) in Tables 4.1 to 4.4) actually increases with increasing pin diameter.

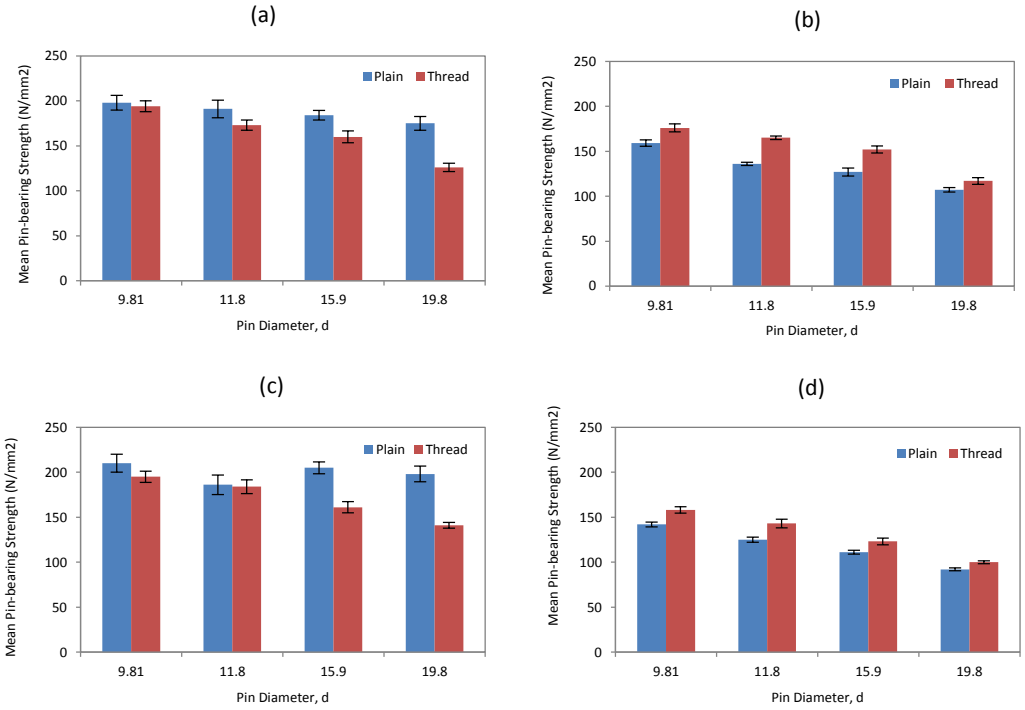

Figure 4.9: Mean Pin-bearing Strengths tested with and without Thread in Bearing for (a) Web 0°, (b) Web 90°, (c) Flange 0° and (d) Flange 90°

The 45° batches (not plotted) give a similar strength variation with plain and threaded pins, with the exception that threaded values are slightly (by ≈ 3.5%) higher than the non-threaded. This can be inferred simply by inspection of the middle rows in Tables 4.1 and 4.2.

The results in Figures 4.8a and 4.8c show that there is a strength reduction with thread for 0^o material. This can be contrasted with threaded values for 90^o material given in Figures 4.8b and 4.8d as they are higher than plain. This implies that, material tested with thread and < 45° orientation will give lower strengths, whereas material tested with thread and > 45° orientation will give higher strengths than when the pin has a smooth cylindrical shaft. A

physical reason for this emerging relationship could be that the failure mechanism with thread in bearing is affected by the material orientation. To confirm this proposal a specific investigation is needed to find out if SuperStructural® material has a critical material orientation at which the threaded mean strength changes from being lower than the plain mean strength to being higher. For both 0^o web and flange materials it can generally be seen from Figures 4.8a and 4.8c that the strength difference between thread and non-thread increases with respect to *d*. Conversely, it is seen from Figures 4.8b and 4.8d that with the 90^o material this strength difference has decreased at the largest pin size.

Shown in Figures 4.9 and 4.10 are typical load-stroke plots, using the same axis scales. On the abscissa of the graphs is the machine stroke, which is indicative of the specimen deformation (although machine and fixture movements that are relatively small are included) and the ordinate is for the compressive load; taken to be positive. This set of graphs is used to show, for the four pin sizes, their typical load-stroke curves. There the same line type is used in the figure parts for a specific bolt size. The stroke is that measured by the DARTEC 9500 testing machine and because of the much higher axial stiffness of test fixtures, steel pin, and testing machine this stroke measurement is dominated by the compressive deformation of the (80 – d_n/2) mm high PFRP specimen; d_n is for the hole diameter including clearance. Figure 4.9 shows the typical load-stroke curves for web material tested for the three material orientations, relative to the pultrusion axis, of 0, 45 and 90° with a plain pin in parts (a), (c) and (e) and a threaded pin in parts (b), (d) and (f), respectively. Similarly, in Figure 4.10 for flange material with parts (a) and (b) showing longitudinal tests with and without thread and parts (c) and (d) transverse tests with and without thread in bearing, respectively. In general, the load-stroke plots show an initial 'bedding in' stage to 0.3 mm or lower stroke, after which there is a nearly linear increase to the maximum load (R_{br}), when bearing failure occurs and there can be a sudden loss in specimen resistance.

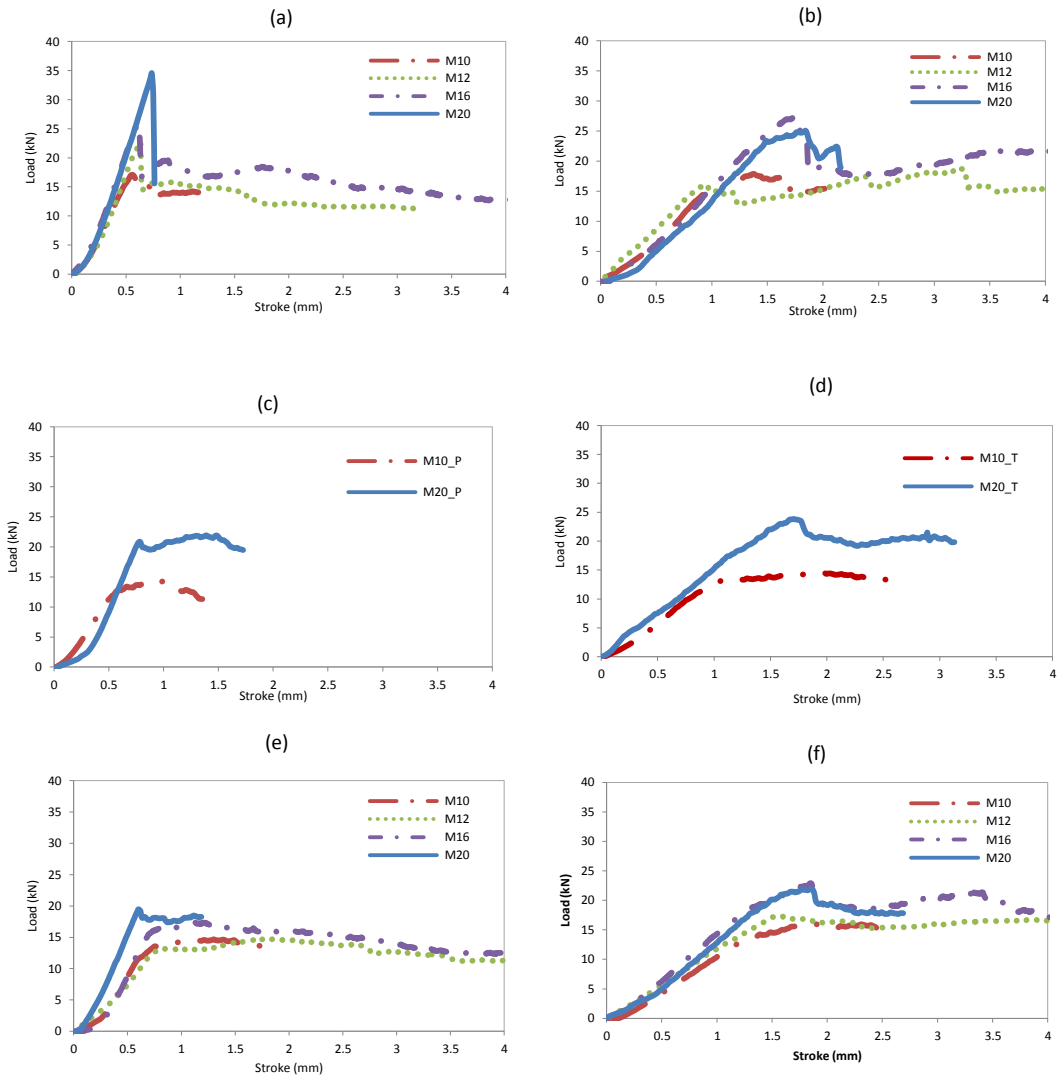

Figure 4.10: Typical Load-Stroke Curves for Web Material tested with a (a) Plain Pin at 0°, (b) Threaded Pin at 0, (c) Plain Pin at 45°, (d) Threaded Pin at 45°, (e) Plain Pin at 90°, (f) Threaded Pin at 90°,

All curves in Figures 4.9 and 4.10 for thread and plain pins, and 45° and 90° materials show a form of 'ductility', whereby the progressive behaviour in the load-stroke response is signified by the maximum load being higher than the first peak. With thread a common feature is for the curve to have a knee point (where a discernible change in stiffness occurs) at approximately 5 kN load. This finding shall be expanded on in the discussion section.

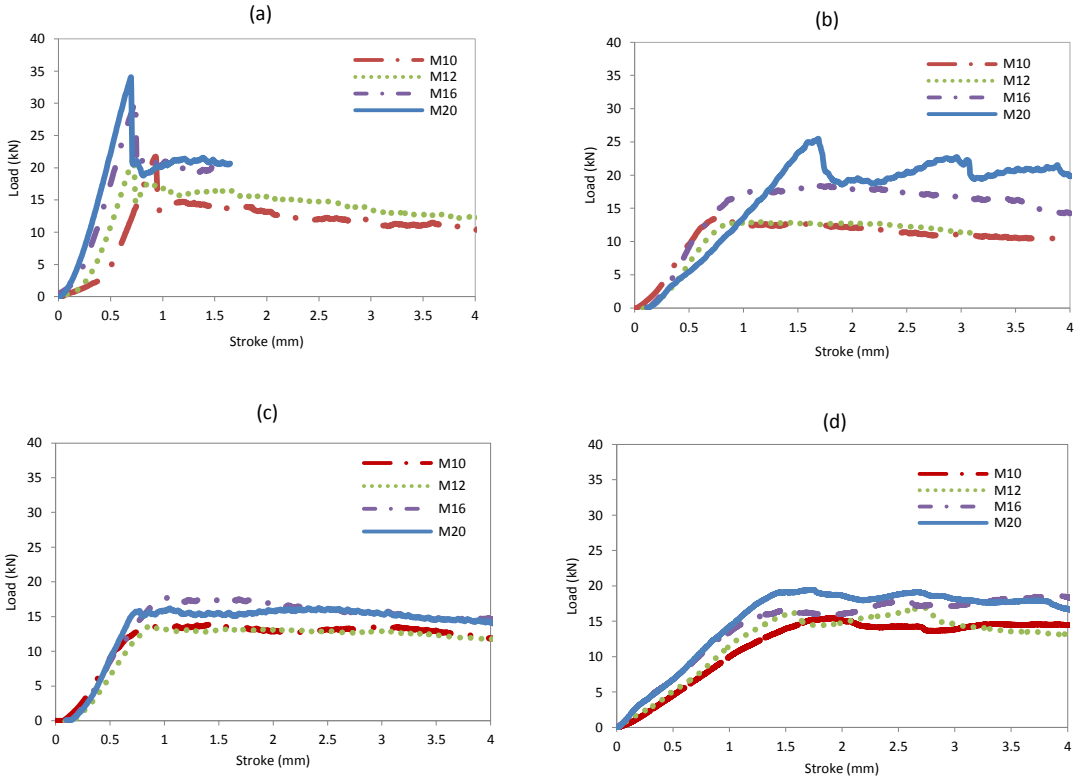

Figure 4.11: Typical Load-Stroke Curves for Flange Material tested with a (a) Plain Pin at 0°, (b) Threaded Pin at 0, (c) Plain Pin at 90° and (d) Threaded Pin at 90°

Presented in Tables 4.5 and 4.6 is a summary for a first failure evaluation of the load-stroke plots for 0^{o} and 90^{o} web material with and without thread in bearing. Columns (1) to (4) are used to enter *d*, *t* (mean), the mean maximum failure load ($R_{br,mn}$) and its Standard Deviation (SD_{mn}). Given in columns (5) and (6) are the mean first failure load ($R_{br,ff}$) and its Standard Deviation (SD_{ff}). The load is defined by either the first peak on the load-stroke curve or the point of deviation from linearity. Column (7) in the table is for the percentage difference given by $((R_{br,mn} - R_{br,ff})\times 100)/ R_{br,mn}$.

It is seen, for web material, that $R_{br,ff}$ is lower than $R_{br,mn}$ by 1 to 16% , accompanied by an increasing SD with increasing *d*. By choosing the $R_{br,ff}$ measure to determine the 'maximum' bearing load the characteristic strength can be forced to be a more conservative value than

reported in Tables 4.1 to 4.4. The full evaluation, including results for the flange material, is given in Appendix C.

Table 4.5: Summary of First Failure Load Analysis for Web Material without thread in Bearing

Pin Diameter, d (mm) (1)	Mean Thickness, t (mm) (2)	Mean Max. Failure Load, $R_{br,mn}$ (kN) (3)	Standard Deviation, SD_{mn} (kN) (4)	Mean First Failure Load $R_{br,ff}$ (kN) (5)	Standard Deviation, SD_{ff} (kN) (6)	Difference between Max. and First Failure Load (%) (7)
Longitudinal (0°)						
9.81 (M10)	9.61	18.7	1.05	17.4	1.88	6.9
11.8 (M12)	9.63	21.7	1.70	20.8	1.79	4.0
15.8 (M16)	9.63	28.1	1.63	27.7	1.24	1.5
19.8 (M20)	9.65	33.5	2.23	33.0	3.66	1.5
Transverse (90°)						
9.81 (M10)	9.62	15.0	0.66	12.6	0.72	16.1
11.8 (M12)	9.64	15.5	0.39	13.2	0.72	15.0
15.8 (M16)	9.63	19.4	1.33	17.0	2.00	12.3
19.8 (M20)	9.64	20.3	0.96	18.9	2.29	8.4

Table 4.6: Summary of First Failure Load Analysis for Web Material with thread in Bearing

Pin Diameter, d (mm) (1)	Mean Thickness, t (mm) (2)	Mean Max. Failure Load, $R_{br,mn}$ (kN) (3)	Standard Deviation, SD_{mn} (kN) (4)	Mean First Failure Load $R_{br,ff}$ (kN) (5)	Standard Deviation, SD_{ff} (kN) (6)	Difference between Max and First Failure Load (%) (7)
Longitudinal (0°)						
9.81 (M10)	9.61	18.3	1.20	16.6	1.74	9.4
11.8 (M12)	9.62	19.6	0.99	18.2	1.61	6.0
15.8 (M16)	9.63	24.3	1.43	22.2	1.37	6.7
19.8 (M20)	9.64	24.1	1.70	23.2	2.18	3.7
Transverse (90°)						
9.81 (M10)	9.61	16.6	0.84	14.9	1.11	10.3
11.8 (M12)	9.63	18.7	0.50	17.3	1.70	7.6
15.8 (M16)	9.63	23.2	1.14	21.3	2.14	8.3
19.8 (M20)	9.63	22.3	1.39	19.9	2.83	10.5

The mean strengths for both web and flange material with plain pins show a decrease of 4% and 12% for the 0^o and 90^o orientations, respectively, between $R_{br,ff}$ and $R_{br,mn}$. This reflects the responses (shown by the load-stroke plots in Figures 4.9 and 4.10) of the 0^o failure being 'brittle', with the first failure and maximum loads being the same. The transverse behaviour as plotted in Figures 4.9e and 4.9f and 4.10c and 4.10d is seen to be more 'ductile' and progressive, and hence there are intermittent 'first peaks' or non-linear deviations in the load-stroke path. It should be noted that during a test there was little signs of Acoustic Emissions (AE), and as noted by Evernden (2006) this would indicate a lack of intermittent fracturing

within the UD roving bundles. A similar comparison for threaded pin sets shows that longitudinal and transverse web (Figures 4.9b and 4.9f) and transverse flange (Figure 4.10d) have an average load difference of 8% between the first failure load and the maximum load. The mean percentage reduction in strength from the first failure pin-bearing strength when compared to the mean maximum pin-bearing strength for 0^{o} flange material was found to be 13%.

4.4.2. Thread Pitch Study

The main pin-bearing test series has considered threaded pins which represent the thread section of a bolt for common sizes of M10 to M20, as found in current practise, and used by PFRP fabricators (in Europe) in designs to reduce the cost of specific bolting to accommodate thickness changes. It was observed that the standard thread pitch is not the same for each of the pin sizes tested and may have an impact on the pin-bearing strength considering the strength reduction was more prominent for the largest pin size, which also had the largest thread pitch. The contribution of the thread pitch to this reduction factor and its effect on pin-bearing strength is unknown. Therefore, a novel study of the effect of thread pitch on the pin-bearing resistance of the SuperStructural® WF section was conducted using flange material only (due to the limited web material available). Testing was conducted in both the longitudinal and transverse directions for all four pin sizes (M10 to M20) with a non-standard thread pitch. It should be noted that the basic thread form for an ISO Metric (M) bolt is similar to the (American) Unified Coarse (UNC) designated bolts which use threads per inch (TPI) instead of thread pitch. The various major dimensions associated with the bolt thread are shown in Figure 4.11.

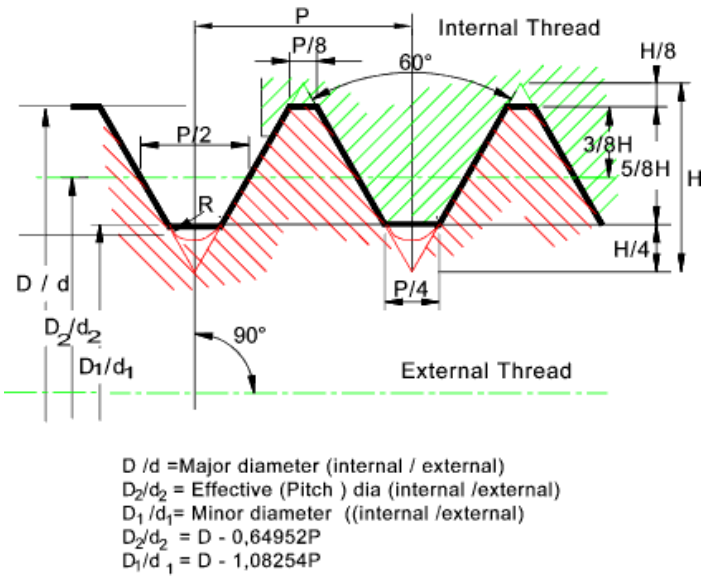

Figure 4.12: Basic Profile for an ISO Metric Course Thread
(http://www.roymech.co.uk/Useful_Tables/Screws/Thread_tol.html)

A total of 120 Specimens were tested with three non-standard pitch sizes for each pin size of M10, M12, M16 and M20. The four thread pitches, *P*, investigated were 1.5, 1.75, 2 and 2.5 mm. The standard size thread pitch (1.5 for M10, 1.75 for M12, 2 for M16 and 2.5 for M20) was not tested again. In order to directly compare the values within the main pin-bearing strength study the nominal clearance between the outer pin diameter and hole remained 1.6 mm, plus the maximum allowable tolerance (in line with the ASCE Pre-standard, 2012). The same specimen preparation, test procedure and methodology as specified in Sections 4.2 and 4.3, respectively, were employed. The non-standard pins were prepared in-house and cut from A4 stainless steel bar using thread cutting apparatus on a metal turning lathe; the accuracy of the thread was checked using a thread pitch gauge. It should be noted that the thread profile on a standard bolt is often formed using a rolled thread process instead of cutting threads; the difference being that the rolled thread can be stiffer than the cut thread method due to material being displaced into shape instead of removed. The same basic thread template as shown in Figure 4.11 was used to give an ISO metric profile.

Table 4.7: Results Summary of Thread Pitch Study with Longitudinal Material

Diameter of Pin, d (mm) (1)	Material Thickness, t, (mm) (2)	Thread Pitch, P (mm) (3)	Mean Max. Failure Load, $R_{br,mn}$ (kN) (4)	Mean Pin-bearing Strength, F_{ϑ}^{br} (N/mm^2) (5)	Standard Deviation, (N/mm^2) (6)	Coefficient of Variation, (%) (7)	Characteristic Value, $F_{k,\vartheta}^{br}$ (N/mm^2) (8)
9.81 (M10)	9.70	1.50	18.7	195	12.5	6.4	174
	9.84	1.75	18.5	189	18.4	9.7	157
	9.54	2.00	17.7	186	5.60	3.0	176
	9.94	2.50	17.9	181	7.26	4.0	168
11.8 (M12)	9.62	1.50	21.2	184	13.7	7.4	160
	9.70	1.75	21.0	184	15.2	8.3	158
	9.71	2.00	20.5	177	8.28	4.7	163
	9.69	2.50	20.2	174	1.93	1.1	171
15.8 (M16)	9.81	1.50	26.3	168	9.47	5.6	152
	9.94	1.75	26.9	169	9.81	5.8	153
	9.78	2.00	24.9	161	12.6	7.8	139
	9.86	2.50	24.1	153	15.2	9.9	127
19.8 (M20)	9.84	1.50	28.6	149	11.5	7.6	129
	9.83	1.75	28.9	147	9.36	6.4	131
	9.80	2.00	28.1	144	6.22	4.3	133
	9.64	2.50	27.0	141	6.21	4.4	130

Presented in Tables 4.7 and 4.8 is a summary of test results for pin-bearing strength tests conducted with non-standard thread pitches for the longitudinal and transverse directions, respectively. Given in columns (1) and (2) are the threaded pin diameter and material thickness, respectively. Column (3) reports the thread pitch, P as shown in Figure 4.11; this correlates to TPI calculated as (P (mm) divided by 25.4 mm (1")) giving 16.9, 14.5, 12.7 and 10.2 for 1.5, 1.75, 2.0 and 2.5 mm thread pitch, correspondingly. Columns (4) to (7) follow the same convention as used in Tables 4.1 and 4.2 with columns (3) to (6). In column (8) of the tables the characteristic strengths for the batches, determined in accordance with Annex D7 of BS EN 1990:2002) are given. This strength value is determined with the assumption that the CoV is known. Based on the procedure for a known CoV and a batch size of five specimens the characteristic value is equal to (mean – 1.8×SD); where k_n is 1.8.

Table 4.8: Results Summary of Thread Pitch Study with Transverse Material

Diameter of Pin, d (mm) (1)	Material Thickness, t, (mm) (2)	Thread Pitch, p (mm) (3)	Mean Max. Failure Load, $R_{br,mn}$ (kN) (4)	Mean Pin-bearing Strength, F_{ϑ}^{br} (N/mm^2) (5)	Standard Deviation, (N/mm^2) (6)	Coefficient of Variation, (%) (7)	Characteristic Value, $F_{k,\vartheta}^{br}$ (N/mm^2) (8)
9.81	9.96	1.50	15.4	158	7.27	4.6	146
	9.85	1.75	15.3	156	6.17	4.0	145
	9.79	2.00	14.2	145	12.5	8.6	123
	9.78	2.50	13.5	141	9.57	6.8	125
11.8	9.67	1.50	15.3	132	5.16	3.9	123
	9.82	1.75	16.5	143	9.35	6.6	126
	9.59	2.00	14.9	130	4.90	3.8	122
	9.58	2.50	14.5	127	5.84	4.6	117
15.8	9.69	1.50	18.9	122	8.99	7.4	107
	9.73	1.75	18.0	116	7.43	6.4	103
	9.65	2.00	18.8	123	7.70	6.2	110
	9.56	2.50	17.3	114	6.98	6.2	102
19.8	9.92	1.50	20.4	105	5.50	5.2	96
	9.83	1.75	18.5	94	4.92	5.2	86
	9.82	2.00	18.6	95	7.36	7.7	83
	10.3	2.50	20.4	100	3.31	3.3	94

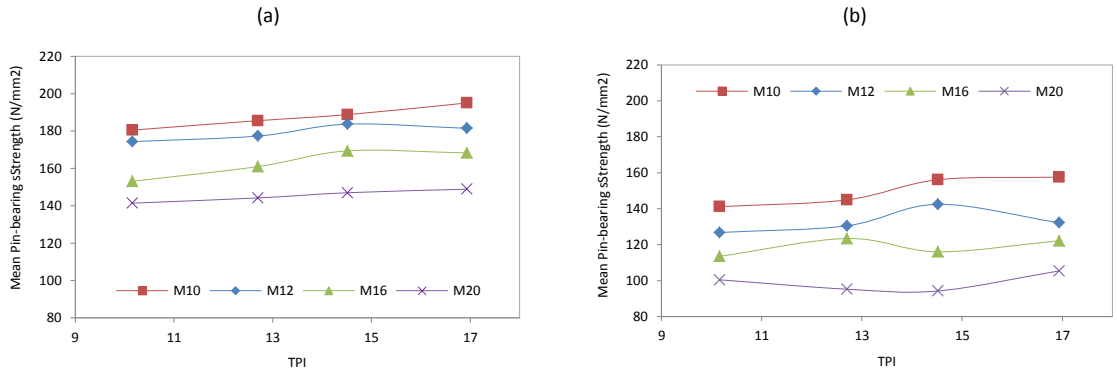

Figure 4.13: Thread Pitch Study Test Results with Mean Pin-bearing Strength plotted against Threads per Inch (TPI) for (a) Longitudinal Material and (b) Transverse Material

Presented in Figure 4.12 are graphs of Threads per Inch (TPI) against the mean threaded pin-bearing strength for longitudinal material in part (a) and transverse material in part (b) for the test results presented in Tables 4.7 and 4.8. The line indicated between points is added only for presentation purposes and doesn't reflect the real trend between values. Clearly, it can be seen from Figure 4.12 that as the TPI increases (or as thread pitch decreases) the pin-bearing strength increases as well, and taking the largest pin size and 0^o material it can be seen that and almost linear trend exists; the trend is less apparent for 90^o orientation. From threaded

pin-bearing values in Tables 4.7 and 4.8 and using the trends in Figure 4.12, it can be calculated that a 1 mm increase in thread pitch results in an average decrease to pin-bearing strength of between 4 to 8%. This suggests the likely contribution the thread pitch has in the reduction factor to pin-bearing strength with thread in bearing is not substantial. Our attention next, shall turn to another factor known to significantly affect the strength value – that is the material orientation.

4.4.3. Material Orientation Study

A PFRP material in a plate-to-plate bolted connection is often orientated at various angles with respect to the pultrusion angle depending on the design of the member or structure. In steel construction this would be of little consequence for the design of connections for bearing due to the isotropic nature of the material. With orthotropic PFRP material this is not the case. As shown in the new test results of this chapter there is a significant change (reduction) in pin-bearing strength due to change in material orientation from 0 to 90°. Although previous studies have given evidence to a trend (Ascione *et al*., 2009 and Zafari and Mottram, 2012a), it is unclear so far for the SuperStructural® material. One question to answer is does the tri-axial mat reinforcement have a different influence on off-axis strength to when there is continuous filament mat in pultruded prismatic sections (Zafari and Mottram 2012b).

Shown in Figure 4.13 is the relationship between the material orientation at 0, 45 and 90° and its effect on pin-bearing strength for web material and all pin sizes. Upon examination of the overall trend it can be seen that a decrease in strength is clearly observed as the orientation increases from 0 to 90°. Previous studies (Zafari and Mottram, 2012b) have eluded that for design values between 0 and 5° the 0^{o} strength value should be used and from 5 to 90° the 90^{o} value is taken to produce a safe design, thereby needing only two strengths characterized.

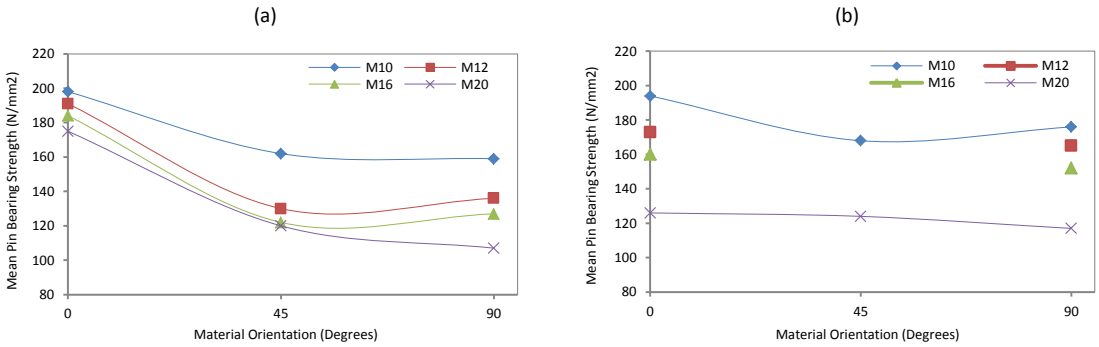

Figure 4.14: Material Orientation plotted against Mean Pin-bearing Strength for Pin Sizes M10 to M20 with a (a) Plain Pin and (b) Thread Pin

An extended study was conducted for the largest and smallest pin sizes of M10 and M20, to determine the behaviour of pin-bearing strength value for the complex fibre architecture web material from the WF sections. The specimens were cut with the material orientation, relative to the pultrusion axis, at 5°, 7.5°, 10°, 12.5°, 15°, 20° and 30° from the 203 x 203 x 9.53 mm SuperStructural® shape.

Table 4.9: Summary of Material Orientation Study with an M10 and M20 size plain Pin

Diameter of Pin, d (mm)	Material Thickness, t, (mm)	Material Orientation, ϑ (degrees)	Mean Max. Failure Load, $R_{br,mn}$ (kN)	Mean Pin-bearing Strength, F_{ϑ}^{br} (N/mm^2)	Standard Deviation, (N/mm^2)	Coefficient of Variation, (%)	Characteristic Value, $F_{k,\vartheta}^{br}$ (N/mm^2)
(1)	(2)	(3)	(4)	(5)	(6)	(7)	(8)
9.81 (M10)	9.61	0	18.7	198	16.3	8.2	170
	9.53	5	17.6	156	6.49	4.2	145
	9.51	7.5	15.1	134	3.14	2.3	128
	9.52	10	15.2	135	7.88	5.8	121
	9.54	12.5	14.8	131	3.80	2.9	124
	9.52	15	14.2	126	6.89	5.5	114
	9.51	20	14.3	127	6.86	5.4	115
	9.51	30	14.7	130	2.21	1.7	127
	9.63	45	15.3	162	4.94	3.0	154
	9.62	90	15.0	159	7.09	4.5	146
19.8 (M20)	9.65	0	33.5	176	15.5	8.8	149
	9.52	5	30.9	164	22.3	14	124
	9.52	7.5	27.8	148	12.2	8.3	126
	9.51	10	25.5	136	9.29	6.8	119
	9.51	12.5	25.5	136	26.4	19	88
	9.53	15	27.1	144	11.2	7.7	124
	9.52	20	24.6	131	9.27	7.1	114
	9.52	30	23.5	125	4.47	3.6	117
	9.66	45	22.9	120	4.85	4.0	112
	9.64	90	20.3	106	5.01	4.7	98

A summary of the test results is given in Table 4.9 using the standard column headers; the 0, 45 and 90° values from Table 4.1 are included to produce the full set of data.

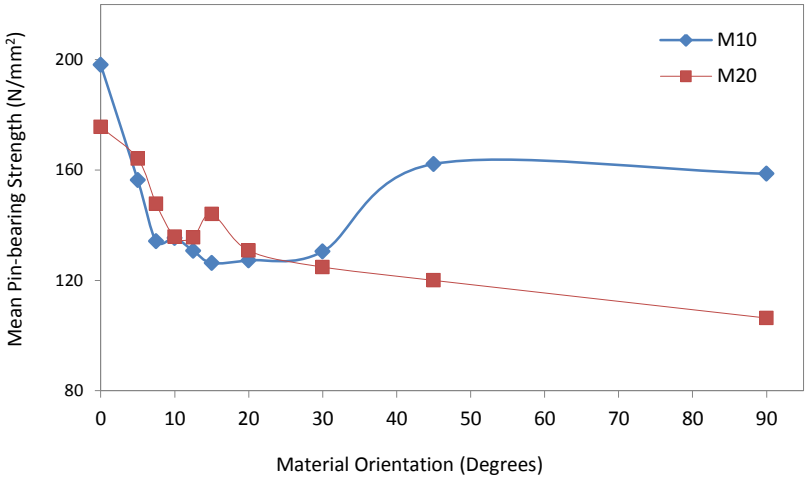

Figure 4.15: Material Orientation plotted against Mean Pin-bearing Strength for an M10 and M20 size Plain Pin

Plotted in Figure 4.14 is the mean pin-bearing strength for an M10 (blue diamond symbols and blue solid line) and M20 (red square symbols and red solid line) size pin for material orientations, with respect to the pultrusion axis, between 0^{o} and 90°. The curved lines are added indicatively and are for presentation only. The initial part of each curve between 0^{o} and 10° there is a sharp strength drop as the orientation angle increases, after which a slight kink (shown by an increase in strength) occurs. The pattern for pin-bearing strength for the two pin sizes is considerably different with orientations from 20 to 90°. A key observation is the lowest value for pin-bearing strength for the M10 size pin is not 90°, it is at 15°. Secondly, although the characteristic 'kink' has been observed in a previous test series by Zafari and Mottram (2012b) it was not as pronounced as can be seen in Figure 4.14.

4.5. Discussion of Non-aged Pin-bearing Strength Test Results

Our discussion shall focus on several key parameters for the determination of pin-bearing strength, namely the: effect of pin size; material orientation; material type; thread. In the course of this research programme it was decided to conduct several complimentary studies, which (looked to) widen our knowledge and understanding of the influence of a particular parameter. These studies involved varying the parameters of thread pitch and of orientation. Firstly, the discussion will deal with the effect of pin diameter, *d* and PFRP material architecture.

The effect of pin size has been discussed to some extent within Section 4.4 and shall be expanded on in what follows next. It is noted that for all test sets (material orientation and pin type), the generic trend of an increase in *d* results in a decrease in pin-bearing strength. Presented in Figures 4.15a to 4.15d are the characteristic strengths against *d*/*t* ratio. In these figure parts the symbols of blue diamond, red square and green triangle are for values taken from Tables 4.1 to 4.4 for the material orientations of 0^{o}, 45^{o} and 90^{o}. In parts (b) and (d) it can be seen that when there is thread in bearing the relationship between the strength and *d*/*t* is virtually linear for all orientations.

Using mean values from Table 4.1 for the M20 plain pin and web material the largest F_0^{br} / F_{90}^{br} is 1.52. This can be seen to be higher and different to the mean of 1.23 (from four batches) from a previous WUTS test series by Mottram and Zafari (2011) with web material cut from a standard wide flange shape, also from CP. The change can be attributed to the differences in the fibre architecture between the two PFRP shapes. It is of interest to note that F_0^{br} / F_{90}^{br} for flange material and M20 plain pin is slightly higher at 2.15; the fibre architecture gives this SuperStructural® material significantly higher strength and stiffness in the direction of

pultrusion. It is therefore, significantly more orthotropic than the web material, which contains four layers of tri-axial mat reinforcement. A means of quantifying the difference in strength with orientation might be to use the Hankinson formula (Hankinson, 1921) that is commonly used with structural timber. Zafari (2012) has shown that the curve created by the Hankinson formula that requires only 0^{o} and 90^{o} strengths does not correspond to the variation of pin-bearing strength with orientation.

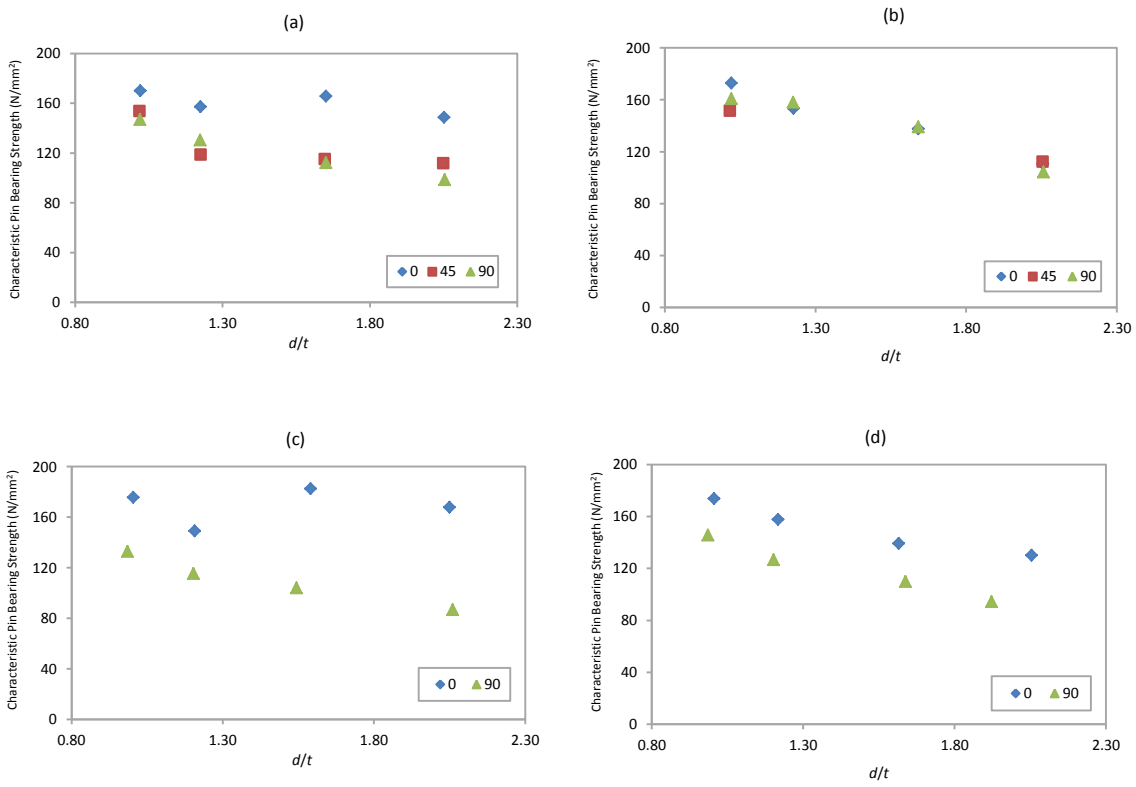

Figure 4.16: Characteristic Pin-bearing Strength and *d*/*t* ratio for (a) Web Material with a Plain Pin (b) Web Material with a Threaded Pin (c) Flange Material with a Plain Pin and (d) Flange Material with a Threaded Pin

From the study relating to the effect of orientation it was found that the web material has a distinct effect upon the pin-bearing strength. Presented in Figure 4.16 are normalised pin-bearing strengths plotted for the material orientation between 0^{o} to 90° with data taken from Ascione, *et al* (2009) and Zafari (2012). Previous studies by Collings (1977) and Cooper and Turvey (1995) have noted that in composite materials with low levels of ± 45° reinforcement

fibres a shear type failure governs a bolted connection. It is known that as the amount of ± 45° fibre reinforcement increases, the shear strength increases until bearing becomes the critical mode of failure. Considering, in the longitudinal direction, the ± 45° reinforcement fibres within the complex tri-axial mat are orientated to resist the bearing force, it is unsurprising that as the material is rotated from 0 to 90° a decrease in strength occurs. This adverse effect on bearing strength is most prominent in Figure 4.16 with the largest reduction of 46% in bearing strength for the M20 size pin (results from Table 4.9), shown by the solid square symbols. The effect of material orientation is seen to be far greater for the web material studied by the author than those of previous research. Note that the FRP material tested by Ascione was not pultruded; it does have similar orthotropic elastic constants. The task of curve fitting is seen to be equally different between the different data sets.

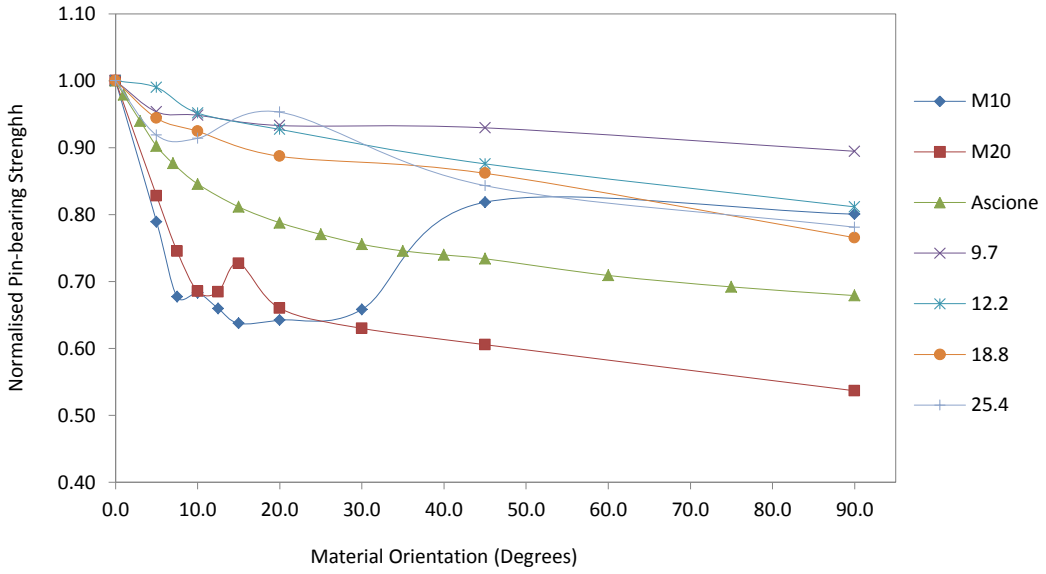

Figure 4.17: Material Orientation plotted against the Normalised Pin-bearing Strength with Data from Ascione et al (2009) and Zafari, PhD thesis (2012)

The key implication on determining the design values from only the 0^{o} and 90^{o} values, as is proposed in the LRFD Pre-standard (ASCE, 2012), is that the lowest strength may not be in the 90^{o} direction. For the type of web material in WF SuperStructural® sections having a complex

mat reinforcement, it seems advisable to measure strength at orientations of 15 to 30°. The additional reduction in this range is up to 20 % of mean F_{90}^{br} and 35 % for characteristic F_{90}^{br}.

Moving on from assessing the influence of orientation, the one apparent irregularity within the data set that doesn't follow the linear trend in Figure 4.15c is the 0^{o} characteristic for M12 plain pin and flange material. This strength at 149 N/mm^2 is seen to be approximately 10% lower than what would be expected had the characteristic value followed a linear relationship with d/t. This unexpected finding was initially investigated by conducting five more nominally identical tests to consider if the relative sample size had any effect on values of predicted mean and characteristic. As has already been mentioned, a contribution from Zureick *et al.* (2006) lead to the recommendation of a minimum of 10 specimens per batch, as this is the minimum batch size required to use ASTM D7290 to determine characteristic values on assuming a Weibull distribution. For an introduction to, and application of, ASTM D7290 there is the MSc thesis by D'Alessandro (2009). Table 4.7 is used to report the means for failure load ($R_{br,mn}$) and pin-bearing strength in columns (2) and (3). Column (1) shows that the table is for three batches having 5, 10 and 15 specimens. Using the method in Eurocode 0 Annex D (British Standards Institute, 2002) the SD and CoV are computed for batches consisting of the five new specimens (first row) and the maximum of 15 specimens (third row). The characteristic value for the five specimen batch is given by (mean - 1.8×SD); k_n is 1.8, and, similarly, for the 15 specimen batch it is calculated from (mean - 1.7×SD).

The results reported in Table 4.7 clearly show that there is, at ≈ 2 to 4 %, no significant difference between the characteristic strength with 5, 10 or 15 specimen batches. Although the mean failure load is slightly lower for the largest batch size, SD remains above 11%. One possible influence for why there is the low failure load with the M12 pin could be the existence of a relationship between the UD fibre roving bundle geometry and the pin size. In the

longitudinal direction it is the UD fibres that govern strength. It can be speculated that if the true bearing area (which is not the projected area *dt*) just happens to coincide with the bundle spacing geometry, premature failure might occur by delamination failure initiating at the fibre bundle roving intervals across the width direction. This proposition has yet to be confirmed and would need to be the subject of a new study on failure mechanisms under bearing action.

Table 4.10: Summary of further Plain Pin-bearing Tests to Varying Batch Size with Longitudinal Flange Material

Batch Size (1)	Mean Failure Load (kN) (2)	Mean Pin-bearing Strength (N/mm^2) (3)	SD (N/mm^2) (4)	CoV (%) (5)	Characteristic strength (N/mm^2) (6)
5 Specimens	19.8	180	14.7	8.7	143
10 Specimens	21.5	186	21.5	11.6	149
15 Specimens	20.9	169	20.7	11.5	146

Let us now consider the bearing area. It is of interest that the mean bearing strength is, always, calculated from the projected area. The actual (unknown) bearing area is smaller, and it is convenience that allows us to deal with the (known) projected area in design, via Eq. (2.1). A measure of the actual area was conducted for the largest pin size (M20) and web material at 0°, 45° and 90° orientations. The method was to use a vernier calliper to measure the width of the pin-imprint (< *d*) left on the bearing surface. It was found that the measured mean average widths, for batches of 10 specimens are 13.8 mm (70%), 17.5 mm (88%) and 17.6 mm (89%), respectively. The bracketed values are for the percentage of *d* (= 19.8 mm). If the measured '*d*' was used instead of the pin *d* the mean strengths for the 0°, 45° and 90° web material would increase by 30%, 13% and 12%, respectively.

It should be noted that this is not a precise method to determine the true bearing area, given that it, for example, neglects any out-of-plane deformation caused in the bearing pressure and the Poisson's ratio effect. Furthermore, the stress field through-the-thickness is not uniform and will increase at the material edges should pin flexure occur, as will be exist in real bolted

connections. Clearly, this indicates that the actual bearing stress causing failure is somewhat higher for the off-axis values and particularly higher than the design strength (F_0^{br}) used in design of a bolted connection.

Considering that the pin-bearing strength measured in this investigation is the compressive force exerted upon a semi-circular notched specimen with a stainless steel pin, it is not unreasonable that a comparison be drawn between the material's compressive strength and the pin-bearing measure. This would aid an understanding of the quantitative difference between pin-bearing stress over the 'actual' area (as measured using the vernier callipers) and characteristic compression strength, as given in Chapter 3. Furthermore, there is anecdotal evidence that practitioners choose the compression strength when the former is available to them and the bearing strength (whatever measure) is not. Strongwell (2013) have an admissible stress factor of 3 for this design approach.

The measured characteristic 0° compression strengths for the web and flange material in Table 13 of Chapter 3 are 270 (258) and 309 (316) N/mm^2, respectively. For comparison the bracketed values are taken form a table in the Design Manual (Creative Pultrusions, 2010). The author's compression strengths offer design bearing strengths of 90 and 105 N/mm^2. Comparing these 0^o values with the lowest equivalent strengths in Tables 4.1 and 4.3 of 148 and 168 N/mm^2 for the M20 sized pin, it is found that there is a significant difference of ≈40%. The difference will be higher still if these values are adjusted (increased) to account for the measured bearing area. It can be observed from this evaluation that the design approach using the compression strength is not unreliable and gives design bearing strengths on the low side.

Although the projected area, given by *dt*, is an acceptable deviation from the actual bearing area, it is important to understand that changing *d* makes a significant difference to the pin-

bearing strength. Pultruders providing material strengths currently do so in the form of tables within in-house design manuals, and in America these maximum bearing strengths are determined by the ASTM D953 test method. This standard stipulated a single pin size of 6.35 mm (1/4 inch) with no clearance hole. These parameters will give a d/t ratio of 0.67 for a 9.53 mm nominal material thickness. Such a relatively low d/t ratio is a reason why the author's WUTS characterization is giving lower values (Tables 4.1 to 4.4) than does CP. Given that increasing d/t always lowers a pin-bearing strength it is concluded that the most severe parameters to be found on-site must be used when specifying what F_{ϑ}^{br} is in Eq. (2.1).

Before the discussion focuses on thread in bearing, a brief exploration to the contribution of reinforcement shall be given. In this study there are two fibre architectures, with the web having three UD reinforcement layers and four tri-axial mat layers and the flange material having two UD layers and three of the mat layers. Note that the thicknesses of the UD layers are not necessarily constant. Differences in architecture are reflected within the strength differences for the two materials, with the web having higher characteristic strength in the transverse direction and the flange giving higher strength at 0^{o}. It is observed that CP has used a thicker UD layer within the flange material on the top most side relative to the mid-surface; to increase the flexural rigidity of the section under flexure. This asymmetrical layering for the flange panel may be having a significant influence on the scatter in pin-bearing strength results. In particular, the through-thickness stress field could be more localised and more non-uniform across the thickness than would be situation with the common symmetrical lay-up found in pultrudates.

4.5.1. The Effect of Thread in Bearing

The main objective has been to characterise the laterally unrestrained bearing strength with and without thread to find out whether or not a reduction factor is required to obtain the threaded characteristic strength from the equivalent pin-bearing value. Presented in Table 4.8 are the normalised mean and characteristic strength reduction factors between plain and threaded pin-bearing strengths for all sets of data tested in the main study of Section 4.4. Column (1) gives the pin size and columns (2) and (3) are for the web material and columns (3) and (4) are for the flange material. Using the results reported in both Tables 4.1 and 4.2 and row 4 in column (3) of Table 4.8 says that there is a 26% reduction for 0^{o} web and M20 bolting. The second highest reduction of 24% is given in column (5) row 3 with two changes being it is for flange material and M16 pin size. In an independent series of tests by Troutman and Mostoller (2010) the mean reduction reported was 30%. Note that their test method is different and was in the spirit of following the clauses in ASTM D953.

Troutman and Mostoller (2010) conducted pin-bearing tests for longitudinal material only, as outlined in Chapter 2, and showed that the largest reduction in bearing strength due to thread in bearing as 37%. The study used UNC bolts of size 0.5” (12.7 mm) and 0.625” (15.9 mm) which have TPI values of 13 and 11, respectively. The largest reduction was found for a laterally unrestrained 12.7 mm pin with a 6.35 mm thick polyester resin matrix pultrusion (the fibre architecture is unknown). The relative d/t ratios for the two pin sizes are 2.0 and 2.5, respectively. It is interesting that the (smaller) 12.7 mm threaded pin with a higher TPI (and smaller pitch) gave a larger reduction in pin-bearing strength. Figure 4.12 gives a clear indication that with 0° SuperStructural® flange an increase in TPI corresponds to a higher bearing strength. A plain pin could be thought of as a threaded pin with an infinitely high TPI value. It should be noted that Troutman and Mostoller found for the thicker material of 12.7

mm that the largest reduction of 34% was found with a 15.9 mm diameter pin. For the smaller pin diameter the reduction was 28%. This suggests that the *d*/*t* ratio for a threaded pin plays a significant role in the level of reduction from the plain pin value.

Table 4.11: Thread Reduction for Mean and Characteristic Values of Web and Flange Material

	Web		Flange	
Pin Size (mm)	Reduction in Mean Bearing Strength (%)	Reduction in Characteristic Strength Value (%)	Reduction in Mean Bearing Strength (%)	Reduction in Characteristic Strength Value (%)
1	2	3	4	5
Longitudinal (0°)				
9.81 (M10)	0.98	1.02	0.93	0.99
11.8 (M12)	0.91	0.98	0.99	1.06
15.8 (M16)	0.87	0.83	0.79	0.76
19.8 (M20)	0.72	0.74	0.71	0.78
45°				
9.81	1.04	0.99	-	-
19.8	1.03	1.00	-	-
Transverse (90°)				
9.81	1.11	1.09	1.11	1.10
11.8	1.21	1.21	1.14	1.10
15.8	1.20	1.24	1.11	1.06
19.8	1.09	1.06	1.09	1.09

On comparing the test results presented in Tables 4.1 to 4.4 it is found that thread gives higher than plain for mean and characteristic strengths with the 45° material, and significantly higher for flange and web at the 90° orientation. This is contradictory to the previously held viewpoint that having thread in bearing would only adversely lower a pin-bearing strength. This can be seen as one reason why it has been advocated by Zafari (2012) not to be allowed in practice. Although, threaded strength is higher in the 90^{o} direction, it should be noted that the maximum load was specified by satisfying the failure criterion used to determine the strength from Equ. (2.1). In particular, at 90^{o} there can be significant damage as progressive failure has developed with the maximum load existing at a significantly greater stroke than at first failure load. This suggests that the criterion for selecting the failure load with thread should not be the maximum load. This opposed the recommendation by Mottram and Zafari (2011) that the maximum load is the only practical load to choose when determining a bearing strength for a

PFRP material. It is important to recognize that this 2011 recommendation was made of the assumption that the bolt shaft is always plain.

If the maximum load is not the appropriate failure load criterion when there is thread there's a need to establish what load should be used. This knowledge would be useful in us understanding the difference in the failure mechanism with and without thread. Shown in Figures 4.17a and 4.17b are bisected specimens, after being tested, without and with thread in the bearing area. A failed specimen was sectioned using a Metaserv cut-off machine equipped with a circular diamond coated blade and soluble cutting fluid. The blade was off-set to the centreline to enable the centreline section to be photographed for observation of internal damage, as seen in the figures.

In Figure 4.17, a red dashed line is introduced where the failure cracks exist. It is noted that both images are after the maximum load and a considerably stroke in the threaded situation. In part (a) the failure mode resembles the laterally unrestrained type situation shown by Wang *et al* (1996) using a carbon fibre reinforced epoxy resin material with various fibre layups and a dowel bearing type test set-up similar to the WUTS. The damage pattern features distinctive through-thickness shear cracks and delamination between the UD and mat intersections. The cracks in Figure 4.17a are formed from the accumulative damage within the PFRP layers and the 'double v' shape have each are aligned at approximately 45^{o} to the direction of resultant compressive force. The location at which the pair of cracks reaches the free surface is approximately at half the thickness (i.e. $t/2$). Between the cracks and the free surface is an area of local fibre buckling. This type of failure was found for many of the specimens tested with plain pins.

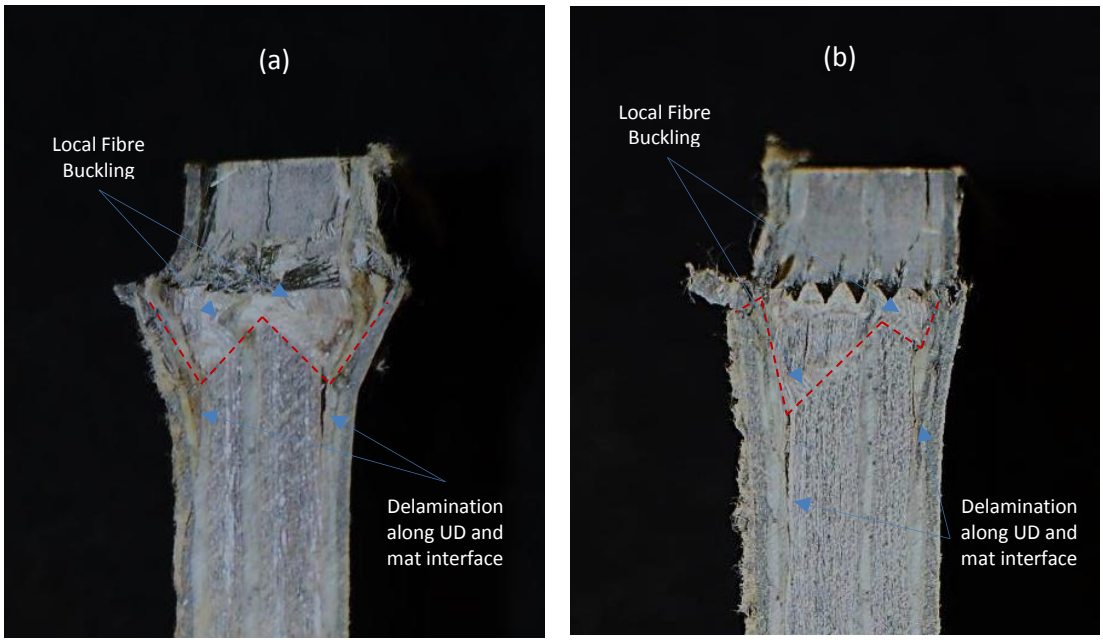

Figure 4.18: Bisected Pin-bearing Flange 0° Specimens for an M12 (a) Plain Pin and (b) Threaded Pin

Although part (b) resembles a similar overall failure as in part (a) the pattern of the shear cracks is altogether different. The same local buckling as in part (a) occurs now at the pin-material interface and further into the specimen's depth. It seems that cracking originates at the free surface at the root of the embedded imprint of the thread. A possible explanation for the difference is that to overcome the through-thickness tension strength there is an additional resistance when thread is present. The localized bearing deformation is now seen to inhibit, to a certain extent, the form of deformation and creation of the shear type cracks exhibited in part (a). This may be a contribution factor to the observed 'increase' in strength from the plain pin with 90° material. Clearly, to investigate the specific causes of failure due to thread in bearing and aid this preliminary discussion a study of the through-thickness tension strength is required in future work. Considering the difference in failure and the level of damage with and without thread in bearing, the most appropriate failure criterion is not the maximum load. An alternative would be, in the opinion of the author, the first peak failure load as it is a common feature in the load-stroke curve, and is thought to correspond to the initiation of local fibre buckling as found observed in both plain and threaded failed specimens.

The propagation of the failure from the tip of the thread (and the root of the threaded indent), as shown in Figure 4.17b, is certainly a point from which the various first peak failures occur as seen in the load-stroke curves in parts of Figures 4.9 and 4.10. Another prominent feature for thread in bearing is a kink or knee on almost all load stroke graphs in Figures 4.9 parts (b), (d) and (f) and 4.10 parts (b) and (d), which this is thought to be the point at which there is full embedment of the thread profiles. The Barcol hardness as determined by CP by ASTM D2483 uses a conical indenter with a flat end of 0.156 mm diameter and faces angled at 26°. The material is indented using a uniform force on a level flat surface and a reading taken from a scale of 0 to 100, with each denomination equating to 0.0076 mm. The material used in this study has a Barcol hardness of 33 (Creative Pultrusions, 2010). This would indicate an embedment of approximately 0.251 mm. From inspection of the load-stroke plots for threaded pins, it is observed that the kink occurs at approximately this stroke and so the analysis gives a satisfactory explanation for the point in testing at which full thread embedment occurs.

The discussion so far has highlighted that thread within the bearing area can have a significant effect on the pin-bearing strength, load-stroke behaviour and failure mechanisms for both the web and flange material characterized. Next, a short digression into the effect of thread in aggressive environments is given before the end of chapter summary. Regardless of the form of the thread in bearing, it is to be recognised that should a bolted connection, in a frame structure, be exposed to an aggressive environment, over its service life, the presence of thread embedment from working connection forces is probably going to impair the bolted connection strength over the long-term. This represents another reason why it could be counterproductive in practice to plan for design working lives of, say, 50 years with threads in bearing. However, without empirical evidence this durability issue has not been resolved, and hence the application of threaded bolting in the bearing thickness when the environment is hostile is explored in Chapter 5.

4.6. Summary

This chapter has presented an extensive investigation into the pin-bearing strength measure for use in the design of PFRP bolted connections. The in-house test method (WUTS) is shown to be very suitable for the determination of pin-bearing strengths for both flange and web materials sourced from pultruded structural shapes. In particular, use of testing with and without thread in bearing and for various material orientations with respect to the direction of pultrusion is applicable with this set-up. Manufacturers and researchers are encouraged to adopt a similar loading device and specimen geometry for the determination of pin-bearing strengths to accommodate the relevant material orientations, thicknesses, pin and clearance-hole diameters. Given that the current analysis methods cannot be relied upon to predict bearing failure (Department of Defence, USA, 2002) the design method should include statistically verified bearing strengths obtained from reliable test results, such as presented in this chapter.

The most influential parameter found in this study is the effect of material orientation with respect to the pultrusion direction. It has been found that the longitudinal and transverse pin-bearing strengths differ considerably for a web and flange material, and, in particular, when determined with the largest pin size of M20. A key observation from the new results is that the pin-bearing strength at material orientations between 10^{o} to 30° may be lower than at 45° and 90^{o}, by almost 35%. The web and flange materials have significantly different mechanical properties in the two principal directions due to the fibre architecture, and this in turn influences how pin-bearing strength varies with orientation of material to bearing force.

Mottram and Zafari (2011) showed that the influence of d/t is prominent and this investigation with different PFRP materials confirms the finding. The adverse effect of this ratio on strength

is found to hold true for tests with and without thread in bearing, with an almost linear relationship for the latter condition. The largest differences between the largest and smallest pin sizes were found for threaded pins and 90^{o} material. A difference of 35% was found between the smallest, M10, and largest, M20, sized pins for threaded bearing strengths in the transverse direction for both web and flange. The smallest variation, at 6% was found for longitudinal material with a plain pin. A contribution to the difference between web and flange material is the tri-axial mat reinforcement, which has a higher volume fraction in the web material.

The main investigation has looked to characterise the pin-bearing strength measure with and without thread. It has been found that when thread is present a reduction of 0.7 can be applied to the characteristic pin-bearing strength (for SuperStructural material) for purpose of using Eq. (2.1) to establish per bolt the bearing failure resistance force. This affirms the current mandatory design guidance in the PFRP LRFD Pre-standard. However, there is reason to believe from this study that for the threaded situation the criterion for selecting the failure load should not be the maximum load. This opposed the recommendation by Mottram and Zafari (2011), when thread is being excluded, that this is the only practical method when determining a bearing strength for a PFRP material.

CHAPTER 5

Effect of Environmental Conditioning on Pin-Bearing Strength

5.1. Introduction

The design of bolted connections of FRP is critical in ensuring sound structural performance and involves a fundamental understanding of failure modes. Due to the orthotropic and layered nature of PFRP these failure modes can vary significantly (Mottram and Turvey, 2003). As developed in this thesis, damage and mode of failure are dependent on connection detailing, material and fastener specifications, such as geometry, fibre volume fraction, and bolt tightening, etc. In addition, it is recognized with FRP materials that material-based resistances can be lowered by exposure to aggressive environments, which influence the material and its structural properties (Karbhari, 2007). Presented in this chapter are test results of a study pertaining to the reduction in pin-bearing strength due to the effect of hot-wet conditioning on specimens cut from the 254 x 254 x 9.53 mm SuperStructural shape, as detailed in Chapter 3.

Environmental degradation involves influences from temperature, UV radiation, water or moisture. As explained in the chapters of the book edited by Karbhari (2007) material changes affect the ability of any FRP to maintain its short-term mechanical properties over time. Any durability issue is a concern to structural engineers as design lives in civil engineering works are measured in decades, say 30, 50 or 100 years. It is essential for confidence in durability performance that there is characterisation work with PFRPs' to understand the material's long-term performance (strength and stiffness) under adverse environmental conditions. It can be expected that years of (continuous) exposure in an aggressive environment in the field will cause irreversible and detrimental changes within the FRP material. Irreversible changes can be within the polymer matrix, to the interface between fibre and matrix and on the surface of the glass fibres themselves. The various mechanisms causing the deterioration are known to be complex and FRP material specific (Karbhari, 2007).

Previous environmental conditioning studies that are summarized in the literature review in Chapter 2 have highlighted the importance of both moisture and temperature exposure on the mechanical properties of PFRP, and other FRP materials. The severity of these two factors will depend on geographical location and climatic (changing) conditions, and needs to be taken into account during the structural design process if there is going to be quantifiable reliability in the performance of PFRP structures. Failure, insofar as the material, or component, or sub-assembly with connections (Mosallam, 2011), or structures is no longer fit-for-purpose, could occur due to cumulative damage to the polymer matrix, interfacial bond degradation, and chemical/stress attack to the glass reinforcing fibres. Indeed, the overall environmental degradation occurs as a complex combination of two or more of these processes (Karbhari, 2007), with the net effect resulting in loss of mechanical integrity.

Undoubtedly, the key to wider exploitation of PFRP materials in Civil Engineering is knowledge of long-term performance, which will in turn allow both safe and economical design. In the absence of long-term pin-bearing strength data from field studies (and there are none on-going) to assess durability and structural performance of bolted connections (Bank *et al*., 1998), alternative methods must be employed, namely by accelerated aging. Maxwell (2005) of the National Physical Laboratory, showed that accelerated (or artificial) aging has been used for many years in the UK by the materials engineering community as a means of predicting long-term behaviour of polymeric composites. By this test approach establishing the thermo-chemical properties of an FRP it allows estimation of the lifetime degradation, due to a process transformation, to be calculated using temperature driven relationships, such as the Arrhenius principles (Karbhari, 2007 and Bank *et al*, 2003).

Presented in this chapter are test results of a study pertaining to the reduction in pin-bearing strength due to the effect of hot-wet conditioning on specimens cut from a polyester matrix based pultruded FRP structural shape. A total of 280 coupons (for 56 batches of five) were immersed in distilled water for three and six months at a constant temperature of 30, 40, 50°C for both flange and web material. After conditioning the specimens were load tested using stainless steel 'pins' of M10, M12, M16 or M20 sizes with material orientations of 0^{o}, 45^{o} and 90^{o} to the direction of pultrusion. Not all combinations of temperatures and material type, pin type and material orientations were used. Only flange material was used for 30 and 50°C hot-wet conditioning (refer to Section 5.2 for specific batch conditions and testing variables). The test series considered the effect of loading with and without bolt thread in the bearing zone. Testing employed the non-standard WUTS. An evaluation of the salient results provides characteristic bearing strength values (in accordance with Annex D of EN1990) and comparisons are drawn between equivalent strengths for non-aged (zero months) material from the test series presented in Chapter 4. The degree of strength reduction is found to be

influenced by both the 'pin' size and type, and observations are drawn towards the safe and reliable design of bolted connections.

The discussion in this chapter will establish a viable indication of the level of pin-bearing strength retention exhibited by PFRP materials having been exposed to commonly found aggressive environments such as high temperature and moisture. The moisture sorption test results reported in Chapter 3 have been used to establish the specific diffusion coefficients for each temperature and material. These coefficients in turn can be used in empirical formulae to determine the activation energy for use in long-term performance analysis. This will allow an evaluation to be made for the justification of having a reduction (knock-down) factor to the short-term pin-bearing strength to account for on-site aging, as specified in the ASCE LRFD design standard for PFRP standard shapes (ASCE, 2012).

5.2. Environmental Conditioning of Specimens

Specimens were prepared using the same cutting and drilling procedures as outlined in Section 4.2 for the non-aged pin-bearing strength characterisation work. The clearance hole diameter, d_n, were measured using an inside micrometer screw gauge for each hole prior to final cutting. The largest variation is an under-sizing of the clearance hole by a maximum value of 0.02 mm. The thickness of each specimen was measured using an outside micrometer screw gauge to the nearest 0.01 mm with average thicknesses being reported in Tables 5.1 and 5.2. The web material thickness ranged from 9.58 to 9.84 mm, and the flange between 9.57 mm and 10.4 mm. The breakdown of each specimen measurement is given in Appendix B. A similar labelling convention was used as previously, with the addition of an 'A' (for aged) before the identification string.

5.2.1. Hot-wet Conditioning of Pin-bearing Specimens

Environmental conditioning of the specimens was conducted by full-immersion in heated Grant SUB36 baths containing distilled water, as shown in Figure 5.1, at temperatures of 30, 40 and 50°C for periods of three (2160 hours) and six months (4320 hours). The specimens were separated by standing them upright in specifically designed stainless steel racks that allowed all surfaces of the specimen to be conditioned and in contact with the heated distilled water. The full surface of the semi-circular notch was in contact with the heated water for the full duration of the immersion. In the opinion of the author this represents a relative worst case scenario with regards to what an unloaded/unstressed bolted connection could experience under field conditions. Although, the worst case would include a specimen under load as well as hot-wet conditioning cycles, the method chosen will drive moisture diffusion and lead to more advanced degradation mechanisms.

In accelerated aging studies reported in Karbhari (2007) it has been noted that conditioning of FRP at temperatures close to the glass transition temperature (T_g) can cause detrimental effects that are not representative of aging at service temperatures. This is due to different levels of mechanical and chemical degradation that does not happen at lower temperatures (Bank *et al*, 2003). The immersion temperatures used within this study were at least 50^{o}C below the T_g for the SuperStructural materials. It has been established on a number of occasions by others (Karbhari and Zhang, 2003 and Bank *et al.*, 2003) that distilled water can offer a more aggressive environment than tap or salt water. This is because of the ability of the free radicals (from the composite resin matrix) reacting and diluting readily in the distilled water as opposed to other solutions.

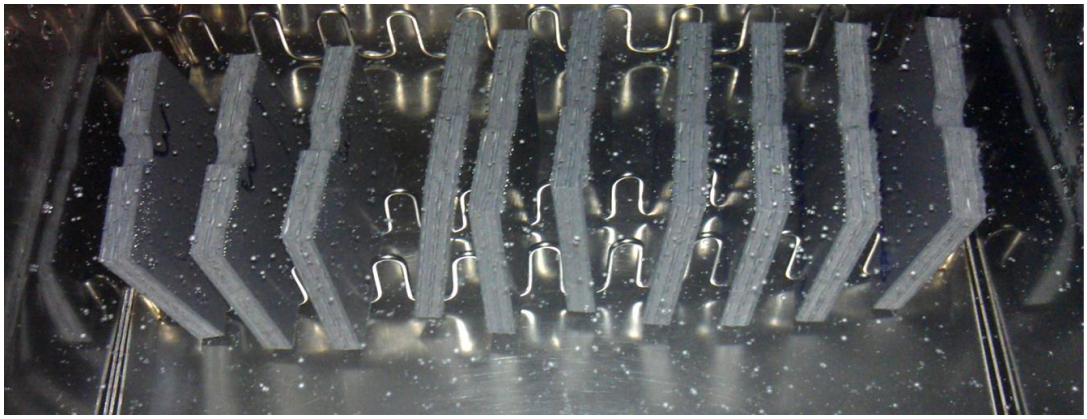

Figure 5.1: PFRP Test Specimens immersed in Distilled Water

Most studies indicate that the moisture uptake should be assessed to some extent, as it can be a viable indicator of the level of degradation, and so specimens were weighed prior to both conditioning and prior to strength testing. A mass balance with a sensitivity of 0.01 g was used, and after removal from the water baths, the wet surfaces of the specimen were wiped before being weighed. It should be noted that this is not a specific study into the diffusion behaviour and moisture uptake process, as was outlined in Chapter 3. The mass change determined can only give a qualitative relationship between the moisture uptake and strength degradation.

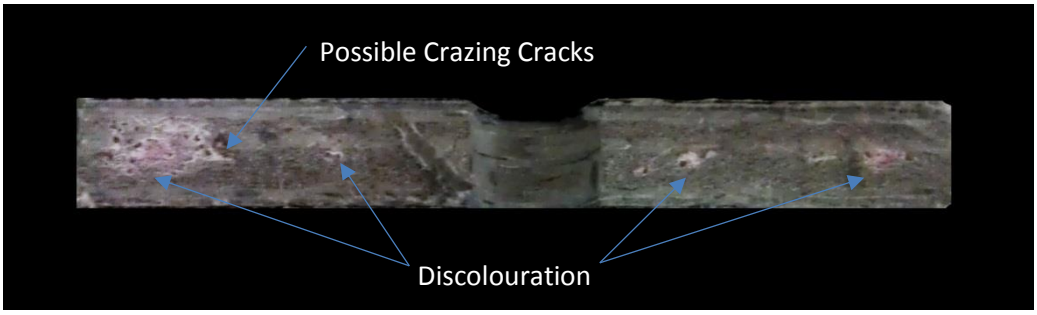

Figure 5.2: Discolouration and Possible Crazing Cracks shown at the Cut Edges of a Pre-test Pin-bearing Strength Specimen after Hot-wet Conditioning at 50°C

It was observed that following the hot-wet aging there were several specimens with slight discolouration and possible crazing cracks, as shown in Figure 5.2, predominately on the (unprotected) cut edges. Similar cracks were found for the moisture sorption study for the

same material as presented in Chapter 3, with a build-up of white extravasation as shown in Figure 5.3. This might be deposits of styrene which is a constituent of the matrix.

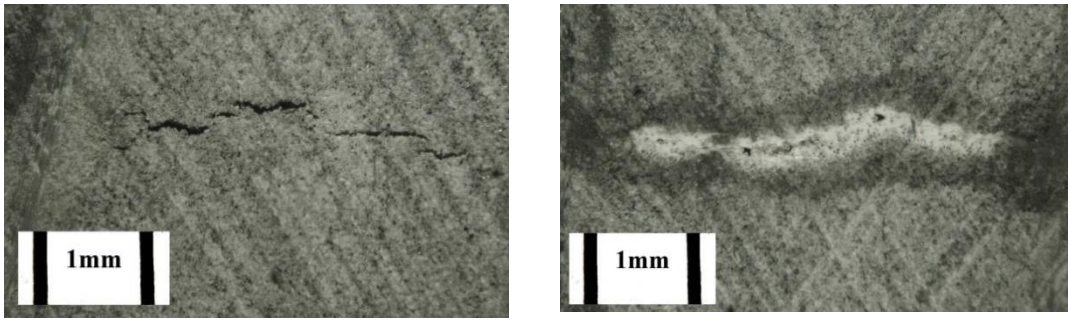

Figure 5.3: Photographs of Hot-wet Conditioned Specimens in distilled water showing (a) Small cracks on the surface for 40°C Specimen and (b) Crazing and White Extravasation for 50°C Specimen

The colour change was found in batches artificially aged at the two temperatures of 40 and 50°C, it did not occur in the 30°C condition. This suggests that there may have been some form of chemical change to the polymer based matrix, and could be what was found in previous work with PFRP material by Nishizakhi and Meirarashi (2002). The specific reason is unknown and would be of direct understanding to an item of future work to explain the materials science and chemical process change of the PFRP material but is not dealt with any further here.

5.3. Test Matrix and Configuration

A total of 280 specimens were tested to determine the effect of 'pin' type, plain or threaded, on the bearing failure load after specimens had been conditioned in distilled water at 40°C. This gave 56 batches having five nominally identical specimens. Web material was tested with respect to three orientations of 0, 45 and 90° and flange material for the 0 and 90^{o} directions only. This was because the flange outstand width at 120 mm is too small for the 45^{o} coupon. The threaded pins, were cut from standard A2 stainless steel bolts of M10, M12, M16 and M20

size diameter (*d*), with 1.5, 1.75, 2 and 2.5 mm (coarse) pitch size, respectively. The web material was tested with the largest and smallest pin sizes only, due to limited available material for the number of specimens; the flange material was tested with all four pin sizes. A clearance hole of 1.6 mm, plus the maximum allowable tolerance of 0.4 mm or 0.8 mm was used to give hole diameters of 12.0 mm, 14.4, 18.4 and 22.4 mm, for the four pin sizes. The measured 'pin' diameters, for both plain and threaded types are given in column (1) of Tables 5.1 and 5.2.

Experimental research by Karbhari (2006) had found that the effect of temperature and immersion in water to be a significant conditioning for accelerated aging and its associated effect on changing strength properties of PFRP material. Consequently, an expanded set of temperatures was chosen within this present study (as compared to the single temperature used by Zafari and Mottram, 2012a) to develop a meaningful data set for prediction purposes. A further series of tests was conducted at 30 and 50°C with flange material, the largest and smallest pin diameters (M10 and M20) and in the longitudinal and transverse directions. Only plain pins were used in this supplementary (durability) study having a total of 80 specimens (in 16 batches of five specimens). Threaded pins or web material were not used due to limited time and material available. To distinguish the specimens for the three test-temperature conditions, the prefix '30A' or '50A' was appended to the test label instead of 'A' to identify the 30 and 50°C specimens, respectively.

Pin-bearing compression testing was conducted straight after a specimen had been removed from the water baths, and followed the same procedure detailed in Section 4.3. The procedure is summarised next. Monotonic load testing was conducted using a DARTEC servo-hydraulic testing machine with a 250 kN load cell equipped with the compression die set for bearing strength tests. The uniaxial compressive load is applied under a constant stroke rate of 0.01

mm/s with load and machine stroke recorded once every half a second by data acquisition software; the failure load is defined as the maximum recorded load (Mottram and Zafari, 2011). Stroke is predominately governed by the deformation of the specimen, due to the relatively high axial stiffness of the metallic testing machine, test fixtures and pins. The maximum compressive force inclusively accounts for the dead weight of the top plate and rocker fixture, at 0.321 kN.

5.4. Test Results

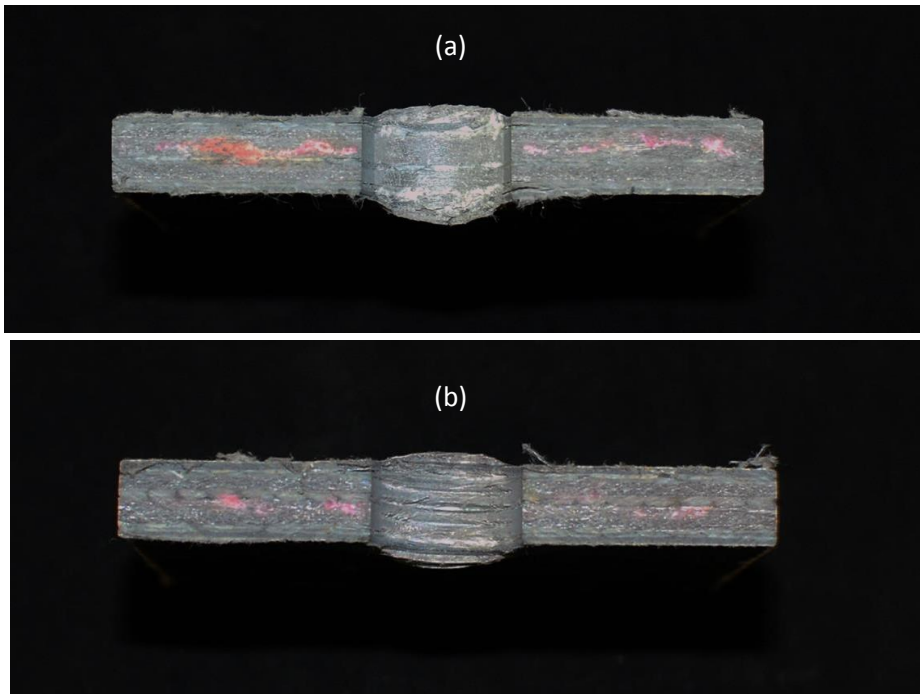

Figure 5.4: A Failed Pin-bearing Specimen of Flange Material after Hot-wet Conditioning in Distilled Water at 40°C for 6 months and tested with a (a) Plain Pin and (b) Threaded Pin

It was observed that failed specimens, which had been tested after being immersed in a hot-wet condition for 3 or 6 months, resembled the failed specimens of the non-aged studies in Chapter 4. They exhibited the typical out-of-plane splaying ('brooming') of the laminated material at the material-steel pin interface, if not to a greater degree than the non-aged material in some cases. Typical visual failure in aged specimens can be seen in the photograph

in Figure 5.4. The specimen chosen has the material discolouration (on cut surfaces) that was mentioned previously.

Summarized in Tables 5.1 and 5.2 are the salient test results from the 56 batches subjected to hot-wet conditioning at 40°C. These two tables have a similar format to Tables 4.1 to 4.4; except column (1) is for the material type and orientation. Table 5.1 is for the plain pin situation and Table 5.2 when bearing is with thread. Both tables reported results at 3 and 6 months aging times. The first column (1) gives the material type, either web or flange and the orientation. In Columns (2) and (3) are reported the measured pin diameter (d) and the mean specimen thickness (t). The average ratio of diameter-to-thickness for the hot-wet conditioned specimen tests is 1.01, 1.19, 1.60 and 2.04 for the pin of size M10, M12, M16 and M20. These values for d/t correspond to the first four rows, and are in same order for subsequent four rows down a table. The mean maximum failure load ($R_{br,mn}$ in kN) is given in column (4). Using the individual R_{br}s for the batch the mean pin-bearing strength in N/mm^2 (MPa) is calculated using Eq. (2.1), and is reported in column (5). For each batch the Standard Deviation (SD) is given in column (6) and its Coefficient of Variation (CoV) in column (7). The full set of specimen results are given in Appendix C for the main results summarised in Tables 5.1 and 5.2.

In column (8) of the tables the characteristic strengths for the batches, determined in accordance with Annex D7 of BS EN 1990:2001 are given. This strength value is determined with the assumption that the CoV is known a priori. Based on the procedure for a known CoV and a batch size of five specimens the characteristic value is equal to (mean – 1.8×SD); where k_n is 1.8. It is observed that the characteristic values are generally lower than the mean value but with a variation between 6 and 50 % for plain pins and between 4 and 23 % for threaded pins than reported in Tables 4.1 to 4.4 and 4.7 for the non-aged materials. The largest variation

(of 50%) for plain pins occurs with the specimens tested with a M12 size pin for flange material with the material orientated in the longitudinal direction. The cause of this difference between mean and characteristic values is a result of a large spread of results within individual batches and is most apparent (upon inspection of CoV in Table 5.1) for all longitudinal flange material specimens tested with a plain pin and after 6 months conditioning. The batch tested with flange material orientated in the transverse direction and tested with a M16 size pin showed the largest difference between mean pin-bearing strengths and CoV (of 23%) for the threaded case.

Table 5.1: Plain bearing strength results for 40°C hot-wet conditioned PFRP Web and Flange Material

Material Type and Orientation (1)	Pin Diameter, d (mm) (2)	Specimen thickness, t (mm) (3)	Mean Max. Failure Load, $R_{br,mn}$ (kN) (4)	Mean Pin-bearing Strength, F_{ϑ}^{br} (N/mm^2) (5)	Standard Deviation, SD (N/mm^2) (6)	Coefficient of Variation, CoV (%) (7)	Characteristic Value, $F_{k,\vartheta}^{br}$ (N/mm^2) (8)
3 Months							
Flange 0°	9.81 (M10)	9.70	16.6	174	12	6.8	153
	11.8 (M12)	9.65	19.6	172	21	12	135
	15.9 (M16)	9.93	26.0	165	8.8	5.4	149
	19.8 (M20)	9.76	30.2	157	5.2	3.3	147
Flange 90°	9.81 (M10)	10.3	13.0	129	7.8	6.1	115
	11.8 (M12)	10.1	13.4	112	5.6	5.0	102
	15.9 (M16)	10.3	15.9	97.3	4.3	4.4	89.6
	19.8 (M20)	10.0	16.8	84.8	3.2	3.8	79.1
Web 0°	9.81 (M10)	9.66	16.3	172	14	7.9	148
	19.8 (M20)	9.65	28.3	148	6.3	4.2	137
Web 45°	9.81 (M10)	9.63	13.2	140	7.7	5.5	126
	19.8 (M20)	9.66	20.2	106	3.2	3.1	99.9
Web 90°	9.81 (M10)	9.62	13.1	139	4.9	3.5	130
	19.8 (M20)	9.61	19.0	100	4.9	4.9	91.2
6 Months							
Flange 0°	9.81 (M10)	9.60	18.4	195	25	12	151
	11.8 (M12)	9.95	20.4	173	32	19	115
	15.9 (M16)	9.71	28.7	186	19	10	153
	19.8 (M20)	9.76	29.1	151	11	7.5	130
Flange 90°	9.81 (M10)	10.1	12.2	123	6.8	5.5	111
	11.8 (M12)	9.74	12.3	107	8.2	7.7	92.1
	15.9 (M16)	9.72	15.5	101	5.9	5.8	90.1
	19.8 (M20)	9.67	16.0	83.3	7.7	9.3	69.4
Web 0°	9.81 (M10)	9.67	16.6	174	13	7.3	152
	19.8 (M20)	9.65	30.1	158	23	14.3	117
Web 45°	9.81 (M10)	9.64	14.0	148	4.4	3.0	140
	19.8 (M20)	9.60	20.4	107	3.3	3.1	101
Web 90°	9.81 (M10)	9.62	12.4	131	4.9	3.7	123
	19.8 (M20)	9.62	18.6	97.7	4.5	4.6	89.5

Table 5.2: Threaded bearing strength results for 40°C hot-wet conditioned PFRP Web and Flange Material

Material Type and Orientation (1)	Pin Diameter, d (mm) (2)	Specimen thickness, t (mm) (3)	Mean Max. Failure Load, $R_{br,mn}$ (kN) (4)	Mean Pin-bearing Strength, F_{ϑ}^{br} (N/mm^2) (5)	Standard Deviation, SD (N/mm^2) (6)	Coefficient of Variation, CoV (%) (7)	Characteristic Value, $F_{k,\vartheta}^{br}$ (N/mm^2) (8)
3 Months							
Flange 0°	9.81 (M10)	9.69	16.4	172	12	7.0	150
	11.8 (M12)	9.83	19.0	164	7.4	4.5	151
	15.9 (M16)	9.66	22.3	146	8.3	5.7	131
	19.8 (M20)	9.93	25.5	132	6.8	5.2	119
Flange 90°	9.81 (M10)	10.1	13.6	138	5.2	3.8	128
	11.8 (M12)	9.96	15.6	133	6.4	4.8	121
	15.9 (M16)	9.98	17.3	110	9.1	8.3	93.3
	19.8 (M20)	10.3	20.2	99.7	6.4	6.4	88.2
Web 0°	9.81 (M10)	9.63	14.8	156	10	6.7	138
	19.8 (M20)	9.66	22.8	119	10	8.6	101
Web 45°	9.81 (M10)	9.62	14.6	155	3.4	2.2	149
	19.8 (M20)	9.64	21.6	113	7.0	6.2	101
Web 90°	9.81 (M10)	9.62	14.4	153	6.4	4.2	142
	19.8 (M20)	9.61	20.7	109	3.8	3.5	102
6 Months							
Flange 0°	9.81 (M10)	9.78	17.4	181	12	6.9	159
	11.8 (M12)	9.69	18.5	162	6.9	4.3	149
	15.9 (M16)	10.0	23.9	151	9.0	6.0	134
	19.8 (M20)	9.81	26.7	138	8.8	6.4	122
Flange 90°	9.81 (M10)	9.77	12.8	134	7.1	5.3	121
	11.8 (M12)	10.2	15.7	131	6.7	5.1	119
	15.9 (M16)	10.2	17.1	106	11.3	11	86.0
	19.8 (M20)	9.67	16.0	106	8.4	7.9	91.0
Web 0°	9.81 (M10)	9.82	20.6	168	9.6	5.7	151
	19.8 (M20)	9.63	15.9	119	7.8	6.6	105
Web 45°	9.81 (M10)	9.63	15.1	159	8.9	5.6	143
	19.8 (M20)	9.64	21.8	114	7.4	6.5	101
Web 90°	9.81 (M10)	9.62	14.7	155	7.5	4.8	142
	19.8 (M20)	9.62	20.6	108	8.2	7.6	93.4

An overview of the results in Tables 5.1 and 5.2 is given next. From here-on the three conditioning time periods of 0, 3 and 6 months shall be used to represent a non-conditioned test batch from Chapter 4 and a 3 or 6 month duration of hot-wet conditioning as described in Tables 5.1 and 5.2, respectively. The clear distinction between mean pin-bearing strengths for web and flange material is that the latter are higher for 0° material and the former are higher for the 90° material for all batches (with and without hot-wet conditioning). The web material pin-bearing strengths are on average 10% higher than flange material strengths for the transverse direction and equally lower than the flange material in the longitudinal direction by the same amount. The relationship between the fibre architecture and pin-bearing strength is similar for values reported in Chapter 4 (that showed 10% difference between flange and web

values), and therefore hot-wet conditioning may not significantly influence the effect fibre architecture has on pin-bearing strength. The tri-axial mat is seen to play an important role in providing off-axis strength and UD rovings provide higher strength when orientated parallel to the direction of the force. Considering, the flange material has a 27% higher content of UD reinforcement than the web material and conversely the web material has a 21% higher content of tri-axial mat reinforcement, the observed relationship between flange and web material and the associated effect of the material architecture on pin-bearing strength is as expected.

A large variation is found for flange material for all batches tested with a plain pin after hot-wet conditioning and for an M16 size threaded pin after 6 months conditioning and tested in the transverse direction, with a CoV of 11%. In particular, the largest variation of 19% is for the batch tested with a M12 plain pin at 0° after 6 months hot-wet conditioning. It should be noted that the mean average of CoVs for all hot-wet conditioned batches is 6.4%. This finding confirms the assumption that this value is known priori tor calculation of characteristic values.

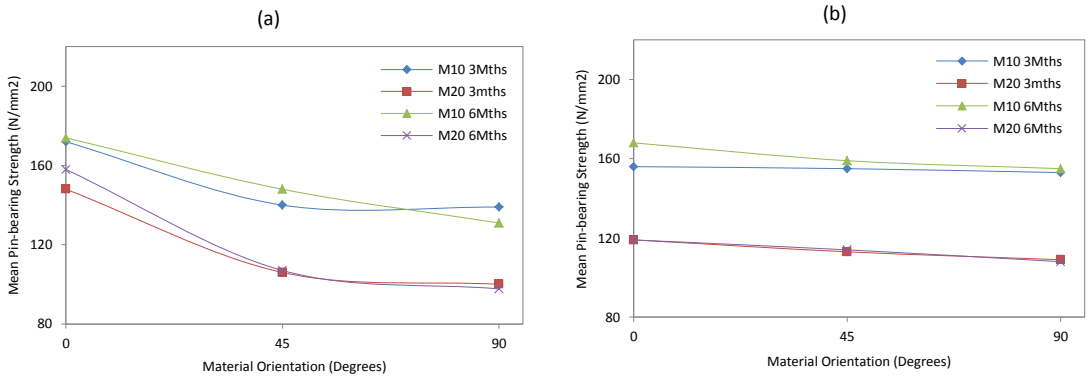

Figure 5.5: Mean Pin-bearing Strength plotted against the Material Orientation with 3 and 6 months Hot-wet Conditioning and tested with M10 and M20 Sized (a) Plain Pins and (b) Threaded Pins

Presented in Figure 5.5 are the mean pin-bearing strengths for material conditioned for 3 and 6 months and tested with a M10 or M20 size pin, plotted for the three material orientations of

0, 45 and 90°. Part (a) shows the trends for a plain and part (b) for threaded pins; the line between points is shown only for presentation. The figure shows that for threaded values there is little difference between the three material orientations, this is in contrast to the values for plain pins, particularly for the trend between 0 and 45°. The longitudinal values are on average 20 and 40% higher than the 45° strengths for the M10 and M20 pin sizes, respectively. The change in strength between 45° and transverse direction show little difference for the plain pins. Comparing results plotted in Figure 5.5 for the hot-wet conditioned specimens with those plotted in Figure 4.13 there seems to be similar trends for both non-aged and conditioned specimens.

The relative strength properties of PFRP material in the 0^o and 90^o directions differ as shown in Figure 4.12 for the non-aged situation, and these are often quantified by strength ratios for the principal axes, as a measure of how orthotropic the material is. Creative Pultrusions (2010) in their design manual give maximum mean pin-bearing strengths (using ASTM D953, 2002) for non-aged (0 months conditioning) WF SuperStructural sections of 227 and 158 N/mm^2 for 0^o and 90^o Flange material and 234 and 206 N/mm^2 for 0^o and 90^o web. The 0°/90° ratios can be computed as 1.43 and 1.13 for flange and web material, respectively. Next the author reports a comparison shall be presented for 0°/90° and 45°/90° ratios using the mean strength values from the WUTS.

Firstly, if we compare 0°/90° ratios for mean pin-bearing strengths for the largest pin size, M20, (the pin *d* known to give the lowest strengths from the four sizes used) using results in from Tables 4.1 to 4.4, 5.1 and 5.2 for flange material tested after 0, 3 and 6 months of conditioning at 40°C with a plain pin. These ratios are 2.15, 1.85 and 1.81 and with a threaded pin there are 1.41, 1.32 and 1.30. Similarly, for web material with a plain pin they are 1.64, 1.48 and 1.62 and with a threaded pin they are 1.08, 1.09 and 1.10. It can be seen that as the

duration of hot-wet conditioning is increased the difference between the 0^o and 90^o strengths converge, with the exception of the web material tested with a threaded pin, which gives similar results for all three time durations. For the strength ratio that is not likely to be governed by the presence of UD reinforcement the 45°/90° for web material with M20 size are 1.12, 1.06, and 1.10 for a plain pin and are 1.06, 1.04 and 1.06 for the thread case. The change with aging time is not significant.

It has been shown that for non-aged material there occurs a difference in thread pin-bearing strength between flange and web materials. Furthermore, this can affect the level of strength reduction, if any (depending on material orientation), between plain and threaded cases. Our next consideration therefore shall be given to the strength characteristics of hot-wet aged specimens with threaded pins and how they differ for both material architectures, when compared with their equivalent plain pin batches. In the 0^o direction, web and flange materials show a reduction in strength due to thread in bearing for the three conditioning time periods. From column (7) in Tables 4.1 and 4.2 the as-received web material with M20 pin has characteristic strengths of 148 and 112 N/mm^2 without and with thread. From column (7) in Tables 5.1 and 5.2 the equivalent aged strengths are, after 3 months of aging found to be 137 and 101 N/mm^2, and after six months they are 117 and 105 N/mm^2. This represents a reduction in characteristic strength after 3 months of 7 and 10 %, and similarly after 6 months of 21 and 6%. In contrast, in the 90^o direction a strength increase is exhibited, with a larger difference in strength observed between the two pin types with web material than with flange material. This trend is not dissimilar to the pin-bearing strength characterisation for the non-aged specimens. The average increases in strength due to a M20 thread in bearing for the three aging times and flange are found to be 9, 15 and 20% and for the web are 9, 8 and 10%.

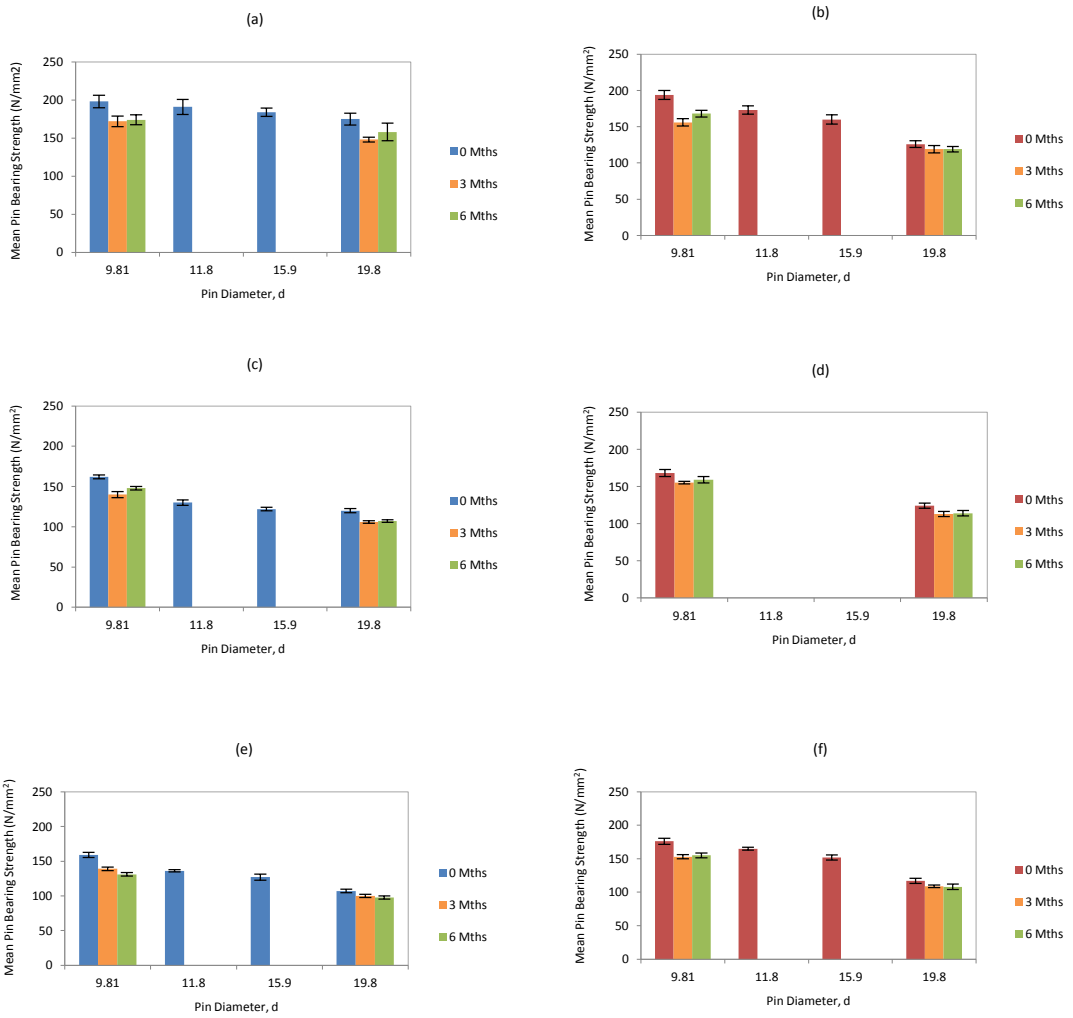

Figure 5.6: Mean Pin-bearing Strengths for Non-aged and 3 months and 6 months Hot-wet Conditioned Web material Specimens of a (a) Plain pin at 0°, (b) Threaded pin at 0°, (c) Plain pin at 45°, (d) Threaded pin at 45°, (e) Plain pin at 90° and (f) Threaded pin at 90°

Plotted in the bar charts in Figures 5.6a to 5.6f and 5.7a to 5.7d are the mean strengths and corresponding standard deviations for the batches conditioned for 0, 3 and 6 months. The batch variation about its mean is given by an error bar in the figures. Comparing strength results presented in Tables 5.1 and 5.2, or as presented in Figures 5.6 and 5.7, it is obvious that after three months a measureable strength reduction is found for all batches. This reduction is on average 15%. Furthermore, this reduction is more prominent with the 0^{o} material having an average reduction in flange and web materials of 15%. The trend for the six month conditioned specimens is less perceptible, although, they all show a reduction when compared to 0 month

values. When compared to the 3 months results a reduction occurs for most batches, except for 0^{o} with M10 and M20 plain pins and M10 with threaded. Generally, the higher mean values correlate to a larger batch variation, as given in Tables 5.1 and 5.2 by higher SDs (or CoVs) in columns (6) and (7), and shown in Figures 5.6 and 5.7 by the taller (longer) error bars.

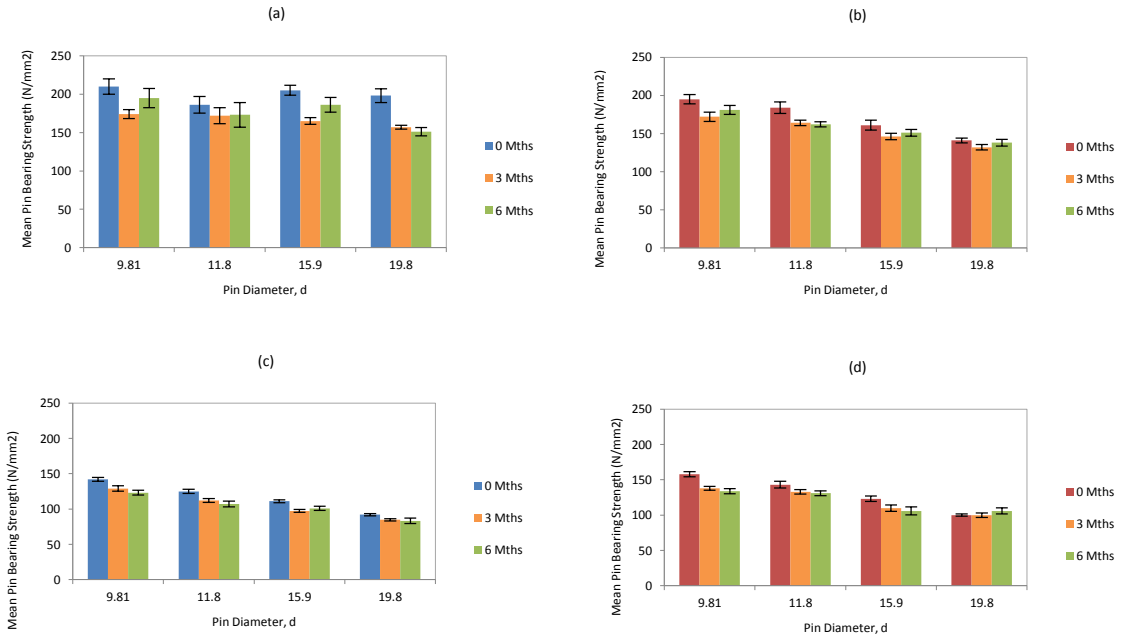

Figure 5.7: Mean Pin-bearing Strengths for Non-aged and 3 months and 6 months Hot-wet Conditioned web material Specimens of a (a) plain pin at 0°, (b) Threaded pin at 0°, (c) Plain pin at 90° and (d) Threaded pin at 90°

Figures 5.6 and 5.7 show that due to an increase in *d* there is a decrease in pin-bearing strength for 0, 3 and 6 months with and without thread. A smaller variation in the mean strength shown by the error bars (SD) and from inspection of data in Tables 5.1 and 5.2 (CoV) is found for the largest pin size of M20, with CoVs below 10%. The difference between the largest and smallest plain pins increases for each of the hot-wet batches at 0, 3 and 6 months as the material is orientated from 0 to 90°. This finding can be seen for the conditioned specimens in Figures 5.6a, 5,6c and 5.6e for web material and Figures 5.7a and 5.7c for flange.

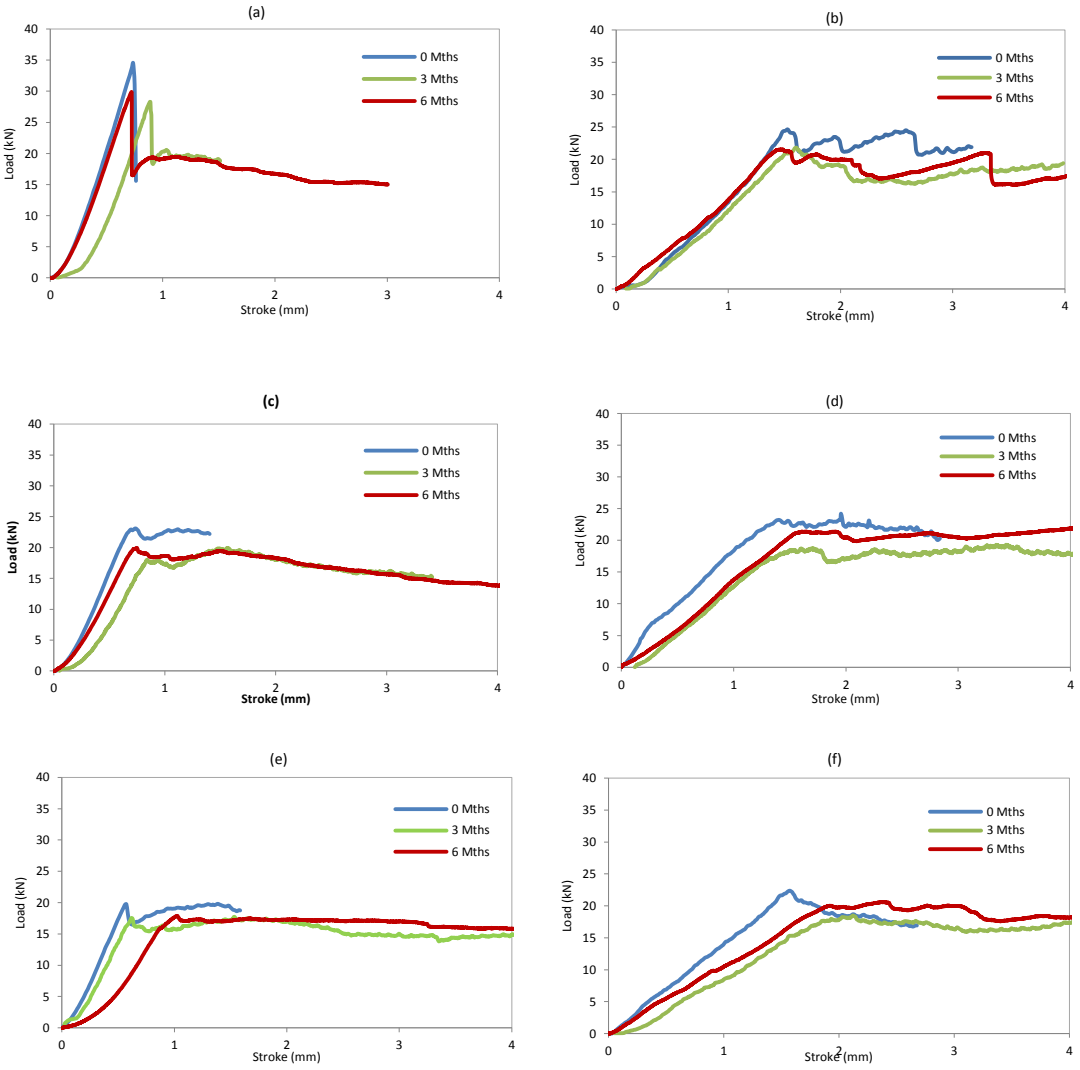

Figure 5.8: Typical Load against Stroke Curves for a M10 sized pin for non-aged and 3 and 6 months Hot-wet conditioned Web Material at 40C with a (a) Plain Pin at 0°, (b) Threaded Pin at 0°, (c) Plain Pin at 45°, (d) Threaded Pin at 45°, (e) Plain Pin at 90° and (f) Threaded Pin at 90°

It would be expected that hot-wet aging may cause a softening of the resin matrix (could be due to bond degradation too), and hence this would cause a change in the load-stroke response of the aged specimen. Presented in Figures 5.8a to 5.8f are six plots having three typical load-stroke curves for the non-aged (0 months) and aged (3 and 6 months) conditionings, with web material and the M20 pin. Parts (a), (c) and (e) are for the plain situation and parts (b), (d) and (f) for the threaded case. The alphabetical order of the three parts per pin type is for the material orientations of 0^{o}, 45^{o} and 90^{o}. Similar load-stroke characteristics were exhibited by specimens in the other batches whose key test results are

given in Tables 5.1 and 5.2. The load-stroke behaviour emerging from assessing the curves in Figures 5.8 is of an initial 'bedding-in' stage, after which there is a nearly linear (probably elastic) increase to the maximum load. When the maximum is reached there is bearing failure, when there can be a sudden loss in resistance.

From inspection, the specimen stiffness determined from the initial part of the load-stroke plots in Figure 5.8 is considerably lower (parts (b), (d) and (f)) when thread is present. This is due to the thread embedment process into the contact area. It is noted that for the threaded case, the post-failure load-stroke response shows a small, if any, loss in bearing capacity. Even for the 0° material in Figure 5.8(a) there is a 30% loss when compared to a plain situation. The measured stiffness for specimens subjected to 6 months hot-wet conditioning does not significantly deviate from the 0 month material. The overall shapes of the three load-stroke curves in Figures 5.8 (a) to (f) remain similar after the hot-wet aging.

Having reviewed the results for material subjected to the 40°C conditioning in distilled water, our attention is next drawn to the other two temperatures considered in the test matrix. This study was conducted in order to provide both a wider set of data and draw more meaningful comparisons for use in long-term degradation predictions for environmental aging in pultruded structures. Presented in Tables 5.3 and 5.4 are summaries of the results for the 16 batches of five specimens following the 30 and 50°C immersion durations at 3 and 6 months. The same convention for column content is observed as in Tables 5.1 and 5.2. The full breakdown of each individual test is given in Appendix C. To accompany the two tables, presented in Figure 5.9 are the mean pin-bearing strength results along with non-aged values from Chapter 4 for 0^{o} and 90^{o} flange material. It should be noted that the dotted line between points is only added for presentation reasons; it cannot be interpreted as the trend between the three points.

Table 5.3: Plain bearing strength results for 30°C hot-wet conditioned PFRP material

Material Type and Orientation (1)	Pin Diameter, d (mm) (2)	Specimen thickness, t (mm) (3)	Mean Max. Failure Load, $R_{br,mn}$ (kN) (4)	Mean Pin-bearing Strength, F_{ϑ}^{br} (N/mm^2) (5)	Standard Deviation, SD (N/mm^2) (6)	Coefficient of Variation, CoV (%) (7)	Characteristic Value, $F_{k,\vartheta}^{br}$ (N/mm^2) (8)
3 Months							
Flange 0°	9.81 (M10)	9.70	16.0	169	19	11	134
	19.8 (M20)	9.78	28.2	146	13	9.1	122
Flange 90°	9.81 (M10)	9.64	11.3	120	3.4	2.8	114
	19.8 (M20)	9.78	16.8	87.0	4.9	5.6	78.2
6 Months							
Flange 0°	9.81 (M10)	9.71	15.3	161	13	7.8	138
	19.8 (M20)	9.97	30.9	157	15	9.5	130
Flange 90°	9.81 (M10)	9.65	10.9	115	5.9	5.2	104
	19.8 (M20)	9.82	16.4	84.3	6.6	7.8	72.4

Table 5.4: Plain bearing strength results for 50°C hot-wet conditioned PFRP material

Material Type and Orientation (1)	Pin Diameter, d (mm) (2)	Specimen thickness, t (mm) (3)	Mean Max. Failure Load, $R_{br,mn}$ (kN) (4)	Mean Pin-bearing Strength, F_{ϑ}^{br} (N/mm^2) (5)	Standard Deviation, SD (N/mm^2) (6)	Coefficient of Variation, CoV (%) (7)	Characteristic Value, $F_{k,\vartheta}^{br}$ (N/mm^2) (8)
3 Months							
Flange 0°	9.81 (M10)	9.81	17.0	176	27	15	127
	19.8 (M20)	9.84	35.9	185	15	8.2	157
Flange 90°	9.81 (M10)	9.61	11.1	117	8.1	6.9	103
	19.8 (M20)	9.82	16.0	82.0	7.9	9.7	67.7
6 Months							
Flange 0°	9.81 (M10)	9.68	16.9	178	7.7	4.3	164
	19.8 (M20)	10.1	31.9	160	13.1	8.2	136
Flange 90°	9.81 (M10)	9.55	11.1	119	5.0	4.2	110
	19.8 (M20)	9.87	16.7	85.5	3.9	4.6	78.4

The distinct trend for the material tested with the material orientated in the transverse direction is that there is little difference between three temperatures, particularly for M20 in part (b) of Figure 5.9. In stark contrast, however, the results for the longitudinal flange material are distinctly varied from the test results. It should be noted the CoVs from Tables 5.3 and 5.4 for the 0° flange conditioned at 3 and 6 months are considerably higher than the other batches, with an average of 11%. It would seem from the M20 results that the strength after 3 months immersion decreases as the test temperature decreases and this trend reverses for the 6 month aging, although the difference between values for the three temperatures is minimal. The M10 results show similar strengths for all three temperatures after 3 months and

a wider range after 6 months (having the highest strength for the batches conditioned at 40°, the second highest at 50° and the lowest at 30°).

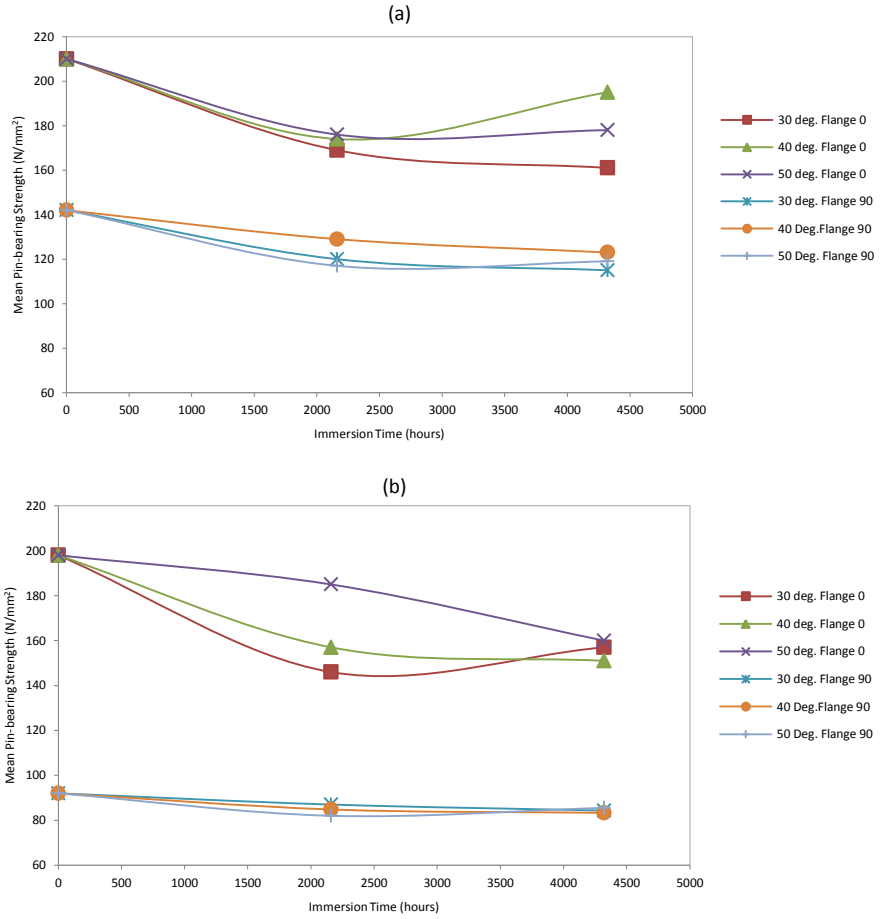

Figure 5.9: Flange 0° and 90° Hot-wet conditioned Pin-bearing Test Results for Non-aged, 3 and 6 months conditioning for 30, 40 and 50°C tested with a (a) M10 Plain Pin and (b) M20 Plain Pin

5.5. Discussion of Hot-wet Conditioned Pin-bearing Strength Test Results

In what follows shall be a discussion of the salient test result from Chapter 4 and the results presented for hot-wet aged specimens after durations of 3 and 6 months and for constant temperatures of 30, 40 and 50°C. Firstly, the focus shall be the aging mechanisms and their associated effects on pin-bearing strength, with comparisons being drawn between the

moisture sorption, as detailed in Chapter 3, and here calculated specifically for each pin-bearing strength specimen. An exploration of the effects of material type and thread in bearing shall be presented. Both of these aspects have not significantly featured within previous research, which mainly considered plain pins and PFRP materials (Zafari and Mottram, 2012a and Wang, 2004). Furthermore, the effect of temperature and duration of hot-wet conditioning upon the pin-bearing strength measure is deliberated. Finally, a lifetime prediction using Arrhenius principles is presented with an attempt to relate the accelerated aging tests within this chapter to a reduction in strength expected due to real-life service conditions.

The degradation of PFRP materials has been shown by Chu and Karbhari (2005) to include mechanisms that involve failure of the resin matrix due to plasticization in short periods of immersion. In longer periods of hot-wet conditioning they found that degradation includes hydrolysis with micro-crack progression from internal water pressure, often observed by swelling of specimens. However, it must be noted that any reduction in the level of cure induces residual stress due to this swelling that can lead to a retardation of failure, and so not all moisture induced effects are known to be adverse (Bach, 1996).

The most significant factor in causing irreversible reduction in strength and material performance is a breakdown of the fibre-resin matrix interface due to the wicking of moisture from capillary action and or from shrinking away of the matrix from the fibres. The crazing cracks shown in Figure 5.3 are certainly the result of Environmental Stress Cracking (ESC), which involves development of a network of micro-cracks that is driven by the moisture absorption process. Therefore, it is speculated that the driving force behind the degradation of the PFRP material is a combination of the matrix failure mechanisms and fibre-matrix de-bonding. At the higher temperatures, the rate of moisture diffusion is generally greater and

hence it can be expected that a decrease in performance and strength occurs under this conditioning environment.

Firstly, to evaluate the level of material degradation, it would be beneficial to have a brief discourse on the moisture uptake over the duration period. Karbhari (2006) has indicated that moisture diffusion is often related directly to loss in material strength due to the lowering of the glass transition temperature (T_g) of the polymer based matrix. Moreover, the lowering of the T_g is associated with the effect of hydrolysis and loss of mechanical strength (Chu and Karbhari, 2005). Although, it should be noted that Cabral-Fonseca *et al*. (2012) found, for a pultruded polyester and vinylester material, the T_g can increase by 4 and 7%, respectively, after 3000 hours exposure in a QUV chamber to variety of water, heat and UV regimes.

Presented next are the relative amounts of moisture diffusion due to distilled water uptake for the hot-wet conditioned specimens at the three temperatures. The percentage change in mass was determined using Eq. (3.4) for all the hot-wet batches; this is the same procedure used in the moisture absorption study presented in Chapter 3. In Eq. (3.4), M_{cond} is the specimen mass after the hot-wet conditioning and M_{dry} is the mass of the dry material immediately prior to exposing a specimen to the aging process. The mass uptake is calculated as a percentage of M_{dry}. The key assumption, in employing Eq. (3.4) to establish mass gain, is that there is no loss in water-soluble matter over the aging process. If necessary a correction can be made to account for a dissolution phenomenon. A simple way to address the level and composition of leachate from the hot-wet aging process would be to characterise the distilled water after removing specimens. Samples of the distilled water from the water baths after removal of specimens were taken to address this issue. However, due to limited time and not the specific need to address the analysis of the chemical process this correction cannot be made herein.

Table 5.5: Average mass gain of hot-wet conditioned PFRP after 3 and 6 months immersion in distilled water at 40°C

	0°		45°		90°	
Batch	%M(3)	%M(6)	%M(3)	%M(6)	%M(3)	%M(6)
(1)	(2)	(3)	(4)	(5)	(6)	(7)
Flange M10	0.81	1.06	-	-	0.83	1.07
Flange M12	0.76	1.02	-	-	0.86	1.06
Flange M16	0.83	1.02	-	-	0.88	1.07
Flange M20	0.82	1.03	-	-	0.88	1.10
Web M10	0.84	1.00	0.92	1.16	0.78	1.02
Web M20	0.87	0.97	0.97	1.15	0.84	1.02

The change in specimen mass from moisture uptake after hot-wet conditioning is presented in Table 5.5 for 40°C and combined in Table 5.6 with 30 and 50°C. The average mass change (%M (*time*)) due to the distilled water that diffuses into the material during the immersion period of months (*time*) is given separately for each bolt size and web and flange material. The plain and threaded specimens for the M10 and M20 notches have been combined into single batches for mass gain evaluation, as they have the same wetted surface area.

Table 5.6: Average mass gain of hot-wet conditioned PFRP after 3 and 6 months immersion in distilled water at 30, 40 and 50°C

		0°		90°	
Temperature	Batch	%M(3)	%M(6)	%M(3)	%M(6)
(1)	(2)	(3)	(4)	(5)	(6)
30	M10	0.73	0.98	0.73	0.90
	M20	0.75	0.95	0.73	0.92
40	M10	0.81	1.06	0.83	1.07
	M20	0.82	1.03	0.88	1.10
50	M10	0.92	1.09	0.90	1.10
	M20	0.98	1.10	0.95	1.10

The results from Tables 5.5 and 5.6 have been combined with the results from the moisture sorption study presented in Chapter 3 to create the moisture uptake curves plotted in Figure 5.10. From Table 5.5 the mass gain for the 14 batches at three months ranges from 0.76 to 0.88% and at six months from 0.97 to 1.16%. From inspection of Figure 5.10, and given that doubling the time has increased the water intake by 25%, there is evidence that the moisture gain is reducing as is predicted by the Fickian diffusion model (Karbhari, 2006). In the third and fifth column of Table 5.6, for 3 month, it is observed that as the temperature increases from 30 to 50°C the rate of moisture absorption increases proportionally (10% increase for every 10°C).

The change due to temperature is less pronounced for the batches conditioned to 6 months, with almost similar percentage moisture uptake at 40 and 50°C. This supports the assumption that the moisture diffusion process is Fickian in nature, and can be directly correlated to temperature as often found in using the Arrhenius principles.

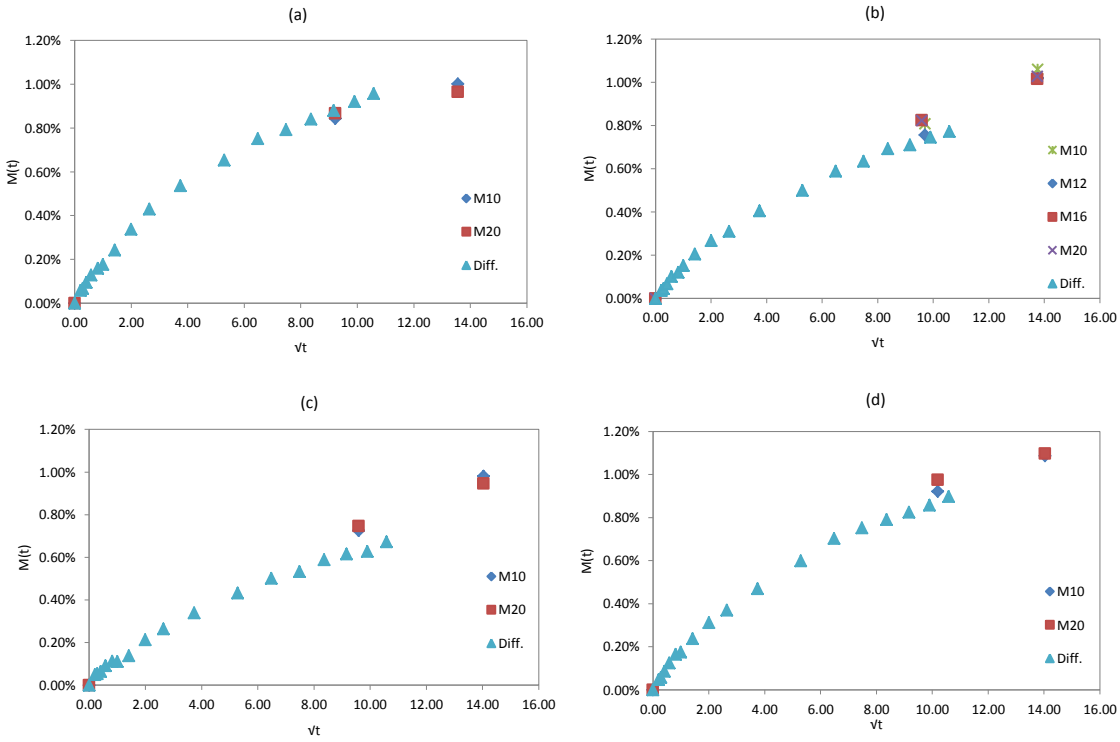

Figure 5.10: Average Moisture Absorption over the Square Root of time (in days) for (a) Web Material at 40°C, (b) Flange Material at 40°C, (c) Flange Material at 30°C and (d) Flange Material at 50°C

In the process of the supplementary conditioning programme (at 30 and 50°C), several additional specimens, which were hot-wet conditioned but not tested for pin-bearing strength, were periodically weighed over a period of several weeks after removal from the water baths. This allowed a preliminary assessment of the level of desorption. The weight change (gain) after being immersed for 3 months at 30°C with a moisture uptake of 0.73%; the weight had reduced after 1, 2 and 2.5 weeks later to 0.59, 0.46 and 0.16%. This shows that a rapid desorption of moisture occurs once specimens are removed from the water baths.

There is a markedly similar level of moisture uptake for both web and flange material, in comparing the results plotted in Figures 5.10a and 5.10b, which would initially suggest that a similar level of moisture diffusion. Hence it may be assumed that degradation has occurred in both of two different fibre reinforcement architectures. Purnell (2008) notes that for GRP samples there is poor correlation between moisture uptake and strength loss, as the rate of change of the former is positive and negative for the latter. It is found, that the flange presents higher pin-bearing strengths in 0° direction, relative to the pultrusion axis, and lower strengths in 90° than web. Both 3 and 6 month values for flange and web are lower than the equivalent non-aged batches strengths. The author finds that the effect of hot-wet conditioning has not significantly affected the pin-bearing strength characteristics for the two material architectures, as this trend was also found in the non-aged characterisation, presented in Chapter 4.

Having considered the kinematic moisture characteristics, next attention shall be drawn to one of the most significant parameters affecting pin-bearing strength, as found in Chapter 4, namely the pin diameter-to-thickness ratio. It was found that as d/t increases a decrease in strength is found for all batches tested and with both material architectures. Presented in Figures 5.11a to 5.11h present characteristic pin-bearing strengths, for plain and threaded batches after hot-wet conditioning, plotted against d/t. Parts (a) to (d) are plots for web material tested with plain pins after 3 and 6 months aging and, similarly, for threaded pins, respectively. Flange material batches are shown in parts (e) to (h), using the same convention. The plot results in Figure 5.11 can be compared with those in Figure 4.15 for the equivalent non-aged test batches.

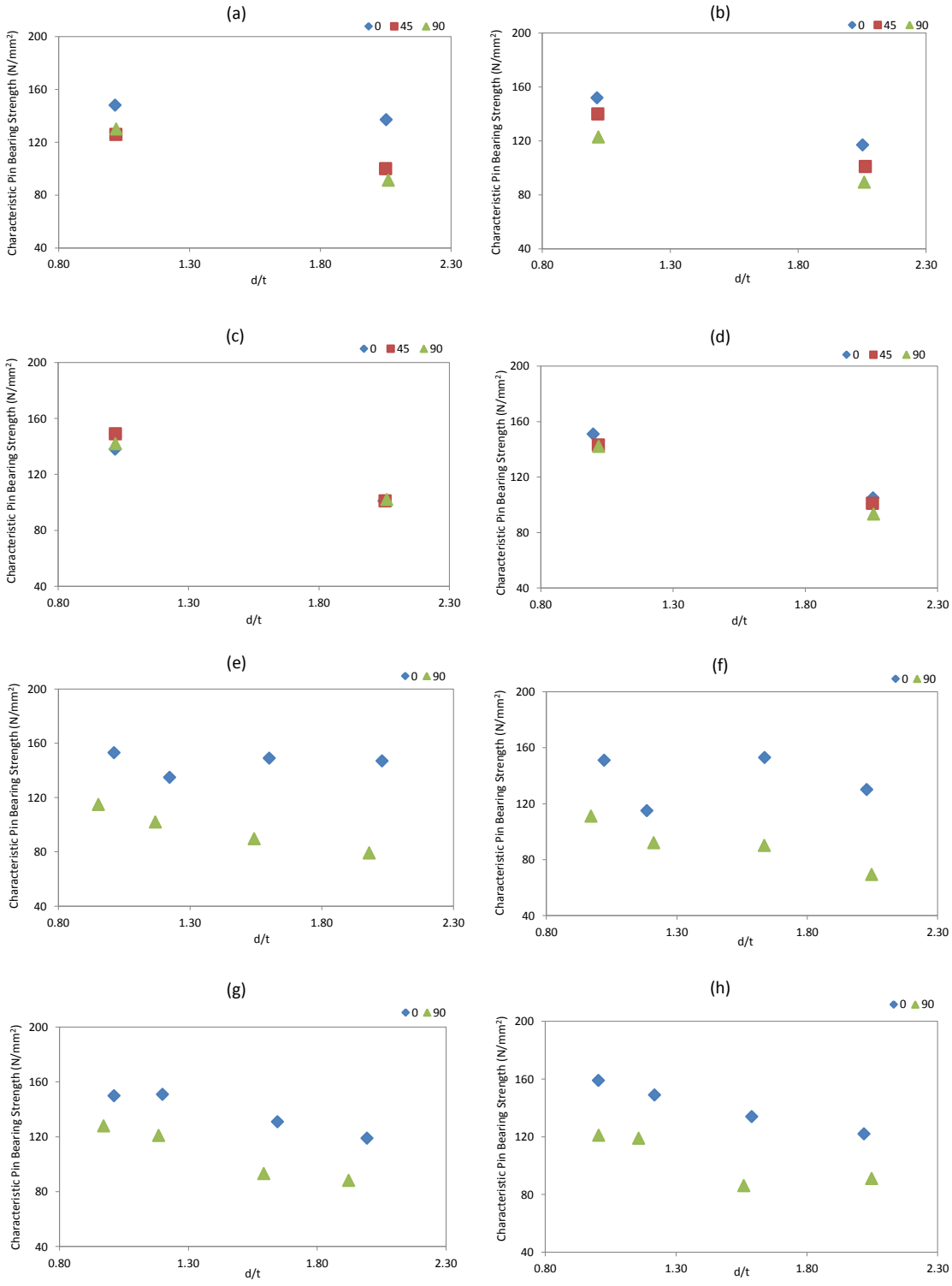

Figure 5.11: Characteristic Pin-bearing Strengths with *d*/*t* ratio: for (a) Web, Plain Pin at 3 Months; (b) Web, Plain Pin at 6 Months; (c) Web, Threaded Pin at 3 Months; (d) Web, Threaded Pin at 6 Months; (e) Flange, Plain Pin at 3 Months; (f) Flange, Plain Pin at 6 Months; (g) Flange, Threaded Pin at 3 Months; (h) Flange, Threaded Pin at 6 Months

Figures 4.15 and 5.11 both show a trend exists of an increase *d*/*t* leading to a lower bearing strength. The difference, as described in the Section 5.4, in strength between the largest and smallest *d*/*t* ratio for conditioned specimens is slightly less than those found for non-aged. The *d*/*t* ratio has a more significant effect on the web material than the flange material between what has been determined to be the largest and smallest values. The trend holds true for all material orientations as shown in Figure 5.11 for 0° (blue diamond symbol), 45° (red square symbol) and 90° (green triangle symbol). Therefore, the recommendation can be made that a standard test methodology for pin-bearing strengths established for use with Eq. (2.1) should account for the largest *d*/*t* ratio and clearance-hole size, as specified in practice. This finding supports a previous set of evidence provided by Zafari and Mottram (2012a).

It should be noted that Creative Pultrusions (2010) stipulate that should their pultruded polyester based material be constantly exposed to an elevated temperature of 38°C (100°F) the ultimate stress should be taken as 85% of specified values tabulated in their design manual. The reduced maximum non-aged pin-bearing strengths from the manufacturer for 38°C elevated temperatures would be for web material F_0^{br} = 199 N/mm^2 and F_{90}^{br} = 175 N/mm^2 and for flange material F_0^{br} = 193 N/mm^2 and F_{90}^{br} = 134 N/mm^2. Immediately, it is observed these values are not as conservative compared to strengths determined using the WUTS. CP use standard test method D953 and a 6.35mm pin with no clearance (ASTM, 2002). However, if a comparison is drawn using the average reduction between characteristic values, it may be determined if 0.85 is an appropriate reduction factor. Taking the largest *d*/*t* ratio, the largest reduction in CV (with a CoV of 7.5%) of 23% is found after 40°C aging of the flange material for 6 months, with 0° orientation and plain pin. It should be noted that the manufacturer has specified that the 15% reduction is due to a sustained service temperature only, with no information of accounting for moisture uptake. Moreover, most specimen

batches do agree with the guidance of a characteristic strength reduction of 5% less than specified by CP for pin diameters greater than the single 1/4in. in ASTM D953:2002.

In addition, the standard EN 13706 for PFRP (standard) materials specifies the minimum pin-bearing strengths required to give a Grade 23 material, and they are F_0^{br} = 150 N/mm^2 and F_{90}^{br} = 70 N/mm^2. The test results for characteristic strengths listed in Tables 5.1 and 5.2, and from inspection of results reported in Figure 5.11, particularly for the largest *d*/*t* ratio, show that the 0^o strengths are in violation of this standard requirement (clause) after hot-wet conditioning, but the 90^o strengths are generally 15% greater than the minimum required.

Similar to the *d*/*t* ratio, the previous chapter highlighted the importance of thread in bearing with regards to reduction in pin-bearing strength. It was theorised that a worst case scenario could be presented with both hot-wet conditioning and a thread in bearing. Therefore, in what follows due consideration is given to the effect of thread and aging upon the strength measure. It was noted within the previous chapter that environmentally degraded PFRP material could be adversely affected by damage cause by thread embedment. Presented in Table 5.8 is the change in mean characteristic strength on dividing the threaded value by the plain value. Column (1) lists the batch ID and columns (2) to (4) give the ratio for the zero, three and six months of hot-wet conditioning. It is seen that 14 out of 42 batches show an increase in strength with three batches (F/90/M10, F/90/M12 and W/90/M20) showing a 10% increase at 0 months. At all three ages the largest reduction from having a thread in bearing is with batches W/0/M20. A reduction of nearly 30% is found for the three batches exposed to three aging times. Within the batches tested using flange material, the largest reduction is found with M20 and 0^o material, with a mean reduction from the three F/0/M20 batches of 25%.

From the results in Table 5.8 there does not seem to be a general trend for the level of strength reduction, due to thread in bearing, when comparing the three time durations of hot-wet conditioning. This is despite expectations that there would be a larger reduction in strength found after increased durations. This finding may be due to the failure criterion for the selection of the load value for the pin-bearing strength test being the maximum attained load. The threaded load-stroke curves in Figure 5.8 show that there is a significant stroke when this maximum load is attained. The load in Eq. (2.1) for the pin-bearing strength would be expected to be lower if the first failure criterion is used. A key feature with the flange material is the reduction, or in this case the lack of decline in strength for M12 batches in both the longitudinal and transverse directions. All the ratios in Table 5.8 are seen to be close to 1.0, and on the high side.

Table 5.7: Normalised Strength Reduction due to Thread to the Characteristic Bearing Strength Values for 0, and 3 and 6 months Hot-wet conditioned at 40°C

Test Batch ID (1)	0 months (2)	3 months (3)	6 months (4)
F/0/M10	0.99	0.85	0.90
F/0/M12	1.06	1.01	1.00
F/0/M16	0.76	0.72	0.74
F/0/M20	0.77	0.71	0.73
F/90/M10	1.10	0.96	0.91
F/90/M12	1.10	1.05	1.03
F/90/M16	1.06	0.90	0.83
F/90/M20	1.08	1.01	1.04
W/0/M10	1.02	0.81	0.89
W/0/M20	**0.74**	**0.68**	**0.71**
W/45/M10	0.98	0.97	0.93
W/45/M20	1.00	0.90	0.90
W/90/M10	1.10	0.97	0.97
W/90/M20	1.06	1.04	0.96
Mean	0.99	0.90	0.90

Having considered the effect of thread and hot-wet conditioning on pin-bearing strength, discussion shall now turn to the ‘aging’ variables of time and temperature. As developed by Bank (2003) an increase in immersion duration is known to adversely affect the strength and performance of PFRPs; his experience would have been with materials without the tri-axial reinforcement. All three month strengths from this series of tests (using WUTS) show a

decrease in strength when compared to the 0 month values, as expected. The material aged for 6 months, although found to have lower strengths than with aging, do, in some cases, show a slight increase from the 3 month results. The specific physical cause, if it may be assumed to be singular in nature (Karbhari, 2007), of this deviation from the anticipated continual lowering (or, maybe, levelling off) for the 6 month strength is discussed now. A factor known from Chapter 4 to contribute to a significant change in strength determination is the smaller specimen batch size of five when compared to 10 per batch in the non-aged tests. Nevertheless, the variation in strength results is somewhat compensated for by computing the characteristic values in accordance with EN 1990 for five specimen batches (British Standards Institute, 2001), such as given in columns (8) of Tables 5.3 and 5.4.

Presented in Figures 5.12a to 5.12d are the mean normalised retentions of characteristic strengths plotted for 0^o and 90^o materials, and tested with the largest and smallest pin sizes over the three immersion durations. Parts (a) to (c) are for flange batches and the three temperatures of 30, 40 and 50°C, respectively. Part (d) shows the values for web material at 40°C. It was anticipated that an increase in conditioning temperature would increase the level of degradation and hence lower the retention of pin-bearing strength over time. As shown in Figure 5.12 it is seen that this expectation is not the case for all batches. In particular, the batches in parts (a) to (c) with for M20 pin reported by the red square symbols (flange 0°) and purple circle symbols (flange 90°) have a normalised strength close to 1.0 or higher.

It has been known by Karbhari (2007) that a level of post-cure is achieved at lower aging temperatures than the T_g. Additional curing of the resin matrix will affect the pin-bearing strength retention positively, and this could explain to a certain extent the large variation in results found. The T_g of the SuperStructural pultruded material in above 100^oC. A larger variation in CoVs is found for batches tested in the 0^o direction. The two plots for 40°C in

Figure 5.12b for flange and in Figure 5.12d for web generally do follow a linear decrease in strength with respect to time. A limitation of the present study is that non-aged (or 0 month) values are for material not subjected to prior immersion in distilled water, and instead were as-received material with an unknown history for environmental conditioning. It would be useful to separate the two environmental parameters of moisture and temperature as part of an item of future work.

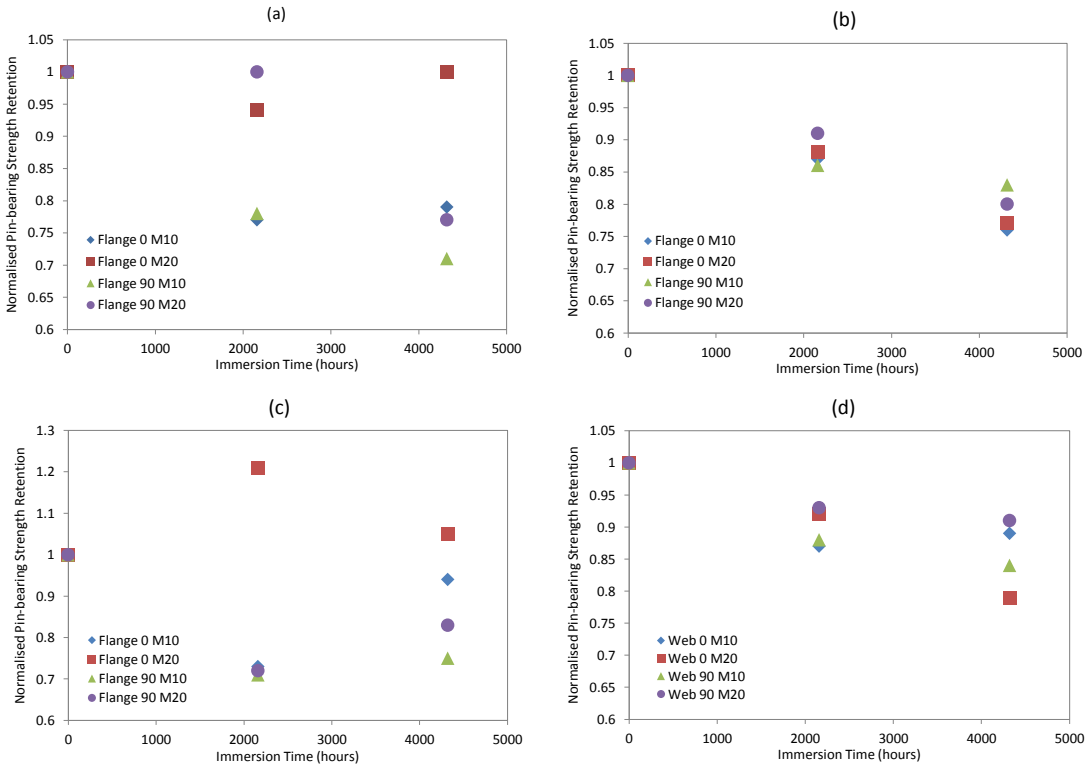

Figure 5.12: Normalised Characteristic Pin-bearing Strengths for Hot-wet conditioned Specimens at Temperatures of: (a) 30°C Flange; (b) 40°C Flange; (c) 50°C Flange; (d) 40°C Web Material.

It is of interest to consider how the conditioning relates to field conditions and Zafari and Mottram (2012a) presented a preliminary investigation into how to relate the hot-wet aging to service time in the field. As in the previous work the specimens here (see Tables 5.2 and 5.33) were fully immersed in distilled water with the full (unstressed) bearing area exposed. A bolted connection between two or more plates of PFRP will be expected to include bolt tightening (Mottram and Turvey, 2003) and washers (of diameter twice the bolt diameter) on either side

of the connected plates. This arrangement is most likely to give a physical barrier that can severely impede, if not prevent, moisture ingress for there to be continuous water contact over the bearing surface. Also the contact surface area where the steel bears into the FRP cannot have a surface layer of water. As a consequence the moisture uptake from the macro scale measurements (see Table 5.5) can be classified as a worst case situation. In addition, it is well known (Karbhari, 2007) that the moisture absorption rate increases as a result of higher temperatures. Without further information it can be assumed that moisture gains for hot-wet exposure at 40°C will be speculative against real service life conditions. It is recognized that FRP components will, depending on geographical location, be exposed to prolonged periods of either (rain or river or sea) water or humidity. PFRP structures with bolted connections will have the capability to absorb water to their maximum capacity (saturation) regardless of diffusion rates (Karbhari, 2007). Therefore, it would be of interest to estimate the relationship between the accelerated aging results for the WF material presented in this chapter and expected performance (degradation) at a lower service life temperature.

It is well established that chemical processes are accelerated as a function of temperature and in the case of accelerated aging of PFRP materials using the Arrhenius law this function is assumed to be exponential. The common and widely referenced form of the Arrhenius equation is given by Eq. (5.1). The reaction rate (k_r) is calculated for a particular reaction using an experimentally found activation energy (E_a) and acceleration constant (A). The other variables include the gas constant (R) of 8.31 J/mol and the absolute temperature (T) in Kelvin (K).

$$k_r = Ae^{-(\frac{E_\mathrm{a}}{RT})} \tag{5.1}$$

It is possible to relate the ratio of two reaction rates using Eq. (5.2) at two different temperatures of (T_1) and (T_2) with the acceleration constant cancelling out. It is this equation that can be used for relating the artificially aged tests to a lower service life temperature.

$$\frac{k_1}{k_2} = e^{-(\frac{E_a}{R})(\frac{1}{T_1}-\frac{1}{T_2})} \tag{5.2}$$

The diffusion coefficients calculated in Chapter 3 are used to determine the activation energy using the Arrhenius plot method developed in Surathi and Karbhari (2006), and details are given in Appendix A. The activation energies for web and flange materials were found to be 59 and 46 kJ/mol, respectively. In comparison, for a wider set of data and using an analytical method, Purnell (2008) presents calculated activation energy for a similar E-glass polyester matrix PFRP of 54 kJ/mol, which is approximately the average value for the two experimentally determined values. Purnell's E_a is used in the following calculations for predicting the comparable time at the lower temperature for the process that took 6 months (i.e. 0.5 years) under the accelerated aging temperature. Using Eq. (5.2) with the test temperatures of 30°C (303 K), 40°C (313 K) and 50°C (323 K), the reduction in pin-bearing strength is found for an assumed average service life temperature of 10.5°C in the UK (Zafari and Mottram, 2012a). For the three aforementioned conditioning temperatures, the estimated times at the lower service temperature are 2.1, 4.2 and 7.8 years, correspondingly. The largest average strength reduction in characteristic pin-bearing strengths are taken from each of the test temperatures giving 23%, 25% and 28% after 2.1, 4.2 and 7.8 years, respective constant exposure to a wet environment.

The LRFD pre-standard for PFRP materials (ASCE, 2012) states in Section 2.4.4 that the characteristic strength should be determined using reference strength multiplied by the adjustment factors. The corresponding adjustment factors to the strength values for a polyester based matrix material at service temperatures between 38 and 60°C, are: for

moisture 0.8; temperature, 1.9 - 0.01T (Fahrenheit). The overall adjustment to the characteristic strength is 0.8×(1.9 – 0.01×(104)) = 0.69 (for the 40°C conditioning). Similarly, at 30 and 50°C the 'knock-down' factor is 0.83 and 0.54. In comparing the total reduction required as determined using the results in this chapter to the pre-standard requirements there is a difference of -8% (30^{o}C), 9% (40^{o}C) and 33% (50^{o}C). It should be noted that the reduction in pin-bearing strength found at 30°C is a lower bound value from eight batches tested and several of these batches exhibited a much higher strength, the author concludes that the guidance given by the LRFD standard is acceptable and likely to be reliable too.

5.6. Summary

An experimental investigation to examine the effect of hot-wet conditioning upon the laterally unrestrained pin-bearing strength has been described and discussed in this chapter. A total of 72 batches of five specimens have been hot-wet conditioned at constant temperatures of 30°C (8 batches), 40°C (65 batches) or 50°C (8 batches), and subsequently tested to determine pin-bearing strengths. Presented are novel test results for materials sourced from a WF pultruded section, with and without a threaded pin in bearing. The non-standard test methodology employed for the strength measurements is the WUTS, which includes a range of pin sizes, and specimens having maximum clearance-hole sizes that can be found in (American) practice.

It has been found that a reduction factor due to thread in bearing is unchanged from the non-aged recommendation of 0.7 for the environmentally conditioned situation. The largest reduction for the threaded strength was found for material tested parallel to the pultrusion direction. The load-stroke stiffness was discernibly lower for the threaded situation. The recommended reduction factor from the characteristic strengths of 30% supports the currently

proposed clause for pin-bearing strength in bolted connections within the ASCE pre-standard for LRFD of PFRP structures (ASCE, 2012).

The influence of the hot-wet conditioning causes a reduction in characteristic strength for all batches conditioned for three months when compared to their non-conditioned equivalents. A less obvious trend occurs for the batches after six months of continuous conditioning. Eleven, out of 28 paired (3 and 6 months) batches now show an increase in mean strength for the temperature of 40°C. Similarly, half of the 30 and 50°C test batches exhibited this same trend. The specific cause of the increase between the two immersion periods is unknown, but possible influences include the small (five) number of specimens per batch and post curing of the resin over the higher time duration. A reduction has been found when the material is loaded in the 0^{o} direction with the largest at 30% for the mean and 28% for the characteristic. The effects of temperature and the specific causes of the increase in strengths between the two immersion durations will require further scientific investigation.

It is observed that increasing the d/t ratio for specimens tested after hot-wet conditioning causes a decrease in pin-bearing strength. This finding is similar to that reported in Chapter 4 for the non-aged material. The lowest strengths are found for the largest pin size (M20), which strengthens the case for the determination of pin-bearing strength to use a standard test methodology that tests the worst case scenario for d/t, and includes the clearance hole size allowing for fabrication tolerance. Moreover, the guidance provided by the pultruder in the company's design manual that, following employment of test standard ASTM D953:2010 for the determination of pin-bearing strength, stipulates a 15% reduction has been shown to be acceptable for non-aged material; although this finding is generally adhered to it is violated by test results from a number of batches.

The water mass uptake due to immersion for six months at 40°C is found to be 25% higher than the change after three months. There is reason to believe the moisture absorption follows the (linear) Fickian diffusion curve, and so the moisture results were used to calculate using the Arrhenius equation an equivalent service-life time period at a lower service temperature. The accelerated aging regimes and long-term strength prediction modelling has shown a mean pin-bearing strength reduction of up to 25% over 7.8 years, at the UK mean service temperature of 10.5°C. This value is found to lie within the bounds set by the American LRFD pre-standard (ASCE, 2012) and gives confidence to the mandatory design requirements.

CHAPTER 6

Bolted Connections in Pultruded FRP

6.1. Introduction

The design of bolted connections in PFRP materials is more multifaceted than for traditional structural materials such as steel. Pultruded materials, often connected with stainless steel bolting due to the ease of assembly and maintenance when compared to adhesive bonding, require a fundamental understanding of the failure modes to produce safe and reliable designs. A typical example of a railway platform assembly of PFRP material is shown in Figure 6.1, with connection details of using simple bolted connections.

Bolted connections not only cause discontinuities in the reinforcing fibres and hence reduce the overall strength of the material, but also introduce complex stress concentrations, which encourage fracture. Furthermore, due to the orthotropic and layered nature of the material, the through thickness stress fields are varied and failure modes can differ significantly. There have been various research endeavours, particularly in the past decade as summarized by

Thoppul *et al* (2009) and Mottram and Turvey (2003), to explore the strength and behaviour of FRP bolted connections. Despite this extensive research database, there are still considerable gaps in knowledge, which hinder the preparation of verified and reliable design clauses for PFRP bolted connections (Mottram, 2009a).

Figure 6.1: Example of Bolted Connections used in a Railway Platform Assembly (Courtesy of Access Design and Engineering Ltd.)

Previous studies (Rosner, 1992; Wang, 2004) have been conducted on plate material which can be somewhat different in fibre architecture and fibre volume fraction to that of structural profiles as used in many PFRP structures, such as shown in Figure 6.1. A summary of previous connections tests has been given in Chapter 2 with key areas of study being split into three areas, as first suggested by Godwin and Matthews (1980), which affect connections, namely, (i) Material parameters, (ii) Fastener parameters and (iii) Design parameters. The material parameters include variables such as fibre architecture (UD, CFM, Mat etc.) of the pultrudate, fibre volume fraction and resin type. Fastener parameters include the level of applied torque, the size of a fastener and use of washers. It should be noted, a significant volume of literature has been concerned with the design parameters of bolted connections which include geometries such as end and side distances, connection type (single-lap, double-lap etc.), number of bolts and hole-pattern.

Researchers have often selected an aspect of the three parameters identified by Godwin and Matthews (1980) and studied it such that the results are not directly applicable for use in design as the geometries were unrealistic or not measured and reliable strength values were not reported with connection tests, particularly for pin bearing strengths. The difficulty, therefore, lies in combining the dissimilar research that has been conducted into a meaningful data set for use, specifically in the preparation of design guidance. Mottram (2009a) found that although some individual connection details from the literature have configurations that adhere to the LRFD Pre-Standard (ASCE, 2012) these are too few to validate the design clauses reliably, specifically for the pin-bearing strength measure.

Presented in this chapter is a study of 325 tension tests conducted with both single and multi-bolted plate-to-plate connections in PFRP material sourced from the web and flange of a WF SuperStructural section specifically targeted to address several key knowledge gaps. These include the possibility of specifying a single bolt connection in designs of PFRP connections, and the strength reduction factor found for single-lap shear connections when compared to double-lap configurations. The aim of study, presented in this chapter, was to investigate the various failure modes known to be associated with bolted connections, in particular the bearing failure mode. The key objective was to use the test results of the bolted connections failing in bearing along with the statistically determined characteristic bearing strengths, presented in Chapter 4, to calibrate a material partial safety factor. This preliminary analysis is presented later in this chapter, for the bearing failure mode for use in design, and is useful for comparison with current specified values with less reliable (Mottram, 2009a) material strengths.

In what follows, firstly, an outline of specimen preparation and the test matrix is given for the bolted connection study. The author's investigations have studied the behavioural effects of

single and double-lap configurations, the number of bolts and their pattern, material type and the geometric end and side distances of the connection. Following the presentation of the salient test results is a discussion of the specific knowledge gaps addressed by this investigation. Conclusions are drawn from the discussion and evaluation of all the test results which look to provide guidance in the design of bolted connections. Finally, a preliminary analysis of a partial factor for the pin-bearing strength measure in accordance with Eurocode procedures outlined in EN 1990 (British Standards Institute, 2001) is given.

6.2. Test Specimen Preparation

Preparation of material for bolted connection test specimens followed a similar procedure as that explained in Section 4.2 to firstly manufacture section blanks from the flange and web material of either 203 x 203 mm or 254 x 254 mm by 9.53 mm SuperStructural sections. The flange and web material was separated by removal of the T-section of resin rich material between the two, using a diamond coated circular saw. The use of soluble oil was used to remove airborne dust and improve the machinability of the material. The prepared sections from the WF profiles were then further cut down to the approximate dimensions for each test specimen, as detailed later, before the bolt-holes and final sizing of specimens using a milling operation. The material has not been conditioned prior to testing, other than stated during the manufacture of specimens, and so has effectively been tested as-received from Creative Pultrusion Inc.

Figure 6.2 shows the convention for dimensions used in the study which followed the PFRP LRFD Pre-Standard (ASCE, 2012) with the geometry defined as follows. The dimensions from the edge of the specimen are the end distance (e_1) and side distance (e_2) from the bolt-hole. The thickness of the specimen (t) is nominally 9.53 mm for all test specimens. Specimen width,

(w) which equals either: ($2e_2$) or ($2e_2$ plus g), where the distance (horizontally) between bolts is the gauge distance (g) or the staggered gauge distance (g_s). Similarly, the distance between bolt rows is the pitch distance (p) and where there are staggered bolting this value becomes the stagger distance (l_s). The specific bolting arrangements are detailed within the next section. The length of the specimens was based on the bolting arrangement in order to be economical with material having a minimum distance of 8d or approximately 100 mm (for the M12 bolt size) maintained between the bolt in a single bolt case or the second row of bolts in the multi-bolt case and the top of the machine grip in all test specimens.

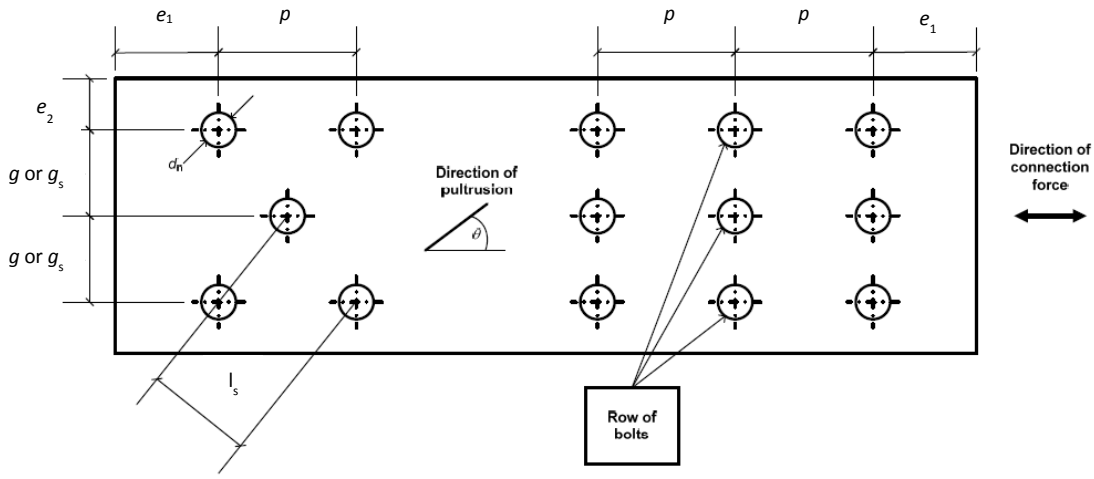

Figure 6.2: Connection Geometry and Definitions in accordance with Section 8.2.5. LRFD Pre-Standard (ASCE, 2012)

The bolt-holes in the test specimens were prepared in two operations, firstly, by drilling a M10 size hole with stub drill at a speed of 2500 rpm and a feed rate of 500 mm/min leaving a 10 mm hole; secondly a finishing hole with a M12 four flute end mill at a speed of 1600 rpm and a feed rate of 637 mm/min. This operation produced the finished hole-size of 13.6 mm ± 0.1mm. The finished dimensions of specimen were achieved by milling around the outside of the perimeter specimen with a four flute end mill at a speed of 1500 rpm and feed rate of 300

mm/min, to the precise end and side distances as well as length required by each specimen batch configuration as detailed in the next section. The specimen was held in place in jig and milled relative to the bolt-hole positions. All drilling and milling operations were done using water soluble coolant with the specific speed and feed rates chosen to both minimise damage to the specimen and ensure longevity of the milling and drill bits. Specimens were supported on the tool exit side by an aluminium plate during the machining process to minimise fibre surface rupture caused by the tool exit.

Specimens that formed a part of a single-lap configuration, and subject to eccentricity, were further processed to include an end tab, which is a packing block (equal to the thickness of a half lap) bonded to the end (opposite to the bolt) of each specimen. This ensures that the joint remains initially straight when held within the grips of the testing machine. It is noted that when a single-lap connection test is initiated the machine grips move apart and the specimen is under both tension and bending – with the initial bending moment equal to the tensile load multiplied by the thickness of one half lap of the single lap connection. The specimens were first abraded to remove an area of surface veil equal to the just larger than the packing block, the surfaces were then cleaned. The end tabs were bonded to the half-lap with Araldite 2015 epoxy adhesive with several short strips of metal wire (nominal diameter of 1 mm) added as between the specimen and the end tab to ensure uniform thickness of adhesive over the bonded area. The end tabs and specimens were clamped and left for at least 24 hours until the adhesive was fully cured.

The specimens were measured prior to testing. The tolerance in specimen dimensions was between ± 0.1 mm for the width, length, side and end distances. This was achieved due to the milling procedure and the precise setting out of the specimen. The thickness of each specimen was measured using an external micrometer to the nearest 0.01 mm, and found to range from

9.36 mm to 9.63 mm (0.27 mm) for web material and 9.48 mm to 10.00 mm (0.52 mm) for flange material.

6.3. Test Matrix

A total of 325 specimens were tested with 65 Series of five specimen batches for the bolted connection investigation. Three types of test configuration were employed including a single-lap shear connection, a double-lap shear connection with either steel or PFRP outer plates. Figure 6.3 shows the two different test configurations employed. Specimens were prepared from material sourced from the flange and web of the of either a 254 x 254 x 9.53 mm or 203 x 203 x 9.53 mm WF SuperStructural sections, as described in Chapter 3. Almost all tests (60 test series of the 65) were conducted with material orientated in the longitudinal direction, relative to the axis of pultrusion. A series of five batches were tested in the transverse direction with four series using a single bolt and one series using two bolts in a row.

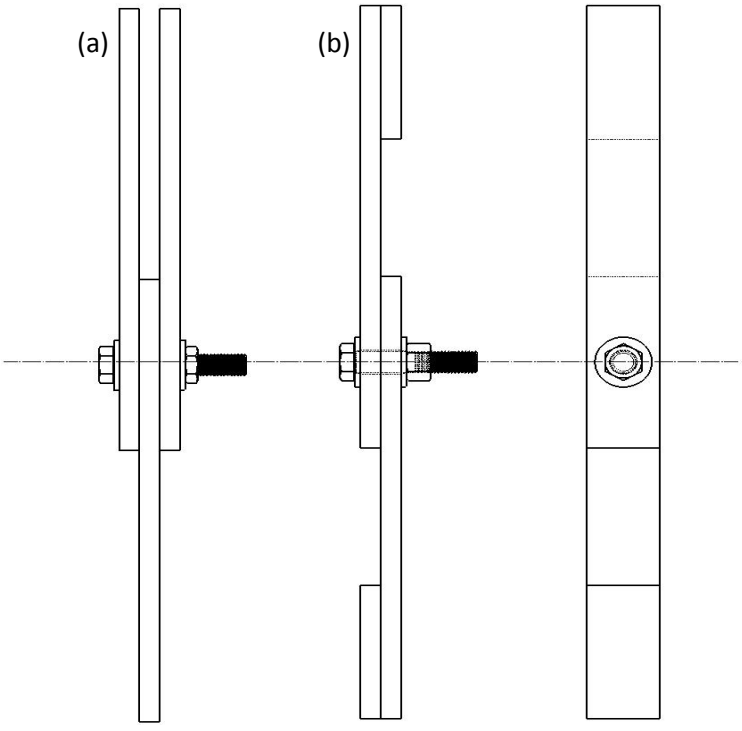

Figure 6.3: Schematic of (a) Double-Lap and (b) Single-Lap Test Configuration for PFRP Bolted Connections

Table 6.1: Minimum requirements for bolted connection geometries in accordance with LRFD Pre-Standard (ASCE, 2012)

Notation (1)	Definition (2)	Minimum Required Spacing (3)	M12 Distance (mm) (4)
e_1	End Distance	4*d* (single) 2*d* (multi)	48 24
e_2	Side Distance	1.5*d*	18
p	Pitch Spacing	4*d*	48
g	Gauge Spacing	4*d*	48
g_s	Staggered Gauge Spacing	2*d*	24
l_s	Stagger Distance	3*d*	36

The specimens were sized in accordance with Table 6.1 and Figure 6.2 in line with *Section "8.2.5. Connection Geometry Requirements"* of the LRFD Pre-standard (ASCE, 2012). It is known (Rosner and Rizkalla, 1995a) that varying the end and side distances it is possible to encourage a bolted connection to fail in a particular failure mode. Although it is not possible to always predict the specific failure mode and indeed mixed modes can occur, the approach to vary both end and side distances was employed in this investigation. Consequently, the key variable investigated was the effect of end distance and side distance upon the failure mode of the bolted connection, with values of 1.5*d*, 2*d* and 4*d* for each distance. The pitch, gauge and staggered pitch (and gauge) distances were not varied from the values specified in column (4) of Table 6.1.

Four (A2) stainless steel bolt sizes were employed for the single bolt tests sized M10, M12, M16 and M20. The multi-bolt tests used a M12 sized bolt only. All tests used 2*d* sized stainless steel washers at least 2.4 mm thick at both the head of the bolt and at the nut in accordance with the LRFD Pre-Standard (ASCE, 2012). A minimal 'finger-tight' level of torque was applied in each test. A clearance of 1.6 mm was used in each test specimen. However, no additional tolerance, as specified with the pin-bearing strength characterisation in Chapters 4 and 5, was used.

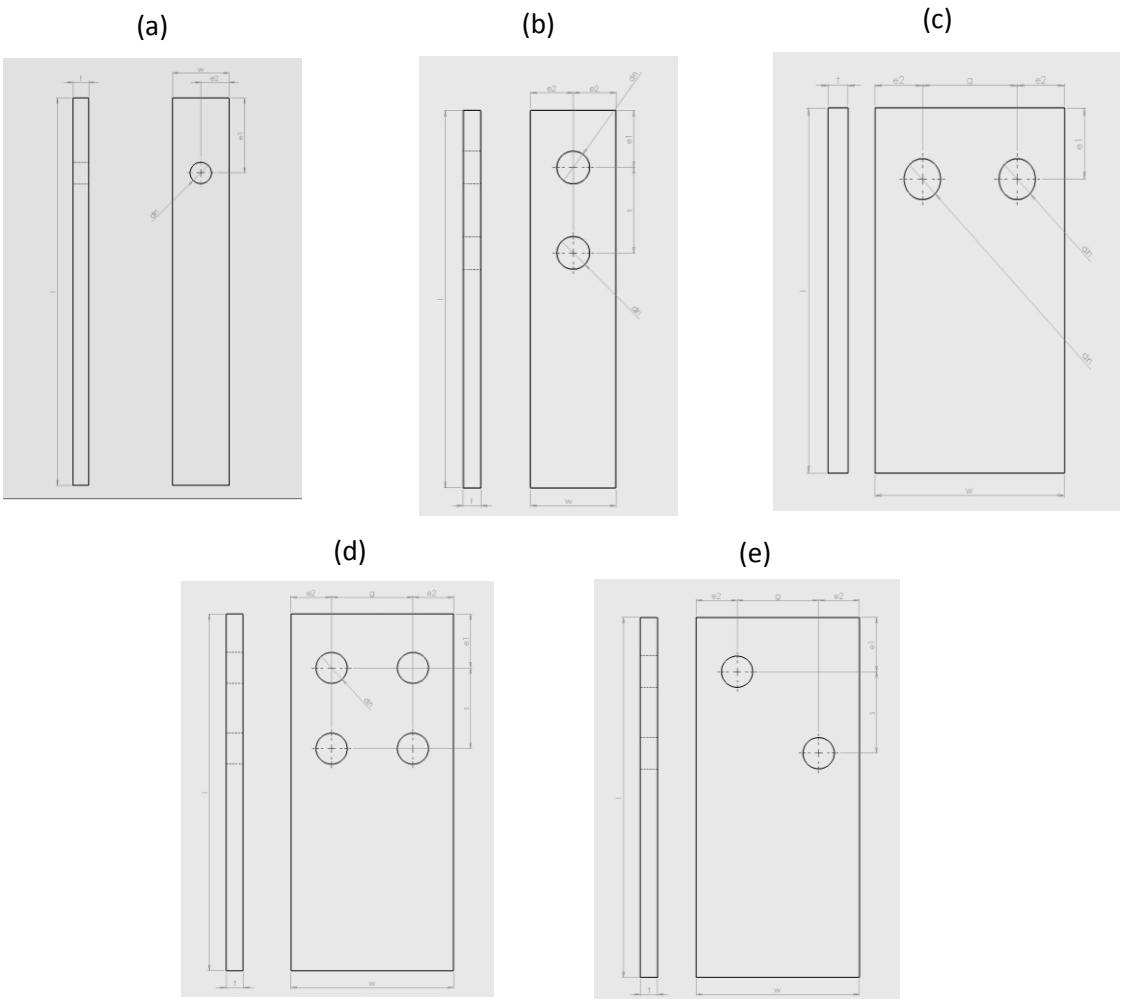

Figure 6.4: Schematic and Major Dimensions of Bolting Arrangements (A) to (E) with (a) Single Bolt, (b) Two Bolts in a Column, (c) Two Bolts in a Row, (d) Four Bolts (2 x 2) and (e) Two Staggered Bolts

Five different bolting patterns were selected in this investigation with a single bolt, two bolts in a row (2 x 1), two bolts in a column (1 x 2), four bolts (2 x 2) and two bolts in a staggered arrangement. The five different bolt-hole arrangements are shown in Figure 6.4. The majority of tests were conducted with either a single bolt or two bolts in a column (1 x 2) arrangement. The five bolting arrangements were labelled from (A) to (E), in order of the configurations stated previously, followed by a batch number (which was sequential without a specific designation for end or side distances) and specimen number for each individual test specimen, for example A1-01. Configurations utilising the single-lap arrangement were labelled with an (a) or (b) after the specimen number for the two parts to the connection and similarly for a

double-lap specimen for three plates of PFRP with (c) for the inner plate, for example B6-01c is an inner plate of a double-lap connection with two bolts in a column.

It should be noted that not all combinations of material, bolt arrangement and test configuration were tested, a full set of test groups are given Table 6.2 and 6.3. Column (1) shows the bolt arrangement, as described previously, for A to E. Column (2) shows the test configuration of either single lap or double connection. The batches were tested with both steel and FRP side plates are indicated with an asterisk in Column (5), which also indicates the material type used. Columns (3) and (4) give the non-dimensional ratio of side distance-to-diameter and end distance-to-diameter, respectively for each test batch. The values marked with a (+) are the minimum values specified within the ASCE Pre-standard (ASCE, 2012).

Table 6.2: Single-bolt Connection Test Matrix

Bolt Arrangement (1)	Test Configuration (2)	e_1/d (3)	e_2/d (4)	Material Type (5)
A (Single Bolt)	Single	1.5	2 4^+	W and F W and F
		2	2 4	W W and F
		4	4	W
	Double	1.5	2 4^+	W* and F W and F
		2	2 4	W* and F W* and F
		4	2 4	W W

In addition to the main study, a supplementary investigation for single bolts were conducted for four different bolt sizes of M10 to M20 with both flange and web material. The side distance was fixed at 2.5*d* and end distance at 5*d*, this was to ensure the connection would fail in bearing, but was not too dissimilar to the minimum specifications of the Pre-standard (ASCE, 2012) to be an unrealistic connection as found in practice. The web material was tested in both the longitudinal (0°) and transverse (90°) directions. The labelling convention was different for this series of single bolt connections with specimen ID in the format of configuration

(A)/material orientation (0 or 90°)/bolt size (M10 to M20). For example the label A/0/M16 would indicate a single bolt tested with a M16 size bolt and the material orientation, with respect to the pultrusion axis and loading direction were parallel.

Table 6.3: Multi-bolt Connection Test Matrix

Bolt Arrangement (1)	Test Configuration (2)	e_1/d (3)	e_2/d (4)	Material Type (5)
B (Row x Column: 2 x 1)	Single	1.5	2^+	W and F
		2	2	W
			4	W and F
	Double	1.5	2^+	W* and F
		2	2	W*
			4	W and F
		4	2	W
			4	W
C (1 x 2)	Single	1.5	2^+	W and F
	Double	1.5	2^+	W, W90 and F
		2	2	W
			4	W
		4	2	W
D (2 x 2)	Single	1.5	2^+	W and F
	Double	1.5	2^+	W and F
		2	2	W
			4	W
E (2 staggered)	Double	1.5	2^+	W and F
		2	2	W
		4	2	W

In total 33 batches (of five specimens) were tested for bolt configuration (A), 14 batches for (B), 8 batches for (C), 6 batches for (D) and 4 for (E). The main emphasis of the study was the characterisation of single and two bolt connections and their associated failure loads and modes.

6.4. Experimental Procedure

The majority of tests were conducted using the double-lap shear configuration with a single inner plate of PFRP material and a steel top fixture made up of three plates of (tool) steel. This configuration has been commonly used by many previous research studies (Mottram and Turvey, 2003) and reduces the number of specimens required. The fixture was made to

accommodate all the test configurations (A) to (D), by machining six bolt-holes with the appropriate distances to accommodate the four test configurations. A second set of steel side plates for the tension loading fixture were machined to accommodate the staggered bolt arrangement (E) and specimens for supplementary single bolt connection study with the four different bolt sizes of M10 to M20. An oversized hole of 25 mm diameter was machined out of the side plates and four pairs of (tool) steel bushings with inner diameters of nominally 10, 12, 16 and 20 mm were produced to house the bolts. This reduced the need for individual side plates for the different pin sizes. The bushings were close fitting (< 0.5 mm) and when located in the over-size hole sat flush with the inner face of the outer side plates of the double-lap fixture. Photographs of the steel tension loading fixtures are shown in Figures 6.5 and 6.6, for the main study and the staggered and single bolt study, respectively.

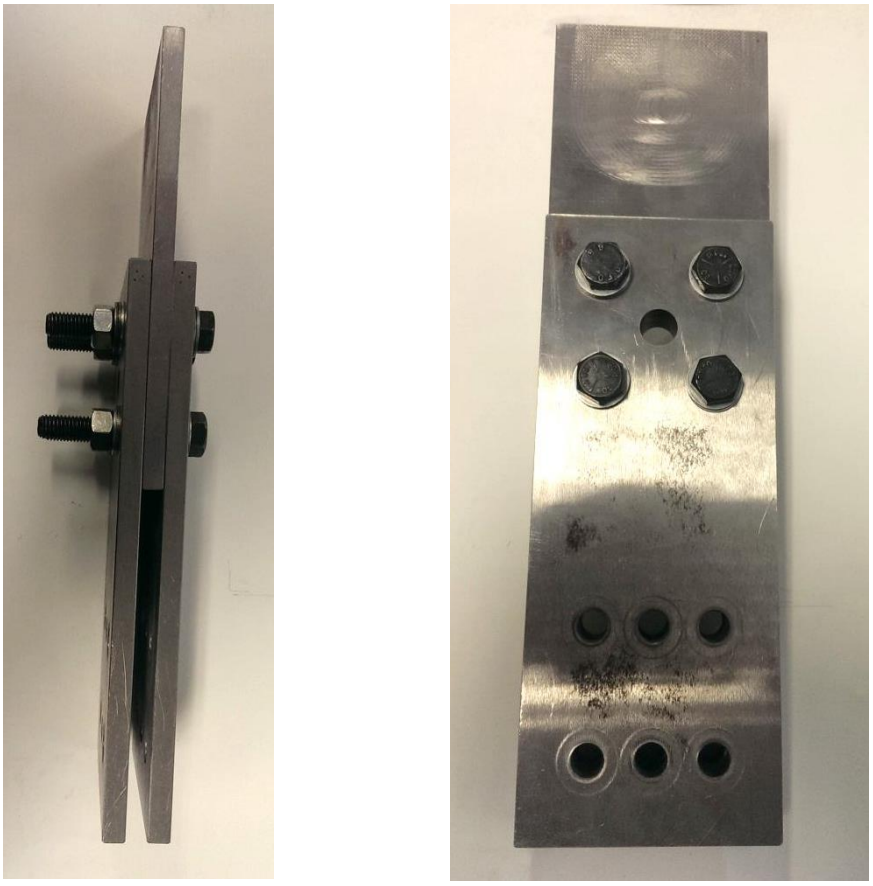

Figure 6.5: Steel Tension Loading Fixture for (A) to (D) Type Bolted Connections Tested with an M12 size Bolt

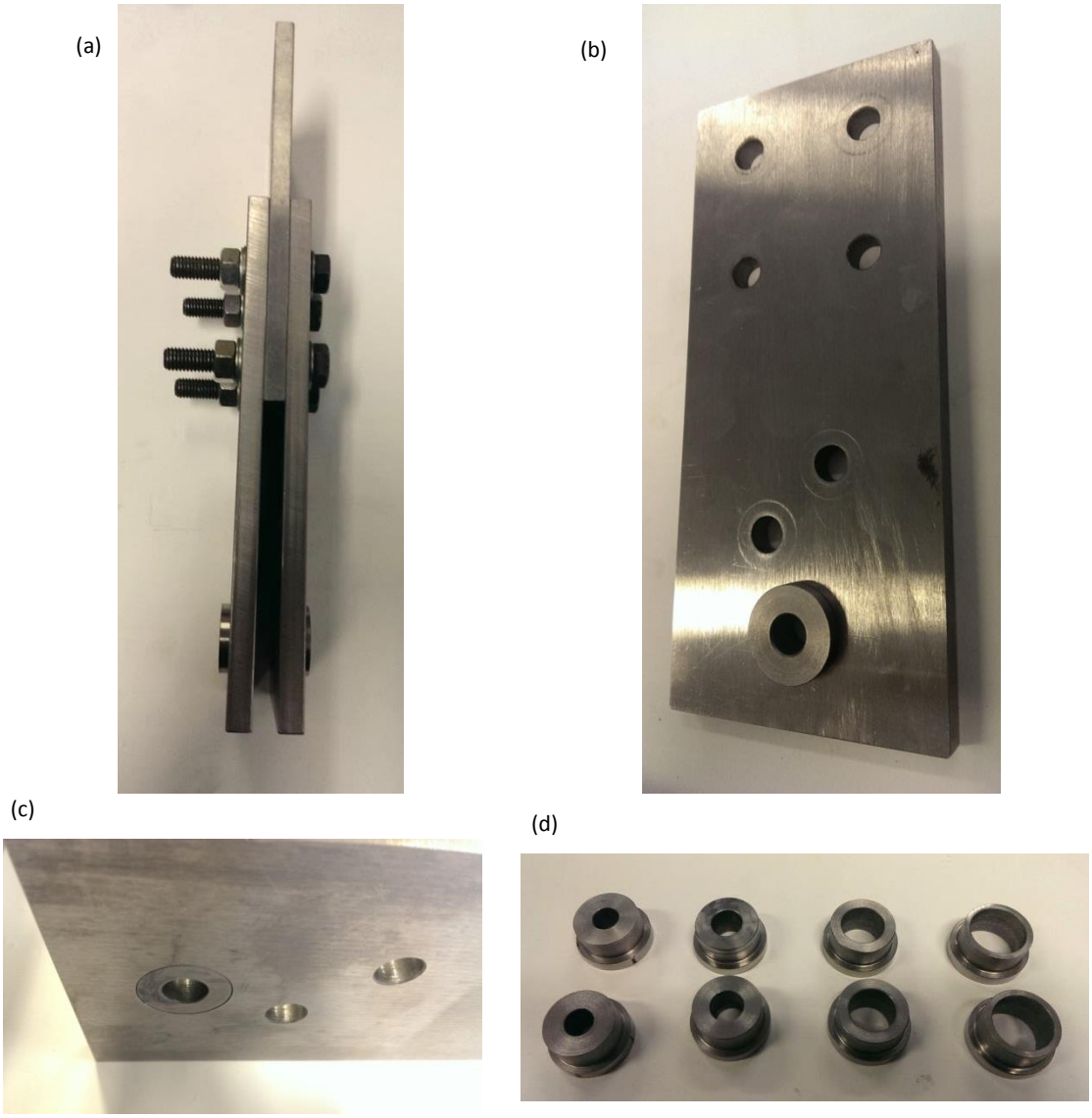

Figure 6.6: Steel Tension Loading Fixture for (A) Type Bolted Connections Tested with Different Bolt Sizes showing (a) The full fixture, (b) An outer plate with a M12 size bushing, (C) the inner face of the plate with a bushing and (d) Bushings with M10 to M20 size inner diameters

Each bolted connection test was conducted under tensile loading on a DARTEC 9500 servo-hydraulic testing machine with a 250 kN load cell. The test procedure involved, firstly, either the steel test fixture or the single lap connection being placed in the top grip, aligned in the fixed top crosshead, and centrally located with pre-marked centrelines on the specimen and grip surface. The top grip was then closed and the lower actuator was raised to meet the lower inner plate of the connection, and gripped. The bolting was in contact with PFRP material prior to commencing the test, however there was some clearance found by an initial displacement

under no load from the load-stroke plots. The load and stroke readings were zeroed and the static strength test was commenced. An example of a bolted connection test just prior to commencement of loading is shown in Figure 6.7.

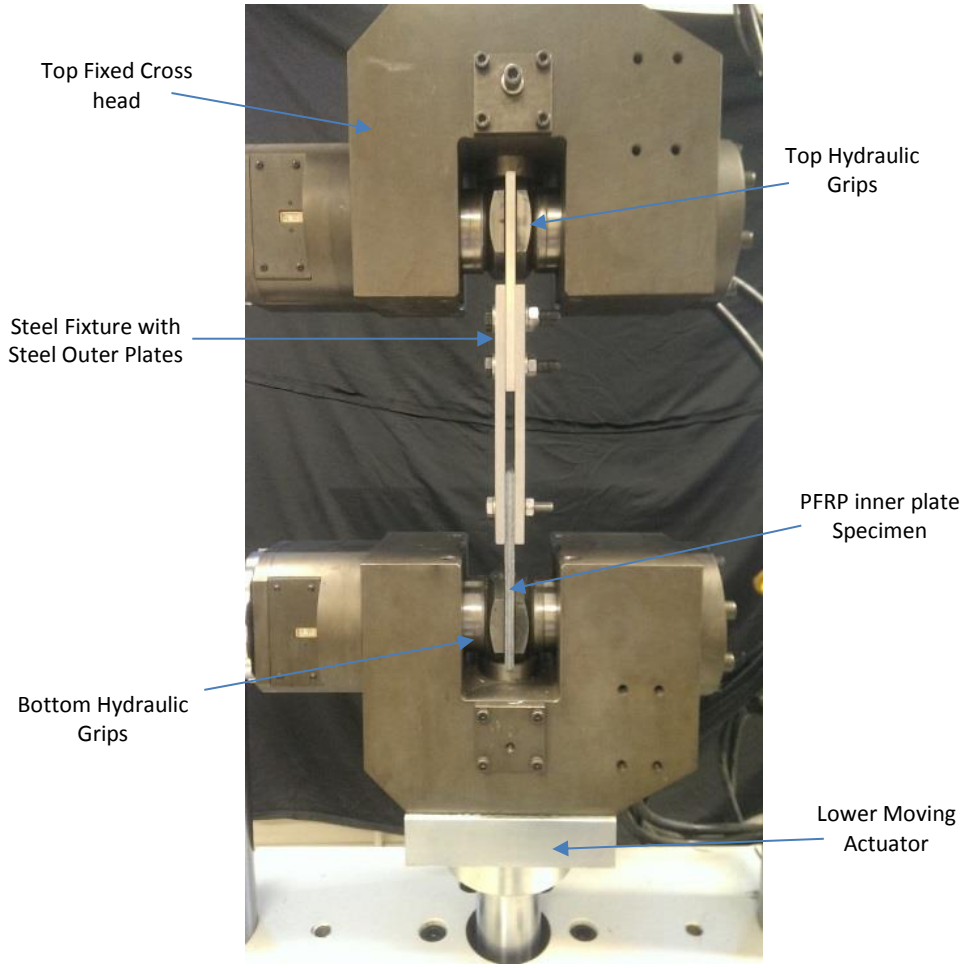

Figure 6.7: Double-Lap Shear Bolted Connection with Steel Outer Plates in the DARTEC 9500 universal Testing Machine prior to Tensile Test

Loading transfer was in-plane for all double-lap connections as the grips moved away from one another with the uniaxial tensile deformation applied under a constant stroke rate of 0.01 mm/s. It should be noted that for the single lap connections the load path, although initially in-plane, became more eccentric as the grips moved apart. The load and machine stroke was recorded once every second by the Cubus software application, which also controlled the machine. The failure load was recorded and the (Cubus) data exported to form load-stroke

plots. The specimens were tested to failure, defined as the load that caused a precipitous drop in the load/displacement plot. First failure is defined as first peak in the linearity of the load-stroke plot. The arrangement of the DARTEC 9500 testing machine and Cubus test setup is shown in Figure 6.8.

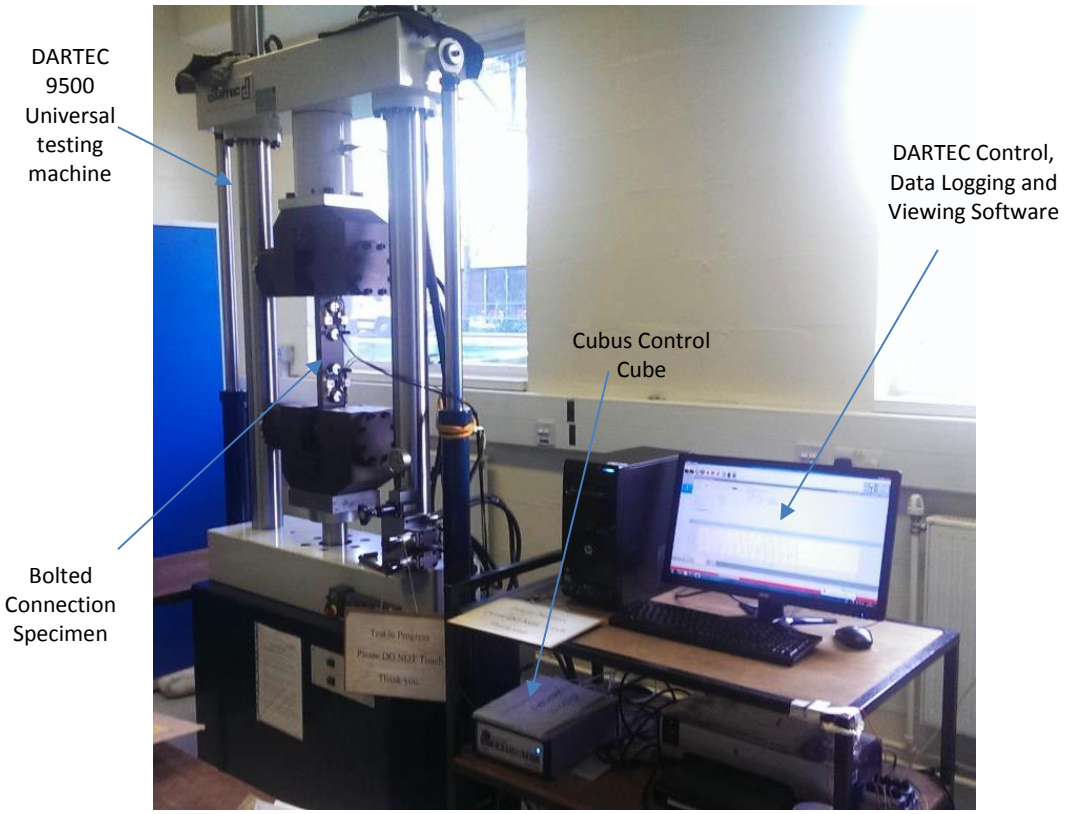

Figure 6.8: Bolted Connection Test Setup and Equipment

It should be noted that not all specimens were able to be tested using the DARTEC 9500 servo-hydraulic testing machine, due to an issue with the upper limit placed on the load, which could not exceed 100kN. This affected specimens with multi-bolt arrangements and particularly bolt configuration (D) with four bolts. The alternative testing arrangement was to use an Amsler Testing machine with the capability to test up to 40 tonnes (≈ 400 kN) under load control. The machine took only load readings in metric tonnes and these were converted to kilonewtons as transcribed within the results tables found in the next section. The same procedure was

executed for tests conducted using this secondary test setup, shown in Figure 6.9, as for the DARTEC 9500 machine setup, with the exception of the machine control and data capture being done manually, and a rate of approximately 10kN/min which matched the time taken in the tests conducted with the DARTEC 9500.

(a) (b)

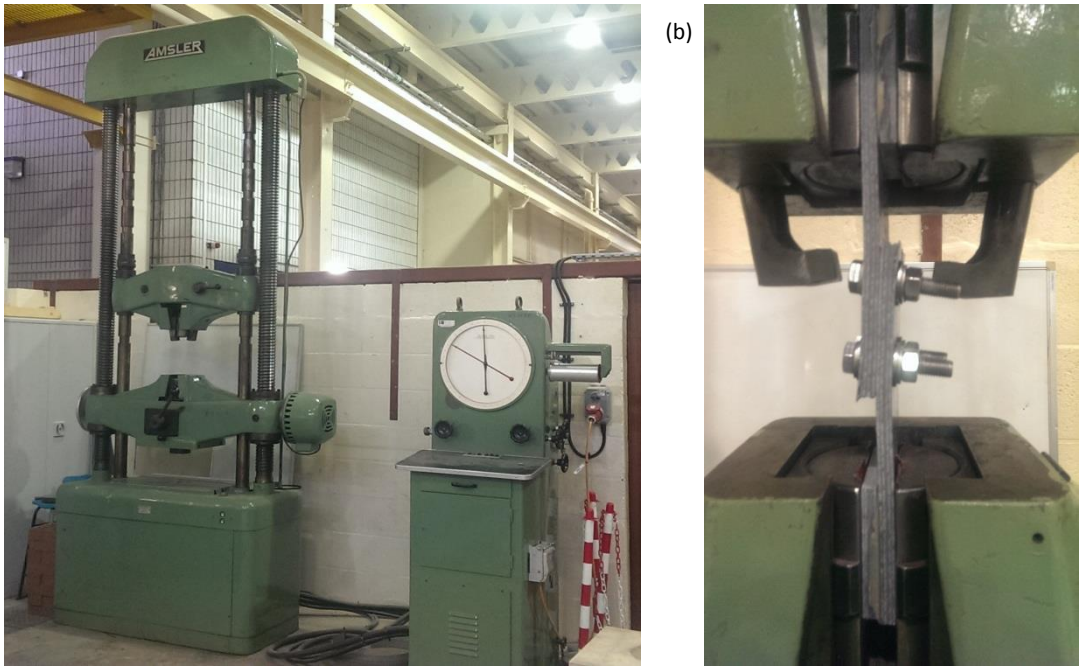

Figure 6.9: Amsler Test Setup with (a) The Testing Machine, Control and Reading Station and (b) A Four Bolt Single-lap Bolted Connection in the Machine Grips

6.5. Test Results and Discussion

Presented in this section are the results from the 65 batches of 5 specimens for the five different bolting arrangements. Each bolt arrangement is dealt with in turn, and the failure modes and loads are reported along with observations of the key trends. During the connection tests both the initial damage (from observation or a precipitous drop in load) and maximum failure loads were recorded. In some tests, linear load-stroke behaviour was observed up until the 'damage' load with the ultimate failure occurring simultaneously. Figure 6.10 shows the some of the failure modes observed from the bolted connection series of tests.

In each section result for each bolt arrangement, due to the large number of batches tested, photographs of the failed specimens with the minimum geometries (ASCE, 2012) are shown. To aid discussion from here-on the abbreviations DL and SL are used to describe the double-lap and single-lap connection configurations, respectively.

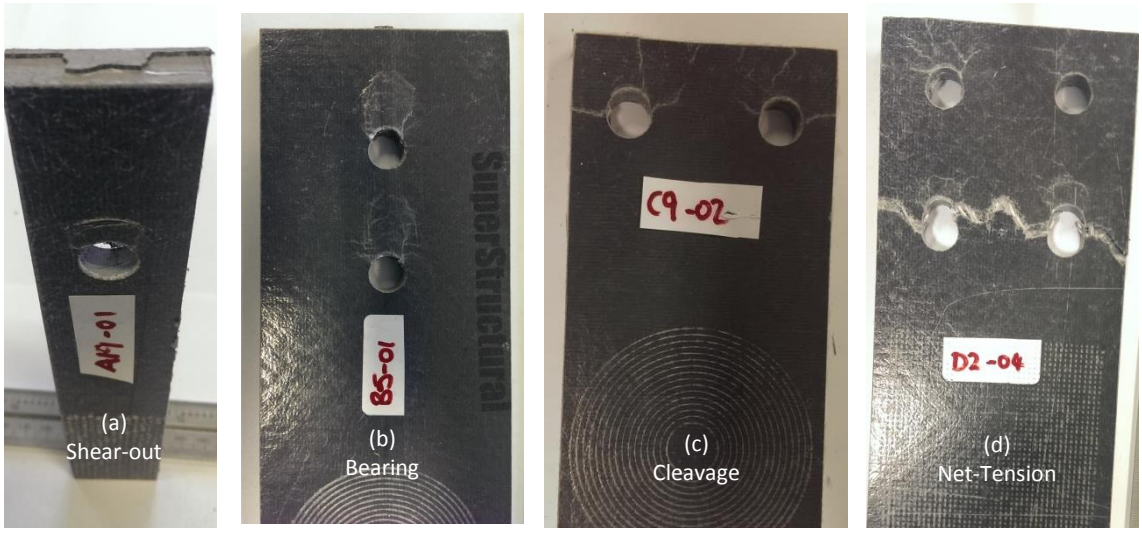

Figure 6.10: Distinct Failure modes of PFRP bolted connections with a WF section showing (a) Shear-out, (b) Bearing, (c) Cleavage and (d) Net-tension failure

Typical load-stroke plots, shown in Figure 6.11, are presented next for the minimum geometries for bolting arrangements (A), (B), (C) and (E) (no load-stroke data was captured using the Amsler testing machine for group (D)). The initial displacement of the specimen is attributed to the bolts not being in contact with the test fixture or specimen bolt hole. In the plots, the load-stroke behaviour of a connection is almost linear until the first failure shown by an initial drop in load or peak in the curve. This was the point at which the load and the failure mode, if visible, were recorded. A limitation of the DL configuration, with steel side plates, is that the initial damage failure mode is not always observable without stopping the test, although the damage load can be found from the first peak in the load-stroke curve. Hereafter, the connection continues to resist the load until ultimate failure, shown by the sudden drop in the load. From inspection, the SL (PFRP to PFRP plate) connection has a far lower stiffness than the DL using the steel side plate fixtures.

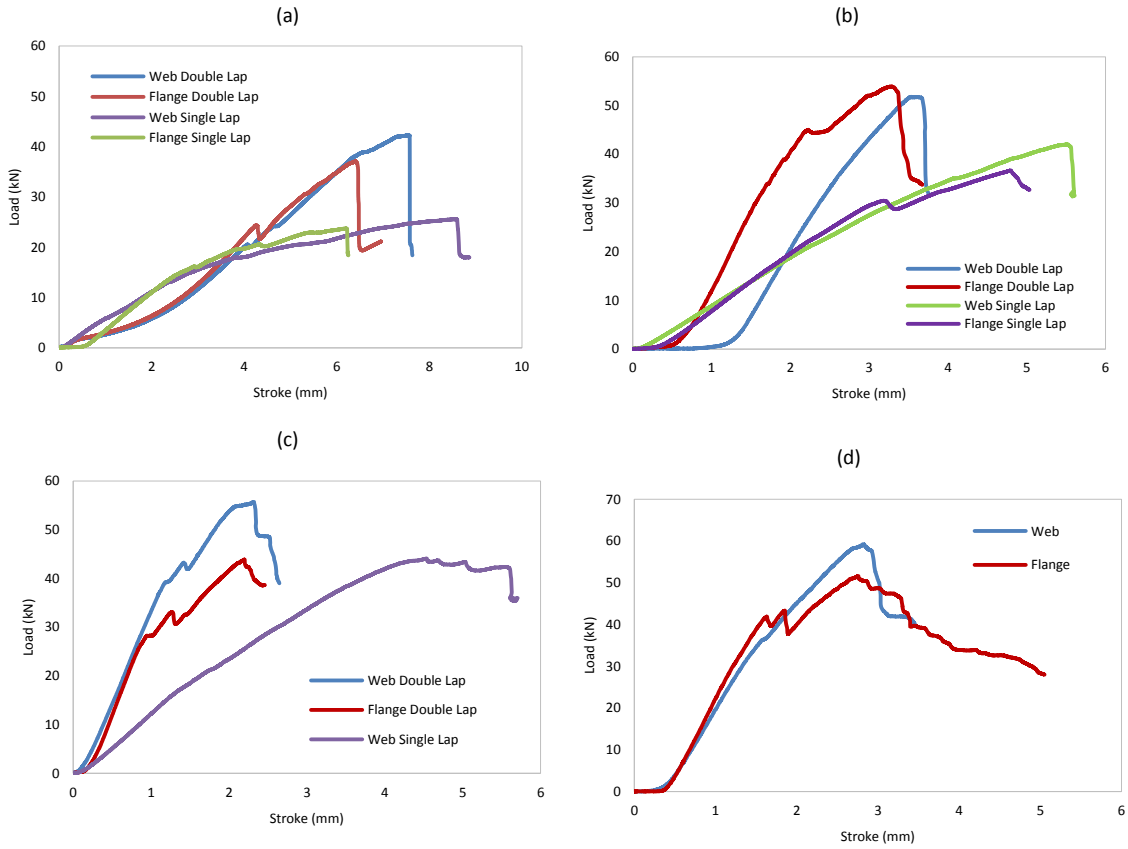

Figure 6.11: Typical Load-Stroke Plots for DL and SL connections with (a) Single Bolts (A), (b) Two Bolts in a Column (B), (c) Two Bolts in a Row (C) and (d) Two Staggered Bolts (E)

The mean for both damage and maximum load of five specimen batches are presented in Tables 6.4 to 6.8 and each bolt configuration is discussed in turn. Each Table (6.4 to 6.8) follows the same convention for data presentation. Column (1) gives the test batch label (ID) along with the material types of either web or flange in column (2). The batches which conform to the minimum requirements ASCE Pre-standard are indicted with a (*) after the test batch label in column (1). Note, the rows have not been arranged in sequential order of test label (column (1)) but with respect to the test set-up, shown in column (3), for double-lap with steel outer plates (Double Lap-S) or PFRP outer plates (Double Lap-F) and single-lap joints (Single Lap). Furthermore, they are arranged firstly in order of end distance, e_1, in column (5) and then side distance, e_2, found in column (6).

As previously, noted, the damage load, shown in column (8) and the associated first failure mode in column (10) were recorded along with the ultimate load, given in column (9), and mode in (11). The abbreviations for failure modes given in columns (10) and (11) are: BR (Bearing); NT (Net-tension); SO (Shear-out) and CL (Cleavage). Note, only the predominant failure mode was recorded at the damage and ultimate failure loads, although as discussed in Chapter 2, multiple failure modes can (and did) occur simultaneously. In the following sub-sections, firstly, the single bolt tests are considered with both the M12 bolt test series and then multiple bolt series with both longitudinal and transverse web material and 0° flange. Finally, the results for two bolt arrangements are given followed by the four bolt case.

6.5.1. Single Bolt Connections

Figure 6.12 shows typical failures in single bolt connections with an end distance of 4*d* and side distance of 1.5*d* (minimum ASCE, 2012 geometry). Parts (a) and (b) are for web material for a double-lap and the single lap specimen, respectively. Parts (c) and (d) are double and single lap flange specimens. The typical failure mode for web material is firstly bearing at the bolt-hole for both DL and SL connections, followed by net-tension.

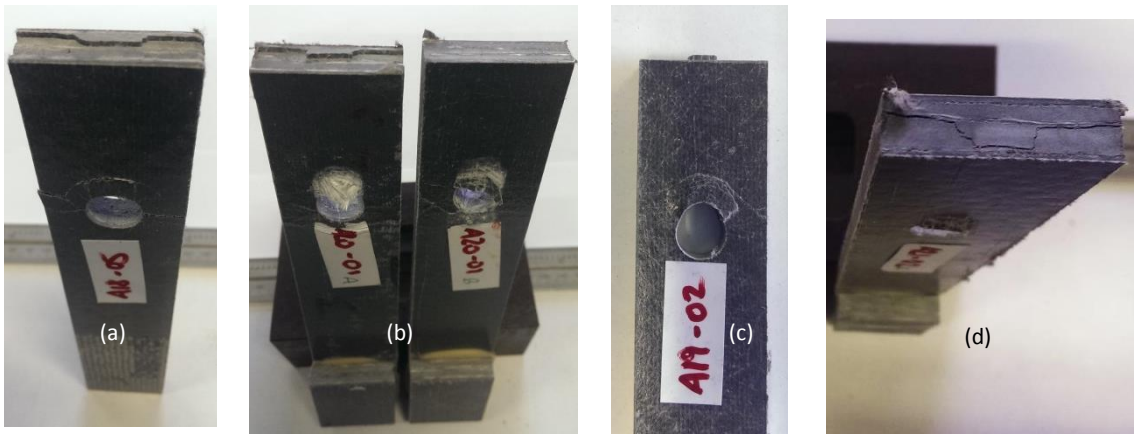

Figure 6.12: Single Bolt Failed Specimens for (a) Web DL, (b) Web SL, (c) Flange DL and (d) Flange SL

In the flange material the ultimate failure is shear-out, this can be attributed to the larger proportion of UD fibres in the flange than the web.

A summary of single bolt connections of web and flange material is given in Table 6.4. The coefficient of variation for this test series ranges from 2.6 to 21% with a mean of 9.8% for all batches. The largest variation is found for batches A17 and A18, which failure primarily in bearing. From Table 6.4, the predominant first failure modes of bearing and shear-out are found for all batches, with a larger end distance changing the mode from shear-out to bearing.

Table 6.4: Mean Batch Test Results for Single Bolt Connections (A)

Test Label (1)	Material (2)	Test Setup (3)	Specimen Thickness, t (mm) (4)	End Distance, e_1 (mm) (5)	Side Distance, e_2 (mm) (6)	Width, w (mm) (7)	Damage Load (kN) (8)	Maximum Load (kN) (9)	1st Failure Mode (10)	2nd Failure Mode (11)
A1	Web	Double Lap-S	9.37	24.0	18.0	36.0	21.2	27.2	SO	NT
A2	Web	Double Lap-S	9.46	24.0	24.0	48.0	18.0	27.6	SO	NT
A3	Web	Double Lap-S	9.40	24.0	48.0	96.0	18.3	27.6	SO	SO
A18*	Web	Double Lap-S	9.53	48.0	18.0	36.0	22.3	38.5	BR	NT
A4	Web	Double Lap-S	9.40	48.0	24.0	48.0	19.6	50.0	BR	SO
A5	Web	Double Lap-S	9.39	48.0	48.0	96.0	32.8	56.4	BR	SO
A13	Flange	Double Lap-S	9.49	24.0	18.0	36.0	14.5	21.5	SO	-
A14	Flange	Double Lap-S	9.48	24.0	24.0	48.0	14.5	21.5	SO	-
A15	Flange	Double Lap-S	9.48	48.0	24.0	48.0	22.2	35.8	BR	-
A19*	Flange	Double Lap-S	9.50	48.0	18.0	36.0	24.1	34.9	BR	SO
A6	Web	Double Lap-F	9.38	24.0	18.0	36.0	18.8	21.9	BR	SO
A7	Web	Double Lap-F	9.54	24.0	24.0	48.0	14.0	18.8	SO	-
A11	Web	Double Lap-F	9.43	48.0	24.0	48.0	21.3	44.8	BR	-
A8	Web	Single Lap	9.55	24.0	18.0	36.0	15.8	-	SO	-
A9	Web	Single Lap	9.52	24.0	24.0	48.0	17.7	-	SO	-
A20*	Web	Single Lap	9.54	48.0	18.0	36.0	14.1	22.0	BR	NT
A10	Web	Single Lap	9.53	48.0	24.0	48.0	13.8	21.4	BR	-
A12	Web	Single Lap	9.45	48.0	48.0	96.0	20.8	29.8	BR	-
A16	Flange	Single Lap	9.52	24.0	24.0	48.0	12.6	13.6	SO	-
A17	Flange	Single Lap	9.49	48.0	24.0	48.0	21.0	24.5	BR	SO
A21*	Flange	Single Lap	9.57	48.0	18.0	36.0	15.8	22.8	BR	SO

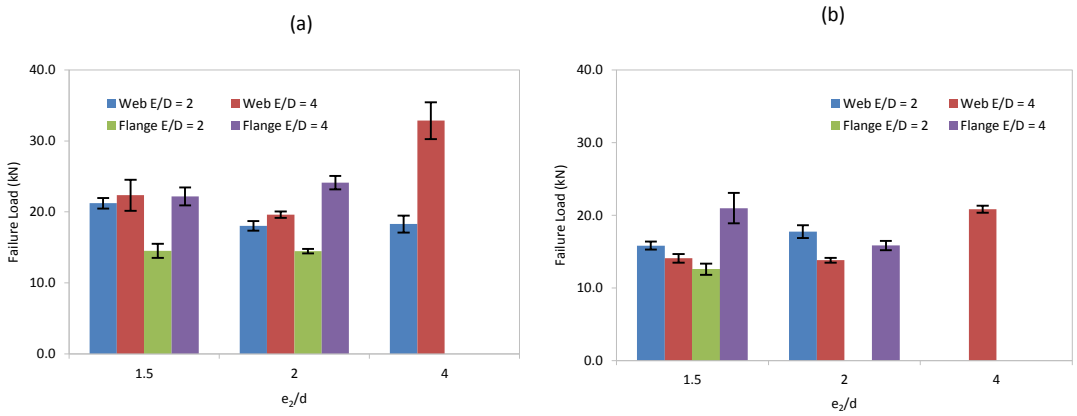

Figure 6.13: Failure loads for Single Bolt Connections, (A) series, with a M12 bolt for various side distance-to-bolt diameter (e_2/d) ratios tested in (a) DL and (b) SL

Figure 6.13 shows the failure loads for the three (e_2/d) ratios of 1.5, 2 and 4. For web material and DL arrangement (Figure 6.13a) a reduction in strength is found as (e_2/d) increases for the constant 2d end distance. The opposite trend occurs for the SL arrangement, with the same parameters for the web batch, with an increase in strength with larger (e_2/d) ratios. Strength values for flange material is similar for (e_1/d) = 2 in the DL and SL cases. Generally, the SL batch test mean results are 37% lower than the DL equivalent.

Table 6.5 presents the test result for the supplementary series of tests with configuration (A) bolt configuration. All specimens failed in the bearing mode with the ultimate failure of Web 90° being net-section. As the UD fibre rovings are orientated parallel to the net-section plane, it is unsurprising that failure is in tension across the section. Note, a (-) signifies no result was recorded or occurred for the particular value and batch.

Table 6.5: Mean Batch Test Results for Single Bolt Connections (A) tested with a M10 to M20 size bolts

Test Label	Material	Test Setup	Specimen Thickness, t (mm)	End Distance, e_1 (mm)	Side Distance, e_2 (mm)	Width, w (mm)	Damage Load (kN)	Maximum Load (kN)	Failure Mode	2nd Failure Mode
(1)	(2)	(3)	(4)	(5)	(6)	(7)	(8)	(9)	(10)	(11)
A/0/M10	Flange	Double Lap-S	9.59	50.0	25.0	50.0	23.1	-	BR	-
A/0/M12	Flange	Double Lap-S	10.0	60.0	30.0	60.0	24.9	-	BR	-
A/0/M16	Flange	Double Lap-S	9.86	80.0	40.0	80.0	30.4	-	BR	-
A/0/M20	Flange	Double Lap-S	9.99	100	50.0	100	40.4	-	BR	-
A/0/M10	Web	Double Lap-S	9.63	50.0	25.0	50.0	23.7	-	BR	-
A/0/M12	Web	Double Lap-S	9.63	60.0	30.0	60.0	23.0	-	BR	-
A/0/M16	Web	Double Lap-S	9.62	80.0	40.0	80.0	28.1	-	BR	-
A/0/M20	Web	Double Lap-S	9.62	100	50.0	100	41.0	-	BR	-
A/90/M10	Web 90	Double Lap-S	9.61	50.0	25.0	50.0	26.1	26.5	BR	NT
A/90/M12	Web 90	Double Lap-S	9.62	60.0	60.0	30.0	24.9	31.6	BR	NT
A/90/M16	Web 90	Double Lap-S	9.62	80.0	40.0	80.0	37.4	43.8	BR	NT
A/90/M20	Web 90	Double Lap-S	9.62	100	50.0	100	47.3	50.8	BR	NT

Figure 6.14 shows that as the bolt diameter increases the failure load increases. It is found that an average 12% higher load is exhibited by web 90° batches when compared to web 0° for all bolt sizes. Flange and web material have similar failure loads in bearing (in the longitudinal direction) for all bolt sizes.

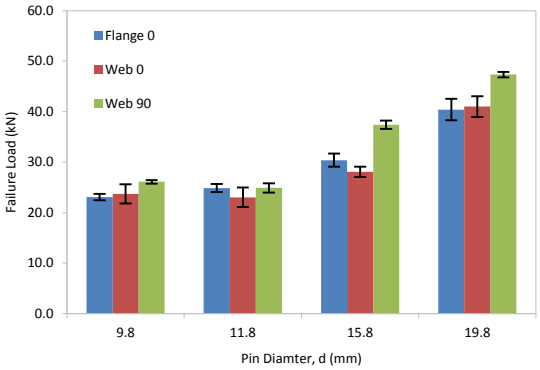

Figure 6.14: Failure loads for Single Bolt Connections, (A) series, with a M10 to M20 bolt sizes

6.5.2. Two bolt Connections

6.5.2.1. Two Bolts in a Column

Figure 6.15 shows the typical failed specimens for bolting arrangement (B). Similar failure trends are exhibited as single bolt connections, with most first failures being shear-out or bearing failure. The difference is the ultimate failure of the connections with a small ≤2d (e_2) are in net-section failure, shown in Figure 6.15 parts (a) and (b), across the first bolt row.

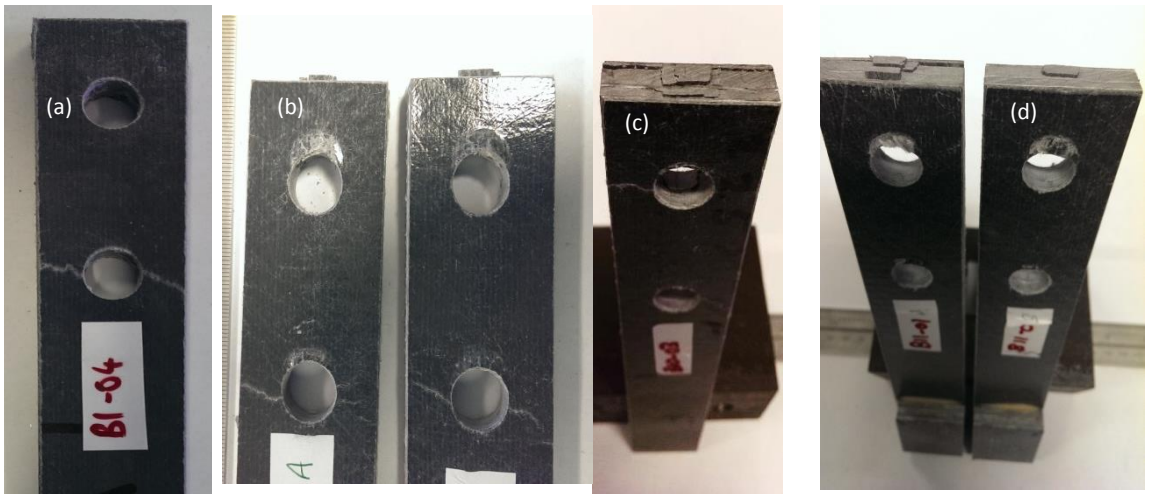

Figure 6.15: Two Bolt in a Column Failed Specimens for (a) Web DL, (b) Web SL, (c) Flange DL and (d) Flange SL

Table 6.6 gives a summary of the test results from the two bolts in a column series, with the mean failure loads plotted in Figure 6.16 for the different end and side distances.

Table 6.6: Mean Batch Test Results for Two Bolt in a Column Connections (B)

Test Label (1)	Material (2)	Test Setup (3)	Specimen Thickness, t (mm) (4)	End Distance, e_1 (mm) (5)	Side Distance, e_2 (mm) (6)	Width, w (mm) (7)	Damage Load (kN) (8)	Maximum Load (kN) (9)	1st Failure Mode (10)	2nd Failure Mode (11)
B1*	Web	Double Lap-S	9.53	24.0	18.0	36.0	32.5	48.1	SO	NT
B2	Web	Double Lap-S	9.51	24.0	24.0	48.0	36.3	64.4	SO	NT
B3	Web	Double Lap-S	9.38	24.0	48.0	96.0	41.8	72.5	BR	SO
B4	Web	Double Lap-S	9.44	48.0	24.0	48.0	46.1	80.8	BR	NT
B5	Web	Double Lap-S	9.46	48.0	48.0	96.0	80.0	-	BR	-
B10*	Flange	Double Lap-S	9.50	24.0	18.0	36.0	51.3	-	SO	NT
B12	Flange	Double Lap-S	9.48	48.0	24.0	48.0	39.8	70.8	BR	SO
B6*	Web	Double Lap-F	9.54	24.0	18.0	36.0	29.8	45.9	SO	NT
B7	Web	Double Lap-F	9.53	24.0	24.0	48.0	34.9	54.4	BR	NT
B8*	Web	Single Lap	9.46	24.0	18.0	36.0	29.3	38.4	SO	-
B9	Web	Single Lap	9.42	24.0	24.0	48.0	33.7	49.0	SO	-
B13	Web	Single Lap	9.41	48.0	24.0	48.0	30.2	55.0	BR	NT
B11*	Flange	Single Lap	9.48	24.0	18.0	36.0	34.1	50.1	SO	-
B14	Flange	Single Lap	9.48	48.0	24.0	48.0	27.0	44.1	BR	-

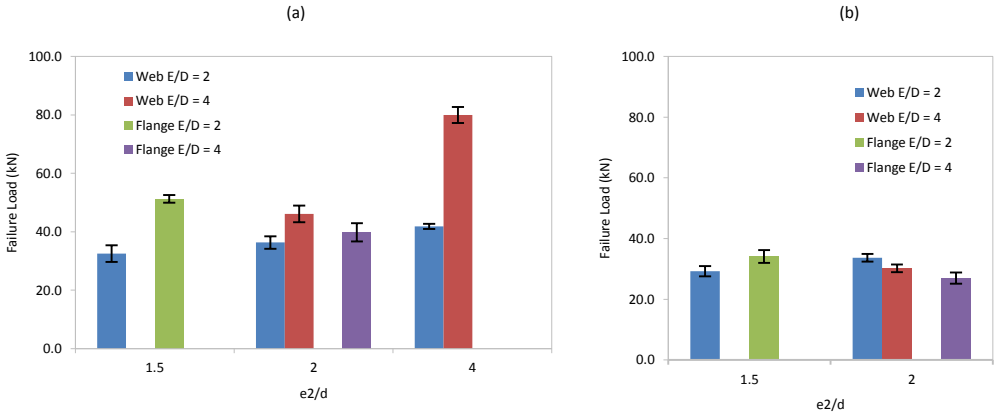

Figure 6.16: Failure loads for Two Bolt Connections, (B) series, for various side distance-to-bolt diameter (e_2/d) ratios tested in (a) DL and (b) SL

6.5.2.2. Two in a Single Row

Figure 6.17 shows the typical failed specimens from the two bolts in a single row (C) test series. Part (a) shows a web specimen that has failed first in shear-out and subsequently in net-

tension. It is observed the net-tension failure cracks propagate along and up towards the area of shear-out, similar, but, not as fully developed as found in block shear. Part (b) shows a typical shear-out failure for the flange material. This would be found in part (a) but the TSFM is causing failure modes dissimilar to those found for PFRP plate (Rosner, 1995).

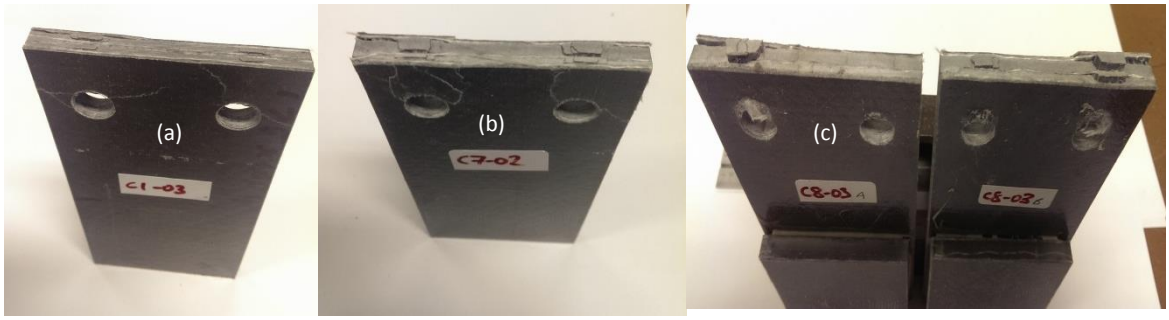

Figure 6.17: Two Bolt in a Row Failed Specimens for (a) Web DL, (b) Flange DL and (c) Flange SL

Presented in Tables 6.7 are the salient test results from the series of two bolts in a row connection tests, with the mean failure loads plotted in the bar chart in Figure 6.18. It can be seen that the side distance has little effect on the load for web material with an end distance of 2*d*, with specimens all failing in shear-out for these specific geometric relations. In contrast when e_2/d = 4 and e_1/d = 2, the strength of web material connections is almost 2.5 times higher than the e_2/d = 2 situation. The only test batch to fail in cleavage is found for web material orientated at 90° to the pultrusion axis. Considering that an end distance of ≤ 2*d* propagates shear-out failure, and at 90° the UD rovings act as stress arrestors as noted by Turvey (1998), it is unsurprising that the cracks develop to form a cleavage-type failure.

The difference between the flange and web material with the minimum geometric relations (ASCE. 2012) shows the former is 26% and 40% higher than the latter for DL and SL configurations, respectively. The reduction in strength values of SL compared to DL is 6% for web and 23% for flange. The larger proportions of TSFM in the web and more uniform

architecture improve materials ability to resist the out-of-plane deformations and stresses caused by the SL configuration. Furthermore, Figure 6.17c shows the shear out failure propagating in the thicker UD layer of the flange, leading to the understanding that the complex TSFM and fibre architecture, in general, have a significant influence on the failure modes and loads especially for the single-lap configuration with two bolts in a row.

Table 6.7: Mean Batch Test Results for Two Bolt in a Row Connections (C)

Test Label (1)	Material (2)	Test Setup (3)	Specimen Thickness, t (mm) (4)	End Distance, e_1 (mm) (5)	Side Distance, e_2 (mm) (6)	Width, w (mm) (7)	Damage Load (kN) (8)	Maximum Load (kN) (9)	1st Failure Mode (10)	2nd Failure Mode (11)
C1*	Web	Double Lap-S	9.41	24.0	18.0	84.0	39.4	56.6	SO	NT
C2	Web	Double Lap-S	9.39	24.0	24.0	96.0	33.8	56.0	SO	-
C3	Web	Double Lap-S	9.51	24.0	48.0	144.0	32.6	50.3	SO	-
C4	Web	Double Lap-S	9.36	48.0	24.0	96.0	90.6	106	BR	NT
C7*	Flange	Double Lap-S	9.51	24.0	18.0	84.0	29.0	39.0	SO	NT
C9*	Web 90	Double Lap-S	9.53	24.0	18.0	84.0	48.1	-	CL	-
C6*	Web	Single Lap	9.43	24.0	18.0	84.0	37.0	40.1	SO	-
C8*	Flange	Single Lap	9.48	24.0	18.0	84.0	22.3	28.1	SO	-

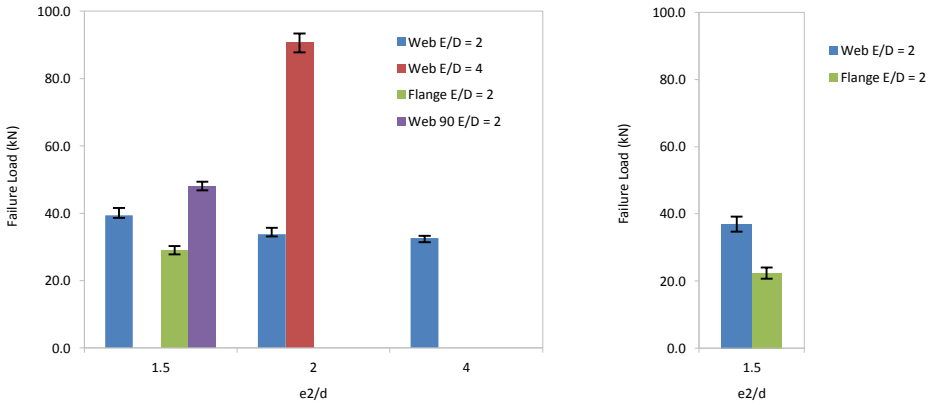

Figure 6.18: Failure loads for Two Bolt Connections, (C) series, for various side distance-to-bolt diameter (e_2/d) ratios tested in (a) DL and (b) SL

6.5.2.3. Two Staggered Bolts

Figure 6.19 presents the typical failure of specimens found for each batch of the two staggered bolt series. The result of the staggered bolt connection tests are given in Table 6.8 and failure loads shown in Figure 6.19. It can be seen that (e_2/d) doesn't significantly affect the failure

load; however for the largest value of this ratio a block shear type failure is found. This (E3) is the only batch from the entire bolted connection study to fail in this manner.

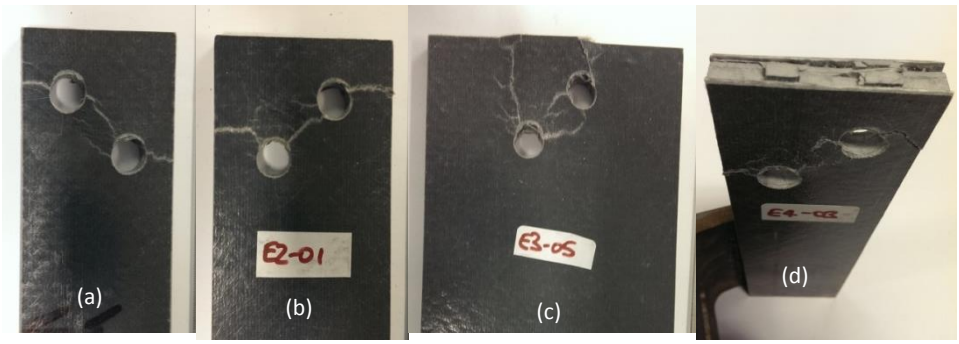

Figure 6.19: Two Staggered Bolt Failed Specimens for batch (a) E1 (b) E2, (c) E3 and (d) E4

Further work is required to explore this type of failure and in particular the failure modes associated with the staggered bolt arrangement. Considering there is a need to support mandatory clauses in the ASCE Pre-standard (2012) for staggered bolt arrangement failure modes, and the limited number of tests presented here, it would be most useful if future bolted connection research characterises a wider range of variables (geometric relations, bolt sizes etc.) of staggered bolt arrangements with PFRP shapes.

Table 6.8: Mean Batch Test Results for Two Staggered Bolt Connections (E)

Test Label (1)	Material (2)	Test Setup (3)	Specimen Thickness, t (mm) (4)	End Distance, e_1 (mm) (5)	Side Distance, e_2 (mm) (6)	Width, w (mm) (7)	Damage Load (kN) (8)	Maximum Load (kN) (9)	1st Failure Mode (10)	2nd Failure Mode (11)
E1*	Web	Double Lap-S	9.51	24.0	18.0	60.0	38.9	59.1	SO	NT
E2	Web	Double Lap-S	9.53	24.0	24.0	72.0	41.6	63.1	SO	NT
E3	Web	Double Lap-S	9.52	24.0	48.0	120	37.5	62.9	SO	BS
E4*	Flange	Double Lap-S	9.51	24.0	18.0	60.0	40.4	51.4	SO	NT

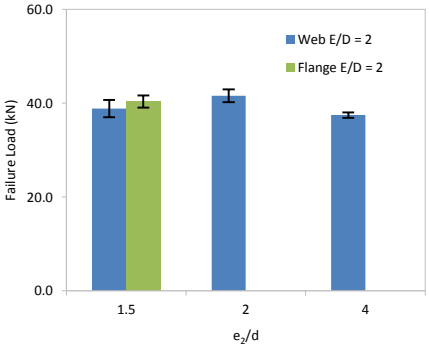

Figure 6.20: Failure loads for Two Bolt Connections, (E) series, for various side distance-to-bolt diameter (e_2/d) ratios tested in DL

6.5.3. Four Bolt Connections

Figure 6.21: Four Bolt Failed Specimens for (a) Web DL, (b) Web SL, (c) Flange DL and (d) Flange SL

Figure 6.21 presents the typical failure modes for four bolt DL and SL bolted connections to the Pre-standard minimum geometries (ASCE, 2012). In comparing 6.21a and 6.21c for the DL configuration it can be seen that the material architecture makes a significant difference on the failure mode of the connection. Part (a) for web material shows a specimen plate that has failed in net-tension, after the initial shear-out, whereas part (c) for the same geometry with flange material, shows a unique double shear-out/cleavage failure at the ultimate strength. The SL configuration in parts (b) and (d) are quite similar with shear-out being the dominant initial failure mode. Due to the rotation of the bolt, as shown in Figure 6.22, causing a local

bearing stress concentration on the bolt-hole edge and surface region, a cleavage failure occurs at the ultimate load value, with the rupture of the outer face of the specimens.

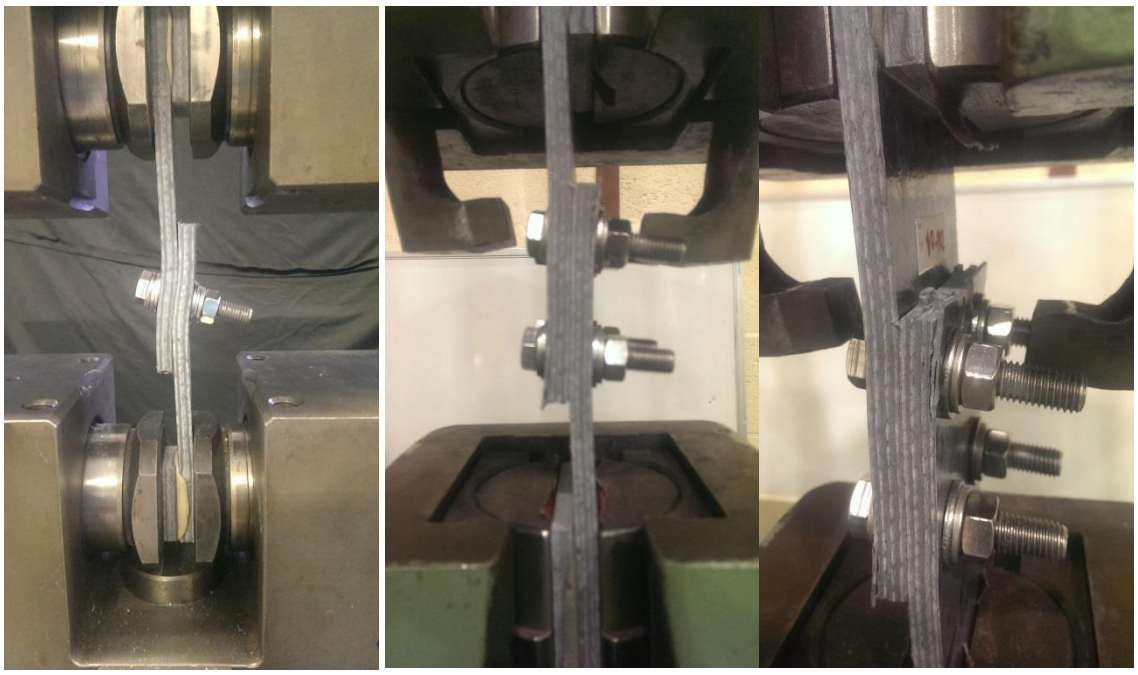

Figure 6.22: Rotation of the bolt in a Single-lap Shear Connection Test

Presented in Table 6.9 are the mean batch results for the four bolt test configuration and associated failure loads plotted for end and side distances in Figure 6.23. It can be seen from comparing Figure 6.23a to 6.23b the failure loads are significantly lower for the SL connections when compared to the DL. The average reduction is found to be 30 and 34% for web and flange materials, respectively, with the same specimen geometry. It is an aim of this investigation to establish the highest reduction found between the SL and DL test configurations in order to validate the mandatory guidance in the ASCE Pre-standard (2012) that a reduction of 0.6 to strength values based on a DL shear configuration when designing for a SL connection. Hart-Smith (1978) found a 20% reduction for aerospace laminates which are thinner than PFRP. The current 40% reduction is the same as the value specified within BS EN 1993-1-8:2005 for steel structures. The mean normalised reduction in connection failure

load between the DL and SL test configurations is plotted in Figure 6.24, for all batches of specimens studied with both setups.

Table 6.9: Mean Batch Test Results for Four Bolt Connections (D)

Test Label (1)	Material (2)	Test Setup (3)	Specimen Thickness, t (mm) (4)	End Distance, e_1 (mm) (5)	Side Distance, e_2 (mm) (6)	Width, w (mm) (7)	Damage Load (kN) (8)	Maximum Load (kN) (9)	1st Failure Mode (10)	2nd Failure Mode (11)
D1*	Web	Double Lap-S	9.39	24.0	18.0	84.0	97.8	121	SO	NT
D2	Web	Double Lap-S	9.40	24.0	24.0	96.0	119	146	SO	NT
D3	Web	Double Lap-S	9.39	48.0	24.0	96.0	70.1	157	BR	NT
D7*	Flange	Double Lap-S	9.51	24.0	18.0	84.0	74.4	99.2	SO	CL
D6*	Web	Single Lap	9.51	24.0	18.0	84.0	68.6	85.8	SO	CL
D8*	Flange	Single Lap	9.50	24.0	18.0	84.0	47.7	65.6	SO	CL

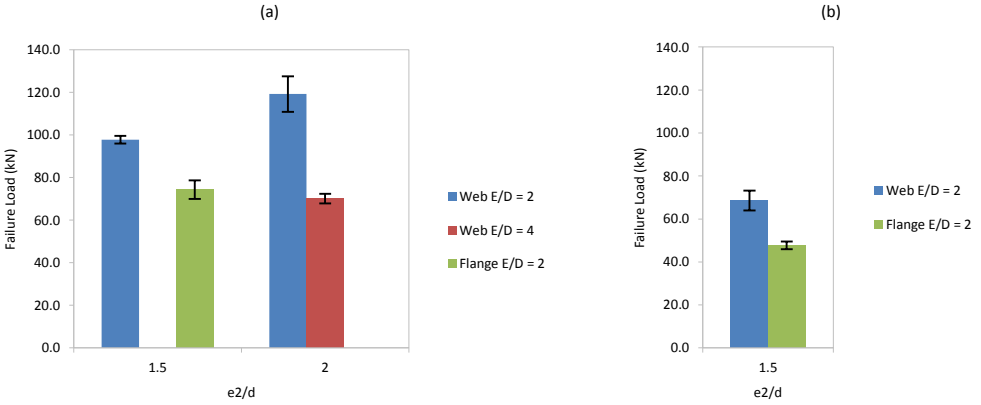

Figure 6.23: Failure loads for Four Bolt Connections, (D) series, for various side distance-to-bolt diameter (e_2/d) ratios tested in (a) DL and (b) SL

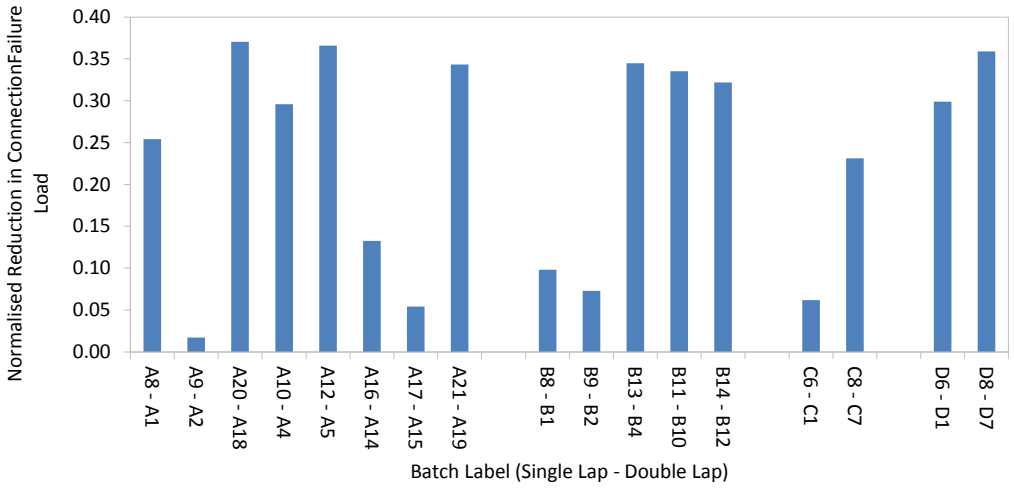

Figure 6.24: Normalised Reduction in Connection Strength for Single-Lap Shear Connections compared with equivalent geometry Double-Lap Shear Connections

The largest reduction is found to be 37% for the single bolt connection with web material and so the recommendation based on the current set of data is the 0.6 factor for SL connection details is appropriate. Next the final section of this chapter is presented for a partial safety factor calibration for bearing strength.

6.6. Partial Safety Factor for Bearing Strengths of PFRP Bolted Connections

Presented next is a preliminary calibration of a partial safety factor, γ_M, for the bearing mode of failure. There are nine steps involved in calibrating a partial safety factor in accordance with Annex D of BS EN 1990:2002. In what follows is a step by step application of the calibration procedure. The combination of test results from Chapter 4 for characteristic pin-bearing strength values are used in conjunction with experimental tests on bolted connections, presented in this chapter, to calibrate a partial safety factor.

Step 1: E*stablishing a 'design model'*

This is Equation (2.1) for the pin-bearing resistance of a bolted connection per bolt (ASCE, 2012). Presented hereafter are the remaining nine steps for the calibration procedure (British Standards Institute, 2001).

Step 2: *Compare experimental and theoretical values*

The theoretical bearing resistance, r_t (i = 1 to n, where n is the number of tests) is found for each bolt configuration presented in Tables 6.4 to 6.8, by substituting the characteristic pin-bearing strength, $F_{\theta,k}^{br}$, (found in Chapter 4) into the resistance formula (Eq 2.1) with the

nominal bolt diameter, *d* and material thickness, *t*. The experimental resistance, r_e is taken as the damage load for each bolted connection test. (A full set of data for each bolted connection test is found in Appendix D). Reported in Tables 6.10 and 6.11 are the experimental and theoretical bearing resistances for single and multi-bolt configurations found to fail in bearing. In Column (1) is the specimen label and columns (2) to (5) are for bolt diameter (d_i), material thickness (t_i), experimental resistance (r_e) and theoretical resistance (r_t), respectively.

Table 6.10: Experimental and Theoretical Bearing Resistances of Single and Multi-bolt Connections

Specimen (1)	d_i (mm) (2)	t_i (mm) (3)	r_e (kN) (4)	r_t (kN) (5)	Specimen (1)	d_i (mm) (2)	t_i (mm) (3)	r_e (kN) (4)	r_t (kN) (5)
B3-01	11.8	9.4	38.7	35.0	WA/0/M10-01	9.8	9.6	18.9	16.4
B3-02	11.8	9.4	42.3	35.1	WA/0/M10-02	9.8	9.6	21.5	16.3
B3-03	11.8	9.3	42.9	35.0	WA/0/M10-03	9.8	9.7	29.0	16.4
B3-04	11.8	9.4	40.9	35.3	WA/0/M10-04	9.8	9.6	24.8	16.4
B3-05	11.8	9.4	44.0	35.1	WA/0/M10-05	9.8	9.6	24.4	16.4
B4-01	11.8	9.5	45.9	35.7	WA/0/M12-01	11.8	9.6	19.6	18.0
B4-02	11.8	9.4	39.6	35.0	WA/0/M12-02	11.8	9.6	25.7	18.0
B4-03	11.8	9.5	41.0	35.7	WA/0/M12-03	11.8	9.6	18.0	18.0
B4-04	11.8	9.4	48.5	35.1	WA/0/M12-04	11.8	9.6	25.6	18.0
B4-05	11.8	9.4	55.6	35.2	WA/0/M12-05	11.8	9.6	26.3	18.0
B12-01	11.8	9.6	44.4	34.2	WA/0/M16-01	15.8	9.6	27.7	25.5
B12-02	11.8	9.5	28.9	33.9	WA/0/M16-02	15.8	9.6	30.5	25.6
B12-03	11.8	9.5	43.0	34.1	WA/0/M16-03	15.8	9.6	28.5	25.6
B12-04	11.8	9.4	45.9	33.7	WA/0/M16-04	15.8	9.6	24.9	25.5
B12-05	11.8	9.4	36.7	33.6	WA/0/M16-05	15.8	9.6	28.9	25.6
B7-01	11.8	9.5	32.0	35.7	WA/0/M20-01	19.8	9.6	40.8	28.6
B7-02	11.8	9.5	32.8	35.6	WA/0/M20-02	19.8	9.6	42.6	28.7
B7-03	11.8	9.6	37.1	35.8	WA/0/M20-03	19.8	9.6	46.3	28.6
B7-04	11.8	9.5	31.7	35.6	WA/0/M20-04	19.8	9.6	40.5	28.7
B7-05	11.8	9.5	41.0	35.7	WA/0/M20-05	19.8	9.6	34.9	28.7
B13-01	11.8	9.5	23.9	21.4	FA//0/M10-01	9.8	9.5	24.2	16.7
B13-02	11.8	9.4	29.9	21.1	FA/0/M10-02	9.8	9.6	21.1	16.8
B13-03	11.8	9.4	37.3	21.0	FA/0/M10-03	9.8	9.7	22.7	16.9
B13-04	11.8	9.4	30.9	21.0	FA/0/M10-04	9.8	9.6	23.5	16.7
B13-05	11.8	9.4	29.0	21.1	FA/0/M10-05	9.8	9.6	23.9	16.8
B14-01	11.8	9.5	25.2	20.5	FA/0/M12-01	11.8	9.6	23.7	17.1
B14-02	11.8	9.5	25.7	20.5	FA/0/M12-02	11.8	10.3	23.7	18.4
B14-03	11.8	9.4	22.3	20.2	FA/0/M12-03	11.8	10.3	25.5	18.3
B14-04	11.8	9.4	33.0	20.2	FA/0/M12-04	11.8	10.3	27.5	18.4
B14-05	11.8	9.5	28.8	20.3	FA/0/M12-05	11.8	9.6	24.0	17.1
FA/0/M20-01	19.8	9.6	35.8	32.3	FA/0/M16-01	15.8	10.3	32.3	30.3
FA/0/M20-02	19.8	9.6	44.0	32.2	FA/0/M16-02	15.8	9.6	26.7	28.0
FA/0/M20-03	19.8	10.2	38.2	34.2	FA/0/M16-03	15.8	9.6	30.5	28.0
FA/0/M20-04	19.8	10.3	45.7	34.6	FA/0/M16-04	15.8	10.2	29.3	29.9
FA/0/M20-05	19.8	10.3	38.2	34.6	FA/0/M16-05	15.8	9.6	33.2	28.2
D3-03	11.8	9.5	70.1	71.0					

Figure 6.24 is a plot of r_e vs r_t for the data presented in Tables 6.10 and 6.11. The linear line of $r_e = r_t$ is to indicate a perfect (ideal) 'design model'. If the model is exact and complete then all

points would lie on this line. As normally found in practice, there is some scatter, with the design model predicting conservative values for bearing resistances.

Table 6.11: Experimental and Theoretical Bearing Resistances of Single Bolt Connections

Specimen (1)	d_i (mm) (2)	t_i (mm) (3)	r_e (kN) (4)	r_t (kN) (5)	Specimen (1)	d_i (mm) (2)	t_i (mm) (3)	r_e (kN) (4)	r_t (kN) (5)
A18-01	11.8	9.7	26.7	18.1	A11-01	11.8	9.4	29.0	17.6
A18-02	11.8	9.5	29.2	17.8	A11-02	11.8	9.4	19.9	17.7
A18-03	11.8	9.4	20.6	17.6	A11-03	11.8	9.4	19.0	17.6
A18-04	11.8	9.5	16.2	17.8	A11-04	11.8	9.4	19.8	17.7
A18-05	11.8	9.6	19.1	18.0	A11-05	11.8	9.5	18.9	17.8
A4-01	11.8	9.4	19.6	17.5	A20-01	11.8	9.5	13.3	10.7
A4-02	11.8	9.5	19.5	17.8	A20-02	11.8	9.6	14.4	10.7
A4-03	11.8	9.4	20.1	17.6	A20-03	11.8	9.5	12.3	10.7
A4-04	11.8	9.3	20.8	17.5	A20-04	11.8	9.6	14.4	10.7
A4-05	11.8	9.4	18.0	17.5	A20-05	11.8	9.5	15.9	10.7
A5-01	11.8	9.4	27.2	17.5	A10-01	11.8	9.5	13.3	10.7
A5-02	11.8	9.3	36.1	17.5	A10-02	11.8	9.5	14.8	10.7
A5-03	11.8	9.4	38.5	17.6	A10-03	11.8	9.6	13.0	10.7
A5-04	11.8	9.4	36.4	17.5	A10-04	11.8	9.5	14.4	10.7
A5-05	11.8	9.5	26.1	17.8	A10-05	11.8	9.5	13.6	10.7
A15-01	11.8	9.5	20.8	16.9	A12-01	11.8	9.4	21.6	10.6
A15-02	11.8	9.5	21.4	16.9	A12-02	11.8	9.5	20.8	10.6
A15-03	11.8	9.5	26.8	16.9	A12-03	11.8	9.4	19.2	10.6
A15-04	11.8	9.5	19.3	16.9	A12-04	11.8	9.4	21.8	10.6
A15-05	11.8	9.5	22.6	16.9	A12-05	11.8	9.5	20.8	10.6
A19-01	11.8	9.5	24.4	16.9	A17-01	11.8	9.5	26.5	10.2
A19-02	11.8	9.5	22.3	16.9	A17-02	11.8	9.5	16.9	10.1
A19-03	11.8	9.5	22.5	16.9	A17-03	11.8	9.5	16.6	10.2
A19-04	11.8	9.6	27.7	16.9	A17-04	11.8	9.5	19.4	10.2
A19-05	11.8	9.4	23.8	16.9	A17-05	11.8	9.5	25.5	10.2
A6-01	11.8	9.4	18.3	17.5	A21-01	11.8	9.6	13.9	10.3
A6-02	11.8	9.4	19.4	17.6	A21-02	11.8	9.6	15.7	10.3
A6-03	11.8	9.4	18.2	17.5	A21-03	11.8	9.6	16.3	10.3
A6-04	11.8	9.4	19.2	17.5	A21-04	11.8	9.5	17.4	10.2
A6-05	11.8	9.4	18.8	17.6	A21-05	11.8	9.5	23.9	10.2

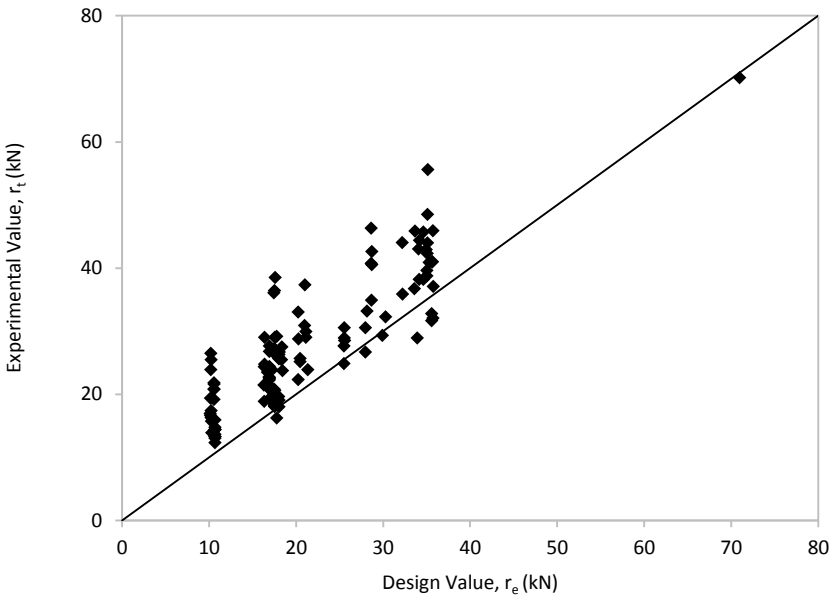

Figure 6.25: Plot of r_e vs r_t for all bolted connections failing in Bearing

Step 3: *Estimate the mean value correction factor* b_m

The mean correction factor b_m is estimated using:

$$b_m = \frac{\sum r_e \, r_t}{\sum {r_t}^2} \qquad (6.\ 2)$$

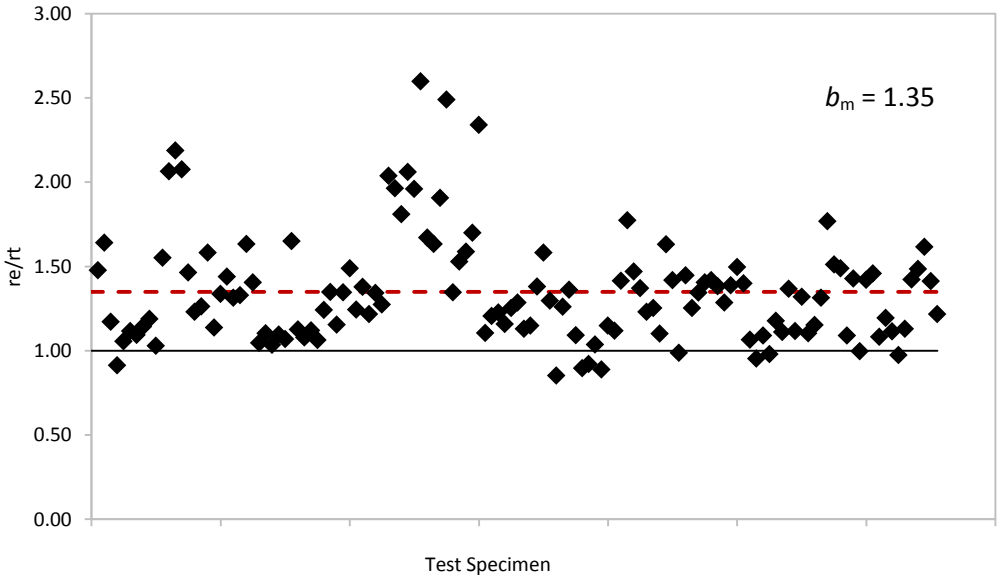

Figure 6.26: Experimental vs. Theoretical Values plotted for all Bolted Connections

The mean correction factor, b_m is 1.35 for the test results in Tables 6.10 and 6.11. It can be seen from Figure 6.26 that seven out of 135 test results are below the predicted values. Specifically, the points that lie (> 4%) beneath the theoretical prediction threshold are for two bolts in a column for (PFRP-to-PFRP) double-lap shear connections. Furthermore, the majority of results at 94% allow confidence in the expression for r_t to give a 'safe' design prediction.

Step 4: *Estimate the coefficient of variation of the errors*

The error term δ_i (i = 1 to n) for each test result r_{ei} is calculated by

$$\delta_i = \frac{r_{ei}}{b_m r_{ti}} \qquad (6.2)$$

Estimation for the coefficient of variation for the error V_δ is given by:

$$V_\delta = \sqrt{\exp(s_\Delta{}^2) - 1} \qquad (6.3.)$$

where

$$s_\Delta{}^2 = \frac{1}{n-1}\sum_{i=1}^{n}(\Delta_i - \bar{\Delta})^2 \qquad (6.4.)$$

Within Equation (6.4), $\Delta_i = \ln(\delta_i)$ and $\bar{\Delta} = \frac{1}{n}\sum_{i=1}^{n}\Delta_i$. Presented in Tables 6.12 and 6.13 are δ_i and Δ_i for the results reported in Tables 6.10 and 6.11, respectively.

Table 6.12: δ_i and Δ_i for Single and Multi-Bolt Connection Tests

Specimen (1)	δ (2)	Δ_i (3)	Specimen (1)	δ (2)	Δ_i (3)
B3-01	0.817	-0.203	WA/0/M10-01	0.852	-0.161
B3-02	0.891	-0.116	WA/0/M10-02	0.971	-0.029
B3-03	0.906	-0.099	WA/0/M10-03	1.306	0.267
B3-04	0.855	-0.156	WA/0/M10-04	1.117	0.110
B3-05	0.926	-0.077	WA/0/M10-05	1.100	0.096
B4-01	0.949	-0.052	WA/0/M12-01	0.805	-0.217
B4-02	0.835	-0.181	WA/0/M12-02	1.055	0.054
B4-03	0.849	-0.164	WA/0/M12-03	0.737	-0.305
B4-04	1.020	0.020	WA/0/M12-04	1.049	0.048
B4-05	1.168	0.156	WA/0/M12-05	1.077	0.074
B12-01	0.959	-0.042	WA/0/M16-01	0.800	-0.223
B12-02	0.630	-0.463	WA/0/M16-02	0.882	-0.125
B12-03	0.932	-0.070	WA/0/M16-03	0.824	-0.194
B12-04	1.006	0.006	WA/0/M16-04	0.719	-0.329
B12-05	0.807	-0.214	WA/0/M16-05	0.835	-0.180
B7-01	0.663	-0.411	WA/0/M20-01	1.051	0.050
B7-02	0.680	-0.385	WA/0/M20-02	1.097	0.092
B7-03	0.766	-0.266	WA/0/M20-03	1.194	0.177
B7-04	0.657	-0.420	WA/0/M20-04	1.044	0.043
B7-05	0.848	-0.164	WA/0/M20-05	0.900	-0.106
B13-01	0.827	-0.190	FA//0/M10-01	1.069	0.066
B13-02	1.045	0.044	FA/0/M10-02	0.926	-0.077
B13-03	1.311	0.270	FA/0/M10-03	0.994	-0.006
B13-04	1.086	0.083	FA/0/M10-04	1.038	0.038
B13-05	1.014	0.013	FA/0/M10-05	1.048	0.047
B14-01	0.909	-0.096	FA/0/M12-01	1.022	0.021
B14-02	0.927	-0.076	FA/0/M12-02	0.950	-0.051
B14-03	0.813	-0.206	FA/0/M12-03	1.026	0.026
B14-04	1.206	0.187	FA/0/M12-04	1.106	0.101
B14-05	1.048	0.046	FA/0/M12-05	1.035	0.034
FA/0/M20-01	0.821	-0.197	FA/0/M16-01	0.787	-0.239
FA/0/M20-02	1.010	0.010	FA/0/M16-02	0.704	-0.350
FA/0/M20-03	0.825	-0.192	FA/0/M16-03	0.806	-0.216
FA/0/M20-04	0.975	-0.025	FA/0/M16-04	0.724	-0.323
FA/0/M20-05	0.815	-0.205	FA/0/M16-05	0.870	-0.140
D3-03	0.730	-0.315			

Table 6.13: δi and Δi for Single Bolt Connection Tests

Specimen (1)	δ (2)	Δ_i (5)	Specimen (1)	δ (2)	Δ_i (5)
A18-01	1.092	0.088	A11-01	1.220	0.199
A18-02	1.212	0.192	A11-02	0.832	-0.183
A18-03	0.866	-0.144	A11-03	0.797	-0.227
A18-04	0.675	-0.394	A11-04	0.828	-0.189
A18-05	0.781	-0.248	A11-05	0.786	-0.241
A4-01	0.826	-0.192	A20-01	0.918	-0.086
A4-02	0.809	-0.212	A20-02	0.996	-0.004
A4-03	0.845	-0.169	A20-03	0.853	-0.159
A4-04	0.878	-0.130	A20-04	0.995	-0.005
A4-05	0.761	-0.274	A20-05	1.100	0.095
A5-01	1.146	0.136	A10-01	0.919	-0.085
A5-02	1.525	0.422	A10-02	1.019	0.019
A5-03	1.617	0.480	A10-03	0.900	-0.106
A5-04	1.534	0.428	A10-04	0.991	-0.009
A5-05	1.082	0.079	A10-05	0.941	-0.061
A15-01	0.909	-0.095	A12-01	1.505	0.409
A15-02	0.932	-0.070	A12-02	1.451	0.372
A15-03	1.169	0.156	A12-03	1.337	0.291
A15-04	0.840	-0.174	A12-04	1.522	0.420
A15-05	0.988	-0.012	A12-05	1.449	0.371
A19-01	1.063	0.061	A17-01	1.920	0.652
A19-02	0.972	-0.029	A17-02	1.234	0.211
A19-03	0.982	-0.018	A17-03	1.207	0.188
A19-04	1.206	0.188	A17-04	1.409	0.343
A19-05	1.039	0.038	A17-05	1.840	0.610
A6-01	0.773	-0.258	A21-01	0.995	-0.005
A6-02	0.815	-0.205	A21-02	1.129	0.121
A6-03	0.765	-0.268	A21-03	1.174	0.160
A6-04	0.810	-0.211	A21-04	1.256	0.228
A6-05	0.791	-0.235	A21-05	1.729	0.547

The error term, δ_i and estimator Δ_i, are given in columns (2) and (3), and used in Equation (6.4) to in turn estimate V_δ from Eq. (6.3). V_δ is found to be 0.221 from all 131 bolted connection test results for bearing failure, i.e. the coefficient of variation for the error terms is close to 20%.

Step 5: *Analyse Compatibility*

Due to the preliminary nature of this study for calibration of γ_M this stage has not been included, although it is recognised that the compatibility of the test results with the assumptions in the 'design model' such as use of the projected area, should be examined when a more rigorous factor from a wider data set is to be determined. The reason for the large scatter is because the whole population has been treated together. It would be beneficial

when more data is available for bolted connections, with statistically verified pin-bearing strengths, that the variables can be separated and a sensitivity analysis conducted. This would establish the influence of individual parameters on the scatter.

Step 6: *Determine the coefficients of variation of the basic variables*, V_{Xi}

The coefficient of variation V_{xi} in this analysis is 0.067 with individual CoV values for the bolt diameter of 0.005 (Trumpf, 2006), 0.03 for material thickness, and from testing 0.06 for characteristic pin bearing strengths.

Steps 7 to 9 were followed to determine the characteristic value of the resistance and finally the partial safety factor. The preliminary value for the partial safety factor for bearing strength in bolted connection of PFRP material is computed to be 1.3. This can be compared to the inverse of the ASCE Pre-standard (2012) resistance factor of 0.8 giving 1.25. There seems to be good agreement with this value and is considerably more reliable than the 2.15 value from the EUROCOMP design manual (Clarke, 1996), which uses an estimate of three other so-called material factors for 'predicting' the partial safety factor.

6.7. Summary

Presented in this chapter is a study of 325 individual bolted shear connections. The test series has considered a double and single-lap test configuration for both the flange and web of a SuperStructural PFRP section. Five different bolting patterns have been used with single bolt and multi-bolted arrangements including two bolts in a row, in a column and staggered as well as four bolts (2 x 2). The test series has identified that using the minimum geometric

requirements for the LRFD Pre-standard (2012); all the distinct failure modes to PFRP material can be observed.

The salient results from the 65 batches of 5 specimens have shown that the damage mode a total of

- 140 failed in bearing, of which 131 have recorded damage loads at bearing failure.
- 35 failed in net-tension, with the first failure being either shear-out or bearing.
- 140 failed in shear-out, with subsequent mixed modes occurring after the initial failure.
- 5 failed in cleavage for the 2 bolts in a row arrangement.
- 5 failed in block-shear for the two staggered bolts arrangement and a large side distance.

The test series has highlighted the importance of the TSFM reinforcement in influencing the failure modes and loads especially for the single-lap configuration with two bolts in a row. The largest reduction found to connection loads from the test series was 37%. Therefore, a reduction factor to the double-lap shear arrangement for use in the design of single-lap joints has been recommended of 0.6. This supports the current mandatory guidance for the single-lap situation which had not been previously verified with specific strength test results.

The 131 bolted connection strength tests that failed in bearing have been used in a preliminary calibration of a partial safety factor, γ_M,for the bearing strength of a WF PFRP material. The characteristic values, computed in Chapter 4, specifically for the SuperStructural material have been used to establish a partial safety factor of 1.3.

CHAPTER 7

Concluding Remarks and Further Work

6.1. Introduction

It is often said that a thesis is a piece of research which has not been finished, but instead abandoned somewhere along the way; this aptly describes the current endeavour. Despite the efforts of testing and analysing many Pultruded Fibre Reinforced Polymer (PFRP) coupons and bolted connections, this research thesis has left many unanswered queries, and in turn opened various new challenges for future research initiatives. In this chapter the author presents the concluding remarks drawn from the PhD work for the two substantial experimental programmes for characterisation of pin-bearing strength and resistance of plate-to-plate bolted connections. Suggestions are made at the end of the chapter for further research that will enhance and contribute to the discussion on aspects of bolted connections in PFRP structures.

First, an overview of the closing comments in Chapter 3 is given. An investigation of the material properties for SuperStructural polyester based Wide-Flange (WF) shapes having E-glass fibre reinforcement (pultruded by Creative Pultrusions Inc., USA), has shown this product

exhibits a complex material architecture. The material has a tri-axial stitched fabric mat that provides off-axis strength and both flange and web materials differ significantly in their fibre architecture. A fibre volume fraction of about 50% is found through resin burn-off analysis. It is found that the flange material has two unidirectional fibre layers that are not of the same thickness, which has a significant influence upon the mechanical properties. The web has a nominally symmetrical fibre lay-up and a higher amount of mat reinforcement; four layers against three in the flanges.

A series of compression coupon tests have been successfully conducted using a non-standard compression test rig, developed by Mottram (1994). Compression strengths for flange and web materials in the two principal directions were characterized. The advantages of loading the rectangular coupons through the ends are an elimination of end effects, no need for end tabs and failure occurring within the gauge length. It has been shown that the majority of specimens failed with a characteristic 45° shear crack throughout the thickness, with the exception of flange material loaded in the pultrusion direction. In this situation the compression failure mechanism gave a double shear crack as a V-shape through the coupon thickness. The mean strengths are found to be on average 20% higher than the four values tabulated in the pultruder's on-line design manual.

Tensile tests have produced characteristic and mean strengths which were further employed in the determination of open-hole tension strength, as required for the by-pass load in multi-row bolted connections. The Hart-Smith method (1979) for determining the open-hole correlation coefficient has been applied and found not to be suitable. The method, when applied with the new test results, does not satisfactorily give the assumed linear relationship between the isotropic stress concentration factor and the orthotropic stress concentration factor. The previously thought material 'constant' of the open hole correlation coefficient is

shown to vary significantly with bolt diameter-to- (plate) width ratio. The implication of this finding is that it brings into question the reliability of using the Hart-Smith approach (1979) to calculate the design resistance of bolted connections that fail with the net-section mode.

Moisture diffusion tests have been used to establish the diffusion coefficients of the materials (2.2-3.0x10^{-9} mm/s) when immersed in distilled water. The semi-empirical approach has been successful in establishing the activation energy for web and flange materials (46 to 59 kJ per mol) that could be used in a Chapter 6 analysis towards understanding the long-term effect of environmental conditioning on lowering pin-bearing strength.

6.2. Pin Bearing Strength Characterisation

6.2.1. Characteristic Pin Bearing Strengths

An extensive experimental investigation into the pin-bearing strength measure for use in the design of PFRP bolted connections has been conducted with more than 500 individual coupon tests. In the programme the four bolt sizes used were M10, M12, M16 and M20. The in-house test method (WUTS) is shown to be suitable for the strength determination for both flange and web materials sourced from SuperStructural WF shapes. Other variables scoped in this series of tests included with and without thread in bearing and material orientation (with respect to the pultrusion direction). The test results are novel as this is the first major study to consider both thread and plain bearing contacts. Manufacturers and researchers are encouraged to adopt a similar loading device and specimen geometry for the determination of pin-bearing strengths as it can accommodate the relevant material orientations, thicknesses, and pin and clearance-hole diameters. Given that computational or other analysis methods cannot be relied upon to predict the bearing mode of failure (Department of Defence, USA, 2002), any

design method used in practice should include statistically verified bearing strengths obtained from reliable test results, such as presented in Chapters 4 and 5.

The most influential parameter found from evaluation of the Chapter 4 results (on as-received material) is the effect of material orientation. It has been found that the longitudinal and transverse strengths differ considerably for a web and flange materials, and, in particular, when determined with the largest pin size of M20; there are their lowest too. A key observation from the new results is that the strength at orientations between 10^{o} to 30° may be lower than for orientations from 45° to 90^{o}, by almost 35%. The web and flange materials have significantly different mechanical properties in the two principal directions due to the fibre architecture, and this in turn influences how pin-bearing strength varies with material orientation.

Mottram and Zafari (2011) showed that the influence of bolt diameter-to-thickness ratio is prominent, and this investigation with different PFRP materials confirms the finding. The adverse effect of this ratio on strength is found to hold true for tests with and without thread in bearing, with an almost linear relationship for the latter condition. The largest differences between the largest and smallest pin sizes were found for threaded pins and transverse material. A difference of 35% was found between the smallest, M10, and largest, M20, sized pins for threaded bearing strengths in the transverse direction for both web and flange. The smallest variation, at 6% was found for longitudinal material with a plain pin. A contribution to the difference between web and flange material is the tri-axial mat reinforcement, which has a higher volume fraction in the web material.

In terms of actual strength values the testing established that for the plain pin situation that the lowest characteristic strengths are: for web material, 148 N/mm^2 in longitudinal direction,

112 N/mm^2 for 45^o orientation and 98 N/mm^2 in transverse direction; for flange material, 168 N/mm^2 in longitudinal direction and 87 N/mm^2 in transverse direction. When thread is present (not constant pitch) the equivalent pin-bearing characteristic strengths were found to be: for web material, 111 N/mm^2 in longitudinal direction, 112 N/mm^2 for 45^o orientation and 104 N/mm^2 in transverse direction; for flange material, 130 N/mm^2 in longitudinal direction and 94 N/mm^2 in transverse direction.

The main investigation has looked to characterise the strength measure with and without thread. It has been found that when thread is present a reduction of 0.7 can be applied to the characteristic pin-bearing strength (for SuperStructural material) for purpose of using Eq. (2.1) to establish, per bolt, the bearing failure force. This affirms the current mandatory design guidance in a PFRP LRFD pre-standard that is currently being developed for publication as an American Society of Civil Engineers standard. There is, however, reason to believe from the results presented in Chapter 4 that for the threaded situation the criterion for selecting the failure load should not be the maximum load. This finding opposes the recommendation by Mottram and Zafari (2011), when thread is being excluded, that this is the only practical load when determining a bearing strength for PFRP material.

6.2.2. The Effect of Environmental Conditioning on Pin-bearing Strength

An experimental investigation to examine the effect of hot-wet conditioning upon the laterally unrestrained pin-bearing strength has been described and discussed in Chapter 5. A total of 72 batches of five specimens (360 in total) have been hot-wet conditioned at constant temperatures of 30°C (8 batches), 40°C (65 batches) or 50°C (8 batches), and subsequently tested to determine pin-bearing strengths. Presented are novel test results with and without a

threaded pin in bearing. Testing followed the research and test methodology in Chapter 4 the study with as-received material.

It has been found that a reduction factor due to thread in bearing is unchanged from the non-aged recommendation of 0.7 for the environmentally conditioned situation. The largest reduction for the threaded strength was found for material tested parallel to the pultrusion direction. The load-stroke stiffness was found to be discernibly lower for the threaded situation. The recommended reduction factor from the characteristic strengths of 30% supports the currently proposed clause for pin-bearing strength in bolted connections within the ASCE pre-standard for LRFD of PFRP structures (ASCE, 2012).

The influence of the hot-wet conditioning causes a reduction in characteristic strength for all batches conditioned for three months when compared to their non-conditioned equivalents. A less obvious trend occurs for the batches after six months (the maximum aging time) of continuous conditioning. Eleven, out of 28 paired (3 and 6 months) batches now showed an increase in mean strength for the temperature of 40°C. Similarly, half of the 30 and 50°C test batches exhibited this same trend. The specific cause of the increase between the two immersion periods is unknown, but possible influences include the small (five) number of specimens per batch and post curing of the resin over the higher time duration. A reduction has been found when the material is loaded in the 0^{o} direction with the largest at 30% for the mean and 28% for the characteristic. The effects of temperature and the specific causes of the increase in strengths between the two immersion durations will require further scientific investigation.

It is observed that increasing the bolt diameter-to-thickness ratio for specimens tested after hot-wet conditioning causes a decrease in strength. This finding is similar to that reported in

Chapter 4 for the non-aged material. The lowest strengths are found, again, for the largest pin size (M20), which strengthens the case for the determination of pin-bearing strength to use a standard test methodology that tests the worst case scenario for bolt diameter-to-thickness, and includes the clearance hole size allowing for fabrication tolerance. Moreover, the guidance provided by Creative Pultrusions Inc. in the (online) design manual that, following employment of test standard ASTM D953:2002 for the determination of pin-bearing strength, stipulates a 15% reduction has been shown to be acceptable for non-aged material. Although this finding is generally adhered to it is violated by test results from a number of batches.

The water mass uptake due to immersion for six months at 40°C is found to be 25% higher than the change after three months. There is reason to believe the moisture absorption follows the (linear) Fickian diffusion curve, and so the moisture results were used to calculate, using the Arrhenius equation, an equivalent service-life time period at a lower service temperature. The accelerated aging regimes and long-term strength prediction modelling has shown a mean pin-bearing strength reduction of up to 25% over 7.8 years, at the UK mean service temperature of 10.5°C. This level of reduction is found to lie within the bounds set by the American LRFD pre-standard (ASCE, 2012), and gives confidence to the mandatory design requirements.

6.3. Bolted Connections

A study of 325 individual bolted connections, with 65 batches of five specimens, has been presented. The test series considered double and single-lap test configurations for flange and web material from a SuperStructural PFRP section. Five different bolting patterns were used with single bolt and multi-bolted arrangements of two bolts in a row, two bolts in a column

and two staggered bolts. In addition, a series of four bolt tests (2 x 2) were conducted. The test series has identified that using the minimum geometric requirements for the LRFD Pre-standard (2012); all the distinct failure modes can be observed in PFRP material.

The salient results have shown the influence of end and side distance upon the failure loads a breakdown of the modes of failure can be given thus:

- 140 failed in bearing, of which 131 have recorded damage loads at bearing failure.
- 35 failed in net-tension, with the first failure being either shear-out or bearing.
- 140 failed in shear-out, with subsequent mixed modes occurring after the initial failure.
- 5 failed in cleavage for the 2 bolts in a row arrangement.
- 5 failed in block-shear for the two staggered bolts arrangement and a side distance >2*d*.

From an appraisal of the bolted connection failure modes, the TSFM reinforcement found in three layers for the web (and two layers in the flange) has significant influence on the failure modes and loads, especially for the single-lap configuration with two bolts in a row. Moreover, the largest reduction found to failure loads of single-lap connections when compared to the equivalent double lap configuration is 37%. Therefore, a reduction factor to the double-lap shear arrangement for use in the design of single-lap joints has been recommended of 0.6. This supports the current mandatory guidance for the single-lap situation which had not been previously verified with specific strength test results for pultruded materials.

The 140 bolted connection strength tests that failed in bearing have been used in a preliminary calibration of a partial safety factor, γ_M,for the bearing strength of a WF PFRP material. The

characteristic values, computed in Chapter 4, specifically for the SuperStructural material have been used to establish a partial safety factor of 1.3. This value is more conservative than the current resistance factor of 1.25 found for use with the bearing resistance formula but, more reliable than the EUROCOMP design guidelines (Clarke, 1996) factor of 2.15.

6.4. Recommendations for Further Work

The following section suggests further work that may be useful in addressing new and unanswered questions.

- A considerable database of pin bearing strengths has been generated with over 500 individual non-aged specimens and more than 350 artificially aged strength values. It is suggested that artificial neural networks for prediction of pin-bearing strengths be explored with validation being possible for variables such as thread in bearing and material orientation, from the new strength test result presented in this thesis.
- The thread in bearing study has highlighted the need to develop an understanding of the threaded pin-bearing failure mechanism in order to develop reliable failure identification from test results as well as a fundamental understanding of failure progression. One Non-destructive approach would be the use of ultrasonic wave detection procedures. The determination of the initiation of bearing failure would aid the development of FEA models as well as more reliable bearing strengths. Furthermore, if the results could be combined with Digital Image Correlation (DIC) the through thickness stress field from variations on the specimens surface could be characterised.

- The preliminary evaluation of a partial safety factor would be aided by a parametric study of the design equation using the Eurocode approach for sensitivity modelling. The use of structural reliability first order reliability methods could be integrated with Monte Carlo simulations of variables in order to assess the individual parameters found in the bearing strength design model.
- Finally, the environmentally conditioned pin bearing strengths require verification from long term weathered specimens and this would allow the reliability of artificial aging regimes to be assessed. This would be of interest to the facade engineering community that executes design in PFRP materials.

Appendix A – Moisture Absorption Experiments and Analysis

A.1 Introduction

Presented in this appendix are analyses and test results of a series of moisture absorption experiments on the PFRP material described in Chapter 3. Firstly, in Tables A.1, A.2 and A.3 are presented the mean (of 5 specimens) moisture absorption test results over a period of 16 weeks for both flange and web material. The columns labelled A, B and C represents the specimen sizes of 40 x 40 mm, 60 x 60 mm and 100 x 100 mm, respectively. The maximum moisture content, M_m, has been estimated by curve fitting the results plotted in Figures A.1, A.2 and A.3 and taken the asymptotic value of the curve. It can be seen in figures A.1, A.2 and A.3 that as the temperature increases the rate of diffusion increases as indicated by the increase in moisture content over time.

Following on from the moisture absorption test results, the calculation of the short-term moisture diffusion co-efficient is given in Tables A.4, A.5 and A.6 for flange and web material. The procedure is outlined in Chapter 3. The results of the short term diffusion co-efficient analysis are plotted in Figures A.4 and A.5. A further analysis of these figures in conducted to establish the apparent (long term) diffusion co-efficient of the material presented in Tables A.7 and A.8. These results are in term is used to plot the Arrhenius plots in Figures A.6 and A.7 for flange and web material, respectively, from the condensed results given in Tables A.9 and A.10. Finally the estimation of the activation energy is given in Table A.11.

A.2 Moisture Absorption Test Results

Table A.1: Percentage (%) Moisture Content of Flange Material from immersion in Distilled water at 22°C and 30°C and estimated Maximum Moisture Content

	22°C			30°C		
Time, √t (days)	A	B	C	A	B	C
0.00	0.00	0.00	0.00	0.00	0.00	0.00
0.20	0.14	0.12	0.07	0.12	0.07	0.05
0.29	0.20	0.13	0.12	0.09	0.08	0.05
0.41	0.25	0.17	0.12	0.12	0.09	0.06
0.58	0.18	0.19	0.19	0.14	0.11	0.09
0.82	0.19	0.13	0.11	0.16	0.15	0.11
1.00	0.03	0.23	0.18	0.18	0.15	0.11
1.41	0.26	0.24	0.18	0.24	0.20	0.14
2.00	0.29	0.25	0.20	0.31	0.25	0.21
2.65	0.39	0.30	0.26	0.37	0.31	0.26
3.74	0.48	0.39	0.33	0.50	0.42	0.34
5.29	0.59	0.51	0.43	0.61	0.54	0.43
6.48	0.67	0.55	0.48	0.68	0.62	0.50
7.48	0.71	0.64	0.54	0.71	0.67	0.53
8.37	0.75	0.68	0.58	0.80	0.74	0.59
9.17	0.76	0.70	0.58	0.84	0.78	0.62
9.90	0.79	0.72	0.61	0.85	0.78	0.63
10.58	0.81	0.76	0.64	0.89	0.83	0.67
M_m	0.87	0.82	0.7	1.01	1.06	0.86

Table A.2: Percentage (%) Moisture Content of Flange Material from immersion in Distilled water at 40°C, 50°C and 60°C and estimated Maximum Moisture Content

	40°C			50°C			60°C		
Time, √t (days)	A	B	C	A	B	C	A	B	C
0.00	0.00	0.00	0.00	0.00	0.00	0.00	0.00	0.00	0.00
0.20	0.07	0.05	0.04	0.07	0.05	0.05	0.08	0.05	0.05
0.29	0.08	0.05	0.05	0.09	0.07	0.06	0.10	0.07	0.07
0.41	0.14	0.07	0.07	0.19	0.11	0.09	0.14	0.11	0.10
0.58	0.14	0.13	0.10	0.23	0.16	0.13	0.23	0.15	0.13
0.82	0.19	0.14	0.12	0.27	0.19	0.17	0.27	0.20	0.18
1.00	0.24	0.17	0.15	0.27	0.21	0.18	0.27	0.22	0.19
1.41	0.31	0.22	0.21	0.37	0.28	0.24	0.38	0.30	0.26
2.00	0.39	0.31	0.27	0.45	0.37	0.31	0.49	0.40	0.34
2.65	0.47	0.38	0.31	0.52	0.44	0.37	0.57	0.49	0.42
3.74	0.60	0.50	0.41	0.62	0.56	0.47	0.70	0.61	0.55
5.29	0.73	0.62	0.50	0.75	0.69	0.60	0.88	0.79	0.70
6.48	0.83	0.71	0.59	0.90	0.82	0.70	0.95	0.84	0.77
7.48	0.87	0.77	0.64	0.95	0.86	0.75	1.02	0.94	0.86
8.37	0.92	0.85	0.69	0.95	0.88	0.79	1.02	0.96	0.88
9.17	0.97	0.86	0.71	0.98	0.92	0.83	1.02	0.99	0.90
9.90	1.00	0.89	0.75	1.00	0.95	0.86	1.07	1.06	0.93
10.58	1.01	0.92	0.77	1.03	1.00	0.90	1.06	1.06	0.91
M_m	1.12	1.14	0.94	1.06	1.11	1.06	1.12	1.2	1.07

Table A.3: Percentage (%) Moisture Content of Web Material from immersion in Distilled water at 30°C, 40°C, 50°C and 60°C and estimated Maximum Moisture Content

	30°C			40°C			50°C			60°C		
Time, √t (days)	A	B	C	A	B	C	A	B	C	A	B	C
0.00	0.00	0.00	0.00	0.00	0.00	0.00	0.00	0.00	0.00	0.00	0.00	0.00
0.20	0.08	0.07	0.05	0.06	0.06	0.06	0.07	0.04	0.05	0.07	0.07	0.05
0.29	0.07	0.08	0.06	0.10	0.08	0.07	0.09	0.06	0.07	0.10	0.08	0.08
0.41	0.09	0.11	0.08	0.16	0.11	0.10	0.10	0.10	0.10	0.14	0.13	0.10
0.58	0.14	0.13	0.10	0.19	0.14	0.13	0.20	0.14	0.13	0.18	0.20	0.16
0.82	0.17	0.16	0.13	0.23	0.19	0.16	0.24	0.19	0.17	0.30	0.27	0.22
1.00	0.19	0.18	0.15	0.27	0.21	0.18	0.27	0.21	0.19	0.32	0.30	0.25
1.41	0.29	0.24	0.20	0.34	0.28	0.24	0.35	0.32	0.27	0.41	0.40	0.33
2.00	0.33	0.33	0.28	0.45	0.39	0.34	0.47	0.43	0.36	0.58	0.53	0.46
2.65	0.41	0.40	0.33	0.55	0.49	0.43	0.52	0.52	0.45	0.65	0.62	0.54
3.74	0.55	0.53	0.45	0.66	0.61	0.54	0.66	0.65	0.56	0.88	0.83	0.73
5.29	0.64	0.67	0.57	0.77	0.77	0.65	0.82	0.83	0.73	1.02	0.96	0.86
6.48	0.75	0.77	0.68	0.89	0.88	0.75	0.89	0.91	0.80	1.12	1.06	0.97
7.48	0.77	0.82	0.73	0.93	0.92	0.79	0.96	0.98	0.89	1.12	1.09	1.01
8.37	0.85	0.89	0.79	0.99	0.98	0.84	0.98	1.02	0.92	1.18	1.16	1.08
9.17	0.85	0.90	0.82	1.02	1.01	0.88	0.97	1.02	0.94	1.21	1.20	1.13
9.90	0.90	0.95	0.86	1.04	1.05	0.92	1.03	1.08	1.00	1.24	1.24	1.17
10.58	0.91	0.98	0.91	1.09	1.09	0.96	1.11	1.13	1.03	1.26	1.23	1.15
M_m	1.02	1.18	1.22	1.13	1.25	1.09	1.12	1.25	1.2	1.31	1.32	1.32

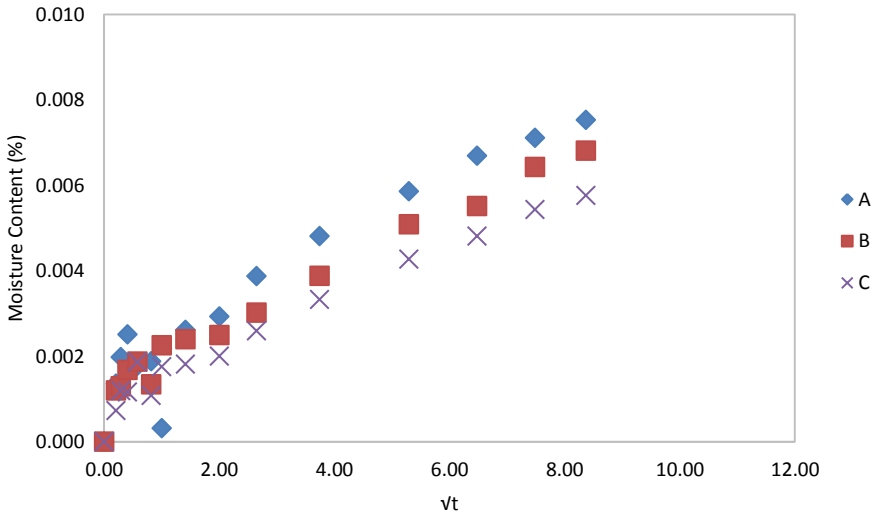

Figure A.1: Percentage Moisture Content over time of Flange Material from immersion in Distilled water at 22°C

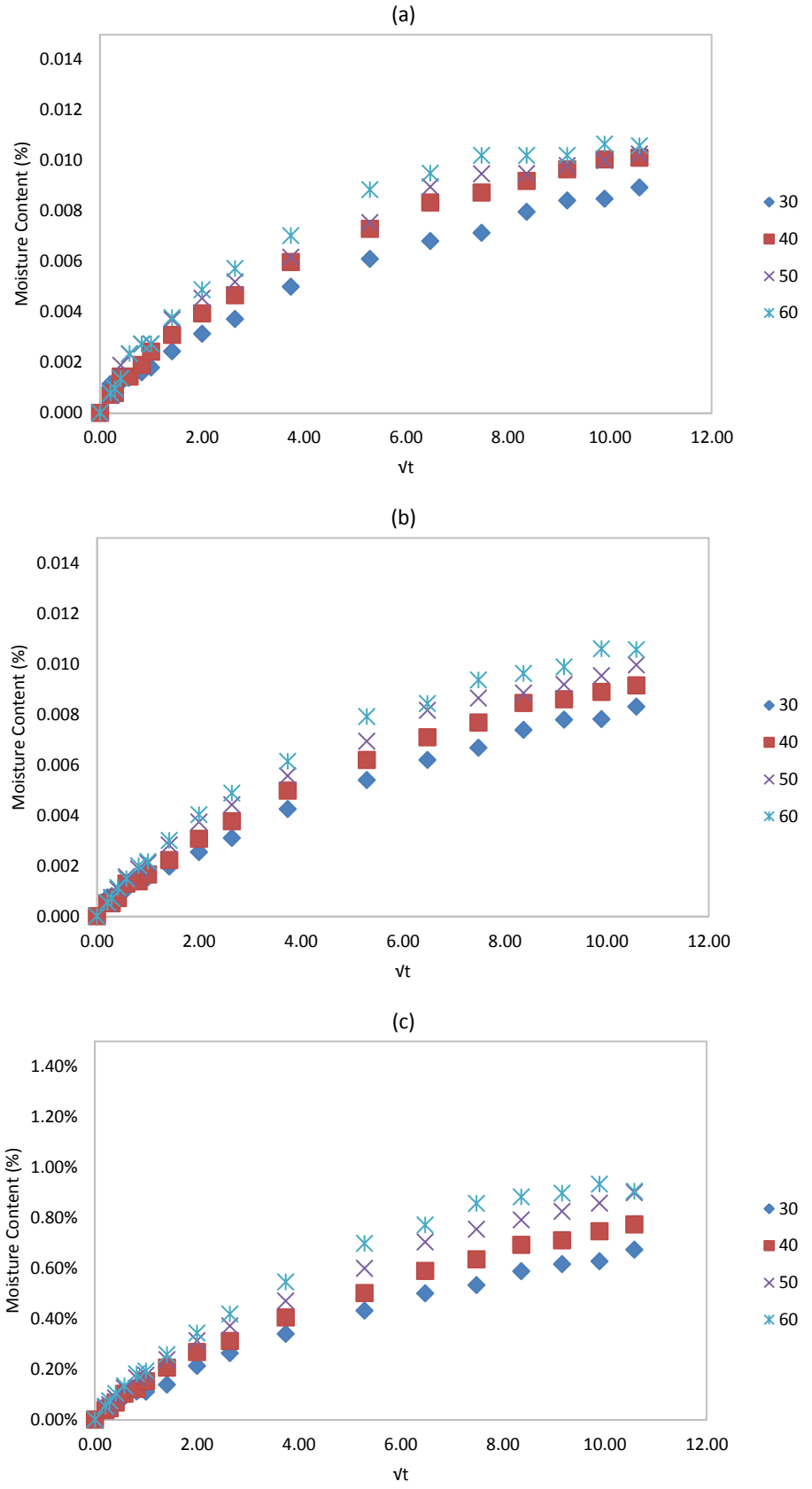

Figure A.2: Percentage Moisture Content over time of Flange Material from immersion in Distilled water for (a) 40 x 40 mm Specimens, (b) 60 x 60 mm Specimens and (c) 100 x 100 mm Specimens

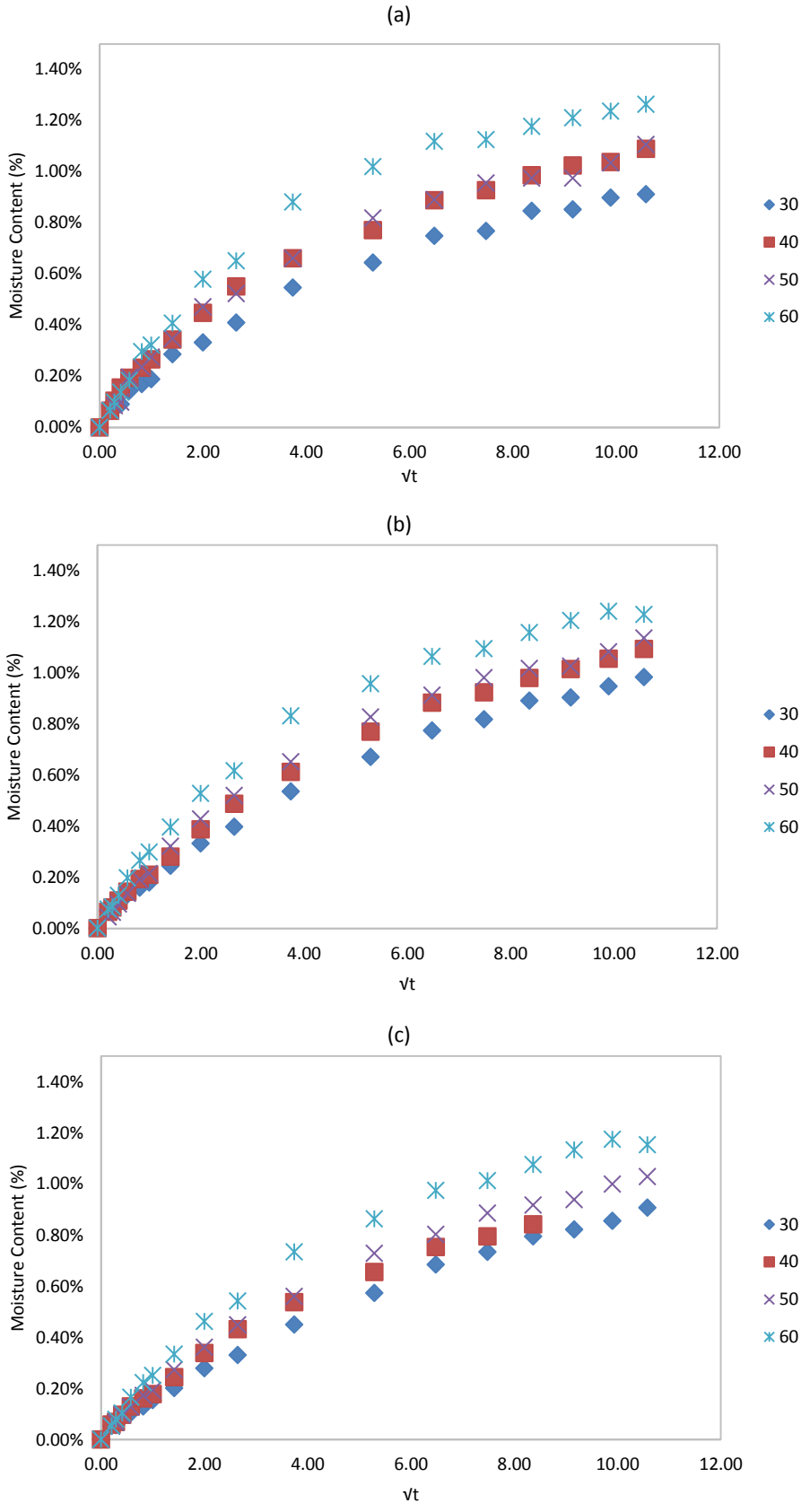

Figure A.3: Percentage Moisture Content over time of Web Material from immersion in Distilled water for (a) 40 x 40 mm Specimens, (b) 60 x 60 mm Specimens and (c) 100 x 100 mm Specimens

A.3 Moisture Diffusion Calculation

Table A.4: Short Term Moisture Diffusion Prediction for Flange Material immersed in Distilled Water at 22°C and 30°C

	22°C			30°C		
$4/h^2\pi(\sqrt{t})$	A	B	C	A	B	C
0.00	0.0000	0.0000	0.0000	0.0000	0.0000	0.0000
0.03	0.0016	0.0015	0.0010	0.0011	0.0007	0.0006
0.04	0.0023	0.0016	0.0017	0.0009	0.0008	0.0006
0.06	0.0029	0.0020	0.0017	0.0012	0.0008	0.0007
0.08	0.0020	0.0023	0.0027	0.0014	0.0010	0.0011
0.11	0.0022	0.0016	0.0015	0.0016	0.0015	0.0013
0.14	0.0004	0.0027	0.0025	0.0018	0.0015	0.0013
0.20	0.0030	0.0029	0.0026	0.0024	0.0019	0.0016
0.28	0.0034	0.0030	0.0029	0.0031	0.0024	0.0025
0.37	0.0045	0.0037	0.0037	0.0037	0.0029	0.0031
0.52	0.0055	0.0047	0.0047	0.0050	0.0040	0.0039
0.73	0.0067	0.0062	0.0061	0.0060	0.0051	0.0050
0.90	0.0077	0.0067	0.0069	0.0067	0.0058	0.0058
1.04	0.0082	0.0078	0.0078	0.0071	0.0063	0.0062
1.16	0.0087	0.0083	0.0082	0.0079	0.0070	0.0068
1.27	0.0088	0.0085	0.0083	0.0083	0.0073	0.0072
1.37	0.0091	0.0088	0.0087	0.0084	0.0074	0.0073
1.46	0.0093	0.0092	0.0091	0.0088	0.0078	0.0078

Table A.5: Short Term Moisture Diffusion Prediction for Flange Material immersed in Distilled Water at 30°C , 40°C , 50°C and 60°C

	40°C			50°C			60°C		
$4/h^2\pi(\sqrt{t})$	A	B	C	A	B	C	A	B	C
0.00	0.0000	0.0000	0.0000	0.0000	0.0000	0.0000	0.0000	0.0000	0.0000
0.03	0.0006	0.0005	0.0004	0.0007	0.0005	0.0004	0.0007	0.0005	0.0005
0.04	0.0007	0.0005	0.0005	0.0009	0.0007	0.0006	0.0009	0.0006	0.0007
0.06	0.0013	0.0006	0.0007	0.0018	0.0010	0.0008	0.0012	0.0010	0.0010
0.08	0.0013	0.0011	0.0011	0.0022	0.0014	0.0012	0.0021	0.0012	0.0013
0.11	0.0017	0.0012	0.0013	0.0026	0.0017	0.0016	0.0024	0.0017	0.0017
0.14	0.0022	0.0014	0.0016	0.0026	0.0019	0.0017	0.0024	0.0018	0.0018
0.20	0.0028	0.0020	0.0022	0.0035	0.0025	0.0022	0.0034	0.0025	0.0024
0.28	0.0035	0.0027	0.0028	0.0043	0.0034	0.0029	0.0044	0.0034	0.0032
0.37	0.0042	0.0033	0.0033	0.0049	0.0040	0.0035	0.0051	0.0041	0.0039
0.52	0.0053	0.0044	0.0043	0.0058	0.0050	0.0044	0.0063	0.0051	0.0051
0.73	0.0065	0.0054	0.0053	0.0071	0.0062	0.0057	0.0079	0.0066	0.0065
0.90	0.0074	0.0062	0.0063	0.0085	0.0073	0.0066	0.0085	0.0070	0.0072
1.04	0.0078	0.0067	0.0068	0.0089	0.0078	0.0071	0.0091	0.0078	0.0080
1.16	0.0082	0.0074	0.0074	0.0089	0.0080	0.0075	0.0091	0.0080	0.0082
1.27	0.0086	0.0075	0.0076	0.0092	0.0083	0.0078	0.0091	0.0082	0.0084
1.37	0.0090	0.0078	0.0079	0.0094	0.0086	0.0081	0.0095	0.0088	0.0087
1.46	0.0090	0.0080	0.0082	0.0097	0.0090	0.0085	0.0095	0.0088	0.0085

Table A.6: Short Term Moisture Diffusion Prediction for Web Material immersed in Distilled Water at 30°C , 40°C , 50°C and 60°C

	40°C			50°C			60°C		
$4/h^2\pi(\sqrt{t})$	A	B	C	A	B	C	A	B	C
0.00	0.0000	0.0000	0.0000	0.0000	0.0000	0.0000	0.0000	0.0000	0.0000
0.03	0.0006	0.0006	0.0006	0.0006	0.0004	0.0005	0.0006	0.0006	0.0005
0.04	0.0009	0.0007	0.0007	0.0008	0.0006	0.0006	0.0009	0.0007	0.0007
0.06	0.0014	0.0009	0.0010	0.0009	0.0009	0.0009	0.0012	0.0011	0.0010
0.08	0.0017	0.0013	0.0014	0.0019	0.0012	0.0012	0.0016	0.0016	0.0015
0.11	0.0021	0.0017	0.0017	0.0022	0.0017	0.0016	0.0026	0.0022	0.0021
0.14	0.0024	0.0018	0.0019	0.0026	0.0019	0.0018	0.0029	0.0025	0.0023
0.20	0.0031	0.0025	0.0026	0.0033	0.0029	0.0026	0.0036	0.0033	0.0031
0.28	0.0040	0.0034	0.0036	0.0044	0.0039	0.0034	0.0052	0.0044	0.0043
0.37	0.0049	0.0043	0.0046	0.0049	0.0047	0.0042	0.0058	0.0051	0.0051
0.52	0.0059	0.0054	0.0057	0.0062	0.0059	0.0053	0.0079	0.0069	0.0069
0.73	0.0069	0.0067	0.0070	0.0077	0.0074	0.0069	0.0091	0.0080	0.0081
0.90	0.0079	0.0077	0.0080	0.0084	0.0082	0.0076	0.0100	0.0089	0.0091
1.04	0.0083	0.0081	0.0084	0.0090	0.0088	0.0083	0.0100	0.0091	0.0095
1.16	0.0088	0.0086	0.0090	0.0092	0.0092	0.0086	0.0105	0.0096	0.0101
1.27	0.0091	0.0089	0.0094	0.0092	0.0092	0.0088	0.0108	0.0100	0.0106
1.37	0.0093	0.0092	0.0098	0.0098	0.0097	0.0094	0.0110	0.0103	0.0110
1.46	0.0097	0.0096	0.0102	0.0104	0.0102	0.0097	0.0113	0.0102	0.0108

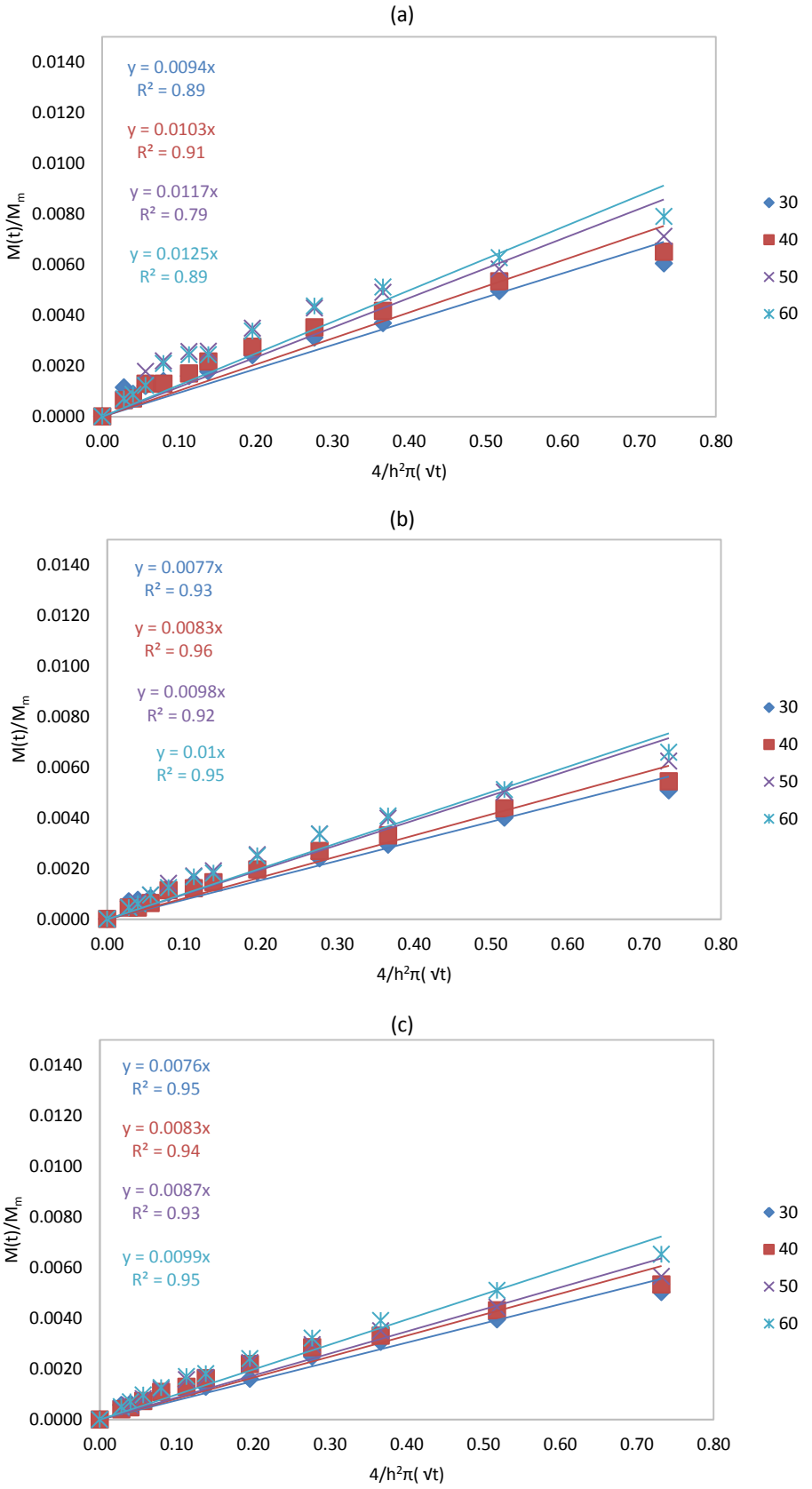

Figure A.4: Short Term Moisture Diffusion Prediction for Flange Material immersed in Distilled Water at 30°C , 40°C , 50°C and 60°C for (a) 40 x 40 mm Specimens, (b) 60 x 60 mm Specimens and (c) 100 x 100 mm Specimens

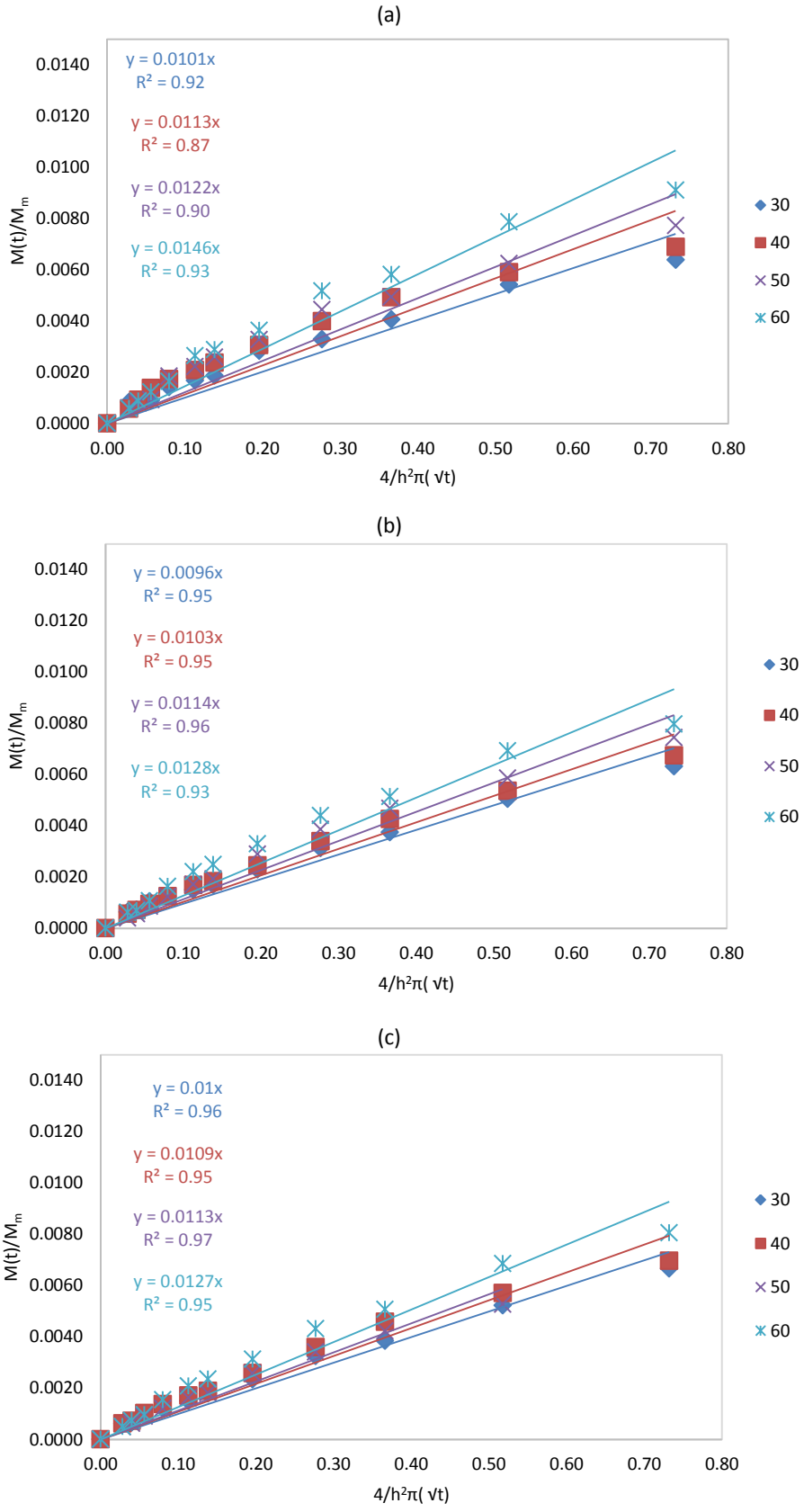

Figure A.5: Short Term Moisture Diffusion Prediction for Web Material immersed in Distilled Water at 30°C , 40°C , 50°C and 60°C for (a) 40 x 40 mm Specimens, (b) 60 x 60 mm Specimens and (c) 100 x 100 mm Specimens

A.4 Calculation of Diffusion Co-efficient

Table A.7: Calculation of the Diffusion Co-efficient at 30, 40, 50 and 60°C for Flange Material

Temp (°C)	Specimen Size	Estimated Saturation, M_m (%)	Slope	Apparent Diffusion Coefficient, D_a (mm/day)	Apparent Diffusion Coefficient, D_a (mm/s)	D_x with Edge Correction $D_x=D_a*\sqrt{(1+(l/h)+(l/n)}$
30	A	1.01	0.0094	0.000088	1.02 E-09	2.55 E-09
	B	1.01	0.0081	0.000066	7.59 E-10	2.19 E-09
	C	0.86	0.0076	0.000058	6.69 E-10	2.16 E-09
40	A	1.12	0.0103	0.000106	1.23 E-09	3.06 E-09
	B	1.14	0.0083	0.000069	7.97 E-10	2.30 E-09
	C	0.94	0.0083	0.000069	7.97 E-10	2.57 E-09
50	A	1.06	0.0117	0.000137	1.58 E-09	3.94 E-09
	B	1.11	0.0098	0.000096	1.11 E-09	3.20 E-09
	C	1.06	0.0087	0.000076	8.76 E-10	2.82 E-09
60	A	1.12	0.0125	0.000156	1.81 E-09	4.50 E-09
	B	1.20	0.0100	0.000100	1.16 E-09	3.33 E-09
	C	1.07	0.0090	0.000081	9.38 E-10	3.02 E-09

Table A.8: Calculation of the Diffusion Co-efficient at 30, 40, 50 and 60°C for Web Material

Temp (°C)	Specimen Size	Estimated Saturation, M_m (%)	Slope	Apparent Diffusion Coefficient, D_a (mm/day)	Apparent Diffusion Coefficient, D_a (mm/s)	D_x with Edge Correction $D_x=D_a*\sqrt{(1+(l/h)+(l/n)}$
30	A	1.02	0.0101	0.000102	1.18 E-09	2.94 E-09
	B	1.18	0.0096	0.000092	1.07 E-09	3.07 E-09
	C	1.22	0.0100	0.000100	1.16 E-09	3.73 E-09
40	A	1.13	0.0113	0.000128	1.48 E-09	3.68 E-09
	B	1.25	0.0103	0.000106	1.23 E-09	3.54 E-09
	C	1.09	0.1090	0.011881	1.38 E-07	4.43 E-07
50	A	1.12	0.0122	0.000149	1.72 E-09	4.29 E-09
	B	1.25	0.0114	0.000130	1.50 E-09	4.33 E-09
	C	1.20	0.0113	0.000128	1.48 E-09	4.76 E-09
60	A	1.31	0.0146	0.000213	2.47 E-09	6.14 E-09
	B	1.32	0.0128	0.000164	1.90 E-09	5.46 E-09
	C	1.32	0.0127	0.000161	1.87 E-09	6.02 E-09

A.5 Calculation of Activation Energy

Table A.9: Variables for Arrhenius Plot at 30, 40, 50 and 60°C for Flange Material

Specimen Size	ln D_x	1000/T (K^{-1})
30°		
A	-19.79	0.122
B	-19.94	0.122
C	-19.96	0.122
40°		
A	-19.61	0.091
B	-19.89	0.091
C	-19.78	0.091
50°		
A	-19.35	0.073
B	-19.56	0.073
C	-19.69	0.073
30°		
A	-19.22	0.061
B	-19.52	0.061
C	-19.62	0.061

Table A.10: Variables for Arrhenius Plot at 30, 40, 50 and 60°C for Web Material

Specimen Size	ln D_x	1000/T (K^{-1})
30°		
A	-19.65	0.122
B	-19.60	0.122
C	-19.41	0.122
40°		
A	-19.42	0.091
B	-19.46	0.091
C	-19.23	0.091
50°		
A	-19.27	0.073
B	-19.26	0.073
C	-19.16	0.073
60°		
A	-18.91	0.061
B	-19.03	0.061
C	-18.93	0.061

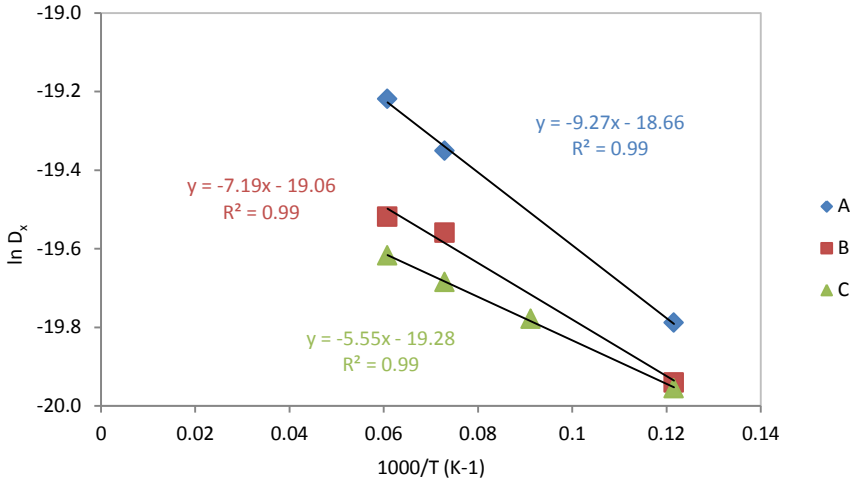

Figure A.6: Arrhenius Plot of Diffusion Coefficients for 40 x 40 mm, 60 x 60 mm and 100 x 100 mm sized Flange Material Specimens

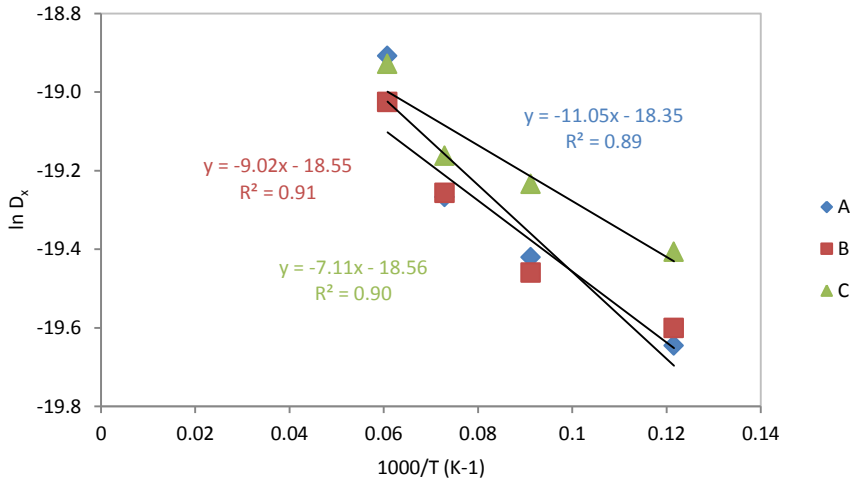

Figure A.7: Arrhenius Plot of Diffusion Coefficients for 40 x 40 mm, 60 x 60 mm and 100 x 100 mm sized Web Material Specimens

Table A.11: Estimation of Activation Energy for Flange and Web Material for Specimens immersed in Distilled Water

Batch	Slope ($-E_a/R$)	Intercept (LnD_0)	E_a (kJ mol^{-1})	D_0
Flange Material				
A	-9.27	-18.66	77.0	7.84 E-09
B	-7.19	-19.06	59.8	5.27 E-09
C	-5.55	-19.28	46.1	4.24 E-09
Web Material				
A	-11.1	-18.35	91.9	1.07 E-08
B	-9.02	-18.55	75.0	8.75 E-09
C	-7.11	-18.57	59.1	8.64 E-09

Appendix B – Aged and Non-aged Pin-bearing Test Specimen Measurements

B.1 Introduction

Presented in this appendix are measurements taken from the pin bearing specimens used in the studies described within Chapters 4 and 5. The measurements are presented in Tables B.1 to B.10 for non-aged and B.12 to B.32 for aged specimens. In each table column (1) Specimen (Identification: ID) Designation; (2) Clearance Hole Diameter, d_n; (3) Specimen Thickness, t; (4) Specimen Width, w; (5) Specimen Length, l; (6) Width to hole edge, w_h; (7) Length to hole edge, l_h; (8) Notch Depth, w_{notch}; (9) Notch Diameter, d_{notch}; (10) Distance to Notch Centre, l_{notch}; (11) Calculated Offset from Middle of Specimen, $(w - l_{notch})/2$. Only the dimensions given in columns (2) to (7) were measured with the dimensions in columns (8) to (11) being calculated using the simple geometric relationships.

The measurements of aged specimen batches in Tables B.12 to B32 include weight and percentage moisture gain for each specimen. All measurements within this appendix are given in millimetres (mm) for dimensions and grams (g) for weights. Each individual value is the average of three measured readings.

B.2 Non- Aged Pin Bearing Specimen Measurements

Table B.1: Pin-bearing Test Specimen Measurements for Flange Material tested with a Plain Pin in the Longitudinal Direction

Specimen ID	Diameter of Hole, d_n	Thickness of Specimen, t	Width of Specimen, w	Length of Specimen, l	Width to Hole Edge, w_h	Length to Hole Edge, l_h	Notch Depth, w_{notch}	Notch Diameter, d_{notch}	Notch Centre, l_{notch}	Offset, $(w - l_{notch})/2$
F/0/P/M10-01	11.99	9.60	80.19	80.18	33.98	74.86	5.32	11.91	39.94	-0.16
F/0/P/M10-02	11.99	9.84	80.15	80.16	34.34	74.59	5.57	11.96	40.32	0.24
F/0/P/M10-03	11.99	9.85	80.23	80.16	34.19	74.24	5.92	11.99	40.18	0.07
F/0/P/M10-04	11.99	9.89	79.86	80.19	34.00	74.15	6.04	11.99	39.99	0.06
F/0/P/M10-05	11.99	9.59	80.10	80.14	34.04	74.21	5.93	11.99	40.03	-0.02
F/0/P/M10-06	11.99	9.59	80.21	80.21	34.21	74.29	5.92	11.98	40.20	0.10
F/0/P/M10-07	11.99	9.57	80.29	80.89	34.33	74.26	6.63	11.92	40.29	0.14
F/0/P/M10-08	11.99	9.96	80.08	80.14	33.89	74.28	5.86	11.99	39.88	-0.16
F/0/P/M10-09	11.99	10.19	80.25	80.06	34.34	74.16	5.90	11.98	40.33	0.21
F/0/P/M10-10	11.99	9.60	80.08	80.08	34.04	74.53	5.55	11.96	40.02	-0.02
Mean	11.99	9.77	80.14	80.11	34.14	74.36	5.86	11.97	40.12	-
SD	0.00	0.21	0.12	0.24	0.17	0.23	0.35	0.03	0.17	-
CoV (%)	0.01	2.16	0.15	0.30	0.49	0.31	5.99	0.25	0.41	-
F/0/P/M12-01	14.39	9.60	80.25	80.01	32.81	73.14	6.87	14.38	40.00	-0.13
F/0/P/M12-02	14.39	9.62	79.90	80.07	32.84	72.89	7.18	14.39	40.03	0.08
F/0/P/M12-03	14.40	9.60	80.29	80.01	33.14	73.10	6.91	14.38	40.33	0.19
F/0/P/M12-04	14.39	9.63	80.18	80.17	32.98	72.89	7.28	14.39	40.17	0.08
F/0/P/M12-05	14.39	9.61	80.13	80.24	32.94	73.03	7.21	14.39	40.13	0.07
F/0/P/M12-06	14.39	9.85	80.27	80.16	32.98	73.23	6.93	14.38	40.17	0.04
F/0/P/M12-07	14.40	9.87	80.20	80.15	33.49	73.00	7.15	14.39	40.69	0.59
F/0/P/M12-08	14.39	10.19	80.28	80.14	32.80	72.99	7.15	14.39	39.99	-0.15
F/0/P/M12-09	14.39	9.84	80.24	80.13	33.01	73.19	6.94	14.38	40.20	0.08
F/0/P/M12-10	14.40	9.88	80.13	80.08	32.81	73.07	7.01	14.39	40.01	-0.06
F/0/P/M12-11	14.40	10.20	80.14	81.50	33.13	74.70	6.80	14.38	40.32	0.25
F/0/P/M12-12	14.40	9.55	79.83	80.84	32.90	73.31	7.53	14.38	40.09	0.18
F/0/P/M12-13	14.40	9.56	79.92	82.51	32.85	75.06	7.45	14.39	40.05	0.09
F/0/P/M12-14	14.40	9.82	79.95	79.86	32.83	73.29	6.57	14.34	40.00	0.03
F/0/P/M12-15	14.40	10.26	80.09	81.62	33.00	74.80	6.82	14.38	40.19	0.14
Mean	14.39	9.81	80.12	80.50	32.97	73.45	7.05	14.38	40.16	-
SD	0.00	0.24	0.15	0.77	0.18	0.74	0.26	0.01	0.18	-
CoV (%)	0.03	2.49	0.19	0.96	0.55	1.01	3.66	0.08	0.46	-
F/0/P/M16-01	18.40	9.86	80.19	80.25	30.77	70.83	9.42	18.39	39.96	-0.13
F/0/P/M16-02	18.39	9.87	80.15	80.29	31.04	70.72	9.57	18.37	40.23	0.15
F/0/P/M16-03	18.39	10.19	80.23	80.30	31.02	70.98	9.32	18.39	40.21	0.10
F/0/P/M16-04	18.39	10.20	80.26	80.28	30.78	71.17	9.11	18.39	39.97	-0.16
F/0/P/M16-05	18.40	9.89	80.21	80.29	30.75	70.92	9.37	18.39	39.95	-0.16
F/0/P/M16-06	18.40	9.85	80.16	80.32	30.97	71.18	9.14	18.39	40.17	0.09
F/0/P/M16-07	18.40	10.17	80.25	80.30	31.10	71.07	9.23	18.39	40.30	0.17
F/0/P/M16-08	18.40	10.20	80.00	80.21	30.89	71.13	9.08	18.39	40.09	0.09
F/0/P/M16-09	18.40	10.18	80.16	80.17	30.88	71.27	8.90	18.39	40.07	-0.01
F/0/P/M16-10	18.40	9.67	80.32	80.15	30.87	70.99	9.16	18.39	40.07	-0.09
Mean	18.39	10.01	80.19	80.26	30.91	71.03	9.23	18.39	40.10	-
SD	0.00	0.20	0.09	0.06	0.12	0.17	0.19	0.01	0.12	-
CoV (%)	0.01	1.99	0.11	0.07	0.39	0.24	2.10	0.03	0.30	-
F/0/P/M20-01	22.40	9.60	80.23	80.28	28.91	69.31	10.97	22.39	40.11	-0.01
F/0/P/M20-02	22.40	9.62	80.24	80.41	29.13	69.10	11.31	22.39	40.33	0.21
F/0/P/M20-03	22.39	9.61	80.25	80.30	29.07	69.05	11.25	22.39	40.26	0.14
F/0/P/M20-04	22.39	9.87	80.04	80.31	28.69	68.93	11.38	22.38	39.88	-0.14
F/0/P/M20-05	22.40	9.61	80.25	80.33	28.74	68.84	11.49	22.39	39.93	-0.19
F/0/P/M20-06	22.40	9.62	80.30	80.37	29.06	68.98	11.39	22.39	40.26	0.11
F/0/P/M20-07	22.39	9.59	80.24	80.32	28.43	69.03	11.29	22.39	39.62	-0.50
F/0/P/M20-08	22.39	9.93	80.05	80.29	28.81	68.99	11.30	22.39	40.00	-0.02
F/0/P/M20-09	22.39	9.62	80.18	80.33	28.95	69.33	11.00	22.39	40.14	0.05
F/0/P/M20-10	22.40	9.54	80.26	80.39	28.80	69.11	11.28	22.39	40.00	-0.13
Mean	22.39	9.66	80.20	80.33	28.86	69.07	11.27	22.39	40.05	-
SD	0.00	0.13	0.09	0.04	0.21	0.16	0.16	0.00	0.21	-
CoV (%)	0.02	1.33	0.11	0.05	0.73	0.22	1.45	0.02	0.53	-

Table B.2: Pin-bearing Test Specimen Measurements for Flange Material tested with a Threaded pin in the Longitudinal Direction

Specimen ID	Diameter of Hole, d_n	Thickness of Specimen, t	Width of Specimen, w	Length of Specimen, l	Width to Hole Edge, w_h	Length to Hole Edge, l_h	Notch Depth, w_{notch}	Notch Diameter, d_{notch}	Notch Centre, l_{notch}	Offset, $(w - l_{notch})/2$
F/0/T/M10-01	11.99	9.60	79.97	80.04	34.74	74.29	5.75	11.98	40.73	0.74
F/0/T/M10-02	11.98	9.62	80.33	80.13	34.64	74.06	6.07	11.98	40.63	0.47
F/0/T/M10-03	11.99	9.86	80.22	80.18	34.06	74.19	5.99	11.98	40.05	-0.06
F/0/T/M10-04	11.99	9.59	80.06	80.15	34.16	74.59	5.56	11.95	40.14	0.11
F/0/T/M10-05	11.99	9.62	80.04	80.06	34.05	74.53	5.53	11.95	40.02	0.00
F/0/T/M10-06	11.99	9.61	80.26	80.11	34.27	74.60	5.51	11.95	40.24	0.11
F/0/T/M10-07	11.99	10.19	80.28	80.19	34.30	74.21	5.98	11.99	40.29	0.15
F/0/T/M10-08	11.99	9.82	80.26	80.10	34.13	74.34	5.76	11.98	40.12	-0.01
F/0/T/M10-09	11.99	9.83	80.16	80.13	34.32	74.29	5.84	11.98	40.31	0.23
F/0/T/M10-10	11.99	9.89	79.96	80.12	34.07	74.20	5.92	11.99	40.06	0.08
Mean	11.99	9.76	80.15	80.12	34.27	74.33	5.79	11.97	40.26	-
SD	0.00	0.19	0.14	0.05	0.24	0.18	0.20	0.02	0.24	-
CoV (%)	0.01	1.98	0.17	0.06	0.70	0.25	3.53	0.14	0.60	-
F/0/T/M12-01	14.40	9.71	80.26	80.10	32.86	73.14	6.96	14.39	40.05	-0.08
F/0/T/M12-02	14.40	9.91	80.02	80.11	32.95	72.89	7.22	14.40	40.15	0.14
F/0/T/M12-03	14.40	9.59	80.26	80.14	33.07	73.10	7.04	14.40	40.27	0.14
F/0/T/M12-04	14.40	9.89	79.99	80.11	32.63	72.89	7.22	14.40	39.83	-0.17
F/0/T/M12-05	14.40	9.60	80.28	80.14	32.84	73.03	7.11	14.39	40.04	-0.10
F/0/T/M12-06	14.40	9.61	80.22	80.16	33.06	73.23	6.93	14.39	40.25	0.14
F/0/T/M12-07	14.40	9.85	80.25	80.17	33.02	73.00	7.17	14.40	40.22	0.09
F/0/T/M12-08	14.40	9.61	80.15	80.12	32.64	72.99	7.13	14.39	39.84	-0.24
F/0/T/M12-09	14.40	9.59	80.27	80.11	33.12	73.19	6.92	14.38	40.31	0.18
F/0/T/M12-10	14.39	9.62	80.05	80.09	32.97	73.07	7.02	14.39	40.16	0.14
Mean	14.40	9.70	80.18	80.13	32.92	73.05	7.07	14.39	40.11	-
SD	0.00	0.13	0.11	0.03	0.17	0.12	0.11	0.01	0.17	-
CoV (%)	0.02	1.37	0.14	0.03	0.52	0.16	1.62	0.05	0.43	-
F/0/T/M16-01	18.39	9.58	79.93	80.15	30.75	71.31	8.84	18.38	39.94	-0.03
F/0/T/M16-02	18.39	9.62	80.14	80.17	31.01	71.46	8.71	18.36	40.19	0.12
F/0/T/M16-03	18.39	10.20	80.28	80.20	31.12	71.13	9.07	18.38	40.31	0.17
F/0/T/M16-04	18.39	9.61	80.28	80.27	30.90	70.93	9.34	18.38	40.09	-0.05
F/0/T/M16-05	18.39	9.62	80.29	80.30	30.89	70.81	9.49	18.38	40.08	-0.06
F/0/T/M16-06	18.39	9.59	80.18	80.17	30.99	70.99	9.18	18.38	40.18	0.09
F/0/T/M16-07	18.39	9.88	80.22	80.32	31.05	70.89	9.43	18.38	40.24	0.13
F/0/T/M16-08	18.39	9.61	80.31	80.34	30.82	70.93	9.41	18.38	40.01	-0.14
F/0/T/M16-09	18.39	9.87	79.87	80.32	30.99	70.95	9.37	18.38	40.18	0.25
F/0/T/M16-10	18.39	10.18	80.28	80.27	30.78	71.27	9.00	18.38	39.97	-0.17
Mean	18.39	9.78	80.18	80.25	30.93	71.07	9.18	18.38	40.12	-
SD	0.00	0.24	0.16	0.07	0.12	0.21	0.27	0.01	0.12	-
CoV (%)	0.01	2.50	0.20	0.09	0.39	0.30	2.94	0.03	0.30	-
F/0/T/M20-01	22.40	9.59	80.26	80.23	28.76	69.04	11.19	22.39	39.96	-0.17
F/0/T/M20-02	22.40	9.61	80.28	80.24	29.09	69.27	10.97	22.39	40.29	0.15
F/0/T/M20-03	22.40	9.60	80.37	80.28	28.94	68.95	11.33	22.39	40.14	-0.05
F/0/T/M20-04	22.40	9.59	80.25	80.33	28.82	68.90	11.43	22.39	40.02	-0.11
F/0/T/M20-05	22.40	9.64	79.95	80.23	28.78	68.99	11.24	22.39	39.98	0.00
F/0/T/M20-06	22.40	9.62	80.00	80.31	28.75	69.24	11.07	22.39	39.95	-0.05
F/0/T/M20-07	22.40	9.85	80.08	80.29	28.96	69.06	11.23	22.39	40.16	0.12
F/0/T/M20-08	22.40	9.71	80.25	80.23	28.94	68.90	11.33	22.39	40.14	0.01
F/0/T/M20-09	22.40	9.60	80.15	80.22	28.87	69.08	11.14	22.39	40.07	-0.01
F/0/T/M20-10	22.40	9.59	80.43	80.21	28.77	69.09	11.12	22.39	39.97	-0.25
Mean	22.40	9.64	80.20	80.26	28.87	69.05	11.21	22.39	40.06	-
SD	0.00	0.08	0.15	0.04	0.11	0.13	0.14	0.00	0.11	-
CoV (%)	0.00	0.85	0.19	0.05	0.39	0.18	1.22	0.01	0.28	-

Table B.3: Pin-bearing Test Specimen Measurements for Flange Material tested with a Plain Pin in the Transverse Direction

Specimen ID	Diameter of Hole, d_n	Thickness of Specimen, t	Width of Specimen, w	Length of Specimen, l	Width to Hole Edge, w_h	Length to Hole Edge, l_h	Notch Depth, w_{notch}	Notch Diameter, d_{notch}	Notch Centre, l_{notch}	Offset, $(w - l_{notch})/2$
F/90/P/M10-01	11.99	10.27	80.15	80.05	34.04	73.91	6.14	11.98	40.03	-0.04
F/90/P/M10-02	11.99	9.75	80.20	80.07	34.29	74.06	6.01	11.99	40.28	0.18
F/90/P/M10-03	11.98	10.25	80.24	80.10	34.18	74.01	6.09	11.98	40.17	0.05
F/90/P/M10-04	11.98	9.59	80.16	80.11	33.94	73.94	6.17	11.97	39.93	-0.15
F/90/P/M10-05	11.98	9.58	80.12	80.14	33.87	73.94	6.20	11.97	39.86	-0.20
F/90/P/M10-06	11.98	9.59	80.17	80.08	34.09	73.85	6.23	11.97	40.08	-0.01
F/90/P/M10-07	11.99	10.29	80.16	80.05	34.19	74.07	5.98	11.98	40.18	0.10
F/90/P/M10-08	11.98	10.30	80.20	80.07	34.06	74.06	6.01	11.98	40.05	-0.05
F/90/P/M10-09	11.98	10.31	80.01	80.09	33.97	73.94	6.15	11.98	39.96	-0.05
F/90/P/M10-10	11.98	9.62	80.26	80.02	33.99	73.76	6.26	11.97	39.97	-0.16
Mean	11.98	9.96	80.17	80.08	34.06	73.95	6.12	11.98	40.05	-
SD	0.00	0.35	0.07	0.03	0.13	0.10	0.10	0.01	0.13	-
CoV (%)	0.02	3.52	0.09	0.04	0.38	0.14	1.60	0.05	0.33	-
F/90/P/M12-01	14.39	9.60	80.33	80.29	32.83	72.80	7.49	14.38	40.02	-0.15
F/90/P/M12-02	14.39	9.59	80.19	80.30	32.98	72.83	7.47	14.37	40.17	0.07
F/90/P/M12-03	14.39	9.59	80.14	80.30	32.82	72.76	7.54	14.37	40.01	-0.06
F/90/P/M12-04	14.39	9.80	80.25	80.31	32.79	72.75	7.56	14.37	39.98	-0.15
F/90/P/M12-05	14.39	9.89	80.12	80.28	32.81	72.66	7.62	14.36	39.99	-0.07
F/90/P/M12-06	14.40	10.32	80.01	80.27	32.80	72.85	7.42	14.39	40.00	-0.01
F/90/P/M12-07	14.39	9.58	80.02	80.25	33.19	72.72	7.53	14.37	40.38	0.37
F/90/P/M12-08	14.39	10.31	80.32	80.23	33.04	72.75	7.48	14.38	40.23	0.07
F/90/P/M12-09	14.39	9.62	80.19	80.22	32.92	72.93	7.29	14.39	40.11	0.02
F/90/P/M12-10	14.39	9.88	79.97	80.27	32.80	72.84	7.43	14.38	39.99	0.01
Mean	14.39	9.82	80.15	80.27	32.90	72.79	7.48	14.38	40.09	-
SD	0.00	0.29	0.13	0.03	0.13	0.08	0.09	0.01	0.13	-
CoV (%)	0.03	2.94	0.16	0.04	0.41	0.11	1.22	0.06	0.33	-
F/90/P/M16-01	18.39	10.29	80.09	80.15	30.80	70.77	9.38	18.39	39.99	-0.05
F/90/P/M16-02	18.40	10.26	80.21	80.20	30.91	70.78	9.42	18.39	40.10	0.00
F/90/P/M16-03	18.40	10.27	80.05	80.23	30.77	70.81	9.42	18.39	39.96	-0.06
F/90/P/M16-04	18.39	10.34	79.85	80.37	30.96	70.79	9.58	18.37	40.15	0.22
F/90/P/M16-05	18.39	10.25	80.22	80.31	30.87	70.51	9.80	18.35	40.05	-0.06
F/90/P/M16-06	18.39	10.30	80.02	80.21	30.91	70.79	9.42	18.38	40.10	0.09
F/90/P/M16-07	18.40	10.26	80.25	80.28	31.36	70.73	9.55	18.38	40.55	0.43
F/90/P/M16-08	18.39	10.30	80.12	80.21	30.91	70.74	9.47	18.38	40.10	0.04
F/90/P/M16-09	18.40	10.28	80.01	80.29	30.74	70.73	9.56	18.38	39.93	-0.07
F/90/P/M16-10	18.40	10.17	80.19	80.35	30.78	70.82	9.53	18.38	39.97	-0.12
Mean	18.39	10.27	80.10	80.26	30.90	70.75	9.51	18.38	40.09	-
SD	0.00	0.04	0.12	0.07	0.18	0.09	0.12	0.01	0.18	-
CoV (%)	0.01	0.43	0.15	0.09	0.57	0.13	1.29	0.06	0.44	-
F/90/P/M20-01	22.40	9.68	80.04	80.18	28.78	68.86	11.32	22.39	39.98	-0.04
F/90/P/M20-02	22.40	9.66	80.13	80.21	28.71	68.77	11.44	22.39	39.90	-0.16
F/90/P/M20-03	22.39	9.59	80.01	80.24	28.70	68.74	11.50	22.38	39.89	-0.11
F/90/P/M20-04	22.39	9.63	80.15	80.19	28.73	68.73	11.46	22.38	39.92	-0.15
F/90/P/M20-05	22.39	9.59	80.21	80.23	29.05	68.70	11.53	22.38	40.24	0.13
F/90/P/M20-06	22.39	9.57	80.16	80.21	28.86	68.74	11.47	22.38	40.05	-0.03
F/90/P/M20-07	22.40	9.60	80.21	80.19	28.77	68.72	11.47	22.39	39.96	-0.14
F/90/P/M20-08	22.40	9.58	80.13	80.18	28.89	68.84	11.34	22.39	40.09	0.02
F/90/P/M20-09	22.40	9.59	80.09	80.24	28.86	68.79	11.45	22.39	40.05	0.01
F/90/P/M20-10	22.40	9.58	80.45	80.16	29.39	68.78	11.38	22.39	40.59	0.36
Mean	22.39	9.61	80.16	80.20	28.87	68.77	11.44	22.39	40.07	-
SD	0.00	0.04	0.12	0.03	0.21	0.05	0.07	0.00	0.21	-
CoV (%)	0.01	0.39	0.15	0.03	0.73	0.08	0.60	0.02	0.52	-

Table B.4: Pin-bearing Test Specimen Measurements for Flange Material tested with a Threaded pin in the Transverse Direction

Specimen ID	Diameter of Hole, d_n	Thickness of Specimen, t	Width of Specimen, w	Length of Specimen, l	Width to Hole Edge, w_h	Length to Hole Edge, l_h	Notch Depth, w_{notch}	Notch Diameter, d_{notch}	Notch Centre, l_{notch}	Offset, $(w - l_{notch})/2$
F/90/T/M10-01	11.98	10.30	80.01	80.09	33.99	74.04	6.05	11.98	39.98	-0.03
F/90/T/M10-02	11.98	10.15	80.11	80.10	34.16	74.03	6.07	11.98	40.15	0.10
F/90/T/M10-03	11.98	10.14	80.17	80.17	34.29	74.01	6.16	11.97	40.28	0.19
F/90/T/M10-04	11.98	9.61	80.22	80.04	33.94	73.97	6.07	11.98	39.93	-0.18
F/90/T/M10-05	11.98	10.20	80.28	80.08	33.83	73.89	6.19	11.98	39.82	-0.32
F/90/T/M10-06	11.98	10.23	79.66	80.01	33.65	73.02	6.99	11.81	39.56	-0.27
F/90/T/M10-07	11.99	10.18	80.02	80.05	33.80	73.93	6.12	11.98	39.79	-0.22
F/90/T/M10-08	11.98	9.62	79.97	80.12	33.98	73.94	6.18	11.97	39.97	-0.02
F/90/T/M10-09	11.98	9.60	80.13	80.03	34.01	74.07	5.96	11.98	40.00	-0.06
F/90/T/M10-10	11.98	9.60	80.11	80.08	33.95	73.97	6.11	11.98	39.94	-0.12
Mean	11.98	9.96	80.07	80.08	33.96	73.89	6.19	11.96	39.94	-
SD	0.00	0.31	0.17	0.05	0.18	0.31	0.29	0.05	0.20	-
CoV (%)	0.02	3.10	0.22	0.06	0.53	0.42	4.67	0.44	0.49	-
F/90/T/M12-01	14.39	9.60	80.23	80.25	32.89	72.53	7.72	14.35	40.07	-0.05
F/90/T/M12-02	14.39	9.59	80.11	80.18	32.88	72.68	7.50	14.37	40.07	0.01
F/90/T/M12-03	14.39	9.59	80.14	80.13	32.93	72.63	7.50	14.37	40.12	0.05
F/90/T/M12-04	14.39	9.80	80.21	80.09	32.87	72.66	7.43	14.38	40.06	-0.05
F/90/T/M12-05	14.39	9.89	80.15	80.06	32.84	72.71	7.35	14.39	40.03	-0.04
F/90/T/M12-06	14.39	10.32	80.01	80.10	32.69	73.14	6.96	14.38	39.88	-0.12
F/90/T/M12-07	14.40	9.58	80.33	80.12	33.31	72.97	7.15	14.39	40.51	0.34
F/90/T/M12-08	14.40	10.31	80.21	79.88	32.96	72.74	7.14	14.39	40.16	0.05
F/90/T/M12-09	14.39	9.62	80.25	80.27	32.98	72.75	7.52	14.38	40.17	0.04
F/90/T/M12-10	14.40	9.88	80.14	80.15	32.77	72.84	7.31	14.39	39.97	-0.10
Mean	14.39	9.82	80.18	80.12	32.91	72.77	7.36	14.38	40.10	-
SD	0.00	0.29	0.09	0.11	0.16	0.18	0.22	0.01	0.17	-
CoV (%)	0.03	2.94	0.11	0.14	0.50	0.24	3.05	0.09	0.41	-
F/90/T/M16-01	18.39	9.58	80.18	80.17	30.70	70.55	9.62	18.37	39.88	-0.21
F/90/T/M16-02	18.39	9.59	80.14	80.20	30.94	70.60	9.60	18.37	40.12	0.05
F/90/T/M16-03	18.38	9.64	80.23	80.28	31.03	70.70	9.58	18.36	40.21	0.10
F/90/T/M16-04	18.39	9.58	80.27	80.17	30.77	70.84	9.33	18.38	39.96	-0.17
F/90/T/M16-05	18.39	9.60	80.17	80.23	30.83	70.64	9.59	18.37	40.02	-0.07
F/90/T/M16-06	18.39	9.79	80.26	80.27	31.02	70.82	9.45	18.38	40.21	0.08
F/90/T/M16-07	18.39	9.78	80.09	80.23	30.77	70.91	9.32	18.38	39.96	-0.08
F/90/T/M16-08	18.90	9.58	80.26	80.27	30.79	70.68	9.59	18.90	40.24	0.11
F/90/T/M16-09	18.40	9.80	80.12	80.27	30.84	70.73	9.54	18.38	40.03	-0.03
F/90/T/M16-10	18.39	9.60	80.15	80.24	30.77	70.86	9.38	18.38	39.96	-0.11
Mean	18.44	9.65	80.19	80.23	30.85	70.73	9.50	18.43	40.06	-
SD	0.16	0.10	0.06	0.04	0.11	0.12	0.12	0.17	0.13	-
CoV (%)	0.88	0.99	0.08	0.05	0.37	0.17	1.25	0.90	0.32	-
F/90/T/M20-01	22.40	10.28	80.19	80.21	28.83	68.75	11.46	22.39	40.02	-0.07
F/90/T/M20-02	22.40	10.25	80.08	80.31	28.78	68.82	11.49	22.39	39.97	-0.07
F/90/T/M20-03	22.39	10.27	80.12	80.25	28.74	68.78	11.47	22.38	39.93	-0.13
F/90/T/M20-04	22.40	10.26	80.09	80.32	28.73	68.74	11.58	22.38	39.92	-0.12
F/90/T/M20-05	22.40	10.25	80.29	80.26	28.81	68.78	11.48	22.39	40.00	-0.14
F/90/T/M20-06	22.40	10.26	80.27	80.12	29.01	68.71	11.41	22.39	40.21	0.07
F/90/T/M20-07	22.39	10.29	80.20	80.21	29.02	68.78	11.43	22.39	40.21	0.11
F/90/T/M20-08	22.39	10.27	80.13	80.20	28.81	68.72	11.48	22.38	40.00	-0.06
F/90/T/M20-09	22.40	10.28	80.09	80.19	28.85	68.73	11.46	22.39	40.04	0.00
F/90/T/M20-10	22.40	10.25	80.18	80.20	28.80	68.71	11.49	22.39	39.99	-0.10
Mean	22.39	10.27	80.16	80.23	28.84	68.75	11.48	22.39	40.03	-
SD	0.00	0.01	0.07	0.06	0.10	0.04	0.05	0.00	0.10	-
CoV (%)	0.01	0.14	0.09	0.07	0.35	0.05	0.39	0.01	0.25	-

Table B.5: Pin-bearing Test Specimen Measurements for Web Material tested with a Plain Pin in the Longitudinal Direction

Specimen ID	Diameter of Hole, d_n	Thickness of Specimen, t	Width of Specimen, w	Length of Specimen, l	Width to Hole Edge, w_h	Length to Hole Edge, l_h	Notch Depth, w_{notch}	Notch Diameter, d_{notch}	Notch Centre, l_{notch}	Offset, $(w - l_{notch})/2$
W/0/P/M10-01	11.98	9.59	80.03	80.08	33.94	74.04	6.04	11.98	39.93	-0.09
W/0/P/M10-02	11.98	9.63	80.04	80.16	34.03	74.38	5.78	11.97	40.02	0.00
W/0/P/M10-03	11.98	9.60	79.98	80.08	33.90	74.10	5.98	11.98	39.89	-0.10
W/0/P/M10-04	11.99	9.64	80.03	80.11	34.02	74.47	5.64	11.97	40.00	-0.01
W/0/P/M10-05	11.99	9.59	79.90	80.02	33.58	74.38	5.64	11.97	39.56	-0.39
W/0/P/M10-06	11.99	9.60	79.97	80.17	34.12	74.48	5.69	11.98	40.11	0.12
W/0/P/M10-07	11.99	9.58	79.98	80.11	34.10	74.34	5.77	11.98	40.09	0.10
W/0/P/M10-08	11.99	9.59	80.01	80.18	34.01	74.37	5.81	11.98	40.00	0.00
W/0/P/M10-09	11.99	9.61	80.20	80.14	34.14	74.36	5.78	11.98	40.13	0.03
W/0/P/M10-10	11.98	9.63	79.93	80.13	33.85	74.24	5.89	11.98	39.84	-0.12
Mean	11.99	9.61	80.01	80.12	33.97	74.32	5.80	11.98	39.96	-
SD	0.00	0.02	0.08	0.05	0.17	0.15	0.13	0.01	0.17	-
CoV (%)	0.04	0.22	0.10	0.06	0.49	0.20	2.32	0.04	0.42	-
W/0/P/M12-01	14.40	9.62	80.16	80.32	32.89	72.92	7.40	14.39	40.09	0.01
W/0/P/M12-02	14.39	9.61	79.87	80.31	32.81	72.80	7.51	14.38	40.00	0.06
W/0/P/M12-03	14.39	9.61	80.14	80.26	32.76	73.11	7.15	14.39	39.95	-0.12
W/0/P/M12-04	14.39	9.60	80.21	80.27	32.95	72.85	7.42	14.38	40.14	0.04
W/0/P/M12-05	14.39	9.65	80.09	80.29	32.79	72.90	7.39	14.38	39.98	-0.06
W/0/P/M12-06	14.39	9.61	80.17	80.27	33.01	72.99	7.28	14.38	40.20	0.12
W/0/P/M12-07	14.40	9.62	79.94	80.33	33.29	73.07	7.26	14.39	40.49	0.52
W/0/P/M12-08	14.40	9.66	80.17	80.31	32.89	73.06	7.25	14.39	40.09	0.00
W/0/P/M12-09	14.39	9.63	80.09	80.29	32.87	73.07	7.22	14.39	40.06	0.02
W/0/P/M12-10	14.40	9.65	80.23	80.27	32.93	73.21	7.06	14.39	40.13	0.01
Mean	14.39	9.63	80.11	80.29	32.92	73.00	7.29	14.39	40.11	-
SD	0.00	0.02	0.12	0.02	0.15	0.13	0.14	0.01	0.15	-
CoV (%)	0.03	0.21	0.15	0.03	0.46	0.18	1.87	0.04	0.38	-
W/0/P/M16-01	18.40	9.63	79.94	80.30	30.88	71.17	9.13	18.39	40.08	0.11
W/0/P/M16-02	18.39	9.65	80.05	80.29	30.77	71.12	9.17	18.39	39.96	-0.06
W/0/P/M16-03	18.39	9.58	80.01	80.26	30.80	71.31	8.95	18.38	39.99	-0.01
W/0/P/M16-04	18.39	9.61	79.95	80.22	30.87	71.27	8.95	18.38	40.06	0.08
W/0/P/M16-05	18.39	9.61	80.15	80.20	30.79	70.86	9.34	18.39	39.98	-0.09
W/0/P/M16-06	18.39	9.65	80.13	80.27	30.77	71.03	9.24	18.39	39.96	-0.10
W/0/P/M16-07	18.39	9.63	80.12	80.24	30.96	71.06	9.18	18.38	40.15	0.09
W/0/P/M16-08	18.39	9.65	80.00	80.24	30.93	70.95	9.29	18.38	40.12	0.12
W/0/P/M16-09	18.39	9.61	80.09	80.23	30.81	71.03	9.20	18.39	40.00	-0.04
W/0/P/M16-10	18.39	9.65	80.01	80.26	30.82	71.12	9.14	18.39	40.01	0.01
Mean	18.39	9.63	80.05	80.25	30.84	71.09	9.16	18.39	40.03	-
SD	0.00	0.02	0.07	0.03	0.07	0.14	0.13	0.00	0.07	-
CoV (%)	0.02	0.25	0.09	0.04	0.22	0.19	1.40	0.02	0.17	-
W/0/P/M20-01	22.40	9.70	80.24	80.26	28.81	68.95	11.31	22.39	40.01	-0.11
W/0/P/M20-02	22.40	9.63	80.06	80.24	28.95	68.99	11.25	22.39	40.15	0.12
W/0/P/M20-03	22.39	9.75	80.15	80.22	28.88	69.28	10.94	22.38	40.07	0.00
W/0/P/M20-04	22.39	9.60	79.98	80.28	28.76	69.04	11.24	22.39	39.95	-0.04
W/0/P/M20-05	22.40	9.66	80.08	80.27	28.82	69.07	11.20	22.39	40.02	-0.02
W/0/P/M20-06	22.39	9.62	80.00	80.24	28.98	69.88	10.36	22.33	40.14	0.14
W/0/P/M20-07	22.39	9.62	80.17	80.26	29.01	69.21	11.05	22.39	40.20	0.12
W/0/P/M20-08	22.40	9.63	80.03	80.31	28.84	69.08	11.23	22.39	40.04	0.02
W/0/P/M20-09	22.39	9.63	79.99	80.40	28.73	69.29	11.11	22.39	39.92	-0.07
W/0/P/M20-10	22.40	9.67	80.09	80.19	28.93	69.03	11.16	22.39	40.13	0.08
Mean	22.39	9.65	80.08	80.27	28.87	69.18	11.09	22.39	40.06	-
SD	0.00	0.05	0.09	0.06	0.09	0.27	0.28	0.02	0.09	-
CoV (%)	0.01	0.47	0.11	0.07	0.33	0.39	2.50	0.09	0.23	-

Table B.6: Pin-bearing Test Specimen Measurements for Web Material tested with a Threaded Pin in the Longitudinal Direction

Specimen ID	Diameter of Hole, dn	Thickness of Specimen, t	Width of Specimen, w	Length of Specimen, l	Width to Hole Edge, wh	Length to Hole Edge, lh	Notch Depth, wnotch	Notch Diameter, dnotch	Notch Centre, lnotch	Offset, (w - lnotch)/ 2
W/0/T/M10-01	12.00	9.62	80.08	80.06	34.05	74.07	5.99	11.99	40.05	0.01
W/0/T/M10-02	11.99	9.62	79.87	80.08	33.85	74.63	5.45	11.94	39.82	-0.11
W/0/T/M10-03	11.99	9.63	79.85	80.12	33.76	74.08	6.04	11.99	39.76	-0.17
W/0/T/M10-04	11.99	9.63	79.98	80.14	34.01	74.16	5.98	11.99	40.01	0.02
W/0/T/M10-05	11.99	9.60	80.08	80.16	33.95	74.01	6.15	11.99	39.94	-0.10
W/0/T/M10-06	11.99	9.61	80.06	80.15	34.16	74.45	5.70	11.98	40.15	0.12
W/0/T/M10-07	11.99	9.62	80.01	80.08	34.05	74.15	5.93	11.99	40.05	0.04
W/0/T/M10-08	11.99	9.60	79.99	80.09	33.97	74.31	5.78	11.98	39.96	-0.03
W/0/T/M10-09	11.99	9.61	80.00	80.15	33.99	74.26	5.89	11.99	39.99	-0.01
W/0/T/M10-10	11.99	9.59	80.19	80.13	34.04	74.27	5.86	11.99	40.04	-0.06
Mean	11.99	9.61	80.01	80.12	33.98	74.24	5.88	11.98	39.98	-
SD	0.00	0.01	0.10	0.04	0.11	0.19	0.20	0.02	0.11	-
CoV (%)	0.01	0.14	0.13	0.04	0.33	0.26	3.36	0.13	0.29	-
W/0/T/M12-01	14.39	9.64	80.07	80.33	32.80	72.84	7.49	14.37	39.99	-0.05
W/0/T/M12-02	14.39	9.63	80.02	79.97	32.89	73.07	6.90	14.37	40.08	0.07
W/0/T/M12-03	14.39	9.61	80.17	80.19	32.88	72.87	7.32	14.39	40.07	-0.01
W/0/T/M12-04	14.39	9.64	79.99	80.33	32.79	73.24	7.09	14.38	39.98	-0.01
W/0/T/M12-05	14.39	9.63	79.99	80.27	32.88	73.22	7.05	14.38	40.07	0.08
W/0/T/M12-06	14.39	9.63	79.97	80.32	32.85	73.28	7.04	14.38	40.04	0.06
W/0/T/M12-07	14.39	9.62	80.03	80.35	32.83	73.16	7.19	14.38	40.02	0.01
W/0/T/M12-08	14.39	9.62	80.17	80.29	32.91	73.09	7.20	14.38	40.10	0.02
W/0/T/M12-09	14.39	9.61	80.01	80.27	32.88	73.18	7.09	14.39	40.07	0.07
W/0/T/M12-10	14.39	9.60	80.19	80.33	32.82	73.16	7.17	14.39	40.01	-0.08
Mean	14.39	9.62	80.06	80.27	32.85	73.11	7.15	14.38	40.04	-
SD	0.00	0.01	0.08	0.11	0.04	0.15	0.16	0.01	0.04	-
CoV (%)	0.02	0.14	0.11	0.14	0.13	0.20	2.29	0.04	0.10	-
W/0/T/M16-01	18.40	9.63	79.92	80.08	30.81	71.26	8.82	18.38	40.00	0.04
W/0/T/M16-02	18.39	9.64	80.09	80.11	30.82	71.13	8.98	18.38	40.01	-0.03
W/0/T/M16-03	18.40	9.61	80.01	80.09	30.97	71.05	9.04	18.39	40.17	0.16
W/0/T/M16-04	18.40	9.65	80.11	80.13	30.67	70.82	9.31	18.39	39.87	-0.19
W/0/T/M16-05	18.40	9.63	80.06	80.06	30.85	70.92	9.14	18.39	40.05	0.02
W/0/T/M16-06	18.40	9.61	80.11	80.08	30.88	71.04	9.04	18.39	40.08	0.02
W/0/T/M16-07	18.40	9.62	80.00	80.09	30.76	70.99	9.10	18.40	39.96	-0.04
W/0/T/M16-08	18.40	9.62	80.03	79.97	30.89	70.92	9.05	18.39	40.09	0.07
W/0/T/M16-09	18.40	9.64	80.09	80.11	30.98	71.24	8.87	18.39	40.17	0.13
W/0/T/M16-10	18.40	9.60	80.15	80.13	30.93	71.10	9.03	18.39	40.13	0.05
Mean	18.40	9.63	80.06	80.09	30.86	71.05	9.04	18.39	40.05	-
SD	0.00	0.02	0.07	0.05	0.10	0.14	0.14	0.01	0.10	-
CoV (%)	0.02	0.16	0.08	0.06	0.31	0.20	1.51	0.03	0.24	-
W/0/T/M20-01	22.40	9.68	80.11	80.22	28.41	69.35	10.87	22.39	39.60	-0.45
W/0/T/M20-02	22.39	9.62	79.96	80.27	28.97	69.23	11.04	22.39	40.16	0.18
W/0/T/M20-03	22.40	9.72	80.00	80.21	28.82	69.06	11.15	22.39	40.02	0.02
W/0/T/M20-04	22.39	9.61	79.94	80.78	28.85	69.05	11.73	22.36	40.03	0.06
W/0/T/M20-05	22.40	9.60	80.09	80.22	28.83	68.84	11.38	22.39	40.03	-0.02
W/0/T/M20-06	22.40	9.62	80.10	80.27	28.83	69.21	11.06	22.39	40.03	-0.02
W/0/T/M20-07	22.40	9.65	79.97	80.26	28.93	68.93	11.33	22.39	40.13	0.14
W/0/T/M20-08	22.40	9.67	80.02	80.29	28.84	69.09	11.20	22.39	40.04	0.03
W/0/T/M20-09	22.39	9.63	80.17	80.31	29.02	68.79	11.52	22.38	40.21	0.13
W/0/T/M20-10	22.39	9.62	80.03	80.36	28.77	69.36	11.00	22.39	39.96	-0.05
Mean	22.39	9.64	80.04	80.32	28.83	69.09	11.23	22.39	40.02	-
SD	0.00	0.04	0.08	0.17	0.17	0.20	0.26	0.01	0.17	-
CoV (%)	0.01	0.39	0.09	0.21	0.57	0.29	2.34	0.04	0.41	-

Table B.7: Pin-bearing Test Specimen Measurements for Web Material tested with a Plain Pin in the 45° Direction

Specimen ID	Diameter of Hole, d_n	Thickness of Specimen, t	Width of Specimen, w	Length of Specimen, l	Width to Hole Edge, w_h	Length to Hole Edge, l_h	Notch Depth, w_{notch}	Notch Diameter, d_{notch}	Notch Centre, l_{notch}	Offset, $(w - l_{notch})/2$
W/45/P/M10-01	11.98	9.64	80.05	80.10	34.09	74.09	6.01	11.98	40.08	0.06
W/45/P/M10-02	11.98	9.61	79.94	80.19	33.94	74.14	6.05	11.98	39.93	-0.04
W/45/P/M10-03	11.98	9.61	80.02	80.18	33.84	74.03	6.15	11.98	39.83	-0.18
W/45/P/M10-04	11.99	9.63	80.02	80.16	34.07	74.00	6.16	11.98	40.06	0.05
W/45/P/M10-05	11.98	9.62	80.00	80.13	34.02	74.07	6.06	11.98	40.01	0.01
W/45/P/M10-06	11.99	9.62	79.57	80.16	33.86	74.52	5.64	11.97	39.84	0.06
W/45/P/M10-07	11.99	9.66	79.80	80.15	33.81	74.08	6.07	11.98	39.80	-0.10
W/45/P/M10-08	11.99	9.64	79.92	80.11	34.15	74.30	5.81	11.98	40.14	0.18
W/45/P/M10-09	11.98	9.62	79.98	80.17	33.93	74.21	5.96	11.98	39.92	-0.07
W/45/P/M10-10	11.99	9.64	79.96	80.16	33.98	74.23	5.93	11.98	39.97	-0.01
Mean	11.98	9.63	79.93	80.15	33.97	74.17	5.98	11.98	39.96	-
SD	0.00	0.02	0.14	0.03	0.11	0.16	0.16	0.01	0.11	-
CoV (%)	0.02	0.17	0.18	0.04	0.33	0.21	2.66	0.04	0.29	-
W/45/P/M12-01	14.40	9.64	80.20	80.79	33.20	73.06	7.73	14.36	40.38	0.28
W/45/P/M12-02	14.40	9.60	79.89	80.81	32.62	73.01	7.80	14.35	39.79	-0.15
W/45/P/M12-03	14.40	9.60	80.03	80.80	32.87	72.90	7.90	14.33	40.04	0.02
W/45/P/M12-04	14.40	9.64	80.00	80.20	32.81	72.88	7.32	14.40	40.01	0.01
W/45/P/M12-05	14.40	9.62	80.15	80.80	32.93	72.81	7.99	14.31	40.09	0.01
W/45/P/M12-06	14.40	9.61	80.44	80.74	33.24	72.83	7.91	14.33	40.40	0.18
W/45/P/M12-07	14.40	9.61	80.08	80.71	32.83	72.82	7.89	14.33	40.00	-0.04
W/45/P/M12-08	14.40	9.60	80.28	80.80	32.83	72.92	7.88	14.34	40.00	-0.14
W/45/P/M12-09	14.40	9.61	80.03	80.81	32.85	72.90	7.91	14.33	40.01	0.00
W/45/P/M12-10	14.40	9.62	80.01	80.80	32.70	72.84	7.96	14.32	39.86	-0.15
Mean	14.40	9.62	80.11	80.73	32.89	72.90	7.83	14.34	40.06	-
SD	0.00	0.02	0.16	0.19	0.20	0.08	0.19	0.02	0.20	-
CoV (%)	0.00	0.16	0.20	0.23	0.60	0.11	2.47	0.17	0.49	-
W/45/P/M16-01	18.40	9.60	80.06	80.79	30.68	70.90	9.89	18.35	39.85	-0.18
W/45/P/M16-02	18.40	9.61	79.96	80.81	30.71	70.83	9.98	18.33	39.88	-0.10
W/45/P/M16-03	18.40	9.00	80.28	80.88	31.10	70.76	10.12	18.31	40.25	0.11
W/45/P/M16-04	18.40	9.67	80.02	80.88	30.79	70.89	9.99	18.33	39.96	-0.05
W/45/P/M16-05	18.40	9.68	80.16	80.88	30.93	71.00	9.88	18.35	40.10	0.02
W/45/P/M16-06	18.40	9.66	80.20	80.87	30.94	70.84	10.03	18.32	40.10	0.00
W/45/P/M16-07	18.40	9.60	79.83	80.81	30.78	70.83	9.98	18.33	39.95	0.03
W/45/P/M16-08	18.40	9.67	80.11	80.82	30.91	70.95	9.87	18.35	40.09	0.03
W/45/P/M16-09	18.40	9.65	80.07	80.87	30.87	70.93	9.94	18.34	40.04	0.01
W/45/P/M16-10	18.40	9.61	80.51	80.79	31.38	70.91	9.88	18.35	40.55	0.30
Mean	18.40	9.58	80.12	80.84	30.91	70.88	9.96	18.34	40.08	-
SD	0.00	0.20	0.19	0.04	0.21	0.07	0.08	0.01	0.21	-
CoV (%)	0.00	2.14	0.23	0.05	0.67	0.10	0.81	0.07	0.52	-
W/45/P/M20-01	22.40	9.62	80.24	80.10	28.89	69.25	10.85	22.38	40.08	-0.04
W/45/P/M20-02	22.39	9.67	80.26	80.12	29.07	69.20	10.92	22.38	40.26	0.13
W/45/P/M20-03	22.40	9.66	80.29	80.15	28.95	69.16	10.99	22.39	40.15	0.00
W/45/P/M20-04	22.39	9.62	80.17	80.18	28.79	69.10	11.08	22.39	39.98	-0.10
W/45/P/M20-05	22.39	9.68	80.26	80.16	28.89	69.24	10.92	22.38	40.08	-0.05
W/45/P/M20-06	22.39	9.66	80.27	80.20	29.07	69.69	10.51	22.35	40.24	0.11
W/45/P/M20-07	22.39	9.74	80.29	80.14	29.04	69.10	11.04	22.39	40.23	0.09
W/45/P/M20-08	22.39	9.63	80.34	80.09	28.94	69.13	10.96	22.39	40.13	-0.04
W/45/P/M20-09	22.39	9.62	80.25	80.01	28.95	69.02	10.99	22.39	40.14	0.02
W/45/P/M20-10	22.40	9.69	80.06	80.04	28.89	69.28	10.76	22.38	40.08	0.05
Mean	22.39	9.66	80.24	80.12	28.95	69.22	10.90	22.38	40.14	-
SD	0.00	0.04	0.08	0.06	0.09	0.18	0.17	0.01	0.09	-
CoV (%)	0.01	0.40	0.10	0.08	0.31	0.27	1.52	0.06	0.22	-

Table B.8: Pin-bearing Test Specimen Measurements for Web Material tested with a Threaded Pin in the 45° Direction

Specimen ID	Diameter of Hole, d_n	Thickness of Specimen, t	Width of Specimen, w	Length of Specimen, l	Width to Hole Edge, w_h	Length to Hole Edge, l_h	Notch Depth, w_{notch}	Notch Diameter, d_{notch}	Notch Centre, l_{notch}	Offset, $(w - l_{notch})/2$
W/45/T/M10-01	11.99	9.64	80.32	80.17	33.97	74.33	5.84	11.99	39.96	-0.20
W/45/T/M10-02	11.99	9.63	80.23	80.05	34.25	74.49	5.56	11.96	40.23	0.11
W/45/T/M10-03	11.99	9.61	79.94	80.21	33.94	74.34	5.87	11.99	39.93	-0.04
W/45/T/M10-04	11.99	9.61	80.27	80.16	33.93	74.49	5.67	11.97	39.92	-0.22
W/45/T/M10-05	11.99	9.66	80.14	80.23	34.04	74.27	5.96	11.99	40.03	-0.04
W/45/T/M10-06	11.99	9.67	80.14	80.16	34.09	74.21	5.95	11.99	40.08	0.01
W/45/T/M10-07	11.99	9.67	80.20	80.20	34.23	74.51	5.69	11.98	40.22	0.12
W/45/T/M10-08	12.00	9.67	80.21	80.20	34.02	74.46	5.74	11.98	40.01	-0.09
W/45/T/M10-09	11.99	9.64	80.18	80.14	34.16	74.37	5.77	11.98	40.15	0.06
W/45/T/M10-10	11.99	9.66	79.96	80.17	34.03	74.62	5.55	11.96	40.01	0.03
Mean	11.99	9.65	80.16	80.17	34.07	74.41	5.76	11.98	40.06	-
SD	0.00	0.02	0.12	0.05	0.11	0.13	0.15	0.01	0.11	-
CoV (%)	0.02	0.25	0.15	0.06	0.34	0.17	2.54	0.10	0.28	-
W/45/T/M12-01	14.40	9.63	80.07	80.59	32.83	72.86	7.73	14.36	40.01	-0.02
W/45/T/M12-02	14.40	9.63	79.97	80.74	32.84	72.99	7.75	14.36	40.02	0.03
W/45/T/M12-03	14.40	9.60	80.23	80.87	33.05	72.90	7.97	14.32	40.21	0.09
W/45/T/M12-04	14.40	9.62	80.07	80.86	32.83	72.81	8.05	14.30	39.98	-0.06
W/45/T/M12-05	14.40	9.66	80.15	80.80	32.91	72.92	7.88	14.34	40.08	0.00
W/45/T/M12-06	14.40	9.63	80.00	80.81	32.75	72.97	7.84	14.34	39.92	-0.08
W/45/T/M12-07	14.40	9.61	80.07	80.86	32.89	72.94	7.92	14.33	40.05	0.02
W/45/T/M12-08	14.40	9.61	80.18	80.80	32.77	72.81	7.99	14.31	39.93	-0.16
W/45/T/M12-09	14.40	9.62	80.00	80.86	32.53	72.70	8.16	14.27	39.67	-0.33
W/45/T/M12-10	14.40	9.61	80.06	80.86	32.79	72.79	8.07	14.29	39.94	-0.09
Mean	14.40	9.62	80.08	80.81	32.82	72.87	7.94	14.32	39.98	-
SD	0.00	0.02	0.08	0.09	0.13	0.09	0.14	0.03	0.14	-
CoV (%)	0.00	0.18	0.10	0.11	0.40	0.13	1.76	0.20	0.35	-
W/45/T/M16-01	18.40	9.64	80.02	80.76	30.73	71.04	9.72	18.37	39.92	-0.09
W/45/T/M16-02	18.40	9.66	80.07	80.82	30.75	71.07	9.75	18.37	39.93	-0.10
W/45/T/M16-03	18.40	9.69	80.12	80.80	30.91	70.93	9.87	18.35	40.09	0.03
W/45/T/M16-04	18.40	9.64	80.09	80.79	30.77	71.00	9.79	18.36	39.95	-0.09
W/45/T/M16-05	18.40	9.68	80.20	80.85	30.96	70.66	10.19	18.29	40.11	0.01
W/45/T/M16-06	18.40	9.64	79.99	80.74	30.80	70.93	9.81	18.36	39.98	-0.02
W/45/T/M16-07	18.40	9.63	80.22	80.76	30.78	70.98	9.78	18.36	39.96	-0.15
W/45/T/M16-08	18.40	9.65	80.01	80.73	30.83	70.93	9.80	18.36	40.01	0.01
W/45/T/M16-09	18.40	9.63	80.31	80.76	30.85	70.80	9.96	18.34	40.02	-0.14
W/45/T/M16-10	18.40	9.67	80.20	80.67	31.10	70.96	9.71	18.37	40.29	0.19
Mean	18.40	9.65	80.12	80.77	30.85	70.93	9.84	18.35	40.02	-
SD	0.00	0.02	0.11	0.05	0.11	0.12	0.14	0.02	0.11	-
CoV (%)	0.00	0.22	0.13	0.06	0.37	0.17	1.46	0.13	0.28	-
W/45/T/M20-01	22.38	9.63	79.90	80.09	28.85	68.88	11.21	22.38	40.04	0.09
W/45/T/M20-02	22.38	9.62	80.10	80.04	28.92	69.43	10.61	22.35	40.09	0.04
W/45/T/M20-03	22.39	9.64	79.98	80.11	28.71	69.03	11.08	22.38	39.90	-0.09
W/45/T/M20-04	22.39	9.63	79.97	80.03	28.82	68.96	11.07	22.38	40.01	0.03
W/45/T/M20-05	22.38	9.66	79.93	80.04	28.81	68.85	11.19	22.38	40.00	0.03
W/45/T/M20-06	22.38	9.63	80.15	80.14	28.93	69.05	11.09	22.38	40.12	0.04
W/45/T/M20-07	22.38	9.64	79.93	80.06	28.64	69.21	10.85	22.37	39.82	-0.14
W/45/T/M20-08	22.39	9.63	80.06	80.01	28.97	69.03	10.98	22.38	40.16	0.13
W/45/T/M20-09	22.38	9.64	80.10	80.07	28.81	69.05	11.02	22.38	40.00	-0.05
W/45/T/M20-10	22.39	9.63	80.13	80.09	28.82	69.02	11.07	22.38	40.01	-0.05
Mean	22.38	9.64	80.03	80.07	28.83	69.05	11.02	22.38	40.02	-
SD	0.00	0.01	0.09	0.04	0.10	0.17	0.18	0.01	0.10	-
CoV (%)	0.01	0.11	0.12	0.05	0.35	0.24	1.59	0.05	0.25	-

Table B.9: Pin-bearing Test Specimen Measurements for Web Material tested with a Plain Pin in the Transverse Direction

Specimen ID	Diameter of Hole, d_n	Thickness of Specimen, t	Width of Specimen, w	Length of Specimen, l	Width to Hole Edge, w_h	Length to Hole Edge, l_h	Notch Depth, w_{notch}	Notch Diameter, d_{notch}	Notch Centre, l_{notch}	Offset, $(w - l_{notch})/2$
W/90/P/M10-01	11.99	9.63	79.98	80.09	33.36	73.85	6.24	11.98	39.35	-0.64
W/90/P/M10-02	11.98	9.60	80.40	80.12	34.46	73.93	6.19	11.98	40.45	0.25
W/90/P/M10-03	11.99	9.65	80.38	80.18	34.29	74.02	6.16	11.99	40.28	0.09
W/90/P/M10-04	11.99	9.60	80.09	80.05	34.11	74.42	5.63	11.96	40.09	0.05
W/90/P/M10-05	11.98	9.60	80.36	80.09	34.09	74.32	5.77	11.98	40.08	-0.10
W/90/P/M10-06	11.99	9.62	80.35	80.11	34.43	74.12	5.99	11.99	40.42	0.25
W/90/P/M10-07	11.99	9.64	80.19	80.09	34.32	74.07	6.02	11.98	40.31	0.22
W/90/P/M10-08	11.98	9.63	80.58	80.07	34.14	74.14	5.93	11.98	40.13	-0.16
W/90/P/M10-09	11.98	9.62	80.35	80.10	34.30	74.07	6.03	11.98	40.29	0.12
W/90/P/M10-10	11.99	9.63	80.31	80.11	33.93	74.03	6.08	11.99	39.92	-0.23
Mean	11.99	9.62	80.30	80.10	34.14	74.10	6.00	11.98	40.13	-
SD	0.00	0.02	0.17	0.03	0.32	0.17	0.19	0.01	0.32	-
CoV (%)	0.02	0.18	0.21	0.04	0.94	0.23	3.15	0.06	0.80	-
W/90/P/M12-01	14.40	9.62	80.14	79.97	32.83	72.84	7.13	14.39	40.03	-0.04
W/90/P/M12-02	14.39	9.63	79.85	80.09	32.71	72.64	7.45	14.38	39.90	-0.02
W/90/P/M12-03	14.39	9.61	80.50	80.15	33.30	73.05	7.10	14.39	40.49	0.24
W/90/P/M12-04	14.39	9.66	80.19	80.07	32.78	72.67	7.40	14.38	39.97	-0.12
W/90/P/M12-05	14.40	9.65	79.92	79.96	32.87	72.43	7.53	14.38	40.06	0.10
W/90/P/M12-06	14.40	9.63	79.90	80.11	32.77	72.79	7.32	14.39	39.97	0.02
W/90/P/M12-07	14.40	9.66	80.21	80.13	32.92	72.81	7.32	14.39	40.12	0.01
W/90/P/M12-08	14.40	9.65	80.13	80.12	32.95	73.09	7.03	14.39	40.15	0.08
W/90/P/M12-09	14.40	9.65	80.17	80.11	32.94	72.93	7.18	14.39	40.14	0.05
W/90/P/M12-10	14.40	9.63	80.34	80.07	32.86	72.85	7.22	14.39	40.06	-0.11
Mean	14.39	9.64	80.14	80.08	32.89	72.81	7.27	14.39	40.09	-
SD	0.00	0.02	0.20	0.06	0.16	0.20	0.16	0.01	0.16	-
CoV (%)	0.02	0.18	0.25	0.08	0.50	0.27	2.24	0.04	0.41	-
W/90/P/M16-01	18.39	9.64	80.15	80.10	30.89	70.70	9.40	18.39	40.08	0.01
W/90/P/M16-02	18.40	9.65	80.17	80.11	30.92	70.95	9.16	18.39	40.12	0.03
W/90/P/M16-03	18.39	9.63	79.92	80.10	30.88	70.63	9.47	18.38	40.07	0.11
W/90/P/M16-04	18.39	9.66	79.79	80.09	30.81	70.65	9.44	18.38	40.00	0.11
W/90/P/M16-05	18.39	9.64	80.01	80.10	30.85	70.91	9.19	18.39	40.04	0.04
W/90/P/M16-06	18.39	9.63	79.87	80.09	30.75	70.82	9.27	18.39	39.94	0.01
W/90/P/M16-07	18.40	9.63	80.19	80.20	30.98	70.89	9.31	18.39	40.18	0.08
W/90/P/M16-08	18.40	9.59	79.83	80.18	30.90	70.74	9.44	18.39	40.09	0.18
W/90/P/M16-09	18.39	9.63	80.18	80.13	31.07	70.79	9.34	18.39	40.26	0.17
W/90/P/M16-10	18.40	9.62	79.95	80.15	30.81	70.80	9.35	18.39	40.01	0.03
Mean	18.39	9.63	80.01	80.13	30.89	70.79	9.34	18.39	40.08	-
SD	0.00	0.02	0.16	0.04	0.09	0.11	0.11	0.00	0.09	-
CoV (%)	0.01	0.19	0.19	0.05	0.30	0.15	1.14	0.02	0.23	-
W/90/P/M20-01	22.40	9.66	80.12	80.23	28.13	68.85	11.38	22.39	39.33	-0.73
W/90/P/M20-02	22.39	9.65	80.28	80.22	29.21	69.14	11.08	22.39	40.40	0.26
W/90/P/M20-03	22.39	9.64	80.08	80.23	28.82	68.99	11.24	22.39	40.01	-0.03
W/90/P/M20-04	22.39	9.63	80.46	80.21	28.81	68.96	11.25	22.39	40.00	-0.23
W/90/P/M20-05	22.39	9.61	80.01	80.19	28.80	68.83	11.36	22.39	39.99	-0.01
W/90/P/M20-06	22.39	9.63	79.88	80.25	28.93	68.89	11.36	22.39	40.12	0.18
W/90/P/M20-07	22.39	9.64	80.15	80.20	29.09	68.83	11.37	22.39	40.28	0.21
W/90/P/M20-08	22.39	9.63	80.05	80.27	28.79	68.47	11.80	22.35	39.97	-0.06
W/90/P/M20-09	22.39	9.60	80.04	80.34	28.98	69.13	11.21	22.38	40.17	0.15
W/90/P/M20-10	22.39	9.66	80.05	80.28	28.76	68.73	11.55	22.38	39.95	-0.08
Mean	22.39	9.64	80.11	80.24	28.83	68.88	11.36	22.38	40.02	-
SD	0.00	0.02	0.16	0.04	0.29	0.20	0.20	0.01	0.29	-
CoV (%)	0.01	0.20	0.20	0.06	1.00	0.28	1.75	0.05	0.72	-

Table B.10: Pin-bearing Test Specimen Measurements for Web Material tested with a Threaded Pin in the Transverse Direction

Specimen ID	Diameter of Hole, d_n	Thickness of Specimen, t	Width of Specimen, w	Length of Specimen, l	Width to Hole Edge, w_h	Length to Hole Edge, l_h	Notch Depth, w_{notch}	Notch Diameter, d_{notch}	Notch Centre, l_{notch}	Offset, $(w - l_{notch})/2$
W/90/T/M10-01	11.99	9.61	80.17	80.10	34.01	74.36	5.74	11.97	40.00	-0.09
W/90/T/M10-02	11.98	9.60	80.43	80.18	34.45	74.00	6.18	11.98	40.44	0.22
W/90/T/M10-03	11.99	9.60	80.13	80.08	33.95	73.99	6.09	11.98	39.94	-0.12
W/90/T/M10-04	11.98	9.64	79.99	80.13	34.08	73.97	6.16	11.97	40.07	0.07
W/90/T/M10-05	11.98	9.65	80.16	80.25	34.04	73.94	6.31	11.97	40.02	-0.06
W/90/T/M10-06	11.98	9.61	80.22	80.15	34.23	73.81	6.34	11.96	40.21	0.10
W/90/T/M10-07	11.99	9.61	80.02	80.13	33.95	74.00	6.13	11.98	39.94	-0.07
W/90/T/M10-08	11.99	9.58	80.04	80.07	34.06	73.93	6.14	11.98	40.05	0.03
W/90/T/M10-09	11.98	9.60	80.56	80.14	34.49	74.08	6.06	11.98	40.48	0.20
W/90/T/M10-10	11.99	9.64	80.33	80.00	34.02	74.09	5.91	11.98	40.01	-0.15
Mean	11.98	9.61	80.21	80.12	34.13	74.02	6.11	11.98	40.12	-
SD	0.00	0.02	0.19	0.07	0.20	0.14	0.18	0.01	0.20	-
CoV (%)	0.03	0.23	0.23	0.08	0.58	0.19	2.90	0.07	0.49	-
W/90/T/M12-01	14.39	9.66	80.49	80.30	32.71	72.83	7.47	14.38	39.90	-0.35
W/90/T/M12-02	14.39	9.64	80.00	80.31	32.90	72.80	7.51	14.37	40.09	0.09
W/90/T/M12-03	14.40	9.63	80.35	80.24	33.07	72.69	7.55	14.38	40.26	0.08
W/90/T/M12-04	14.39	9.64	80.36	80.26	32.83	72.66	7.60	14.36	40.01	-0.17
W/90/T/M12-05	14.39	9.62	79.91	80.22	32.77	72.77	7.45	14.38	39.96	0.01
W/90/T/M12-06	14.39	9.60	80.03	80.24	32.86	73.18	7.06	14.38	40.05	0.04
W/90/T/M12-07	14.39	9.60	80.53	80.33	33.48	73.02	7.31	14.39	40.67	0.41
W/90/T/M12-08	14.39	9.67	80.43	80.27	32.84	72.71	7.56	14.37	40.02	-0.19
W/90/T/M12-09	14.39	9.61	79.93	80.28	32.86	72.83	7.45	14.38	40.05	0.08
W/90/T/M12-10	14.39	9.64	80.35	80.17	32.81	72.81	7.36	14.39	40.00	-0.17
Mean	14.39	9.63	80.24	80.26	32.91	72.83	7.43	14.38	40.10	-
SD	0.00	0.02	0.24	0.05	0.22	0.16	0.16	0.01	0.22	-
CoV (%)	0.02	0.25	0.30	0.06	0.67	0.22	2.13	0.06	0.55	-
W/90/T/M16-01	18.39	9.62	80.61	80.05	30.79	70.95	9.10	18.38	39.98	-0.32
W/90/T/M16-02	18.38	9.66	80.21	80.19	31.06	71.13	9.06	18.38	40.25	0.14
W/90/T/M16-03	18.38	9.65	80.59	80.12	30.94	70.94	9.18	18.38	40.13	-0.17
W/90/T/M16-04	18.38	9.61	80.20	80.21	30.91	70.92	9.29	18.38	40.10	0.00
W/90/T/M16-05	18.38	9.61	80.55	80.01	31.34	71.06	8.95	18.37	40.53	0.25
W/90/T/M16-06	18.39	9.63	80.43	79.98	31.23	70.99	8.99	18.38	40.42	0.21
W/90/T/M16-07	18.38	9.62	80.21	80.08	31.02	70.67	9.41	18.37	40.21	0.10
W/90/T/M16-08	18.38	9.61	80.34	80.03	32.58	70.70	9.33	18.38	41.77	1.60
W/90/T/M16-09	18.38	9.65	80.23	80.10	30.97	71.03	9.07	18.38	40.16	0.04
W/90/T/M16-10	18.38	9.63	80.05	80.05	30.82	70.84	9.21	18.38	40.01	-0.02
Mean	18.38	9.63	80.34	80.08	31.17	70.92	9.16	18.38	40.36	-
SD	0.00	0.02	0.19	0.07	0.53	0.15	0.15	0.00	0.52	-
CoV (%)	0.01	0.19	0.24	0.09	1.69	0.21	1.65	0.02	1.30	-
W/90/T/M20-01	22.39	9.63	80.12	80.24	28.83	68.81	11.43	22.38	40.02	-0.04
W/90/T/M20-02	22.39	9.70	80.22	80.26	29.04	68.87	11.39	22.38	40.23	0.12
W/90/T/M20-03	22.39	9.67	79.90	80.33	28.65	68.67	11.66	22.37	39.83	-0.12
W/90/T/M20-04	22.39	9.61	79.95	80.25	28.86	68.76	11.49	22.38	40.05	0.07
W/90/T/M20-05	22.39	9.59	80.07	80.31	28.82	69.13	11.18	22.38	40.01	-0.02
W/90/T/M20-06	22.39	9.59	80.55	80.34	29.47	69.14	11.20	22.38	40.66	0.39
W/90/T/M20-07	22.39	9.60	80.00	80.25	28.84	69.01	11.24	22.38	40.03	0.03
W/90/T/M20-08	22.39	9.64	80.45	80.31	28.80	69.78	10.53	22.35	39.97	-0.25
W/90/T/M20-09	22.38	9.63	80.10	80.23	28.86	68.57	11.66	22.36	40.04	-0.01
W/90/T/M20-10	22.38	9.67	80.05	80.32	28.76	68.80	11.52	22.37	39.95	-0.08
Mean	22.38	9.63	80.14	80.28	28.89	68.95	11.33	22.37	40.08	-
SD	0.00	0.04	0.21	0.04	0.22	0.34	0.33	0.01	0.23	-
CoV (%)	0.01	0.39	0.26	0.05	0.78	0.50	2.91	0.06	0.57	-

B.3 Hot-wet Conditioned Pin Bearing Specimen Measurements

Table B.11: Pin-bearing Test Specimen Measurements for Flange Material tested with a Plain Pin in the Longitudinal Direction and Hot-wet Conditioned at 40°C for 3 Months

Specimen ID	Diameter of Hole, d_n	Thickness of Specimen, t	Width of Specimen, w	Length of Specimen, l	Width to Hole Edge, w_h	Length to Hole Edge, l_h	Notch Depth, w_{notch}	Notch Diameter, d_{notch}	Notch Centre, l_{notch}	Offset, $(w - l_{notch})/2$	Weight Before (g)	Weight After (g)	Weight Change (g)	Moisture Gain (%)
A/F/0/P/M10-01	11.99	9.88	79.98	80.05	33.95	74.26	5.79	11.98	39.94	-0.05	123.28	124.19	0.91	0.738%
A/F/0/P/M10-02	11.99	9.85	80.11	80.08	34.08	74.22	5.86	11.98	40.07	0.02	122.11	123.11	1.00	0.819%
A/F/0/P/M10-03	11.98	9.57	80.16	80.12	34.01	74.34	5.78	11.97	40.00	-0.08	120.07	121.15	1.08	0.899%
A/F/0/P/M10-04	11.98	9.61	79.98	80.11	34.04	74.11	6.00	11.98	40.03	0.04	122.32	123.40	1.08	0.883%
A/F/0/P/M10-05	11.98	9.58	80.11	80.09	34.16	74.20	5.89	11.98	40.15	0.09	121.77	122.86	1.09	0.895%
Mean	11.98	9.70	80.07	80.09	34.05	74.23	5.86	11.98	40.04	-	121.91	122.94	1.03	0.847%
SD	0.00	0.15	0.08	0.03	0.08	0.08	0.09	0.00	0.08	-	1.17	1.12	0.08	0.00
CoV (%)	0.03	1.58	0.10	0.03	0.23	0.11	1.52	0.03	0.20	-	0.96	0.91	7.49	8.14
A/F/0/P/M12-01	14.39	9.63	80.21	79.97	32.94	73.01	6.96	14.38	40.13	0.03	120.11	120.91	0.80	0.666%
A/F/0/P/M12-02	14.39	9.63	80.16	80.14	33.04	73.06	7.08	14.39	40.23	0.15	121.25	122.16	0.91	0.751%
A/F/0/P/M12-03	14.40	9.61	80.16	80.17	32.80	72.95	7.22	14.39	40.00	-0.08	122.24	123.28	1.04	0.851%
A/F/0/P/M12-04	14.39	9.72	80.03	80.12	32.92	73.04	7.08	14.39	40.11	0.10	120.94	121.85	0.91	0.752%
A/F/0/P/M12-05	14.39	9.68	80.06	80.13	32.89	72.99	7.14	14.39	40.08	0.05	121.14	122.04	0.90	0.743%
Mean	14.39	9.65	80.12	80.11	32.92	73.01	7.10	14.39	40.11	-	121.14	122.05	0.91	0.753%
SD	0.00	0.05	0.08	0.08	0.09	0.04	0.10	0.00	0.09	-	0.76	0.85	0.09	0.00
CoV (%)	0.02	0.47	0.09	0.10	0.26	0.06	1.34	0.03	0.21	-	0.63	0.69	9.35	8.72
A/F/0/P/M16-01	18.39	10.21	80.02	80.13	30.98	71.15	8.98	18.38	40.17	0.16	126.56	127.48	0.92	0.727%
A/F/0/P/M16-02	18.39	9.86	80.03	80.15	30.94	71.04	9.11	18.38	40.13	0.12	120.80	121.82	1.02	0.844%
A/F/0/P/M16-03	18.39	9.70	80.20	80.12	31.05	71.00	9.12	18.39	40.24	0.14	118.48	119.55	1.07	0.903%
A/F/0/P/M16-04	18.40	9.64	79.81	80.15	30.88	70.97	9.18	18.39	40.08	0.17	119.84	120.80	0.96	0.801%
A/F/0/P/M16-05	18.39	10.23	80.15	80.14	30.97	71.01	9.13	18.38	40.16	0.09	126.51	127.62	1.11	0.877%
Mean	18.39	9.93	80.04	80.14	30.96	71.03	9.10	18.39	40.16	-	122.44	123.45	1.02	0.831%
SD	0.00	0.28	0.15	0.01	0.06	0.07	0.07	0.01	0.06	-	3.83	3.82	0.08	0.00
CoV (%)	0.02	2.81	0.19	0.02	0.20	0.10	0.82	0.03	0.15	-	3.13	3.10	7.64	8.35
A/F/0/P/M20-01	22.39	9.71	80.10	80.01	28.82	69.29	10.72	22.37	40.00	-0.05	117.27	118.09	0.82	0.699%
A/F/0/P/M20-02	22.39	9.64	80.18	80.10	29.07	69.32	10.78	22.37	40.25	0.16	118.01	119.08	1.07	0.907%
A/F/0/P/M20-03	22.39	9.65	80.19	80.12	29.37	68.96	11.16	22.38	40.56	0.47	117.94	119.01	1.07	0.907%
A/F/0/P/M20-04	22.38	9.90	80.17	80.12	28.89	68.90	11.22	22.38	40.08	-0.01	118.95	119.93	0.98	0.824%
A/F/0/P/M20-05	22.38	9.88	80.15	80.14	28.90	69.15	10.99	22.38	40.09	0.01	119.09	120.08	0.99	0.831%
Mean	22.38	9.76	80.16	80.10	29.01	69.12	10.97	22.38	40.20	-	118.25	119.24	0.99	0.834%
SD	0.00	0.13	0.04	0.05	0.22	0.19	0.22	0.01	0.22	-	0.76	0.80	0.10	0.00
CoV (%)	0.02	1.29	0.04	0.06	0.76	0.27	2.02	0.03	0.56	-	0.64	0.67	10.36	10.20

Table B.12: Pin-bearing Test Specimen Measurements for Flange Material tested with a Threaded Pin in the Longitudinal Direction and Hot-wet Conditioned at 40°C for 3 Months

Specimen ID	Diameter of Hole, d_n	Thickness of Specimen, t	Width of Specimen, w	Length of Specimen, l	Width to Hole Edge, w_h	Length to Hole Edge, l_h	Notch Depth, w_{notch}	Notch Diameter, d_{notch}	Notch Centre, l_{notch}	Offset, (w - l_{notch})/2	Weight Before (g)	Weight After (g)	Weight Change (g)	Moisture Gain (%)
A/F/0/T/M10-01	11.98	9.59	80.13	80.09	34.07	74.27	5.82	11.98	40.06	-0.01	122.60	123.44	0.84	0.685%
A/F/0/T/M10-02	11.98	9.59	80.08	80.08	34.05	74.08	6.00	11.98	40.04	0.00	122.47	123.50	1.03	0.841%
A/F/0/T/M10-03	11.98	9.83	80.12	80.12	34.01	74.31	5.81	11.98	40.00	-0.06	122.21	123.19	0.98	0.802%
A/F/0/T/M10-04	11.98	9.85	80.09	80.13	33.99	74.28	5.85	11.98	39.98	-0.07	121.69	122.67	0.98	0.805%
A/F/0/T/M10-05	11.98	9.59	80.15	80.13	33.97	74.30	5.83	11.97	39.96	-0.12	121.53	122.41	0.88	0.724%
Mean	11.98	9.69	80.11	80.11	34.02	74.25	5.86	11.98	40.01	-	122.10	123.04	0.94	0.772%
SD	0.00	0.14	0.03	0.02	0.04	0.10	0.08	0.00	0.04	-	0.47	0.48	0.08	0.00
CoV (%)	0.03	1.41	0.04	0.03	0.12	0.13	1.34	0.02	0.11	-	0.39	0.39	8.37	8.35
A/F/0/T/M12-01	14.39	9.85	80.15	80.07	32.86	72.86	7.21	14.38	40.05	-0.02	122.04	122.79	0.75	0.615%
A/F/0/T/M12-02	14.39	9.86	79.83	80.12	32.58	72.92	7.20	14.38	39.77	-0.14	121.54	122.49	0.95	0.782%
A/F/0/T/M12-03	14.38	9.62	80.13	80.16	32.87	72.96	7.20	14.38	40.06	-0.01	120.91	121.81	0.90	0.744%
A/F/0/T/M12-04	14.39	9.89	80.05	80.14	32.89	73.00	7.14	14.38	40.08	0.06	123.14	124.17	1.03	0.836%
A/F/0/T/M12-05	14.40	9.93	80.17	80.15	32.87	72.94	7.21	14.39	40.07	-0.02	122.96	123.97	1.01	0.821%
Mean	14.39	9.83	80.07	80.13	32.81	72.94	7.19	14.39	40.01	-	122.12	123.05	0.93	0.760%
SD	0.01	0.12	0.14	0.04	0.13	0.05	0.03	0.01	0.13	-	0.94	1.00	0.11	0.00
CoV (%)	0.04	1.24	0.17	0.04	0.40	0.07	0.41	0.04	0.33	-	0.77	0.81	12.06	11.68
A/F/0/T/M16-01	18.39	9.61	79.95	80.13	30.95	71.16	8.97	18.38	40.14	0.17	121.09	121.92	0.83	0.685%
A/F/0/T/M16-02	18.39	9.64	80.11	80.10	31.04	71.13	8.97	18.38	40.23	0.18	118.45	119.48	1.03	0.870%
A/F/0/T/M16-03	18.39	9.59	80.21	80.10	30.96	71.26	8.84	18.38	40.15	0.04	118.87	119.88	1.01	0.850%
A/F/0/T/M16-04	18.39	9.61	80.20	80.12	30.91	71.10	9.02	18.39	40.10	0.00	118.88	119.92	1.04	0.875%
A/F/0/T/M16-05	18.40	9.85	80.17	80.16	30.94	71.03	9.13	18.39	40.14	0.05	120.61	121.60	0.99	0.821%
Mean	18.39	9.66	80.13	80.12	30.96	71.14	8.99	18.39	40.15	-	119.58	120.56	0.98	0.820%
SD	0.00	0.11	0.11	0.02	0.05	0.08	0.10	0.01	0.05	-	1.18	1.11	0.09	0.00
CoV (%)	0.01	1.11	0.13	0.03	0.16	0.12	1.16	0.04	0.12	-	0.99	0.92	8.78	9.53
A/F/0/T/M20-01	22.39	9.94	80.07	80.04	28.80	68.95	11.09	22.38	39.99	-0.04	119.73	120.49	0.76	0.635%
A/F/0/T/M20-02	22.39	9.59	80.13	80.12	29.05	69.02	11.10	22.39	40.24	0.18	118.83	119.77	0.94	0.791%
A/F/0/T/M20-03	22.36	9.65	80.03	80.13	28.91	69.02	11.11	22.36	40.09	0.07	117.44	118.47	1.03	0.877%
A/F/0/T/M20-04	22.38	10.24	79.96	80.09	28.93	69.07	11.02	22.37	40.12	0.14	124.75	125.86	1.11	0.890%
A/F/0/T/M20-05	22.39	10.25	80.17	80.11	29.13	69.16	10.95	22.38	40.32	0.23	124.89	125.98	1.09	0.873%
Mean	22.38	9.93	80.07	80.10	28.96	69.04	11.05	22.38	40.15	-	121.13	122.11	0.99	0.813%
SD	0.01	0.31	0.08	0.04	0.13	0.08	0.07	0.01	0.13	-	3.47	3.55	0.14	0.00
CoV (%)	0.05	3.15	0.10	0.04	0.44	0.11	0.62	0.05	0.32	-	2.86	2.91	14.46	13.16

Table B.13: Pin-bearing Test Specimen Measurements for Flange Material tested with a Plain Pin in the Longitudinal Direction and Hot-wet Conditioned at 40°C for 6 Months

Specimen ID	Diameter of Hole, d_n	Thickness of Specimen, t	Width of Specimen, w	Length of Specimen, l	Width to Hole Edge, w_h	Length to Hole Edge, l_h	Notch Depth, w_{notch}	Notch Diameter, d_{notch}	Notch Centre, l_{notch}	Offset, (w - l_{notch})/2	Weight Before (g)	Weight After (g)	Weight Change (g)	Moisture Gain (%)
A/F/0/P/M10-06	11.98	9.62	80.21	80.12	34.22	74.18	5.94	11.98	40.21	0.10	121.18	122.38	1.20	0.990%
A/F/0/P/M10-07	11.98	9.58	80.26	80.14	34.30	74.49	5.65	11.96	40.28	0.15	122.66	124.04	1.38	1.125%
A/F/0/P/M10-08	11.98	9.60	80.21	80.15	34.20	74.19	5.96	11.98	40.19	0.08	120.93	122.26	1.33	1.100%
A/F/0/P/M10-09	11.98	9.61	80.31	80.12	34.27	74.29	5.83	11.97	40.26	0.10	120.19	121.57	1.38	1.148%
A/F/0/P/M10-10	11.98	9.59	80.27	80.12	34.04	74.40	5.72	11.97	40.02	-0.11	122.45	123.79	1.34	1.094%
Mean	11.98	9.60	80.25	80.13	34.21	74.31	5.82	11.97	40.19	-	121.48	122.81	1.33	1.092%
SD	0.00	0.02	0.04	0.01	0.10	0.13	0.14	0.01	0.10	-	1.05	1.06	0.07	0.00
CoV (%)	0.01	0.16	0.05	0.02	0.29	0.18	2.32	0.06	0.25	-	0.86	0.86	5.58	5.55
A/F/0/P/M12-06	14.39	10.26	80.09	80.14	32.95	73.14	7.00	14.38	40.14	0.10	127.32	128.67	1.35	1.060%
A/F/0/P/M12-07	14.40	9.66	80.12	80.17	32.90	73.11	7.06	14.39	40.10	0.04	120.94	122.11	1.17	0.967%
A/F/0/P/M12-08	14.40	9.94	80.14	80.19	32.84	73.18	7.01	14.39	40.04	-0.03	123.22	124.55	1.33	1.079%
A/F/0/P/M12-09	14.39	9.66	80.20	80.01	32.94	73.04	6.97	14.38	40.13	0.03	120.98	122.15	1.17	0.967%
A/F/0/P/M12-10	14.40	10.25	80.11	80.14	32.82	73.17	6.97	14.39	40.01	-0.04	127.31	128.68	1.37	1.076%
Mean	14.39	9.95	80.13	80.13	32.89	73.13	7.00	14.39	40.08	-	123.95	125.23	1.28	1.030%
SD	0.00	0.30	0.04	0.07	0.06	0.06	0.04	0.00	0.06	-	3.20	3.29	0.10	0.00
CoV (%)	0.02	2.99	0.05	0.09	0.18	0.08	0.53	0.03	0.14	-	2.58	2.63	7.79	5.61
A/F/0/P/M16-06	18.39	9.61	80.18	80.11	31.09	71.05	9.06	18.39	40.28	0.19	120.08	121.20	1.12	0.933%
A/F/0/P/M16-07	18.39	9.58	80.13	80.13	31.67	70.99	9.14	18.39	40.86	0.80	118.39	119.67	1.28	1.081%
A/F/0/P/M16-08	18.40	9.88	80.05	80.18	30.94	71.04	9.14	18.39	40.14	0.11	121.99	123.30	1.31	1.074%
A/F/0/P/M16-09	18.40	9.61	80.22	80.08	31.12	71.09	8.99	18.39	40.32	0.21	120.22	121.37	1.15	0.957%
A/F/0/P/M16-10	18.39	9.87	80.05	80.06	30.90	71.08	8.98	18.38	40.09	0.07	120.51	121.70	1.19	0.987%
Mean	18.39	9.71	80.13	80.11	31.14	71.05	9.06	18.39	40.34	-	120.24	121.45	1.21	1.006%
SD	0.00	0.15	0.08	0.05	0.31	0.04	0.08	0.01	0.31	-	1.28	1.30	0.08	0.00
CoV (%)	0.02	1.56	0.10	0.06	0.99	0.06	0.86	0.03	0.77	-	1.07	1.07	6.79	6.74
A/F/0/P/M20-06	22.39	9.89	80.16	80.08	28.92	68.98	11.10	22.39	40.11	0.03	120.67	121.95	1.28	1.061%
A/F/0/P/M20-07	22.39	9.91	79.99	80.08	28.89	69.00	11.08	22.39	40.08	0.09	120.81	122.13	1.32	1.093%
A/F/0/P/M20-08	22.39	9.73	80.15	80.19	28.92	69.10	11.09	22.38	40.11	0.04	118.88	120.03	1.15	0.967%
A/F/0/P/M20-09	22.39	9.61	79.93	80.11	28.69	69.16	10.95	22.38	39.88	-0.09	118.38	119.51	1.13	0.955%
A/F/0/P/M20-10	22.38	9.65	80.08	80.15	28.93	69.18	10.97	22.38	40.12	0.08	117.37	118.58	1.21	1.031%
Mean	22.39	9.76	80.06	80.12	28.87	69.08	11.04	22.38	40.06	-	119.22	120.44	1.22	1.021%
SD	0.00	0.14	0.10	0.05	0.10	0.09	0.07	0.01	0.10	-	1.49	1.55	0.08	0.00
CoV (%)	0.02	1.40	0.13	0.06	0.35	0.13	0.65	0.03	0.26	-	1.25	1.29	6.71	5.81

Table B.14: Pin-bearing Test Specimen Measurements for Flange Material tested with a Threaded Pin in the Longitudinal Direction and Hot-wet Conditioned at 40°C for 6 Months

Specimen ID	Diameter of Hole, d_n	Thickness of Specimen, t	Width of Specimen, w	Length of Specimen, l	Width to Hole Edge, w_h	Length to Hole Edge, l_h	Notch Depth, w_{notch}	Notch Diameter, d_{notch}	Notch Centre, l_{notch}	Offset, (w - l_{notch})/2	Weight Before (g)	Weight After (g)	Weight Change (g)	Moisture Gain (%)
A/F/0/T/M10-06	11.99	9.87	80.07	80.19	34.02	74.18	6.01	11.99	40.01	-0.02	121.23	122.50	1.27	1.048%
A/F/0/T/M10-07	11.98	9.63	80.20	80.11	34.34	74.27	5.84	11.98	40.33	0.23	120.69	121.99	1.30	1.077%
A/F/0/T/M10-08	11.99	9.86	80.08	80.11	34.05	74.33	5.78	11.98	40.04	0.00	122.19	123.41	1.22	0.998%
A/F/0/T/M10-09	11.98	9.61	79.99	80.06	33.98	74.34	5.72	11.97	39.96	-0.03	121.45	122.60	1.15	0.947%
A/F/0/T/M10-10	11.98	9.91	80.18	80.09	34.07	74.30	5.79	11.97	40.06	-0.03	123.72	125.05	1.33	1.075%
Mean	11.98	9.78	80.10	80.11	34.09	74.28	5.83	11.98	40.08	-	121.86	123.11	1.25	1.029%
SD	0.00	0.14	0.09	0.05	0.14	0.06	0.11	0.01	0.14	-	1.17	1.20	0.07	0.00
CoV (%)	0.03	1.47	0.11	0.06	0.42	0.09	1.89	0.06	0.36	-	0.96	0.97	5.66	5.42
A/F/0/T/M12-06	14.39	9.66	80.13	80.11	32.88	73.15	6.96	14.38	40.07	0.00	122.21	123.51	1.30	1.064%
A/F/0/T/M12-07	14.39	9.61	80.31	80.17	33.20	72.96	7.21	14.38	40.39	0.24	119.70	121.02	1.32	1.103%
A/F/0/T/M12-08	14.39	9.70	80.09	80.07	32.93	72.97	7.10	14.39	40.12	0.08	120.79	121.93	1.14	0.944%
A/F/0/T/M12-09	14.39	9.90	79.74	80.13	32.63	73.14	6.99	14.38	39.82	-0.05	120.56	121.67	1.11	0.921%
A/F/0/T/M12-10	14.39	9.60	80.16	80.14	32.98	73.13	7.01	14.39	40.17	0.09	121.51	122.73	1.22	1.004%
Mean	14.39	9.69	80.09	80.12	32.92	73.07	7.05	14.38	40.12	-	120.95	122.17	1.22	1.007%
SD	0.00	0.12	0.21	0.04	0.20	0.10	0.10	0.00	0.21	-	0.95	0.97	0.09	0.00
CoV (%)	0.02	1.26	0.26	0.05	0.62	0.13	1.44	0.03	0.51	-	0.79	0.79	7.67	7.67
A/F/0/T/M16-06	18.39	9.84	80.02	80.18	30.96	71.08	9.10	18.39	40.15	0.14	120.10	121.34	1.24	1.032%
A/F/0/T/M16-07	18.40	10.34	80.10	80.13	31.10	71.12	9.01	18.39	40.30	0.25	126.42	127.77	1.35	1.068%
A/F/0/T/M16-08	18.39	9.85	79.88	80.10	31.02	70.97	9.13	18.39	40.21	0.27	120.58	121.78	1.20	0.995%
A/F/0/T/M16-09	18.40	9.86	80.21	80.12	31.09	71.18	8.94	18.39	40.28	0.18	120.72	121.94	1.22	1.011%
A/F/0/T/M16-10	18.39	10.23	80.12	80.15	30.93	71.12	9.03	18.39	40.12	0.06	126.65	127.94	1.29	1.019%
Mean	18.39	10.02	80.07	80.14	31.02	71.09	9.04	18.39	40.21	-	122.89	124.15	1.26	1.025%
SD	0.00	0.24	0.12	0.03	0.08	0.08	0.08	0.00	0.08	-	3.33	3.39	0.06	0.00
CoV (%)	0.01	2.41	0.15	0.04	0.24	0.11	0.83	0.01	0.19	-	2.71	2.73	4.79	2.69
A/F/0/T/M20-06	22.39	9.74	80.15	80.03	29.01	68.99	11.04	22.39	40.20	0.13	117.47	118.71	1.24	1.056%
A/F/0/T/M20-07	22.39	10.22	80.05	80.04	28.92	69.13	10.91	22.38	40.11	0.08	124.64	125.96	1.32	1.059%
A/F/0/T/M20-08	22.40	9.62	80.09	80.11	28.85	69.15	10.96	22.39	40.04	0.00	118.84	119.95	1.11	0.934%
A/F/0/T/M20-09	22.40	9.61	80.17	80.05	29.07	68.88	11.17	22.40	40.27	0.18	120.80	122.10	1.30	1.076%
A/F/0/T/M20-10	22.39	9.88	80.23	80.09	28.81	69.01	11.08	22.38	40.00	-0.11	117.76	118.99	1.23	1.044%
Mean	22.39	9.81	80.14	80.06	28.93	69.03	11.03	22.39	40.13	-	119.90	121.14	1.24	1.034%
SD	0.01	0.25	0.07	0.03	0.11	0.11	0.10	0.01	0.11	-	2.95	3.00	0.08	0.00
CoV (%)	0.03	2.57	0.09	0.04	0.37	0.16	0.92	0.04	0.28	-	2.46	2.48	6.63	5.51

Table B.15: Pin-bearing Test Specimen Measurements for Flange Material tested with a Plain Pin in the Transverse Direction and Hot-wet Conditioned at 40°C for 3 Months

Specimen ID	Diameter of Hole, d_n	Thickness of Specimen, t	Width of Specimen, w	Length of Specimen, l	Width to Hole Edge, w_h	Length to Hole Edge, l_h	Notch Depth, w_{notch}	Notch Diameter, d_{notch}	Notch Centre, l_{notch}	Offset, (w - l_{notch})/2	Weight Before (g)	Weight After (g)	Weight Change (g)	Moisture Gain (%)
A/F/90/P/M10-01	11.98	10.30	80.13	79.94	34.05	74.16	5.78	11.97	40.03	-0.03	127.92	128.83	0.91	0.711%
A/F/90/P/M10-02	11.98	10.29	80.14	80.01	34.15	74.06	5.95	11.98	40.14	0.07	127.76	128.88	1.12	0.877%
A/F/90/P/M10-03	11.98	10.29	80.04	80.07	34.02	74.12	5.95	11.98	40.01	-0.01	127.41	128.52	1.11	0.871%
A/F/90/P/M10-04	11.98	10.30	80.17	79.90	34.08	74.09	5.81	11.97	40.06	-0.02	127.99	129.10	1.11	0.867%
A/F/90/P/M10-05	11.98	10.29	80.05	79.94	34.09	74.22	5.72	11.96	40.07	0.05	127.54	128.66	1.12	0.878%
Mean	11.98	10.29	80.11	79.97	34.08	74.13	5.84	11.97	40.06	-	127.72	128.80	1.07	0.841%
SD	0.00	0.01	0.06	0.07	0.05	0.06	0.10	0.01	0.05	-	0.25	0.22	0.09	0.00
CoV (%)	0.01	0.05	0.07	0.08	0.14	0.08	1.78	0.05	0.12	-	0.19	0.17	8.55	8.63
A/F/90/P/M12-01	14.39	10.37	80.01	79.99	32.77	72.97	7.02	14.38	39.96	-0.04	127.22	128.13	0.91	0.715%
A/F/90/P/M12-02	14.39	10.19	80.06	79.96	32.85	73.02	6.94	14.38	40.04	0.01	126.97	128.18	1.21	0.953%
A/F/90/P/M12-03	14.39	10.26	80.02	80.07	32.74	73.03	7.04	14.39	39.93	-0.08	127.03	128.18	1.15	0.905%
A/F/90/P/M12-04	14.39	10.25	80.07	80.03	32.86	73.07	6.96	14.38	40.05	0.01	127.07	128.20	1.13	0.889%
A/F/90/P/M12-05	14.40	9.61	79.74	80.01	32.89	73.01	7.00	14.39	40.08	0.21	116.06	117.12	1.06	0.913%
Mean	14.39	10.14	79.98	80.01	32.82	73.02	6.99	14.38	40.01	-	124.87	125.96	1.09	0.875%
SD	0.00	0.30	0.14	0.04	0.06	0.04	0.04	0.00	0.06	-	4.93	4.94	0.11	0.00
CoV (%)	0.03	2.97	0.17	0.05	0.19	0.05	0.59	0.03	0.16	-	3.94	3.92	10.53	10.56
A/F/90/P/M16-01	18.39	10.22	79.81	80.03	30.89	71.00	9.03	18.39	40.08	0.18	115.08	115.93	0.85	0.739%
A/F/90/P/M16-02	18.39	10.23	80.09	79.98	30.94	70.87	9.11	18.39	40.13	0.09	121.91	122.99	1.08	0.886%
A/F/90/P/M16-03	18.40	10.33	80.17	80.13	30.78	71.21	8.92	18.39	39.97	-0.11	126.43	127.59	1.16	0.918%
A/F/90/P/M16-04	18.39	10.33	79.93	79.97	30.74	70.98	8.99	18.39	39.93	-0.03	121.95	123.04	1.09	0.894%
A/F/90/P/M16-05	18.40	10.27	80.04	80.14	30.72	70.89	9.25	18.39	39.92	-0.10	126.37	127.49	1.12	0.886%
Mean	18.39	10.28	80.01	80.05	30.81	70.99	9.06	18.39	40.01	-	122.35	123.41	1.06	0.864%
SD	0.00	0.05	0.14	0.08	0.10	0.14	0.13	0.00	0.10	-	4.64	4.75	0.12	0.00
CoV (%)	0.01	0.51	0.18	0.10	0.31	0.19	1.39	0.02	0.24	-	3.79	3.85	11.46	8.27
A/F/90/P/M20-01	22.40	10.21	80.03	80.01	28.74	69.14	10.87	22.39	39.93	-0.08	124.98	125.90	0.92	0.736%
A/F/90/P/M20-02	22.40	9.58	80.03	80.01	29.05	68.86	11.15	22.39	40.25	0.23	119.63	120.76	1.13	0.945%
A/F/90/P/M20-03	22.39	10.21	79.90	80.00	28.57	69.04	10.96	22.39	39.76	-0.19	124.42	125.58	1.16	0.932%
A/F/90/P/M20-04	22.40	10.20	80.13	80.04	28.73	68.95	11.09	22.39	39.93	-0.14	124.82	125.98	1.16	0.929%
A/F/90/P/M20-05	22.40	9.90	80.01	79.95	28.70	68.86	11.09	22.39	39.90	-0.11	119.22	120.30	1.08	0.906%
Mean	22.39	10.02	80.02	80.00	28.76	68.97	11.03	22.39	39.95	-	122.61	123.70	1.09	0.890%
SD	0.00	0.28	0.08	0.03	0.18	0.12	0.11	0.00	0.18	-	2.92	2.91	0.10	0.00
CoV (%)	0.01	2.79	0.10	0.04	0.61	0.18	1.03	0.02	0.45	-	2.38	2.35	9.22	9.77

Table B.16: Pin-bearing Test Specimen Measurements for Flange Material tested with a Threaded Pin in the Transverse Direction and Hot-wet Conditioned at 40°C for 3 Months

Specimen ID	Diameter of Hole, d_n	Thickness of Specimen, t	Width of Specimen, w	Length of Specimen, l	Width to Hole Edge, w_h	Length to Hole Edge, l_h	Notch Depth, w_{notch}	Notch Diameter, d_{notch}	Notch Centre, l_{notch}	Offset, (w - l_{notch})/2	Weight Before (g)	Weight After (g)	Weight Change (g)	Moisture Gain (%)
A/F/90/T/M10-01	11.98	10.23	80.11	79.99	34.08	74.19	5.80	11.97	40.07	0.01	127.81	128.75	0.94	0.735%
A/F/90/T/M10-02	11.97	10.29	80.07	80.18	34.15	74.15	6.03	11.97	40.14	0.10	127.89	128.87	0.98	0.766%
A/F/90/T/M10-03	11.98	10.34	79.97	80.03	34.24	75.13	4.90	11.78	40.13	0.14	128.49	129.60	1.11	0.864%
A/F/90/T/M10-04	11.97	9.63	80.12	80.05	33.97	74.10	5.95	11.97	39.96	-0.10	122.13	123.21	1.08	0.884%
A/F/90/T/M10-05	11.98	9.79	80.10	80.04	33.90	73.98	6.06	11.98	39.89	-0.16	123.93	124.99	1.06	0.855%
Mean	11.98	10.06	80.07	80.06	34.07	74.31	5.75	11.93	40.04	-	126.05	127.08	1.03	0.821%
SD	0.00	0.32	0.06	0.07	0.14	0.47	0.48	0.09	0.11	-	2.84	2.81	0.07	0.00
CoV (%)	0.03	3.21	0.08	0.09	0.40	0.63	8.43	0.72	0.27	-	2.25	2.21	6.89	8.02
A/F/90/T/M12-01	14.38	9.54	79.58	79.97	32.77	72.89	7.08	14.38	39.96	0.17	118.88	119.69	0.81	0.681%
A/F/90/T/M12-02	14.39	9.57	79.77	79.99	32.58	72.88	7.11	14.38	39.77	-0.11	119.20	120.25	1.05	0.881%
A/F/90/T/M12-03	14.39	10.31	80.11	79.95	32.84	72.92	7.03	14.38	40.03	-0.02	127.20	128.30	1.10	0.865%
A/F/90/T/M12-04	14.40	10.19	80.08	80.15	32.77	72.77	7.38	14.39	39.97	-0.07	126.73	127.89	1.16	0.915%
A/F/90/T/M12-05	14.39	10.21	79.95	80.07	32.94	72.84	7.23	14.39	40.13	0.16	126.94	128.06	1.12	0.882%
Mean	14.39	9.96	79.90	80.03	32.78	72.86	7.17	14.38	39.97	0.02	123.79	124.84	1.05	0.845%
SD	0.01	0.38	0.22	0.08	0.13	0.06	0.14	0.01	0.13	0.13	4.34	4.45	0.14	0.00
CoV (%)	0.04	3.78	0.28	0.10	0.40	0.08	1.96	0.04	0.33	567.20	3.51	3.57	13.25	11.04
A/F/90/T/M16-01	18.39	9.63	79.97	79.98	30.77	71.22	8.76	18.37	39.95	-0.03	125.93	126.90	0.97	0.770%
A/F/90/T/M16-02	18.39	9.81	80.12	80.04	31.01	71.58	8.46	18.33	40.18	0.12	126.45	127.64	1.19	0.941%
A/F/90/T/M16-03	18.39	10.31	80.09	80.14	30.70	70.93	9.21	18.39	39.89	-0.15	126.19	127.34	1.15	0.911%
A/F/90/T/M16-04	18.39	9.82	79.99	79.96	30.85	70.89	9.07	18.39	40.04	0.05	126.20	127.36	1.16	0.919%
A/F/90/T/M16-05	18.40	10.35	80.13	80.02	30.83	70.87	9.15	18.39	40.03	-0.04	125.81	126.98	1.17	0.930%
Mean	18.39	9.98	80.06	80.03	30.83	71.10	8.93	18.37	40.02	-0.01	126.12	127.24	1.13	0.894%
SD	0.00	0.33	0.07	0.07	0.12	0.30	0.31	0.03	0.11	0.10	0.25	0.30	0.09	0.00
CoV (%)	0.01	3.26	0.09	0.09	0.37	0.43	3.52	0.14	0.26	-940.32	0.20	0.24	7.94	7.86
A/F/90/T/M20-01	22.40	10.36	79.89	79.92	28.61	69.48	10.44	22.34	39.78	-0.16	125.31	126.21	0.90	0.718%
A/F/90/T/M20-02	22.40	10.31	80.05	79.91	28.93	69.14	10.77	22.38	40.12	0.09	124.90	126.02	1.12	0.897%
A/F/90/T/M20-03	22.39	10.20	80.09	80.01	28.94	68.88	11.13	22.39	40.13	0.09	124.33	125.48	1.15	0.925%
A/F/90/T/M20-04	22.40	10.21	80.12	79.95	28.75	68.94	11.01	22.39	39.95	-0.11	124.59	125.74	1.15	0.923%
A/F/90/T/M20-05	22.39	10.20	80.11	79.94	28.88	69.12	10.82	22.38	40.07	0.01	124.71	125.87	1.16	0.930%
Mean	22.39	10.26	80.05	79.95	28.82	69.11	10.83	22.38	40.01	-0.02	124.77	125.86	1.10	0.879%
SD	0.00	0.07	0.09	0.04	0.14	0.23	0.26	0.02	0.15	0.12	0.37	0.28	0.11	0.00
CoV (%)	0.01	0.73	0.12	0.05	0.49	0.34	2.43	0.09	0.37	-742.34	0.29	0.22	10.09	10.31

Table B.17 Pin-bearing Test Specimen Measurements for Flange Material tested with a Plain Pin in the Transverse Direction and Hot-wet Conditioned at 40°C for 6 Months

Specimen ID	Diameter of Hole, d_n	Thickness of Specimen, t	Width of Specimen, w	Length of Specimen, l	Width to Hole Edge, w_h	Length to Hole Edge, l_h	Notch Depth, w_{notch}	Notch Diameter, d_{notch}	Notch Centre, l_{notch}	Offset, (w - l_{notch})/2	Weight Before (g)	Weight After (g)	Weight Change (g)	Moisture Gain (%)
A/F/90/P/M10-06	11.98	10.16	80.17	80.22	34.23	74.35	5.87	11.97	40.22	0.13	127.52	128.87	1.35	1.059%
A/F/90/P/M10-07	11.98	10.18	80.16	80.14	34.22	74.39	5.75	11.97	40.20	0.12	127.72	129.08	1.36	1.065%
A/F/90/P/M10-08	11.98	10.19	80.18	80.16	34.05	74.21	5.95	11.97	40.04	-0.05	127.37	128.75	1.38	1.083%
A/F/90/P/M10-09	11.97	10.32	80.12	80.13	34.09	74.08	6.05	11.97	40.08	0.02	127.89	129.21	1.32	1.032%
A/F/90/P/M10-10	11.97	9.60	79.98	79.81	33.95	74.16	5.65	11.95	39.93	-0.06	122.11	123.42	1.31	1.073%
Mean	11.97	10.09	80.12	80.09	34.11	74.24	5.85	11.97	40.09	-	126.52	127.87	1.34	1.062%
SD	0.00	0.28	0.08	0.16	0.12	0.13	0.16	0.01	0.12	-	2.47	2.49	0.03	0.00
CoV (%)	0.01	2.79	0.10	0.20	0.35	0.17	2.71	0.07	0.30	-	1.96	1.95	2.14	1.82
A/F/90/P/M12-06	14.39	9.59	79.83	79.99	32.59	72.92	7.07	14.39	39.78	-0.13	119.42	120.65	1.23	1.030%
A/F/90/P/M12-07	14.39	9.93	80.05	80.08	32.82	72.81	7.27	14.39	40.01	-0.01	121.53	122.85	1.32	1.086%
A/F/90/P/M12-08	14.40	9.92	80.07	80.02	32.81	72.86	7.16	14.39	40.01	-0.03	121.54	122.83	1.29	1.061%
A/F/90/P/M12-09	14.39	9.62	79.67	80.10	32.52	73.02	7.08	14.39	39.71	-0.12	116.31	117.59	1.28	1.101%
A/F/90/P/M12-10	14.39	9.66	79.73	80.04	32.82	73.14	6.90	14.38	40.01	0.14	116.90	118.14	1.24	1.061%
Mean	14.39	9.74	79.87	80.05	32.71	72.95	7.10	14.39	39.91	-	119.14	120.41	1.27	1.068%
SD	0.00	0.17	0.18	0.04	0.15	0.13	0.14	0.01	0.15	-	2.48	2.50	0.04	0.00
CoV (%)	0.02	1.72	0.23	0.06	0.44	0.18	1.91	0.04	0.36	-	2.08	2.08	2.91	2.53
A/F/90/P/M16-06	18.40	9.88	80.05	80.19	30.85	71.01	9.18	18.39	40.05	0.02	126.55	127.86	1.31	1.035%
A/F/90/P/M16-07	18.39	9.58	80.05	79.99	30.88	70.95	9.04	18.39	40.07	0.05	120.66	122.02	1.36	1.127%
A/F/90/P/M16-08	18.39	9.89	79.96	80.07	30.81	70.85	9.22	18.39	40.00	0.02	125.62	126.99	1.37	1.091%
A/F/90/P/M16-09	18.40	9.59	80.15	79.99	30.91	70.87	9.12	18.39	40.11	0.03	126.53	127.86	1.33	1.051%
A/F/90/P/M16-10	18.40	9.65	80.08	80.14	30.78	71.05	9.09	18.39	39.98	-0.06	126.41	127.76	1.35	1.068%
Mean	18.39	9.72	80.06	80.08	30.85	70.95	9.13	18.39	40.04	-	125.15	126.50	1.34	1.074%
SD	0.00	0.15	0.07	0.09	0.05	0.09	0.07	0.00	0.05	-	2.54	2.53	0.02	0.00
CoV (%)	0.01	1.59	0.09	0.11	0.17	0.12	0.78	0.02	0.13	-	2.03	2.00	1.79	3.34
A/F/90/P/M20-01	22.40	10.21	80.03	80.01	28.74	69.14	10.87	22.39	39.93	-0.08	124.98	125.90	0.92	0.736%
A/F/90/P/M20-02	22.40	9.58	80.03	80.01	29.05	68.86	11.15	22.39	40.25	0.23	119.63	120.76	1.13	0.945%
A/F/90/P/M20-03	22.39	10.21	79.90	80.00	28.57	69.04	10.96	22.39	39.76	-0.19	124.42	125.58	1.16	0.932%
A/F/90/P/M20-04	22.40	10.20	80.13	80.04	28.73	68.95	11.09	22.39	39.93	-0.14	124.82	125.98	1.16	0.929%
A/F/90/P/M20-05	22.40	9.90	80.01	79.95	28.70	68.86	11.09	22.39	39.90	-0.11	119.22	120.30	1.08	0.906%
Mean	22.39	10.02	80.02	80.00	28.76	68.97	11.03	22.39	39.95	-	122.61	123.70	1.09	0.890%
SD	0.00	0.28	0.08	0.03	0.18	0.12	0.11	0.00	0.18	-	2.92	2.91	0.10	0.00
CoV (%)	0.01	2.79	0.10	0.04	0.61	0.18	1.03	0.02	0.45	-	2.38	2.35	9.22	9.77

Table B.18: Pin-bearing Test Specimen Measurements for Flange Material tested with a Threaded Pin in the Transverse Direction and Hot-wet Conditioned at 40°C for 6 Months

Specimen ID	Diameter of Hole, d_n	Thickness of Specimen, t	Width of Specimen, w	Length of Specimen, l	Width to Hole Edge, w_h	Length to Hole Edge, l_h	Notch Depth, w_{notch}	Notch Diameter, d_{notch}	Notch Centre, l_{notch}	Offset, (w - l_{notch})/2	Weight Before (g)	Weight After (g)	Weight Change (g)	Moisture Gain (%)
A/F/90/T/M10-06	11.97	9.91	80.05	80.06	34.11	74.11	5.95	11.97	40.10	0.07	122.18	123.48	1.30	1.064%
A/F/90/T/M10-07	11.98	9.57	80.13	80.08	35.09	74.21	5.87	11.98	41.08	1.01	121.91	123.24	1.33	1.091%
A/F/90/T/M10-08	11.98	9.60	80.00	80.04	34.02	74.13	5.91	11.97	40.01	0.01	121.88	123.23	1.35	1.108%
A/F/90/T/M10-09	11.97	9.59	80.07	79.99	34.10	74.26	5.73	11.96	40.08	0.04	122.72	124.03	1.31	1.067%
A/F/90/T/M10-10	11.97	10.20	80.17	80.19	34.04	74.14	6.05	11.97	40.03	-0.06	127.69	129.07	1.38	1.081%
Mean	11.97	9.77	80.08	80.07	34.27	74.17	5.90	11.97	40.26	-	123.28	124.61	1.33	1.082%
SD	0.00	0.28	0.07	0.07	0.46	0.06	0.12	0.01	0.46	-	2.49	2.51	0.03	0.00
CoV (%)	0.03	2.83	0.08	0.09	1.34	0.08	1.98	0.06	1.14	-	2.02	2.02	2.41	1.65
A/F/90/T/M12-06	14.39	10.34	80.19	80.13	33.04	72.87	7.26	14.38	40.23	0.14	127.56	128.88	1.32	1.035%
A/F/90/T/M12-07	14.39	10.30	80.05	80.10	32.94	73.43	6.67	14.35	40.12	0.09	127.67	129.00	1.33	1.042%
A/F/90/T/M12-08	14.39	9.75	79.91	79.99	32.84	72.91	7.08	14.39	40.03	0.08	120.18	121.47	1.29	1.073%
A/F/90/T/M12-09	14.39	10.19	80.13	80.11	33.11	72.98	7.13	14.39	40.30	0.24	127.15	128.49	1.34	1.054%
A/F/90/T/M12-10	14.39	10.30	80.00	79.86	32.95	72.95	6.91	14.38	40.14	0.14	127.06	128.38	1.32	1.039%
Mean	14.39	10.18	80.06	80.04	32.98	73.03	7.01	14.38	40.17	-	125.92	127.24	1.32	1.049%
SD	0.00	0.24	0.11	0.11	0.10	0.23	0.23	0.02	0.11	-	3.22	3.24	0.02	0.00
CoV (%)	0.02	2.40	0.14	0.14	0.31	0.31	3.25	0.11	0.26	-	2.56	2.54	1.42	1.49
A/F/90/T/M16-06	18.39	10.31	80.03	79.99	30.91	70.89	9.10	18.39	40.10	0.09	120.26	121.55	1.29	1.073%
A/F/90/T/M16-07	18.40	9.63	79.85	80.04	30.74	71.27	8.77	18.38	39.93	0.00	119.07	120.34	1.27	1.067%
A/F/90/T/M16-08	18.39	10.21	80.02	79.95	30.82	70.96	8.99	18.38	40.01	0.00	120.15	121.45	1.30	1.082%
A/F/90/T/M16-09	18.40	10.35	79.72	80.07	30.52	71.05	9.02	18.39	39.72	-0.14	115.16	116.42	1.26	1.094%
A/F/90/T/M16-10	18.39	10.33	79.79	79.88	30.72	70.95	8.93	18.38	39.91	0.02	118.31	119.52	1.21	1.023%
Mean	18.39	10.17	79.88	79.99	30.74	71.02	8.96	18.38	39.93	-	118.59	119.86	1.27	1.068%
SD	0.00	0.30	0.14	0.08	0.14	0.15	0.12	0.01	0.14	-	2.08	2.10	0.04	0.00
CoV (%)	0.02	2.99	0.17	0.09	0.47	0.21	1.38	0.04	0.36	-	1.75	1.75	2.77	2.54
A/F/90/T/M20-06	22.39	10.19	80.05	79.97	28.90	69.00	10.97	22.39	40.09	0.07	124.37	125.85	1.48	1.190%
A/F/90/T/M20-07	22.38	9.59	80.04	79.92	28.92	68.85	11.07	22.38	40.11	0.09	119.92	121.24	1.32	1.101%
A/F/90/T/M20-08	22.40	9.89	79.99	80.02	28.73	68.79	11.23	22.39	39.93	-0.07	119.13	120.50	1.37	1.150%
A/F/90/T/M20-09	22.40	9.59	80.05	80.01	28.88	68.89	11.12	22.39	40.08	0.05	119.43	120.75	1.32	1.105%
A/F/90/T/M20-10	22.39	9.84	79.98	79.85	28.73	68.42	11.43	22.39	39.92	-0.07	120.71	122.05	1.34	1.110%
Mean	22.39	9.82	80.02	79.95	28.83	68.79	11.16	22.39	40.03	-	120.71	122.08	1.37	1.131%
SD	0.01	0.25	0.03	0.07	0.09	0.22	0.18	0.01	0.09	-	2.13	2.19	0.07	0.00
CoV (%)	0.03	2.54	0.04	0.09	0.33	0.32	1.57	0.03	0.23	-	1.76	1.79	4.90	3.38

Table B.19: Pin-bearing Test Specimen Measurements for Web Material tested with a Plain and Threaded Pin in the Longitudinal Direction and Hot-wet Conditioned at 40°C for 3 Months

Specimen ID	Diameter of Hole, d_n	Thickness of Specimen, t	Width of Specimen, w	Length of Specimen, l	Width to Hole Edge, w_h	Length to Hole Edge, l_h	Notch Depth, w_{notch}	Notch Diameter, d_{notch}	Notch Centre, l_{notch}	Offset, (w - l_{notch})/2	Weight Before (g)	Weight After (g)	Weight Change (g)	Moisture Gain (%)
Plain														
A/W/0/P/M10-01	11.97	9.58	80.08	80.10	34.04	74.30	5.80	11.97	40.02	-0.02	118.97	119.80	0.83	0.698%
A/W/0/P/M10-02	11.97	9.66	80.22	80.15	34.47	74.15	6.00	11.97	40.46	0.35	118.84	119.91	1.07	0.900%
A/W/0/P/M10-03	11.97	9.81	80.18	80.20	34.00	74.34	5.86	11.97	39.99	-0.10	119.37	120.46	1.09	0.913%
A/W/0/P/M10-04	11.97	9.65	80.17	80.11	34.06	74.01	6.10	11.97	40.04	-0.04	119.29	120.36	1.07	0.897%
A/W/0/P/M10-05	11.97	9.60	80.16	80.17	34.09	74.11	6.06	11.97	40.08	0.00	119.24	120.22	0.98	0.822%
Mean	11.97	9.66	80.16	80.15	34.13	74.18	5.96	11.97	40.12	-	119.14	120.15	1.01	0.846%
SD	0.00	0.09	0.05	0.04	0.19	0.14	0.13	0.00	0.19	-	0.23	0.29	0.11	0.00
CoV (%)	0.01	0.93	0.06	0.05	0.56	0.18	2.17	0.02	0.48	-	0.19	0.24	10.74	10.68
A/W/0/P/M20-01	22.38	9.62	80.15	79.95	28.82	69.01	10.94	22.37	40.01	-0.07	116.62	117.47	0.85	0.729%
A/W/0/P/M20-02	22.39	9.74	80.12	80.15	28.95	69.33	10.82	22.37	40.14	0.08	116.20	117.37	1.17	1.007%
A/W/0/P/M20-03	22.38	9.62	80.22	80.07	28.98	68.95	11.12	22.38	40.17	0.06	116.24	117.28	1.04	0.895%
A/W/0/P/M20-04	22.38	9.64	80.11	80.09	28.76	69.03	11.06	22.38	39.95	-0.11	116.03	117.09	1.06	0.914%
A/W/0/P/M20-05	22.38	9.65	80.15	80.07	28.79	68.92	11.15	22.38	39.98	-0.10	116.57	117.64	1.07	0.918%
Mean	22.38	9.65	80.15	80.07	28.86	69.05	11.02	22.38	40.05	-	116.33	117.37	1.04	0.892%
SD	0.00	0.05	0.04	0.07	0.10	0.16	0.14	0.00	0.10	-	0.25	0.21	0.12	0.00
CoV (%)	0.01	0.52	0.05	0.09	0.34	0.24	1.24	0.01	0.25	-	0.22	0.18	11.22	11.34
Threaded														
A/W/0/T/M10-01	11.98	9.68	80.08	80.11	33.93	73.99	6.12	11.97	39.92	-0.12	119.50	120.32	0.82	0.686%
A/W/0/T/M10-02	11.97	9.63	79.97	80.17	34.05	74.18	5.99	11.97	40.04	0.05	118.83	119.84	1.01	0.850%
A/W/0/T/M10-03	11.97	9.64	80.06	80.14	34.00	74.16	5.98	11.97	39.99	-0.04	118.74	119.87	1.13	0.952%
A/W/0/T/M10-04	11.97	9.62	80.13	80.20	33.91	74.34	5.86	11.97	39.90	-0.17	119.29	120.32	1.03	0.863%
A/W/0/T/M10-05	11.97	9.60	80.13	80.05	34.07	74.06	5.99	11.97	40.06	-0.01	118.95	119.98	1.03	0.866%
Mean	11.97	9.63	80.07	80.13	33.99	74.15	5.99	11.97	39.98	-	119.06	120.07	1.00	0.843%
SD	0.00	0.03	0.07	0.06	0.07	0.13	0.09	0.00	0.07	-	0.32	0.24	0.11	0.00
CoV (%)	0.02	0.31	0.08	0.07	0.21	0.18	1.54	0.02	0.18	-	0.27	0.20	11.26	11.46
A/W/0/T/M20-01	22.38	9.64	80.15	80.11	28.52	69.52	10.59	22.35	39.69	-0.38	116.75	117.53	0.78	0.668%
A/W/0/T/M20-02	22.38	9.63	80.12	80.12	29.03	68.98	11.14	22.37	40.22	0.16	116.32	117.37	1.05	0.903%
A/W/0/T/M20-03	22.38	9.71	80.15	80.09	28.91	68.90	11.19	22.37	40.10	0.02	116.60	117.66	1.06	0.909%
A/W/0/T/M20-04	22.38	9.65	80.22	80.11	29.02	69.10	11.01	22.37	40.21	0.10	116.08	117.12	1.04	0.896%
A/W/0/T/M20-05	22.37	9.67	80.02	80.15	28.87	69.31	10.84	22.36	40.05	0.04	116.69	117.67	0.98	0.840%
Mean	22.38	9.66	80.13	80.12	28.87	69.16	10.95	22.37	40.05	-	116.49	117.47	0.98	0.843%
SD	0.00	0.03	0.07	0.02	0.21	0.25	0.24	0.01	0.21	-	0.28	0.23	0.12	0.00
CoV (%)	0.02	0.33	0.09	0.03	0.72	0.37	2.23	0.05	0.53	-	0.24	0.20	11.93	12.06

Table B.20: Pin-bearing Test Specimen Measurements for Web Material tested with a Plain and Threaded Pin in the Longitudinal Direction and Hot-wet Conditioned at 40°C for 6 Months

Specimen ID	Diameter of Hole, d_n	Thickness of Specimen, t	Width of Specimen, w	Length of Specimen, l	Width to Hole Edge, w_h	Length to Hole Edge, l_h	Notch Depth, w_{notch}	Notch Diameter, d_{notch}	Notch Centre, l_{notch}	Offset, $(w - l_{notch})/2$	Weight Before (g)	Weight After (g)	Weight Change (g)	Moisture Gain (%)
Plain														
A/W/0/P/M10-06	11.98	9.64	80.17	80.14	34.13	73.93	6.21	11.97	40.11	0.03	118.98	120.18	1.20	1.009%
A/W/0/P/M10-07	11.98	9.64	80.14	80.17	34.12	74.31	5.86	11.97	40.11	0.04	119.17	120.43	1.26	1.057%
A/W/0/P/M10-08	11.98	9.84	80.18	80.14	34.01	74.36	5.78	11.97	40.00	-0.09	118.84	120.06	1.22	1.027%
A/W/0/P/M10-09	11.98	9.61	80.22	80.07	34.27	74.30	5.77	11.97	40.25	0.14	118.78	119.97	1.19	1.002%
A/W/0/P/M10-10	11.98	9.62	80.11	80.11	34.01	74.37	5.74	11.97	39.99	-0.06	119.17	120.37	1.20	1.007%
Mean	10.13	8.26	67.84	67.82	28.93	62.82	5.19	10.13	33.99	-	118.99	120.20	1.21	1.020%
SD	4.49	3.44	30.08	30.08	12.67	27.81	1.85	4.49	14.94	-	0.18	0.20	0.03	0.00
CoV (%)	44.36	41.69	44.34	44.35	43.81	44.27	35.59	44.34	43.94	-	0.15	0.16	2.30	2.23
A/W/0/P/M20-06	22.38	9.69	80.17	80.03	28.93	69.01	11.02	22.38	40.12	0.03	116.54	117.67	1.13	0.970%
A/W/0/P/M20-07	22.39	9.64	80.09	80.10	28.89	68.94	11.16	22.38	40.08	0.04	116.09	117.20	1.11	0.956%
A/W/0/P/M20-08	22.39	9.65	80.17	80.02	28.84	69.05	10.97	22.38	40.03	-0.05	116.37	117.49	1.12	0.962%
A/W/0/P/M20-09	22.39	9.63	80.11	80.02	28.88	68.89	11.13	22.38	40.07	0.02	115.91	117.06	1.15	0.992%
A/W/0/P/M20-10	22.38	9.62	80.12	80.13	28.71	69.12	11.01	22.38	39.90	-0.16	115.86	117.03	1.17	1.010%
Mean	18.94	8.21	67.82	67.76	24.45	58.44	9.44	18.94	33.91	-	116.15	117.29	1.14	0.978%
SD	8.40	3.52	30.08	30.04	10.75	25.85	3.89	8.40	14.97	-	0.29	0.28	0.02	0.00
CoV (%)	44.37	42.87	44.35	44.33	43.98	44.23	41.22	44.36	44.16	-	0.25	0.24	2.12	2.29
Threaded														
A/W/0/T/M10-06	11.98	9.65	79.91	80.17	34.01	74.33	5.84	11.97	40.00	0.04	118.75	120.01	1.26	1.061%
A/W/0/T/M10-07	11.98	9.63	79.96	80.14	33.94	74.11	6.03	11.98	39.93	-0.05	119.33	120.48	1.15	0.964%
A/W/0/T/M10-08	11.97	9.63	79.99	80.19	33.85	74.08	6.11	11.97	39.84	-0.16	118.98	120.05	1.07	0.899%
A/W/0/T/M10-09	11.97	9.62	80.15	80.17	34.19	74.37	5.80	11.97	40.17	0.10	118.91	120.07	1.16	0.976%
A/W/0/T/M10-10	11.97	9.64	79.89	80.19	33.92	74.26	5.93	11.97	39.91	-0.04	118.88	120.10	1.22	1.026%
Mean	10.13	8.18	67.73	67.83	28.78	62.80	5.17	10.13	33.84	-	118.97	120.14	1.17	0.985%
SD	4.49	3.56	30.03	30.08	12.71	27.80	1.96	4.49	14.97	-	0.22	0.19	0.07	0.00
CoV (%)	44.34	43.47	44.33	44.34	44.17	44.27	37.87	44.34	44.22	-	0.18	0.16	6.19	6.29
A/W/0/T/M20-06	22.38	9.62	80.13	80.17	28.98	69.10	11.07	22.37	40.17	0.10	116.31	117.40	1.09	0.937%
A/W/0/T/M20-07	22.37	9.60	80.11	80.15	28.95	69.39	10.76	22.35	40.13	0.07	115.98	117.08	1.10	0.948%
A/W/0/T/M20-08	22.38	9.62	80.16	80.12	28.71	69.19	10.93	22.37	39.90	-0.18	116.49	117.61	1.12	0.961%
A/W/0/T/M20-09	22.38	9.63	79.99	80.08	28.84	69.08	11.00	22.37	40.03	0.03	115.81	116.93	1.12	0.967%
A/W/0/T/M20-10	22.38	9.69	80.10	80.08	28.71	69.00	11.08	22.37	39.90	-0.15	116.49	117.60	1.11	0.953%
Mean	18.93	8.19	67.80	67.80	24.49	58.57	9.46	18.93	33.94	-	116.22	117.32	1.11	0.953%
SD	8.40	3.56	30.06	30.08	10.66	25.86	3.68	8.39	14.90	-	0.31	0.31	0.01	0.00
CoV (%)	44.36	43.42	44.33	44.37	43.55	44.15	38.85	44.30	43.90	-	0.27	0.26	1.18	1.22

Table B.21: Pin-bearing Test Specimen Measurements for Web Material tested with a Plain and Threaded Pin in the 45° Direction and Hot-wet Conditioned at 40°C for 3 Months

Specimen ID	Diameter of Hole, d_n	Thickness of Specimen, t	Width of Specimen, w	Length of Specimen, l	Width to Hole Edge, w_h	Length to Hole Edge, l_h	Notch Depth, w_{notch}	Notch Diameter, d_{notch}	Notch Centre, l_{notch}	Offset, $(w - l_{notch})/2$	Weight Before (g)	Weight After (g)	Weight Change (g)	Moisture Gain (%)
Plain														
A/W/45/P/M10-01	11.97	9.64	80.30	80.13	34.07	74.25	5.88	11.97	40.05	-0.10	118.87	119.77	0.90	0.757%
A/W/45/P/M10-02	11.97	9.61	80.24	80.19	34.37	74.30	5.89	11.97	40.35	0.23	118.51	119.62	1.11	0.937%
A/W/45/P/M10-03	11.97	9.64	80.20	80.25	34.05	74.26	5.99	11.96	40.03	-0.07	119.20	120.34	1.14	0.956%
A/W/45/P/M10-04	11.97	9.64	80.29	80.21	34.02	74.30	5.91	11.97	40.00	-0.14	118.54	119.69	1.15	0.970%
A/W/45/P/M10-05	11.97	9.63	80.40	80.27	34.06	74.37	5.90	11.97	40.04	-0.16	119.69	120.84	1.15	0.961%
Mean	11.97	9.63	80.29	80.21	34.11	74.30	5.91	11.97	40.10	-	118.96	120.05	1.09	0.916%
SD	0.00	0.01	0.08	0.05	0.14	0.05	0.04	0.00	0.14	-	0.49	0.52	0.11	0.00
CoV (%)	0.01	0.14	0.09	0.07	0.42	0.06	0.74	0.01	0.36	-	0.42	0.44	9.86	9.80
A/W/45/P/M20-01	22.39	9.65	80.20	80.20	28.80	69.47	10.73	22.37	39.99	-0.11	116.56	117.46	0.90	0.772%
A/W/45/P/M20-02	22.40	9.68	80.31	80.15	29.20	69.35	10.80	22.38	40.39	0.24	116.97	118.14	1.17	1.000%
A/W/45/P/M20-03	22.39	9.64	80.34	80.16	29.05	69.11	11.05	22.39	40.24	0.07	117.19	118.37	1.18	1.007%
A/W/45/P/M20-04	22.39	9.62	80.26	80.19	28.85	69.13	11.06	22.38	40.04	-0.09	115.84	117.01	1.17	1.010%
A/W/45/P/M20-05	22.39	9.69	80.26	80.13	28.91	69.19	10.94	22.38	40.10	-0.03	116.11	117.23	1.12	0.965%
Mean	22.39	9.66	80.27	80.17	28.96	69.25	10.92	22.38	40.15	-	116.53	117.64	1.11	0.951%
SD	0.00	0.03	0.05	0.03	0.16	0.15	0.15	0.01	0.16	-	0.57	0.59	0.12	0.00
CoV (%)	0.02	0.30	0.07	0.04	0.56	0.22	1.36	0.03	0.41	-	0.49	0.50	10.71	10.68
Threaded														
A/W/45/T/M10-01	11.97	9.62	80.11	80.22	34.10	74.23	5.99	11.96	40.08	0.03	118.74	119.66	0.92	0.775%
A/W/45/T/M10-02	11.96	9.63	79.82	80.20	33.96	74.10	6.10	11.96	39.94	0.03	119.11	120.25	1.14	0.957%
A/W/45/T/M10-03	11.97	9.58	79.73	80.25	33.62	74.33	5.92	11.97	39.60	-0.26	117.84	118.99	1.15	0.976%
A/W/45/T/M10-04	11.97	9.64	80.16	80.25	33.95	74.11	6.14	11.96	39.93	-0.15	119.05	120.18	1.13	0.949%
A/W/45/T/M10-05	11.97	9.61	80.07	80.22	34.08	74.16	6.06	11.97	40.06	0.03	119.13	120.23	1.10	0.923%
Mean	11.97	9.62	79.98	80.23	33.94	74.19	6.04	11.96	39.92	-	118.77	119.86	1.09	0.916%
SD	0.00	0.02	0.19	0.02	0.19	0.10	0.09	0.00	0.19	-	0.55	0.55	0.10	0.00
CoV (%)	0.02	0.24	0.24	0.03	0.57	0.13	1.45	0.02	0.48	-	0.46	0.45	8.80	8.86
A/W/45/T/M20-01	22.40	9.65	79.88	80.07	28.87	68.96	11.11	22.39	40.07	0.13	115.41	116.32	0.91	0.996%
A/W/45/T/M20-02	22.40	9.62	80.13	80.11	29.04	69.15	10.96	22.39	40.23	0.17	115.46	116.61	1.15	1.027%
A/W/45/T/M20-03	22.40	9.64	80.16	80.14	28.85	69.27	10.87	22.39	40.04	-0.04	115.87	117.06	1.19	1.004%
A/W/45/T/M20-04	22.40	9.65	80.22	80.09	28.81	69.00	11.09	22.39	40.01	-0.10	115.58	116.74	1.16	0.983%
A/W/45/T/M20-05	22.40	9.66	80.28	80.10	28.86	69.10	11.00	22.39	40.06	-0.08	117.02	118.17	1.15	0.960%
Mean	22.40	9.64	80.13	80.10	28.89	69.10	11.01	22.39	40.08	-	115.87	116.98	1.11	0.994%
SD	0.00	0.02	0.15	0.03	0.09	0.12	0.10	0.00	0.09	-	0.67	0.72	0.11	0.00
CoV (%)	0.00	0.16	0.19	0.03	0.31	0.18	0.89	0.02	0.22	-	0.58	0.61	10.26	2.51

Table B.22: Pin-bearing Test Specimen Measurements for Web Material tested with a Plain and Threaded Pin in the 45° Direction and Hot-wet Conditioned at 40°C for 6 Months

Specimen ID	Diameter of Hole, d_n	Thickness of Specimen, t	Width of Specimen, w	Length of Specimen, l	Width to Hole Edge, w_h	Length to Hole Edge, l_h	Notch Depth, w_{notch}	Notch Diameter, d_{notch}	Notch Centre, l_{notch}	Offset, $(w - l_{notch})/2$	Weight Before (g)	Weight After (g)	Weight Change (g)	Moisture Gain (%)
Plain														
A/W/45/P/M10-06	11.98	9.66	80.12	80.24	34.09	74.32	5.92	11.97	40.08	0.02	119.65	121.01	1.36	1.137%
A/W/45/P/M10-07	11.97	9.61	80.20	80.21	34.25	74.26	5.95	11.97	40.23	0.13	118.32	119.70	1.38	1.166%
A/W/45/P/M10-08	11.97	9.64	80.34	80.25	34.10	74.40	5.85	11.96	40.08	-0.09	118.83	120.24	1.41	1.187%
A/W/45/P/M10-09	11.97	9.65	79.95	80.22	33.96	74.17	6.05	11.97	39.94	-0.03	118.54	119.92	1.38	1.164%
A/W/45/P/M10-10	11.97	9.64	80.20	80.26	33.97	74.39	5.87	11.97	39.95	-0.15	118.87	120.23	1.36	1.144%
Mean	10.13	8.16	67.90	67.89	28.89	62.88	5.07	10.13	33.95	-	118.84	120.22	1.38	1.160%
SD	4.49	3.59	30.10	30.10	12.70	27.88	2.08	4.49	14.96	-	0.50	0.50	0.02	0.00
CoV (%)	44.35	43.98	44.33	44.34	43.95	44.34	41.05	44.36	44.05	-	0.42	0.41	1.49	1.70
A/W/45/P/M20-06	22.39	9.65	80.22	80.18	29.25	69.97	10.21	22.30	40.40	0.29	116.49	117.82	1.33	1.142%
A/W/45/P/M20-07	22.39	9.59	80.30	80.18	29.05	69.33	10.85	22.37	40.24	0.09	115.89	117.25	1.36	1.174%
A/W/45/P/M20-08	22.39	9.64	80.17	80.21	28.76	69.11	11.10	22.39	39.95	-0.13	117.32	118.66	1.34	1.142%
A/W/45/P/M20-09	22.39	9.62	80.21	80.16	28.94	69.18	10.98	22.38	40.13	0.03	115.99	117.34	1.35	1.164%
A/W/45/P/M20-10	22.39	9.63	80.28	80.14	28.77	69.18	10.96	22.38	39.96	-0.18	116.05	117.40	1.35	1.163%
Mean	18.95	8.18	67.92	67.84	24.56	58.67	9.32	18.93	34.01	-	116.35	117.69	1.35	1.157%
SD	8.40	3.56	30.12	30.09	10.74	25.95	3.81	8.40	14.97	-	0.59	0.58	0.01	0.00
CoV (%)	44.35	43.50	44.34	44.36	43.73	44.24	40.95	44.34	44.01	-	0.51	0.50	0.85	1.23
Threaded														
A/W/45/T/M10-06	11.97	9.62	79.98	80.20	34.01	74.12	6.08	11.96	39.99	0.00	117.82	119.23	1.41	1.197%
A/W/45/T/M10-07	11.97	9.67	80.05	80.21	34.13	74.20	6.01	11.97	40.11	0.09	119.32	120.70	1.38	1.157%
A/W/45/T/M10-08	11.98	9.63	79.92	80.16	33.97	74.15	6.01	11.97	39.96	0.00	118.33	119.70	1.37	1.158%
A/W/45/T/M10-09	11.96	9.61	79.91	80.24	33.90	74.28	5.96	11.96	39.88	-0.07	118.05	119.44	1.39	1.177%
A/W/45/T/M10-10	11.96	9.64	80.02	80.23	34.01	74.22	6.01	11.96	39.99	-0.02	119.34	120.67	1.33	1.114%
Mean	10.13	8.16	67.71	67.88	28.80	62.79	5.22	10.13	33.86	-	118.57	119.95	1.38	1.161%
SD	4.49	3.57	29.95	30.12	12.62	27.82	2.00	4.49	14.88	-	0.72	0.69	0.03	0.00
CoV (%)	44.34	43.67	44.24	44.37	43.80	44.30	38.22	44.33	43.94	-	0.60	0.58	2.16	2.64
A/W/45/T/M20-06	22.40	9.67	80.23	80.11	29.05	69.23	10.88	22.39	40.24	0.13	116.46	117.85	1.39	1.131%
A/W/45/T/M20-07	22.40	9.64	80.21	80.12	29.06	69.11	11.01	22.39	40.26	0.15	117.59	118.92	1.33	1.142%
A/W/45/T/M20-08	22.40	9.65	80.09	80.14	28.85	69.13	11.01	22.39	40.05	0.00	117.34	118.68	1.34	1.164%
A/W/45/T/M20-09	22.40	9.63	80.25	80.07	29.02	69.11	10.96	22.39	40.21	0.09	116.02	117.37	1.35	1.142%
A/W/45/T/M20-10	22.40	9.62	80.28	80.36	28.70	69.19	11.17	22.39	39.90	-0.24	116.46	117.79	1.33	1.154%
Mean	18.95	8.17	67.86	67.81	24.49	58.51	9.39	18.95	33.96	-	116.77	118.12	1.35	1.147%
SD	8.41	3.59	30.04	30.08	10.78	25.90	3.95	8.40	15.00	-	0.66	0.65	0.02	0.00
CoV (%)	44.38	43.91	44.27	44.36	44.02	44.27	42.09	44.36	44.18	-	0.57	0.55	1.85	1.10

Table B.23: Pin-bearing Strength Test Specimens for Web Material tested with a Plain and Threaded Pin in the Transverse Direction and Hot-wet Conditioned at 40°C for 3 Months

Specimen ID	Diameter of Hole, d_n	Thickness of Specimen, t	Width of Specimen, w	Length of Specimen, l	Width to Hole Edge, w_h	Length to Hole Edge, l_h	Notch Depth, w_{notch}	Notch Diameter, d_{notch}	Notch Centre, l_{notch}	Offset, $(w - l_{notch})/2$	Weight Before (g)	Weight After (g)	Weight Change (g)	Moisture Gain (%)
Plain														
A/W/90/P/M10-01	11.97	9.63	80.06	80.15	34.06	74.08	6.07	11.97	40.04	0.01	118.64	119.42	0.78	0.657%
A/W/90/P/M10-02	11.97	9.66	80.04	80.13	34.07	74.01	6.12	11.97	40.05	0.03	118.58	119.56	0.98	0.826%
A/W/90/P/M10-03	11.97	9.60	80.01	80.18	33.81	74.04	6.14	11.97	39.79	-0.21	119.41	120.41	1.00	0.837%
A/W/90/P/M10-04	11.97	9.60	79.92	80.16	33.94	74.02	6.14	11.97	39.92	-0.04	118.43	119.41	0.98	0.827%
A/W/90/P/M10-05	11.97	9.61	79.93	80.12	33.97	74.14	5.98	11.97	39.95	-0.01	118.35	119.28	0.93	0.786%
Mean	11.97	9.62	79.99	80.15	33.97	74.06	6.09	11.97	39.95	-	118.68	119.62	0.93	0.787%
SD	0.00	0.03	0.06	0.02	0.11	0.05	0.07	0.00	0.11	-	0.42	0.45	0.09	0.00
CoV (%)	0.01	0.27	0.08	0.03	0.31	0.07	1.11	0.01	0.26	-	0.36	0.38	9.62	9.54
A/W/90/P/M20-01	22.39	9.61	80.15	79.88	28.82	68.70	11.18	22.39	40.01	-0.06	115.94	116.71	0.77	0.664%
A/W/90/P/M20-02	22.39	9.61	79.91	79.94	29.05	68.80	11.14	22.38	40.24	0.29	115.82	116.81	0.99	0.855%
A/W/90/P/M20-03	22.90	9.61	80.62	80.05	29.34	68.74	11.31	22.90	40.79	0.48	116.77	117.79	1.02	0.874%
A/W/90/P/M20-04	22.39	9.62	80.23	79.98	28.92	68.82	11.16	22.38	40.11	0.00	116.81	117.80	0.99	0.848%
A/W/90/P/M20-05	22.39	9.61	80.04	80.00	28.96	69.03	10.97	22.38	40.15	0.13	116.37	117.37	1.00	0.859%
Mean	22.49	9.61	80.19	79.97	29.02	68.82	11.15	22.49	40.26	-	116.34	117.30	0.95	0.820%
SD	0.23	0.00	0.27	0.06	0.20	0.13	0.12	0.23	0.31	-	0.46	0.52	0.10	0.00
CoV (%)	1.02	0.05	0.34	0.08	0.68	0.19	1.09	1.02	0.76	-	0.39	0.44	10.86	10.68
Threaded														
A/W/90/T/M10-01	11.97	9.63	80.27	80.09	34.04	73.89	6.20	11.96	40.02	-0.11	119.55	120.30	0.75	0.627%
A/W/90/T/M10-02	11.97	9.59	79.81	80.15	33.87	74.31	5.84	11.97	39.85	-0.05	119.14	120.14	1.00	0.839%
A/W/90/T/M10-03	11.97	9.61	79.91	80.05	33.83	73.83	6.22	11.96	39.81	-0.14	118.39	119.37	0.98	0.828%
A/W/90/T/M10-04	11.97	9.63	80.23	80.16	34.00	74.04	6.12	11.97	39.98	-0.13	119.39	120.38	0.99	0.829%
A/W/90/T/M10-05	11.97	9.64	80.28	80.15	34.10	74.19	5.96	11.97	40.09	-0.05	120.48	121.43	0.95	0.789%
Mean	11.97	9.62	80.10	80.12	33.97	74.05	6.07	11.97	39.95	-	119.39	120.32	0.93	0.782%
SD	0.00	0.02	0.22	0.05	0.11	0.20	0.16	0.00	0.12	-	0.75	0.74	0.10	0.00
CoV (%)	0.01	0.21	0.28	0.06	0.34	0.27	2.69	0.04	0.29	-	0.63	0.61	11.19	11.35
A/W/90/T/M20-01	22.39	9.64	80.27	80.09	28.64	68.87	11.22	22.39	39.83	-0.30	117.13	117.89	0.76	0.859%
A/W/90/T/M20-02	22.39	9.60	80.07	80.04	28.99	69.05	10.99	22.39	40.18	0.15	116.41	117.41	1.00	0.863%
A/W/90/T/M20-03	22.39	9.62	80.40	80.13	29.18	69.00	11.13	22.38	40.37	0.17	116.97	117.98	1.01	0.856%
A/W/90/T/M20-04	22.38	9.60	79.90	79.99	28.86	68.88	11.11	22.38	40.05	0.10	115.69	116.68	0.99	0.884%
A/W/90/T/M20-05	22.39	9.60	79.96	80.04	28.86	68.98	11.06	22.38	40.05	0.07	116.50	117.53	1.03	0.822%
Mean	22.39	9.61	80.12	80.06	28.91	68.96	11.10	22.38	40.10	-	116.54	117.50	0.96	0.857%
SD	0.00	0.02	0.21	0.05	0.20	0.08	0.09	0.00	0.20	-	0.56	0.52	0.11	0.00
CoV (%)	0.02	0.19	0.26	0.07	0.69	0.11	0.77	0.02	0.49	-	0.48	0.44	11.66	2.61

Table B.24: Pin-bearing Test Specimen Measurements for Web Material tested with a Plain and Threaded Pin in the Transverse Direction and Hot-wet Conditioned at 40°C for 6 Months

Specimen ID	Diameter of Hole, d_n	Thickness of Specimen, t	Width of Specimen, w	Length of Specimen, l	Width to Hole Edge, w_h	Length to Hole Edge, l_h	Notch Depth, w_{notch}	Notch Diameter, d_{notch}	Notch Centre, l_{notch}	Offset, $(w - l_{notch})/2$	Weight Before (g)	Weight After (g)	Weight Change (g)	Moisture Gain (%)
Plain														
A/W/90/P/M10-06	11.97	9.60	80.02	80.17	33.93	74.12	6.05	11.97	39.92	-0.09	119.16	120.36	1.20	1.007%
A/W/90/P/M10-07	11.97	9.62	80.06	80.16	34.09	74.14	6.02	11.97	40.08	0.05	119.12	120.32	1.20	1.007%
A/W/90/P/M10-08	11.97	9.63	80.12	80.11	34.04	74.35	5.76	11.96	40.02	-0.04	118.44	119.62	1.18	0.996%
A/W/90/P/M10-09	11.97	9.65	80.14	80.12	34.23	74.22	5.90	11.97	40.22	0.15	118.82	120.01	1.19	1.002%
A/W/90/P/M10-10	11.97	9.62	80.09	80.13	33.89	74.13	6.00	11.97	39.88	-0.17	118.73	119.94	1.21	1.019%
Mean	10.13	8.16	67.73	67.82	28.80	62.73	5.19	10.13	33.86	-	118.85	120.05	1.20	1.006%
SD	4.49	3.56	30.03	30.09	12.69	27.81	2.05	4.49	14.95	-	0.30	0.30	0.01	0.00
CoV (%)	44.36	43.60	44.33	44.36	44.06	44.34	39.59	44.35	44.14	-	0.25	0.25	0.95	0.85
A/W/90/P/M20-06	22.39	9.61	80.19	80.02	29.00	69.07	10.95	22.38	40.19	0.10	116.32	117.47	1.15	0.989%
A/W/90/P/M20-07	22.39	9.62	80.10	80.03	28.96	68.70	11.33	22.38	40.15	0.10	115.55	116.71	1.16	1.004%
A/W/90/P/M20-08	22.39	9.61	79.75	80.02	28.91	69.12	10.90	22.38	40.10	0.22	115.56	116.75	1.19	1.030%
A/W/90/P/M20-09	22.39	9.63	79.91	80.02	28.63	68.94	11.08	22.39	39.82	-0.13	116.29	117.50	1.21	1.041%
A/W/90/P/M20-10	22.39	9.64	79.86	80.16	28.83	69.15	11.01	22.38	40.02	0.09	116.11	117.29	1.18	1.016%
Mean	19.09	8.14	67.81	67.71	24.56	58.32	9.49	19.08	34.07	-	115.97	117.14	1.18	1.016%
SD	8.20	3.60	29.96	30.02	10.71	25.82	3.95	8.20	14.89	-	0.38	0.39	0.02	0.00
CoV (%)	42.94	44.24	44.18	44.33	43.59	44.26	41.62	42.94	43.69	-	0.33	0.33	2.03	2.02
Threaded														
A/W/90/T/M10-06	11.97	9.62	79.93	80.41	33.84	74.32	6.09	11.97	39.83	-0.14	118.74	119.94	1.20	1.011%
A/W/90/T/M10-07	11.97	9.62	79.95	80.19	33.90	74.03	6.16	11.96	39.88	-0.09	119.02	120.19	1.17	0.983%
A/W/90/T/M10-08	11.97	9.63	80.34	80.13	33.95	74.08	6.05	11.97	39.93	-0.24	119.93	121.26	1.33	1.109%
A/W/90/T/M10-09	11.97	9.60	79.87	80.13	33.72	74.11	6.02	11.97	39.70	-0.23	118.52	119.73	1.21	1.021%
A/W/90/T/M10-10	11.97	9.65	80.36	80.05	33.97	73.91	6.14	11.97	39.95	-0.23	120.39	121.68	1.29	1.072%
Mean	10.13	8.16	67.81	67.83	28.74	62.71	5.36	10.13	33.80	-	119.32	120.56	1.24	1.039%
SD	4.49	3.57	29.99	30.08	12.66	27.73	1.82	4.49	14.91	-	0.80	0.86	0.07	0.00
CoV (%)	44.35	43.76	44.22	44.35	44.03	44.21	34.01	44.29	44.12	-	0.67	0.71	5.41	4.86
A/W/90/T/M20-06	22.39	9.64	80.25	80.00	28.88	68.96	11.04	22.38	40.07	-0.05	116.23	117.43	1.20	1.024%
A/W/90/T/M20-07	22.39	9.59	79.90	80.05	28.65	69.05	11.00	22.39	39.84	-0.11	116.24	117.43	1.19	0.997%
A/W/90/T/M20-08	22.39	9.63	79.94	80.01	28.55	69.00	11.01	22.38	39.74	-0.23	116.31	117.47	1.16	1.045%
A/W/90/T/M20-09	22.39	9.60	79.95	80.06	28.74	68.66	11.40	22.38	39.93	-0.04	115.82	117.03	1.21	0.989%
A/W/90/T/M20-10	22.39	9.66	80.08	80.42	28.84	68.68	11.74	22.36	40.02	-0.02	116.28	117.43	1.15	1.017%
Mean	18.94	8.15	67.79	67.77	24.46	58.33	9.51	18.94	33.91	-	116.18	117.36	1.18	1.014%
SD	8.40	3.57	29.98	30.05	10.66	25.84	4.04	8.40	14.90	-	0.20	0.18	0.03	0.00
CoV (%)	44.35	43.83	44.23	44.34	43.59	44.31	42.47	44.36	43.93	-	0.17	0.16	2.19	2.18

Table B.25: Pin-bearing Test Specimen Measurements for Flange Material tested with a Plain and Threaded Pin in the Longitudinal Direction and Hot-wet Conditioned at 30°C for 3 Months

Specimen ID	Diameter of Hole, d_n	Thickness of Specimen, t	Width of Specimen, w	Length of Specimen, l	Width to Hole Edge, w_h	Length to Hole Edge, l_h	Notch Depth, w_{notch}	Notch Diameter, d_{notch}	Notch Centre, l_{notch}	Offset, $(w - l_{notch})/2$	Weight Before (g)	Weight After (g)	Weight Change (g)	Moisture Gain (%)
Plain														
30A/F/0/P/M10-01	12.00	9.79	80.32	80.03	34.26	74.37	5.66	11.98	40.25	0.09	121.83	122.69	0.86	0.706%
30A/F/0/P/M10-02	12.00	9.82	80.11	80.26	34.35	74.51	5.75	11.98	40.34	0.29	122.63	123.54	0.91	0.742%
30A/F/0/P/M10-03	11.99	9.58	80.22	80.08	34.05	74.30	5.78	11.98	40.04	-0.07	121.70	122.59	0.89	0.731%
30A/F/0/P/M10-04	12.00	9.79	80.30	80.12	34.31	74.24	5.88	12.00	40.31	0.16	122.42	123.31	0.89	0.727%
30A/F/0/P/M10-05	12.00	9.53	80.30	80.13	34.27	74.37	5.76	11.99	40.26	0.11	122.57	123.44	0.87	0.710%
Mean	12.00	9.70	80.25	80.12	34.25	74.36	5.77	11.99	40.24	-	122.23	123.11	0.88	0.723%
SD	0.00	0.14	0.09	0.09	0.12	0.10	0.08	0.01	0.12	-	0.43	0.44	0.02	0.00
CoV (%)	0.03	1.40	0.11	0.11	0.34	0.14	1.36	0.07	0.29	-	0.35	0.36	2.21	2.09
30A/F/0/P/M20-01	22.39	9.83	80.15	80.20	28.89	69.04	11.16	22.38	40.08	0.01	119.97	120.88	0.91	0.759%
30A/F/0/P/M20-02	22.39	9.58	80.28	80.06	29.20	69.13	10.93	22.38	40.39	0.25	119.94	120.86	0.92	0.767%
30A/F/0/P/M20-03	22.39	9.81	80.15	80.08	28.73	69.11	10.97	22.38	39.92	-0.15	119.79	120.72	0.93	0.776%
30A/F/0/P/M20-04	22.39	9.83	80.00	80.10	28.65	69.03	11.07	22.38	39.84	-0.16	119.39	120.30	0.91	0.762%
30A/F/0/P/M20-05	22.38	9.83	80.10	80.08	29.13	68.89	11.19	22.38	40.32	0.27	119.73	120.64	0.91	0.760%
Mean	22.38	9.78	80.14	80.10	28.92	69.04	11.06	22.38	40.11	-	119.76	120.68	0.92	0.765%
SD	0.00	0.11	0.10	0.06	0.24	0.09	0.11	0.00	0.24	-	0.23	0.23	0.01	0.00
CoV (%)	0.01	1.12	0.13	0.07	0.83	0.14	1.03	0.01	0.60	-	0.19	0.19	0.98	0.94
Threaded														
30A/F/0/T/M10-01	11.96	9.58	79.96	80.19	34.49	76.11	4.08	11.34	40.16	0.18	121.12	121.96	0.84	0.694%
30A/F/0/T/M10-02	11.95	9.64	79.89	80.25	34.34	76.06	4.19	11.40	40.04	0.10	121.25	122.08	0.83	0.685%
30A/F/0/T/M10-03	11.95	9.57	80.19	80.15	33.95	74.73	5.42	11.89	39.90	-0.20	119.43	120.36	0.93	0.779%
30A/F/0/T/M10-04	11.95	9.62	79.99	80.20	34.04	74.48	5.72	11.93	40.01	0.01	121.87	122.78	0.91	0.747%
30A/F/0/T/M10-05	11.97	9.59	79.84	80.14	33.87	74.33	5.81	11.96	39.85	-0.07	122.07	122.96	0.89	0.729%
Mean	11.95	9.60	79.97	80.19	34.14	75.14	5.04	11.71	39.99	-	121.15	122.03	0.88	0.727%
SD	0.01	0.03	0.13	0.04	0.27	0.87	0.84	0.31	0.12	-	1.04	1.03	0.04	0.00
CoV (%)	0.07	0.30	0.17	0.05	0.78	1.16	16.72	2.64	0.30	-	0.86	0.84	4.95	5.33
30A/F/0/T/M20-01	22.37	9.94	80.08	80.06	29.06	70.46	9.60	22.14	40.13	0.09	118.52	119.35	0.83	0.700%
30A/F/0/T/M20-02	22.38	10.28	80.09	80.16	28.59	69.09	11.07	22.38	39.78	-0.27	124.58	125.51	0.93	0.747%
30A/F/0/T/M20-03	22.37	10.28	79.93	80.09	28.79	69.28	10.81	22.36	39.97	0.00	124.44	125.35	0.91	0.731%
30A/F/0/T/M20-04	22.37	10.29	80.12	80.08	29.16	70.72	9.36	22.07	40.19	0.13	125.55	126.44	0.89	0.709%
30A/F/0/T/M20-05	22.37	9.57	80.04	80.05	29.02	70.20	9.85	22.21	40.12	0.10	120.16	121.07	0.91	0.757%
Mean	22.37	10.07	80.05	80.09	28.92	69.95	10.14	22.23	40.04	-	122.65	123.54	0.89	0.729%
SD	0.01	0.32	0.07	0.04	0.23	0.73	0.76	0.14	0.17	-	3.11	3.13	0.04	0.00
CoV (%)	0.03	3.15	0.09	0.05	0.80	1.04	7.48	0.61	0.42	-	2.53	2.53	4.30	3.32

Table B.26: Pin-bearing Test Specimen Measurements for Web Material tested with a Plain and Threaded Pin in the Longitudinal Direction and Hot-wet Conditioned at 30°C for 6 Months

Specimen ID	Diameter of Hole, d_n	Thickness of Specimen, t	Width of Specimen, w	Length of Specimen, l	Width to Hole Edge, w_h	Length to Hole Edge, l_h	Notch Depth, w_{notch}	Notch Diameter, d_{notch}	Notch Centre, l_{notch}	Offset, $(w - l_{notch})/2$	Weight Before (g)	Weight After (g)	Weight Change (g)	Moisture Gain (%)
Plain														
30A/F/0/P/M10-06	12.00	9.82	80.45	79.93	33.88	74.09	5.84	11.99	39.88	-0.35	122.20	123.86	1.66	1.358%
30A/F/0/P/M10-07	12.00	9.54	79.99	79.91	34.21	74.17	5.74	11.98	40.20	0.21	121.82	123.76	1.94	1.593%
30A/F/0/P/M10-08	11.99	9.54	80.43	80.06	33.78	74.08	5.98	11.99	39.77	-0.44	122.79	123.97	1.18	0.961%
30A/F/0/P/M10-09	12.00	9.76	80.62	80.06	34.60	74.19	5.87	11.99	40.60	0.29	123.14	124.73	1.59	1.291%
30A/F/0/P/M10-10	11.99	9.87	80.21	80.00	34.43	74.33	5.67	11.97	40.42	0.31	122.05	124.01	1.96	1.606%
Mean	11.99	9.71	80.34	79.99	34.18	74.17	5.82	11.99	40.17	-	122.40	124.07	1.67	1.362%
SD	0.00	0.16	0.24	0.07	0.35	0.10	0.12	0.01	0.35	-	0.55	0.38	0.32	0.00
CoV (%)	0.02	1.61	0.30	0.09	1.02	0.14	2.06	0.07	0.87	-	0.45	0.31	19.06	19.37
30A/F/0/P/M20-06	22.39	10.15	80.34	80.12	29.05	69.08	11.04	22.38	40.24	0.07	125.08	126.23	1.15	0.919%
30A/F/0/P/M20-07	22.38	10.16	80.33	80.02	29.17	68.90	11.12	22.38	40.36	0.19	124.89	126.12	1.23	0.985%
30A/F/0/P/M20-08	22.38	9.85	80.05	80.01	29.10	69.09	10.92	22.37	40.29	0.26	119.59	120.74	1.15	0.962%
30A/F/0/P/M20-09	22.38	9.54	80.20	80.10	28.66	69.12	10.98	22.38	39.85	-0.25	119.91	121.05	1.14	0.951%
30A/F/0/P/M20-10	22.38	10.17	79.82	80.14	28.88	69.19	10.95	22.37	40.07	0.16	124.03	125.23	1.20	0.968%
Mean	22.38	9.97	80.15	80.08	28.97	69.08	11.00	22.38	40.16	-	122.70	123.87	1.17	0.957%
SD	0.00	0.28	0.22	0.06	0.20	0.11	0.08	0.00	0.21	-	2.72	2.75	0.04	0.00
CoV (%)	0.01	2.78	0.27	0.07	0.71	0.16	0.72	0.02	0.51	-	2.22	2.22	3.33	2.54
Threaded														
30A/F/0/T/M10-06	11.97	9.60	80.04	80.21	34.55	77.05	3.16	10.55	39.82	-0.20	123.27	124.51	1.24	1.006%
30A/F/0/T/M10-07	11.98	9.63	80.03	80.15	34.03	74.64	5.51	11.94	40.00	-0.01	121.12	122.23	1.11	0.916%
30A/F/0/T/M10-08	11.96	9.64	79.97	80.16	34.07	74.43	5.73	11.94	40.04	0.06	122.34	123.53	1.19	0.973%
30A/F/0/T/M10-09	11.97	9.60	79.89	80.16	33.84	74.26	5.90	11.97	39.82	-0.12	121.56	122.86	1.30	1.069%
30A/F/0/T/M10-10	11.97	9.59	79.89	80.01	34.02	74.56	5.45	11.92	39.98	0.03	121.66	122.83	1.17	0.962%
Mean	11.97	9.61	79.96	80.14	34.10	74.99	5.15	11.66	39.93	-	121.99	123.19	1.20	0.985%
SD	0.01	0.02	0.07	0.08	0.27	1.16	1.13	0.62	0.10	-	0.84	0.87	0.07	0.00
CoV (%)	0.08	0.23	0.09	0.09	0.78	1.55	21.88	5.34	0.26	-	0.69	0.71	5.98	5.78
30A/F/0/T/M20-06	22.36	9.65	79.94	80.14	28.92	71.22	8.92	21.89	39.87	-0.10	117.84	118.97	1.13	0.959%
30A/F/0/T/M20-07	22.37	9.62	79.83	80.07	29.06	71.31	8.76	21.83	39.98	0.06	116.70	117.82	1.12	0.960%
30A/F/0/T/M20-08	22.37	10.28	80.25	80.09	29.06	69.05	11.04	22.37	40.24	0.12	124.81	125.95	1.14	0.913%
30A/F/0/T/M20-09	22.36	10.31	80.21	80.08	28.83	68.90	11.18	22.36	40.01	-0.09	123.85	124.99	1.14	0.920%
30A/F/0/T/M20-10	22.36	10.24	80.10	80.03	28.96	69.13	10.90	22.35	40.14	0.09	124.16	125.31	1.15	0.926%
Mean	22.36	10.02	80.07	80.08	28.97	69.92	10.16	22.16	40.05	-	121.47	122.61	1.14	0.936%
SD	0.01	0.35	0.18	0.04	0.10	1.23	1.21	0.27	0.15	-	3.87	3.88	0.01	0.00
CoV (%)	0.03	3.52	0.22	0.05	0.34	1. 76	11.91	1.23	0.36	-	3.19	3.17	1.00	2.35

Table B.27: Pin-bearing Test Specimen Measurements for Flange Material tested with a Plain and Threaded Pin in the Transverse Direction and Hot-wet Conditioned at 30°C for 3 Months

Specimen ID	Diameter of Hole, d_n	Thickness of Specimen, t	Width of Specimen, w	Length of Specimen, l	Width to Hole Edge, w_h	Length to Hole Edge, l_h	Notch Depth, w_{notch}	Notch Diameter, d_{notch}	Notch Centre, l_{notch}	Offset, $(w - l_{notch})/2$	Weight Before (g)	Weight After (g)	Weight Change (g)	Moisture Gain (%)
Plain														
30A/F/90/P/M10-01	12.00	9.76	80.40	80.40	34.29	74.20	6.20	11.99	40.28	0.08	124.58	125.57	0.99	0.795%
30A/F/90/P/M10-02	12.00	9.56	80.41	80.17	34.14	74.28	5.89	11.99	40.14	-0.07	122.71	123.68	0.97	0.790%
30A/F/90/P/M10-03	11.99	9.58	80.09	79.88	34.34	74.23	5.65	11.97	40.33	0.28	119.78	120.64	0.86	0.718%
30A/F/90/P/M10-04	12.00	9.56	80.34	80.05	33.93	74.21	5.84	11.99	39.93	-0.24	122.78	123.72	0.94	0.766%
30A/F/90/P/M10-05	12.00	9.76	80.39	79.83	34.72	74.34	5.49	11.96	40.70	0.50	124.01	124.96	0.95	0.766%
Mean	12.00	9.64	80.33	80.07	34.28	74.25	5.81	11.98	40.27	-	122.77	123.71	0.94	0.767%
SD	0.00	0.11	0.13	0.23	0.29	0.06	0.27	0.02	0.28	-	1.85	1.90	0.05	0.00
CoV (%)	0.03	1.10	0.17	0.29	0.85	0.08	4.61	0.13	0.71	-	1.51	1.54	5.28	3.98
30A/F/90/P/M20-01	22.39	10.18	80.12	80.01	28.90	68.90	11.11	22.38	40.09	0.03	124.58	125.51	0.93	0.747%
30A/F/90/P/M20-02	22.38	9.55	80.16	80.06	28.75	68.94	11.12	22.38	39.94	-0.14	117.22	118.07	0.85	0.725%
30A/F/90/P/M20-03	22.38	9.54	80.00	80.29	28.97	68.97	11.32	22.37	40.16	0.16	118.94	119.82	0.88	0.740%
30A/F/90/P/M20-04	22.38	9.83	80.01	80.11	28.73	68.87	11.24	22.37	39.92	-0.09	116.47	117.40	0.93	0.798%
30A/F/90/P/M20-05	22.38	9.78	80.42	80.02	28.68	69.07	10.95	22.37	39.86	-0.35	121.61	122.58	0.97	0.798%
Mean	22.38	9.78	80.14	80.10	28.81	68.95	11.15	22.38	39.99	-	119.76	120.68	0.91	0.762%
SD	0.00	0.26	0.17	0.11	0.12	0.08	0.14	0.01	0.12	-	3.34	3.36	0.05	0.00
CoV (%)	0.02	2.67	0.21	0.14	0.43	0.11	1.26	0.03	0.31	-	2.79	2.79	5.17	4.50
Threaded														
30A/F/90/T/M10-01	12.00	10.29	80.07	80.16	34.05	74.26	5.90	11.99	40.05	0.01	127.79	128.67	0.88	0.689%
30A/F/90/T/M10-02	12.00	9.58	80.14	80.17	34.06	74.37	5.80	11.99	40.05	-0.02	122.21	123.04	0.83	0.679%
30A/F/90/T/M10-03	11.97	9.61	80.17	80.27	34.24	74.36	5.91	11.96	40.22	0.14	121.90	122.70	0.80	0.656%
30A/F/90/T/M10-04	11.96	10.17	80.15	80.23	34.09	74.24	5.99	11.96	40.07	-0.01	127.58	128.47	0.89	0.698%
30A/F/90/T/M10-05	11.98	9.59	79.96	80.20	33.99	74.37	5.83	11.97	39.98	0.00	118.02	118.89	0.87	0.737%
Mean	11.98	9.85	80.10	80.21	34.09	74.32	5.89	11.98	40.07	-	123.50	124.35	0.85	0.692%
SD	0.02	0.35	0.09	0.05	0.09	0.06	0.07	0.01	0.09	-	4.16	4.18	0.04	0.00
CoV (%)	0.14	3.57	0.11	0.06	0.27	0.09	1.26	0.12	0.23	-	3.37	3.36	4.43	4.29
30A/F/90/T/M20-01	22.36	10.16	79.95	80.11	28.79	68.94	11.17	22.36	39.97	-0.01	124.37	125.25	0.88	0.708%
30A/F/90/T/M20-02	22.36	10.27	80.11	80.12	28.78	68.70	11.42	22.35	39.95	-0.10	124.14	125.00	0.86	0.693%
30A/F/90/T/M20-03	22.36	9.89	80.10	80.15	28.87	68.88	11.27	22.35	40.05	0.00	119.65	120.50	0.85	0.710%
30A/F/90/T/M20-04	22.35	9.58	80.01	80.15	28.76	68.91	11.24	22.34	39.93	-0.07	118.63	119.45	0.82	0.691%
30A/F/90/T/M20-05	22.35	9.55	80.19	80.17	28.92	69.00	11.17	22.34	40.09	0.00	118.88	119.71	0.83	0.698%
Mean	22.35	9.89	80.07	80.14	28.82	68.89	11.25	22.35	40.00	-	121.13	121.98	0.85	0.700%
SD	0.01	0.33	0.09	0.02	0.07	0.11	0.10	0.01	0.07	-	2.87	2.90	0.02	0.00
CoV (%)	0.03	3.31	0.12	0.03	0.24	0.16	0.91	0.03	0.17	-	2.37	2.37	2.82	1.23

Table B.28: Pin-bearing Test Specimen Measurements for Flange Material tested with a Plain and Threaded Pin in the Transverse Direction and Hot-wet Conditioned at 30°C for 6 Months

Specimen ID	Diameter of Hole, d_n	Thickness of Specimen, t	Width of Specimen, w	Length of Specimen, l	Width to Hole Edge, w_h	Length to Hole Edge, l_h	Notch Depth, w_{notch}	Notch Diameter, d_{notch}	Notch Centre, l_{notch}	Offset, $(w - l_{notch})/2$	Weight Before (g)	Weight After (g)	Weight Change (g)	Moisture Gain (%)
Plain														
30A/F/90/P/M10-06	12.00	9.52	80.27	80.11	34.05	74.43	5.68	11.98	40.04	-0.09	122.68	123.39	0.71	0.579%
30A/F/90/P/M10-07	12.00	9.82	80.21	80.14	34.15	74.26	5.88	11.99	40.15	0.04	122.62	122.92	0.30	0.245%
30A/F/90/P/M10-08	11.99	9.55	80.29	80.11	34.12	74.31	5.80	11.98	40.11	-0.03	122.80	123.96	1.16	0.945%
30A/F/90/P/M10-09	12.00	9.81	80.25	80.11	34.14	74.15	5.96	11.99	40.14	0.01	121.98	125.96	3.98	3.263%
30A/F/90/P/M10-10	12.00	9.54	80.37	80.19	33.90	74.37	5.82	11.99	39.89	-0.29	122.87	123.30	0.43	0.350%
Mean	12.00	9.65	80.28	80.13	34.07	74.30	5.83	11.99	40.07	-	122.59	123.91	1.32	1.076%
SD	0.00	0.15	0.06	0.03	0.10	0.11	0.10	0.01	0.10	-	0.35	1.21	1.53	0.01
CoV (%)	0.03	1.58	0.07	0.04	0.30	0.14	1.78	0.04	0.26	-	0.29	0.97	115.90	116.29
30A/F/90/P/M20-06	22.38	9.89	80.46	80.16	29.14	68.88	11.28	22.38	40.33	0.10	119.81	121.02	1.21	1.010%
30A/F/90/P/M20-07	22.39	9.86	80.46	80.10	29.20	68.80	11.30	22.39	40.39	0.16	119.69	120.94	1.25	1.044%
30A/F/90/P/M20-08	22.38	9.76	80.03	80.01	28.78	68.82	11.19	22.37	39.97	-0.05	119.76	120.89	1.13	0.944%
30A/F/90/P/M20-09	22.39	9.81	79.98	80.18	28.91	68.80	11.38	22.38	40.10	0.11	116.02	117.16	1.14	0.983%
30A/F/90/P/M20-10	22.39	9.79	80.38	80.17	28.86	69.02	11.15	22.38	40.05	-0.14	119.52	120.78	1.26	1.054%
Mean	22.38	9.82	80.26	80.12	28.98	68.86	11.26	22.38	40.17	-	118.96	120.16	1.20	1.007%
SD	0.01	0.05	0.24	0.07	0.18	0.09	0.09	0.01	0.18	-	1.65	1.68	0.06	0.00
CoV (%)	0.03	0.54	0.30	0.09	0.63	0.14	0.81	0.02	0.46	-	1.38	1.40	5.06	4.51
Threaded														
30A/F/90/T/M10-06	12.00	10.26	80.23	80.07	34.46	74.19	5.88	11.99	40.46	0.34	127.52	128.60	1.08	0.847%
30A/F/90/T/M10-07	12.00	9.90	80.03	79.98	34.12	74.25	5.73	11.98	40.11	0.10	121.95	123.12	1.17	0.959%
30A/F/90/T/M10-08	11.97	9.57	80.28	80.26	33.99	74.17	6.09	11.97	39.97	-0.17	122.24	123.33	1.09	0.892%
30A/F/90/T/M10-09	11.99	10.25	80.13	80.16	34.08	74.17	5.99	11.98	40.07	0.01	127.17	128.28	1.11	0.873%
30A/F/90/T/M10-10	11.98	9.57	80.22	79.98	34.39	74.16	5.82	11.97	40.38	0.27	121.89	122.98	1.09	0.894%
Mean	11.98	9.91	80.18	80.09	34.21	74.19	5.90	11.98	40.20	-	124.15	125.26	1.11	0.893%
SD	0.01	0.34	0.10	0.12	0.21	0.04	0.14	0.01	0.21	-	2.92	2.91	0.04	0.00
CoV (%)	0.10	3.46	0.12	0.15	0.60	0.05	2.39	0.09	0.52	-	2.35	2.32	3.28	4.67
30A/F/90/T/M20-06	22.35	9.57	80.13	80.17	28.94	69.07	11.10	22.34	40.11	0.05	119.47	120.45	0.98	0.820%
30A/F/90/T/M20-07	22.33	10.25	80.14	80.13	28.88	68.96	11.17	22.32	40.04	-0.03	124.38	125.34	0.96	0.772%
30A/F/90/T/M20-08	22.34	9.84	80.17	80.12	28.73	68.91	11.21	22.33	39.90	-0.19	121.25	122.32	1.07	0.882%
30A/F/90/T/M20-09	22.35	10.15	80.08	80.16	28.87	68.98	11.18	22.35	40.04	0.00	124.20	125.24	1.04	0.837%
30A/F/90/T/M20-10	22.33	9.56	80.12	80.17	28.92	68.95	11.22	22.33	40.08	0.02	119.36	120.41	1.05	0.880%
Mean	22.34	9.87	80.13	80.15	28.87	68.97	11.18	22.34	40.04	-	121.73	122.75	1.02	0.838%
SD	0.01	0.32	0.03	0.02	0.08	0.06	0.05	0.01	0.08	-	2.45	2.44	0.05	0.00
CoV (%)	0.05	3.24	0.04	0.03	0.29	0.09	0.42	0.05	0.21	-	2.02	1.99	4.65	5.47

Table B.29: Pin-bearing Test Specimen Measurements for Flange Material tested with a Plain and Threaded Pin in the Longitudinal Direction and Hot-wet Conditioned at 50°C for 3 Months

Specimen ID	Diameter of Hole, d_n	Thickness of Specimen, t	Width of Specimen, w	Length of Specimen, l	Width to Hole Edge, w_h	Length to Hole Edge, l_h	Notch Depth, w_{notch}	Notch Diameter, d_{notch}	Notch Centre, l_{notch}	Offset, $(w - l_{notch})/2$	Weight Before (g)	Weight After (g)	Weight Change (g)	Moisture Gain (%)
Plain														
50A/F/0/P/M10-06	11.99	9.58	80.08	80.63	34.35	74.39	6.24	11.98	40.34	0.30	123.16	124.35	1.19	0.966%
50A/F/0/P/M10-07	11.98	9.59	80.09	80.77	34.27	74.01	6.76	11.88	40.21	0.17	122.76	123.98	1.22	0.994%
50A/F/0/P/M10-08	11.99	10.23	79.99	80.83	33.99	74.02	6.81	11.88	39.93	-0.07	128.50	129.72	1.22	0.949%
50A/F/0/P/M10-09	11.99	9.82	80.02	80.86	34.01	74.13	6.73	11.90	39.96	-0.05	121.72	122.80	1.08	0.887%
50A/F/0/P/M10-10	11.99	9.82	79.88	80.64	34.17	74.15	6.49	11.95	40.14	0.20	121.45	122.57	1.12	0.922%
Mean	11.99	9.81	80.01	80.75	34.16	74.14	6.61	11.92	40.12	-	123.52	124.68	1.17	0.944%
SD	0.00	0.26	0.08	0.11	0.16	0.15	0.24	0.04	0.17	-	2.87	2.91	0.06	0.00
CoV (%)	0.04	2.69	0.11	0.13	0.46	0.21	3.62	0.38	0.43	-	2.33	2.34	5.41	4.34
50A/F/0/P/M20-06	22.40	9.59	80.00	80.76	28.54	69.12	11.64	22.38	39.73	-0.27	119.83	120.86	1.03	0.860%
50A/F/0/P/M20-07	22.40	10.24	80.20	80.73	28.98	69.11	11.62	22.38	40.17	0.07	125.56	126.80	1.24	0.988%
50A/F/0/P/M20-08	22.40	9.56	79.94	80.74	28.68	68.93	11.81	22.37	39.86	-0.11	119.85	121.03	1.18	0.985%
50A/F/0/P/M20-09	22.40	9.57	79.83	80.73	28.36	68.95	11.78	22.37	39.54	-0.37	119.21	120.36	1.15	0.965%
50A/F/0/P/M20-10	22.39	10.23	79.98	80.81	28.75	68.92	11.89	22.35	39.92	-0.07	124.75	126.05	1.30	1.042%
Mean	22.40	9.84	79.99	80.75	28.66	69.01	11.75	22.37	39.85	-	121.84	123.02	1.18	0.968%
SD	0.00	0.36	0.13	0.03	0.23	0.10	0.12	0.02	0.23	-	3.05	3.13	0.10	0.00
CoV (%)	0.02	3.69	0.17	0.04	0.81	0.15	0.98	0.07	0.58	-	2.50	2.54	8.62	6.92
Threaded														
50A/F/0/T/M10-06	12.00	9.79	79.81	80.89	34.09	74.13	6.76	11.90	40.04	0.14	122.03	123.17	1.14	0.934%
50A/F/0/T/M10-07	11.99	9.56	80.21	80.78	34.57	74.01	6.77	11.89	40.51	0.41	119.96	121.05	1.09	0.909%
50A/F/0/T/M10-08	11.98	9.59	79.90	80.84	34.02	74.08	6.76	11.88	39.96	0.01	122.69	123.73	1.04	0.848%
50A/F/0/T/M10-09	11.99	9.81	79.96	80.96	34.28	74.32	6.64	11.92	40.24	0.26	121.32	122.37	1.05	0.865%
50A/F/0/T/M10-10	11.99	10.23	79.95	80.91	34.07	74.17	6.74	11.90	40.02	0.04	127.94	129.15	1.21	0.946%
Mean	11.99	9.80	79.97	80.88	34.21	74.14	6.73	11.90	40.16	-	122.79	123.89	1.11	0.900%
SD	0.01	0.27	0.15	0.07	0.23	0.12	0.05	0.02	0.23	-	3.05	3.11	0.07	0.00
CoV (%)	0.06	2.73	0.19	0.09	0.66	0.16	0.80	0.13	0.57	-	2.49	2.51	6.35	4.73
50A/F/0/T/M20-06	22.40	9.82	79.91	80.76	28.81	68.93	11.83	22.36	39.99	0.04	119.18	120.34	1.16	0.973%
50A/F/0/T/M20-07	22.40	9.56	80.16	80.74	28.76	68.92	11.82	22.37	39.94	-0.14	120.19	121.44	1.25	1.040%
50A/F/0/T/M20-08	22.40	9.54	79.95	80.73	28.79	68.94	11.79	22.37	39.97	0.00	119.12	120.27	1.15	0.965%
50A/F/0/T/M20-09	22.40	9.58	79.79	80.83	28.64	68.89	11.94	22.35	39.82	-0.08	120.18	121.34	1.16	0.965%
50A/F/0/T/M20-10	22.40	9.56	80.02	80.80	28.84	68.84	11.96	22.35	40.01	0.00	116.53	117.66	1.13	0.970%
Mean	22.40	9.61	79.97	80.77	28.77	68.90	11.87	22.36	39.95	-	119.04	120.21	1.17	0.983%
SD	0.00	0.12	0.14	0.04	0.08	0.04	0.08	0.01	0.08	-	1.50	1.53	0.05	0.00
CoV (%)	0.00	1.22	0.17	0.05	0.27	0.06	0.65	0.04	0.20	-	1.26	1.27	3.96	3.28

Table B.30: Pin-bearing Test Specimen Measurements for Flange Material tested with a Plain and Threaded Pin in the Longitudinal Direction and Hot-wet Conditioned at 50°C for 6 Months

Specimen ID	Diameter of Hole, d_n	Thickness of Specimen, t	Width of Specimen, w	Length of Specimen, l	Width to Hole Edge, w_h	Length to Hole Edge, l_h	Notch Depth, w_{notch}	Notch Diameter, d_{notch}	Notch Centre, l_{notch}	Offset, $(w - l_{notch})/2$	Weight Before (g)	Weight After (g)	Weight Change (g)	Moisture Gain (%)
Plain														
50A/F/0/P/M10-01	12.00	9.54	80.33	80.02	34.10	74.34	5.68	11.98	40.09	-0.08	122.74	124.02	1.28	1.043%
50A/F/0/P/M10-02	12.00	9.55	80.26	80.15	34.48	74.35	5.80	11.99	40.48	0.35	121.47	122.72	1.25	1.029%
50A/F/0/P/M10-03	11.99	10.16	80.21	80.16	34.27	74.45	5.71	11.98	40.26	0.15	127.51	128.86	1.35	1.059%
50A/F/0/P/M10-04	11.99	9.55	80.38	80.10	34.28	74.45	5.65	11.97	40.27	0.08	122.65	124.06	1.41	1.150%
50A/F/0/P/M10-05	12.00	9.59	80.24	80.17	34.20	74.31	5.86	11.99	40.20	0.08	121.68	122.98	1.30	1.068%
Mean	11.99	9.68	80.28	80.12	34.27	74.38	5.74	11.98	40.26	-	123.21	124.53	1.32	1.070%
SD	0.00	0.27	0.07	0.06	0.14	0.07	0.09	0.01	0.14	-	2.47	2.50	0.06	0.00
CoV (%)	0.03	2.79	0.09	0.08	0.41	0.09	1.52	0.08	0.35	-	2.00	2.00	4.78	4.40
50A/F/0/P/M20-01	22.38	10.17	80.22	80.09	28.72	69.19	10.90	22.37	39.91	-0.20	124.95	126.32	1.37	1.096%
50A/F/0/P/M20-02	22.38	9.85	80.18	80.14	28.78	69.05	11.09	22.37	39.97	-0.12	119.98	121.20	1.22	1.017%
50A/F/0/P/M20-03	22.38	10.16	80.28	80.12	28.49	69.15	10.97	22.37	39.68	-0.46	124.89	126.26	1.37	1.097%
50A/F/0/P/M20-04	22.38	10.23	80.07	80.08	28.27	69.02	11.06	22.37	39.46	-0.58	124.47	125.83	1.36	1.093%
50A/F/0/P/M20-05	22.38	10.18	80.16	80.09	29.16	69.14	10.95	22.37	40.34	0.26	124.62	125.97	1.35	1.083%
Mean	22.38	10.12	80.18	80.10	28.68	69.11	10.99	22.37	39.87	-	123.78	125.12	1.33	1.077%
SD	0.00	0.15	0.08	0.03	0.33	0.07	0.08	0.00	0.33	-	2.13	2.20	0.06	0.00
CoV (%)	0.01	1.50	0.10	0.03	1.16	0.10	0.72	0.01	0.84	-	1.72	1.76	4.82	3.18
Threaded														
50A/F/0/T/M10-01	11.97	9.62	80.19	80.18	34.04	75.28	4.90	11.77	39.93	-0.17	122.61	124.04	1.43	1.166%
50A/F/0/T/M10-02	11.97	10.27	80.08	80.20	33.86	74.29	5.91	11.97	39.84	-0.20	127.67	129.09	1.42	1.112%
50A/F/0/T/M10-03	11.96	9.60	80.01	80.26	34.09	74.23	6.03	11.96	40.07	0.06	119.05	120.42	1.37	1.151%
50A/F/0/T/M10-04	11.97	9.62	80.23	80.19	34.28	74.58	5.61	11.94	40.25	0.14	122.00	123.28	1.28	1.049%
50A/F/0/T/M10-05	11.96	9.60	79.90	80.27	34.07	74.23	6.04	11.95	40.05	0.10	121.72	123.00	1.28	1.052%
Mean	11.96	9.74	80.08	80.22	34.07	74.52	5.70	11.92	40.03	-	122.61	123.97	1.36	1.106%
SD	0.01	0.30	0.13	0.04	0.15	0.45	0.48	0.08	0.15	-	3.14	3.17	0.07	0.00
CoV (%)	0.05	3.03	0.17	0.05	0.44	0.60	8.40	0.70	0.39	-	2.56	2.56	5.38	4.92
50A/F/0/T/M20-01	22.38	10.23	79.95	80.11	28.76	67.77	12.34	22.26	39.89	-0.08	118.98	120.25	1.27	1.067%
50A/F/0/T/M20-02	22.37	9.90	80.20	80.04	28.77	69.29	10.75	22.35	39.94	-0.16	116.39	117.70	1.31	1.126%
50A/F/0/T/M20-03	22.37	10.24	79.95	80.12	28.78	68.98	11.14	22.36	39.96	-0.01	119.40	120.79	1.39	1.164%
50A/F/0/T/M20-04	22.37	10.24	79.97	80.15	29.05	69.21	10.94	22.36	40.23	0.24	120.05	121.39	1.34	1.116%
50A/F/0/T/M20-05	22.35	10.22	80.15	80.04	29.07	70.11	9.93	22.21	40.18	0.10	120.14	121.49	1.35	1.124%
Mean	22.37	10.17	80.04	80.09	28.89	69.07	11.02	22.31	40.04	-	118.99	120.32	1.33	1.119%
SD	0.01	0.15	0.12	0.05	0.16	0.84	0.87	0.07	0.15	-	1.53	1.55	0.04	0.00
CoV (%)	0.05	1.46	0.15	0.06	0.55	1.22	7.89	0.31	0.38	-	1.29	1.29	3.37	3.09

Table B.31: : Pin-bearing Test Specimen Measurements for Flange Material tested with a Plain and Threaded Pin in the Transverse Direction and Hot-wet Conditioned at 50°C for 3 Months

Specimen ID	Diameter of Hole, d_n	Thickness of Specimen, t	Width of Specimen, w	Length of Specimen, l	Width to Hole Edge, w_h	Length to Hole Edge, l_h	Notch Depth, w_{notch}	Notch Diameter, d_{notch}	Notch Centre, l_{notch}	Offset, (w - l_{notch})/2	Weight Before (g)	Weight After (g)	Weight Change (g)	Moisture Gain (%)
Plain														
50A/F/90/P/M10-06	11.99	9.57	80.18	80.68	33.97	74.14	6.54	11.94	39.94	-0.15	122.64	123.81	1.17	0.954%
50A/F/90/P/M10-07	12.00	9.55	80.09	80.82	34.20	74.20	6.62	11.94	40.17	0.12	121.26	122.31	1.05	0.866%
50A/F/90/P/M10-08	12.00	9.80	80.20	80.76	34.33	74.16	6.60	11.94	40.30	0.20	124.41	125.53	1.12	0.900%
50A/F/90/P/M10-09	12.00	9.54	79.98	80.95	33.96	74.12	6.83	11.88	39.90	-0.09	118.73	119.80	1.07	0.901%
50A/F/90/P/M10-10	12.00	9.58	80.29	80.76	34.44	74.12	6.64	11.93	40.41	0.26	123.34	124.54	1.20	0.973%
Mean	12.00	9.61	80.15	80.79	34.18	74.15	6.65	11.93	40.14	-	122.08	123.20	1.12	0.919%
SD	0.00	0.11	0.12	0.10	0.21	0.03	0.11	0.02	0.22	-	2.19	2.23	0.06	0.00
CoV (%)	0.04	1.13	0.15	0.12	0.63	0.05	1.65	0.20	0.55	-	1.80	1.81	5.69	4.75
50A/F/90/P/M20-06	22.39	9.53	80.12	80.83	28.88	68.88	11.95	22.34	40.05	-0.01	119.31	120.46	1.15	0.964%
50A/F/90/P/M20-07	22.39	9.59	80.21	80.85	28.79	68.98	11.87	22.35	39.96	-0.14	120.14	121.35	1.21	1.007%
50A/F/90/P/M20-08	22.39	9.57	80.08	80.79	28.89	68.89	11.90	22.35	40.06	0.02	115.98	117.11	1.13	0.974%
50A/F/90/P/M20-09	22.40	10.24	80.21	80.83	28.86	68.71	12.12	22.32	40.02	-0.08	124.78	125.91	1.13	0.906%
50A/F/90/P/M20-10	22.39	10.15	80.07	80.94	28.86	68.53	12.41	22.26	39.99	-0.05	124.82	126.02	1.20	0.961%
Mean	22.39	9.82	80.14	80.85	28.86	68.80	12.05	22.32	40.02	-	121.01	122.17	1.16	0.962%
SD	0.00	0.35	0.07	0.06	0.04	0.18	0.22	0.04	0.04	-	3.80	3.81	0.04	0.00
CoV (%)	0.02	3.55	0.09	0.07	0.14	0.26	1.85	0.17	0.10	-	3.14	3.12	3.31	3.81
Threaded														
50A/F/90/T/M10-06	11.99	9.78	80.20	80.66	34.42	74.05	6.61	11.93	40.38	0.28	124.61	125.75	1.14	0.915%
50A/F/90/T/M10-07	11.99	10.22	80.21	80.80	34.44	74.09	6.71	11.90	40.39	0.29	127.65	128.70	1.05	0.823%
50A/F/90/T/M10-08	11.99	10.24	80.10	80.84	34.29	74.28	6.56	11.94	40.26	0.21	127.88	128.92	1.04	0.813%
50A/F/90/T/M10-09	12.00	9.53	80.13	80.73	34.22	74.26	6.47	11.96	40.20	0.14	122.05	123.14	1.09	0.893%
50A/F/90/T/M10-10	11.99	9.89	80.01	80.77	34.03	74.13	6.64	11.92	39.99	-0.01	123.05	124.22	1.17	0.951%
Mean	11.99	9.93	80.13	80.76	34.28	74.16	6.60	11.93	40.25	-	125.05	126.15	1.10	0.879%
SD	0.00	0.30	0.08	0.07	0.17	0.10	0.09	0.02	0.16	-	2.64	2.60	0.06	0.00
CoV (%)	0.04	3.04	0.10	0.09	0.49	0.14	1.36	0.18	0.41	-	2.11	2.06	5.13	6.77
50A/F/90/T/M20-06	22.40	10.12	80.13	80.88	28.94	69.00	11.88	22.36	40.12	0.05	124.84	125.98	1.14	0.913%
50A/F/90/T/M20-07	22.40	9.79	80.20	80.88	29.08	68.92	11.96	22.35	40.25	0.15	122.06	123.22	1.16	0.950%
50A/F/90/T/M20-08	22.39	10.22	80.16	80.73	29.03	69.05	11.68	22.37	40.21	0.13	125.03	126.16	1.13	0.904%
50A/F/90/T/M20-09	22.40	9.88	79.96	80.77	28.82	68.89	11.88	22.36	40.00	0.02	120.11	121.22	1.11	0.924%
50A/F/90/T/M20-10	22.40	9.57	80.12	80.81	28.85	68.97	11.84	22.36	40.03	-0.03	120.07	121.28	1.21	1.008%
Mean	22.40	9.92	80.11	80.81	28.94	68.97	11.85	22.36	40.12	-	122.42	123.57	1.15	0.940%
SD	0.00	0.26	0.09	0.07	0.11	0.06	0.10	0.01	0.11	-	2.43	2.42	0.04	0.00
CoV (%)	0.02	2.62	0.11	0.08	0.39	0.09	0.87	0.03	0.28	-	1.99	1.96	3.31	4.44

Table B.32: Pin-bearing Test Specimen Measurements for Flange Material tested with a Plain and Threaded Pin in the Transverse Direction and Hot-wet Conditioned at 50°C for 6 Months

Specimen ID	Diameter of Hole, d_n	Thickness of Specimen, t	Width of Specimen, w	Length of Specimen, l	Width to Hole Edge, w_h	Length to Hole Edge, l_h	Notch Depth, w_{notch}	Notch Diameter, d_{notch}	Notch Centre, l_{notch}	Offset, $(w - l_{notch})/2$	Weight Before (g)	Weight After (g)	Weight Change (g)	Moisture Gain (%)
Plain														
50A/F/90/P/M10-01	12.00	9.54	79.87	79.87	34.17	74.18	5.69	11.98	40.16	0.22	122.52	123.92	1.40	1.143%
50A/F/90/P/M10-02	11.99	9.55	79.87	79.87	34.04	74.19	5.68	11.97	40.03	0.09	122.43	123.83	1.40	1.144%
50A/F/90/P/M10-03	11.99	9.53	80.13	80.13	34.30	74.22	5.91	11.99	40.29	0.23	122.04	123.36	1.32	1.082%
50A/F/90/P/M10-04	11.99	9.57	80.15	80.15	34.06	74.34	5.81	11.98	40.05	-0.02	120.15	121.40	1.25	1.040%
50A/F/90/P/M10-05	11.99	9.54	80.16	80.16	33.77	74.07	6.09	11.99	39.76	-0.32	121.62	122.86	1.24	1.020%
Mean	11.99	9.55	80.04	80.04	34.07	74.20	5.84	11.98	40.06	-	121.75	123.07	1.32	1.086%
SD	0.00	0.02	0.15	0.15	0.20	0.10	0.17	0.01	0.20	-	0.96	1.03	0.08	0.00
CoV (%)	0.02	0.16	0.19	0.19	0.58	0.13	2.92	0.05	0.49	-	0.79	0.83	5.87	5.26
50A/F/90/P/M20-01	22.38	9.90	80.03	79.91	28.84	68.96	10.95	22.37	40.03	0.01	116.19	117.51	1.32	1.136%
50A/F/90/P/M20-02	22.39	9.86	80.46	79.83	29.44	69.03	10.80	22.38	40.63	0.40	119.49	120.90	1.41	1.180%
50A/F/90/P/M20-03	22.38	9.83	80.00	79.92	28.85	68.91	11.01	22.38	40.04	0.04	116.21	117.52	1.31	1.127%
50A/F/90/P/M20-04	22.38	10.24	80.08	79.80	28.63	68.81	10.99	22.38	39.82	-0.22	124.82	126.14	1.32	1.058%
50A/F/90/P/M20-05	22.38	9.52	79.93	80.10	28.99	68.98	11.12	22.37	40.18	0.21	118.49	119.68	1.19	1.004%
Mean	22.38	9.87	80.10	79.91	28.95	68.94	10.97	22.38	40.14	-	119.04	120.35	1.31	1.101%
SD	0.01	0.26	0.21	0.12	0.30	0.08	0.12	0.00	0.30	-	3.54	3.55	0.08	0.00
CoV (%)	0.02	2.59	0.26	0.15	1.05	0.12	1.06	0.00	0.75	-	2.97	2.95	5.99	6.33
Threaded														
50A/F/90/T/M10-01	12.00	9.92	80.13	80.22	34.14	74.10	6.12	11.99	40.14	0.07	122.76	124.21	1.45	1.181%
50A/F/90/T/M10-02	11.97	10.14	80.18	80.27	34.03	74.22	6.05	11.97	40.01	-0.08	127.02	128.43	1.41	1.110%
50A/F/90/T/M10-03	11.95	10.11	80.03	80.26	33.98	74.23	6.03	11.95	39.95	-0.06	126.95	128.32	1.37	1.079%
50A/F/90/T/M10-04	11.98	10.24	80.11	80.19	33.92	74.21	5.98	11.97	39.91	-0.15	127.24	128.57	1.33	1.045%
50A/F/90/T/M10-05	11.98	10.30	80.23	80.26	33.96	74.08	6.18	11.97	39.95	-0.17	128.18	129.62	1.44	1.123%
Mean	11.97	10.14	80.14	80.24	34.01	74.17	6.07	11.97	39.99	-	126.43	127.83	1.40	1.108%
SD	0.02	0.15	0.08	0.03	0.08	0.07	0.08	0.02	0.09	-	2.11	2.09	0.05	0.00
CoV (%)	0.14	1.44	0.09	0.04	0.25	0.10	1.29	0.13	0.22	-	1.67	1.63	3.57	4.59
50A/F/90/T/M20-01	22.37	9.58	80.05	80.07	28.80	69.18	10.89	22.36	39.98	-0.05	119.77	121.09	1.32	1.102%
50A/F/90/T/M20-02	22.39	9.59	80.08	80.09	28.93	69.07	11.02	22.38	40.12	0.08	124.90	126.33	1.43	1.145%
50A/F/90/T/M20-03	22.35	9.87	80.20	80.14	28.73	69.13	11.01	22.35	39.90	-0.20	119.18	120.42	1.24	1.040%
50A/F/90/T/M20-04	22.36	9.58	80.04	80.19	28.86	68.93	11.26	22.36	40.04	0.02	121.58	122.92	1.34	1.102%
50A/F/90/T/M20-05	22.36	9.57	80.03	80.19	28.78	68.90	11.29	22.36	39.96	-0.06	119.65	120.98	1.33	1.112%
Mean	22.36	9.64	80.08	80.14	28.82	69.04	11.09	22.36	40.00	-	121.02	122.35	1.33	1.100%
SD	0.01	0.13	0.07	0.06	0.08	0.12	0.17	0.01	0.08	-	2.36	2.42	0.07	0.00
CoV (%)	0.06	1.35	0.09	0.07	0.27	0.18	1.56	0.06	0.21	-	1.95	1.97	5.08	3.43

Appendix C – Aged and Non-aged Pin-bearing Strength Test Results

C.1 Introduction

Presented in this appendix is the full set of strength test results from the pin-bearing experimental programme described in Chapters 4 and 5. Firstly, in Tables C.1 to C.16 are the strength test results for non-aged material. The first failure load, displacement and criterion for selection of failure load are given as obtained from the load-stroke data. The maximum failure load and corresponding displacement is tabulated, along with the calculated first failure and maximum bearing strength.

The Chauvenet criterion, as described in Chapter 3, is applied to the test results for non-aged material only. This criterion identifies outliers within a selected test batch. The re-adjusted values for mean, standard deviation and co-efficient of variation are computed, if there is an outlier identified. A comparison of the non-adjusted values and those computed after the analysis is presented by way of a percentage difference.

Presented in Tables C.17 to C.36 are the strength test results for the hot-wet conditioned material at 40°C. Tables C.37 to C.40 and C41 to C.44 present the results for 30 and 50°C, respectively.

C.2 Non-aged Pin-bearing Strength Test Results

Table C.1: Pin-bearing Strength Test Results for Web Material tested in the Longitudinal Direction with a Plain Pin

Specimen	Pin Size (mm)	Clearance (mm)	Thickness (mm)	First Failure Load (kN)	Disp. at First Failure (mm)	First Failure Criterion	Max Failure Load (kN)	Disp. at Max Failure (mm)	Bearing Strength (N/mm^2)	FF Bearing Strength (N/mm^2)
W/0/P/M10-01	9.81	2.17	9.63	12.8	0.58	DFL	14.6	0.74	155	166
W/0/P/M10-02	9.81	2.17	9.60	14.1	0.58	FP	14.7	0.67	156	214
W/0/P/M10-03	9.81	2.18	9.65	12.6	0.59	DFL	14.2	1.48	150	172
W/0/P/M10-04	9.81	2.15	9.60	12.1	0.60	FP	14.3	0.83	152	183
W/0/P/M10-05	9.81	2.17	9.60	11.8	0.70	FP	16.1	1.02	171	189
W/0/P/M10-06	9.81	2.18	9.62	12.4	0.56	FP	14.8	0.76	157	217
W/0/P/M10-07	9.81	2.17	9.64	12.4	0.50	DFL	14.7	1.03	155	198
W/0/P/M10-08	9.81	2.17	9.63	13.4	0.68	FP	14.8	1.48	157	167
W/0/P/M10-09	9.81	2.17	9.62	11.8	0.57	DFL	15.7	0.94	166	159
W/0/P/M10-10	9.81	2.18	9.63	12.3	0.60	DFL	15.9	1.29	168	180
W/0/P/M12-01	11.8	2.56	9.62	13.7	0.71	FP	15.4	1.47	136	162
W/0/P/M12-02	11.8	2.55	9.63	13.9	0.74	FP	15.0	1.93	132	171
W/0/P/M12-03	11.8	2.56	9.61	12.5	0.95	DFL	15.4	2.10	136	205
W/0/P/M12-04	11.8	2.55	9.66	12.2	0.51	FP	15.8	1.48	139	182
W/0/P/M12-05	11.8	2.55	9.65	13.4	0.75	FP	15.9	1.73	140	194
W/0/P/M12-06	11.8	2.56	9.63	14.6	0.56	FP	15.9	1.84	140	196
W/0/P/M12-07	11.8	2.56	9.66	13.1	0.57	FP	15.8	1.10	139	196
W/0/P/M12-08	11.8	2.56	9.65	13.0	0.58	DFL	15.3	1.47	134	156
W/0/P/M12-09	11.8	2.56	9.65	12.8	0.59	FP	15.8	1.47	139	180
W/0/P/M12-10	11.8	2.56	9.63	12.7	0.66	DFL	14.8	1.2	130	188
W/0/P/M16-01	15.9	2.53	9.64	14.2	0.45	FP	17.4	1.73	114	178
W/0/P/M16-02	15.9	2.53	9.65	18.7	1.01	DFL	20.0	1.12	130	175
W/0/P/M16-03	15.9	2.52	9.63	16.6	0.56	DFL	19.3	0.69	126	183
W/0/P/M16-04	15.9	2.52	9.66	21.5	0.55	-	21.5	0.55	140	193
W/0/P/M16-05	15.9	2.53	9.64	16.2	0.69	DFL	18.0	1.12	117	180
W/0/P/M16-06	15.9	2.53	9.63	17.5	0.55	DFL	19.1	2.47	125	176
W/0/P/M16-07	15.9	2.53	9.63	16.7	0.54	FP	19.6	0.73	128	185
W/0/P/M16-08	15.9	2.53	9.59	16.5	0.57	FP	20.7	1.30	136	168
W/0/P/M16-09	15.9	2.53	9.63	15.1	0.57	DFL	17.9	0.92	117	179
W/0/P/M16-10	15.9	2.53	9.62	17.3	0.57	FP	20.6	1.47	135	195
W/0/P/M20-01	19.8	2.61	9.66	18.0	0.53	FP	20.7	1.49	108	175
W/0/P/M20-02	19.8	2.61	9.65	20.7	0.85	FP	20.9	1.49	109	178
W/0/P/M20-03	19.8	2.61	9.64	17.8	0.58	DFL	20.1	0.65	105	128
W/0/P/M20-04	19.8	2.61	9.63	13.9	0.46	DFL	17.7	0.61	92.8	163
W/0/P/M20-05	19.8	2.61	9.61	21.1	0.75	-	21.1	0.75	111	186
W/0/P/M20-06	19.8	2.61	9.63	19.3	0.51	FP	20.8	0.93	109	187
W/0/P/M20-07	19.8	2.61	9.64	16.8	0.47	DFL	20.6	1.01	108	193
W/0/P/M20-08	19.8	2.57	9.63	20.5	0.56	FP	20.5	1.37	108	167
W/0/P/M20-09	19.8	2.60	9.60	20.1	0.60	-	20.1	0.60	106	191
W/0/P/M20-10	19.8	2.60	9.66	20.8	0.58	-	20.8	0.58	109	161

Table C.2: Chauvenet Criterion applied to Pin-bearing Strength Test Results for Web Material tested in the Longitudinal Direction with a Plain Pin

Specimen	x_i-x_m	(x_i-x_m)/σ	Outlier ?		Chauvenet x_m	% Diff (Chauvenet - x)
W/0/P/M10-01	0.9	0.58	FALSE	17.8	18.31	-2.0%
W/0/P/M10-02	1.5	0.99	FALSE	20.2	1.05	-31.4%
W/0/P/M10-03	0.7	0.44	FALSE	18	5.73%	
W/0/P/M10-04	0.8	0.51	FALSE	17.9		
W/0/P/M10-05	0.4	0.25	FALSE	18.3		
W/0/P/M10-06	3.3	2.17	TRUE	0		
W/0/P/M10-07	0.1	0.05	FALSE	18.6		
W/0/P/M10-08	1.6	1.03	FALSE	17.1		
W/0/P/M10-09	1.5	0.97	FALSE	17.2		
W/0/P/M10-10	1.0	0.67	FALSE	19.7		
W/0/P/M12-01	3.3	1.46	FALSE	18.4	21.65	0.0%
W/0/P/M12-02	2.3	1.01	FALSE	19.4	1.70	-23.9%
W/0/P/M12-03	3.8	1.68	FALSE	25.4	7.85%	
W/0/P/M12-04	0.2	0.07	FALSE	21.8		
W/0/P/M12-05	0.5	0.20	FALSE	22.1		
W/0/P/M12-06	1.9	0.83	FALSE	23.5		
W/0/P/M12-07	2.5	1.10	FALSE	24.1		
W/0/P/M12-08	2.3	1.01	FALSE	19.4		
W/0/P/M12-09	0.6	0.29	FALSE	21		
W/0/P/M12-10	0.3	0.11	FALSE	21.4		
W/0/P/M16-01	0.9	0.58	FALSE	27.2	28.14	0.0%
W/0/P/M16-02	1.3	0.82	FALSE	26.8	1.63	0.0%
W/0/P/M16-03	0.6	0.34	FALSE	28.7	5.81%	
W/0/P/M16-04	1.4	0.83	FALSE	29.5		
W/0/P/M16-05	0.1	0.09	FALSE	28		
W/0/P/M16-06	1.1	0.70	FALSE	27		
W/0/P/M16-07	3.0	1.81	FALSE	31.1		
W/0/P/M16-08	2.3	1.43	FALSE	25.8		
W/0/P/M16-09	0.7	0.45	FALSE	27.4		
W/0/P/M16-10	1.8	1.08	FALSE	29.9		
W/0/P/M20-01	0.7	0.24	FALSE	34.2	33.51	0.0%
W/0/P/M20-02	0.5	0.17	FALSE	34	2.23	-22.4%
W/0/P/M20-03	5.0	1.74	FALSE	28.5	6.66%	
W/0/P/M20-04	2.6	0.91	FALSE	30.9		
W/0/P/M20-05	2.0	0.69	FALSE	35.5		
W/0/P/M20-06	2.1	0.73	FALSE	35.6		
W/0/P/M20-07	3.8	1.32	FALSE	37.3		
W/0/P/M20-08	1.7	0.59	FALSE	31.8		
W/0/P/M20-09	3.0	1.04	FALSE	36.5		
W/0/P/M20-10	2.7	0.94	FALSE	30.8		

Table C.3: Pin-bearing Strength Test Results for Flange Material tested in the Longitudinal Direction with a Plain Pin

Specimen	Pin Size (mm)	Clearance (mm)	Thickness (mm)	First Failure Load (kN)	Disp. at First Failure (mm)	First Failure Criterion	Max Failure Load (kN)	Disp. at Max Failure (mm)	Bearing Strength (N/mm^2)	FF Bearing Strength (N/mm^2)
F/0/P/M10-01	9.81	2.16	9.60	22.5	0.93	-	22.5	0.93	239	239
F/0/P/M10-02	9.81	2.15	9.84	19.5	0.70	-	19.5	0.70	202	202
F/0/P/M10-03	9.81	2.18	9.85	17.6	0.72	-	17.6	0.72	182	182
F/0/P/M10-04	9.81	2.18	9.89	19.3	0.63	-	19.3	0.63	199	199
F/0/P/M10-05	9.81	2.18	9.59	17.3	0.56	DFL	20.6	0.78	219	184
F/0/P/M10-06	9.81	2.17	9.59	21.4	0.74	-	21.4	0.74	227	227
F/0/P/M10-07	9.81	2.11	9.57	18.9	0.86	FP	19.3	0.94	206	201
F/0/P/M10-08	9.81	2.18	9.96	18.1	0.56	FP	18.7	0.62	191	185
F/0/P/M10-09	9.81	2.17	10.2	22.3	0.76	FP	23.7	0.88	237	223
F/0/P/M10-10	9.81	2.15	9.60	18.2	0.74	-	18.2	0.69	193	193
F/0/P/M12-01	11.8	2.55	9.60	17.9	0.95	-	18.7	0.95	165	158
F/0/P/M12-02	11.8	2.56	9.62	19.7	0.60	-	20.4	0.60	180	174
F/0/P/M12-03	11.8	2.55	9.60	19.6	0.98	-	26.5	0.98	234	173
F/0/P/M12-04	11.8	2.56	9.63	17.9	0.55	-	19.2	0.55	169	158
F/0/P/M12-05	11.8	2.56	9.61	17.7	0.57	FP	22.7	0.78	200	156
F/0/P/M12-06	11.8	2.55	9.85	23.2	0.84	-	23.2	0.84	200	200
F/0/P/M12-07	11.8	2.56	9.87	20.1	0.70	-	20.1	0.70	173	173
F/0/P/M12-08	11.8	2.56	10.2	22.1	0.72	-	22.1	0.72	184	184
F/0/P/M12-09	11.8	2.55	9.84	17.7	0.69	FP	20.2	0.76	174	152
F/0/P/M12-10	11.8	2.56	9.88	20.2	0.54	DFL	22.5	0.59	193	173
F/0/P/M16-01	15.9	2.53	9.86	31.3	0.78	-	31.3	0.78	200	200
F/0/P/M16-02	15.9	2.51	9.87	25.1	0.69	DFL	35.0	0.90	223	160
F/0/P/M16-03	15.9	2.53	10.2	33.7	0.83	-	33.7	0.83	208	208
F/0/P/M16-04	15.9	2.53	10.2	31.4	0.93	DFL	34.7	1.02	214	194
F/0/P/M16-05	15.9	2.53	9.89	30.2	0.77	FP	32.7	0.83	208	192
F/0/P/M16-06	15.9	2.53	9.85	26.8	0.64	DFL	31.3	0.74	200	171
F/0/P/M16-07	15.9	2.53	10.2	29.1	0.67	DFL	33.9	0.77	209	179
F/0/P/M16-08	15.9	2.53	10.2	30.3	0.76	-	30.3	0.76	187	187
F/0/P/M16-09	15.9	2.53	10.2	35.9	0.84	-	35.9	0.84	221	221
F/0/P/M16-10	15.9	2.53	9.67	22.5	0.58	DFL	28.3	0.7	184	146
F/0/P/M20-01	19.8	2.61	9.60	40.4	0.91	-	40.4	0.91	213	213
F/0/P/M20-02	19.8	2.61	9.62	37.1	0.79	-	37.1	0.79	195	195
F/0/P/M20-03	19.8	2.61	9.61	38.4	0.79	FP	39.5	0.82	208	202
F/0/P/M20-04	19.8	2.60	9.87	39.8	0.79	-	39.8	0.79	204	204
F/0/P/M20-05	19.8	2.61	9.61	30.1	0.67	FP	31.7	0.77	167	158
F/0/P/M20-06	19.8	2.61	9.62	41.5	0.90	-	41.5	0.90	218	218
F/0/P/M20-07	19.8	2.61	9.59	40.1	0.88	-	40.1	0.88	211	211
F/0/P/M20-08	19.8	2.61	9.93	34.7	0.70	-	34.7	0.70	176	176
F/0/P/M20-09	19.8	2.61	9.62	34.7	0.65	-	34.7	0.65	182	182
F/0/P/M20-10	19.8	2.61	9.54	36.6	0.73	FP	39.9	0.80	211	194

Table C.4: Chauvenet Criterion applied to Pin-bearing Strength Test Results for Flange Material tested in the Longitudinal Direction with a Plain Pin

Specimen	x_i- x_m	(x_i- x_m)/σ	Outlier ?		Chauvenet x_m	% Diff (Chauvenet - x)
F/0/P/M10-01	2.4	1.24	FALSE	22.5	20.08	0.0%
F/0/P/M10-02	0.6	0.30	FALSE	19.5	1.56	-19.7%
F/0/P/M10-03	2.5	1.27	FALSE	17.6	7.79%	
F/0/P/M10-04	0.8	0.40	FALSE	19.3		
F/0/P/M10-05	0.5	0.27	FALSE	20.6		
F/0/P/M10-06	1.3	0.68	FALSE	21.4		
F/0/P/M10-07	0.8	0.40	FALSE	19.3		
F/0/P/M10-08	1.4	0.71	FALSE	18.7		
F/0/P/M10-09	3.6	1.86	FALSE	23.7		
F/0/P/M10-10	1.9	0.97	FALSE	18.2		
F/0/P/M12-01	2.9	1.23	FALSE	18.7	21.01	-2.5%
F/0/P/M12-02	1.2	0.50	FALSE	20.4	1.49	-36.0%
F/0/P/M12-03	4.9	2.12	TRUE	0	7.09%	
F/0/P/M12-04	2.4	1.02	FALSE	19.2		
F/0/P/M12-05	1.1	0.49	FALSE	22.7		
F/0/P/M12-06	1.6	0.71	FALSE	23.2		
F/0/P/M12-07	1.5	0.63	FALSE	20.1		
F/0/P/M12-08	0.5	0.23	FALSE	22.1		
F/0/P/M12-09	1.4	0.58	FALSE	20.2		
F/0/P/M12-10	0.9	0.40	FALSE	22.5		
F/0/P/M16-01	1.4	0.59	FALSE	31.3	32.71	0.0%
F/0/P/M16-02	2.3	0.96	FALSE	35	1.74	-26.9%
F/0/P/M16-03	1.0	0.42	FALSE	33.7	5.32%	
F/0/P/M16-04	2.0	0.84	FALSE	34.7		
F/0/P/M16-05	0.0	0.00	FALSE	32.7		
F/0/P/M16-06	1.4	0.59	FALSE	31.3		
F/0/P/M16-07	1.2	0.50	FALSE	33.9		
F/0/P/M16-08	2.4	1.01	FALSE	30.3		
F/0/P/M16-09	3.2	1.34	FALSE	35.9		
F/0/P/M16-10	4.4	1.85	FALSE	28.3		
F/0/P/M20-01	2.5	0.76	FALSE	40.4	37.94	0.0%
F/0/P/M20-02	0.8	0.26	FALSE	37.1	1.20	-62.9%
F/0/P/M20-03	1.6	0.48	FALSE	39.5	3.16%	
F/0/P/M20-04	1.9	0.58	FALSE	39.8		
F/0/P/M20-05	6.2	1.93	FALSE	31.7		
F/0/P/M20-06	3.6	1.10	FALSE	41.5		
F/0/P/M20-07	2.2	0.67	FALSE	40.1		
F/0/P/M20-08	3.2	1.00	FALSE	34.7		
F/0/P/M20-09	3.2	1.00	FALSE	34.7		
F/0/P/M20-10	2.0	0.61	FALSE	39.9		

Table C.5: Pin-bearing Strength Test Results for Web Material tested in the Transverse Direction with a Plain Pin

Specimen	Pin Size (mm)	Clearance (mm)	Thickness (mm)	First Failure Load (kN)	Disp. at First Failure (mm)	First Failure Criterion	Max Failure Load (kN)	Disp. at Max Failure (mm)	Bearing Strength (N/mm^2)	FF Bearing Strength (N/mm^2)
W/90/P/M10-01	9.81	2.17	9.63	12.8	0.58	DFL	14.6	0.74	155	135
W/90/P/M10-02	9.81	2.17	9.60	14.1	0.58	FP	14.7	0.67	156	150
W/90/P/M10-03	9.81	2.18	9.65	12.6	0.59	DFL	14.2	1.48	150	133
W/90/P/M10-04	9.81	2.15	9.60	12.1	0.60	FP	14.3	0.83	152	128
W/90/P/M10-05	9.81	2.17	9.60	11.8	0.70	FP	16.1	1.02	171	125
W/90/P/M10-06	9.81	2.18	9.62	12.4	0.56	FP	14.8	0.76	157	131
W/90/P/M10-07	9.81	2.17	9.64	12.4	0.50	DFL	14.7	1.03	155	131
W/90/P/M10-08	9.81	2.17	9.63	13.4	0.68	FP	14.8	1.48	157	142
W/90/P/M10-09	9.81	2.17	9.62	11.8	0.57	DFL	15.7	0.94	166	125
W/90/P/M10-10	9.81	2.18	9.63	12.3	0.60	DFL	15.9	1.29	168	130
W/90/P/M12-01	11.8	2.56	9.62	13.7	0.71	FP	15.4	1.47	136	121
W/90/P/M12-02	11.8	2.55	9.63	13.9	0.74	FP	15.0	1.93	132	122
W/90/P/M12-03	11.8	2.56	9.61	12.5	0.95	DFL	15.4	2.10	136	110
W/90/P/M12-04	11.8	2.55	9.66	12.2	0.51	FP	15.8	1.48	139	107
W/90/P/M12-05	11.8	2.55	9.65	13.4	0.75	FP	15.9	1.73	140	118
W/90/P/M12-06	11.8	2.56	9.63	14.6	0.56	FP	15.9	1.84	140	128
W/90/P/M12-07	11.8	2.56	9.66	13.1	0.57	FP	15.8	1.10	139	115
W/90/P/M12-08	11.8	2.56	9.65	13.0	0.58	DFL	15.3	1.47	134	114
W/90/P/M12-09	11.8	2.56	9.65	12.8	0.59	FP	15.8	1.47	139	112
W/90/P/M12-10	11.8	2.56	9.63	12.7	0.66	DFL	14.8	1.20	130	112
W/90/P/M16-01	15.9	2.53	9.64	14.2	0.45	FP	17.4	1.73	113	93
W/90/P/M16-02	15.9	2.53	9.65	18.7	1.01	DFL	20.0	1.12	130	122
W/90/P/M16-03	15.9	2.52	9.63	16.6	0.56	DFL	19.3	0.69	126	108
W/90/P/M16-04	15.9	2.52	9.66	21.5	0.55	-	21.5	0.55	140	140
W/90/P/M16-05	15.9	2.53	9.64	16.2	0.69	DFL	18.0	1.12	117	106
W/90/P/M16-06	15.9	2.53	9.63	17.5	0.55	DFL	19.1	2.47	125	114
W/90/P/M16-07	15.9	2.53	9.63	16.7	0.54	FP	19.6	0.73	128	109
W/90/P/M16-08	15.9	2.53	9.59	16.5	0.57	FP	20.7	1.30	136	108
W/90/P/M16-09	15.9	2.53	9.63	15.1	0.57	DFL	17.9	0.92	117	99
W/90/P/M16-10	15.9	2.53	9.62	17.3	0.57	FP	20.6	1.47	135	113
W/90/P/M20-01	19.8	2.61	9.66	18.0	0.53	FP	20.7	1.49	108	94
W/90/P/M20-02	19.8	2.61	9.65	20.7	0.85	FP	20.9	1.49	109	108
W/90/P/M20-03	19.8	2.61	9.64	17.8	0.58	DFL	20.1	0.65	105	93
W/90/P/M20-04	19.8	2.61	9.63	13.9	0.46	DFL	17.7	0.61	93	73
W/90/P/M20-05	19.8	2.61	9.61	21.1	0.75	-	21.1	0.75	111	111
W/90/P/M20-06	19.8	2.61	9.63	19.3	0.51	FP	20.8	0.93	109	101
W/90/P/M20-07	19.8	2.61	9.64	16.8	0.47	DFL	20.6	1.01	108	88
W/90/P/M20-08	19.8	2.57	9.63	20.5	0.56	FP	20.5	1.37	108	108
W/90/P/M20-09	19.8	2.60	9.60	20.1	0.60	-	20.1	0.60	106	106
W/90/P/M20-10	19.8	2.60	9.66	20.8	0.58	-	20.8	0.58	109	109

Table C.6: Chauvenet Criterion applied to Pin-bearing Strength Test Results for Web Material tested in the Transverse Direction with a Plain Pin

Specimen	x_i- x_m	(x_i- x_m)/σ	Outlier ?		Chauvenet x_m	% Diff (Chauvenet - x)
W/90/P/M10-01	0.4	0.57	FALSE	14.6	14.98	0.0%
W/90/P/M10-02	0.3	0.42	FALSE	14.7	0.67	0.0%
W/90/P/M10-03	0.8	1.16	FALSE	14.2	4.48%	
W/90/P/M10-04	0.7	1.01	FALSE	14.3		
W/90/P/M10-05	1.1	1.67	FALSE	16.1		
W/90/P/M10-06	0.2	0.27	FALSE	14.8		
W/90/P/M10-07	0.3	0.42	FALSE	14.7		
W/90/P/M10-08	0.2	0.27	FALSE	14.8		
W/90/P/M10-09	0.7	1.07	FALSE	15.7		
W/90/P/M10-10	0.9	1.37	FALSE	15.9		
W/90/P/M12-01	0.1	0.28	FALSE	15.4	15.51	0.0%
W/90/P/M12-02	0.5	1.30	FALSE	15	0.39	0.0%
W/90/P/M12-03	0.1	0.28	FALSE	15.4	2.53%	
W/90/P/M12-04	0.3	0.74	FALSE	15.8		
W/90/P/M12-05	0.4	0.99	FALSE	15.9		
W/90/P/M12-06	0.4	0.99	FALSE	15.9		
W/90/P/M12-07	0.3	0.74	FALSE	15.8		
W/90/P/M12-08	0.2	0.53	FALSE	15.3		
W/90/P/M12-09	0.3	0.74	FALSE	15.8		
W/90/P/M12-10	0.7	1.81	FALSE	14.8		
W/90/P/M16-01	2.0	1.50	FALSE	17.4	19.41	0.0%
W/90/P/M16-02	0.6	0.44	FALSE	20	1.34	0.0%
W/90/P/M16-03	0.1	0.08	FALSE	19.3	6.92%	
W/90/P/M16-04	2.1	1.56	FALSE	21.5		
W/90/P/M16-05	1.4	1.05	FALSE	18		
W/90/P/M16-06	0.3	0.23	FALSE	19.1		
W/90/P/M16-07	0.2	0.14	FALSE	19.6		
W/90/P/M16-08	1.3	0.96	FALSE	20.7		
W/90/P/M16-09	1.5	1.12	FALSE	17.9		
W/90/P/M16-10	1.2	0.89	FALSE	20.6		
W/90/P/M20-01	0.4	0.38	FALSE	20.7	20.62	1.4%
W/90/P/M20-02	0.6	0.58	FALSE	20.9	6.53	567.1%
W/90/P/M20-03	0.2	0.24	FALSE	20.1	31.66%	
W/90/P/M20-04	2.6	2.69	TRUE	0		
W/90/P/M20-05	0.8	0.79	FALSE	21.1		
W/90/P/M20-06	0.5	0.48	FALSE	20.8		
W/90/P/M20-07	0.3	0.28	FALSE	20.6		
W/90/P/M20-08	0.2	0.17	FALSE	20.5		
W/90/P/M20-09	0.2	0.24	FALSE	20.1		
W/90/P/M20-10	0.5	0.48	FALSE	20.8		

Table C.7: Chauvenet Criterion applied to Pin-bearing Strength Test Results for Flange Material tested in the Transverse Direction with a Plain Pin

Specimen	Pin Size (mm)	Clearance (mm)	Thickness (mm)	First Failure Load (kN)	Disp. at First Failure (mm)	First Failure Criterion	Max Failure Load (kN)	Disp. at Max Failure (mm)	Bearing Strength (N/mm^2)	FF Bearing Strength (N/mm^2)
F/90/P/M10-01	9.81	2.17	10.3	11.2	0.56	FP	14.5	1.49	144	111
F/90/P/M10-02	9.81	2.18	9.75	12.5	0.71	DFL	14.1	1.48	147	131
F/90/P/M10-03	9.81	2.17	10.3	12.5	0.74	DFL	13.8	1.48	137	124
F/90/P/M10-04	9.81	2.16	9.59	11.3	0.66	DFL	13.1	0.93	139	120
F/90/P/M10-05	9.81	2.16	9.58	10.2	0.66	DFL	13.7	1.48	146	109
F/90/P/M10-06	9.81	2.16	9.59	9.60	0.80	DFL	13.3	1.48	141	102
F/90/P/M10-07	9.81	2.17	10.3	10.5	0.49	DFL	14.8	0.93	146	104
F/90/P/M10-08	9.81	2.17	10.3	10.8	0.58	DFL	14.8	1.47	146	107
F/90/P/M10-09	9.81	2.17	10.3	12.6	0.60	DFL	13.9	0.71	138	125
F/90/P/M10-10	9.81	2.16	9.62	9.90	0.52	DFL	12.7	1.84	135	105
F/90/P/M12-01	11.8	2.55	10.3	14.8	0.93	DFL	15.2	1.48	125	122
F/90/P/M12-02	11.8	2.54	9.60	11.8	0.77	FP	13.8	1.49	122	104
F/90/P/M12-03	11.8	2.54	9.57	12.9	0.66	DFL	14.3	1.47	127	114
F/90/P/M12-04	11.8	2.54	9.58	11.8	0.66	DFL	15.0	1.22	132	104
F/90/P/M12-05	11.8	2.53	9.86	11.7	0.67	DFL	13.7	1.58	118	101
F/90/P/M12-06	11.8	2.56	9.87	13.0	0.73	FP	14.0	1.57	120	112
F/90/P/M12-07	11.8	2.54	9.79	14.1	0.85	-	14.1	0.85	122	122
F/90/P/M12-08	11.8	2.55	9.87	11.4	0.67	DFL	13.8	1.22	118	98
F/90/P/M12-09	11.8	2.56	9.86	11.8	0.68	DFL	15.5	1.38	133	101
F/90/P/M12-10	11.8	2.55	9.77	12.9	0.67	DFL	14.9	0.94	129	112
F/90/P/M16-01	15.9	2.53	10.3	15.2	0.77	DFL	17.5	1.58	107	93
F/90/P/M16-02	15.9	2.53	10.3	18.5	0.94	DFL	19.6	1.59	120	113
F/90/P/M16-03	15.9	2.53	10.3	11.7	0.59	FP	18.4	1.03	112	71
F/90/P/M16-04	15.9	2.51	10.3	11.4	0.54	DFL	18.9	1.59	115	70
F/90/P/M16-05	15.9	2.49	10.3	15.4	0.77	DFL	18.6	1.59	114	94
F/90/P/M16-06	15.9	2.52	10.3	16.8	0.86	FP	17.7	1.59	108	103
F/90/P/M16-07	15.9	2.52	10.3	13.5	0.63	FP	17.6	2.23	107	82
F/90/P/M16-08	15.9	2.52	10.3	15.4	0.69	DFL	18.0	0.95	110	94
F/90/P/M16-09	15.9	2.52	10.3	16.8	0.86	DFL	17.6	0.95	107	103
F/90/P/M16-10	15.9	2.52	10.2	12.4	0.59	DFL	18.2	1.03	112	76
F/90/P/M20-01	19.8	2.61	9.68	17.3	0.86	FP	17.7	1.69	92.3	90
F/90/P/M20-02	19.8	2.61	9.66	12.7	0.72	FP	18.2	1.59	95.2	66
F/90/P/M20-03	19.8	2.60	9.59	13.2	0.68	FP	17.2	1.59	90.6	70
F/90/P/M20-04	19.8	2.60	9.63	16.5	0.73	FP	16.8	2.32	88.1	87
F/90/P/M20-05	19.8	2.60	9.59	17.0	0.77	FP	18.3	1.59	96.4	90
F/90/P/M20-06	19.8	2.60	9.57	13.3	0.58	FP	17.6	1.59	92.9	70
F/90/P/M20-07	19.8	2.61	9.60	14.2	0.64	FP	16.7	1.59	87.9	75
F/90/P/M20-08	19.8	2.61	9.58	16.9	1.00	FP	17.5	1.58	92.3	89
F/90/P/M20-09	19.8	2.61	9.59	15.6	0.96	DFL	18.0	1.96	94.8	82
F/90/P/M20-10	19.8	2.61	9.58	14.9	0.94	FP	18.0	1.95	94.9	79

Table C.8: Chauvenet Criterion applied to Pin-bearing Strength Test Results for Flange Material tested in the Transverse Direction with a Plain Pin

Specimen	x_i-x_m	(x_i-x_m)/σ	Outlier ?		Chauvenet x_m	% Diff (Chauvenet - x)
F/90/P/M10-01	0.6	0.89	FALSE	14.5	13.87	0.0%
F/90/P/M10-02	0.2	0.33	FALSE	14.1	0.71	0.0%
F/90/P/M10-03	0.1	0.10	FALSE	13.8	5.10%	
F/90/P/M10-04	0.8	1.09	FALSE	13.1		
F/90/P/M10-05	0.2	0.24	FALSE	13.7		
F/90/P/M10-06	0.6	0.81	FALSE	13.3		
F/90/P/M10-07	0.9	1.32	FALSE	14.8		
F/90/P/M10-08	0.9	1.32	FALSE	14.8		
F/90/P/M10-09	0.0	0.04	FALSE	13.9		
F/90/P/M10-10	1.2	1.65	FALSE	12.7		
F/90/P/M12-01	0.8	1.17	FALSE	15.2	14.43	0.0%
F/90/P/M12-02	0.6	0.95	FALSE	13.8	0.66	0.0%
F/90/P/M12-03	0.1	0.20	FALSE	14.3	4.57%	
F/90/P/M12-04	0.6	0.86	FALSE	15		
F/90/P/M12-05	0.7	1.11	FALSE	13.7		
F/90/P/M12-06	0.4	0.65	FALSE	14		
F/90/P/M12-07	0.3	0.50	FALSE	14.1		
F/90/P/M12-08	0.6	0.95	FALSE	13.8		
F/90/P/M12-09	1.1	1.62	FALSE	15.5		
F/90/P/M12-10	0.5	0.71	FALSE	14.9		
F/90/P/M16-01	0.7	1.05	FALSE	17.5	16.25	-10.8%
F/90/P/M16-02	1.4	2.05	TRUE	0	5.73	743.8%
F/90/P/M16-03	0.2	0.28	FALSE	18.4	35.26%	
F/90/P/M16-04	0.7	1.02	FALSE	18.9		
F/90/P/M16-05	0.4	0.57	FALSE	18.6		
F/90/P/M16-06	0.5	0.75	FALSE	17.7		
F/90/P/M16-07	0.6	0.90	FALSE	17.6		
F/90/P/M16-08	0.2	0.31	FALSE	18		
F/90/P/M16-09	0.6	0.90	FALSE	17.6		
F/90/P/M16-10	0.0	0.01	FALSE	18.2		
F/90/P/M20-01	0.1	0.18	FALSE	17.7	17.60	0.0%
F/90/P/M20-02	0.6	1.08	FALSE	18.2	0.56	0.0%
F/90/P/M20-03	0.4	0.72	FALSE	17.2	3.17%	
F/90/P/M20-04	0.8	1.43	FALSE	16.8		
F/90/P/M20-05	0.7	1.25	FALSE	18.3		
F/90/P/M20-06	0.0	0.00	FALSE	17.6		
F/90/P/M20-07	0.9	1.61	FALSE	16.7		
F/90/P/M20-08	0.1	0.18	FALSE	17.5		
F/90/P/M20-09	0.4	0.72	FALSE	18		
F/90/P/M20-10	0.4	0.72	FALSE	18		

Table C.9: Pin-bearing Strength Test Results for Web Material tested in the Longitudinal Direction with a Threaded Pin

Specimen	Pin Size (mm)	Clearance (mm)	Thickness (mm)	First Failure Load (kN)	Disp. at First Failure (mm)	First Failure Criterion	Max Failure Load (kN)	Disp. at Max Failure (mm)	Bearing Strength (N/mm^2)	FF Bearing Strength (N/mm^2)
W/0/T/M10-01	9.81	2.18	9.62	15.9	0.84	DFL	17.7	1.06	188	168
W/0/T/M10-02	9.81	2.13	9.62	15.9	0.94	DFL	18.2	1.42	193	168
W/0/T/M10-03	9.81	2.18	9.63	15.9	0.93	DFL	18.4	1.49	195	168
W/0/T/M10-04	9.81	2.18	9.63	14.6	0.92	DFL	17.9	1.50	189	155
W/0/T/M10-05	9.81	2.18	9.60	14.4	0.86	DFL	16.2	2.30	172	153
W/0/T/M10-06	9.81	2.17	9.61	17.4	1.10	FP	18.2	1.76	193	185
W/0/T/M10-07	9.81	2.18	9.62	18.6	1.40	DFL	20.4	1.56	216	197
W/0/T/M10-08	9.81	2.17	9.60	19.9	1.25	-	19.9	1.25	211	211
W/0/T/M10-09	9.81	2.18	9.61	15.9	0.97	FP	18.6	1.37	197	169
W/0/T/M10-10	9.81	2.18	9.59	17.5	1.23	DFL	17.7	1.30	188	186
W/0/T/M12-01	11.8	2.56	9.64	18.3	1.12	FP	19.1	1.29	168	161
W/0/T/M12-02	11.8	2.56	9.63	18.3	1.13	FP	20.8	1.70	183	161
W/0/T/M12-03	11.8	2.58	9.61	15.4	1.03	FP	17.7	6.34	156	136
W/0/T/M12-04	11.8	2.57	9.64	18.1	1.21	FP	20.4	5.61	179	159
W/0/T/M12-05	11.8	2.57	9.63	21.3	1.32	DFL	22.2	1.49	195	187
W/0/T/M12-06	11.8	2.57	9.63	16.8	0.94	FP	19.3	3.29	170	148
W/0/T/M12-07	11.8	2.57	9.62	20.0	1.36	-	20.0	1.36	176	176
W/0/T/M12-08	11.8	2.57	9.62	17.9	1.2	FP	19.1	4.42	168	158
W/0/T/M12-09	11.8	2.58	9.61	17.5	1.02	FP	18.2	1.97	161	154
W/0/T/M12-10	11.8	2.58	9.60	17.9	1.18	FP	19.3	4.42	170	158
W/0/T/M16-01	15.8	2.57	9.63	22.8	1.39	FP	24.1	5.15	158	150
W/0/T/M16-02	15.8	2.57	9.64	21.6	1.50	-	21.6	1.50	142	142
W/0/T/M16-03	15.8	2.58	9.61	21.1	1.50	FP	25.1	3.96	165	139
W/0/T/M16-04	15.8	2.58	9.65	23.2	1.43	DFL	25.2	1.82	165	152
W/0/T/M16-05	15.8	2.58	9.63	19.7	1.02	DFL	22.7	1.40	149	129
W/0/T/M16-06	15.8	2.58	9.61	21.7	1.36	FP	24.5	3.88	161	143
W/0/T/M16-07	15.8	2.59	9.62	24.9	1.50	FP	25.8	1.89	170	164
W/0/T/M16-08	15.8	2.58	9.62	22.1	1.30	DFL	28.4	1.78	187	145
W/0/T/M16-09	15.8	2.58	9.64	22.6	1.34	-	22.6	1.34	148	148
W/0/T/M16-10	15.8	2.58	9.6	22.3	1.54	FP	23.0	7.36	152	147
W/0/T/M20-01	19.8	2.61	9.68	18.8	1.03	FP	21.0	1.44	110	98
W/0/T/M20-02	19.8	2.61	9.62	22.6	1.50	DFL	24.3	2.22	128	119
W/0/T/M20-03	19.8	2.61	9.72	23.3	1.42	DFL	25.0	1.69	130	121
W/0/T/M20-04	19.8	2.58	9.61	26.4	1.78	-	26.4	1.78	139	139
W/0/T/M20-05	19.8	2.61	9.60	20.8	1.28	FP	21.8	1.60	115	109
W/0/T/M20-06	19.8	2.61	9.62	23.1	1.56	-	23.1	1.56	121	121
W/0/T/M20-07	19.8	2.61	9.65	24.5	1.32	-	24.5	1.32	128	128
W/0/T/M20-08	19.8	2.61	9.67	24.1	1.49	DFL	25.7	1.84	134	126
W/0/T/M20-09	19.8	2.60	9.63	23.1	1.38	FP	23.7	2.50	124	121
W/0/T/M20-10	19.8	2.61	9.62	25.3	1.53	-	25.3	1.53	133	133

Table C.10: Chauvenet Criterion applied to Pin-bearing Strength Test Results for Web Material tested in the Longitudinal Direction with a Threaded Pin

Specimen	x_i-x_m	(x_i-x_m)/σ	Outlier ?		Chauvenet x_m	% Diff (Chauvenet - x)
W/0/T/M10-01	0.6	0.53	FALSE	17.7	18.32	0.0%
W/0/T/M10-02	0.1	0.10	FALSE	18.2	1.17	0.0%
W/0/T/M10-03	0.1	0.07	FALSE	18.4	6.40%	
W/0/T/M10-04	0.4	0.36	FALSE	17.9		
W/0/T/M10-05	2.1	1.81	FALSE	16.2		
W/0/T/M10-06	0.1	0.10	FALSE	18.2		
W/0/T/M10-07	2.1	1.77	FALSE	20.4		
W/0/T/M10-08	1.6	1.35	FALSE	19.9		
W/0/T/M10-09	0.3	0.24	FALSE	18.6		
W/0/T/M10-10	0.6	0.53	FALSE	17.7		
W/0/T/M12-01	0.5	0.39	FALSE	19.1	19.32	28.8%
W/0/T/M12-02	1.2	0.91	FALSE	20.8	0.99	31.5%
W/0/T/M12-03	1.9	1.47	FALSE	17.7	5.11%	
W/0/T/M12-04	0.8	0.61	FALSE	20.4		
W/0/T/M12-05	2.6	1.99	TRUE	22.2		
W/0/T/M12-06	0.3	0.24	FALSE	19.3		
W/0/T/M12-07	0.4	0.30	FALSE	20		
W/0/T/M12-08	0.5	0.39	FALSE	19.1		
W/0/T/M12-09	1.4	1.08	FALSE	18.2		
W/0/T/M12-10	0.3	0.24	FALSE	19.3		
W/0/T/M16-01	0.2	0.10	FALSE	24.1	23.84	45.6%
W/0/T/M16-02	2.7	1.37	FALSE	21.6	1.43	54.3%
W/0/T/M16-03	0.8	0.41	FALSE	25.1	5.99%	
W/0/T/M16-04	0.9	0.46	FALSE	25.2		
W/0/T/M16-05	1.6	0.81	FALSE	22.7		
W/0/T/M16-06	0.2	0.10	FALSE	24.5		
W/0/T/M16-07	1.5	0.76	FALSE	25.8		
W/0/T/M16-08	4.1	2.08	TRUE	28.4		
W/0/T/M16-09	1.7	0.86	FALSE	22.6		
W/0/T/M16-10	1.3	0.66	FALSE	23		
W/0/T/M20-01	3.1	1.80	FALSE	21	24.08	0.0%
W/0/T/M20-02	0.2	0.13	FALSE	24.3	1.71	0.0%
W/0/T/M20-03	0.9	0.54	FALSE	25	7.11%	
W/0/T/M20-04	2.3	1.36	FALSE	26.4		
W/0/T/M20-05	2.3	1.33	FALSE	21.8		
W/0/T/M20-06	1.0	0.57	FALSE	23.1		
W/0/T/M20-07	0.4	0.25	FALSE	24.5		
W/0/T/M20-08	1.6	0.95	FALSE	25.7		
W/0/T/M20-09	0.4	0.22	FALSE	23.7		
W/0/T/M20-10	1.2	0.71	FALSE	25.3		

Table C.11: Chauvenet Criterion applied to Pin-bearing Strength Test Results for Flange Material tested in the Longitudinal Direction with a Threaded Pin

Specimen	Pin Size (mm)	Clearance (mm)	Thickness (mm)	First Failure Load (kN)	Disp. at First Failure (mm)	First Failure Criterion	Max Failure Load (kN)	Disp. at Max Failure (mm)	Bearing Strength (N/mm^2)	FF Bearing Strength (N/mm^2)
F/0/T/M10-01	9.81	2.17	9.60	15.2	0.99	DFL	18.7	2.04	199	161
F/0/T/M10-02	9.81	2.17	9.62	16.3	1.27	FP	19.7	2.04	209	173
F/0/T/M10-03	9.81	2.17	9.86	17.3	1.15	DFL	19.6	1.50	203	179
F/0/T/M10-04	9.81	2.14	9.59	16.8	1.21	FP	17.9	1.89	190	179
F/0/T/M10-05	9.81	2.14	9.62	17.0	1.18	-	17.0	1.18	180	180
F/0/T/M10-06	9.81	2.14	9.61	15.6	1.01	FP	19.1	1.77	203	165
F/0/T/M10-07	9.81	2.18	10.2	18.5	1.05	DFL	20.8	1.49	208	185
F/0/T/M10-08	9.81	2.17	9.82	15.8	1.10	FP	18.8	3.33	195	164
F/0/T/M10-09	9.81	2.17	9.83	14.8	1.00	FP	18.7	1.82	194	153
F/0/T/M10-10	9.81	2.18	9.89	15.3	1.07	FP	16.4	1.39	169	158
F/0/T/M12-01	11.8	2.58	9.71	20.9	1.41	FP	23.4	2.23	204	182
F/0/T/M12-02	11.8	2.59	9.91	18.2	1.19	FP	19.6	1.75	168	156
F/0/T/M12-03	11.8	2.59	9.59	20.1	1.44	FP	22.2	2.02	196	178
F/0/T/M12-04	11.8	2.59	9.89	15.1	1.11	FP	20.0	2.69	171	129
F/0/T/M12-05	11.8	2.58	9.60	17.0	1.19	FP	22.4	2.42	198	150
F/0/T/M12-06	11.8	2.58	9.61	20.7	1.40	FP	21.6	2.31	190	183
F/0/T/M12-07	11.8	2.59	9.85	18.0	0.81	FP	19.6	1.50	169	155
F/0/T/M12-08	11.8	2.58	9.61	18.1	1.13	DFL	19.7	5.34	174	160
F/0/T/M12-09	11.8	2.57	9.59	20.8	1.35	DFL	22.7	1.78	201	184
F/0/T/M12-10	11.8	2.58	9.62	17.9	0.99	FP	19.1	4.67	168	158
F/0/T/M16-01	15.8	2.57	9.58	20.3	1.40	FP	26.4	5.10	174	134
F/0/T/M16-02	15.8	2.55	9.62	22.4	1.47	FP	23.4	2.37	154	147
F/0/T/M16-03	15.8	2.57	10.2	22.2	1.85	FP	28.6	2.80	177	138
F/0/T/M16-04	15.8	2.57	9.61	22.8	1.41	FP	24.4	2.65	161	150
F/0/T/M16-05	15.8	2.57	9.62	19.3	1.12	FP	24.9	2.11	164	127
F/0/T/M16-06	15.8	2.57	9.59	22.6	1.29	FP	26.1	2.49	172	149
F/0/T/M16-07	15.8	2.57	9.88	21.0	1.16	FP	23.6	2.55	151	135
F/0/T/M16-08	15.8	2.57	9.61	23.1	1.17	-	23.1	1.17	152	152
F/0/T/M16-09	15.8	2.57	9.87	16.4	0.99	FP	21.4	2.92	137	105
F/0/T/M16-10	15.8	2.57	10.2	22.3	1.15	FP	27.0	1.85	168	139
F/0/T/M20-01	19.8	2.61	9.59	20.9	1.39	FP	25.8	1.78	136	110
F/0/T/M20-02	19.8	2.61	9.61	22.7	1.35	DFL	26.0	2.45	137	119
F/0/T/M20-03	19.8	2.61	9.60	23.3	1.60	FP	26.2	4.53	138	123
F/0/T/M20-04	19.8	2.61	9.59	23.8	1.70	FP	26.5	2.13	140	125
F/0/T/M20-05	19.8	2.61	9.64	22.8	1.48	FP	26.5	8.46	139	119
F/0/T/M20-06	19.8	2.61	9.62	21.8	1.51	FP	27.2	3.25	143	114
F/0/T/M20-07	19.8	2.61	9.85	25.7	1.60	FP	26.0	1.69	133	132
F/0/T/M20-08	19.8	2.61	9.71	28.9	1.60	-	28.9	1.60	150	150
F/0/T/M20-09	19.8	2.61	9.60	21.8	1.33	DFL	27.9	2.40	147	115
F/0/T/M20-10	19.8	2.61	9.59	27.0	1.69	FP	28.7	1.88	151	142

Table C.12: Chauvenet Criterion applied to Pin-bearing Strength Test Results for Flange Material tested in the Longitudinal Direction with a Threaded Pin

Specimen	x_i-x_m	(x_i-x_m)/σ	Outlier ?		Chauvenet x_m	% Diff (Chauvenet - x)
F/0/T/M10-01	0.0	0.02	FALSE	18.7	18.67	0.0%
F/0/T/M10-02	1.0	0.79	FALSE	19.7	1.30	0.0%
F/0/T/M10-03	0.9	0.72	FALSE	19.6	6.96%	
F/0/T/M10-04	0.8	0.59	FALSE	17.9		
F/0/T/M10-05	1.7	1.28	FALSE	17		
F/0/T/M10-06	0.4	0.33	FALSE	19.1		
F/0/T/M10-07	2.1	1.64	FALSE	20.8		
F/0/T/M10-08	0.1	0.10	FALSE	18.8		
F/0/T/M10-09	0.0	0.02	FALSE	18.7		
F/0/T/M10-10	2.3	1.75	FALSE	16.4		
F/0/T/M12-01	2.4	1.49	FALSE	23.4	21.03	0.0%
F/0/T/M12-02	1.4	0.90	FALSE	19.6	1.59	0.0%
F/0/T/M12-03	1.2	0.74	FALSE	22.2	7.54%	
F/0/T/M12-04	1.0	0.65	FALSE	20		
F/0/T/M12-05	1.4	0.86	FALSE	22.4		
F/0/T/M12-06	0.6	0.36	FALSE	21.6		
F/0/T/M12-07	1.4	0.90	FALSE	19.6		
F/0/T/M12-08	1.3	0.84	FALSE	19.7		
F/0/T/M12-09	1.7	1.05	FALSE	22.7		
F/0/T/M12-10	1.9	1.22	FALSE	19.1		
F/0/T/M16-01	1.5	0.70	FALSE	26.4	24.89	0.0%
F/0/T/M16-02	1.5	0.69	FALSE	23.4	2.15	0.0%
F/0/T/M16-03	3.7	1.73	FALSE	28.6	8.62%	
F/0/T/M16-04	0.5	0.23	FALSE	24.4		
F/0/T/M16-05	0.0	0.00	FALSE	24.9		
F/0/T/M16-06	1.2	0.56	FALSE	26.1		
F/0/T/M16-07	1.3	0.60	FALSE	23.6		
F/0/T/M16-08	1.8	0.83	FALSE	23.1		
F/0/T/M16-09	3.5	1.63	FALSE	21.4		
F/0/T/M16-10	2.1	0.98	FALSE	27		
F/0/T/M20-01	1.2	1.02	FALSE	25.8	26.97	0.0%
F/0/T/M20-02	1.0	0.84	FALSE	26	1.15	0.0%
F/0/T/M20-03	0.8	0.67	FALSE	26.2	4.27%	
F/0/T/M20-04	0.5	0.41	FALSE	26.5		
F/0/T/M20-05	0.5	0.41	FALSE	26.5		
F/0/T/M20-06	0.2	0.20	FALSE	27.2		
F/0/T/M20-07	1.0	0.84	FALSE	26		
F/0/T/M20-08	1.9	1.68	FALSE	28.9		
F/0/T/M20-09	0.9	0.81	FALSE	27.9		
F/0/T/M20-10	1.7	1.50	FALSE	28.7		

Table C.13: Pin-bearing Strength Test Results for Web Material tested in the Transverse Direction with a Threaded Pin

Specimen	Pin Size (mm)	Clearance (mm)	Thickness (mm)	First Failure Load (kN)	Disp. at First Failure (mm)	First Failure Criterion	Max Failure Load (kN)	Disp. at Max Failure (mm)	Bearing Strength (N/mm^2)	FF Bearing Strength (N/mm^2)
W/90/T/M10-01	9.81	2.16	9.61	16.6	1.33	-	16.6	1.33	176	176
W/90/T/M10-02	9.81	2.17	9.60	13.3	0.96	DFL	16.0	1.32	170	141
W/90/T/M10-03	9.81	2.17	9.60	13.8	1.21	DFL	16.8	1.86	178	147
W/90/T/M10-04	9.81	2.16	9.64	16.4	1.30	-	16.4	1.30	173	173
W/90/T/M10-05	9.81	2.16	9.65	14.4	1.01	DFL	16.2	1.93	171	152
W/90/T/M10-06	9.81	2.15	9.61	14.7	1.04	DFL	18.0	2.04	191	156
W/90/T/M10-07	9.81	2.17	9.61	15.9	1.22	DFL	17.1	2.23	181	169
W/90/T/M10-08	9.81	2.17	9.58	14.1	1.12	DFL	17.1	1.59	182	150
W/90/T/M10-09	9.81	2.17	9.60	14.9	1.40	DFL	16.6	2.22	176	158
W/90/T/M10-10	9.81	2.17	9.64	14.4	1.02	FP	14.8	2.24	157	152
W/90/T/M12-01	11.8	2.57	9.66	16.4	1.48	DFL	19.0	3.42	167	144
W/90/T/M12-02	11.8	2.56	9.64	15.5	1.52	DFL	19.1	5.88	168	136
W/90/T/M12-03	11.8	2.57	9.63	18.0	1.60	-	18.0	1.60	158	158
W/90/T/M12-04	11.8	2.55	9.64	18.8	1.58	-	18.8	1.58	165	165
W/90/T/M12-05	11.8	2.57	9.62	18.6	1.59	DFL	19.2	2.95	169	164
W/90/T/M12-06	11.8	2.57	9.60	18.4	1.49	-	18.1	1.49	160	162
W/90/T/M12-07	11.8	2.58	9.60	18.6	1.73	-	18.6	1.73	164	164
W/90/T/M12-08	11.8	2.56	9.67	18.6	1.68	FP	19.5	3.42	171	163
W/90/T/M12-09	11.8	2.57	9.61	13.9	1.20	DFL	18.3	2.35	161	123
W/90/T/M12-10	11.8	2.58	9.64	16.1	1.53	FP	18.5	4.60	163	142
W/90/T/M16-01	15.8	2.57	9.62	20.4	1.97	DFL	22.3	2.40	147	134
W/90/T/M16-02	15.8	2.57	9.66	22.8	1.65	-	22.8	1.65	149	149
W/90/T/M16-03	15.8	2.57	9.65	22.1	1.75	-	22.1	1.75	145	145
W/90/T/M16-04	15.8	2.57	9.61	21.6	1.94	FP	22.3	2.28	147	142
W/90/T/M16-05	15.8	2.56	9.61	24.4	1.76	-	24.4	1.76	161	161
W/90/T/M16-06	15.8	2.57	9.63	23.1	1.78	FP	24.3	3.42	160	152
W/90/T/M16-07	15.8	2.56	9.62	19.4	1.38	DFL	22.0	1.99	145	128
W/90/T/M16-08	15.8	2.57	9.61	17.4	1.25	DFL	22.8	1.94	150	115
W/90/T/M16-09	15.8	2.57	9.65	19.1	1.28	DFL	23.5	1.86	154	125
W/90/T/M16-10	15.8	2.57	9.63	22.2	1.84	DFL	25.3	2.84	166	146
W/90/T/M20-01	19.8	2.60	9.63	17.3	1.24	DFL	22.3	1.92	117	91
W/90/T/M20-02	19.8	2.60	9.70	19.5	1.48	DFL	23.9	2.18	124	102
W/90/T/M20-03	19.8	2.59	9.67	17.2	1.51	DFL	19.6	2.58	102	90
W/90/T/M20-04	19.8	2.60	9.61	23.7	2.34	-	23.7	2.34	125	125
W/90/T/M20-05	19.8	2.60	9.59	22.6	1.76	-	22.6	1.76	119	119
W/90/T/M20-06	19.8	2.60	9.59	18.5	1.32	DFL	22.6	1.87	119	97
W/90/T/M20-07	19.8	2.60	9.60	23.1	1.85	-	23.1	1.85	122	122
W/90/T/M20-08	19.8	2.57	9.64	17.5	1.50	DFL	21.8	2.04	114	92
W/90/T/M20-09	19.8	2.58	9.63	23.0	1.57	-	23.0	1.57	121	121
W/90/T/M20-10	19.8	2.59	9.67	17.0	1.20	FP	20.3	1.79	106	89

Table C.14: Chauvenet Criterion applied to Pin-bearing Strength Test Results for Web Material tested in the Transverse Direction with a Threaded Pin

Specimen	x_i- x_m	(x_i- x_m)/σ	Outlier ?		Chauvenet x_m	% Diff (Chauvenet - x)
W/90/T/M10-01	0.0	0.05	FALSE	16.6	16.56	0.0%
W/90/T/M10-02	0.6	0.67	FALSE	16	0.84	0.0%
W/90/T/M10-03	0.2	0.29	FALSE	16.8	5.05%	
W/90/T/M10-04	0.2	0.19	FALSE	16.4		
W/90/T/M10-05	0.4	0.43	FALSE	16.2		
W/90/T/M10-06	1.4	1.72	FALSE	18		
W/90/T/M10-07	0.5	0.65	FALSE	17.1		
W/90/T/M10-08	0.5	0.65	FALSE	17.1		
W/90/T/M10-09	0.0	0.05	FALSE	16.6		
W/90/T/M10-10	1.8	2.11	TRUE	14.8		
W/90/T/M12-01	0.3	0.59	FALSE	19	18.71	0.0%
W/90/T/M12-02	0.4	0.79	FALSE	19.1	0.50	0.0%
W/90/T/M12-03	0.7	1.43	FALSE	18	2.65%	
W/90/T/M12-04	0.1	0.18	FALSE	18.8		
W/90/T/M12-05	0.5	0.99	FALSE	19.2		
W/90/T/M12-06	0.6	1.23	FALSE	18.1		
W/90/T/M12-07	0.1	0.22	FALSE	18.6		
W/90/T/M12-08	0.8	1.59	FALSE	19.5		
W/90/T/M12-09	0.4	0.83	FALSE	18.3		
W/90/T/M12-10	0.2	0.42	FALSE	18.5		
W/90/T/M16-01	0.9	0.77	FALSE	22.3	23.18	0.0%
W/90/T/M16-02	0.4	0.33	FALSE	22.8	1.14	0.0%
W/90/T/M16-03	1.1	0.95	FALSE	22.1	4.93%	
W/90/T/M16-04	0.9	0.77	FALSE	22.3		
W/90/T/M16-05	1.2	1.07	FALSE	24.4		
W/90/T/M16-06	1.1	0.98	FALSE	24.3		
W/90/T/M16-07	1.2	1.03	FALSE	22		
W/90/T/M16-08	0.4	0.33	FALSE	22.8		
W/90/T/M16-09	0.3	0.28	FALSE	23.5		
W/90/T/M16-10	2.1	1.86	FALSE	25.3		
W/90/T/M20-01	0.0	0.01	FALSE	22.3	22.29	0.0%
W/90/T/M20-02	1.6	1.16	FALSE	23.9	1.39	0.0%
W/90/T/M20-03	2.7	1.94	FALSE	19.6	6.23%	
W/90/T/M20-04	1.4	1.01	FALSE	23.7		
W/90/T/M20-05	0.3	0.22	FALSE	22.6		
W/90/T/M20-06	0.3	0.22	FALSE	22.6		
W/90/T/M20-07	0.8	0.58	FALSE	23.1		
W/90/T/M20-08	0.5	0.35	FALSE	21.8		
W/90/T/M20-09	0.7	0.51	FALSE	23		
W/90/T/M20-10	2.0	1.43	FALSE	20.3		

Table C.15: Pin-bearing Strength Test Results for Flange Material tested in the Transverse Direction with a Threaded Pin

Specimen	Pin Size (mm)	Clearance (mm)	Thickness (mm)	First Failure Load (kN)	Disp. at First Failure (mm)	First Failure Criterion	Max Failure Load (kN)	Disp. at Max Failure (mm)	Bearing Strength (N/mm^2)	FF Bearing Strength (N/mm^2)
F/90/T/M10-01	9.81	2.17	10.3	15.8	1.61	FP	16.5	2.32	163	156
F/90/T/M10-02	9.81	2.17	10.2	16.0	1.37	-	16.0	1.37	161	161
F/90/T/M10-03	9.81	2.16	10.1	16.1	1.41	-	16.1	1.41	162	162
F/90/T/M10-04	9.81	2.17	9.61	14.5	1.83	-	14.5	1.83	154	154
F/90/T/M10-05	9.81	2.17	10.2	16.0	1.92	-	16.0	1.92	160	160
F/90/T/M10-06	9.81	2.16	10.2	15.2	1.45	DFL	16.4	2.24	163	151
F/90/T/M10-07	9.81	2.17	10.2	16.0	1.36	-	16.0	1.36	160	160
F/90/T/M10-08	9.81	2.16	9.62	14.7	1.38	DFL	15.3	1.78	162	156
F/90/T/M10-09	9.81	2.17	9.60	13.4	1.36	FP	13.4	3.34	142	142
F/90/T/M10-10	9.81	2.17	9.60	12.1	1.19	FP	13.9	3.96	148	128
F/90/T/M12-01	11.8	2.54	9.60	13.9	1.58	FP	16.2	4.30	143	123
F/90/T/M12-02	11.8	2.56	9.59	16.1	1.83	-	16.1	1.83	142	142
F/90/T/M12-03	11.8	2.56	9.59	16.0	1.65	-	16.0	1.65	141	141
F/90/T/M12-04	11.8	2.57	9.80	16.2	1.34	DFL	18.3	1.93	158	140
F/90/T/M12-05	11.8	2.58	9.89	16.8	1.60	FP	17.2	2.75	147	144
F/90/T/M12-06	11.8	2.57	10.3	14.3	1.09	DFL	17.7	1.70	145	117
F/90/T/M12-07	11.8	2.58	9.58	15.5	1.45	DFL	16.5	1.86	146	137
F/90/T/M12-08	11.8	2.58	10.3	16.5	1.45	DFL	16.7	2.44	137	136
F/90/T/M12-09	11.8	2.57	9.62	14.6	1.34	DFL	16.3	4.72	144	129
F/90/T/M12-10	11.8	2.58	9.88	14.1	1.40	-	14.1	1.40	121	121
F/90/T/M16-01	15.8	2.56	9.58	20.6	2.13	-	20.6	2.13	136	136
F/90/T/M16-02	15.8	2.56	9.59	18.6	1.70	FP	19.4	4.10	128	123
F/90/T/M16-03	15.8	2.55	9.64	16.2	1.55	FP	20.3	4.25	133	106
F/90/T/M16-04	15.8	2.57	9.58	17.2	1.27	FP	18.9	1.86	125	114
F/90/T/M16-05	15.8	2.56	9.60	17.5	1.74	-	17.5	1.74	115	115
F/90/T/M16-06	15.8	2.57	9.79	11.8	0.99	FP	18.6	2.15	120	76
F/90/T/M16-07	15.8	2.57	9.78	17.2	1.25	DFL	18.9	3.92	122	111
F/90/T/M16-08	15.8	2.58	9.58	13.6	0.98	DFL	18.9	1.78	125	90
F/90/T/M16-09	15.8	2.57	9.80	17.2	1.53	-	17.2	1.53	111	111
F/90/T/M16-10	15.8	2.57	9.60	13.5	0.55	DFL	18.0	1.25	119	89
F/90/T/M20-01	19.8	2.61	10.3	19.8	1.42	-	19.8	1.42	97	97
F/90/T/M20-02	19.8	2.61	10.3	17.9	1.42	DFL	19.9	5.36	98	88
F/90/T/M20-03	19.8	2.60	10.3	19.6	1.64	FP	20.3	5.47	100	96
F/90/T/M20-04	19.8	2.60	10.3	18.3	1.56	FP	20.2	3.27	99	90
F/90/T/M20-05	19.8	2.61	10.3	18.3	1.39	DFL	20.5	1.76	101	90
F/90/T/M20-06	19.8	2.61	10.3	18.2	1.38	DFL	21.8	1.97	107	90
F/90/T/M20-07	19.8	2.61	10.3	19.8	1.43	FP	20.9	1.99	103	97
F/90/T/M20-08	19.8	2.60	10.3	16.9	1.04	FP	20.6	2.00	101	83
F/90/T/M20-09	19.8	2.61	10.3	19.4	1.70	-	19.4	1.70	95	95
F/90/T/M20-10	19.8	2.61	10.3	16.2	1.15	DFL	20.7	4.00	102	80

Table C.16: Chauvenet Criterion applied to Pin-bearing Strength Test Results for Flange Material tested in the Transverse Direction with a Threaded Pin

Specimen	x_i- x_m	(x_i- x_m)/σ	Outlier ?		Chauvenet x_m	% Diff (Chauvenet - x)
F/90/T/M10-01	1.1	0.99	FALSE	16.5	15.41	0.0%
F/90/T/M10-02	0.6	0.54	FALSE	16	1.10	0.0%
F/90/T/M10-03	0.7	0.63	FALSE	16.1	7.12%	
F/90/T/M10-04	0.9	0.83	FALSE	14.5		
F/90/T/M10-05	0.6	0.54	FALSE	16		
F/90/T/M10-06	1.0	0.90	FALSE	16.4		
F/90/T/M10-07	0.6	0.54	FALSE	16		
F/90/T/M10-08	0.1	0.10	FALSE	15.3		
F/90/T/M10-09	2.0	1.83	FALSE	13.4		
F/90/T/M10-10	1.5	1.38	FALSE	13.9		
F/90/T/M12-01	0.3	0.27	FALSE	16.2	16.78	-26.8%
F/90/T/M12-02	0.4	0.36	FALSE	16.1	0.79	33.6%
F/90/T/M12-03	0.5	0.45	FALSE	16	4.74%	
F/90/T/M12-04	1.8	1.58	FALSE	18.3		
F/90/T/M12-05	0.7	0.61	FALSE	17.2		
F/90/T/M12-06	1.2	1.05	FALSE	17.7		
F/90/T/M12-07	0.0	0.01	FALSE	16.5		
F/90/T/M12-08	0.2	0.17	FALSE	16.7		
F/90/T/M12-09	0.2	0.19	FALSE	16.3		
F/90/T/M12-10	2.4	2.13	TRUE	14.1		
F/90/T/M16-01	1.8	1.62	FALSE	20.6	18.83	0.0%
F/90/T/M16-02	0.6	0.52	FALSE	19.4	1.10	0.0%
F/90/T/M16-03	1.5	1.34	FALSE	20.3	5.82%	
F/90/T/M16-04	0.1	0.06	FALSE	18.9		
F/90/T/M16-05	1.3	1.21	FALSE	17.5		
F/90/T/M16-06	0.2	0.21	FALSE	18.6		
F/90/T/M16-07	0.1	0.06	FALSE	18.9		
F/90/T/M16-08	0.1	0.06	FALSE	18.9		
F/90/T/M16-09	1.6	1.49	FALSE	17.2		
F/90/T/M16-10	0.8	0.76	FALSE	18		
F/90/T/M20-01	0.6	0.91	FALSE	19.8	20.26	15.4%
F/90/T/M20-02	0.5	0.76	FALSE	19.9	0.48	18.5%
F/90/T/M20-03	0.1	0.16	FALSE	20.3	2.38%	
F/90/T/M20-04	0.2	0.31	FALSE	20.2		
F/90/T/M20-05	0.1	0.13	FALSE	20.5		
F/90/T/M20-06	1.4	2.08	TRUE	21.8		
F/90/T/M20-07	0.5	0.73	FALSE	20.9		
F/90/T/M20-08	0.2	0.28	FALSE	20.6		
F/90/T/M20-09	1.0	1.51	FALSE	19.4		
F/90/T/M20-10	0.3	0.43	FALSE	20.7		

C.3 Aged Pin-bearing Strength Test Results

Table C.17: Pin-bearing Strength Test Results for Flange Material tested in the Longitudinal Direction with a Plain Pin after 3 months conditioning at 40°C

Specimen	Diameter of Pin, d (mm)	Diameter of Hole, d_n (mm)	Clearance (mm)	Thickness of Specimen, t (mm)	Maximum DARTEC load (kN)	Maximum specimen load (kN)	d/t	Bearing Strength (N/mm^2)
A/F/0/P/M10-01	9.81	11.90	2.09	9.88	15.39	15.73	0.99	162.27
A/F/0/P/M10-02	9.81	11.90	2.09	9.85	16.24	16.58	1.00	171.56
A/F/0/P/M10-03	9.81	11.98	2.17	9.57	15.15	15.49	1.03	164.97
A/F/0/P/M10-04	9.81	11.98	2.17	9.61	16.79	17.13	1.02	181.68
A/F/0/P/M10-05	9.81	11.98	2.17	9.58	17.60	17.94	1.02	190.87
Mean	9.81	11.95	2.14	9.70	16.23	16.57	1.01	174.27
A/F/0/P/M12-01	11.83	14.39	2.56	9.63	16.05	16.39	1.23	143.85
A/F/0/P/M12-02	11.83	14.39	2.56	9.63	18.93	19.27	1.23	169.13
A/F/0/P/M12-03	11.83	14.40	2.57	9.61	21.07	21.41	1.23	188.31
A/F/0/P/M12-04	11.83	14.39	2.56	9.72	22.12	22.46	1.22	195.31
A/F/0/P/M12-05	11.83	14.39	2.56	9.68	18.28	18.62	1.22	162.58
Mean	11.83	14.39	2.56	9.65	19.29	19.63	1.23	171.84
A/F/0/P/M16-01	15.86	18.39	2.53	10.21	25.48	25.82	1.55	159.44
A/F/0/P/M16-02	15.86	18.39	2.53	9.86	25.60	25.94	1.61	165.87
A/F/0/P/M16-03	15.86	18.39	2.53	9.70	23.58	23.92	1.64	155.47
A/F/0/P/M16-04	15.86	18.40	2.54	9.64	26.99	27.33	1.65	178.74
A/F/0/P/M16-05	15.86	18.39	2.53	10.23	26.52	26.86	1.55	165.54
Mean	15.86	18.39	2.53	9.93	25.63	25.97	1.60	165.01
A/F/0/P/M20-01	19.78	22.39	2.61	9.71	29.32	29.66	2.04	154.42
A/F/0/P/M20-02	19.78	22.39	2.61	9.64	29.94	30.28	2.05	158.79
A/F/0/P/M20-03	19.78	22.39	2.61	9.65	28.11	28.45	2.05	149.04
A/F/0/P/M20-04	19.78	22.38	2.60	9.90	31.52	31.86	2.00	162.69
A/F/0/P/M20-05	19.78	22.38	2.60	9.88	30.57	30.91	2.00	158.16
Mean	19.78	22.38	2.60	9.76	29.89	30.23	2.03	156.62

Table C.18: Pin-bearing Strength Test Results for Flange Material tested in the Longitudinal Direction with a Threaded Pin after 3 months conditioning at 40°C

Specimen	Diameter of Pin, d (mm)	Diameter of Hole, d_n (mm)	Clearance (mm)	Thickness of Specimen, t (mm)	Maximum DARTEC load (kN)	Maximum specimen load (kN)	d/t	Bearing Strength (N/mm^2)
A/F/0/T/M10-01	9.81	11.98	2.17	9.59	16.15	16.49	1.02	175.26
A/F/0/T/M10-02	9.81	11.98	2.17	9.59	15.73	16.07	1.02	170.79
A/F/0/T/M10-03	9.81	11.98	2.17	9.83	15.41	15.75	1.00	163.31
A/F/0/T/M10-04	9.81	11.98	2.17	9.85	15.15	15.49	1.00	160.28
A/F/0/T/M10-05	9.81	11.98	2.17	9.59	17.63	17.97	1.02	190.99
Mean	9.81	11.98	2.17	9.69	16.01	16.35	1.01	172.13
A/F/0/T/M12-01	11.81	14.39	2.58	9.85	19.00	19.34	1.20	166.24
A/F/0/T/M12-02	11.81	14.39	2.58	9.86	18.19	18.53	1.20	159.11
A/F/0/T/M12-03	11.81	14.38	2.57	9.62	18.97	19.31	1.23	169.95
A/F/0/T/M12-04	11.81	14.39	2.58	9.89	17.61	17.95	1.19	153.66
A/F/0/T/M12-05	11.81	14.40	2.59	9.93	19.71	20.05	1.19	170.95
Mean	11.81	14.39	2.58	9.83	18.70	19.03	1.20	163.98
A/F/0/T/M16-01	15.81	18.39	2.58	9.61	21.96	22.30	1.65	146.76
A/F/0/T/M16-02	15.81	18.39	2.58	9.64	21.30	21.64	1.64	141.97
A/F/0/T/M16-03	15.81	18.39	2.58	9.59	23.68	24.02	1.65	158.41
A/F/0/T/M16-04	15.81	18.39	2.58	9.61	21.94	22.28	1.65	146.63
A/F/0/T/M16-05	15.81	18.40	2.59	9.85	20.80	21.14	1.61	135.74
Mean	15.81	18.39	2.58	9.66	21.94	22.27	1.64	145.90
A/F/0/T/M20-01	19.78	22.39	2.61	9.94	23.62	23.96	1.99	121.85
A/F/0/T/M20-02	19.78	22.39	2.61	9.59	24.43	24.77	2.06	130.57
A/F/0/T/M20-03	19.78	22.36	2.58	9.65	25.84	26.18	2.05	137.15
A/F/0/T/M20-04	19.78	22.38	2.60	10.24	27.84	28.18	1.93	139.12
A/F/0/T/M20-05	19.78	22.39	2.61	10.25	25.99	26.33	1.93	129.86
Mean	19.78	22.38	2.60	9.93	25.54	25.88	1.99	131.71

Table C.19: Pin-bearing Strength Test Results for Flange Material tested in the Longitudinal Direction with a Plain Pin after 6 months conditioning at 40°C

Specimen	Diameter of Pin, d (mm)	Diameter of Hole, d_n (mm)	Clearance (mm)	Thickness of Specimen, t (mm)	Maximum DARTEC load (kN)	Maximum specimen load (kN)	d/t	Bearing Strength (N/mm^2)
A/F/0/P/M10-06	9.81	11.98	2.17	9.62	17.53	17.87	1.02	189.34
A/F/0/P/M10-07	9.81	11.98	2.17	9.58	21.72	22.06	1.02	234.71
A/F/0/P/M10-08	9.81	11.98	2.17	9.60	15.93	16.27	1.02	172.74
A/F/0/P/M10-09	9.81	11.98	2.17	9.61	16.38	16.72	1.02	177.33
A/F/0/P/M10-10	9.81	11.98	2.17	9.59	18.75	19.09	1.02	202.90
Mean	9.81	11.98	2.17	9.60	18.06	18.40	1.02	195.40
A/F/0/P/M12-06	11.83	14.39	2.56	10.26	23.74	24.08	1.15	198.38
A/F/0/P/M12-07	11.83	14.40	2.57	9.66	16.84	17.18	1.22	150.32
A/F/0/P/M12-08	11.83	14.40	2.57	9.94	15.21	15.55	1.19	132.22
A/F/0/P/M12-09	11.83	14.39	2.56	9.66	19.45	19.79	1.22	173.16
A/F/0/P/M12-10	11.83	14.40	2.57	10.25	25.00	25.34	1.15	208.96
Mean	11.83	14.39	2.56	9.95	20.05	20.39	1.19	172.61
A/F/0/P/M16-06	15.86	18.39	2.53	9.61	28.86	29.20	1.65	191.57
A/F/0/P/M16-07	15.86	18.39	2.53	9.58	30.81	31.15	1.66	205.00
A/F/0/P/M16-08	15.86	18.40	2.54	9.88	26.07	26.41	1.61	168.53
A/F/0/P/M16-09	15.86	18.40	2.54	9.61	30.48	30.82	1.65	202.20
A/F/0/P/M16-10	15.86	18.39	2.53	9.87	25.49	25.83	1.61	164.99
Mean	15.86	18.39	2.53	9.71	28.34	28.68	1.63	186.46
A/F/0/P/M20-06	19.78	22.39	2.61	9.89	27.26	27.60	2.00	141.08
A/F/0/P/M20-07	19.78	22.39	2.61	9.91	26.58	26.92	2.00	137.32
A/F/0/P/M20-08	19.78	22.39	2.61	9.73	30.26	30.60	2.03	158.98
A/F/0/P/M20-09	19.78	22.39	2.61	9.61	30.79	31.13	2.06	163.76
A/F/0/P/M20-10	19.78	22.38	2.60	9.65	28.95	29.29	2.05	153.44
Mean	19.78	22.39	2.61	9.76	28.77	29.11	2.03	150.92

Table C.20: Pin-bearing Strength Test Results for Flange Material tested in the Longitudinal Direction with a Threaded Pin after 6 months conditioning at 40°C

Specimen	Diameter of Pin, d (mm)	Diameter of Hole, d_n (mm)	Clearance (mm)	Thickness of Specimen, t (mm)	Maximum DARTEC load (kN)	Maximum specimen load (kN)	d/t	Bearing Strength (N/mm^2)
A/F/0/T/M10-06	9.81	11.99	2.18	9.87	16.38	16.72	0.99	172.66
A/F/0/T/M10-07	9.81	11.98	2.17	9.63	17.22	17.56	1.02	185.86
A/F/0/T/M10-08	9.81	11.99	2.18	9.86	16.78	17.12	0.99	176.97
A/F/0/T/M10-09	9.81	11.98	2.17	9.61	18.59	18.93	1.02	200.78
A/F/0/T/M10-10	9.81	11.98	2.17	9.91	16.20	16.54	0.99	170.11
Mean	9.81	11.98	2.17	9.78	17.03	17.37	1.00	181.28
A/F/0/T/M12-06	11.81	14.39	2.58	9.66	17.82	18.16	1.22	159.16
A/F/0/T/M12-07	11.81	14.39	2.58	9.61	17.99	18.33	1.23	161.49
A/F/0/T/M12-08	11.81	14.39	2.58	9.70	19.55	19.89	1.22	173.61
A/F/0/T/M12-09	11.81	14.39	2.58	9.90	17.85	18.19	1.19	155.56
A/F/0/T/M12-10	11.81	14.39	2.58	9.60	17.72	18.06	1.23	159.28
Mean	11.81	14.39	2.58	9.69	18.19	18.52	1.22	161.82
A/F/0/T/M16-06	15.81	18.39	2.58	9.84	22.65	22.99	1.61	147.77
A/F/0/T/M16-07	15.81	18.40	2.59	10.34	24.63	24.97	1.53	152.73
A/F/0/T/M16-08	15.81	18.39	2.58	9.85	21.31	21.65	1.61	139.01
A/F/0/T/M16-09	15.81	18.40	2.59	9.86	22.99	23.33	1.60	149.65
A/F/0/T/M16-10	15.81	18.39	2.58	10.23	26.17	26.51	1.55	163.90
Mean	15.81	18.39	2.58	10.02	23.55	23.89	1.58	150.61
A/F/0/T/M20-06	19.78	22.39	2.61	9.74	26.97	27.31	2.03	141.74
A/F/0/T/M20-07	19.78	22.39	2.61	10.22	29.25	29.59	1.94	146.37
A/F/0/T/M20-08	19.78	22.40	2.62	9.62	26.80	27.14	2.06	142.62
A/F/0/T/M20-09	19.78	22.40	2.62	9.61	24.85	25.19	2.06	132.51
A/F/0/T/M20-10	19.78	22.39	2.61	9.88	24.03	24.37	2.00	124.69
Mean	19.78	22.39	2.61	9.81	26.38	26.72	2.02	137.59

Table C.21: Pin-bearing Strength Test Results for Flange Material tested in the Transverse Direction with a Plain Pin after 3 months conditioning at 40°C

Specimen	Diameter of Pin, *d* (mm)	Diameter of Hole, d_n (mm)	Clearance (mm)	Thickness of Specimen, *t* (mm)	Maximum DARTEC load (kN)	Maximum specimen load (kN)	*d/t*	Bearing Strength (N/mm^2)
A/F/90/P/M10-01	9.81	11.98	2.17	10.30	11.93	12.27	0.95	121.41
A/F/90/P/M10-02	9.81	11.98	2.17	10.29	13.53	13.87	0.95	137.38
A/F/90/P/M10-03	9.81	11.98	2.17	10.29	13.12	13.46	0.95	133.32
A/F/90/P/M10-04	9.81	11.98	2.17	10.30	10.07	10.41	0.95	103.01
A/F/90/P/M10-05	9.81	11.98	2.17	10.29	12.06	12.40	0.95	122.82
Mean	9.81	11.98	2.17	10.29	12.14	12.48	0.95	123.59
A/F/90/P/M12-01	11.83	14.39	2.56	10.37	12.45	12.79	1.14	104.24
A/F/90/P/M12-02	11.83	14.39	2.56	10.19	12.79	13.13	1.16	108.90
A/F/90/P/M12-03	11.83	14.39	2.56	10.26	13.88	14.22	1.15	117.14
A/F/90/P/M12-04	11.83	14.39	2.56	10.25	13.91	14.25	1.15	117.50
A/F/90/P/M12-05	11.83	14.40	2.57	9.61	12.38	12.72	1.23	111.87
Mean	11.83	14.39	2.56	10.14	13.08	13.42	1.17	111.93
A/F/90/P/M16-01	15.86	18.39	2.53	10.22	14.98	15.32	1.55	94.50
A/F/90/P/M16-02	15.86	18.39	2.53	10.23	14.84	15.18	1.55	93.55
A/F/90/P/M16-03	15.86	18.40	2.54	10.33	16.32	16.66	1.54	101.68
A/F/90/P/M16-04	15.86	18.39	2.53	10.33	15.15	15.49	1.54	94.53
A/F/90/P/M16-05	15.86	18.40	2.54	10.27	16.30	16.64	1.54	102.15
Mean	15.86	18.39	2.53	10.28	15.52	15.86	1.54	97.28
A/F/90/P/M20-01	19.78	22.40	2.62	10.21	17.32	17.66	1.94	87.44
A/F/90/P/M20-02	19.78	22.40	2.62	9.58	15.54	15.88	2.06	83.79
A/F/90/P/M20-03	19.78	22.39	2.61	10.21	16.39	16.73	1.94	82.83
A/F/90/P/M20-04	19.78	22.40	2.62	10.20	16.03	16.37	1.94	81.13
A/F/90/P/M20-05	19.78	22.40	2.62	9.90	17.03	17.37	2.00	88.69
Mean	19.78	22.39	2.61	10.02	16.46	16.80	1.98	84.78

Table C.22: Pin-bearing Strength Test Results for Flange Material tested in the Transverse Direction with a Threaded Pin after 3 months conditioning at 40°C

Specimen	Diameter of Pin, *d* (mm)	Diameter of Hole, d_n (mm)	Clearance (mm)	Thickness of Specimen, *t* (mm)	Maximum DARTEC load (kN)	Maximum specimen load (kN)	*d/t*	Bearing Strength (N/mm^2)
A/F/90/T/M10-01	9.81	11.98	2.17	10.23	12.72	13.06	0.96	130.12
A/F/90/T/M10-02	9.81	11.97	2.16	10.29	14.00	14.34	0.95	142.04
A/F/90/T/M10-03	9.81	11.98	2.17	10.34	14.18	14.52	0.95	143.13
A/F/90/T/M10-04	9.81	11.97	2.16	9.63	12.50	12.84	1.02	135.89
A/F/90/T/M10-05	9.81	11.98	2.17	9.79	12.91	13.25	1.00	137.94
Mean	9.81	11.98	2.17	10.06	13.26	13.60	0.98	137.82
A/F/90/T/M12-01	11.81	14.38	2.57	9.54	15.45	15.79	1.24	140.13
A/F/90/T/M12-02	11.81	14.39	2.58	9.57	15.30	15.64	1.23	138.36
A/F/90/T/M12-03	11.81	14.39	2.58	10.31	15.83	16.17	1.15	132.78
A/F/90/T/M12-04	11.81	14.40	2.59	10.19	14.71	15.05	1.16	125.04
A/F/90/T/M12-05	11.81	14.39	2.58	10.21	15.13	15.47	1.16	128.28
Mean	11.81	14.39	2.58	9.96	15.28	15.62	1.19	132.92
A/F/90/T/M16-01	15.81	18.39	2.58	9.63	17.37	17.71	1.64	116.31
A/F/90/T/M16-02	15.81	18.39	2.58	9.81	14.97	15.31	1.61	98.70
A/F/90/T/M16-03	15.81	18.39	2.58	10.31	17.65	17.99	1.53	110.36
A/F/90/T/M16-04	15.81	18.39	2.58	9.82	18.39	18.73	1.61	120.63
A/F/90/T/M16-05	15.81	18.40	2.59	10.35	16.47	16.81	1.53	102.72
Mean	15.81	18.39	2.58	9.98	16.97	17.31	1.58	109.74
A/F/90/T/M20-01	19.78	22.40	2.62	10.36	21.39	21.73	1.91	106.03
A/F/90/T/M20-02	19.78	22.40	2.62	10.31	20.07	20.41	1.92	100.07
A/F/90/T/M20-03	19.78	22.39	2.61	10.20	19.96	20.30	1.94	100.61
A/F/90/T/M20-04	19.78	22.40	2.62	10.21	20.40	20.74	1.94	102.69
A/F/90/T/M20-05	19.78	22.39	2.61	10.20	17.64	17.98	1.94	89.11
Mean	19.78	22.39	2.61	10.26	19.89	20.23	1.93	99.70

Table C.23: Pin-bearing Strength Test Results for Flange Material tested in the Transverse Direction with a Plain Pin after 6 months conditioning at 40°C

Specimen	Diameter of Pin, d (mm)	Diameter of Hole, d_n (mm)	Clearance (mm)	Thickness of Specimen, t (mm)	Maximum DARTEC load (kN)	Maximum specimen load (kN)	d/t	Bearing Strength (N/mm^2)
A/F/90/P/M10-06	9.81	11.98	2.17	10.16	11.31	11.65	0.97	116.87
A/F/90/P/M10-07	9.81	11.98	2.17	10.18	11.94	12.28	0.96	122.94
A/F/90/P/M10-08	9.81	11.98	2.17	10.19	11.20	11.54	0.96	115.42
A/F/90/P/M10-09	9.81	11.97	2.16	10.32	12.82	13.16	0.95	129.97
A/F/90/P/M10-10	9.81	11.97	2.16	9.60	11.84	12.18	1.02	129.31
Mean	9.81	11.97	2.16	10.09	11.82	12.16	0.97	122.90
A/F/90/P/M12-06	11.83	14.39	2.56	9.59	12.75	13.09	1.23	115.36
A/F/90/P/M12-07	11.83	14.39	2.56	9.93	11.18	11.52	1.19	98.05
A/F/90/P/M12-08	11.83	14.40	2.57	9.92	11.17	11.51	1.19	98.06
A/F/90/P/M12-09	11.83	14.39	2.56	9.62	12.45	12.79	1.23	112.37
A/F/90/P/M12-10	11.83	14.39	2.56	9.66	12.27	12.61	1.22	110.33
Mean	11.83	14.39	2.56	9.74	11.96	12.30	1.21	106.83
A/F/90/P/M16-06	15.86	18.40	2.54	9.88	15.34	15.68	1.61	100.05
A/F/90/P/M16-07	15.86	18.39	2.53	9.58	13.59	13.93	1.66	91.67
A/F/90/P/M16-08	15.86	18.39	2.53	9.89	15.26	15.60	1.60	99.44
A/F/90/P/M16-09	15.86	18.40	2.54	9.59	15.77	16.11	1.65	105.91
A/F/90/P/M16-10	15.86	18.40	2.54	9.65	15.86	16.20	1.64	105.84
Mean	15.86	18.39	2.53	9.72	15.16	15.50	1.63	100.58
A/F/90/P/M20-06	19.78	22.40	2.62	9.83	16.35	16.69	2.01	85.83
A/F/90/P/M20-07	19.78	22.40	2.62	9.80	17.90	18.24	2.02	94.09
A/F/90/P/M20-08	19.78	22.39	2.61	9.57	15.76	16.10	2.07	85.04
A/F/90/P/M20-09	19.78	22.40	2.62	9.59	14.16	14.50	2.06	76.43
A/F/90/P/M20-10	19.78	22.40	2.62	9.58	13.90	14.24	2.06	75.14
Mean	19.78	22.39	2.61	9.67	15.61	15.95	2.04	83.30

Table C.24: Pin-bearing Strength Test Results for Flange Material tested in the Transverse Direction with a Threaded Pin after 6 months conditioning at 40°C

Specimen	Diameter of Pin, d (mm)	Diameter of Hole, d_n (mm)	Clearance (mm)	Thickness of Specimen, t (mm)	Maximum DARTEC load (kN)	Maximum specimen load (kN)	d/t	Bearing Strength (N/mm^2)
A/F/90/T/M10-06	9.81	11.97	2.16	9.91	12.78	13.12	0.99	134.94
A/F/90/T/M10-07	9.81	11.98	2.17	9.57	11.27	11.61	1.03	123.64
A/F/90/T/M10-08	9.81	11.98	2.17	9.60	11.89	12.23	1.02	129.84
A/F/90/T/M10-09	9.81	11.97	2.16	9.59	12.70	13.04	1.02	138.59
A/F/90/T/M10-10	9.81	11.97	2.16	10.20	13.82	14.16	0.96	141.49
Mean	9.81	11.97	2.16	9.77	12.49	12.83	1.00	133.70
A/F/90/T/M12-06	11.81	14.39	2.58	10.34	15.71	16.05	1.14	131.42
A/F/90/T/M12-07	11.81	14.39	2.58	10.30	14.89	15.23	1.15	125.19
A/F/90/T/M12-08	11.81	14.39	2.58	9.75	15.85	16.19	1.21	140.58
A/F/90/T/M12-09	11.81	14.39	2.58	10.19	14.56	14.90	1.16	123.80
A/F/90/T/M12-10	11.81	14.39	2.58	10.30	15.69	16.03	1.15	131.76
Mean	11.81	14.39	2.58	10.18	15.34	15.68	1.16	130.55
A/F/90/T/M16-06	15.81	18.39	2.58	10.31	15.27	15.61	1.53	95.75
A/F/90/T/M16-07	15.81	18.40	2.59	9.63	18.39	18.73	1.64	123.01
A/F/90/T/M16-08	15.81	18.39	2.58	10.21	15.25	15.59	1.55	96.57
A/F/90/T/M16-09	15.81	18.40	2.59	10.35	16.89	17.23	1.53	105.28
A/F/90/T/M16-10	15.81	18.39	2.58	10.33	17.82	18.16	1.53	111.18
Mean	15.81	18.39	2.58	10.17	16.72	17.06	1.56	106.36
A/F/90/T/M20-06	19.78	22.39	2.61	10.19	20.61	20.95	1.94	103.93
A/F/90/T/M20-07	19.78	22.38	2.60	9.59	20.11	20.45	2.06	107.80
A/F/90/T/M20-08	19.78	22.40	2.62	9.89	21.62	21.96	2.00	112.25
A/F/90/T/M20-09	19.78	22.40	2.62	9.59	21.24	21.58	2.06	113.75
A/F/90/T/M20-10	19.78	22.39	2.61	9.84	17.72	18.06	2.01	92.78
Mean	19.78	22.39	2.61	9.82	20.26	20.60	2.02	106.10

Table C.25: Pin-bearing Strength Test Results for Web Material tested in the Longitudinal Direction with a Plain Pin after 3 months conditioning at 40°C

Specimen	Diameter of Pin, d (mm)	Diameter of Hole, d_n (mm)	Clearance (mm)	Thickness of Specimen, t (mm)	Maximum DARTEC load (kN)	Maximum specimen load (kN)	d/t	Bearing Strength (N/mm^2)
A/W/0/P/M10-01	9.81	11.97	2.16	9.58	16.79	17.13	1.02	182.25
A/W/0/P/M10-02	9.81	11.97	2.16	9.66	14.36	14.70	1.02	155.10
A/W/0/P/M10-03	9.81	11.97	2.16	9.81	16.40	16.74	1.00	173.93
A/W/0/P/M10-04	9.81	11.97	2.16	9.65	15.02	15.36	1.02	162.23
A/W/0/P/M10-05	9.81	11.97	2.16	9.60	17.35	17.69	1.02	187.82
Mean	9.81	11.97	2.16	9.66	15.98	16.32	1.02	172.27
A/W/0/P/M20-01	19.78	22.38	2.60	9.62	26.25	26.59	2.06	139.73
A/W/0/P/M20-02	19.78	22.39	2.61	9.74	27.88	28.22	2.03	146.47
A/W/0/P/M20-03	19.78	22.38	2.60	9.62	29.31	29.65	2.06	155.81
A/W/0/P/M20-04	19.78	22.38	2.60	9.64	28.70	29.04	2.05	152.29
A/W/0/P/M20-05	19.78	22.38	2.60	9.65	27.42	27.76	2.05	145.42
Mean	19.78	22.38	2.60	9.65	27.91	28.25	2.05	147.94

Table C.26: Pin-bearing Strength Test Results for Web Material tested in the Longitudinal Direction with a Plain Pin after 3 months conditioning at 40°C

Specimen	Diameter of Pin, d (mm)	Diameter of Hole, d_n (mm)	Clearance (mm)	Thickness of Specimen, t (mm)	Maximum DARTEC load (kN)	Maximum specimen load (kN)	d/t	Bearing Strength (N/mm^2)
A/W/0/T/M10-01	9.81	11.98	2.17	9.68	13.90	14.24	1.01	149.94
A/W/0/T/M10-02	9.81	11.97	2.16	9.63	15.54	15.88	1.02	168.07
A/W/0/T/M10-03	9.81	11.97	2.16	9.64	13.06	13.40	1.02	141.68
A/W/0/T/M10-04	9.81	11.97	2.16	9.62	14.90	15.24	1.02	161.47
A/W/0/T/M10-05	9.81	11.97	2.16	9.60	14.80	15.14	1.02	160.74
Mean	9.81	11.97	2.16	9.63	14.44	14.78	1.02	156.38
A/W/0/T/M20-01	19.78	22.38	2.60	9.64	25.28	25.62	2.05	134.35
A/W/0/T/M20-02	19.78	22.38	2.60	9.63	23.28	23.62	2.05	123.99
A/W/0/T/M20-03	19.78	22.38	2.60	9.71	22.00	22.34	2.04	116.31
A/W/0/T/M20-04	19.78	22.38	2.60	9.65	21.37	21.71	2.05	113.73
A/W/0/T/M20-05	19.78	22.37	2.59	9.67	20.31	20.65	2.05	107.95
Mean	19.78	22.38	2.60	9.66	22.45	22.79	2.05	119.27

Table C.27: Pin-bearing Strength Test Results for Web Material tested in the Longitudinal Direction with a Plain Pin after 6 months conditioning at 40°C

Specimen	Diameter of Pin, d (mm)	Diameter of Hole, d_n (mm)	Clearance (mm)	Thickness of Specimen, t (mm)	Maximum DARTEC load (kN)	Maximum specimen load (kN)	d/t	Bearing Strength (N/mm^2)
A/W/0/P/M10-06	9.81	11.98	2.17	9.64	16.52	16.86	1.02	178.26
A/W/0/P/M10-07	9.81	11.98	2.17	9.64	17.63	17.97	1.02	190.00
A/W/0/P/M10-08	9.81	11.98	2.17	9.84	17.08	17.42	1.00	180.44
A/W/0/P/M10-09	9.81	11.98	2.17	9.61	15.22	15.56	1.02	165.03
A/W/0/P/M10-10	9.81	11.98	2.17	9.62	14.60	14.94	1.02	158.29
Mean	9.81	11.98	2.17	9.67	16.21	16.55	1.01	174.40
A/W/0/P/M20-06	19.78	22.38	2.60	9.69	29.64	29.98	2.04	156.41
A/W/0/P/M20-07	19.78	22.39	2.61	9.64	33.89	34.23	2.05	179.51
A/W/0/P/M20-08	19.78	22.39	2.61	9.65	22.87	23.21	2.05	121.59
A/W/0/P/M20-09	19.78	22.39	2.61	9.63	29.89	30.23	2.05	158.69
A/W/0/P/M20-10	19.78	22.38	2.60	9.62	32.69	33.03	2.06	173.57
Mean	19.78	22.38	2.60	9.65	29.80	30.13	2.05	157.95

Table C.28: Pin-bearing Strength Test Results for Web Material tested in the Longitudinal Direction with a Plain Pin after 6 months conditioning at 40°C

Specimen	Diameter of Pin, *d* (mm)	Diameter of Hole, d_n (mm)	Clearance (mm)	Thickness of Specimen, *t* (mm)	Maximum DARTEC load (kN)	Maximum specimen load (kN)	*d/t*	Bearing Strength (N/mm^2)
A/W/0/T/M10-06	9.81	11.98	2.17	9.65	15.10	15.44	1.02	163.08
A/W/0/T/M10-07	9.81	11.98	2.17	9.63	16.19	16.53	1.02	174.95
A/W/0/T/M10-08	9.81	11.97	2.16	9.63	15.28	15.62	1.02	165.32
A/W/0/T/M10-09	9.81	11.97	2.16	9.62	16.75	17.09	1.02	181.07
A/W/0/T/M10-10	9.81	11.97	2.16	9.64	14.52	14.86	1.02	157.11
Mean	9.81	11.97	2.16	9.63	15.57	15.91	1.02	168.31
A/W/0/T/M20-06	19.78	22.38	2.60	9.62	21.12	21.46	2.06	112.77
A/W/0/T/M20-07	19.78	22.37	2.59	9.60	22.68	23.02	2.06	121.22
A/W/0/T/M20-08	19.78	22.38	2.60	9.62	24.80	25.14	2.06	132.11
A/W/0/T/M20-09	19.78	22.38	2.60	9.63	21.78	22.12	2.05	116.12
A/W/0/T/M20-10	19.78	22.38	2.60	9.69	21.59	21.93	2.04	114.41
Mean	19.78	22.38	2.60	9.63	22.39	22.73	2.05	119.32

Table C.29: Pin-bearing Strength Test Results for Web Material tested in the 45° Direction with a Plain Pin after 3 months conditioning at 40°C

Specimen	Diameter of Pin, *d* (mm)	Diameter of Hole, d_n (mm)	Clearance (mm)	Thickness of Specimen, *t* (mm)	Maximum DARTEC load (kN)	Maximum specimen load (kN)	*d/t*	Bearing Strength (N/mm^2)
A/W/45/P/M10-01	9.81	11.97	2.16	9.64	13.85	14.19	1.02	150.03
A/W/45/P/M10-02	9.81	11.97	2.16	9.61	12.52	12.86	1.02	136.39
A/W/45/P/M10-03	9.81	11.97	2.16	9.64	13.51	13.85	1.02	146.43
A/W/45/P/M10-04	9.81	11.97	2.16	9.64	12.13	12.47	1.02	131.84
A/W/45/P/M10-05	9.81	11.97	2.16	9.63	12.50	12.84	1.02	135.89
Mean	9.81	11.97	2.16	9.63	12.90	13.24	1.02	140.12
A/W/45/P/M20-01	19.78	22.39	2.61	9.65	20.06	20.40	2.05	106.86
A/W/45/P/M20-02	19.78	22.40	2.62	9.68	20.45	20.79	2.04	108.57
A/W/45/P/M20-03	19.78	22.39	2.61	9.64	18.80	19.14	2.05	100.37
A/W/45/P/M20-04	19.78	22.39	2.61	9.62	20.13	20.47	2.06	107.57
A/W/45/P/M20-05	19.78	22.39	2.61	9.69	19.84	20.18	2.04	105.28
Mean	19.78	22.39	2.61	9.66	19.86	20.19	2.05	105.73

Table C.30: Pin-bearing Strength Test Results for Web Material tested in the 45° Direction with a Threaded Pin after 3 months conditioning at 40°C

Specimen	Diameter of Pin, *d* (mm)	Diameter of Hole, d_n (mm)	Clearance (mm)	Thickness of Specimen, *t* (mm)	Maximum DARTEC load (kN)	Maximum specimen load (kN)	*d/t*	Bearing Strength (N/mm^2)
A/W/45/T/M10-01	9.81	11.97	2.16	9.62	14.39	14.73	1.02	156.06
A/W/45/T/M10-02	9.81	11.96	2.15	9.63	14.14	14.48	1.02	153.25
A/W/45/T/M10-03	9.81	11.97	2.16	9.58	14.52	14.86	1.02	158.10
A/W/45/T/M10-04	9.81	11.97	2.16	9.64	13.80	14.14	1.02	149.50
A/W/45/T/M10-05	9.81	11.97	2.16	9.61	14.39	14.73	1.02	156.23
Mean	9.81	11.97	2.16	9.62	14.25	14.59	1.02	154.63
A/W/45/T/M20-01	19.78	22.40	2.62	9.65	21.34	21.68	2.05	113.57
A/W/45/T/M20-02	19.78	22.40	2.62	9.62	20.33	20.67	2.06	108.62
A/W/45/T/M20-03	19.78	22.40	2.62	9.64	23.47	23.81	2.05	124.86
A/W/45/T/M20-04	19.78	22.40	2.62	9.65	20.06	20.40	2.05	106.86
A/W/45/T/M20-05	19.78	22.40	2.62	9.66	21.22	21.56	2.05	112.82
Mean	19.78	22.40	2.62	9.64	21.28	21.62	2.05	113.35

Table C.31: Pin-bearing Strength Test Results for Web Material tested in the 45° Direction with a Plain Pin after 6 months conditioning at 40°C

Specimen	Diameter of Pin, d (mm)	Diameter of Hole, d_n (mm)	Clearance (mm)	Thickness of Specimen, t (mm)	Maximum DARTEC load (kN)	Maximum specimen load (kN)	d/t	Bearing Strength (N/mm^2)
A/W/45/P/M10-06	9.81	11.98	2.17	9.66	13.80	14.14	1.02	149.19
A/W/45/P/M10-07	9.81	11.97	2.16	9.61	12.86	13.20	1.02	140.00
A/W/45/P/M10-08	9.81	11.97	2.16	9.64	13.75	14.09	1.02	148.97
A/W/45/P/M10-09	9.81	11.97	2.16	9.65	13.70	14.04	1.02	148.29
A/W/45/P/M10-10	9.81	11.97	2.16	9.64	13.99	14.33	1.02	151.51
Mean	9.81	11.97	2.16	9.64	13.62	13.96	1.02	147.59
A/W/45/P/M20-06	19.78	22.39	2.61	9.65	19.95	20.29	2.05	106.29
A/W/45/P/M20-07	19.78	22.39	2.61	9.59	20.73	21.07	2.06	111.07
A/W/45/P/M20-08	19.78	22.39	2.61	9.64	19.41	19.75	2.05	103.57
A/W/45/P/M20-09	19.78	22.39	2.61	9.62	20.71	21.05	2.06	110.61
A/W/45/P/M20-10	19.78	22.39	2.61	9.63	19.72	20.06	2.05	105.30
Mean	19.78	22.39	2.61	9.63	20.10	20.44	2.05	107.37

Table C.32: Pin-bearing Strength Test Results for Web Material tested in the 45° Direction with a Threaded Pin after 6 months conditioning at 40°C

Specimen	Diameter of Pin, d (mm)	Diameter of Hole, d_n (mm)	Clearance (mm)	Thickness of Specimen, t (mm)	Maximum DARTEC load (kN)	Maximum specimen load (kN)	d/t	Bearing Strength (N/mm^2)
A/W/45/T/M10-06	9.81	11.97	2.16	9.62	14.55	14.89	1.02	157.76
A/W/45/T/M10-07	9.81	11.97	2.16	9.67	13.90	14.24	1.01	150.09
A/W/45/T/M10-08	9.81	11.98	2.17	9.63	15.61	15.95	1.02	168.81
A/W/45/T/M10-09	9.81	11.96	2.15	9.61	15.56	15.90	1.02	168.64
A/W/45/T/M10-10	9.81	11.96	2.15	9.64	14.05	14.39	1.02	152.14
Mean	9.81	11.97	2.16	9.63	14.73	15.07	1.02	159.49
A/W/45/T/M20-06	19.78	22.40	2.62	9.67	19.56	19.90	2.05	104.03
A/W/45/T/M20-07	19.78	22.40	2.62	9.64	20.68	21.02	2.05	110.23
A/W/45/T/M20-08	19.78	22.40	2.62	9.65	22.01	22.35	2.05	117.08
A/W/45/T/M20-09	19.78	22.40	2.62	9.63	21.97	22.31	2.05	117.11
A/W/45/T/M20-10	19.78	22.40	2.62	9.62	23.15	23.49	2.06	123.44
Mean	19.78	22.40	2.62	9.64	21.47	21.81	2.05	114.38

Table C.33: Pin-bearing Strength Test Results for Web Material tested in the Transverse Direction with a Plain Pin after 3 months conditioning at 40°C

Specimen	Diameter of Pin, d (mm)	Diameter of Hole, d_n (mm)	Clearance (mm)	Thickness of Specimen, t (mm)	Maximum DARTEC load (kN)	Maximum specimen load (kN)	d/t	Bearing Strength (N/mm^2)
A/W/90/P/M10-01	9.81	11.97	2.16	9.63	13.30	13.64	1.02	144.36
A/W/90/P/M10-02	9.81	11.97	2.16	9.66	12.32	12.66	1.02	133.57
A/W/90/P/M10-03	9.81	11.97	2.16	9.60	12.98	13.32	1.02	141.42
A/W/90/P/M10-04	9.81	11.97	2.16	9.60	12.94	13.28	1.02	140.99
A/W/90/P/M10-05	9.81	11.97	2.16	9.61	12.26	12.60	1.02	133.63
Mean	9.81	11.97	2.16	9.62	12.76	13.10	1.02	138.79
A/W/90/P/M20-01	19.78	22.39	2.61	9.61	18.16	18.50	2.06	97.31
A/W/90/P/M20-02	19.78	22.39	2.61	9.61	18.02	18.36	2.06	96.58
A/W/90/P/M20-03	19.78	22.39	2.61	9.61	17.95	18.29	2.06	96.21
A/W/90/P/M20-04	19.78	22.39	2.61	9.62	20.14	20.48	2.06	107.62
A/W/90/P/M20-05	19.78	22.39	2.61	9.61	19.09	19.43	2.06	102.21
Mean	19.78	22.39	2.61	9.61	18.67	19.01	2.06	99.99

Table C.34: Pin-bearing Strength Test Results for Web Material tested in the Transverse Direction with a Threaded Pin after 3 months conditioning at 40°C

Specimen	Diameter of Pin, d (mm)	Diameter of Hole, d_n (mm)	Clearance (mm)	Thickness of Specimen, t (mm)	Maximum DARTEC load (kN)	Maximum specimen load (kN)	d/t	Bearing Strength (N/mm^2)
A/W/90/T/M10-01	9.81	11.97	2.16	9.63	13.95	14.29	1.02	151.24
A/W/90/T/M10-02	9.81	11.97	2.16	9.59	13.59	13.93	1.02	148.05
A/W/90/T/M10-03	9.81	11.97	2.16	9.61	13.49	13.83	1.02	146.68
A/W/90/T/M10-04	9.81	11.97	2.16	9.63	14.94	15.28	1.02	161.72
A/W/90/T/M10-05	9.81	11.97	2.16	9.64	14.55	14.89	1.02	157.43
Mean	9.81	11.97	2.16	9.62	14.10	14.44	1.02	153.02
A/W/90/T/M20-01	19.78	22.39	2.61	9.64	21.53	21.87	2.05	114.68
A/W/90/T/M20-02	19.78	22.39	2.61	9.60	20.22	20.56	2.06	108.26
A/W/90/T/M20-03	19.78	22.39	2.61	9.62	20.45	20.79	2.06	109.25
A/W/90/T/M20-04	19.78	22.38	2.60	9.60	20.27	20.61	2.06	108.53
A/W/90/T/M20-05	19.78	22.39	2.61	9.60	19.41	19.75	2.06	104.00
Mean	19.78	22.39	2.61	9.61	20.38	20.71	2.06	108.94

Table C.35: Pin-bearing Strength Test Results for Web Material tested in the Transverse Direction with a Plain Pin after 6 months conditioning at 40°C

Specimen	Diameter of Pin, d (mm)	Diameter of Hole, d_n (mm)	Clearance (mm)	Thickness of Specimen, t (mm)	Maximum DARTEC load (kN)	Maximum specimen load (kN)	d/t	Bearing Strength (N/mm^2)
A/W/90/P/M10-06	9.81	11.97	2.16	9.60	12.36	12.70	1.02	134.83
A/W/90/P/M10-07	9.81	11.97	2.16	9.62	11.46	11.80	1.02	125.02
A/W/90/P/M10-08	9.81	11.97	2.16	9.63	12.44	12.78	1.02	135.26
A/W/90/P/M10-09	9.81	11.97	2.16	9.65	11.71	12.05	1.02	127.27
A/W/90/P/M10-10	9.81	11.97	2.16	9.62	12.38	12.72	1.02	134.76
Mean	9.81	11.97	2.16	9.62	12.07	12.41	1.02	131.43
A/W/90/P/M20-06	19.78	22.39	2.61	9.61	19.04	19.38	2.06	101.94
A/W/90/P/M20-07	19.78	22.39	2.61	9.62	19.29	19.63	2.06	103.15
A/W/90/P/M20-08	19.78	22.39	2.61	9.61	17.89	18.23	2.06	95.89
A/W/90/P/M20-09	19.78	22.39	2.61	9.63	17.47	17.81	2.05	93.49
A/W/90/P/M20-10	19.78	22.39	2.61	9.64	17.59	17.93	2.05	94.02
Mean	19.78	22.39	2.61	9.62	18.26	18.59	2.06	97.70

Table C.36: Pin-bearing Strength Test Results for Web Material tested in the Transverse Direction with a Threaded Pin after 6 months conditioning at 40°C

Specimen	Diameter of Pin, d (mm)	Diameter of Hole, d_n (mm)	Clearance (mm)	Thickness of Specimen, t (mm)	Maximum DARTEC load (kN)	Maximum specimen load (kN)	d/t	Bearing Strength (N/mm^2)
A/W/90/T/M10-06	9.81	11.97	2.16	9.62	15.13	15.47	1.02	163.90
A/W/90/T/M10-07	9.81	11.97	2.16	9.62	14.10	14.44	1.02	152.99
A/W/90/T/M10-08	9.81	11.97	2.16	9.63	14.23	14.57	1.02	154.21
A/W/90/T/M10-09	9.81	11.97	2.16	9.60	14.82	15.16	1.02	160.95
A/W/90/T/M10-10	9.81	11.97	2.16	9.65	13.37	13.71	1.02	144.80
Mean	9.81	11.97	2.16	9.62	14.33	14.67	1.02	155.37
A/W/90/T/M20-06	19.78	22.39	2.61	9.64	20.61	20.95	2.05	109.86
A/W/90/T/M20-07	19.78	22.39	2.61	9.59	20.11	20.45	2.06	107.80
A/W/90/T/M20-08	19.78	22.39	2.61	9.63	21.62	21.96	2.05	115.28
A/W/90/T/M20-09	19.78	22.39	2.61	9.60	21.24	21.58	2.06	113.64
A/W/90/T/M20-10	19.78	22.39	2.61	9.66	17.72	18.06	2.05	94.51
Mean	19.78	22.39	2.61	9.62	20.26	20.60	2.06	108.22

Table C.37: Pin-bearing Strength Test Results for Flange Material tested in the Longitudinal Direction with a Plain Pin after 3 months conditioning at 30°C

Specimen	Diameter of Pin, d (mm)	Diameter of Hole, d_n (mm)	Clearance (mm)	Thickness of Specimen, t (mm)	Maximum DARTEC load (kN)	Maximum specimen load (kN)	d/t	Bearing Strength (N/mm^2)
30A/F/0/P/M10-01	9.81	12.00	2.19	9.79	14.77	15.11	1.00	157.31
30A/F/0/P/M10-02	9.81	12.00	2.19	9.82	13.69	14.03	1.00	145.62
30A/F/0/P/M10-03	9.81	11.99	2.18	9.58	15.91	16.25	1.02	172.89
30A/F/0/P/M10-04	9.81	12.00	2.19	9.79	16.12	16.46	1.00	171.37
30A/F/0/P/M10-05	9.81	12.00	2.19	9.53	18.02	18.36	1.03	196.36
Mean	9.81	12.00	2.19	9.70	15.70	16.04	1.01	168.71
30A/F/0/P/M20-01	19.78	22.39	2.61	9.83	30.03	30.37	2.01	156.18
30A/F/0/P/M20-02	19.78	22.39	2.61	9.58	30.78	31.12	2.06	164.22
30A/F/0/P/M20-03	19.78	22.39	2.61	9.81	26.33	26.67	2.02	137.43
30A/F/0/P/M20-04	19.78	22.39	2.61	9.83	26.73	27.07	2.01	139.21
30A/F/0/P/M20-05	19.78	22.38	2.60	9.83	25.66	26.00	2.01	133.71
Mean	19.78	22.38	2.60	9.78	27.91	28.24	2.02	146.15

Table C.38: Pin-bearing Strength Test Results for Flange Material tested in the Longitudinal Direction with a Plain Pin after 6 months conditioning at 30°C

Specimen	Diameter of Pin, d (mm)	Diameter of Hole, d_n (mm)	Clearance (mm)	Thickness of Specimen, t (mm)	Maximum DARTEC load (kN)	Maximum specimen load (kN)	d/t	Bearing Strength (N/mm^2)
30A/F/0/P/M10-06	9.81	12.00	2.19	9.82	15.31	15.65	1.00	162.43
30A/F/0/P/M10-07	9.81	12.00	2.19	9.54	15.83	16.17	1.03	172.76
30A/F/0/P/M10-08	9.81	11.99	2.18	9.54	14.30	14.64	1.03	156.41
30A/F/0/P/M10-09	9.81	12.00	2.19	9.76	13.24	13.58	1.01	141.81
30A/F/0/P/M10-10	9.81	11.99	2.18	9.87	16.22	16.56	0.99	171.01
Mean	9.81	11.99	2.18	9.71	14.98	15.32	1.01	160.89
30A/F/0/P/M20-06	19.78	22.39	2.61	10.15	32.64	32.98	1.95	164.26
30A/F/0/P/M20-07	19.78	22.38	2.60	10.16	34.67	35.01	1.95	174.20
30A/F/0/P/M20-08	19.78	22.38	2.60	9.85	26.50	26.84	2.01	137.75
30A/F/0/P/M20-09	19.78	22.38	2.60	9.54	30.21	30.55	2.07	161.89
30A/F/0/P/M20-10	19.78	22.38	2.60	10.17	28.78	29.12	1.94	144.75
Mean	19.78	22.38	2.60	9.97	30.56	30.90	1.98	156.57

Table C.39: Pin-bearing Strength Test Results for Flange Material tested in the Transverse Direction with a Plain Pin after 3 months conditioning at 30°C

Specimen	Diameter of Pin, d (mm)	Diameter of Hole, d_n (mm)	Clearance (mm)	Thickness of Specimen, t (mm)	Maximum DARTEC load (kN)	Maximum specimen load (kN)	d/t	Bearing Strength (N/mm^2)
30A/F/90/P/M10-01	9.81	12.00	2.19	9.76	10.93	11.27	1.01	117.69
30A/F/90/P/M10-02	9.81	12.00	2.19	9.56	10.67	11.01	1.03	117.38
30A/F/90/P/M10-03	9.81	11.99	2.18	9.58	10.68	11.02	1.02	117.24
30A/F/90/P/M10-04	9.81	12.00	2.19	9.56	11.15	11.49	1.03	122.49
30A/F/90/P/M10-05	9.81	12.00	2.19	9.76	11.58	11.92	1.01	124.48
Mean	9.81	12.00	2.19	9.64	11.00	11.34	1.02	119.85
30A/F/90/P/M20-01	19.78	22.39	2.61	10.18	16.26	16.60	1.94	82.43
30A/F/90/P/M20-02	19.78	22.38	2.60	9.55	16.17	16.51	2.07	87.39
30A/F/90/P/M20-03	19.78	22.38	2.60	9.54	15.73	16.07	2.07	85.15
30A/F/90/P/M20-04	19.78	22.38	2.60	9.83	16.16	16.50	2.01	84.85
30A/F/90/P/M20-05	19.78	22.38	2.60	9.78	18.06	18.40	2.02	95.11
Mean	19.78	22.38	2.60	9.78	16.48	16.81	2.02	86.99

Table C.40: Pin-bearing Strength Test Results for Flange Material tested in the Transverse Direction with a Plain Pin after 6 months conditioning at 30°C

Specimen	Diameter of Pin, d (mm)	Diameter of Hole, d_n (mm)	Clearance (mm)	Thickness of Specimen, t (mm)	Maximum DARTEC load (kN)	Maximum specimen load (kN)	d/t	Bearing Strength (N/mm^2)
30A/F/90/P/M10-06	9.81	12.00	2.19	9.52	10.11	10.45	1.03	111.87
30A/F/90/P/M10-07	9.81	12.00	2.19	9.82	11.20	11.54	1.00	119.77
30A/F/90/P/M10-08	9.81	11.99	2.18	9.55	9.81	10.15	1.03	108.32
30A/F/90/P/M10-09	9.81	12.00	2.19	9.81	11.42	11.76	1.00	122.18
30A/F/90/P/M10-10	9.81	12.00	2.19	9.54	10.09	10.43	1.03	111.43
Mean	9.81	12.00	2.19	9.65	10.53	10.86	1.02	114.71
30A/F/90/P/M20-06	19.78	22.38	2.60	9.89	14.37	14.71	2.00	75.18
30A/F/90/P/M20-07	19.78	22.39	2.61	9.86	15.39	15.73	2.01	80.64
30A/F/90/P/M20-08	19.78	22.38	2.60	9.76	16.72	17.06	2.03	88.36
30A/F/90/P/M20-09	19.78	22.39	2.61	9.81	17.53	17.87	2.02	92.08
30A/F/90/P/M20-10	19.78	22.39	2.61	9.79	16.18	16.52	2.02	85.30
Mean	19.78	22.38	2.60	9.82	16.04	16.38	2.01	84.31

Table C.41: Pin-bearing Strength Test Results for Flange Material tested in the Longitudinal Direction with a Plain Pin after 3 months conditioning at 50°C

Specimen	Diameter of Pin, d (mm)	Diameter of Hole, d_n (mm)	Clearance (mm)	Thickness of Specimen, t (mm)	Maximum DARTEC load (kN)	Maximum specimen load (kN)	d/t	Bearing Strength (N/mm^2)
50A/F/0/P/M10-06	9.81	11.99	2.18	9.58	14.70	15.04	1.02	160.01
50A/F/0/P/M10-07	9.81	11.98	2.17	9.59	12.73	13.07	1.02	138.91
50A/F/0/P/M10-08	9.81	11.99	2.18	10.23	19.76	20.10	0.96	200.27
50A/F/0/P/M10-09	9.81	11.99	2.18	9.82	19.15	19.49	1.00	202.30
50A/F/0/P/M10-10	9.81	11.99	2.18	9.82	16.70	17.04	1.00	176.86
Mean	9.81	11.99	2.18	9.81	16.61	16.95	1.00	175.67
50A/F/0/P/M20-06	19.78	22.40	2.62	9.59	35.19	35.53	2.06	187.29
50A/F/0/P/M20-07	19.78	22.40	2.62	10.24	38.15	38.49	1.93	190.02
50A/F/0/P/M20-08	19.78	22.40	2.62	9.56	30.06	30.40	2.07	160.75
50A/F/0/P/M20-09	19.78	22.40	2.62	9.57	37.86	38.20	2.07	201.79
50A/F/0/P/M20-10	19.78	22.39	2.61	10.23	36.64	36.98	1.93	182.74
Mean	19.78	22.40	2.62	9.84	35.58	35.92	2.01	184.52

Table C.42: Pin-bearing Strength Test Results for Flange Material tested in the Longitudinal Direction with a Plain Pin after 6 months conditioning at 50°C

Specimen	Diameter of Pin, d (mm)	Diameter of Hole, d_n (mm)	Clearance (mm)	Thickness of Specimen, t (mm)	Maximum DARTEC load (kN)	Maximum specimen load (kN)	d/t	Bearing Strength (N/mm^2)
50A/F/0/P/M10-01	9.81	12.00	2.19	9.54	17.38	17.72	1.03	189.32
50A/F/0/P/M10-02	9.81	12.00	2.19	9.55	15.65	15.99	1.03	170.66
50A/F/0/P/M10-03	9.81	11.99	2.18	10.16	16.66	17.00	0.97	170.54
50A/F/0/P/M10-04	9.81	11.99	2.18	9.55	16.35	16.69	1.03	178.13
50A/F/0/P/M10-05	9.81	12.00	2.19	9.59	16.50	16.84	1.02	178.98
Mean	9.81	11.99	2.18	9.68	16.51	16.85	1.01	177.53
50A/F/0/P/M20-01	19.78	22.38	2.60	10.17	29.54	29.88	1.94	148.53
50A/F/0/P/M20-02	19.78	22.38	2.60	9.85	28.61	28.95	2.01	148.58
50A/F/0/P/M20-03	19.78	22.38	2.60	10.16	30.50	30.84	1.95	153.45
50A/F/0/P/M20-04	19.78	22.38	2.60	10.23	35.41	35.75	1.93	176.66
50A/F/0/P/M20-05	19.78	22.38	2.60	10.18	33.96	34.30	1.94	170.33
Mean	19.78	22.38	2.60	10.12	31.60	31.94	1.96	159.51

Table C.43: Pin-bearing Strength Test Results for Flange Material tested in the Transverse Direction with a Plain Pin after 3 months conditioning at 50°C

Specimen	Diameter of Pin, d (mm)	Diameter of Hole, d_n (mm)	Clearance (mm)	Thickness of Specimen, t (mm)	Maximum DARTEC load (kN)	Maximum specimen load (kN)	d/t	Bearing Strength (N/mm^2)
50A/F/90/P/M10-06	9.81	11.99	2.18	9.57	9.69	10.03	1.03	106.82
50A/F/90/P/M10-07	9.81	12.00	2.19	9.55	11.72	12.06	1.03	128.71
50A/F/90/P/M10-08	9.81	12.00	2.19	9.80	11.32	11.66	1.00	121.26
50A/F/90/P/M10-09	9.81	12.00	2.19	9.54	10.42	10.76	1.03	114.95
50A/F/90/P/M10-10	9.81	12.00	2.19	9.58	10.50	10.84	1.02	115.32
Mean	9.81	12.00	2.19	9.61	10.73	11.07	1.02	117.41
50A/F/90/P/M20-06	19.78	22.39	2.61	9.53	14.18	14.52	2.08	77.02
50A/F/90/P/M20-07	19.78	22.39	2.61	9.59	13.56	13.90	2.06	73.27
50A/F/90/P/M20-08	19.78	22.39	2.61	9.57	14.67	15.01	2.07	79.28
50A/F/90/P/M20-09	19.78	22.40	2.62	10.24	17.47	17.81	1.93	87.92
50A/F/90/P/M20-10	19.78	22.39	2.61	10.15	18.22	18.56	1.95	92.44
Mean	19.78	22.39	2.61	9.82	15.62	15.96	2.02	81.98

Table C.44: Pin-bearing Strength Test Results for Flange Material tested in the Transverse Direction with a Plain Pin after 6 months conditioning at 50°C

Specimen	Diameter of Pin, d (mm)	Diameter of Hole, d_n (mm)	Clearance (mm)	Thickness of Specimen, t (mm)	Maximum DARTEC load (kN)	Maximum specimen load (kN)	d/t	Bearing Strength (N/mm^2)
50A/F/90/P/M10-01	9.81	12.00	2.19	9.54	10.20	10.54	1.03	112.60
50A/F/90/P/M10-02	9.81	11.99	2.18	9.55	10.48	10.82	1.03	115.47
50A/F/90/P/M10-03	9.81	11.99	2.18	9.53	11.32	11.66	1.03	124.70
50A/F/90/P/M10-04	9.81	11.99	2.18	9.57	11.20	11.54	1.03	122.90
50A/F/90/P/M10-05	9.81	11.99	2.18	9.54	10.76	11.10	1.03	118.58
Mean	9.81	11.99	2.18	9.55	10.79	11.13	1.03	118.85
50A/F/90/P/M20-01	19.78	22.38	2.60	9.90	16.10	16.44	2.00	83.94
50A/F/90/P/M20-02	19.78	22.39	2.61	9.86	15.38	15.72	2.01	80.59
50A/F/90/P/M20-03	19.78	22.38	2.60	9.83	16.51	16.85	2.01	86.65
50A/F/90/P/M20-04	19.78	22.38	2.60	10.24	18.16	18.50	1.93	91.33
50A/F/90/P/M20-05	19.78	22.38	2.60	9.52	15.65	15.99	2.08	84.90
Mean	19.78	22.38	2.60	9.87	16.36	16.70	2.01	85.48

Appendix D – Plate-to-Plate Bolted Connection Strength Test Results

D.1 Introduction

Presented in this appendix are the test results from a series of plate-to-plate bolted connection tests as described in Chapter 6. First, the results for the single bolt tests are given in Tables D.1 to D.6 which is followed by results for two bolt tests in Tables D.7 to D.12. Finally, the four bolt test results are presented in Tables D.13 and D.14.

In each table presented in this appendix the convention used for each column is as follows. Column (1) gives the specimen ID for each individual test conducted. Column (2) and (3) give the bolt diameter and the bolt-hole diameter, respectively. Column (4) is the clearance-hole size, being the bolt-hole minus the bolt diameter. Columns (5) to (8) give the dimensions of the test specimens with specimen thickness, end distance, side distance and width, respectively. Columns (9) and (10) give the maximum load attained by the specimen and the damage load recorded from the load-stroke plots. Finally, columns (11) and (12) show the failure mode found for each test, either the (ultimate) failure at maximum load (12) or the failure at the damage load (11).

D.2 Single Bolt Connections

Table D.1: Single Bolt Double Lap Shear Connection Test Results for Flange and Web Material tested with a M12 size bolt and steel side plates

Test Label	Diameter of Pin, d (mm)	Diameter of Hole, d_n (mm)	Clearance (mm)	Specimen Thickness, t (mm)	End Distance, e_1 (mm)	Side Distance, e_2 (mm)	Width, w (mm)	Maximum Load (kN)	Damage Load (kN)	Failure Mode	2nd Failure Mode
A1-01	11.84	13.60	1.76	9.37	24.00	18.00	36.00	30.07	20.03	SO	NT
A1-02	11.84	13.60	1.76	9.39	24.00	18.00	36.00	26.52	23.66	SO	NT
A1-03	11.84	13.60	1.76	9.36	24.00	18.00	36.00	27.34	22.27	SO	NT
A1-04	11.84	13.60	1.76	9.34	24.00	18.00	36.00	23.76	19.81	SO	NT
A1-05	11.84	13.60	1.76	9.40	24.00	18.00	36.00	28.53	20.32	SO	NT
Mean	11.84	13.60	1.76	9.37	24.00	18.00	36.00	27.24	21.22	-	-
A2-01	11.84	13.60	1.76	9.35	24.00	24.00	48.00	28.77	18.44	SO	NT
A2-02	11.84	13.60	1.76	9.48	24.00	24.00	48.00	27.26	15.75	SO	NT
A2-03	11.84	13.60	1.76	9.52	24.00	24.00	48.00	27.78	18.52	SO	NT
A2-04	11.84	13.60	1.76	9.55	24.00	24.00	48.00	27.14	-	SO	NT
A2-05	11.84	13.60	1.76	9.40	24.00	24.00	48.00	26.97	19.45	SO	NT
Mean	11.84	13.60	1.76	9.46	24.00	24.00	48.00	27.58	18.04	-	-
A3-01	11.84	13.60	1.76	9.49	24.00	48.00	96.00	25.52	14.69	SO	SO
A3-02	11.84	13.60	1.76	9.49	24.00	48.00	96.00	27.36	16.20	SO	SO
A3-03	11.84	13.60	1.76	9.34	24.00	48.00	96.00	27.32	21.04	SO	SO
A3-04	11.84	13.60	1.76	9.35	24.00	48.00	96.00	28.39	19.77	SO	SO
A3-05	11.84	13.60	1.76	9.33	24.00	48.00	96.00	29.23	19.73	SO	SO
Mean	11.84	13.60	1.76	9.40	24.00	48.00	96.00	27.56	18.29	-	-
A4-01	11.84	13.60	1.76	9.36	48.00	24.00	48.00	51.59	19.58	BR	SO
A4-02	11.84	13.60	1.76	9.53	48.00	24.00	48.00	43.31	19.53	BR	SO
A4-03	11.84	13.60	1.76	9.39	48.00	24.00	48.00	53.82	20.10	BR	SO
A4-04	11.84	13.60	1.76	9.34	48.00	24.00	48.00	51.13	20.79	BR	SO
A4-05	11.84	13.60	1.76	9.36	48.00	24.00	48.00	50.15	18.04	BR	SO
Mean	11.84	13.60	1.76	9.40	48.00	24.00	48.00	50.00	19.61	-	-
A5-01	11.84	13.60	1.76	9.37	48.00	48.00	96.00	59.61	27.21	BR	SO
A5-02	11.84	13.60	1.76	9.33	48.00	48.00	96.00	55.97	36.05	BR	SO
A5-03	11.84	13.60	1.76	9.40	48.00	48.00	96.00	58.95	38.51	BR	SO
A5-04	11.84	13.60	1.76	9.37	48.00	48.00	96.00	58.14	36.42	BR	SO
A5-05	11.84	13.60	1.76	9.50	48.00	48.00	96.00	49.13	26.05	BR	SO
Mean	11.84	13.60	1.76	9.39	48.00	48.00	96.00	56.36	32.85	-	-
A13-01	11.84	13.60	1.76	9.45	24.00	18.00	36.00	22.18	16.42	SO	-
A13-02	11.84	13.60	1.76	9.52	24.00	18.00	36.00	22.10	12.91	SO	-
A13-03	11.84	13.60	1.76	9.49	24.00	18.00	36.00	21.51	11.68	SO	-
A13-04	11.84	13.60	1.76	9.48	24.00	18.00	36.00	18.82	14.83	SO	-
A13-05	11.84	13.60	1.76	9.51	24.00	18.00	36.00	23.06	16.80	SO	-
Mean	11.84	13.60	1.76	9.49	24.00	18.00	36.00	21.53	14.53	-	-
A14-01	11.84	13.60	1.76	9.52	24.00	24.00	48.00	22.29	15.37	SO	-
A14-02	11.84	13.60	1.76	9.44	24.00	24.00	48.00	20.62	14.76	SO	-
A14-03	11.84	13.60	1.76	9.44	24.00	24.00	48.00	21.03	13.73	SO	-
A14-04	11.84	13.60	1.76	9.51	24.00	24.00	48.00	22.59	-	SO	-
A14-05	11.84	13.60	1.76	9.49	24.00	24.00	48.00	20.91	14.05	SO	-
Mean	11.84	13.60	1.76	9.48	24.00	24.00	48.00	21.49	14.48	-	-
A15-01	11.84	13.60	1.76	9.47	48.00	24.00	48.00	35.35	20.84	BR	-
A15-02	11.84	13.60	1.76	9.47	48.00	24.00	48.00	36.94	21.37	BR	-
A15-03	11.84	13.60	1.76	9.45	48.00	24.00	48.00	38.47	26.80	BR	-
A15-04	11.84	13.60	1.76	9.47	48.00	24.00	48.00	35.32	19.26	BR	-
A15-05	11.84	13.60	1.76	9.53	48.00	24.00	48.00	32.85	22.64	BR	-
Mean	11.84	13.60	1.76	9.48	48.00	24.00	48.00	35.79	22.18	-	-
A18-01	11.84	13.60	1.76	9.65	48.00	18.00	36.00	39.35	26.70	BR	NT
A18-02	11.84	13.60	1.76	9.50	48.00	18.00	36.00	37.78	29.17	BR	NT
A18-03	11.84	13.60	1.76	9.38	48.00	18.00	36.00	42.23	20.58	BR	NT
A18-04	11.84	13.60	1.76	9.50	48.00	18.00	36.00	35.55	16.24	BR	NT
A18-05	11.84	13.60	1.76	9.63	48.00	18.00	36.00	37.72	19.05	BR	NT
Mean	11.84	13.60	1.76	9.53	48.00	18.00	36.00	38.53	22.35	-	-
A19-01	11.84	13.60	1.76	9.47	48.00	18.00	36.00	37.12	24.37	BR	SO
A19-02	11.84	13.60	1.76	9.49	48.00	18.00	36.00	33.40	22.27	BR	SO
A19-03	11.84	13.60	1.76	9.54	48.00	18.00	36.00	37.60	22.51	BR	SO
A19-04	11.84	13.60	1.76	9.57	48.00	18.00	36.00	31.26	27.65	BR	SO
A19-05	11.84	13.60	1.76	9.43	48.00	18.00	36.00	34.98	23.81	BR	SO
Mean	11.84	13.60	1.76	9.50	48.00	18.00	36.00	34.87	24.12	-	-

Table D.2: Single Bolt Double Lap Shear Connection Test Results for M10 to M20 size bolts and Longitudinal Flange Material

Test Label	Diameter of Pin, d (mm)	Diameter of Hole, d_n (mm)	Clearance (mm)	Thickness of Specimen, t (mm)	End Distance, e_1 (mm)	Side Distance, e_2 (mm)	Width, w (mm)	Damage Load (kN)
WP2-A/F/0/M10-01	9.80	11.60	1.80	9.54	50.00	25.00	50.00	24.15
WP2-A/F/0/M10-02	9.80	11.60	1.80	9.60	50.00	25.00	50.00	21.05
WP2-A/F/0/M10-03	9.80	11.60	1.80	9.66	50.00	25.00	50.00	22.74
WP2-A/F/0/M10-04	9.80	11.60	1.80	9.55	50.00	25.00	50.00	23.49
WP2-A/F/0/M10-05	9.80	11.60	1.80	9.62	50.00	25.00	50.00	23.89
Mean	9.80	11.60	1.80	9.59	50.00	25.00	50.00	23.06
WP2-A/F/0/M12-01	11.84	13.60	1.76	9.59	60.00	30.00	60.00	23.71
WP2-A/F/0/M12-02	11.84	13.60	1.76	10.31	60.00	30.00	60.00	23.71
WP2-A/F/0/M12-03	11.84	13.60	1.76	10.26	60.00	30.00	60.00	25.48
WP2-A/F/0/M12-04	11.84	13.60	1.76	10.27	60.00	30.00	60.00	27.49
WP2-A/F/0/M12-05	11.84	13.60	1.76	9.59	60.00	30.00	60.00	24.01
Mean	11.84	13.60	1.76	10.00	60.00	30.00	60.00	24.88
WP2-A/F/0/M16-01	15.81	17.60	1.79	10.34	80.00	40.00	80.00	32.26
WP2-A/F/0/M16-02	15.81	17.60	1.79	9.55	80.00	40.00	80.00	26.66
WP2-A/F/0/M16-03	15.81	17.60	1.79	9.56	80.00	40.00	80.00	30.54
WP2-A/F/0/M16-04	15.81	17.60	1.79	10.22	80.00	40.00	80.00	29.33
WP2-A/F/0/M16-05	15.81	17.60	1.79	9.62	80.00	40.00	80.00	33.16
Mean	15.81	17.60	1.79	9.86	80.00	40.00	80.00	30.39
WP2-A/F/0/M20-01	19.80	21.60	1.80	9.60	100.00	50.00	100.00	35.84
WP2-A/F/0/M20-02	19.80	21.60	1.80	9.58	100.00	50.00	100.00	44.01
WP2-A/F/0/M20-03	19.80	21.60	1.80	10.17	100.00	50.00	100.00	38.18
WP2-A/F/0/M20-04	19.80	21.60	1.80	10.31	100.00	50.00	100.00	45.72
WP2-A/F/0/M20-05	19.80	21.60	1.80	10.31	100.00	50.00	100.00	38.20
Mean	19.80	21.60	1.80	9.99	100.00	50.00	100.00	40.39

Table D.3: Single Bolt Double Lap Shear Connection Test Results for M10 to M20 size bolts and Longitudinal Web Material

Test Label	Diameter of Pin, d (mm)	Diameter of Hole, d_n (mm)	Clearance (mm)	Thickness of Specimen, t (mm)	End Distance, e_1 (mm)	Side Distance, e_2 (mm)	Width, w (mm)	Damage Load (kN)
WP2-A/W/0/M10-01	9.80	11.60	1.80	9.62	50.00	25.00	50.00	18.85
WP2-A/W/0/M10-02	9.83	11.60	1.77	9.60	50.00	25.00	50.00	21.46
WP2-A/W/0/M10-03	9.80	11.60	1.80	9.65	50.00	25.00	50.00	29.01
WP2-A/W/0/M10-04	9.83	11.60	1.77	9.64	50.00	25.00	50.00	24.77
WP2-A/W/0/M10-05	9.83	11.60	1.77	9.62	50.00	25.00	50.00	24.36
Mean	9.82	11.60	1.78	9.63	50.00	25.00	50.00	23.69
WP2-A/W/0/M12-01	11.84	13.60	1.76	9.62	60.00	30.00	60.00	19.63
WP2-A/W/0/M12-02	11.84	13.60	1.76	9.62	60.00	30.00	60.00	25.72
WP2-A/W/0/M12-03	11.84	13.60	1.76	9.64	60.00	30.00	60.00	18.00
WP2-A/W/0/M12-04	11.84	13.60	1.76	9.63	60.00	30.00	60.00	25.60
WP2-A/W/0/M12-05	11.84	13.60	1.76	9.63	60.00	30.00	60.00	26.28
Mean	11.84	13.60	1.76	9.63	60.00	30.00	60.00	23.05
WP2-A/W/0/M16-01	15.81	17.60	1.79	9.61	80.00	40.00	80.00	27.65
WP2-A/W/0/M16-02	15.81	17.60	1.79	9.62	80.00	40.00	80.00	30.51
WP2-A/W/0/M16-03	15.81	17.60	1.79	9.63	80.00	40.00	80.00	28.52
WP2-A/W/0/M16-04	15.81	17.60	1.79	9.61	80.00	40.00	80.00	24.85
WP2-A/W/0/M16-05	15.81	17.60	1.79	9.62	80.00	40.00	80.00	28.89
Mean	15.81	17.60	1.79	9.62	80.00	40.00	80.00	28.08
WP2-A/W/0/M20-01	19.80	21.60	1.80	9.61	100.00	50.00	100.00	40.75
WP2-A/W/0/M20-02	19.80	21.60	1.80	9.63	100.00	50.00	100.00	42.60
WP2-A/W/0/M20-03	19.80	21.60	1.80	9.61	100.00	50.00	100.00	46.29
WP2-A/W/0/M20-04	19.80	21.60	1.80	9.63	100.00	50.00	100.00	40.54
WP2-A/W/0/M20-05	19.80	21.60	1.80	9.62	100.00	50.00	100.00	34.91
Mean	19.80	21.60	1.80	9.62	100.00	50.00	100.00	41.02

Table D.4: Single Bolt Double Lap Shear Connection Test Results for M10 to M20 size bolts and Transverse Web Material

Test Label	Diameter of Pin, d (mm)	Diameter of Hole, d_n (mm)	Clearance (mm)	Specimen Thickness, t (mm)	End Distance, e_1 (mm)	Side Distance, e_2 (mm)	Width, w (mm)	Maximum Load (kN)	Damage Load (kN)
WP2-A/W/90/M10-01	9.80	11.60	1.80	9.61	50.00	25.00	50.00	26.56	25.75
WP2-A/W/90/M10-02	9.80	11.60	1.80	9.61	50.00	25.00	50.00	24.06	-
WP2-A/W/90/M10-03	9.80	11.60	1.80	9.60	50.00	25.00	50.00	25.27	-
WP2-A/W/90/M10-04	9.80	11.60	1.80	9.63	50.00	25.00	50.00	25.84	-
WP2-A/W/90/M10-05	9.80	11.60	1.80	9.61	50.00	25.00	50.00	28.53	27.15
Mean	9.80	11.60	1.80	9.61	50.00	25.00	50.00	26.05	26.45
WP2-A/W/90/M12-01	11.84	13.60	1.76	9.61	60.00	30.00	60.00	32.22	26.72
WP2-A/W/90/M12-02	11.84	13.60	1.76	9.60	60.00	30.00	60.00	29.92	-
WP2-A/W/90/M12-03	11.84	13.60	1.76	9.62	60.00	30.00	60.00	30.24	-
WP2-A/W/90/M12-04	11.84	13.60	1.76	9.62	60.00	30.00	60.00	34.09	-
WP2-A/W/90/M12-05	11.84	13.60	1.76	9.63	60.00	30.00	60.00	31.35	23.08
Mean	11.84	13.60	1.76	9.62	60.00	60.00	30.00	31.56	24.90
WP2-A/W/90/M16-01	15.81	17.60	1.79	9.62	80.00	40.00	80.00	43.21	20.38
WP2-A/W/90/M16-02	15.81	17.60	1.79	9.61	80.00	40.00	80.00	43.61	24.63
WP2-A/W/90/M16-03	15.81	17.60	1.79	9.64	80.00	40.00	80.00	44.56	20.21
WP2-A/W/90/M16-04	15.81	17.60	1.79	9.62	80.00	40.00	80.00	41.55	21.06
WP2-A/W/90/M16-05	15.81	17.60	1.79	9.63	80.00	40.00	80.00	45.83	22.42
Mean	15.81	17.60	1.79	9.62	80.00	40.00	80.00	43.75	21.74
WP2-A/W/90/M20-01	19.80	21.60	1.80	9.63	100.00	50.00	100.00	50.12	46.79
WP2-A/W/90/M20-02	19.80	21.60	1.80	9.62	100.00	50.00	100.00	48.89	48.89
WP2-A/W/90/M20-03	19.80	21.60	1.80	9.62	100.00	50.00	100.00	51.13	46.33
WP2-A/W/90/M20-04	19.80	21.60	1.80	9.61	100.00	50.00	100.00	54.56	-
WP2-A/W/90/M20-05	19.80	21.60	1.80	9.62	100.00	50.00	100.00	49.35	-
Mean	19.80	21.60	1.80	9.62	100.00	50.00	100.00	50.81	47.34

Table D.5: Single Bolt Double Lap Shear Connection Test Results for Flange and Web Material tested with a M12 size bolt and PFRP side plates

Test Label	Diameter of Pin, d (mm)	Diameter of Hole, d_n (mm)	Clearance (mm)	Specimen Thickness, t (mm)	End Distance, e_1 (mm)	Side Distance, e_2 (mm)	Width, w (mm)	Maximum Load (kN)	Damage Load (kN)	Failure Mode	2nd Failure Mode
A6-01	11.84	13.60	1.76	9.36	24.00	18.00	36.00	21.93	18.33	BR/SO	-
A6-02	11.84	13.60	1.76	9.39	24.00	18.00	36.00	-	19.38	BR/SO	-
A6-03	11.84	13.60	1.76	9.36	24.00	18.00	36.00	-	18.15	BR/SO	-
A6-04	11.84	13.60	1.76	9.37	24.00	18.00	36.00	-	19.22	BR/SO	-
A6-05	11.84	13.60	1.76	9.40	24.00	18.00	36.00	-	18.83	BR/SO	-
Mean	11.84	13.60	1.76	9.38	24.00	18.00	36.00	21.93	18.78	-	-
A7-01	11.84	13.60	1.76	9.54	24.00	24.00	48.00	20.09	14.92	SO	-
A7-02	11.84	13.60	1.76	9.53	24.00	24.00	48.00	17.77	13.16	SO	-
A7-03	11.84	13.60	1.76	9.56	24.00	24.00	48.00	-	13.45	SO	-
A7-04	11.84	13.60	1.76	9.55	24.00	24.00	48.00	18.57	14.58	SO	-
A7-05	11.84	13.60	1.76	9.50	24.00	24.00	48.00	-	13.92	SO	-
Mean	11.84	13.60	1.76	9.54	24.00	24.00	48.00	18.81	14.01	-	-
A11-01	11.84	13.60	1.76	9.39	48.00	24.00	48.00	44.81	29.02	BR	-
A11-02	11.84	13.60	1.76	9.44	48.00	24.00	48.00	-	19.91	BR	-
A11-03	11.84	13.60	1.76	9.39	48.00	24.00	48.00	-	18.97	BR	-
A11-04	11.84	13.60	1.76	9.43	48.00	24.00	48.00	-	19.78	BR	-
A11-05	11.84	13.60	1.76	9.49	48.00	24.00	48.00	-	18.89	BR	-
Mean	11.84	13.60	1.76	9.43	48.00	24.00	48.00	44.81	21.31	-	-

Table D.6: Single Bolt Single Lap Shear Connection Test Results for Flange and Web Material tested with a M12 size bolt and steel side plates

Test Label	Diameter of Pin, d (mm)	Diameter of Hole, d_n (mm)	Clearance (mm)	Plate A Thickness , t (mm)	Plate B Thickness , t (mm)	End Distance, e_1 (mm)	Side Distance, e_2 (mm)	Maximum Load (kN)	Damage Load (kN)	Failure Mode	2nd Failure Mode
A8-01	11.84	13.60	1.76	9.51	9.52	24.00	18.00	-	16.14	SO(A)	-
A8-02	11.84	13.60	1.76	9.50	9.55	24.00	18.00	-	17.76	SO(B)	-
A8-03	11.84	13.60	1.76	9.58	9.55	24.00	18.00	-	15.65	SO(A)	-
A8-04	11.84	13.60	1.76	9.55	9.53	24.00	18.00	15.64	14.92	SO(A)	-
A8-05	11.84	13.60	1.76	9.58	9.59	24.00	18.00	15.37	14.66	SO(A&B)	-
Mean	11.84	13.60	1.76	9.54	9.55	24.00	18.00	15.51	15.83	-	-
A9-01	11.84	13.60	1.76	9.52	9.50	24.00	24.00	-	20.35	SO(B)	-
A9-02	11.84	13.60	1.76	9.50	9.55	24.00	24.00	-	16.45	SO(B)	-
A9-03	11.84	13.60	1.76	9.50	9.52	24.00	24.00	-	19.21	SO	-
A9-04	11.84	13.60	1.76	9.53	9.52	24.00	24.00	-	15.79	SO(A)	-
A9-05	11.84	13.60	1.76	9.56	9.53	24.00	24.00	-	16.86	SO(B)	-
Mean	11.84	13.60	1.76	9.52	9.52	24.00	24.00	-	17.73	-	-
A10-01	11.84	13.60	1.76	9.53	9.51	48.00	24.00	28.95	13.30	BR	-
A10-02	11.84	13.60	1.76	9.55	9.49	48.00	24.00	21.27	14.75	BR	-
A10-03	11.84	13.60	1.76	9.54	9.58	48.00	24.00	18.22	13.02	BR	-
A10-04	11.84	13.60	1.76	9.53	9.51	48.00	24.00	17.03	14.35	BR	-
A10-05	11.84	13.60	1.76	9.51	9.56	48.00	24.00	-	13.62	BR	-
Mean	11.84	13.60	1.76	9.53	9.53	48.00	24.00	21.37	13.81	-	-
A12-01	11.84	13.60	1.76	9.40	9.46	48.00	48.00	35.69	21.58	BR	-
A12-02	11.84	13.60	1.76	9.54	9.51	48.00	48.00	23.99	20.80	BR	-
A12-03	11.84	13.60	1.76	9.50	9.38	48.00	48.00	-	19.17	BR	-
A12-04	11.84	13.60	1.76	9.36	9.35	48.00	48.00	-	21.82	BR	-
A12-05	11.84	13.60	1.76	9.49	9.48	48.00	48.00	-	20.77	BR	-
Mean	11.84	13.60	1.76	9.46	9.44	48.00	48.00	29.84	20.83	-	-
A16-01	11.84	13.60	1.76	9.55	9.61	24.00	24.00	12.63	10.83	SO(A)	-
A16-02	11.84	13.60	1.76	9.48	9.53	24.00	24.00	11.71	11.03	SO(A)	-
A16-03	11.84	13.60	1.76	9.46	9.48	24.00	24.00	15.66	14.51	SO(A)	-
A16-04	11.84	13.60	1.76	9.54	9.46	24.00	24.00	14.46	12.16	SO(A)	-
A16-05	11.84	13.60	1.76	9.54	9.52	24.00	24.00	-	14.27	SO(A&B)	-
Mean	11.84	13.60	1.76	9.51	9.52	24.00	24.00	13.62	12.56	-	-
A17-01	11.84	13.60	1.76	9.55	9.45	48.00	24.00	-	26.49	BR	-
A17-02	11.84	13.60	1.76	9.45	9.45	48.00	24.00	25.07	16.94	BR	-
A17-03	11.84	13.60	1.76	9.48	9.47	48.00	24.00	24.40	16.61	BR	-
A17-04	11.84	13.60	1.76	9.47	9.47	48.00	24.00	24.05	19.38	BR	SO
A17-05	11.84	13.60	1.76	9.56	9.51	48.00	24.00	-	25.47	BR	-
Mean	11.84	13.60	1.76	9.50	9.47	48.00	24.00	24.51	20.98	-	-
A20-01	11.84	13.60	1.76	9.50	9.54	48.00	18.00	25.59	13.28	BR	NT
A20-02	11.84	13.60	1.76	9.63	9.51	48.00	18.00	-	14.42	BR	-
A20-03	11.84	13.60	1.76	9.41	9.64	48.00	18.00	18.36	12.34	BR	-
A20-04	11.84	13.60	1.76	9.65	9.62	48.00	18.00	-	14.40	BR	-
A20-05	11.84	13.60	1.76	9.50	9.40	48.00	18.00	-	15.92	BR	-
Mean	11.84	13.60	1.76	9.54	9.54	48.00	18.00	21.98	14.07	-	-
A21-01	11.84	13.60	1.76	9.70	9.56	48.00	18.00	20.07	13.91	BR	SO
A21-02	11.84	13.60	1.76	9.60	9.60	48.00	18.00	23.09	15.74	BR	SO
A21-03	11.84	13.60	1.76	9.56	9.57	48.00	18.00	23.76	16.30	BR	SO
A21-04	11.84	13.60	1.76	9.58	9.50	48.00	18.00	23.27	17.40	BR	-
A21-05	11.84	13.60	1.76	9.48	9.56	48.00	18.00	23.92	-	BR	-
Mean	11.84	13.60	1.76	9.58	9.56	48.00	18.00	22.82	15.84	-	-

D.3 Two Bolt Connections

Table D.7: Two Bolts in a Column Double Lap Shear Connection Test Results for Flange and Web Material tested with a M12 size bolt and steel side plates

Test Label	Diameter of Pin, d (mm)	Diameter of Hole, d_n (mm)	Clearance (mm)	Specimen Thickness, t (mm)	End Distance, e_1 (mm)	Side Distance, e_2 (mm)	Width, w (mm)	Maximum Load (kN)	Damage Load (kN)	Failure Mode	2nd Failure Mode
B1-01	11.84	13.60	1.76	9.64	24.00	18.00	36.00	38.78	23.30	SO	NT
B1-02	11.84	13.60	1.76	9.51	24.00	18.00	36.00	49.28	-	SO	NT
B1-03	11.84	13.60	1.76	9.51	24.00	18.00	36.00	51.78	33.77	SO	NT
B1-04	11.84	13.60	1.76	9.51	24.00	18.00	36.00	48.38	33.78	SO	NT
B1-05	11.84	13.60	1.76	9.48	24.00	18.00	36.00	52.35	38.97	SO	NT
Mean	11.84	13.60	1.76	9.53	24.00	18.00	36.00	48.11	32.46	-	-
B2-01	11.84	13.60	1.76	9.51	24.00	24.00	48.00	65.98	35.39	SO	NT
B2-02	11.84	13.60	1.76	9.49	24.00	24.00	48.00	64.36	29.07	SO	NT
B2-03	11.84	13.60	1.76	9.53	24.00	24.00	48.00	64.05	36.17	SO	NT
B2-04	11.84	13.60	1.76	9.52	24.00	24.00	48.00	66.84	39.20	SO	NT
B2-05	11.84	13.60	1.76	9.51	24.00	24.00	48.00	60.89	41.66	SO	NT
Mean	11.84	13.60	1.76	9.51	24.00	24.00	48.00	64.42	36.30	-	-
B3-01	11.84	13.60	1.76	9.36	24.00	48.00	96.00	70.86	38.73	BR	SO
B3-02	11.84	13.60	1.76	9.37	24.00	48.00	96.00	70.26	42.30	BR	SO
B3-03	11.84	13.60	1.76	9.34	24.00	48.00	96.00	72.45	42.89	BR	SO
B3-04	11.84	13.60	1.76	9.43	24.00	48.00	96.00	74.87	40.88	BR	SO
B3-05	11.84	13.60	1.76	9.38	24.00	48.00	96.00	74.08	44.00	BR	SO
Mean	11.84	13.60	1.76	9.38	24.00	48.00	96.00	72.50	41.76	-	-
B4-01	11.84	13.60	1.76	9.54	48.00	24.00	48.00	85.00	45.86	BR	NT
B4-02	11.84	13.60	1.76	9.36	48.00	24.00	48.00	80.13	39.63	BR	NT
B4-03	11.84	13.60	1.76	9.53	48.00	24.00	48.00	81.70	40.96	BR	NT
B4-04	11.84	13.60	1.76	9.38	48.00	24.00	48.00	79.17	48.46	BR	NT
B4-05	11.84	13.60	1.76	9.39	48.00	24.00	48.00	78.20	55.62	BR	NT
Mean	11.84	13.60	1.76	9.44	48.00	24.00	48.00	80.84	46.11	-	-
B5-01	11.84	13.60	1.76	9.52	48.00	48.00	96.00	82.37	-	BR	-
B5-02	11.84	13.60	1.76	9.52	48.00	48.00	96.00	77.97	-	BR	-
B5-03	11.84	13.60	1.76	9.38	48.00	48.00	96.00	72.61	-	BR	-
B5-04	11.84	13.60	1.76	9.36	48.00	48.00	96.00	88.81	-	BR	-
B5-05	11.84	13.60	1.76	9.52	48.00	48.00	96.00	78.01	-	BR	-
Mean	11.84	13.60	1.76	9.46	48.00	48.00	96.00	79.95	-	-	
B10-01	11.84	13.60	1.76	9.50	24.00	18.00	36.00	53.33	-	SO	-
B10-02	11.84	13.60	1.76	9.60	24.00	18.00	36.00	46.81	39.75	SO	NT
B10-03	11.84	13.60	1.76	9.47	24.00	18.00	36.00	53.93	-	SO	NT
B10-04	11.84	13.60	1.76	9.48	24.00	18.00	36.00	49.90	-	SO	NT
B10-05	11.84	13.60	1.76	9.47	24.00	18.00	36.00	52.47	-	SO	NT
Mean	11.84	13.60	1.76	9.50	24.00	18.00	36.00	51.29	39.75	-	-
B12-01	11.84	13.60	1.76	9.56	48.00	24.00	48.00	64.42	44.36	BR	SO
B12-02	11.84	13.60	1.76	9.49	48.00	24.00	48.00	71.41	28.92	BR	SO
B12-03	11.84	13.60	1.76	9.53	48.00	24.00	48.00	68.03	43.01	BR	SO
B12-04	11.84	13.60	1.76	9.42	48.00	24.00	48.00	75.60	45.85	BR	SO
B12-05	11.84	13.60	1.76	9.40	48.00	24.00	48.00	74.37	36.74	BR	SO
Mean	11.84	13.60	1.76	9.48	48.00	24.00	48.00	70.77	39.78	-	-

Table D.8: Two Bolts in a Column Double Lap Shear Connection Test Results for Flange and Web Material tested with a M12 size bolt and PFRP side plates

Test Label	Diameter of Pin, d (mm)	Diameter of Hole, d_n (mm)	Clearance (mm)	Specimen Thickness, t (mm)	End Distance, e_1 (mm)	Side Distance, e_2 (mm)	Width, w (mm)	Maximum Load (kN)	Damage Load (kN)	Failure Mode	2nd Failure Mode
B6-01	11.84	13.60	1.76	9.53	24.00	18.00	36.00	46.80	31.27	BR/SO	NT
B6-02	11.84	13.60	1.76	9.57	24.00	18.00	36.00	46.56	27.62	SO	NT
B6-03	11.84	13.60	1.76	9.52	24.00	18.00	36.00	44.75	29.87	SO	NT
B6-04	11.84	13.60	1.76	9.55	24.00	18.00	36.00	45.94	29.34	SO	NT
B6-05	11.84	13.60	1.76	9.51	24.00	18.00	36.00	45.53	30.65	SO	NT
Mean	11.84	13.60	1.76	9.54	24.00	18.00	36.00	45.92	29.75	-	
B7-01	11.84	13.60	1.76	9.54	24.00	24.00	48.00	53.76	32.04	BR	NT
B7-02	11.84	13.60	1.76	9.51	24.00	24.00	48.00	56.19	32.78	BR	NT
B7-03	11.84	13.60	1.76	9.55	24.00	24.00	48.00	53.33	37.08	BR/SO	NT
B7-04	11.84	13.60	1.76	9.51	24.00	24.00	48.00	-	31.66	BR/SO	-
B7-05	11.84	13.60	1.76	9.53	24.00	24.00	48.00	-	40.97	BR/SO	-
Mean	11.84	13.60	1.76	9.53	24.00	24.00	48.00	54.43	34.91	-	-

Table D.9: Two Bolts in a Column Single Lap Shear Connection Test Results for Flange and Web Material tested with a M12 size bolt

Test Label	Diameter of Pin, d (mm)	Diameter of Hole, d_n (mm)	Clearance (mm)	Plate A Thickness , t (mm)	Plate B Thickness , t (mm)	End Distance, e_1 (mm)	Side Distance, e_2 (mm)	Width, w (mm)	Maximum Load (kN)	Damage Load (kN)	Failure Mode	2nd Failure Mode
B8-01	11.84	13.60	1.76	9.39	9.38	24.00	18.00	36.00	42.03	35.09	SO(A)	-
B8-02	11.84	13.60	1.76	9.37	9.37	24.00	18.00	36.00	39.35	26.16	SO(B)	-
B8-03	11.84	13.60	1.76	9.41	9.52	24.00	18.00	36.00	39.04	28.07	SO(B)	-
B8-04	11.84	13.60	1.76	9.53	9.55	24.00	18.00	36.00	35.59	30.61	SO(B)	-
B8-05	11.84	13.60	1.76	9.53	9.54	24.00	18.00	36.00	35.88	26.42	SO(A&B)	-
Mean	11.84	13.60	1.76	9.45	9.47	24.00	18.00	36.00	38.38	29.27	-	-
B9-01	11.84	13.60	1.76	9.54	9.39	24.00	24.00	48.00	43.45	37.61	SO(B)	-
B9-02	11.84	13.60	1.76	9.38	9.42	24.00	24.00	48.00	49.20	31.55	SO(A&B)	-
B9-03	11.84	13.60	1.76	9.36	9.41	24.00	24.00	48.00	52.45	35.86	SO(A)	-
B9-04	11.84	13.60	1.76	9.37	9.48	24.00	24.00	48.00	-	31.27	SO(B)	-
B9-05	11.84	13.60	1.76	9.41	9.42	24.00	24.00	48.00	50.96	32.00	SO(A)	-
Mean	11.84	13.60	1.76	9.41	9.42	24.00	24.00	48.00	49.02	33.66	-	-
B11-01	11.84	13.60	1.76	9.41	9.42	24.00	18.00	36.00	36.69	30.45	SO(A&B)	-
B11-02	11.84	13.60	1.76	9.51	9.47	24.00	18.00	36.00	32.07	24.00	SO(A&B)	-
B11-03	11.84	13.60	1.76	9.47	9.52	24.00	18.00	36.00	-	28.39	SO(A&B)	-
B11-04	11.84	13.60	1.76	9.51	9.52	24.00	18.00	36.00	-	31.32	SO(A&B)	-
B11-05	11.84	13.60	1.76	9.46	9.54	24.00	18.00	36.00	33.61	27.26	SO(A&B)	-
Mean	11.84	13.60	1.76	9.47	9.49	24.00	18.00	36.00	34.12	28.28	-	-
B13-01	11.84	13.60	1.76	9.50	9.51	48.00	24.00	48.00	60.83	23.90	BR	NT
B13-02	11.84	13.60	1.76	9.34	9.48	48.00	24.00	48.00	61.35	29.90	BR	NT
B13-03	11.84	13.60	1.76	9.36	9.37	48.00	24.00	48.00	55.30	37.32	BR	NT
B13-04	11.84	13.60	1.76	9.37	9.33	48.00	24.00	48.00	42.62	30.88	BR	-
B13-05	11.84	13.60	1.76	9.47	9.35	48.00	24.00	48.00	55.10	29.00	BR	NT
Mean	11.84	13.60	1.76	9.41	9.41	48.00	24.00	48.00	55.04	30.20	-	-
B14-01	11.84	13.60	1.76	9.53	9.54	48.00	48.00	48.00	49.06	25.16	BR	-
B14-02	11.84	13.60	1.76	9.55	9.53	48.00	48.00	48.00	27.32	25.67	BR	-
B14-03	11.84	13.60	1.76	9.49	9.38	48.00	48.00	48.00	51.51	22.29	BR	-
B14-04	11.84	13.60	1.76	9.44	9.43	48.00	48.00	48.00	56.49	33.04	BR	-
B14-05	11.84	13.60	1.76	9.45	9.47	48.00	48.00	48.00	35.89	28.78	BR	-
Mean	11.84	13.60	1.76	9.49	9.47	48.00	48.00	48.00	44.05	26.99	-	-

Table D.10: Two Bolts in a Row Double Lap Shear Connection Test Results for Flange and Web Material tested with a M12 size bolt and steel side plates

Test Label	Diameter of Pin, d (mm)	Diameter of Hole, d_n (mm)	Clearance (mm)	Specimen Thickness, t (mm)	End Distance, e_1 (mm)	Side Distance, e_2 (mm)	Width, w (mm)	Maximum Load (kN)	Damage Load (kN)	Failure Mode	2nd Failure Mode
C1-01	11.84	13.60	1.76	9.37	24.00	18.00	84.00	60.79	42.31	SO	NT
C1-02	11.84	13.60	1.76	9.41	24.00	18.00	84.00	59.17	41.78	SO	NT
C1-03	11.84	13.60	1.76	9.36	24.00	18.00	84.00	55.69	43.24	SO	NT
C1-04	11.84	13.60	1.76	9.54	24.00	18.00	84.00	50.89	31.43	SO	NT
C1-05	11.84	13.60	1.76	9.39	24.00	18.00	84.00	56.46	38.37	SO	NT
Mean	11.84	13.60	1.76	9.41	24.00	18.00	84.00	56.60	39.43	-	-
C2-01	11.84	13.60	1.76	9.38	24.00	24.00	96.00	59.90	30.72	SO	-
C2-02	11.84	13.60	1.76	9.50	24.00	24.00	96.00	49.80	33.13	SO	-
C2-03	11.84	13.60	1.76	9.37	24.00	24.00	96.00	55.42	40.44	SO	-
C2-04	11.84	13.60	1.76	9.32	24.00	24.00	96.00	59.65	34.91	SO	-
C2-05	11.84	13.60	1.76	9.37	24.00	24.00	96.00	55.02	29.94	SO	CL
Mean	11.84	13.60	1.76	9.39	24.00	24.00	96.00	55.96	33.83	-	-
C3-01	11.84	13.60	1.76	9.52	24.00	48.00	144.00	51.09	32.20	SO	-
C3-02	11.84	13.60	1.76	9.50	24.00	48.00	144.00	51.30	33.46	SO	-
C3-03	11.84	13.60	1.76	9.49	24.00	48.00	144.00	50.66	30.03	SO	-
C3-04	11.84	13.60	1.76	9.52	24.00	48.00	144.00	49.56	33.81	SO	-
C3-05	11.84	13.60	1.76	9.53	24.00	48.00	144.00	48.84	33.71	SO	-
Mean	11.84	13.60	1.76	9.51	24.00	48.00	144.00	50.29	32.64	-	-
C4-01	11.84	13.60	1.76	9.34	48.00	24.00	96.00	103.01	90.97	BR	NT
C4-02	11.84	13.60	1.76	9.35	48.00	24.00	96.00	101.84	98.10	BR	NT
C4-03	11.84	13.60	1.76	9.36	48.00	24.00	96.00	105.36	95.16	BR	NT
C4-04	11.84	13.60	1.76	9.35	48.00	24.00	96.00	108.89	84.37	BR	NT
C4-05	11.84	13.60	1.76	9.39	48.00	24.00	96.00	111.64	84.37	BR	NT
Mean	11.84	13.60	1.76	9.36	48.00	24.00	96.00	106.15	90.59	-	-
C7-01	11.84	13.60	1.76	9.46	24.00	18.00	84.00	43.89	33.08	SO	NT
C7-02	11.84	13.60	1.76	9.48	24.00	18.00	84.00	40.88	29.00	SO	NT
C7-03	11.84	13.60	1.76	9.52	24.00	18.00	84.00	40.01	29.80	SO	NT
C7-04	11.84	13.60	1.76	9.57	24.00	18.00	84.00	30.49	25.55	SO	NT
C7-05	11.84	13.60	1.76	9.51	24.00	18.00	84.00	39.56	27.80	SO	NT
Mean	11.84	13.60	1.76	9.51	24.00	18.00	84.00	38.97	29.05	-	-
C9-01	11.84	13.60	1.76	9.41	24.00	18.00	84.00	56.59	-	CL	-
C9-02	11.84	13.60	1.76	9.57	24.00	18.00	84.00	44.80	-	CL	-
C9-03	11.84	13.60	1.76	9.57	24.00	18.00	84.00	48.59	-	CL	-
C9-04	11.84	13.60	1.76	9.52	24.00	18.00	84.00	43.81	-	CL	-
C9-05	11.84	13.60	1.76	9.56	24.00	18.00	84.00	46.94	-	CL	-
Mean	11.84	13.60	1.76	9.53	24.00	18.00	84.00	48.15	-	-	-

Table D.11: Two Bolts in a Row Single Lap Shear Connection Test Results for Flange and Web Material tested with a M12 size bolt

Test Label	Diameter of Pin, d (mm)	Diameter of Hole, d_n (mm)	Clearance (mm)	Plate A Thickness , t (mm)	Plate B Thickness , t (mm)	End Distance, e_1 (mm)	Side Distance, e_2 (mm)	Maximum Load (kN)	Damage Load (kN)	Failure Mode	2nd Failure Mode
C6-01	11.84	13.60	1.76	9.63	9.38	24.00	18.00	36.50	35.33	SO(A)	-
C6-02	11.84	13.60	1.76	9.43	9.35	24.00	18.00	44.09	43.63	SO(B)	-
C6-03	11.84	13.60	1.76	9.50	9.37	24.00	18.00	38.56	31.15	SO(A)	-
C6-04	11.84	13.60	1.76	9.37	9.48	24.00	18.00	37.91	34.28	SO(B)	-
C6-05	11.84	13.60	1.76	9.38	9.38	24.00	18.00	43.67	40.42	SO	-
Mean	11.84	13.60	1.76	9.46	9.39	24.00	18.00	40.15	36.96		-
C8-01	11.84	13.60	1.76	9.43	9.56	24.00	18.00	-	-	-	-
C8-02	11.84	13.60	1.76	9.51	9.50	24.00	18.00	-	-	-	-
C8-03	11.84	13.60	1.76	9.41	9.56	24.00	18.00	28.66	26.29	SO(B)	-
C8-04	11.84	13.60	1.76	9.46	9.50	24.00	18.00	29.16	18.10	SO(B)	-
C8-05	11.84	13.60	1.76	9.42	9.48	24.00	18.00	26.62	22.61	SO(A)	-
Mean	11.84	13.60	1.76	9.45	9.52	24.00	18.00	28.15	22.33	-	-

Table D.12: Two Bolt Staggered Double Lap Shear Connection Test Results for Flange and Web Material tested with a M12 size bolt and steel side plates

Test Label	Diameter of Pin, d (mm)	Diameter of Hole, d_n (mm)	Clearance (mm)	Specimen Thickness, t (mm)	End Distance, e_1 (mm)	Side Distance, e_2 (mm)	Width, w (mm)	Maximum Load (kN)	Damage Load (kN)	Failure Mode	2nd Failure Mode
E1-01	11.84	13.60	1.76	9.50	24.00	18.00	60.00	54.69	32.71	SO	NT
E1-02	11.84	13.60	1.76	9.52	24.00	18.00	60.00	61.06	42.09	SO	NT
E1-03	11.84	13.60	1.76	9.50	24.00	18.00	60.00	61.42	42.14	SO	NT
E1-04	11.84	13.60	1.76	9.51	24.00	18.00	60.00	59.21	36.48	SO	NT
E1-05	11.84	13.60	1.76	9.50	24.00	18.00	60.00	-	40.84	SO	NT
Mean	11.84	13.60	1.76	9.51	24.00	18.00	60.00	59.10	38.85	-	-
E2-01	11.84	13.60	1.76	9.50	24.00	24.00	72.00	62.17	39.94	SO	NT
E2-02	11.84	13.60	1.76	9.52	24.00	24.00	72.00	61.58	40.57	SO	NT
E2-03	11.84	13.60	1.76	9.53	24.00	24.00	72.00	64.49	46.54	SO	NT
E2-04	11.84	13.60	1.76	9.50	24.00	24.00	72.00	63.32	38.74	SO	NT
E2-05	11.84	13.60	1.76	9.58	24.00	24.00	72.00	64.08	42.21	SO	NT
Mean	11.84	13.60	1.76	9.53	24.00	24.00	72.00	63.13	41.60	-	-
E3-01	11.84	13.60	1.76	9.49	24.00	48.00	120.00	61.40	35.93	SO	-
E3-02	11.84	13.60	1.76	9.56	24.00	48.00	120.00	60.88	38.11	SO	-
E3-03	11.84	13.60	1.76	9.49	24.00	48.00	120.00	63.52	36.25	SO	-
E3-04	11.84	13.60	1.76	9.52	24.00	48.00	120.00	66.36	38.85	SO	-
E3-05	11.84	13.60	1.76	9.52	24.00	48.00	120.00	62.33	38.33	SO	-
Mean	11.84	13.60	1.76	9.52	24.00	48.00	120.00	62.90	37.49	-	-
E4-01	11.84	13.60	1.76	9.49	24.00	18.00	60.00	50.37	43.55	SO	NT
E4-02	11.84	13.60	1.76	9.53	24.00	18.00	60.00	50.89	41.50	SO	NT
E4-03	11.84	13.60	1.76	9.53	24.00	18.00	60.00	51.58	41.90	SO	NT
E4-04	11.84	13.60	1.76	9.46	24.00	18.00	60.00	52.72	36.42	SO	NT
E4-05	11.84	13.60	1.76	9.52	24.00	18.00	60.00	-	38.48	SO	NT
Mean	11.84	13.60	1.76	9.51	24.00	18.00	60.00	51.39	40.37	-	-

D.4 Four Bolt Connections

Table D.13: Four Bolt Double Lap Shear Connection Test Results for Flange and Web Material tested with a M12 size bolt and steel side plates

Test Label	Diameter of Pin, d (mm)	Diameter of Hole, d_n (mm)	Clearance (mm)	Specimen Thickness, t (mm)	End Distance, e_1 (mm)	Side Distance, e_2 (mm)	Width, w (mm)	Maximum Load (kN)	Damage Load (kN)	Failure Mode	2nd Failure Mode
D1-01	11.84	13.60	1.76	9.33	24.00	18.00	84.00	116.35	93.59	SO	NT
D1-02	11.84	13.60	1.76	9.36	24.00	18.00	84.00	124.19	93.20	SO	NT
D1-03	11.84	13.60	1.76	9.51	24.00	18.00	84.00	115.56	101.04	SO	NT
D1-04	11.84	13.60	1.76	9.35	24.00	18.00	84.00	125.18	100.06	SO	NT
D1-05	11.84	13.60	1.76	9.41	24.00	18.00	84.00	121.45	101.04	SO	NT
Mean	11.84	13.60	1.76	9.39	24.00	18.00	84.00	120.55	97.79	-	-
D2-01	11.84	13.60	1.76	9.36	24.00	24.00	96.00	150.29	118.70	SO	NT
D2-02	11.84	13.60	1.76	9.51	24.00	24.00	96.00	129.88	129.88	SO	NT
D2-03	11.84	13.60	1.76	9.39	24.00	24.00	96.00	151.86	133.51	SO	NT
D2-04	11.84	13.60	1.76	9.39	24.00	24.00	96.00	149.31	126.55	SO	NT
D2-05	11.84	13.60	1.76	9.35	24.00	24.00	96.00	146.56	87.31	SO	NT
Mean	11.84	13.60	1.76	9.40	24.00	24.00	96.00	145.58	119.19	-	-
D3-01	11.84	13.60	1.76	9.34	48.00	24.00	96.00	153.62	-	BR	NT
D3-02	11.84	13.60	1.76	9.32	48.00	24.00	96.00	156.96	-	BR	NT
D3-03	11.84	13.60	1.76	9.48	48.00	24.00	96.00	159.31	70.14	BR	NT
D3-04	11.84	13.60	1.76	9.32	48.00	24.00	96.00	150.09	-	BR	NT
D3-05	11.84	13.60	1.76	9.47	48.00	24.00	96.00	163.43	-	BR	NT
Mean	11.84	13.60	1.76	9.39	48.00	24.00	96.00	156.69	14.03	-	-
D7-01	11.84	13.60	1.76	9.47	24.00	18.00	84.00	102.22	81.42	SO	CL
D7-02	11.84	13.60	1.76	9.50	24.00	18.00	84.00	102.02	84.37	SO	CL
D7-03	11.84	13.60	1.76	9.52	24.00	18.00	84.00	104.38	76.52	SO	CL
D7-04	11.84	13.60	1.76	9.50	24.00	18.00	84.00	97.12	60.33	SO	CL
D7-05	11.84	13.60	1.76	9.55	24.00	18.00	84.00	90.45	69.16	SO	CL
Mean	11.84	13.60	1.76	9.51	24.00	18.00	84.00	99.24	74.36	-	-

Table D.14: Four Bolt Single Lap Shear Connection Test Results for Flange and Web Material tested with a M12 size bolt and steel side plates

Test Label	Diameter of Pin, d (mm)	Diameter of Hole, d_n (mm)	Clearance (mm)	Plate A Thickness , t (mm)	Plate B Thickness , t (mm)	End Distance, e_1 (mm)	Side Distance, e_2 (mm)	Width, w (mm)	Maximum Load (kN)	Damage Load (kN)	Failure Mode	2nd Failure Mode
D6-01	11.84	13.60	1.76	9.51	9.50	24.00	18.00	84.00	88.78	86.33	SO	CL
D6-02	11.84	13.60	1.76	9.50	9.51	24.00	18.00	84.00	85.15	60.82	SO	CL
D6-03	11.84	13.60	1.76	9.51	9.52	24.00	18.00	84.00	84.17	65.24	SO	CL
D6-04	11.84	13.60	1.76	9.52	9.49	24.00	18.00	84.00	85.35	63.27	SO	CL
D6-05	11.84	13.60	1.76	9.49	9.51	24.00	18.00	84.00	85.54	67.20	SO	CL
Mean	11.84	13.60	1.76	9.51	9.51	24.00	18.00	84.00	85.80	68.57	-	-
D8-01	11.84	13.60	1.76	9.46	9.48	24.00	18.00	84.00	70.04	52.97	SO	CL
D8-02	11.84	13.60	1.76	9.53	9.54	24.00	18.00	84.00	60.43	48.56	SO	CL
D8-03	11.84	13.60	1.76	9.49	9.52	24.00	18.00	84.00	68.08	46.11	SO	CL
D8-04	11.84	13.60	1.76	9.45	9.51	24.00	18.00	84.00	74.65	48.56	SO	CL
D8-05	11.84	13.60	1.76	9.58	9.78	24.00	18.00	84.00	54.74	42.18	SO	CL
Mean	11.84	13.60	1.76	9.50	9.57	24.00	18.00	84.00	65.59	47.68	-	-

References

Apicella, A., Migliaresi, C., Nicolais, L., Iaccarino, L. and Roccotelli, S. (1983), The Water Ageing of Unsaturated Polyester-based Composites: Influence of Resin Chemical Structure, *Composites*, **14**(4), 387–392.

ASCE (2013), Code of Standard Practice for Fabrication and Installation of Pultruded FRP Structures, *ANSI Standard*, American Composites Manufacturers Association, 2nd Edition, Arlington, Virginia, USA.

ACSE (2012), Pre-Standard for Load & Resistance Factor Design (LRFD) of Pultruded Fiber Reinforced Polymer (FRP) Structures, American Composites Manufacturers Association, 1st Editon, Arlington, Virginia, USA.

Ascione, F., Feo, L., and Maceri, F. (2009), An Experimental Investigation on the Bearing Failure Load of Glass Fibre/Epoxy Laminates, *Composites Part B: Engineering*, **40**(3), 197-205.

ASTM (2011), D2584-11: Standard Test Method for Ignition Loss of Cured Reinforced Resins, American Society for Testing and Materials International, West Conshohocken, Pennsylvania, USA.

ASTM (2012), D5379/D5379M-12: Standard Test Method for Shear Properties of Composite Materials by the V-Notched Beam Method, American Society for Testing and Materials International, West Conshohocken, Pennsylvania, USA.

ASTM (2013), D5764-97a: Standard Test Method for Evaluating Dowel-Bearing Strength of Wood and Wood-Based Products, American Society for Testing and Materials International, West Conshohocken, Pennsylvania, USA.

ASTM (2013), D 5961-13: Standard Test Method for Bearing Response of Polymer Matrix Composite Laminates, American Society for Testing and Materials International, West Conshohocken, Pennsylvania, USA.

ASTM (2006), D 7290-06: Standard Practice for Evaluating Material Property Characteristic Values for Polymeric Composites for Civil Engineering Structural Applications, American Society for Testing and Materials International, West Conshohocken, Pennsylvania, USA.

ASTM (2010), D 953-10: Standard test method for bearing strength of plastics, American Society for Testing and Materials International, West Conshohocken, Pennsylvania, USA.

ASTM (2014) E84-14: Standard Test Method for Surface Burning Characteristics of Building Materials, American Society for Testing and Materials International, West Conshohocken, Pennsylvania, USA.

Bach, P. W. (1996), The Effect of Moisture on the Fatigue Performance of Glass Fibre Reinforced Polyester Coupons and Bolted Joints, the *Proceedings of the European Community Wind Energy Conference (ECWECI93)*, 8-12 March, Travemünde, Germany.

Bank L. C., Gentry T. R., Thompson B. J. and Russell J. S. (2003), A Model Specification for FRP Composites for Civil Engineering Structures, *Construction and Building Materials*, 17, 405-437.

Bank, L. C., Gentry, T. R., and Barkatt, A. (1995), Accelerated Test Methods to determine the Long-term Behavior of FRP Composite Structures: Environmental Effects, *Journal of Reinforced Plastics and Composites*, **14**(6), 559-587.

Bank L. C. (2006), Composites for Construction: Structural Design with FRP Materials, John Wiley & Sons, Inc., Hoboken, New Jersey, USA.

Barker, A. J., and Balasundarum, V. (1987), Compression testing of Carbon Fibre Reinforced Plastics exposed to Humid Environments, *Composites*, **18**(3), 217-226.

Broughton, W. R., Crocker, L. E. and Gower, M. R. L. (2002), Design Requirements for Bonded and Bolted Composite Structures, National Physical Laboratory Materials Center, *NPL report MATC (A) 65*, January 2002.

BSI (2002), BS EN 13706-2: Reinforced plastic composites – Specification for pultruded profiles – Part 2: Methods of test and general requirements, British Standards Institute, London, UK.

BSI (2002), BS EN 1990: Basis of Structural Design, British Standards Institute, London, UK.

BSI (2005), BS EN 1993-1-8: Eurocode 3: Design of Steel Structures – Design of Joints, British Standards Institute, London, UK.

BSI (1995), BS EN 2378: Fibre Reinforced Plastics – Determination of Water Absorption by Immersion, British Standards Institute, London, UK.

BSI (2008), BS EN ISO 62: Plastics-Determination of Water Absorption, British Standards Institute, London, UK.

Cabral-Fonseca, S., Correia, J. R., Rodrigues, M. P. and Branco, F. A. (2012), Artificial Accelerated Ageing of GFRP Pultruded Profiles made of Polyester and Vinylester Resins: Characterisation of Physical–Chemical and Mechanical Damage, *Strain*, **48**(2) 162-173.

Cadei, J. and Stratford, T. (2002), The Design, Construction and in-service Performance of the All-composite Aberfeldy Footbridge, in the *Proceedings of the 1st International Conference on Advanced Polymer Composites for Structural Applications in Construction*, Thomas Telford, London, UK, Paper 8.1, 445-455.

Chamis, C. C. (1988), Simplified Procedures for Designing Composite Bolted Joints, *Proceedings of the 43rd Annual Conference of the Society of the Plastics Industry*, 1 -5 Feb, Cincinnati, Ohio, Session 23-D.

Chu, W. and Karbhari, V. M. (2005), Effect of Water Sorption on Performance of Pultruded E-Glass Vinylester Composites, *Journal of Materials in Civil Engineering*, 17(1), 63-71.

Clarke, J. L. (Ed.) (1996), Structural Design of Polymer Composites: EUROCOMP Design Code and Handbook, E. and FN Spon, London, UK.

Collings T. A. (1977), The Strength of Bolted Joints in Multi-directional CFRP Laminates, *Composites* **8**(1), 43-54.

Cooper, C. and Turvey, G. J. (1995) Effects of Joint Geometry and Bolt Torque on the Structural Performance of Single Bolt Tension Joints in Pultruded GRP Sheet Material, *Composite Structures*, **32**(1-4) 217-226.

Crank, J. (1995), The Mathematics of Diffusion, 2nd Edition, Oxford University Press, Oxford, UK.

Creative Pultrusions (2010), The New and Improved Pultrex® Pultrusion Design Manual, Creative Pultrusions, Inc., Alum Bank, PA.

D'Alessandro, R.G. (2009), Characteristic Values of Mechanical Properties of Wide-flange Pultruded FRF Beams, MSc Thesis, University of Wisconsin-Madison, USA.

Daniel, R. A. (2003), Environmental Considerations to Structural Material Selection for a Bridge, In *Proceedings of the European Bridge Engineering Conference*, Lightweight Bridge Decks, March, Rotterdam, the Netherlands.

Department of Defence (2002), Composite Material Handbook Volume 3: Polymer Matrix Composites- Materials Usages, Design and Analysis, *Military Handbook - MIL-HDBK-17-3F*, Department of Defence, USA.

Duncan, B. C. and Broughton, W. R. (2007), Absorption and Diffusion of Moisture in Polymeric Materials, *Measurement Good Practice Guide No. 102*, National Physical Laboratory, Teddington, UK, March 2007.

Eriksson, I. (1998), Plate-to-Plate Mechanical: Part I. Analysis and Design, in *State-of-the-art review on design, testing, analysis and application of polymeric composite connections, COST C1 Report*, Mottram, J. T. and Turvey, G. J. (Eds.), DG XII European Commission, Brussels & Luxembourg.

Erki, M. A. (1995), Bolted Glass-fibre-reinforced Plastic Joints, *Canadian Journal of Civil Engineering*, **22**(4), 736-744.

Evernden, M. C. (2006), Structural Evaluation of a Novel Box Beam System of PFRP Shapes, PhD Thesis, University of Warwick, UK.

Ghorbel, I. and Valentin, D. (2004), Hydrothermal Effects on the Physico-chemical Properties of Pure and Glass Fiber Reinforced Polyester and Vinylester Resins, *Polymer Composites*, **14**(4), 324-334.

Godwin, E. W. and Matthews, F. L. (1980), A Review of the Strength of Joints in Fibre Reinforced Plastics: Part 1. Mechanically Fastened Joints, *Composites*, **11**(3), 155-160.

Haeberle, J. and Matthews, F. L. (1990), Studies on Compressive Failure in Unidirectional CFRP using an Improved Test Method, in *Proceedings of the Fourth European Conference on Composites (ECCM-4)*, European Association for Composite Materials, Elsevier, London, UK, 517-523.

Hankinson, R. L. (1921), Investigation of Crushing Strength of Spruce at varying Angles of Grain, *Air Service Information Circular*, **3** (259), No. 130 Material Section Report.

Hart-Smith L. J. (1978), Mechanically Fastened Joints for Advanced Composites Phenomenological Considerations and Simple Analyses, in the *Proceedings of the 4th Conference on Fibrous Composites in Structural Design*, New York, 543-574.

Hassan, N. H., Mohamedien, M. A., and Rizkalla, S. H. (1996), Finite Element Analysis of Bolted Connections for PFRP Composites, *Composites: Part B*, **27**(3-4), 339-349.

Hyer, M. W., Klang, E. C. and Cooper, D. E. (1987), The Effects of Pin Elasticity, Clearance, and Friction on the Stresses in a Pin-loaded Orthotropic Plate, *Journal of Composite Materials*, **21**, 190–206.

Hassan M. and Iskander M. G. (2001), Accelerated Degradation of Recycled Plastic Piling in Aggressive Soils, *Journal of Composites in Construction*, **5**(3) 179-187.

Johnson, M. and Matthews, F. L. (1979), Determination of Safety Factors for use when Designing Bolted Joints in GRP, *Composites*, **10**(2) 155-160.

Karbhari, V. M. (Ed.) (2007), Durability of Composites for Civil Structural Applications, Woodhead Publishing in Civil and Structural Engineering. Cambridge, UK.

Karbhari, V. M., Chin, J. W., Hunston, D., Benmokrane, B., Juska, T., Morgan, R., Lesko, J. J., Sorathia, U. and Reynaud, D. (2003), Durability Gap Analysis for Fiber Reinforced Polymer Composites in Civil Infrastructure, *Journal of Composites for Construction*, **7**(3), 238-247.

Karbhari, V. M. and Zhang, S. (2003), E-Glass/Vinylester Composites in Aqueous Environments – I: Experimental Results, *Applied Composite Materials,* **10**(1) 19-48.

Kennedy, J. B. and Neville, A. M. (1986), Basic Statistical Methods for Engineers and Scientists, 3rd Edition, Harper & Row, London and New York.

Kim, D. H. (Ed.) (1995), Composite Structures for Civil and Architectural Engineering, E & FN Spon, London and New York.

Koerner, R., Lord, A., and Hsuan, Y. (1992), Arrhenius Modeling to Predict Geosynthetic Degradation, *Geotextiles and Geomembranes*, **11**(2), 151-183.

Lane A. (2002), An Experimental Investigation of Buckling Mode Interaction in PFRP Columns, PhD thesis, University of Warwick, UK.

Liao, K., Schultheisz, C. R., and Hunston, D. L. (1999), Effects of Environmental Aging on the Properties of Pultruded GFRP, *Composites Part B: Engineering*, **30**(5), 485-493.

Litherland K. L., Oakly D. R. and Proctor B. A. (1981), The Use of Accelerated Ageing Procedures to Predict the Long Term Strength of GRC Composites. Cement and Concrete Research, **11**(2), 455-466.

Lutz, C. (2006), Structural Integrity of Bolted Joints for Pultruded GRP Profiles, PhD thesis, University of Warwick, UK.

Matharu, N. S. and Mottram, J. T. (2012) Laterally Unrestrained Bolt Bearing Strength: Plain Pin and Threaded Values, in the *Proceedings of the 6th International Conference on FRP Composites in Civil Engineering (CICE 2012)*, Rome, Italy, Section 14: Codes and Design Guidelines, Paper 311.

McCarthy, M. A., McCarthy, C. T., Lawlor, V. P., and Stanley, W. F. (2005), Three-dimensional Finite Element Analysis of Single-bolt, Single-lap Composite Bolted Joints: Part I—Model Development and Validation, *Composite Structures*, **71**(2), 140-158.

Mosallam, A. S. (2011), Design guide for FRP composite connections, *Manuals of Practice (MOP) No. 102*, American Society of Civil Engineers, Reston, USA.

Mottram, J. T., (2010) Prediction of Net–tension Strength for Multi-row Bolted Connections of Pultruded Material using the Hart-Smith Semi-empirical Modeling Approach, *Journal of Composites for Construction*, **14**(1), 105-144.

Mottram, J. T. and Turvey, G. J., (Eds.) (1998), State-of-the-art Review on design, Testing, Analysis and Application of Polymeric Composite Connections, Polymeric Composite Structures Working Group 7, European Commission, Brussels & Luxembourg.

Mottram, J. T. and Turvey G. J. (2003), Physical Test Data for the Appraisal of Design Procedures for Bolted Joints in Pultruded FRP Structural Shapes and Systems, *Progress in Structural Engineering and Materials*, **5**(4), 195-222.

Mottram, J. T. and Zafari, B. (2011), Pin-bearing Strengths for Design of Bolted Connections in Pultruded Structures, *Structures and Buildings*, **164**(5), 291-305.

Mottram, J.T. (1994), Compression Strength of Pultruded Flat Sheet Material, *Journal of Materials in Civil Engineering*, **6**(2), 185-200.

Mottram, J.T. (2001), Analysis and Design of Connections for Pultruded FRP Structures, in the *Proceedings of the International Workshop on Composites in Construction: A Reality*, American Society of Civil Engineers, Special Publication, Reston, 250-257.

Mottram, J. T. (2004). Friction and Load Transfer in Bolted Joints of Pultruded Fibre Reinforced Polymer Section, in the Proceedings of *the 2nd International Conference on FRP Composites in Civil Engineering* (*CICE 2004),* 8-10 December, Adelaide, Australia.

Mottram, J.T. (2009a), Design Guidance for Bolted Connections in Structures of Pultruded Shapes: Gaps in Knowledge, in *Proceedings of the 17th International Conference on Composite Materials (ICCM17)*, 27-31 July 2009, Paper A1:6.

Mottram, J.T. (2009b), Determination of Pin-bearing Strength for the Design of Bolted Connections with Standard Pultruded Profiles, in the *Proceedings of the 4th International Conference on Advanced Composites in Construction (ACIC 2009)*, NetComposites Ltd., Chesterfield, UK, 483-495.

Nishizaki, I. and Meiarashi, S. (2002), Long-term Deterioration of GFRP in Water and Moist Environment, *Journal of Composites for Construction*, 6 (1), 21-27.

Maxwell, A.S. (2005), Review of Techniques for Monitoring the Environmental Degradation of Polymers, Engineering and Process Control Division, National Physical Laboratory, *NPL report DEPC MPR 015,* March 2005.

Purnell, P., Cain, J., van Itterbeeck P. and Lesko, J. (2008), Service Life Modelling of Fibre Composites: A Unified Approach, *Composites Science and Technology*, **68**(15-16) 3330-3336.

RCSC (2009), Specification for Structural Joints Using High-Strength Bolts, *Research Council on Structural Connections Publication*, Chicago, Illinois, USA.

Rosner, C. N. and Rizkalla, S. H. (1995a), Bolted Connections for Fiber-reinforced Composite Structural Members: Experimental Program, *Journal of Materials in Civil Engineering*, **7**(4), 223-231.

Rosner, C. N. and Rizkalla, S. H. (1995b), Bolted Connections for Fiber-Reinforced Composite Structural Members: Analytical Model and Design Recommendations, *Journal of Materials in Civil Engineering*, **7**(4), 232-238.

Robert, M., Wang, P., Cousin, P. and Benmokrane, B. (2010), Temperature as an Accelerating Factor for Long-term Durability Testing of FRPs: Should there be any Limitations? *Journal of Composites for Construction*, **14**(4), 361-367.

Rosner, R. N. (1992), Single-Bolted Connections for Orthotropic Fibre-Reinforced Composite Structural Members, MSc Thesis, the University of Manitoba, USA.

Schutte, C. L. (1994), Environmental Durability of Glass-Fiber Composites, *Materials Science and Engineering: R: Reports*, **13**(7), 265-323.

Shen, C. H. and Springer G. S. (1976), Moisture Absorption and Desorption of Composite Materials, *Journal of Composite Materials*, **10**(1) 2-20.

Shen, C. H. and Springer G. S. (1977), Effects of Moisture and Temperature on the Tensile Strength of Composite Materials, *Journal of Composite Materials*, **11**(1), 2-16.

Singh, I. and Bhatnagar, N. (2006), Drilling-induced Damage in Uni-directional Glass Fiber Reinforced Plastic (UD-GFRP) Composite Laminates, *The International Journal of Advanced Manufacturing Technology*, 27(9-10), 877-882.

Springer, G.S. (1977), Moisture Content of Composites under Transient Conditions, *Journal of Composite Materials*, **11**(1), 107-123.

Sridharan, S., Zureick, A. H., and Muzzy, J. D. (1998), Effect of Hot-wet Environments on E-glass/Vinylester Composites, In the *Proceedings of the 56th Annual Technical Conference of the Society of Plastics Engineers (ANTEC 98)*, Society of Plastics Engineers, Atlanta, Georgia, 26-30 April, Volume II Materials, 2255-2259.

Starr, T. (2000), Pultrusion for Engineers, Woodhead Publishing Ltd, Cambridge.

Strongwell (2013), Strongwell Design Manual, Strongwell Corporation, Bristol, Virginia, USA (http://www.strongwell.com/designmanual) accessed March, 2013.

Surathi, P. and Karbhari, V. M. (2006), Hygrothermal Effects on Durability and Moisture Kinectics of FRP Composites, Structural Systems Research Project, *Interim Report No. SSRP - 06/15*, June 2006.

Thoppul, S. D., Finegan, J. and Gibson, R. F. (2009), Mechanics of Mechanically Fastened Joints in Polymer-matrix Composites – A Review, *Composites Science and Technology*, **69**(3-4) 301-329.

Troutman, D. L. and Mostoller, J. D. (2010), An Investigation of Pin Bearing Strength on Composite Materials, in the *Proceedings of the Cooling Technology Institute Annual Conference 2010*, Cooling Technology Institute, Houston, Texas, 7-11 February, Paper TP10-24 (Materials).

Turvey, G. J. and Wang, P. (2003), Open-hole Tension Strength of Pultruded GRP Plate, *Structures and Buildings*, **156**(1) 93-101.

Turvey, G. J. (1998), Single-bolt Tension Joint Tests on Pultruded GRP Plate – Effects of Tension Direction Relative to Pultrusion Direction, *Composite Structures*, **42**(4), 341-351.

Turvey, G. J. (2000), Bolted Connections in PFRP Structures, *Progress in Structural Engineering and Materials*, **2**(2), 146-156.

Vangrimde, B., and Boukhili, R. (2003), Descriptive Relationships between Bearing Response and Macroscopic Damage in GRP Bolted Joints. *Composites Part B: Engineering*, **34**(7), 593-605.

Wang, H. S., Hung, C. L. and Chang, F. K. (1996), Bearing Failure of Bolted Composite Joints. Part I: Experimental Characterization, *Journal of Composite Materials*, **30**(12), 1284-1313.

Wang, P. (2004), Structural Integrity of Bolted Joints for Pultruded GRP Profiles, PhD Thesis, Lancaster University, UK.

Ye, B. S., Svenson, A. L. and Bank, L. C. (1995), Mass and Volume Fraction Properties of Pultruded Glass Fibre-reinforced Composites, *Composites*, **26**(10), 725-731.

Yuan, R.L., Liu, C.J. and Daley, T. (1996), Study of Mechanical Connection for GFRP Laminated Structures, in the *Proceedings of the 2nd International Conference in Advanced Composite Materials in Bridges and Structures (ACMBS/2)*, The Canadian Society for Civil Engineers (CSCE), Montreal, 951-958.

Zafari, B. and Mottram, J.T. (2012a), Effect of Hot-wet Aging on the Pin-bearing Strength of a Pultruded Material with Polyester Matrix, *Journal of Composites for Construction*, **16**(3), 340-352.

Zafari B. and Mottram, J.T. (2012b), Effect of Orientation on the Pin-bearing Strength for Bolted Connections in Bolted Joints', in the *Proceedings of 6th International Conference on FRP Composites in Civil Engineering (CICE 2012)*, Rome, Section 14: Codes and Design Guidelines, Paper 209.

Zafari, B. (2013), Startlink Building System and Connections for Fibre Reinforced Polymer Structures,' PhD thesis, University of Warwick, UK.

Zureick, A. H., Bennett, R.M. and Ellingwood, B.R. (2006), Statistical Characterization of Fiber-reinforced Polymer Composite Material Properties for Structural Design, *Journal of Structural Engineering*, **132**(8), 1320-1327.